Expanding the Chemical Space of Nitrene Transferases: Biocatalytic Construction of C–N Bonds

Thesis by

Ziyang Qin

In Partial Fulfillment of the Requirements for
the Degree of
Doctor of Philosophy in Chemistry

CALIFORNIA INSTITUTE OF TECHNOLOGY
Pasadena, California

2026
(Defended June 3rd, 2025)

Ziyang Qin
ORCID: 0000-0001-7356-6927

ACKNOWLEDGEMENTS

Five years have passed in the blink of an eye, and I am deeply grateful to have reached this milestone in completing my Ph.D. Reflecting on nearly a decade of scientific training, I have been incredibly fortunate to have been surrounded by inspiring mentors, supportive colleagues, and lifelong friends. None of this journey would have been possible without their guidance, encouragement, and belief in me.

First and foremost, I would like to express my deepest gratitude to my Ph.D. advisor and role model, Prof. Frances H. Arnold. Her unwavering support, mentorship, and encouragement have been pivotal throughout my graduate studies. Starting my Ph.D. journey during the COVID-19 pandemic made international travel incredibly challenging, but Frances was always understanding and did everything she could to help me transition from China to the UK and eventually to Caltech. Joining the Arnold Lab and pursuing research in biocatalysis and protein engineering under her guidance has been one of the most rewarding experiences of my life. Frances's passion for science and her commitment to advancing the scientific community have profoundly inspired me. Her example has taught me not only how to pursue rigorous and impactful research but also how to contribute meaningfully to the broader community.

I am also deeply thankful to my thesis committee members, Prof. Gregory C. Fu, Prof. Mikhail G. Shapiro, and Prof. Lu Wei. I appreciate their time, advice, and consistent support throughout my graduate studies, especially during moments of uncertainty about my future. Each of them has served as a role model in different ways. I vividly remember following Greg's work when I first stepped into enantioselective radical transformations, and later learning from him directly in Ch104 course. It was such an honor to have him as my committee chair. His dedication to mentoring students and his brilliance in synthetic chemistry have had a lasting impact on me. I could not have completed this journey without the support and insights of all my committee members.

A heartfelt thank you goes to Sabine Brinkmann-Chen, our exceptional lab manager. Her guidance, patience, and steady support have been instrumental throughout my time in the Arnold Lab. I have lost count of how many missteps she helped me navigate. From teaching me how to refine my presentation and writing style to always offering a listening ear, Sabine has been both a mentor and a source of strength. I'm also grateful to Cheryl Nakashima, our administrative assistant, for her fast responsiveness and kindness in handling all matters with such care.

To the incredible Arnold Lab community: thank you! Over the past five years, I have had the pleasure of overlapping with more than 40 brilliant scientists. I want to especially thank my mentor, Zhen Liu. From our overlap in the Engle Lab to our years at Caltech, Zhen has been a guiding figure and a true friend, someone I could learn from, share ideas with, and unwind with over games. I am equally indebted to my main collaborators, Ziqi Li, Shilong Gao, and Runze Mao, along with students who worked closely with us, Jan L. Heise, Sophia J. Wu, Orna Mukhopadhyay, Chi Zhang, and James B. Wang. Your contributions made these projects possible. I especially want to acknowledge Ziqi Li for her encouragement, collaboration on multiple projects, and strong support during challenging times. I would also like to thank Yueming Long, Edwin Alfonso, and Katie Sicinski for their helpful discussion, generosity, and insight. A special shout-out goes to Team "Error Prone," particularly our previous captain, Jae L. Kennemur, and current captain, Casey S. Ritts. The Caltech summer softball league has always been one of the highlights each year, and I have really cherished the time spent with teammates, fighting for a win and sharing laughter along the way! Lastly, to my incredible office mates, Jason Yang, Theophile Lambert, and Daniel Roth! Thanks for making SPL327 such an inspiring, supportive, and fun place to work. It is the BEST office! Also, I would like to thank my supervisors at Protomer, Alborz Mahdavi, Jack Steele and Ganesh Sable for their continuous support!

Beyond the lab, I am incredibly grateful for the friendships I have built at Caltech. My heartfelt thanks go to my roommate and longtime friend Ruilin Qian, with whom I shared both undergraduate and graduate experiences. I also want to acknowledge Sihe Chen, Rui Li, Junjie Yang, and Yao Luo, friends who lived with me and made Caltech feel like home. I extend my gratitude to the USTC cohort and our extended "families, " Qianying Wu, Cijin Zhou, Haixu Shen, and Hao Shen. I am especially thankful to my "Honor of Kings" friends, Stella M. Luo, Yan Sun, Jee Won Yang, Changfan Lin, Yuxing Yao, Zhiyang Jin, and Xinhong Chen, who stood by me during the most stressful periods of my Ph.D.

I owe my early passion for chemistry to my undergraduate mentors. Prof. Xisheng Wang, my first advisor, sparked my fascination with research through his dedication and enthusiasm. Rui Wang patiently taught me essential lab skills, even as I bombarded him with endless questions. I am also grateful to Chengyu Wang and Ruoxing Jin for their support during my time in the Wang Lab. I am especially indebted to Professor Keary M. Engle, who has guided me at every stage of my academic journey. Keary exemplifies kindness, integrity, and scientific excellence, and he has profoundly shaped my path. I must also thank my mentor, Tanner C. Jankins, whose creativity and

intellect made every project an exciting challenge. Prof. Alexander T. Radosevich inspired me with his originality and encouragement during my internship. I also wish to thank my MIT mentor, Gen Li, whose passion and mentorship helped me mature from an undergraduate into a graduate researcher.

I am grateful to still be connected with friends from high school and college, whose encouragement has remained a source of strength. In particular, I thank the "Kouyue Forum," formed by my dearest high school friends, Sharon Y. Tang, Gefei Liu, Kane K. Luo, Xinlu Dong, Molly M. Chen, and Rebecca K. Chen. Moreover, I am deeply grateful to my best buddies, Xisong Wang, Michael H. Chen and Bruce Z. Ju, whose steadfast companionship has carried me through ups and downs. I also extend my sincere thanks to my undergraduate friends, Xin Lian, Hongwei Lv, Shiping Sun, and Pei Wang, for their enduring support and camaraderie.

Lastly, I want to thank my parents, who have supported me unconditionally. Although I have always been an independent child and have not spent as much time with them as I would like, they have always stood behind me through every challenge. Their quiet strength and unwavering love have been my most significant source of security.

I want to thank everyone who has been in my life over the past 26 years. Each interaction, each friendship, and each lesson has helped shape the person I am today. I carry your support with deep gratitude.

ABSTRACT

The construction of carbon–nitrogen (C–N) bonds is pivotal to the development of pharmaceuticals, agrochemicals, and advanced materials. While traditional synthetic methods offer robust and efficient solutions, biocatalysis has emerged as a powerful, sustainable alternative for constructing these bonds with precise stereochemical control. Yet, the enzymatic repertoire for C–N bond formation remains limited compared to its chemical counterpart. By leveraging directed evolution and enzyme promiscuity, we have traversed beyond natural enzymatic functions and explored the new-to-nature catalytic landscape of enzymes.

This thesis outlines a suite of strategies that expand the enzymatic toolbox for stereoselective C–N bond construction in two main avenues: the functionalization of more challenging C–H bonds and the development of novel nitrene species. Chapter I reviews contemporary chemical and biocatalytic approaches, highlighting how directed evolution can transcend native enzymatic functions to unlock new reactivities.

Chapter II presents engineered serine-ligated cytochrome P411 variants capable of catalyzing enantioselective propargylic C(sp^3)–H amination, granting streamlined access to chiral propargylamines. Chapter III addresses the long-standing challenge of differentiating minimally distinct alkyl groups, methyl and ethyl substituents, by evolving P411 enzymes that perform enantiospecific functionalization of tertiary C–H bonds to construct methyl-ethyl stereocenters with high selectivity.

Chapter IV expands the scope of enzymatic nitrene transfer, enabling intramolecular alkyl and aryl nitrene C–H insertions to synthesize chiral pyrrolidines and methyl indolines. Subsequent biocatalytic derivatization of these products affords complex molecules bearing multiple chiral centers, showcasing the potential of biocatalysis to rapidly build molecular complexity. Chapter V introduces engineered protoglobins capable of mediating intermolecular methylnitrene transfer using a simple and stable *N*-methyl hydroxylamine recursor. This process uniquely achieves the stereoconvergent conversion

of both (*Z*)- and (*E*)-silyl enol ether isomers, affording enantiopure *N*-methyl-α-aminoketones, which defies conventional limitations of enzyme specificity.

Together, these efforts address critical gaps in biocatalytic C–N bond formation, establishing broadly applicable platforms for sustainable and stereoselective synthesis of *N*-containing molecules. The strategies developed herein not only deepen our understanding of heme-dependent enzymes but also lay the foundation for future innovations in biocatalysis and synthetic biology.

PUBLISHED CONTENT AND CONTRIBUTIONS

1. Liu, Z. [†]; **Qin, Z.-Y.** [†]; Zhu, L. D.; Athavale, S. V.; Sengupta, A.; Jia, Z.-J.; Garcia-Borràs, M.; Houk, K. N.; Arnold, F. H.[*] An Enzymatic Platform for Primary Amination of 1-Aryl-2-alkyl Alkynes. *J. Am. Chem. Soc.* **2022**, *144*, 80–85. https://doi.org/10.1021/jacs.1c11340 († authors contributed equally)

Z.-Y. Q. participated in the execution of the research, including enzyme engineering, enzymatic reactions, substrate scope study, and synthetic applications. Z.-Y. Q. participated in the writing of the supplementary information, and in reviewing and editing the manuscript.

2. **Qin, Z.-Y.** [†]; Gao, S. [†]; Zou, Y.; Liu, Z.; Wang, J. B.; Houk, K. N.; Arnold, F. H. Biocatalytic Construction of Chiral Pyrrolidines and Indolines via Intramolecular C(sp^3)–H Amination. *ACS Cent. Sci.* **2023**, *9*, 2333–2338. https://doi.org/10.1021/acscentsci.3c00516 († authors contributed equally)

Z.-Y. Q. designed the project and discovered the initial activity of intramolecular alkyl/aryl nitrene C–H amination with S. G.. Z.-Y. Q. participated in the design and execution of the research, including enzyme engineering, enzymatic reactions, substrate scope study, mechanistic study and synthetic applications. Z.-Y. Q. participated in the writing and editing of the manuscript and supplementary information.

3. Mao, R. [†]; Gao, S. [†]; **Qin, Z.-Y.** [†]; Rogge, T.; Wu, S. J.; Li, Z.-Q.; Houk, K. N.; Arnold, F. H. Biocatalytic, Enantioenriched Primary Amination of Tertiary C–H Bonds. *Nat. Catal.* **2024**, *7*, 585–592. https://doi.org/10.1038/s41929-024-01149-w (Preprint on *ChemRxiv* **2023**, DOI: 10.26434/chemrxiv-2023-8d2tc, † authors contributed equally)

Z.-Y. Q. participated in the execution of the research, including enzyme engineering, enzymatic reactions, substrate scope study, and mechanistic study. Z.-Y. Q. participated in reviewing and editing the manuscript.

4. **Qin, Z.-Y.** †; Li, Z.-Q. †; Heise, J. L.; Mao, R.; Arnold, F. H. Engineering Stereoconvergent Protoglobins for Enantiodivergent Construction of α-Aminoketones *via* Intermolecular Alkyl Nitrene Transfer. *Manuscript in Preparation*. († authors contributed equally)

Z.-Y. Q. designed the project and discovered the initial activity of this transformation. Z.-Y. Q. participated in the execution of the research, including enzyme engineering, enzymatic reactions, substrate scope study, and mechanistic study. Z.-Y. Q. participated in the writing and editing of the manuscript.

CONTENT NOT INCLUDED IN THESIS

5. Li, Z.-Q.; Wu, S. J.; **Qin, Z.-Y.**; Arnold, F. H. Biocatalytic Domino Amination/Semipinacol Approach to Chiral β-Aminoketones Bearing All-Carbon Quatrnary Centers. *In Preparation*.

Z.-Y. Q. participated in the execution of the directed evolution campaigns.

6. Li, Z.-Q.; Hanley, D. M.; Wu, S. J.; **Qin, Z.-Y.**; Alfonzo, E.; Arnold, F. H. Biocatalytic Amination of Unactivated Alkenes Enables Chemoenzymatic Synthesis of Oxazolidinone Antibiotics. *Manuscript in Preparation*.

Z.-Y. Q. participated in the execution of the directed evolution campaigns.

TABLE OF CONTENTS

LIST OF TABLES

LIST OF FIGURES AND SCHEMES

ABBREVIATIONS

Å	Ångstrom
ACN	acetonitrile
Ac	acetyl
AcOH	acetic acid
ALA	aminolevulinic acid
Ar	aryl
BM3	cytochrome P450 from *Bacillus megaterium* (CYP102A1)
CO	carbon monoxide
CYP	cytochrome P450 monooxygenase identifier
Cys	cystine
DMSO	dimethyl sulfoxide
d.r.	diastereomeric ratio
E. coli	*Escherichia coli*
ee	enantiomeric excess
epPCR	error-prone PCR
e.r.	enantiomeric ratio
Et	ethyl
EtOH	ethanol
GC	gas chromatography
GC-MS	gas chromatography with mass spectrometry
GOx	glucose oxidase
h	hour(s)
HB_{Amp}	Hyper Broth with 0.1 mg/mL ampicillin
HPLC	high performance liquid chromatography
HPLC-MS	high performance liquid chromatography with mass spectrometry
HRMS	high-resolution mass spectrometry
IPTG	isopropyl β-D-1-thiogalactopyranoside

KPi	potassium phosphate buffer
LB_{Amp}	Luria-Bertani medium with 0.1 mg/mL ampicillin
M9-N	M9 minimum media minus nitrogen sources
Me	methyl
MeOH	methanol
min	minute(s)
OD_{600}	optical density at 600 nm
P450	cystine-ligated cytochrome P450 monooxygenase
P411	serine-ligated cytochrome P450 enzymes
PCR	polymerase chain reaction
PDB	Protein Data Bank
RT (or r.t.)	room temperature
s	second(s)
Ser	serine
SSM	site saturation mutagenesis
StEP	staggered extension process
TB_{Amp}	Terrific Broth with 0.1 mg/mL ampicillin
T_R	retention time
TTN	total turnover number
Ts	*para*-toluenesulfonyl
UV-vis	ultraviolet visible
WT	wild type

C h a p t e r I

THE CARBON-NITROGEN (C–N) BOND: A CORNERSTONE OF BIOLOGICAL COMPLEXITY

1.1 Overview

Carbon–nitrogen (C–N) bonds constitute a foundational pillar of molecular complexity in both biological systems and synthetic chemistry (**Figure 1.1**). They serve as the chemical backbone for processes that sustain life and drive pharmaceutical innovation. In living organisms, these bonds are indispensable for encoding the structural and functional diversity of life-sustaining biomolecules: peptides and proteins rely on amide linkages for enzymatic catalysis and cellular architecture; nucleotides utilize nitrogenous bases to store genetic information; and adenosine triphosphate (ATP) harnesses C–N motifs to mediate energy transduction. Beyond their biological ubiquity, C–N bonds are equally critical to pharmaceutical and agrochemical industries, where nitrogen-containing compounds dominate drug candidates, bioactive agents, and crop protection molecules. Nitrogen's versatility in forming hydrogen bonds, ionic interactions, and π-stacking arrangements makes it indispensable for drug-target binding, with around 85% of kinase inhibitors and 70% of antibiotics relying on C–N motifs for bioactivity. Furthermore, the stereochemical precision of these bonds, often exemplified by amino acids and antibiotics, governs their biological activity and therapeutic efficacy.

Hence, the necessity to construct C–N bonds with high efficiency, sustainability, and stereochemical control has driven decades of innovation in synthetic methodology. Transition metal-catalyzed cross-coupling reactions, such as the Buchwald-Hartwig amination, Chan-Lam coupling, and Ullmann reaction, have revolutionized the access to chiral amines and *N*-heterocycles, enabling the scalable synthesis of complex pharmacophores[1–3]. Parallel advances in main-group catalysis, leveraging elements such as phosphorus and boron, have established an orthogonal approach to make challenging

C–N bonds that were previously inaccessible with transition metal catalysis[4,5]. Despite these achievements, persistent challenges remain, including the reliance on precious metals, harsh reaction conditions, and limitations in stereoselectivity—issues that conflict with growing demands for green chemistry and atom-economical processes.

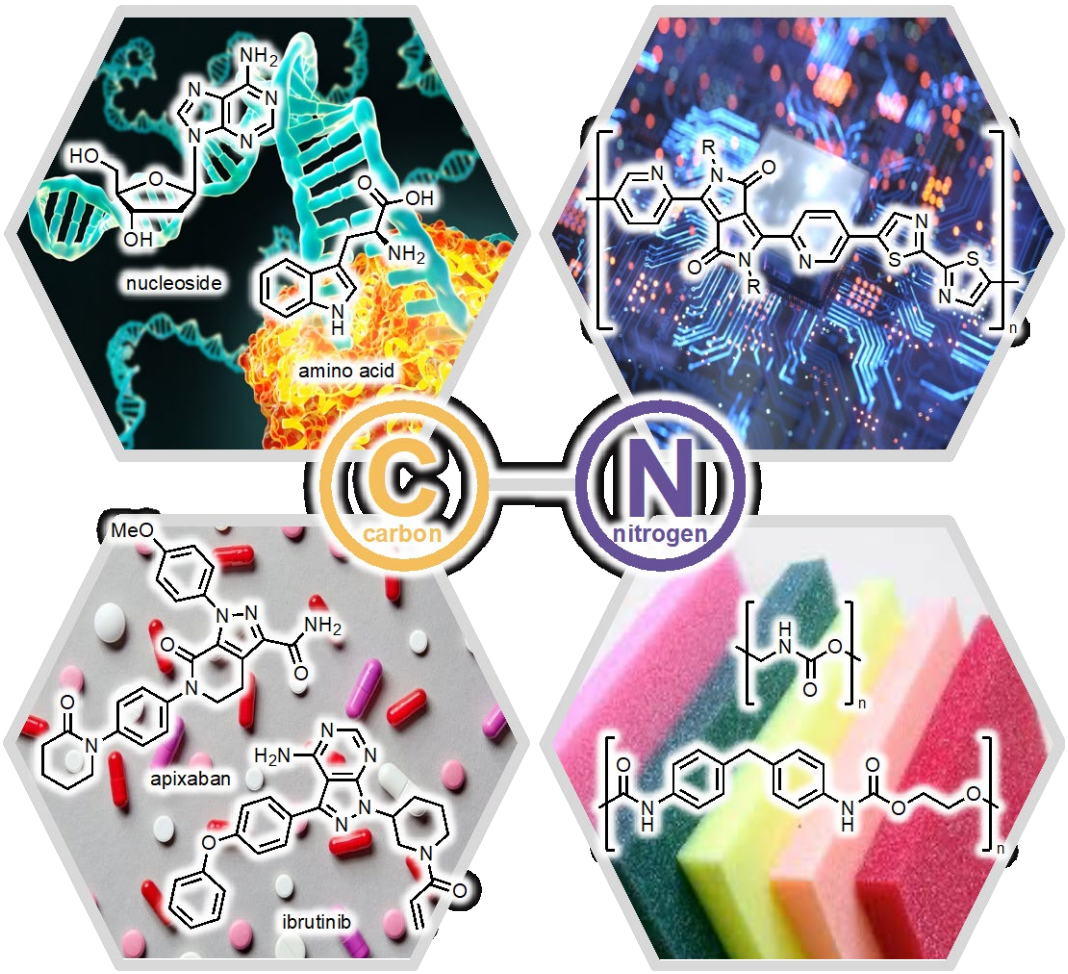

Figure 1.1. The ubiquitous role of C–N bonds in modern society.

Recently, much attention has shifted toward radical-mediated C–N bond-forming strategies and biocatalytic approaches, which offer distinct advantages in sustainability and stereochemical control[6,7]. C–N bond formation strategies involving radical intermediates bypass traditional two-electron mechanisms, unlocking unconventional reactivity and functional group tolerance. Meanwhile, biocatalytic methods, employing enzymes such as

ammonia lyases, transaminases, and nitrene transferases, harness Nature's precision to construct C–N bonds with unparalleled regio- and stereoselectivity under ambient conditions. Together, these research frontiers not only address longstanding synthetic limitations but also bridge the gap between chemical synthesis and biosynthesis, offering transformative potential for drug discovery and sustainable manufacturing.

1.2 Radical-mediated stereoselective construction of C–N bonds

Radical chemistry is distinguished by its unique reactivity, high efficiency under mild conditions, and broad functional group tolerance[8]. These attributes render radical-mediated strategies highly attractive and orthogonal to traditional polar pathways for C–N bond construction. Notably, radical C–N coupling has emerged as a powerful approach to generate quaternary centers stereoselectively and to enable stereoconvergent transformations that are often challenging through classical ionic or organometallic routes.

A pivotal aspect of radical-mediated C–N bond formation is the generation of carbon-centered radicals. These can be categorized into three main mechanistic categories based on their origin (**Figure 1.2**): (1) single-electron transfer (SET) or halogen atom transfer (XAT) from alkyl halides, (2) radical addition to alkenes, and (3) hydrogen atom transfer (HAT) from C–H bonds. Over the past decade, these approaches have enabled the enantioselective transformation of simple feedstocks into value-added chiral *N*-containing compounds. Given the vast and rapidly expanding literature, this section highlights a selection of recent contributions from the past five years.

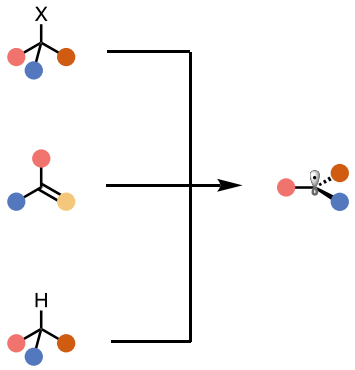

Figure 1.2. Representative categories of radical-based C–N bond formation reactions.

1.2.1 Enantioselective Amination of Alkyl Halides

Pioneering work by the Fu group has laid the foundation for enantioselective radical amination of alkyl halides. In 2021, Fu and coworkers reported a photoinduced, copper-catalyzed enantioconvergent amination of racemic unactivated alkyl bromides[9]. This transformation granted access to structurally diverse secondary amides, including aromatic, aliphatic, and natural product–derived motifs, using a variety of directing groups (e.g., phosphoryl, amide, ester, ketone, sulfone, **Figure 1.3**). The success of this system hinged on the *in situ* assembly of a chiral copper catalyst comprising three ligands: a bidentate phosphine and a phenoxide coordinated to Cu(I) to form a photoactive complex with a sufficiently long-lived excited state and strong reduction potential for C–Br activation; and a bidentate chiral diamine bound to Cu(II) to mediate stereoselective C–N bond formation. In 2022, Fu's group expanded this strategy to the enantioconvergent coupling of racemic tertiary α-substituted α-chloro-/bromo-nitriles with aniline derivatives, enabling efficient access to chiral amines bearing fully substituted stereocenters with high enantioselectivity (**Figure 1.3**)[10].

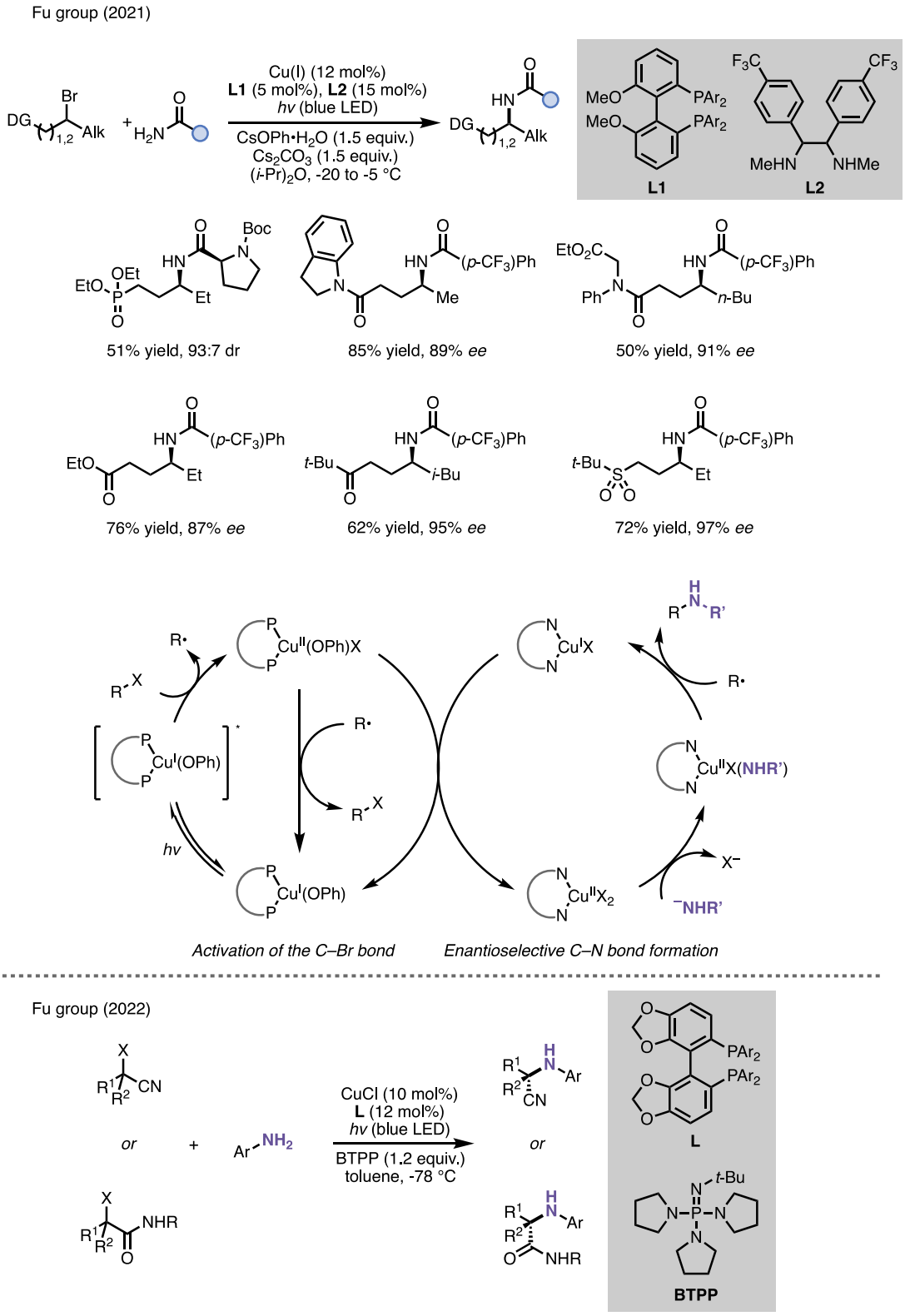

Figure 1.3. Photoinduced, Cu-catalyzed enantioselective amination from alkyl halides.

Parallel advances were made by the Liu group. In 2021, they disclosed a copper-catalyzed enantioconvergent C–N coupling of racemic secondary alkyl halides using electron-rich tridentate anionic *N,N,P*-ligands and sulfoximines as ammonia surrogates (**Figure 1.4**)[11]. This transformation delivered enantioenriched *N*-alkyl sulfoximines bearing stereocenters adjacent to benzyl, propargyl, carbonyl, or cyano groups.

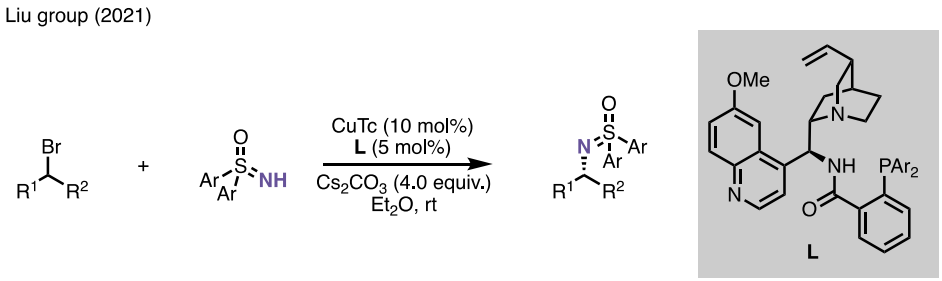

Figure 1.4. Cu-catalyzed enantioselective amination of secondary alkyl halides with *N,N,P*-ligand.

In 2023, Liu and coworkers designed a novel anionic *N,N,N*-ligand with an expansive side arm, enabling efficient C(sp^3)–N bond formation from sterically congested tertiary alkyl halides (**Figure 1.5**)[12]. The same year, the Liu group further developed chiral *N,N,N*-tridentate anionic ligands that enabled Cu-catalyzed enantioconvergent *N*-alkylation of simple aliphatic amines (e.g., ammonia, methylamine, dimethylamine) and α-carbonyl alkyl chlorides[13]. This robust transformation showed exceptional enantioselectivity and functional group tolerance and was successfully applied to late-stage functionalization of pharmaceutically relevant amines. The strong coordination of the tridentate ligand to copper not only prevented catalyst deactivation by nucleophilic amines but also promoted high stereoinduction. Concurrently, Fu and colleagues developed a Cu/chiral isoxazoline-catalyzed enantioconvergent substitution of racemic α-chloro-/bromo-*N*-phenylbutanamides with amines, affording α-amino amides with excellent yields and enantioselectivity[14].

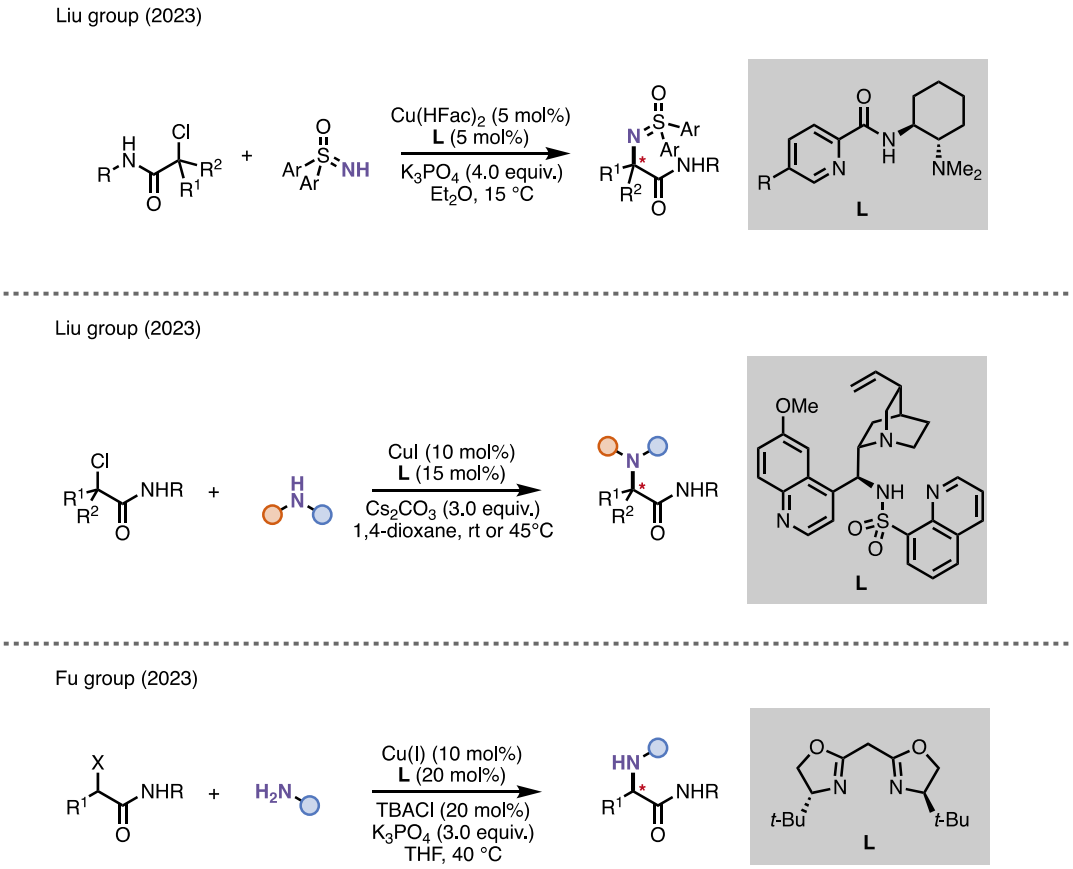

Figure 1.5. Cu-catalyzed enantioconvergent radical C–N cross-coupling.

In 2025, the Fu group introduced a photoinduced Cu-catalyzed method for constructing tertiary alkyl amines *via* coupling between secondary alkyl amines and unactivated secondary or tertiary alkyl halides[15]. They also reported a Cu-catalyzed enantioconvergent synthesis of β-aminoalcohols recently[16]. Most recently, Liu group unveiled a Cu-catalyzed strategy for the enantioselective amination of unactivated, prochiral secondary alkyl radicals (**Figure 1.6**)[17]. This approach relied on specially designed tridentate *N,N,P*-ligands to differentiate between two similar alkyl substituents at the radical center. Drawing inspiration from enzymatic active sites, the authors proposed that the catalyst forms a truncated, cone-shaped chiral pocket around the Cu center, positioning larger groups near the pocket's opening and smaller groups in a more confined

space. This spatial organization promotes outer-sphere enantiodiscrimination during radical substitution between the alkyl radical and a Cu(II)–sulfoximinato complex.

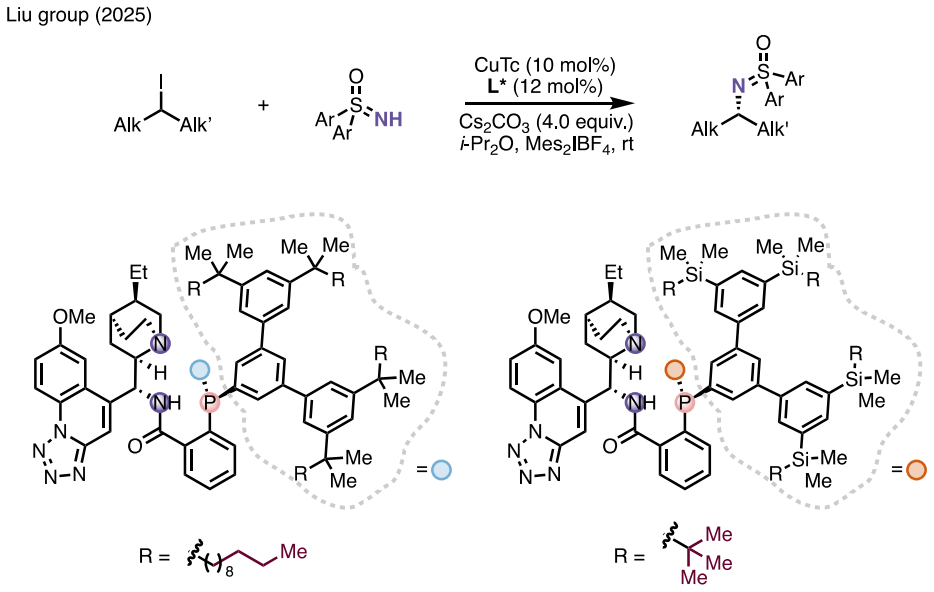

Figure 1.6. Asymmetric amination of alkyl radicals with minimally different alkyl substituents.

Beyond copper, emerging studies have also demonstrated the potential of iron catalysis for enantioselective radical C–N bond formation, opening additional avenues for sustainable and versatile amination strategies[18].

1.2.2 Enantioselective Amination of Alkenes

Alkenes are abundant feedstock chemicals that can be readily utilized as a starting point to rapidly build up molecular complexity. The C=C double bond in alkenes is prone to radical addition, which makes them ideal candidates for radical-mediated reactions. Radical-mediated asymmetric amination of alkenes provided a reliable approach to incorporate electrophilic, nucleophilic, and nitrene-type nitrogen sources into double bonds, providing an efficient and versatile route to access a large diversity of chiral amines.

In 2020, Knowles and coworkers developed a dual-catalytic strategy for the enantioselective hydroamination of olefins using a chiral phosphoric acid (CPA) and a photoredox catalyst (PC)[19]. Mechanistic studies revealed that nitrogen-centered radicals are generated *via* proton-coupled electron transfer (PCET) activation of sulfonamide N–H bonds. These radicals undergo enantioselective *5-exo-trig* cyclization, followed by hydrogen atom transfer (HAT) from a thiol to furnish tetrahydropyrrole derivatives. Enantioselectivity is achieved through noncovalent interactions between the neutral sulfonamidyl radical and the CPA, which mediate the enantio-determining radical addition step (**Figure 1.7**).

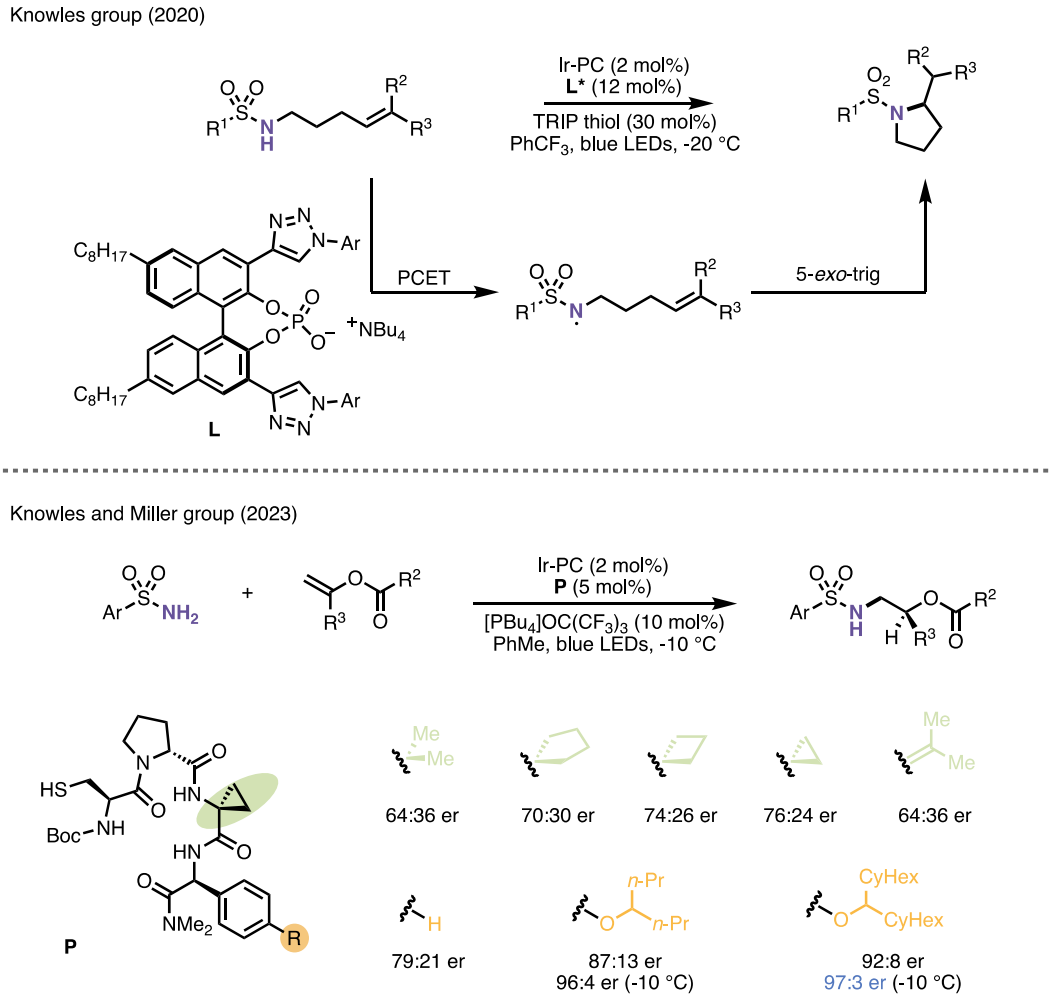

Figure 1.7. CPA/PC or peptide/PC dual-catalyzed enantioselective hydroamination of alkenes *via* PCET.

Building on this work, in 2023, the Knowles and Miller groups jointly reported a peptide-catalyzed enantioselective hydroamination of alkenes[20]. Through systematic variation of both the peptide catalyst and alkene substrates, they established key structure–selectivity relationships that guided the development of an optimized catalyst. Mechanistic insights from both experimental and computational studies revealed that hydrogen bonding, π–π stacking, and London dispersion forces contribute significantly to substrate recognition and enantioinduction.

Another notable class of asymmetric alkene functionalization involves nitrene transfer reactions. In recent years, the Chang group has developed a series of Ni- and Fe-catalyzed transformations employing dioxazolones as nitrene precursors to access diverse α- and β-amino carbonyl compounds and amides[21–23]. A 2023 study reported a Ni-catalyzed intramolecular hydroamidation of alkenes that enables the enantioselective synthesis of chiral β-lactams (**Figure 1.8**)[24]. This method was successfully applied to construct key intermediates *en route* to pharmaceuticals such as sitagliptin and carbapenem antibiotics.

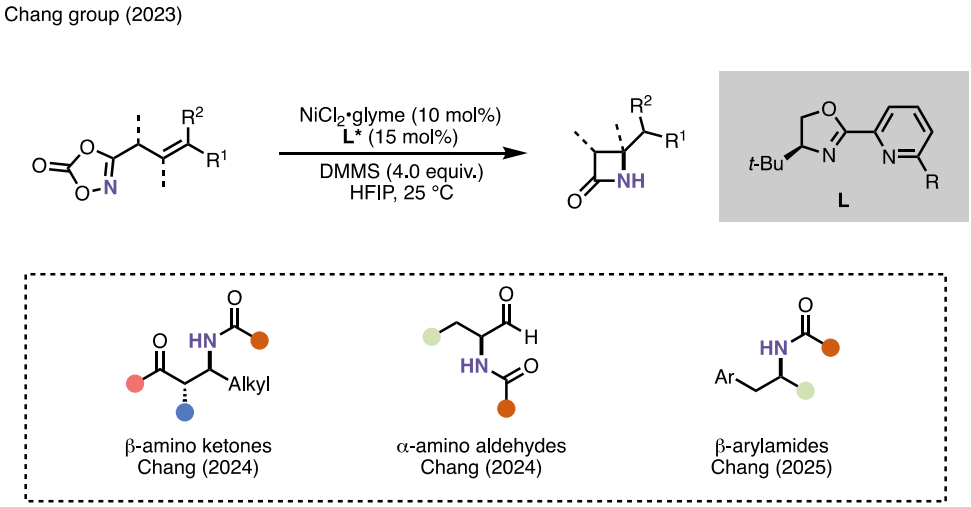

Figure 1.8. Ni- and Fe-catalyzed asymmetric hydroamination reactions *via* nitrene intermediates.

Asymmetric alkene aziridination is also an important class of radical-mediated alkene functionalization transformations. In 2008, Zhang and coworkers pioneered the use of cobalt(II) complexes bearing D_2-symmetric chiral porphyrins for the enantioselective aziridination of olefins, employing diphenylphosphoryl azide (DPPA) as the nitrene source[25]. This represented an early example of cobalt-mediated asymmetric nitrene transfer. More recently, in 2024, the same group reported the development of an enantioselective radical *N*-heterobicyclization reaction using a cobalt(II)-based metalloradical catalysis (MRC) platform[26]. Distinct from previous methodologies, the process proceeds via formation of a Co(III)-aminyl radical intermediate, which undergoes a 6-endo-trig radical addition to a terminal olefin, forming a γ-Co(III)-alkyl radical. This intermediate then undergoes a stereospecific 3-*exo*-tet radical cyclization to forge the N-heterobicyclic framework (**Figure 1.9**). Comprehensive experimental and computational analyses identified two critical steps governing enantioselectivity: enantiofacial-selective radical addition and subsequent stereospecific radical substitution.

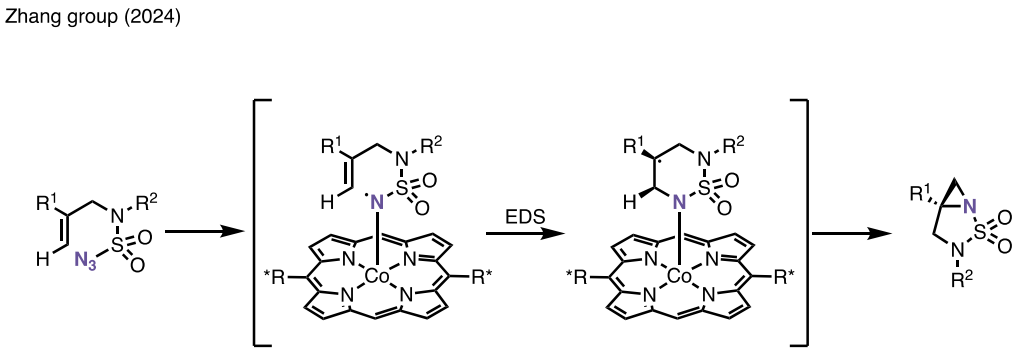

Figure 1.9. Co-porphyrin-catalyzed enantioselective radical bicyclization.

1.2.3 Enantioselective C–H amination to construct C–N bonds

Direct C–H functionalization is vital for constructing C–N bonds as it bypasses the need for pre-functionalized substrates, enabling efficient, step- and atom-economical synthesis of amines, amides, and *N*-heterocycles. By directly activating inert C–H bonds using radical-based methods, it streamlines access to pharmaceuticals, agrochemicals, and

biomolecules while minimizing waste. Pioneering work has been achieved by multiple groups utilizing different transition metals, such as cobalt, copper, iron, nickel, rhodium, ruthenium, iridium, and so on.

Metalloradical catalysis (MRC) has emerged as a powerful strategy for C–H functionalization, leveraging metal-coordinated radical species to activate organic substrates in novel ways[27]. In this context, Zhang and coworkers developed a family of D_2-symmetric chiral cobalt(II) porphyrin complexes that function as stable 1,5-electron metalloradicals. These Co(II)-based MRC systems effectively activate organic azides, generating α-Co(III)-aminyl radicals that undergo 1,5-, 1,6-, or even intermolecular hydrogen atom transfer (HAT) followed by amino radical substitution, enabling the formation of enantioenriched C–N bonds.

Over the past decade, the Zhang group has systematically explored intramolecular C–H amination of sulfamoyl azides *via* 1,5- and 1,6-HAT pathways, affording chiral cyclic sulfonamides with high stereocontrol. The scope of this methodology was further expanded to include intermolecular HAT processes, enabling the enantioselective amination of benzylic and allylic C–H bonds. In 2020, they reported an enantioselective intermolecular radical C–H amination of benzylic substrates bearing ester functionalities, using fluoroaryl azides as nitrogen sources (**Figure 1.10**)[28]. This transformation facilitated the synthesis of valuable α-amino acid derivatives with excellent enantioselectivity.

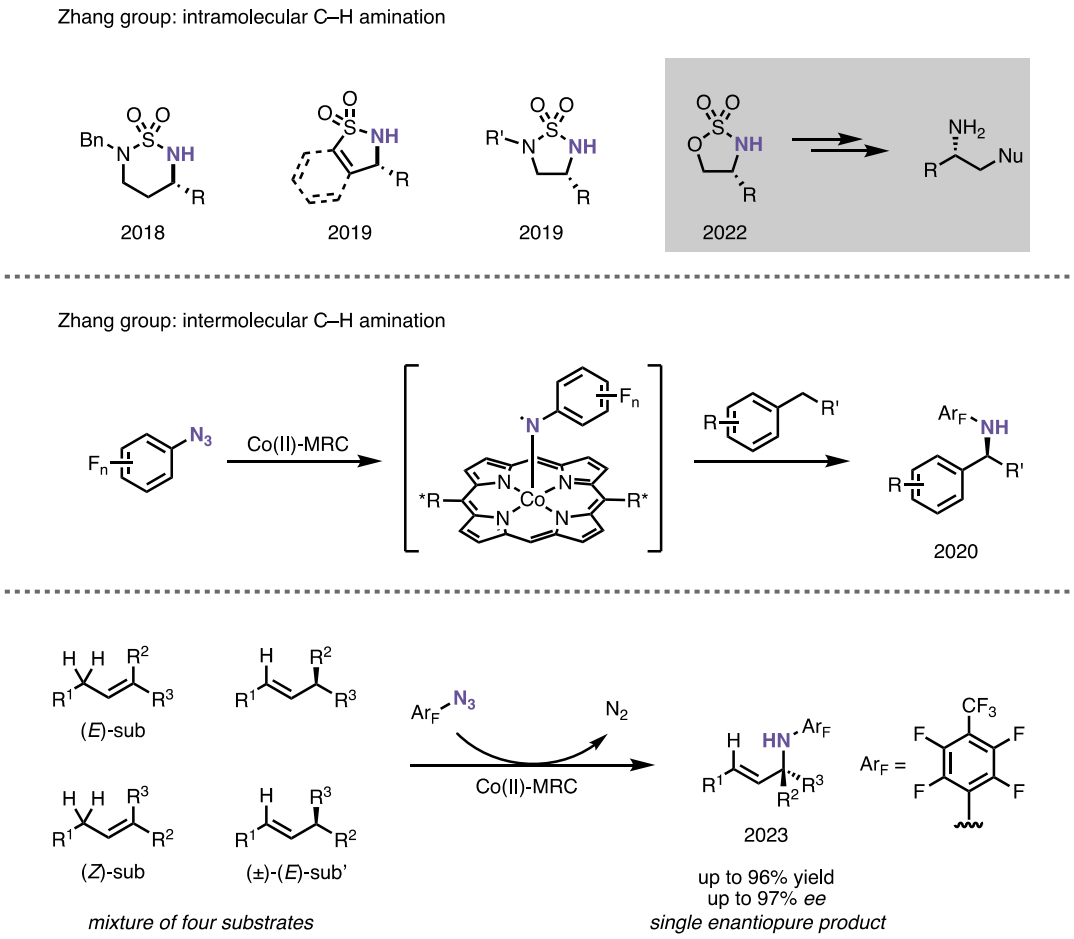

Figure 1.10. Co(II)-porphyrin-catalyzed enantioselective radical C–H amination.

A major synthetic challenge in organic chemistry is the convergent transformation of isomeric alkene mixtures. Addressing this issue, Zhang and coworkers recently developed a cobalt-based MRC approach for the intermolecular enantioselective radical allylic C–H amination of isomeric alkenes (**Figure 1.10**, bottom)[29]. By employing modularly tunable D_2-symmetric chiral amidoporphyrin ligands, this method enables the efficient synthesis of chiral α-tertiary amines from a broad range of fluoroaryl azides and alkene isomers. The high level of regio- and stereocontrol is attributed to the delocalized nature of the allyl radical intermediate and the stepwise nature of the radical mechanism. Mechanistic investigations, including density functional theory (DFT) calculations and kinetic isotope effect (KIE) studies, support a stepwise radical pathway and elucidate key

factors influencing both regioselectivity and enantioselectivity. Crucially, the chemical and stereochemical convergence observed in these transformations is enabled by the dynamic delocalization of the allylic radical intermediate and the precise chiral environment provided by the cobalt catalyst.

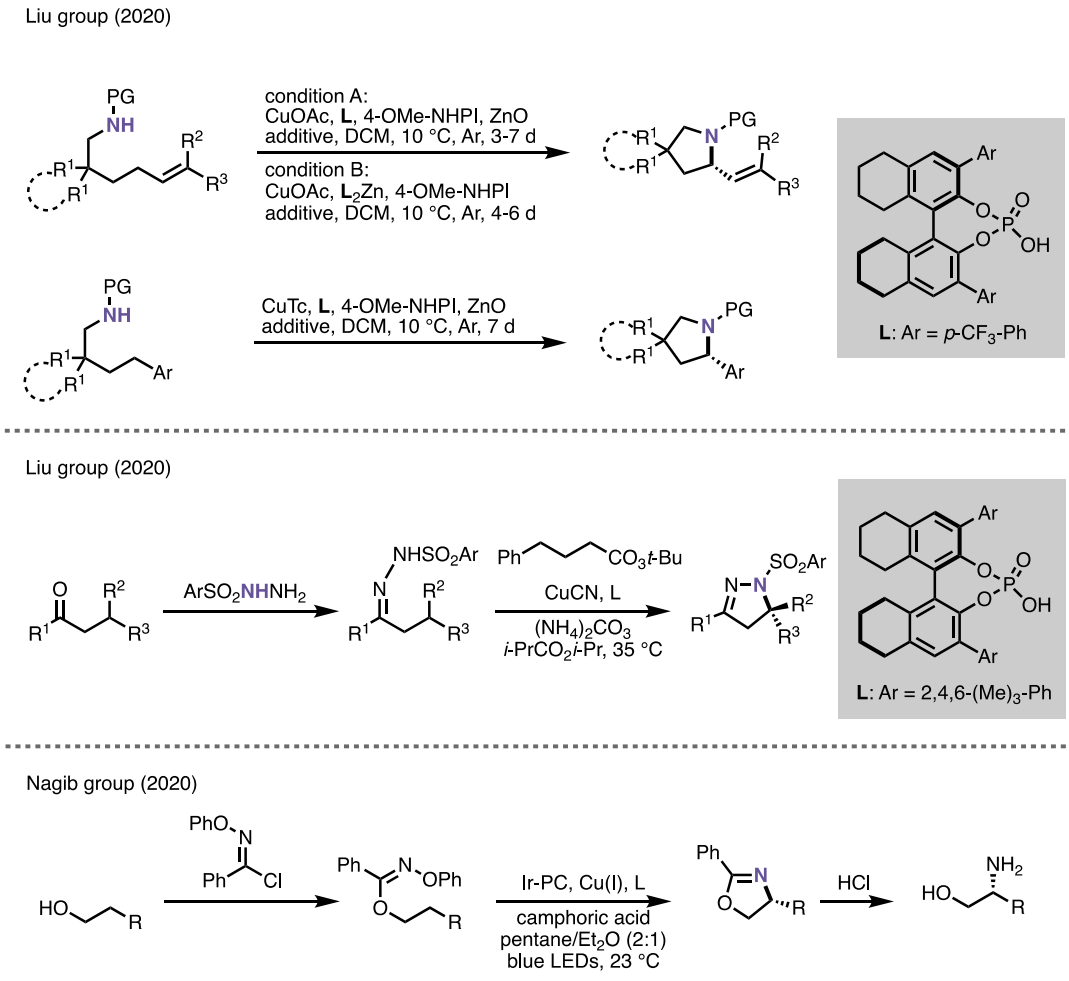

Figure 1.11. Cu-catalyzed intramolecular asymmetric C–H amination.

Beyond cobalt-based systems, copper catalysis has also emerged as a powerful platform for the enantioselective construction of C–N bonds. In 2020, Liu group sequentially reported two notable Cu/chiral phosphoric acid (CPA)-catalyzed transformations: (1) an asymmetric radical intramolecular 1,5-C–H amination of allylic and benzylic substrates[30], and (2) an enantioconvergent intramolecular radical amination

of tertiary β-C(sp³)–H bonds in racemic ketones[31]. Both methods showcased broad substrate scope, high efficiency, and good to excellent enantioselectivities (**Figure 1.11**). Concurrently, the Nagib lab developed a copper/photocatalyst (Cu/PC) dual catalytic system for intramolecular 1,5-C–H amination, enabling the synthesis of chiral β-amino alcohols[32].

In 2023, Chang and coworkers introduced a Cu/chiral bisoxazoline (BOX)-catalyzed regio- and enantioselective δ-C(sp³)–H amidation of dioxazolones (**Figure 1.12**)[33]. This transformation enabled the efficient synthesis of six-membered chiral lactams with excellent regioselectivity and enantiocontrol. The work builds upon their earlier success in iridium-catalyzed intramolecular γ-C–H amidation to access γ-lactams[34,35].

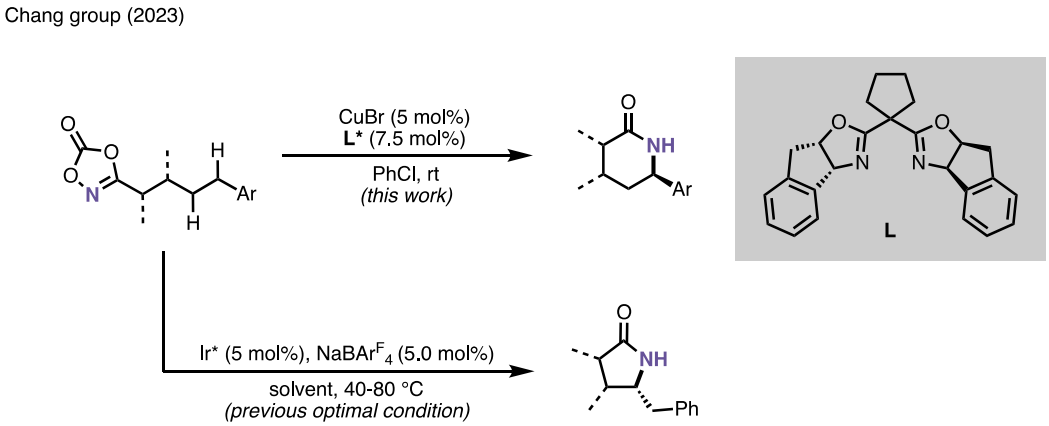

Figure 1.12. Cu-catalyzed intramolecular nitrene C–H insertion to forge δ-lactams.

That same year, Zhou and colleagues reported a Cu/BOX-catalyzed intermolecular enantioselective benzylic C(sp³)–H amination[36]. The strategy employed a peroxide as both oxidant and hydrogen atom transfer (HAT) reagent, with benzamide serving as the nitrogen source. Independently, Lian and Kramer groups developed a copper/photoredox (Cu/PC) dual-catalytic platform for enantioselective benzylic C–H amination and amidation, notable for using the benzylic C–H substrate as the limiting reagent[37].

1.3 Natural biocatalytic construction of C–N bonds

Although a broad range of chemical methods has been developed for constructing C–N bonds selectively, many still suffer from limitations such as sophisticated ligand designs, poor stereoselectivity, or harsh reaction conditions. In contrast, Nature has evolved elegant and efficient enzymatic strategies to form C–N bonds under mild, aqueous, and biocompatible conditions. These biological transformations often proceed *via* mechanisms such as nucleophilic amine addition or radical-mediated pathways, offering high regio- and stereoselectivity with remarkable catalytic efficiency. Moreover, these enzymatic reactions are inherently sustainable, characterized by their leverage of non-toxic reagents, ambient reaction conditions, and minimal environmental footprint. Their capacity to operate with exquisite selectivity while achieving high activity has inspired chemists to adapt and engineer these biocatalysts for use in stereoselective C–N bond construction. As such, biocatalysis represents a promising and complementary platform to traditional synthetic methodologies for the development of chiral amines and *N*-heterocycles.

1.3.1 C–N lyase-catalyzed hydroamination reactions

C–N lyases catalyze the non-hydrolytic, non-oxidative cleavage of C–N bonds *via* elimination reactions, typically resulting in the formation of unsaturated systems or cyclic structures with the release of ammonia or amines. These reactions are inherently reversible, and the equilibrium can be shifted toward C–N bond formation by employing an excess of the amine or alkene substrate. Such thermodynamic control enables the synthetic application of lyases for the biocatalytic, stereoselective construction of C–N bonds.

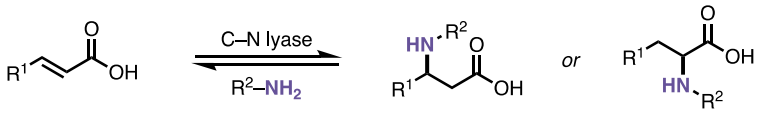

Figure 1.13. General transformation of C–N lyase-catalyzed asymmetric C–N bond formation.

In 2019, Poelarends and coworkers reported the use of ethylenediamine-*N,N'*-disuccinic acid lyase (EDDS lyase) for the synthesis of *N*-arylated aspartic acids and pyrazolidinones (**Figure 1.14**)[38]. This lyase demonstrated broad substrate compatibility, efficiently catalyzing the addition of a wide range of arylamines to fumarate with high conversion rates and excellent enantioselectivity. More recently, Wu and coworkers identified a phenylalanine ammonia lyase (PAL), *Ls*PAL3 from *Lactuca sativa* L., which enabled the kinetic resolution of racemic phenylalanine derivatives and promoted ammonia addition across a diverse panel of cinnamic acid substrates (**Figure 1.14**)[39].

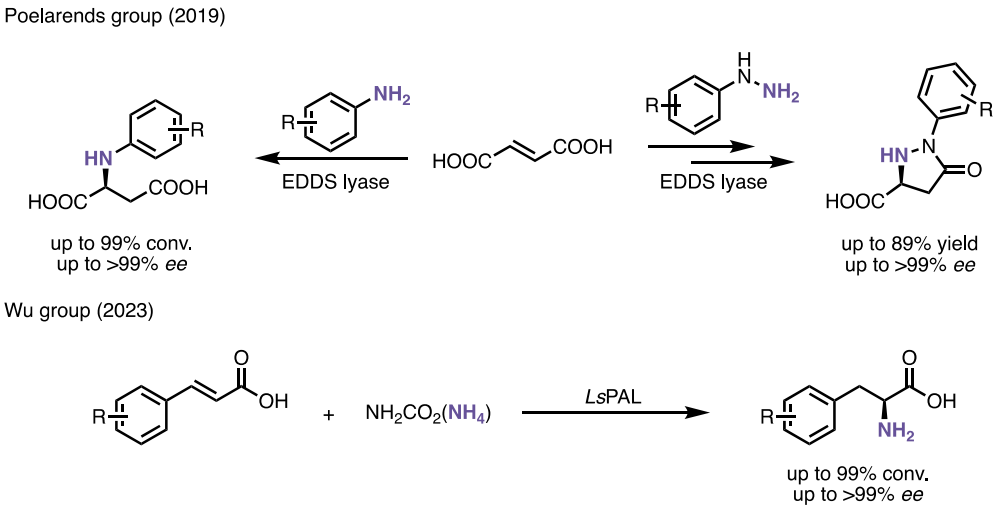

Figure 1.14. Biocatalytic hydroamination catalyzed by natural lyases.

In parallel, another Wu group utilized computational approaches to redesign an aspartase from *Bacillus* sp. YM55-1 (AspB) for the synthesis of β-amino acids (**Figure 1.15**)[40,41]. The engineered variant, B19, exhibited high catalytic activity toward α,β-unsaturated carboxylic acids, with exceptional substrate loading tolerance up to 300 g/L. Building upon this platform, they screened an *in silico*–derived mutant library of B19 to identify AspB variants with expanded activity and substrate scope.

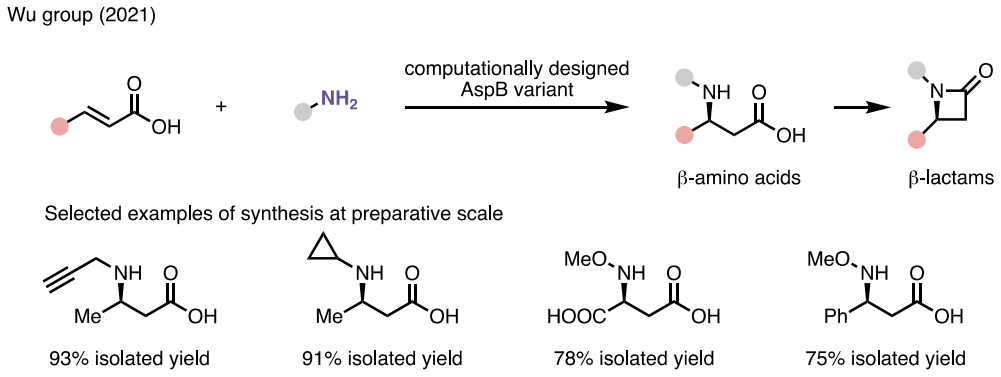

Figure 1.15. Computationally redesigned AspB variant catalyzing β-amino acid synthesis.

These studies highlight the versatility of C–N lyases as powerful biocatalysts for the synthesis of noncanonical amino acids (ncAAs) and other nitrogen-containing scaffolds. Their ability to operate with high stereo- and chemoselectivity under green and scalable conditions underscores their potential for industrial applications in sustainable nitrogen bond construction.

1.3.2 S-adenosyl-L-methionine (SAM)-dependent methyl transferase-catalyzed *N*-alkylation reactions

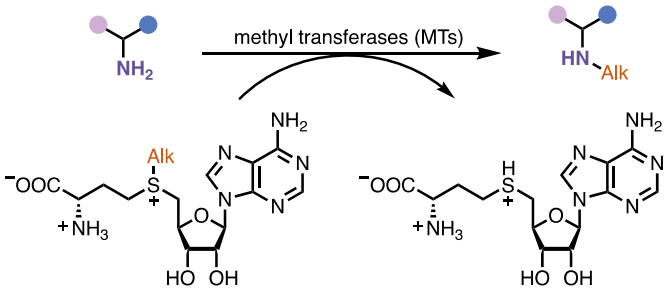

Figure 1.16. General transformation of MT-catalyzed C–N bond formation.

SAM–dependent methyltransferases (MTs) constitute a vast and functionally diverse enzyme superfamily that utilizes SAM as an alkyl donor to catalyze *N*-alkylation

across a wide array of biological substrates, including proteins, nucleic acids, lipids, and small molecules.

Building on this natural reactivity, Seebeck and coworkers demonstrated that halide methyltransferases can be repurposed to generate fluorinated SAM analogues, specifically mono-fluorinated SAM (F-SAM), which enabled site-specific monofluoromethylation of amino acids[42]. This strategy allows for the direct incorporation of fluorine, a valuable pharmacophore, into target molecules, offering another biocatalytic route to fluorinated building blocks for drug discovery.

In parallel, the Hammer group demonstrated a regioselective enzymatic *N*-alkylation strategy for the functionalization of pyrazole scaffolds (**Figure 1.17**)[43]. In a subsequent study, they further developed the methyltransferase system to accommodate a broader scope of *N*-heterocycles, including benzimidazoles, benzotriazoles, imidazoles, and indazoles with remarkable regioselectivity (*rr* > 99:1), regiodivergence, and high catalytic efficiency (up to 99% yield).

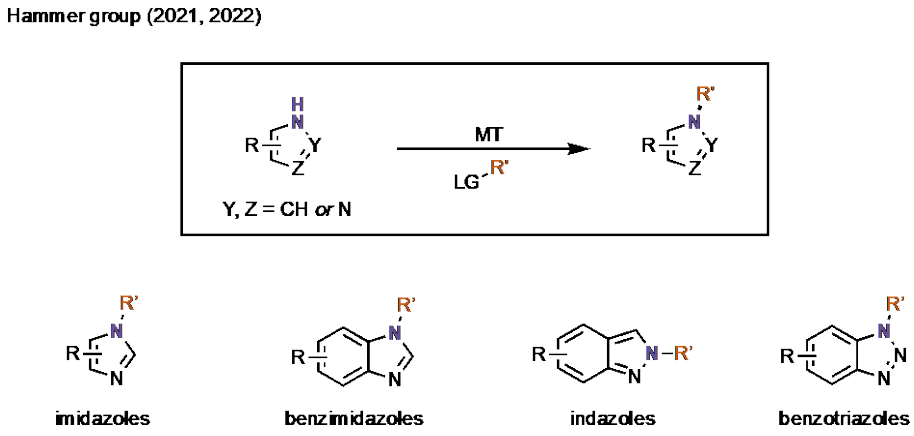

Figure 1.17. Selective MT-catalyzed *N*-alkylation of unsaturated heterocycles.

1.3.3 Transaminase-catalyzed C–N bond construction

Transaminases (TAs), a prominent subclass of transferases, catalyze the reversible transfer of an amino group from an amino acid to a keto acid, yielding a new amino acid

and a corresponding keto acid. This reaction plays a central role in amino acid biosynthesis and catabolism, as well as nitrogen metabolism. Due to their inherent substrate promiscuity and operational robustness, TAs have been extensively investigated in both academic and industrial settings as versatile biocatalysts for the synthesis of diverse amino acid derivatives. These include molecules of significant interest in pharmaceuticals, agrochemicals, and materials science, such as noncanonical α-amino acids, β-amino acids, and D-amino acids.

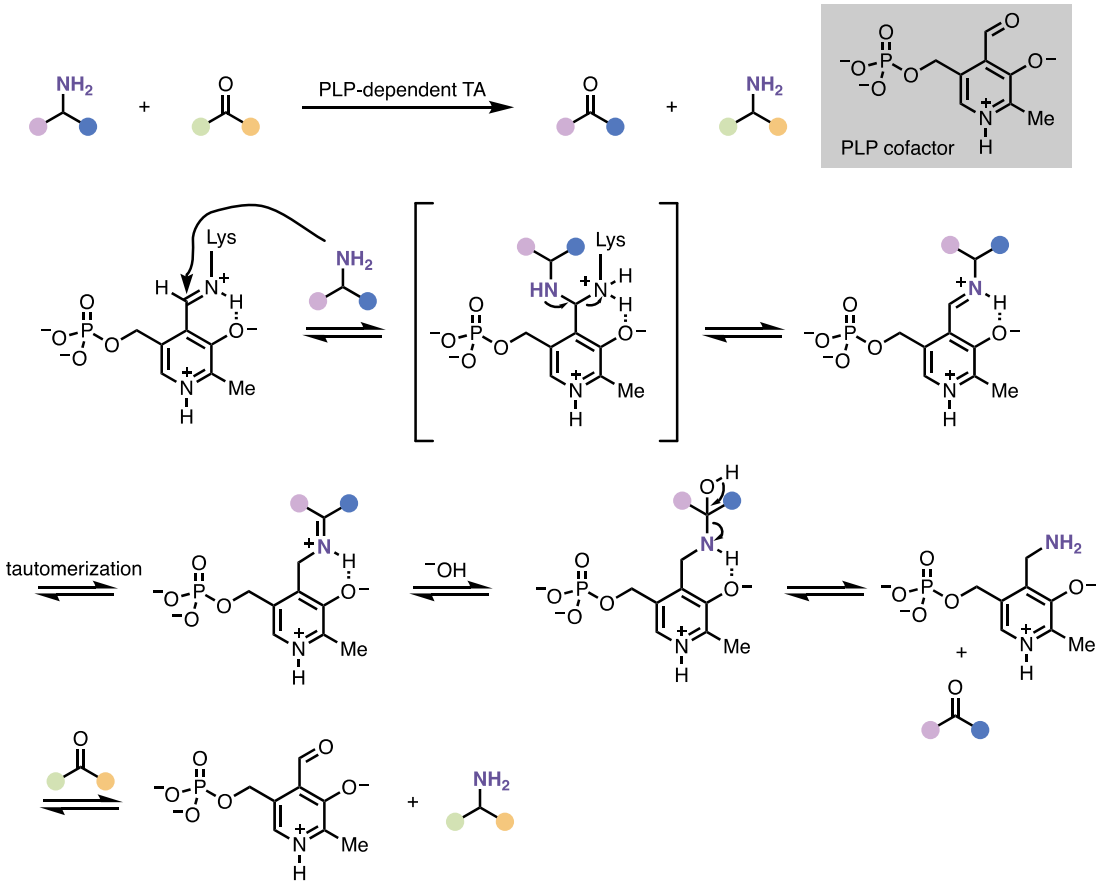

Figure 1.18. General mechanism of TA-catalyzed asymmetric C–N bond formation.

In 2020, Seebeck and coworkers developed a multienzyme cascade combining a transaminase (TA), a methyltransferase (MT), and a halide methyltransferase (HMT) to convert L- or D-α-amino acids into β-methylated α-amino acids[44]. This approach expands

the utility of TAs in value-added amino acid derivatization. Renata and colleagues reported a highly diastereo- and enantioselective TA-based method for the synthesis of aromatic β-branched α-amino acids. Their strategy harnessed a dynamic kinetic resolution (DKR) process to achieve excellent stereoselectivity across a broad substrate scope. Although several substrate classes exhibited reduced reactivity or selectivity, the authors proposed that these limitations could be addressed through genome mining and directed evolution.

In 2024, researchers at Merck reported a novel application of lysine as a "smart" amine donor in TA-catalyzed DKR reactions to access β-branched noncanonical arylalanines[45]. This method enabled the efficient preparation of a wide array of β-branched arylalanines, including those bearing challenging cyclopropyl and isopropyl groups, in high yields and with excellent stereoselectivity (**Figure 1.19**).

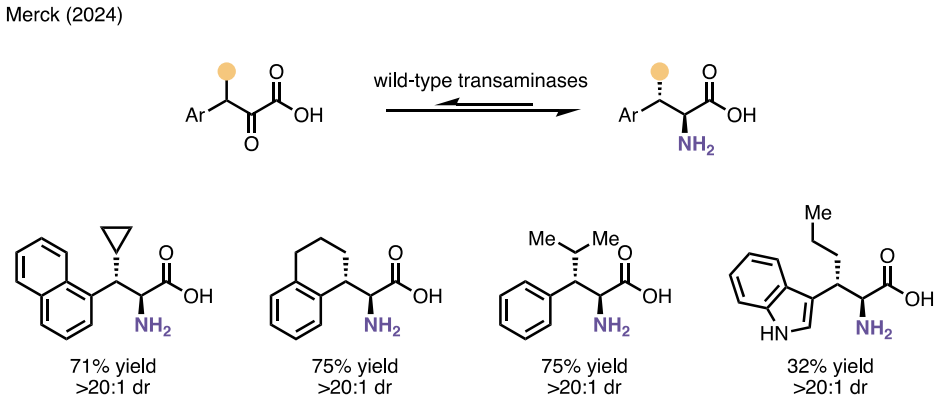

Figure 1.19. TA-catalyzed synthesis of β-branched noncanonical amino acids.

1.3.4 NAD(P)H-dependent imine reduction enzyme-catalyzed C–N bond formation

Chiral amines can also be synthesized by natural enzymes through the reduction of imine intermediates, which typically arise from the condensation of carbonyl compounds and amines. Key enzyme classes capable of reducing imines to furnish chiral amines include amine dehydrogenases (AmDHs)[46], opine dehydrogenases (OpDHs)[47], imine reductases (IREDs), reductive aminases (RedAms)[48], and Pictet–Spenglerases (PSases)[49].

Since the first demonstration of IREDs as competent catalysts for the asymmetric synthesis of chiral amines[50], considerable advancements have been made in expanding their substrate scope and improving catalytic performance[51]. A notable example by Turner and colleagues employed a high-throughput screen of 384 metagenomic IREDs, enabling the enantiocomplementary synthesis of 2-aminotetralin and 3-aminochroman derivatives[52]. Beyond reductive amination, IREDs also catalyze conjugate reductions. The Turner group identified a set of IREDs, named "EneIREDs," capable of catalyzing amine-activated conjugate alkene reduction followed by reductive amination. This enzyme can couple a diverse array of α,β-unsaturated carbonyls with amines to streamline the synthesis of chiral amines bearing multiple stereocenters (**Figure 1.20**). Mechanistic studies indicated a dual EneIRED catalytic cycle, where α,β-unsaturated carbonyls first underwent a conjugate reduction process, generating chiral carbonyls, followed by a reductive amination process to afford the desired products. IREDs have also found industrial relevance, where a team from GlaxoSmithKline medicines successfully engineered an IRED variant for kilogram-scale synthesis of a key intermediate in the production of the LSD1 inhibitor GSK2879552[53].

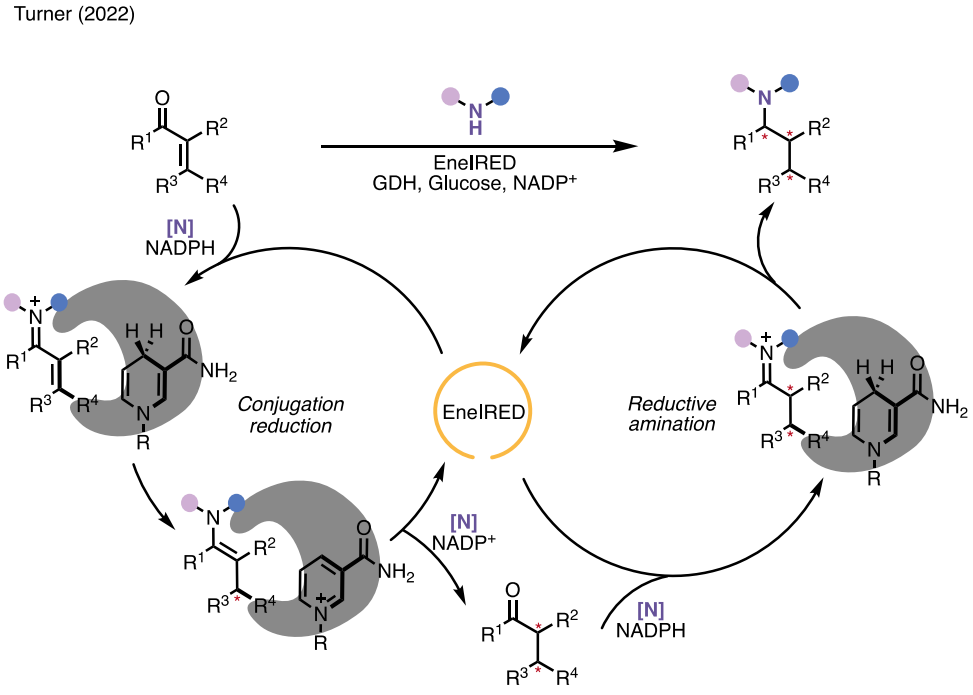

Figure 1.20. Proposed catalytic cycle of productive EneIRE-catalyzed CR and RA.

A common limitation of IRED-catalyzed reactions is their reliance on a large excess of amine nucleophiles (typically 5–50 equivalents) to drive imine formation. Reductive aminases (RedAms), by contrast, catalyze both imine formation and reduction under near-equimolar substrate conditions. In 2017, Turner's group reported a RedAm from *Aspergillus oryzae* (AspRedAm) capable of catalyzing reductive amination under equimolar conditions of ketone and amine substrates[48], significantly enhancing the synthetic utility of these enzymes. In a subsequent study, they developed a dynamic kinetic resolution (DKR) strategy using RedAm variants to access enantioenriched tertiary amines from racemic aldehydes[54]. RedAms accept a diverse range of amine donors, including ammonia, primary alkyl amines, and cyclic secondary amines[55,56]. Pfizer has recently demonstrated the utility of engineered RedAms in the manufacturing of a late-stage clinical candidate, the JAK1 inhibitor abrocitinib[57].

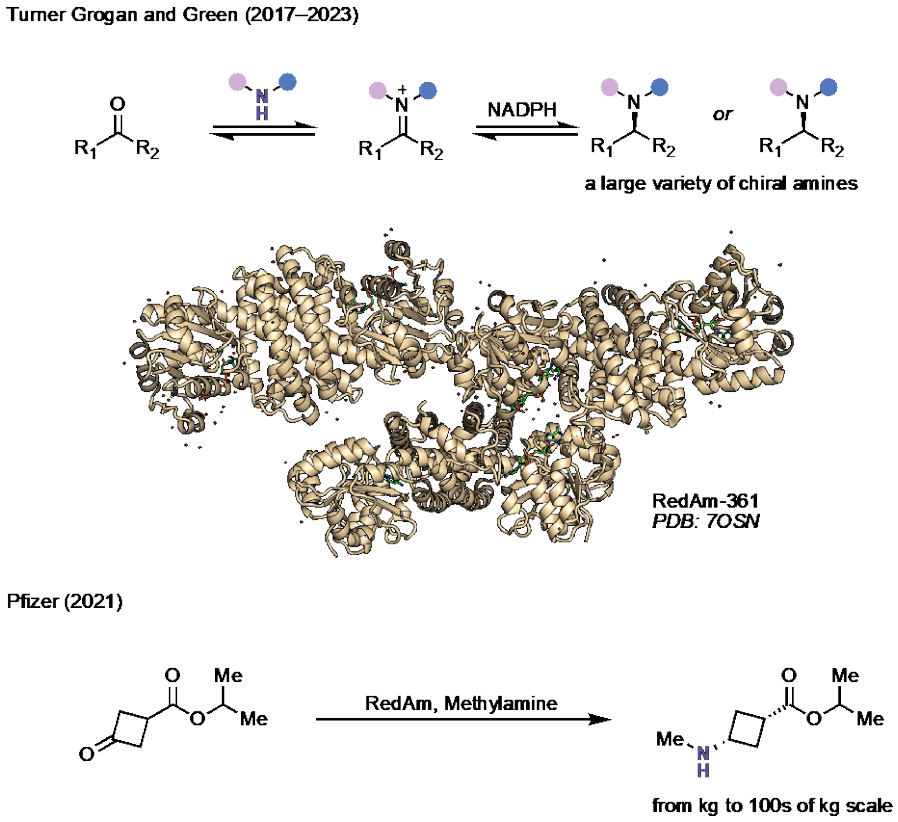

Figure 1.21. RedAm-catalyzed imine reduction to forge chiral amines.

Amine dehydrogenases (AmDHs) represent another versatile class of biocatalysts for reductive amination. Vergne-Vaxelaire, Grogan and coworkers identified a family of native NAD(P)H-dependent AmDHs (natAmDHs) that enable the conversion of ketones and aldehydes using ammonia or methylamine[58]. The Jiang group further engineered an AmDH from *Jeotgalicoccus aerolatus* for the enantioselective synthesis of a wide array of α-(hetero)aryl primary amines[59].

Beyond reductive strategies, imines are also competent electrophiles for carbon nucleophiles. Nature has evolved several remarkable enzymes to exploit this reactivity. Strictosidine synthase (STR) catalyzes the Pictet–Spengler condensation between tryptamine and secologanin to produce (S)-strictosidine, a central precursor in indole alkaloid biosynthesis[49]. In another example, Hai and colleagues uncovered a PLP-dependent Mannich cyclase, LolT, involved in loline biosynthesis (**Figure 1.22**). LolT catalyzes the formation of cyclic α-amino acids bearing quaternary stereocenters, demonstrating Nature's ability to construct highly complex architectures through enzymatic Mannich-type transformations[60].

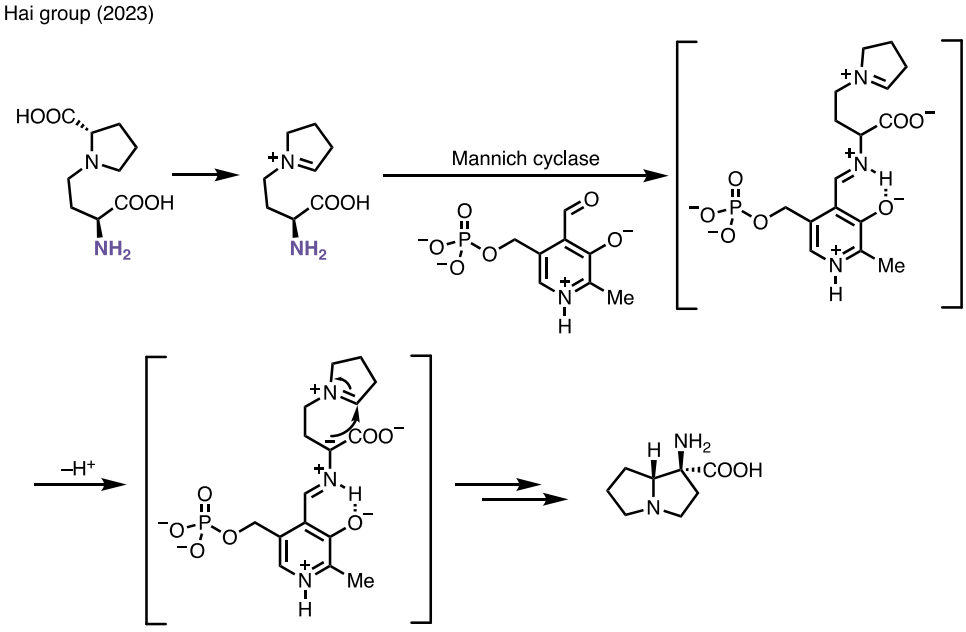

Figure 1.22. PLP-dependent Mannich cyclase-catalyzed aza(bi)cylic synthesis.

1.3.5 Additional natural enzymatic strategies for C–N bond formation

In addition to the aforementioned enzyme classes, enzymes involved in amide bond formation represent another major and well-established category for biocatalytic C–N bond construction. This group includes enzymatic complexes such as ribosomal peptide synthetases and nonribosomal peptide synthetases (NRPSs), both of which facilitate peptide bond formation through highly controlled enzymatic machinery. These systems have been extensively reviewed in the literature and are recognized for their modularity, substrate diversity, and biosynthetic precision in assembling both canonical and noncanonical peptides[61,62].

Beyond traditional peptide biosynthesis, Deska and coworkers introduced an innovative enzymatic strategy for C–N bond formation *via* a biocatalytic nitroso-*ene* reaction[63]. In this system, laccases or an oxidase/peroxidase cascade were employed to generate reactive nitroso intermediates *in situ*. These intermediates subsequently underwent C–N bond formation through an *ene*-type mechanism (**Figure 1.23**). The platform demonstrated high efficiency in both intra- and intermolecular amination reactions, offering a versatile route to nitrogen-containing scaffolds under environmentally benign conditions.

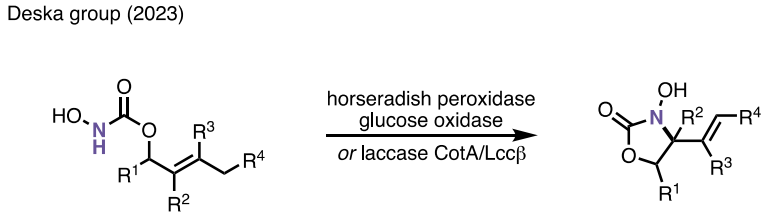

Figure 1.23. HRP- or laccase-catalyzed nitroso-ene-type reaction

Collectively, these additional enzymatic approaches expand the repertoire of biocatalytic tools available for C–N bond construction, further underscoring the potential of Nature's catalysts in modern synthesis.

1.4 New-to-Nature biocatalytic stereoselective construction of C–N bonds

While Nature offers elegant and selective strategies for C–N bond formation, the enzymatic repertoire remains comparatively limited in scope relative to the diversity of chemical transformations available to synthetic chemists. Many synthetically valuable C–N bond-forming reactions, such as nitrene insertions, certain reductive couplings, and cross-coupling processes, lack natural counterparts. Even when natural analogs exist, leveraging them for non-native substrates or reactions is complicated by the intrinsic substrate specificity and mechanistic constraints of enzymes. As a result, achieving high efficiency and selectivity for a desired transformation often necessitates the modification of native enzymes.

Fortunately, Nature is expert at taking one enzyme framework and repurposing it to perform a multitude of chemical transformations. For example, the P450 superfamily consists of structurally similar heme-containing proteins that catalyze C–H oxygenation, alkene epoxidation, oxidative cyclization, aryl-aryl coupling, and nitration, among others. While an enzyme may be optimized to catalyze a specific process, it often exhibits activity for different processes, known as catalytic promiscuity[64]. Evolution can take advantage of these ‘promiscuous’ reactivities in response to a changing environment to create novel enzymes that perform new-to-nature functions (**Figure 1.24**). Researchers are using similar concepts to make, diversify, and optimize new artificial metalloenzymes.

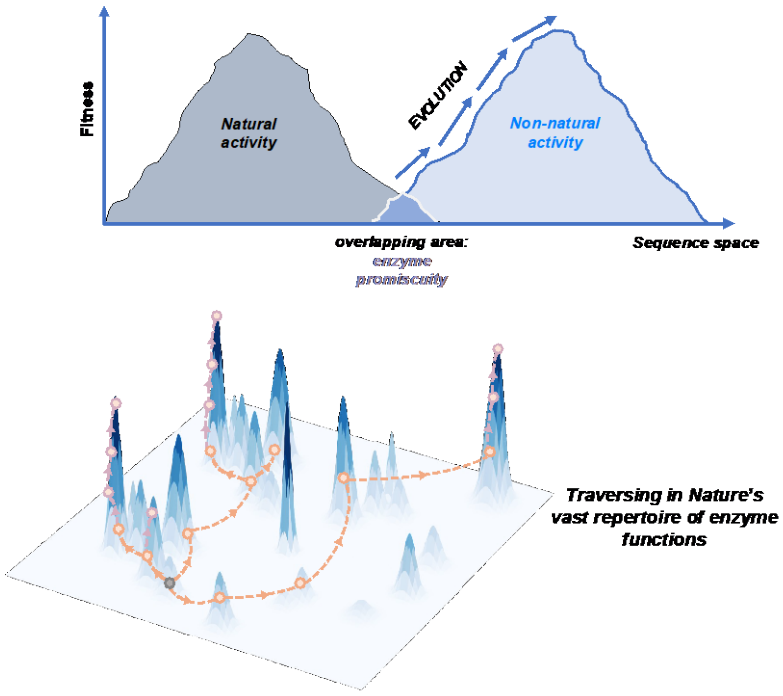

Figure 1.24. Enzyme promiscuity: the capability to exhibit new-to-nature functions.

Directed evolution (**Figure 1.25**), on the other hand, offers a promising method to steer proteins toward desired functions. It is a powerful engineering technique that mimics natural evolution and consists of iterative rounds of mutagenesis and screening or selection[65,66]. This method is able to accumulate beneficial mutations identified by screening libraries at a fast pace, leading to the quick enhancement of desired protein functions. The process involves four key steps: 1) identification of a starting protein (that may have only low levels of the desired property), 2) diversification of the starting protein through mutagenesis of the corresponding DNA sequence, 3) functional screening of the variants to identify improved variants, and repeating steps 2 and 3 until sufficient levels of the desired property are achieved (step 4). These efforts aim to compress evolutionary timescales, which are on the order of billions of years, into laboratory-friendly timeframes. Despite the immense challenge, recent advances in high-throughput screening, structure-guided design, and machine learning have enabled the tailoring of enzymes toward increasingly ambitious catalytic goals.

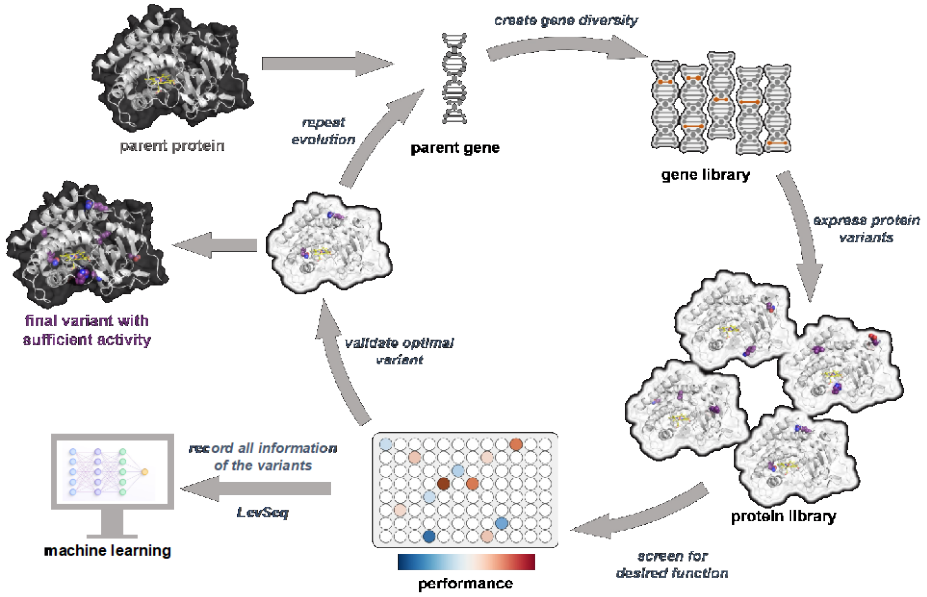

Figure 1.25. Directed evolution: an efficient technique to steer proteins toward desired functions.

1.4.1 Heme-dependent carbene/nitrene transferase-catalyzed C–N bond formation

The selective functionalization of C–H bonds represents a long-standing challenge in synthetic chemistry, largely due to their high bond dissociation energies and ubiquity in organic molecules[67]. Nevertheless, significant progress has been made in harnessing engineered hemoproteins for site-selective C–H amination. Since the pioneering reports of intramolecular C–H amination using engineered hemoproteins [68,69], nitrene-mediated C–H insertion has rapidly gained attention as a powerful strategy in biocatalysis. Over the past five years, a diverse array of enzymatic platforms has been developed by the Arnold group, the Fasan group, and others to facilitate these transformations.

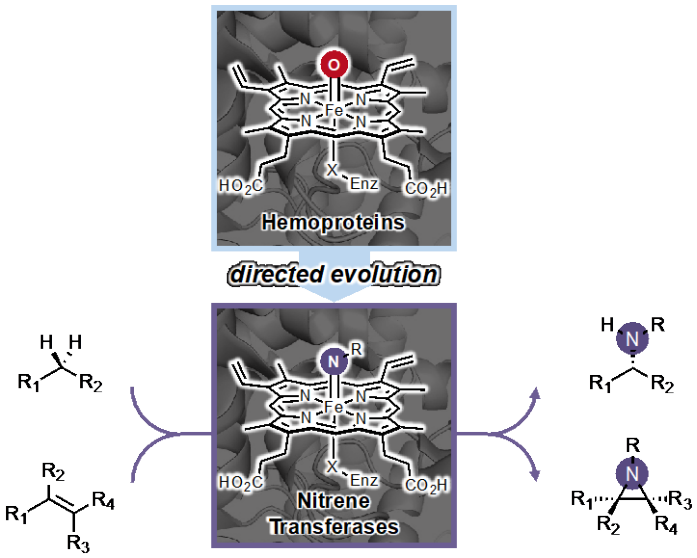

Figure 1.26. Directed evolution enables biocatalytic nitrene C–H insertion and alkene aziridination.

A landmark study by Arnold in 2019 demonstrated the intramolecular cyclization of sulfamoyl azides catalyzed by P411 enzymes, engineered cytochrome P450s bearing a C400S axial ligand mutation[70]. This transformation enabled the efficient formation of primary, secondary, and tertiary C(sp^3)–N bonds (**Figure 1.27**). Remarkably, one evolved variant, P411-Diane4, exhibited the capacity to generate a challenging methyl–ethyl stereocenter, underscoring the exquisite stereocontrol achievable through enzyme engineering.

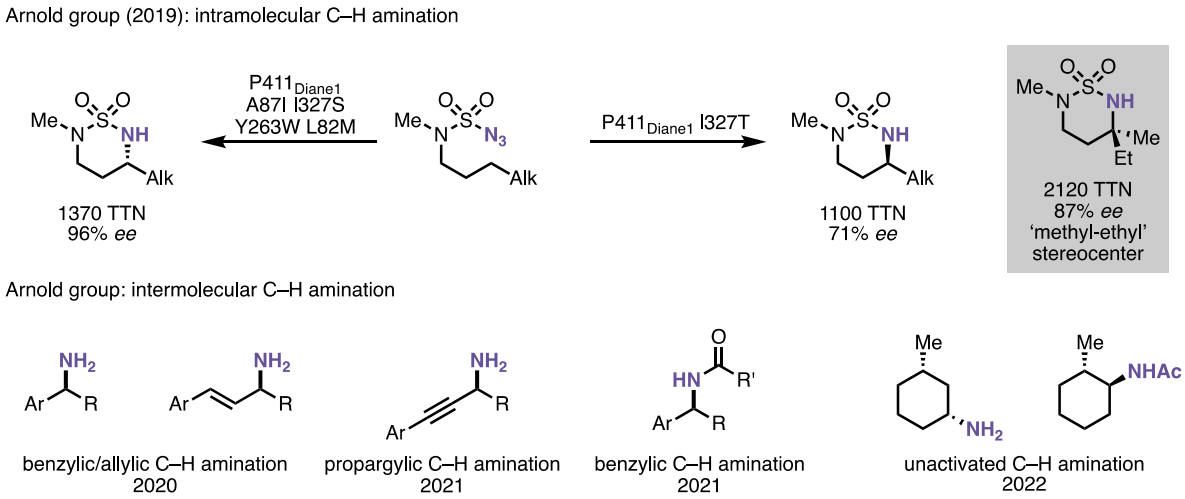

Figure 1.27. Nitrene transferase-catalyzed intramolecular and intermolecular C–H amination.

While intramolecular reactions benefit from entropic advantages, intermolecular C–H amination remains inherently more demanding due to the requirement for precise control over reactive species and site-selectivity. Despite these challenges, extensive protein engineering efforts have yielded hemoprotein variants capable of catalyzing diverse intermolecular nitrene insertion reactions (**Figure 1.27**). These include benzylic/allylic[71], propargylic primary amination[72], and benzylic amidation[73]. Notably, in 2022, Arnold and coworkers reported the biocatalytic amination and amidation of unactivated C(sp^3)–H bonds using P411 variants[74]. Starting from enzymes with negligible activity on methylcyclohexanone, nine rounds of directed evolution led to the identification of robust catalysts capable of functionalizing these otherwise inert sites.

Beyond C–H amination, engineered nitrene transferases have also enabled reactions between nitrene precursors and alkenes (**Figure 1.28**). Two prominent transformations are alkene aziridination and aminohydroxylation[75]. Aminohydroxylation of styrenes has been successfully catalyzed by engineered cytochrome c from *Rhodothermus marinus*[75]. In 2023, Arnold lab has demonstrated that engineered protoglobins can activate simple hydroxylamine as a nitrogen synthon to achieve

aminohydroxylation of alkenes[76]. Despite these achievements, the more ambitious goal of aminohydroxylation across unactivated alkenes remains an outstanding challenge for future enzyme development.

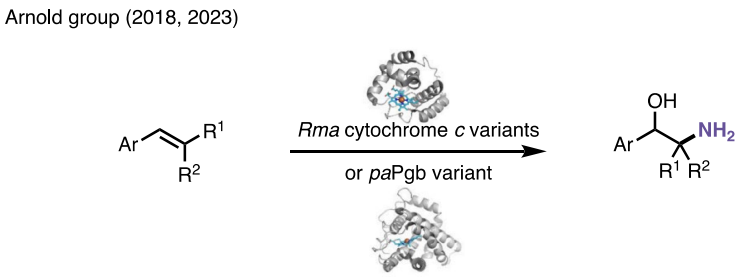

Figure 1.28. Biocatalytic aminohydroxylation of styrene derivatives.

On the other hand, carbene N–H insertion has emerged as a valuable strategy for the synthesis of structurally complex amines in synthetic chemistry. However, achieving high levels of enantioselectivity in these transformations remains a formidable challenge, primarily due to the difficulty in controlling the stereoselective protonation step following carbene insertion. This challenge is exacerbated in enzymatic systems, where reactions are typically performed in aqueous environments that further complicate asymmetric control.

To address this issue, Fasan and coworkers engineered myoglobin (Mb) variants capable of catalyzing N–H insertion reactions between 2-diazopropanate benzyl esters and primary anilines, achieving enantioselectivities of up to 82% *ee* (**Figure 1.29**). Remarkably, through strategic protein engineering, they also developed an enantiocomplementary variant delivering the opposite stereoisomer in up to –63% ee. At the same time, the Arnold group employed a cyclic carbene precursor to improve both enantioselectivity (up to 98% ee) and amine substrate scope[77,78]. In this study, P411 variants **L6_FL** and **L7_FL** exhibited high catalytic efficiency (**Figure 1.29**). Molecular dynamics (MD) simulations and density functional theory (DFT) calculations revealed that a serine residue at position 264 played a key role in determining stereoselectivity *via* hydrogen bonding with the ester moiety of the lactone carbene intermediate. Intriguingly, introducing two mutations (S264S

and V328N) into **L6_FL** inverted the carbene binding orientation, affording variant **L5_FL-B3** with reversed enantioselectivity.

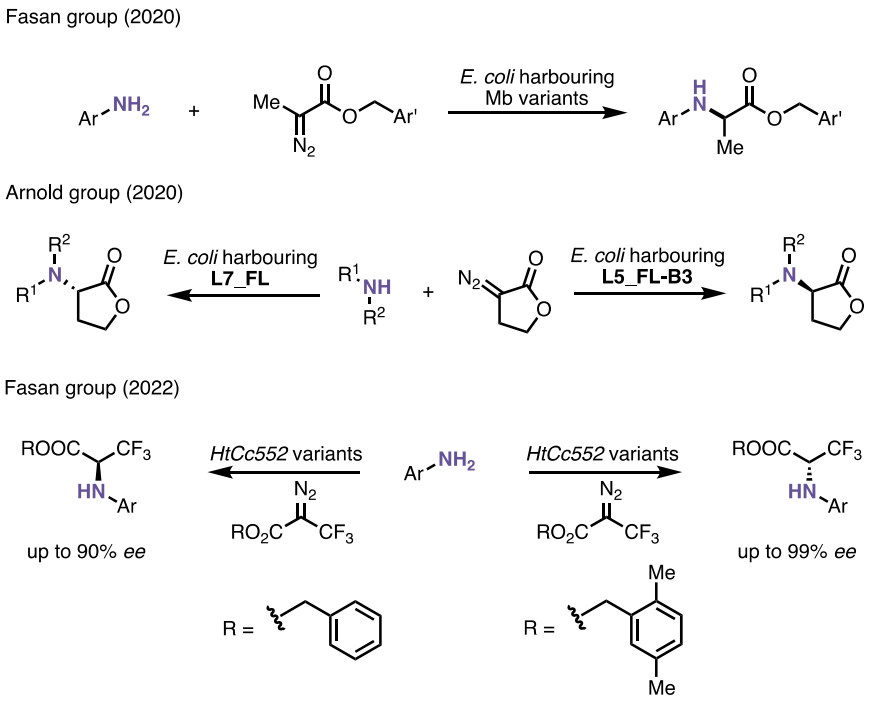

Figure 1.29. Biocatalytic N–H insertion catalyzed by engineered heme-dependent enzymes.

In another notable advance, the Fasan group developed an enzymatic platform for the synthesis of α-trifluoromethyl amines using alkyl 2-diazo-3,3,3-trifluoropropanoates as acceptor–acceptor carbene precursors[79]. Through directed evolution of cytochrome *c552* from *Hydrogenobacter thermophilus*, they obtained a highly efficient biocatalyst for this transformation (**Figure 1.29**), further expanding the biocatalytic repertoire of carbene insertion chemistry.

Beyond N–H insertion, carbene chemistry has enabled the formation of amines through alternative pathways. In 2022, Arnold group reported a P411-catalyzed enantioselective [1,2]-Stevens rearrangement for the synthesis of chiral azetidines[80]. In this transformation, the carbene intermediate effectively inserts into a C–N bond of an aziridine,

promoting a one-carbon ring expansion (**Figure 1.30**). Notably, this novel biocatalytic transformation was successfully performed on a gram scale, highlighting its practical applicability in synthesis.

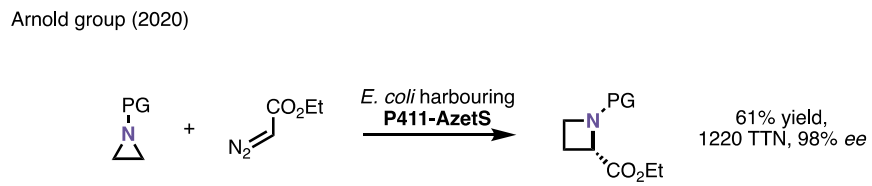

Figure 1.30. Biocatalytic N–H insertion catalyzed by engineered heme-dependent enzymes.

While most carbene transferases have been derived from natural enzymes, recent advances demonstrate that de novo designed proteins can also support carbene-mediated transformations. Stenner and coworkers reported a *de novo* designed peroxidase capable of catalyzing carbene N–H insertion, although the substrates used did not afford chiral products[81]. To date, hemoproteins remain the principal scaffolds for engineering carbene N–H insertion activity, while alternative metalloenzymes, either naturally occurring or synthetically designed, remain underexplored. A notable exception is the recent work by Kumar et al., who identified that the vitamin B_{12}-dependent enzyme MtaC catalyzes the *N*-alkylation of anilines using ethyl diazoacetate (EDA)[82]. However, mechanistic studies suggest that this transformation proceeds *via* a radical pathway, rather than through a metal-carbene intermediate.

1.4.2 Non-heme iron enzyme-catalyzed C–N bond construction

Non-heme iron enzymes also offer unique opportunities to mediate radical-based C–N bond-forming reactions. Controlling high-energy radical intermediates with site- and stereoselectivity has long been a major hurdle in synthetic chemistry. In a recent advance, the Arnold lab reported the first biocatalytic aziridination catalyzed by an engineered α-

ketoglutarate (αKG)-dependent non-heme iron enzyme, *Ps*EFE (PDB: 6CBA)[83], marking a significant milestone in expanding nitrene transfer chemistry beyond hemoproteins (**Figure 1.31**).

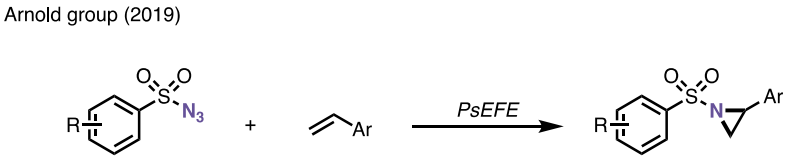

Figure 1.31. Nonheme iron enzyme-catalyzed aziridination of styrenes.

Although enzymes capable of catalyzing C–H azidation have been identified through halogenases[84], few are effective on small molecule substrates with precise regio- and stereocontrol. In 2022, the Huang group described an abiological C(sp^3)–H azidation reaction mediated by engineered non-heme iron enzymes through a radical relay mechanism (**Figure 1.31**)[85]. Starting from a 4-hydroxyphenylpyruvate dioxygenase from *Streptomyces avermitilis* (*Sav* HppD), directed evolution yielded variants capable of activating N–F precursors to generate reactive amidyl radicals within the active site. These radicals underwent a 1,5-hydrogen atom transfer (HAT) to form benzylic radicals, which then selectively rebound with azide over fluoride (**Figure 1.32**). Building on this strategy, the Lewis group demonstrated that an αKG-dependent iron enzyme, *SadA*, could be engineered to perform site-selective azidation on unactivated C–H bonds of succinylated amino acids and amines (**Figure 1.32**)[86]. The resulting azidated products represent valuable intermediates for biological and medicinal chemistry applications. Most recently, the Huang group merged photoredox catalysis with metalloenzymatic transformations to achieve enantioselective decarboxylative C(sp^3)–N_3 bond formation (**Figure 1.32**)[87]. In parallel, similar work was also reported by the Yang group[88].

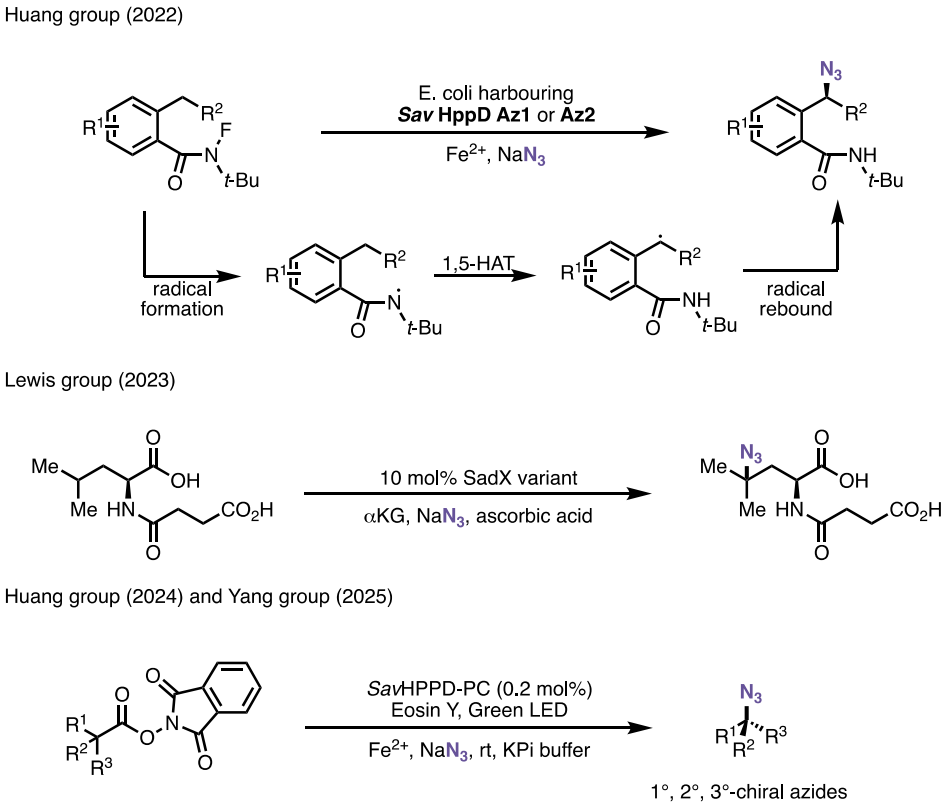

Figure 1.32. Azidation reactions catalyzed by engineered nonheme iron enzymes.

1.4.3 Flavin-dependent ene-reductase-catalyzed enantioselective C–N bond formation

Nitrogen-centered radicals (NCRs) are highly reactive and synthetically versatile intermediates, but their use in asymmetric transformations remains exceptionally challenging. Biocatalysis has recently emerged as a promising solution to harness these reactive species in a stereocontrolled fashion. In a pioneering example, Hyster and coworkers developed a photoenzymatic system for enantioselective hydroamination, coupling flavin-dependent ene-reductases (EREDs) with exogenous photoredox catalysts (**Figure 1.33**)[89]. The *Bacillus subtilis* ERED *YqjM* was engineered to catalyze intramolecular hydroamination reactions, affording lactams with ring sizes ranging from five to eight members. Further engineering of GluER (variant T36A–T231A–G270A) enabled the transformation to proceed intermolecularly, albeit with reduced yields.

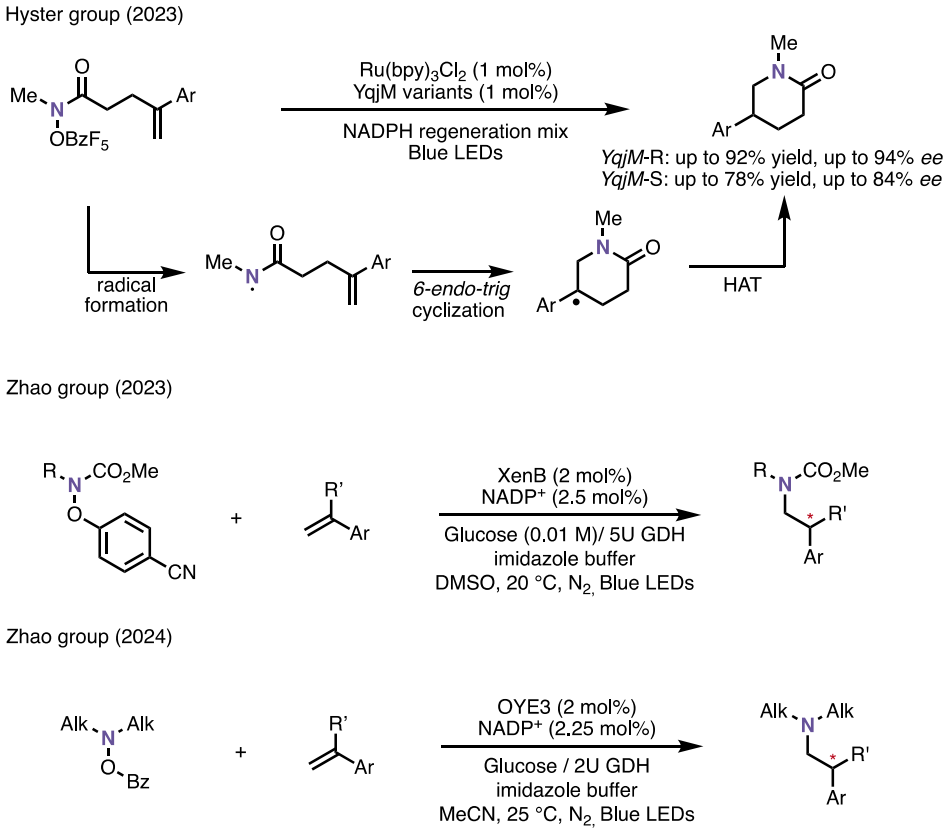

Figure 1.33. Biocatalytic alkene hydroamination reactions *via* nitrogen-centered radical.

Building on this work, the Zhao group engineered another flavin-dependent enzyme, XenB, which displayed enhanced catalytic performance and broader substrate scope in intermolecular styrene hydroamination[90]. In a follow-up paper, they expanded this flavin-dependent ene-reductase platform to generate and control secondary amine radicals for intermolecular hydroamination reactions. Collectively, these photoenzymatic platforms significantly expand the synthetic utility of C–N bond-forming biocatalysts[91].

1.4.4 Miscellaneous unnatural enzymatic strategies for C–N bond formation

In 2024, the Hyster group discovered that flavin-dependent Baeyer–Villiger monooxygenases (BVMOs) can catalyze a photoenzymatic hydroamination of alkenes, enabling the synthesis of 2,2-disubstituted pyrrolidines[92]. Through five rounds of directed evolution, they developed a variant, *Ac*HYAM, exhibiting excellent catalytic activity, high

enantioselectivity, and broad substrate scope. Notably, mechanistic studies revealed a distinct mode of activation involving a through-space interaction between a reductively generated benzylic radical and the lone pair of the amine nitrogen, in contrast with conventional photochemical hydroamination pathways (**Figure 1.34**). Moreover, the evolved enzyme uniquely favored *5-exo-trig* cyclization, overriding the *6-endo-trig* selectivity typically observed in small-molecule catalysis.

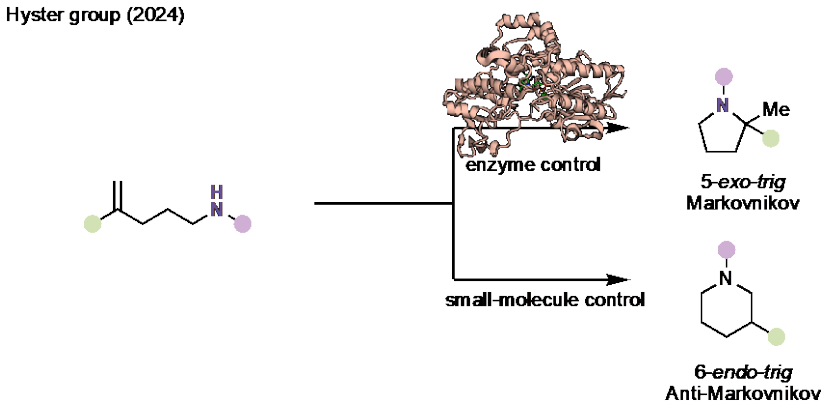

Figure 1.34. Flavoenzyme-catalyzed photoenzymatic intramolecular hydroamination reactions.

1.5 Highlight and outlook

The rapid development of biocatalytic strategies for C–N bond construction, propelled by advancements in high-throughput experimentation, atomic-resolution structural elucidation, and machine learning (ML), signals a transformative era in biocatalytic synthesis. While enzymes have demonstrated a remarkable capacity to forge these bonds, the field needs continued innovation to unlock their full potential. A pivotal frontier lies in expanding the repertoire of natural enzymes to perform more unnatural transformations, a paradigm that merges chemical understanding with biological systems. The engineering of heme-dependent oxygenases into carbene/nitrene transferases exemplifies this approach, illustrating how novel enzyme functions can emerge, evolve, and diversify. One critical aspect that needs to be addressed is the biocatalytic late-stage functionalization of pharmacophores, where enzymatic selectivity and mild reaction conditions could redefine synthetic strategies in pharmaceutical manufacturing. Beyond catalytic activity and stereoselectivity, enzymatic properties, such as thermostability, heterologous expression efficiency, substrate concentration tolerance, and scalability, demand equal attention to align biocatalysis with industrial demands.

Despite the accumulation of vast datasets from directed evolution campaigns, the sequence-function relationship of enzymes remains underutilized. Integrating sequence-function information, molecular dynamics, and structural annotations into ML frameworks offers a promising avenue toward predictive and “rational” protein engineering and even novel function discovery.

Moreover, current engineering efforts often fall short when applied to complex, multidomain enzymes such as RuBisCO, nonribosomal peptide synthetases (NRPS), polyketide synthases (PKS), and nitrogenases. These megasynth(et)ases present unique challenges, including domain cooperativity, substrate channeling, and intricate allosteric regulation. Decoding these features through molecular dynamics, phylogenetic analysis, and mechanistic dissection will be essential for reprogramming Nature’s most

sophisticated enzymatic machinery and enabling the scalable synthesis of structurally complex targets.

Looking forward, biocatalysis will transcend its current confines in small-molecule synthesis. Emerging methodologies are poised to revolutionize the production of biomacromolecules, including peptide therapeutics, oligonucleotides, and glycosylated biologics. By synergizing enzyme engineering, computational design, and bioprocess innovation, the field will anchor its role as a cornerstone of sustainable chemical manufacturing, offering atom-efficient, selective, and environmentally benign solutions to conventional chemical synthesis across molecular scales.

1.6 References

(1) Ruiz-Castillo, P.; Buchwald, S. L. Applications of Palladium-Catalyzed C–N Cross-Coupling Reactions. *Chem. Rev.* **2016**, *116*, 12564–12649.

(2) West, M. J.; Fyfe, J. W. B.; Vantourout, J. C.; Watson, A. J. B. Mechanistic Development and Recent Applications of the Chan–Lam Amination. *Chem. Rev.* **2019**, *119*, 12491–12523.

(3) Seifinoferest, B.; Tanbakouchian, A.; Larijani, B.; Mahdavi, M. Ullmann-Goldberg and Buchwald-Hartwig C−N Cross Couplings: Synthetic Methods to Pharmaceutically Potential N-Heterocycles. *Asian J Org Chem* **2021**, *10*, 1319–1344.

(4) Xie, C.; Smaligo, A. J.; Song, X.-R.; Kwon, O. Phosphorus-Based Catalysis. *ACS Cent. Sci.* **2021**, *7*, 536–558.

(5) Lipshultz, J. M.; Li, G.; Radosevich, A. T. Main Group Redox Catalysis of Organopnictogens: Vertical Periodic Trends and Emerging Opportunities in Group 15. *J. Am. Chem. Soc.* **2021**, *143*, 1699–1721.

(6) Yin, H.-N.; Wang, P.-C.; Liu, Z. Recent Advances in Biocatalytic C–N Bond-Forming Reactions. *Bioorg. Chem*. **2024**, *144*, 107108.

(7) Sun, J.; Zheng, G.; Zhang, G.; Li, Y.; Zhang, Q. Recent Advances in Enantioselective Construction of C–N Bonds Involving Radical Intermediates. *Org. Chem. Front.* **2025**, *12*, 1671–1694.

(8) Yan, M.; Lo, J. C.; Edwards, J. T.; Baran, P. S. Radicals: Reactive Intermediates with Translational Potential. *J. Am. Chem. Soc.* **2016**, *138*, 12692–12714.

(9) Chen, C.; Peters, J. C.; Fu, G. C. Photoinduced Copper-Catalysed Asymmetric Amidation via Ligand Cooperativity. *Nature* **2021**, *596*, 250–256.

(10) Cho, H.; Suematsu, H.; Oyala, P. H.; Peters, J. C.; Fu, G. C. Photoinduced, Copper-Catalyzed Enantioconvergent Alkylations of Anilines by Racemic Tertiary Electrophiles: Synthesis and Mechanism. *J. Am. Chem. Soc.* **2022**, *144*, 4550–4558.

(11) Zhang, Y.-F.; Dong, X.-Y.; Cheng, J.-T.; Yang, N.-Y.; Wang, L.-L.; Wang, F.-L.; Luan, C.; Liu, J.; Li, Z.-L.; Gu, Q.-S.; Liu, X.-Y. Enantioconvergent Cu-Catalyzed Radical C–N Coupling of Racemic Secondary Alkyl Halides to Access α-Chiral Primary Amines. *J. Am. Chem. Soc.* **2021**, *143*, 15413–15419.

(12) Zhang, Y.; Wang, J.; Yang, N.; Chen, Z.; Wang, L.; Gu, Q.; Li, Z.; Liu, X. Copper-Catalyzed Enantioconvergent Radical C(sp^3)−N Cross-Coupling: Access to α,α-Disubstituted Amino Acids. *Angew. Chem. Int. Ed.* **2023**, *62*, e202302983.

(13) Chen, J.-J.; Fang, J.-H.; Du, X.-Y.; Zhang, J.-Y.; Bian, J.-Q.; Wang, F.-L.; Luan, C.; Liu, W.-L.; Liu, J.-R.; Dong, X.-Y.; Li, Z.-L.; Gu, Q.-S.; Dong, Z.; Liu, X.-Y. Enantioconvergent Cu-Catalysed N-Alkylation of Aliphatic Amines. *Nature* **2023**, *618*, 294–300.

(14) Chen, C.; Fu, G. C. Copper-Catalysed Enantioconvergent Alkylation of Oxygen Nucleophiles. *Nature* **2023**, *618*, 301–307.

(15) Cho, H.; Tong, X.; Zuccarello, G.; Anderson, R. L.; Fu, G. C. Synthesis of Tertiary Alkyl Amines via Photoinduced Copper-Catalysed Nucleophilic Substitution. *Nat. Chem.* **2025**, *17*, 271–278.

(16) Mondal, A.; Fu, G. C. Photoinduced, Copper-Catalyzed Enantioconvergent Synthesis of β-Aminoalcohol Derivatives. *J. Am. Chem. Soc.* **2025**, *147*, 10859–10863.

(17) Zhang, Y.-F.; Wang, B.; Chen, Z.; Liu, J.-R.; Yang, N.-Y.; Xiang, J.-M.; Liu, J.; Gu, Q.-S.; Hong, X.; Liu, X.-Y. Asymmetric Amination of Alkyl Radicals with Two Minimally Different Alkyl Substituents. *Science* **2025**, *388*, 283–291.

(18) Wang, K.; Li, Y.; Li, X.; Li, D.; Bao, H. Iron-Catalyzed Asymmetric Decarboxylative Azidation. *Org. Lett.* **2021**, *23*, 8847–8851.

(19) Roos, C. B.; Demaerel, J.; Graff, D. E.; Knowles, R. R. Enantioselective Hydroamination of Alkenes with Sulfonamides Enabled by Proton-Coupled Electron Transfer. *J. Am. Chem. Soc.* **2020**, *142*, 5974–5979.

(20) Hejna, B. G.; Ganley, J. M.; Shao, H.; Tian, H.; Ellefsen, J. D.; Fastuca, N. J.; Houk, K. N.; Miller, S. J.; Knowles, R. R. Catalytic Asymmetric Hydrogen Atom Transfer: Enantioselective Hydroamination of Alkenes. *J. Am. Chem. Soc.* **2023**, *145*, 16118–16129.

(21) Lyu, X.; Jung, H.; Kim, D.; Chang, S. Enantioselective Access to β-Amino Carbonyls via Ni-Catalyzed Formal Olefin Hydroamidation. *J. Am. Chem. Soc.* **2024**, *146*, 14745–14753.

(22) Hore, S.; Jeong, J.; Kim, D.; Chang, S. Visible-Light-Promoted Enantioselective α-Amidation of Aldehydes by Harnessing Organo-Iron Dual Catalysis. *J. Am. Chem. Soc.* **2024**, *146*, 22172–22179.

(23) Lyu, X.; Jeon, E.; Seo, C.; Kim, D.; Chang, S. Nickel-Catalyzed Asymmetric Homobenzylic Hydroamidation of Aryl Alkenes to Access Chiral β-Arylamides. *J. Am. Chem. Soc.* **2025**, *147*, 8928–8938.

(24) Lyu, X.; Seo, C.; Jung, H.; Faber, T.; Kim, D.; Seo, S.; Chang, S. Intramolecular Hydroamidation of Alkenes Enabling Asymmetric Synthesis of β-Lactams via Transposed NiH Catalysis. *Nat. Catal.* **2023**, *6*, 784–795.

(25) Jones, J. E.; Ruppel, J. V.; Gao, G.-Y.; Moore, T. M.; Zhang, X. P. Cobalt-Catalyzed Asymmetric Olefin Aziridination with Diphenylphosphoryl Azide. *J. Org. Chem.* **2008**, *73*, 7260–7265.

(26) Xu, H.; Wang, D.-S.; Zhu, Z.; Deb, A.; Zhang, X. P. New Mode of Asymmetric Induction for Enantioselective Radical N-Heterobicyclization via Kinetically Stable Chiral Radical Center. *Chem* **2024**, *10*, 283–298.

(27) Lee, W. C.; Zhang, X. P. Metalloradical Catalysis: General Approach for Controlling Reactivity and Selectivity of Homolytic Radical Reactions. *Angew. Chem. Int. Ed.* **2024**, *63*, e202320243.

(28) Jin, L.-M.; Xu, P.; Xie, J.; Zhang, X. P. Enantioselective Intermolecular Radical C–H Amination. *J. Am. Chem. Soc.* **2020**, *142*, 20828–20836.

(29) Xu, P.; Xie, J.; Wang, D.-S.; Zhang, X. P. Metalloradical Approach for Concurrent Control in Intermolecular Radical Allylic C−H Amination. *Nat. Chem.* **2023**, *15*, 498–507.

(30) Ye, L.; Tian, Y.; Meng, X.; Gu, Q.; Liu, X. Enantioselective Copper(I)/Chiral Phosphoric Acid Catalyzed Intramolecular Amination of Allylic and Benzylic C−H Bonds. *Angew. Chem. Int. Ed.* **2020**, *59*, 1129–1133.

(31) Yang, C.-J.; Zhang, C.; Gu, Q.-S.; Fang, J.-H.; Su, X.-L.; Ye, L.; Sun, Y.; Tian, Y.; Li, Z.-L.; Liu, X.-Y. Cu-Catalysed Intramolecular Radical Enantioconvergent Tertiary β-C(Sp3)–H Amination of Racemic Ketones. *Nat. Catal.* **2020**, *3*, 539–546.

(32) Nakafuku, K. M.; Zhang, Z.; Wappes, E. A.; Stateman, L. M.; Chen, A. D.; Nagib, D. A. Enantioselective Radical C–H Amination for the Synthesis of β-Amino Alcohols. *Nat. Chem.* **2020**, *12*, 697–704.

(33) Kim, S.; Song, S. L.; Zhang, J.; Kim, D.; Hong, S.; Chang, S. Regio- and Enantioselective Catalytic δ-C–H Amidation of Dioxazolones Enabled by Open-Shell Copper-Nitrenoid Transfer. *J. Am. Chem. Soc.* **2023**, *145*, 16238–16248.

(34) Park, Y.; Chang, S. Asymmetric Formation of γ-Lactams via C–H Amidation Enabled by Chiral Hydrogen-Bond-Donor Catalysts. *Nat. Catal.* **2019**, *2*, 219–227.

(35) Wang, H.; Park, Y.; Bai, Z.; Chang, S.; He, G.; Chen, G. Iridium-Catalyzed Enantioselective C(sp^3)–H Amidation Controlled by Attractive Noncovalent Interactions. *J. Am. Chem. Soc.* **2019**, *141*, 7194–7201.

(36) Dai, L.; Chen, Y.; Xiao, L.; Zhou, Q. Intermolecular Enantioselective Benzylic C(sp^3)−H Amination by Cationic Copper Catalysis. *Angew. Chem. Int. Ed.* **2023**, *62*, e202304427.

(37) Chen, X.; Lian, Z.; Kramer, S. Enantioselective Intermolecular Radical Amidation and Amination of Benzylic C−H Bonds via Dual Copper and Photocatalysis. *Angew. Chem. Int. Ed.* **2023**, *62*, e202217638.

(38) Fu, H.; Prats Luján, A.; Bothof, L.; Zhang, J.; Tepper, P. G.; Poelarends, G. J. Biocatalytic Asymmetric Synthesis of *N* -Aryl-Functionalized Amino Acids and Substituted Pyrazolidinones. *ACS Catal.* **2019**, *9*, 7292–7299.

(39) Zhu, B.-F.; Liu, Y.; Pei, X.-Q.; Wu, Z.-L. Characterization of Phenylalanine Ammonia Lyases from Lettuce (*Lactuca Sativa* L.) as Robust Biocatalysts for the Production of D- and L-Amino Acids. *J. Agric. Food Chem.* **2023**, *71*, 2935–2942.

(40) Li, R.; Wijma, H. J.; Song, L.; Cui, Y.; Otzen, M.; Tian, Y.; Du, J.; Li, T.; Niu, D.; Chen, Y.; Feng, J.; Han, J.; Chen, H.; Tao, Y.; Janssen, D. B.; Wu, B. Computational Redesign of Enzymes for Regio- and Enantioselective Hydroamination. *Nat. Chem. Biol.* **2018**, *14*, 664–670.

(41) Cui, Y.; Wang, Y.; Tian, W.; Bu, Y.; Li, T.; Cui, X.; Zhu, T.; Li, R.; Wu, B. Development of a Versatile and Efficient C–N Lyase Platform for Asymmetric Hydroamination via Computational Enzyme Redesign. *Nat. Catal.* **2021**, *4*, 364–373.

(42) Peng, J.; Liao, C.; Bauer, C.; Seebeck, F. P. Fluorinated *S* -Adenosylmethionine as a Reagent for Enzyme-Catalyzed Fluoromethylation. *Angew. Chem. Int. Ed.* **2021**, *60*, 27178–27183.

(43) Bengel, L. L.; Aberle, B.; Egler-Kemmerer, A.; Kienzle, S.; Hauer, B.; Hammer, S. C. Engineered Enzymes Enable Selective *N* -Alkylation of Pyrazoles with Simple Haloalkanes. *Angew. Chem. Int. Ed.* **2021**, *60*, 5554–5560.

(44) Liao, C.; Seebeck, F. P. Asymmetric β-Methylation of L- and D-α-Amino Acids by a Self-Contained Enzyme Cascade. *Angew. Chem. Int. Ed.* **2020**, *59*, 7184–7187.

(45) Dunham, N. P.; Winston, M. S.; Ray, R.; Eberle, C. M.; Newman, J. A.; Gao, Q.; Cao, Y.; Barrientos, R. C.; Ji, Y.; Reibarkh, M. Y.; Silverman, S. M. Transaminase-Catalyzed Synthesis of β-Branched Noncanonical Amino Acids Driven by a Lysine Amine Donor. *J. Am. Chem. Soc.* **2024**, *146*, 16306–16313.

(46) Liu, J.; Kong, W.; Bai, J.; Li, Y.; Dong, L.; Zhou, L.; Liu, Y.; Gao, J.; Bradshaw Allen, R. T.; Turner, N. J.; Jiang, Y. Amine Dehydrogenases: Current Status and Potential Value for Chiral Amine Synthesis. *Chem Catal*. **2022**, *2*, 1288–1314.

(47) Telek, A.; Molnár, Z.; Vértessy, B. G.; Tasnádi, G. Opine Dehydrogenases, an Underexplored Enzyme Family for the Enzymatic Synthesis of Chiral Amines. *Biotech. & Bioengineering* **2023**, *120*, 2793–2808.

(48) Aleku, G. A.; France, S. P.; Man, H.; Mangas-Sanchez, J.; Montgomery, S. L.; Sharma, M.; Leipold, F.; Hussain, S.; Grogan, G.; Turner, N. J. A Reductive Aminase from Aspergillus Oryzae. *Nat. Chem.* **2017**, *9*, 961–969.

(49) Stöckigt, J.; Zenk, M. H. Strictosidine (Isovincoside): The Key Intermediate in the Biosynthesis of Monoterpenoid Indole Alkaloids. *J. Chem. Soc., Chem. Commun.* **1977**, *18*, 646–648.

(50) Mitsukura, K.; Suzuki, M.; Tada, K.; Yoshida, T.; Nagasawa, T. Asymmetric Synthesis of Chiral Cyclic Amine from Cyclic Imine by Bacterial Whole-Cell Catalyst of Enantioselective Imine Reductase. *Org. Biomol. Chem.* **2010**, *8*, 4533.

(51) Mangas-Sanchez, J.; France, S. P.; Montgomery, S. L.; Aleku, G. A.; Man, H.; Sharma, M.; Ramsden, J. I.; Grogan, G.; Turner, N. J. Imine Reductases (IREDs). *Curr. Opin. in Chem. Biol.* **2017**, *37*, 19–25.

(52) Thorpe, T. W.; Marshall, J. R.; Harawa, V.; Ruscoe, R. E.; Cuetos, A.; Finnigan, J. D.; Angelastro, A.; Heath, R. S.; Parmeggiani, F.; Charnock, S. J.; Howard, R. M.; Kumar, R.; Daniels, D. S. B.; Grogan, G.; Turner, N. J. Multifunctional Biocatalyst for Conjugate Reduction and Reductive Amination. *Nature* **2022**, *604*, 86–91.

(53) Schober, M.; MacDermaid, C.; Ollis, A. A.; Chang, S.; Khan, D.; Hosford, J.; Latham, J.; Ihnken, L. A. F.; Brown, M. J. B.; Fuerst, D.; Sanganee, M. J.; Roiban, G.-D. Chiral Synthesis of LSD1 Inhibitor GSK2879552 Enabled by Directed Evolution of an Imine Reductase. *Nat. Catal.* **2019**, *2*, 909–915.

(54) Burke, A. J.; Lister, T. M.; Marshall, J. R.; Brown, M. J. B.; Lloyd, R.; Green, A. P.; Turner, N. J. Engineered Biocatalysts for Enantioselective Reductive Aminations of Cyclic Secondary Amines. *ChemCatChem* **2023**, *15*, e202300256.

(55) Sharma, M.; Mangas-Sanchez, J.; France, S. P.; Aleku, G. A.; Montgomery, S. L.; Ramsden, J. I.; Turner, N. J.; Grogan, G. A Mechanism for Reductive Amination Catalyzed by Fungal Reductive Aminases. *ACS Catal.* **2018**, *8*, 11534–11541.

(56) Mangas-Sanchez, J.; Sharma, M.; Cosgrove, S. C.; Ramsden, J. I.; Marshall, J. R.; Thorpe, T. W.; Palmer, R. B.; Grogan, G.; Turner, N. J. Asymmetric Synthesis of Primary Amines Catalyzed by Thermotolerant Fungal Reductive Aminases. *Chem. Sci.* **2020**, *11*, 5052–5057.

(57) Kumar, R.; Karmilowicz, M. J.; Burke, D.; Burns, M. P.; Clark, L. A.; Connor, C. G.; Cordi, E.; Do, N. M.; Doyle, K. M.; Hoagland, S.; Lewis, C. A.; Mangan, D.; Martinez, C. A.; McInturff, E. L.; Meldrum, K.; Pearson, R.; Steflik, J.; Rane, A.; Weaver, J. Biocatalytic Reductive Amination from Discovery to Commercial Manufacturing Applied to Abrocitinib JAK1 Inhibitor. *Nat. Catal.* **2021**, *4*, 775–782.

(58) Mayol, O.; Bastard, K.; Beloti, L.; Frese, A.; Turkenburg, J. P.; Petit, J.-L.; Mariage, A.; Debard, A.; Pellouin, V.; Perret, A.; De Berardinis, V.; Zaparucha, A.; Grogan, G.; Vergne-Vaxelaire, C. A Family of Native Amine Dehydrogenases for the Asymmetric Reductive Amination of Ketones. *Nat. Catal.* **2019**, *2*, 324–333.

(59) Kong, W.; Liu, Y.; Huang, C.; Zhou, L.; Gao, J.; Turner, N. J.; Jiang, Y. Direct Asymmetric Reductive Amination of Alkyl (Hetero)Aryl Ketones by an Engineered Amine Dehydrogenase. *Angew. Chem. Int. Ed.* **2022**, *61*, e202202264.

(60) Gao, J.; Liu, S.; Zhou, C.; Lara, D.; Zou, Y.; Hai, Y. A Pyridoxal 5′-Phosphate-Dependent Mannich Cyclase. *Nat. Catal.* **2023**, *6*, 476–486.

(61) Dell, M.; Dunbar, K. L.; Hertweck, C. Ribosome-Independent Peptide Biosynthesis: The Challenge of a Unifying Nomenclature. *Nat. Prod. Rep.* **2022**, *39*, 453–459.

(62) Patel, K. D.; MacDonald, M. R.; Ahmed, S. F.; Singh, J.; Gulick, A. M. Structural Advances toward Understanding the Catalytic Activity and Conformational Dynamics of Modular Nonribosomal Peptide Synthetases. *Nat. Prod. Rep.* **2023**, *40*, 1550–1582.

(63) Jäger, C.; Haase, M.; Koschorreck, K.; Urlacher, V. B.; Deska, J. Aerobic C−N Bond Formation through Enzymatic Nitroso-Ene-Type Reactions. *Angew. Chem. Int. Ed.* **2023**, *62*, e202213671.

(64) Khersonsky, O.; Roodveldt, C.; Tawfik, D. Enzyme Promiscuity: Evolutionary and Mechanistic Aspects. *Curr. Opin. in Chem. Biol.* **2006**, *10*, 498–508.

(65) Arnold, F. H. Directed Evolution: Bringing New Chemistry to Life. *Angew. Chem. Int. Ed.* **2018**, *57*, 4143–4148.

(66) Arnold, F. H. Innovation by Evolution: Bringing New Chemistry to Life (Nobel Lecture). *Angew. Chem. Int. Ed.* **2019**, *58*, 14420–14426.

(67) Collet, F.; Lescot, C.; Dauban, P. Catalytic C–H Amination: The Stereoselectivity Issue. *Chem. Soc. Rev.* **2011**, *40*, 1926.

(68) McIntosh, J. A.; Coelho, P. S.; Farwell, C. C.; Wang, Z. J.; Lewis, J. C.; Brown, T. R.; Arnold, F. H. Enantioselective Intramolecular C–H Amination Catalyzed by Engineered Cytochrome P450 Enzymes In Vitro and In Vivo. *Angew. Chem. Int. Ed.* **2013**, *52*, 9309–9312.

(69) Singh, R.; Bordeaux, M.; Fasan, R. P450-Catalyzed Intramolecular sp^3 C–H Amination with Arylsulfonyl Azide Substrates. *ACS Catal.* **2014**, *4*, 546–552.

(70) Yang, Y.; Cho, I.; Qi, X.; Liu, P.; Arnold, F. H. An Enzymatic Platform for the Asymmetric Amination of Primary, Secondary and Tertiary C(sp^3)–H Bonds. *Nat. Chem.* **2019**, *11*, 987–993.

(71) Jia, Z.-J.; Gao, S.; Arnold, F. H. Enzymatic Primary Amination of Benzylic and Allylic C(sp^3)–H Bonds. *J. Am. Chem. Soc.* **2020**, *142*, 10279–10283.

(72) Liu, Z.; Qin, Z.-Y.; Zhu, L.; Athavale, S. V.; Sengupta, A.; Jia, Z.-J.; Garcia-Borràs, M.; Houk, K. N.; Arnold, F. H. An Enzymatic Platform for Primary Amination of 1-Aryl-2-Alkyl Alkynes. *J. Am. Chem. Soc.* **2022**, *144*, 80–85.

(73) Athavale, S. V.; Gao, S.; Liu, Z.; Mallojjala, S. C.; Hirschi, J. S.; Arnold, F. H. Biocatalytic, Intermolecular C−H Bond Functionalization for the Synthesis of Enantioenriched Amides. *Angew. Chem. Int. Ed.* **2021**, *60*, 24864–24869.

(74) Athavale, S. V.; Gao, S.; Das, A.; Mallojjala, S. C.; Alfonzo, E.; Long, Y.; Hirschi, J. S.; Arnold, F. H. Enzymatic Nitrogen Insertion into Unactivated C–H Bonds. *J. Am. Chem. Soc.* **2022**, *144*, 19097–19105.

(75) Cho, I.; Prier, C. K.; Jia, Z.; Zhang, R. K.; Görbe, T.; Arnold, F. H. Enantioselective Aminohydroxylation of Styrenyl Olefins Catalyzed by an Engineered Hemoprotein. *Angew. Chem. Int. Ed.* **2019**, *58*, 3138–3142.

(76) Gao, S.; Das, A.; Alfonzo, E.; Sicinski, K. M.; Rieger, D.; Arnold, F. H. Enzymatic Nitrogen Incorporation Using Hydroxylamine. *J. Am. Chem. Soc.* **2023**, *145*, 20196–20201.

(77) Liu, Z.; Calvó-Tusell, C.; Zhou, A. Z.; Chen, K.; Garcia-Borràs, M.; Arnold, F. H. Dual-Function Enzyme Catalysis for Enantioselective Carbon–Nitrogen Bond Formation. *Nat. Chem.* **2021**, *13*, 1166–1172.

(78) Calvó-Tusell, C.; Liu, Z.; Chen, K.; Arnold, F. H.; Garcia-Borràs, M. Reversing the Enantioselectivity of Enzymatic Carbene N−H Insertion Through Mechanism-Guided Protein Engineering. *Angew. Chem. Int. Ed.* **2023**, *62*, e202303879.

(79) Nam, D.; Tinoco, A.; Shen, Z.; Adukure, R. D.; Sreenilayam, G.; Khare, S. D.; Fasan, R. Enantioselective Synthesis of α-Trifluoromethyl Amines via Biocatalytic N–H Bond Insertion with Acceptor-Acceptor Carbene Donors. *J. Am. Chem. Soc.* **2022**, *144*, 2590–2602.

(80) Miller, D. C.; Lal, R. G.; Marchetti, L. A.; Arnold, F. H. Biocatalytic One-Carbon Ring Expansion of Aziridines to Azetidines via a Highly Enantioselective [1,2]-Stevens Rearrangement. *J. Am. Chem. Soc.* **2022**, *144*, 4739–4745.

(81) Stenner, R.; Steventon, J. W.; Seddon, A.; Anderson, J. L. R. A de Novo Peroxidase Is Also a Promiscuous yet Stereoselective Carbene Transferase. *Proc. Natl. Acad. Sci. U.S.A.* **2020**, *117*, 1419–1428.

(82) Kumar, A.; Yang, X.; Li, J.; Lewis, J. C. First and Second Sphere Interactions Accelerate Non-Native *N*-Alkylation Catalysis by the Thermostable, Methanol-Tolerant B_{12}-Dependent Enzyme MtaC. *Chem. Commun.* **2023**, *59*, 4798–4801.

(83) Goldberg, N. W.; Knight, A. M.; Zhang, R. K.; Arnold, F. H. Nitrene Transfer Catalyzed by a Non-Heme Iron Enzyme and Enhanced by Non-Native Small-Molecule Ligands. *J. Am. Chem. Soc.* **2019**, *141*, 19585–19588.

(84) Matthews, M. L.; Chang, W.; Layne, A. P.; Miles, L. A.; Krebs, C.; Bollinger, J. M. Direct Nitration and Azidation of Aliphatic Carbons by an Iron-Dependent Halogenase. *Nat. Chem. Biol.* **2014**, *10*, 209–215.

(85) Rui, J.; Zhao, Q.; Huls, A. J.; Soler, J.; Paris, J. C.; Chen, Z.; Reshetnikov, V.; Yang, Y.; Guo, Y.; Garcia-Borràs, M.; Huang, X. Directed Evolution of Nonheme Iron Enzymes to Access Abiological Radical-Relay C(sp^3)−H Azidation. *Science* **2022**, *376*, 869–874.

(86) Gomez, C. A.; Mondal, D.; Du, Q.; Chan, N.; Lewis, J. C. Directed Evolution of an Iron(II)- and α-Ketoglutarate-Dependent Dioxygenase for Site-Selective Azidation of Unactivated Aliphatic C−H Bonds. *Angew. Chem. Int. Ed.* **2023**, *62*, e202301370.

(87) Rui, J.; Mu, X.; Soler, J.; Paris, J. C.; Guo, Y.; Garcia-Borràs, M.; Huang, X. Merging Photoredox with Metalloenzymatic Catalysis for Enantioselective Decarboxylative C(sp^3)–N_3 and C(sp^3)–SCN Bond Formation. *Nat. Catal.* **2024**, *7*, 1394–1403.

(88) Zhao, L.-P.; Lin, K.; Xie, P.-P.; Liu, H.; Xiang, H.; Liu, X.; Zhao, Y.; Liu, P.; Yang, Y. Cooperative Photometallobiocatalysis Enables Nonheme Fe Enzyme-Catalyzed Enantioconvergent Radical Decarboxyla-Tive Azidation, Thiocyanation and Isocyanation of Redox-Active Esters. *ChemRxiv* **2025**, https://doi.org/10.26434/chemrxiv-2025-gp5bn.

(89) Ye, Y.; Cao, J.; Oblinsky, D. G.; Verma, D.; Prier, C. K.; Scholes, G. D.; Hyster, T. K. Using Enzymes to Tame Nitrogen-Centred Radicals for Enantioselective Hydroamination. *Nat. Chem.* **2023**, *15*, 206–212.

(90) Zhang, Z.; Feng, J.; Yang, C.; Cui, H.; Harrison, W.; Zhong, D.; Wang, B.; Zhao, H. Photoenzymatic Enantioselective Intermolecular Radical Hydroamination. *Nat. Catal.* **2023**, *6*, 687–694.

(91) Harrison, W.; Jiang, G.; Zhang, Z.; Li, M.; Chen, H.; Zhao, H. Photoenzymatic Asymmetric Hydroamination for Chiral Alkyl Amine Synthesis. *J. Am. Chem. Soc.* **2024**, *146*, 10716–10722.

(92) Raps, F. C.; Rivas-Souchet, A.; Jones, C. M.; Hyster, T. K. Emergence of a Distinct Mechanism of C–N Bond Formation in Photoenzymes. *Nature* **2025**, *637*, 362–368.

Chapter II

BIOCATALYTIC PRIMARY AMINATION OF PROPARGYLIC C(SP^3)–H BONDS

2.1 Introduction

Propargyl amines are an important class of molecules in organic synthesis and medicinal chemistry.[1–3] This motif is widely observed in many bioactive molecules,[2,3] such as drugs and their analogs (**Scheme 2.1a**). The functional group combination of an alkyne and an amine also makes them versatile synthetic intermediates toward complex structures.[1,4] Popular methods to prepare propargyl amines include propargylic substitution with nitrogen nucleophiles, reductive amination of alkynyl ketones, and imine alkynylation.[1,5] While efficient, these methods require the use of hazardous organometallic reagents or prefunctionalization of the alkyne substrates at the propargylic positions. Direct nitrene C–H insertion reactions represent an attractive alternative strategy to make propargyl amines from simple alkynes;[6] however, selective C–H amination of these substrates is extremely challenging. On the one hand, the highly reactive nitrene species are usually undiscriminating toward different functionalities (e.g., the triple bonds of alkynes are known to react with nitrenes[7]) and C–H bonds, leading to low chemo- and regioselectivity and uncontrolled side reactions. On the other hand, the relatively small steric effect imposed by the alkynyl group can be a problem for enantiotopic differentiation in small-molecule catalysis.[6e,6f] Nonetheless, several catalytic systems based on cobalt,[6c,6d] iridium,[6e,6h] ruthenium[6f,6g] or silver[6i] have been developed for asymmetric intramolecular propargylic amination reactions since 2018 (**Scheme 2.1b**). To the best of our knowledge, however, there is only one example of an enantioselective intermolecular propargylic C(sp^3)–H amination in the literature, which used perfluoroaryl azide as the nitrene precursor.

Since 2013, biocatalytic nitrene transformations have emerged as powerful tools for the construction of nitrogen-containing molecules. Several research groups have demonstrated that enzymatic nitrene C–H insertion reactions can be achieved with excellent efficiency and selectivity on various substrates.[9] In 2020, we reported an unprecedented primary amination reaction of benzylic and allylic C–H bonds using P411 enzymes (cytochromes P450 with serine in place of

cysteine as their axial ligand).[10] The remarkable ability of P411 enzymes to tame highly reactive unprotected nitrene species while also allowing exquisite stereocontrol demonstrates their catalytic potential for other challenging transformations. We therefore hypothesized that P411 enzymes could be suitable catalysts for propargylic amination. In this work, we show that an engineered P411 variant, namely PA-G8, derived from cytochrome P450BM3 and improved by directed evolution, catalyzes an intermolecular propargylic amination reaction (**Scheme 2.1c**) with excellent enantioselectivity and catalytic efficiency (up to 79% yield, >2000 TTN, and 82–96% ee).

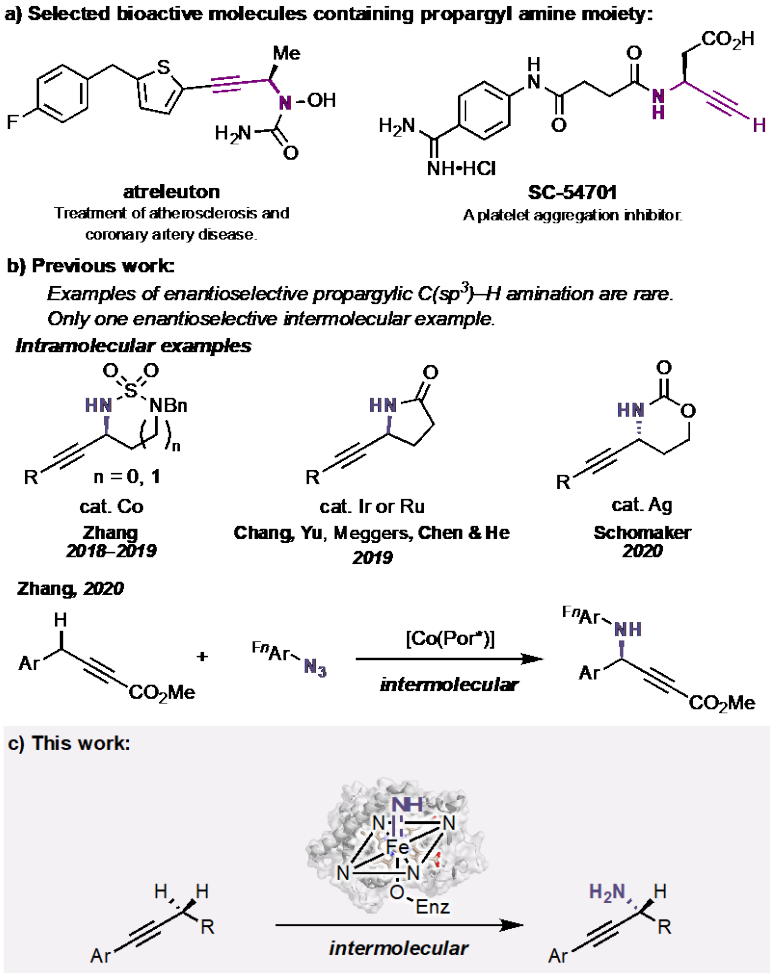

Scheme 2.1. Background and project synopsis

2.2 Results and discussions

We commenced this investigation of enzymatic propargylic amination by focusing on the reaction between 1-phenyl-butyne **1.1a** and *O*-pivaloylhydroxylamine triflic acid **2**[11]. The hydroxylamine-based nitrene precursor is more stable and safer to handle compared to the azide precursors used in our previous work. The expected primary amine product **1.3a** is of biological interest[12] and can be converted easily to other valuable compounds through downstream transformations.[1] The reaction was first evaluated with a panel of hemoproteins, previously evolved for different nitrene and carbene transformations,[13] in the form of whole *Escherichia coli* (*E. coli*) cell catalysts. Although most variants did not show detectable activity toward this reaction, a few of the P411 enzymes from the allylic primary amination lineage indeed showed promising initial activities.[10] The best hit (P411-b4) among them could catalyze the standard reaction with 64% yield, albeit with negligible enantioselectivity (–1% *ee*). The heme domain of P411-b4 has four mutations (A78M, L263M, G268P, and L437G) with respect to our previously reported "**E10**" variant of $P450_{BM3}$ for benzylic C–H tosylamidation, which has a solved crystal structure (PDB ID: 5UCW).[9b]

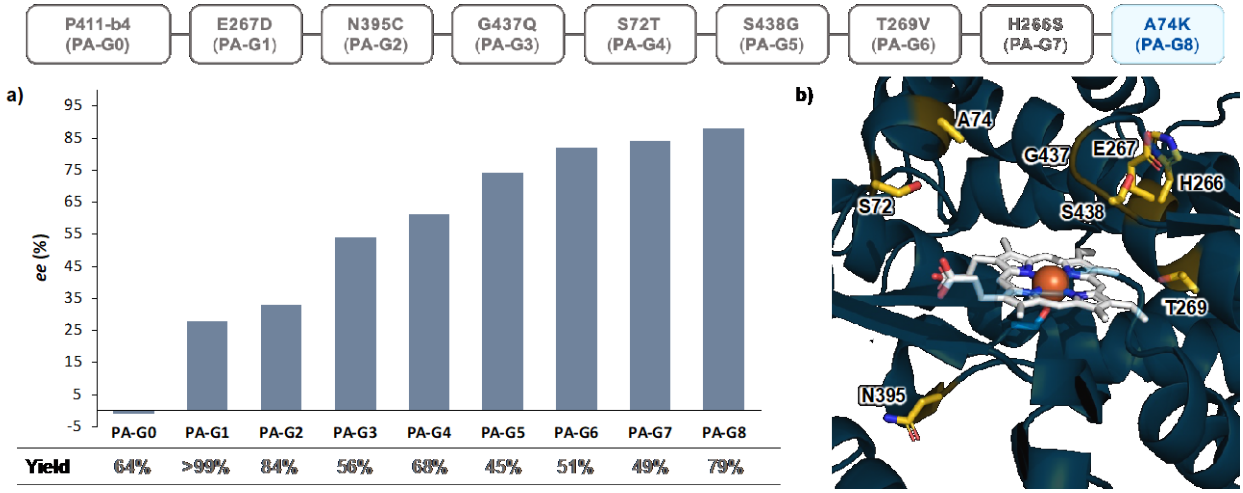

Figure 2.1. Directed evolution for enantioselective propargylic amination. a) Evolutionary trajectory of **PA-G8** for the synthesis of propargyl amine **1.3a**. **PA-G8** was evolved through eight rounds of SSM and screening starting from **PA-G0**. Indicated mutations are relative to **PA-G0**. The experiments were performed using *E. coli* (OD_{600} = 20) that expressed P411 enzymes with 2 mM substrate **1.1a** and 5 mM substrate **1.2** in M9-N buffer (pH = 8.4) at 10 ℃ under anaerobic conditions. Performing reactions at 10 ℃ was found to give higher yields compared to running them at room temperature. Yields were quantified by LC-MS based on the calibration curve of **1.3a**. Enantioselectivities were measured by HPLC on a chiral phase after benzoyl protection. See SI for details. b) The mutated residues (S72, A74, H266, E267, T269, N395, G437, and S438) are highlighted in the active site of P411 variant **E10** (PDB ID: 5UCW).

Variant P411-b4 (named **PA-G0** in this new lineage) was chosen as the parent for a directed evolution campaign (**Figure 2.1aa**). Site-saturation mutagenesis (SSM) libraries were generated and screened by revisiting beneficial sites for previous P411-catalyzed transformations (see **Table A.S1** and **A.S2** in *Supporting Information* (SI) for all the targeted sites in directed evolution). To reduce the screening burden in SSM rounds, only variants which displayed more than 60% activity compared to the parent were assayed for enantioselectivity. Gratifyingly, by introducing a single mutation E267D, we obtained a new variant **PA-G1**, which could catalyze the model reaction with nearly quantitative yield and 28% *ee*. Seven additional rounds of SSM and screening generated the final variant **PA-G8**, which could perform propargylic amination in excellent yield and enantiocontrol (79% analytical yield and 88% *ee*). Mutations E267D, G437Q, and S438G, which reside on the flexible loop and the α-helix directly above the heme cofactor (**Figure 2.1b**), provide the most significant enantioselectivity boosts. All the mutations (E267D, N395C, G437Q, S72T, S438G, T269V, H266S, and A74K) were selected for enhancing enantioselectivity, even though some of them reduce the reaction yield (N395C, G437Q, S438G, and H266S).

After identifying the best variant **PA-G8** for propargylic amination of the model substrate **1.1a**, we next evaluated the enzyme's activity on an array of alkyne substrates (**1.1b–1.1n**) under the standard whole-cell reaction conditions (Figure 2a). In general, **PA-G8** accepts many 1-aryl-2-alkyl alkynes, delivering the desired products with good to excellent enantioselectivity (82–96% *ee*). Alkynes bearing longer alkyl chains could be transformed to the corresponding propargyl amines by **PA-G8**, albeit in lower yields (**1.3b** and **1.3c**). The absolute configurations of **1.3b** and **1.3c** were determined as *R* (see section VIII in the SI for details). Interestingly, increased chain length correlated with improved enantioselectivities (91% and 96% *ee* for **1.3b** and **1.3c**,

respectively). Furthermore, aryl groups with various substitution patterns were well tolerated in this reaction, including substituents with different electronic properties at *ortho*-, *meta*-, and *para*-positions of the aromatic ring (**1.3d–1.3i**). Alkynes containing heteroaromatic rings were competent substrates as well (**1.3j–3l**). This is notable since many transition-metal-based catalytic systems are not compatible with heterocycles, especially pyridines, due to their tendency to deactivate transition-metal catalysts.[14] Besides nitrene insertion into secondary C(sp^3)–H bonds, **PA-G8** could also catalyze the amination reaction of primary and tertiary C–H bonds (**1.3m** and **1.3n**). Although the reaction yields were relatively low for some of the alkynes,[15] we believe they can be improved through further optimization of these "propargylic aminases" (see **Scheme A.S1** in SI for some preliminary efforts). We also tested **PA-G8** with dialkyl alkynes, for example, 3-hexyne. Unfortunately, only trace yields were obtained with such substrates (see **Figure A.S2** in SI for details).

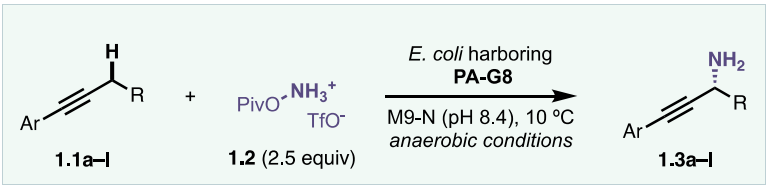

A

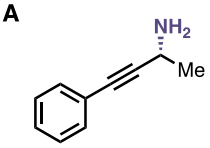

1.3a, 79% yield
1820 TTN, 88% *ee*

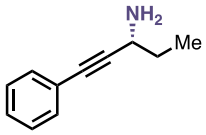

1.3b, 40% yield
919 TTN, 91% *ee*

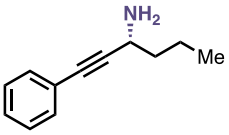

1.3c, 6% yield
219 TTN, 96% *ee*

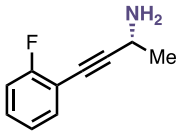

1.3d, 74% yield
2610 TTN, 90% *ee*

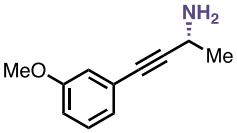

1.3e, 39% yield
901 TTN, 95% *ee*

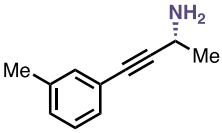

1.3f, 32% yield
1030 TTN, 89% *ee*

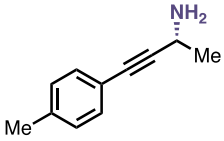

1.3g, 25% yield
884 TTN, 89% *ee*

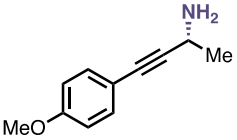

1.3h, 31% yield
1080 TTN, 93% *ee*

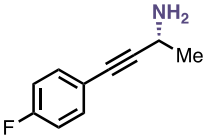

1.3i, 37% yield
1290 TTN, 82% *ee*

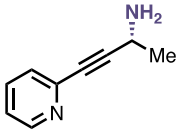

1.3j, 72% yield
2320 TTN, 91% *ee*

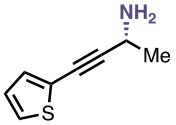

1.3k, 69% yield
1580 TTN, 92% *ee*

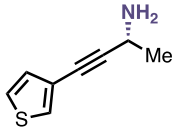

1.3l, 69% yield
2440 TTN, 91% *ee*

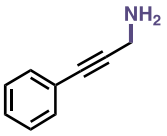

1.3m, 13% yield
442 TTN

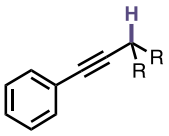

primary C–H bond: R = H
tertiary C–H bond: R = Me

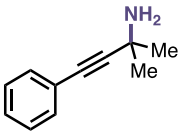

1.3n, 18% yield
649 TTN

B

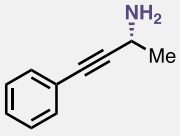

1.3a, 64% isolated yield
1150 TTN, 88% *ee*
[1 mmol scale]

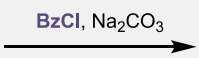

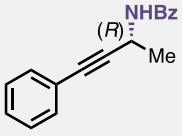

(1)

1.4a, 65% isolated yield
$[\alpha]_D^{21}$ = +49.0 (in $CHCl_3$, *c* = 0.83)

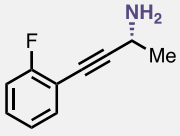

1.3d, 64% isolated yield
1570 TTN, 91% *ee*
[1 mmol scale]

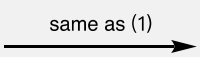

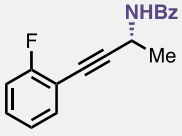

(2)

1.4d, 79% isolated yield
$[\alpha]_D^{21}$ = +52.2 (in $CHCl_3$, *c* = 0.75)

Figure 2.2. Substrate scope studies of propargylic C–H amination. A) Substrate scope of enantioselective propargylic amination. The experiments were performed at analytical scale using *E. coli* (OD_{600} = 20) that expressed the **PA-G8** enzyme with 2 mM substrate (**1.1a–l**) and 5 mM substrate **1.2** in M9-N buffer (pH = 8.4) at 10 °C under anaerobic conditions. Yields were quantified by LC-MS based on the calibration curves of the corresponding reference products. Enantioselectivities were measured by HPLC on a chiral phase after benzoyl protection of the propargyl amine products. See SI for details. B) Preparative-scale synthesis and product derivatization for the determination of absolute stereochemistry. Chiral amides **1.4a** and **1.4d** were obtained from benzoyl protection of amines **1.3a** and **1.3d**. Compound **1.4a** was used to determine the absolute stereochemistry by comparing the optical rotation with the reported value of (*R*)-**1.4a**.[5b]

To demonstrate the synthetic utility of this biocatalytic platform, we performed the enzymatic reactions at 1-mmol scale with alkyne substrates **1.1a** and **1.1d** (Figure 2b). To our delight, propargyl amine **1.3a** was obtained in 64% isolated yield, 1150 TTN, and 88% *ee*. Similarly, product **1.3d** was obtained in 64% yield, 1570 TTN, and 91% *ee*. After benzoyl protection, the optical rotation of amide **4a** was measured as +49.0 (c = 0.83, in $CHCl_3$), which is consistent with the reported value of (*R*)-**4a**, thus establishing the absolute configuration of **1.3a**.[5b]

Finally, density functional theory (DFT) calculations with a truncated system were carried out to explore the nature of the nitrene insertion into propargylic C(sp^3)–H bond using model substrate **1.1a** (see SI for computational details). DFT calculations describe the iron-nitrenoid active species as a triplet ground state, in line with similar reported iron-nitrenoid species.[16] Calculations indicate that nitrene insertion proceeds through a hydrogen atom transfer (HAT) step (TS1 $\Delta G^{\ddagger}$ = 14.7 kcal·mol^{-1}, in the triplet state) to initially form a propargyl radical intermediate, which then undergoes a radical rebound step (TS2 $\Delta G^{\ddagger}$ = 8.2 kcal·mol^{-1}, in the triplet state) generating the final propargyl amine product (**Figure 2.3**, and **Figure A.S3** in the SI). This is similar to what was previously described for inter- and intramolecular nitrene C(sp^3)–H insertion based on sulfonamide and sulfamide Fe-nitrenoids,[16a,17] and acyl Fe-nitrenoids.[16b]

The low energy barrier found for HAT TS1 ($\Delta G^{\ddagger}$ = 7.1 kcal·mol^{-1} from reactant complex, triplet state) reflects the enhanced stability of the propargyl radical being formed due to resonance and the high reactivity of the iron-nitrenoid. Higher activation barriers are found for the HAT step involving benzylic C(sp^3)–H bonds and Fe-acyl-nitrenoids.[16b] DFT calculations also describe that protonation of the axial serine would slightly increase the HAT barrier, favoring the quintet electronic state over the triplet for the HAT and radical rebound steps (see SI discussion and Figures S3 and S4).

The radical rebound step is calculated to be much faster than that for the previously reported enantioconvergent amination of tertiary C(sp^3)–H bond (ca. 10 kcal·mol^{-1} higher).[16a] The rapid capture of the propargyl radical suggests that the rebound process outcompetes radical reorientation and alkyl group rotation in the active site due to steric constraints. Consequently, the substrate (**1.1a**) and propargyl radical have similar orientations in the active site. Enantioselectivity of the amination process would be determined by the orientation of the propargyl radical during

the rebound step. In effect, the selectivity of the amination process would be controlled by the binding pose of the substrate in the **PA-G8** active site relative to the reactive iron-nitrenoid species. This is consistent with the improved enantioselectivities observed for substrates with longer alkyl chains (**1.3b** and **1.3c**, Figure 2), which will be geometrically more constrained in the binding pocket.

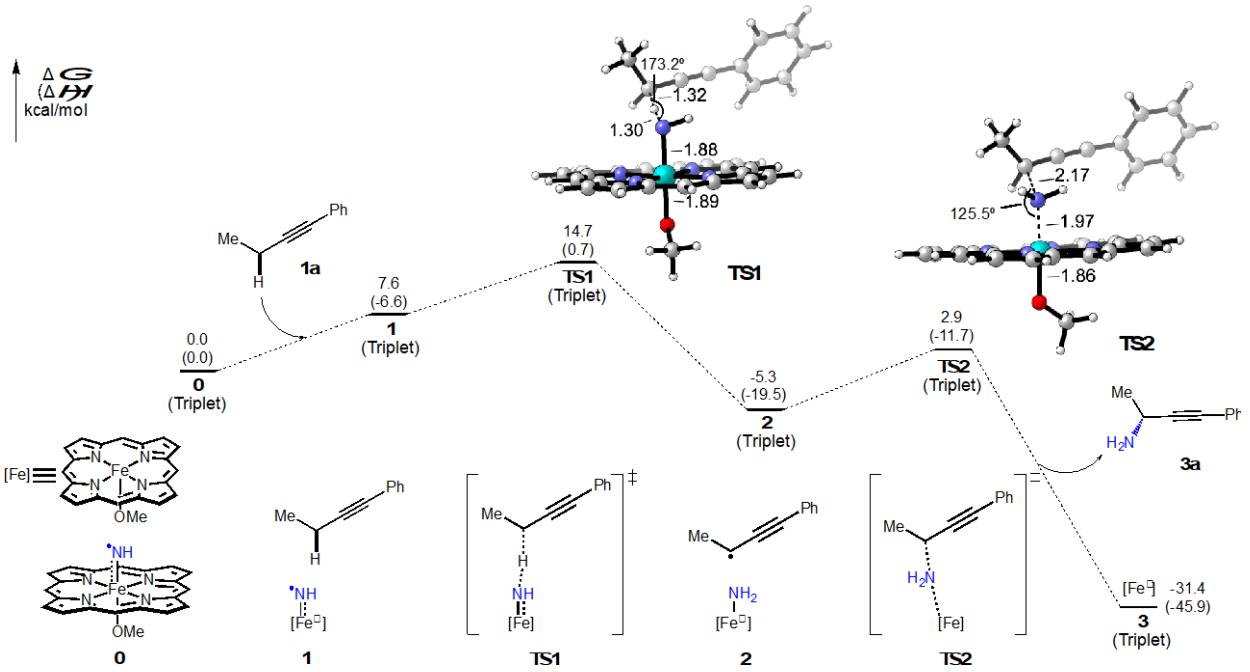

Figure 2.3. DFT computed free energy profile for the iron(II)-porphyrin catalyzed propargylic C(sp^3)–H amination using a truncated computational model and substrate **1.1a**. Gibbs free energies are obtained at the B3LYP-D3(BJ)/Def2TZVP/SMD(ε=4)//B3LYP-D3(BJ)/6-31G(d)-SDD(Fe) level of theory, and are given in kcal·mol^{-1}. Key distances and angles are given in Å and degrees, respectively.

2.3 Conclusion

In summary, we established a biocatalytic platform for highly enantioselective nitrene propargylic C–H insertion reactions to furnish a set of synthetically useful and biologically relevant propargyl amine products. This work represents the first example of an intermolecular propargylic C–H amination reaction via a putative unsubstituted nitrene intermediate. Through eight iterative rounds of directed evolution, we identified a P411 variant **PA-G8** which could catalyze the desired reaction in good efficiency and selectivity (up to 79% yield, >2000 TTN, and 96% ee). In addition, **PA-G8** could accept an array of different substituted alkyne substrates. DFT calculations provided mechanistic insights on the nitrene insertion, suggesting a key role of the enzyme active site in controlling the selectivity of the process by precisely positioning the substrate with respect to the Fe-nitrenoid species. Future work will be focused on engineering "propargylic aminases" for a broader scope of substrates, such as dialkyl alkynes, and investigating the origins of stereoselectivity based on the new mutations introduced during the laboratory evolution. Further characterization of the nitrene intermediate would be valuable for generalizing this process as well. We envision that this enzymatic primary amination system can be applied to the preparation of bioactive chiral amines for synthetic chemistry and drug discovery.

2.4 Experimental Methods

General Procedure

Unless otherwise noted, all chemicals and reagents were obtained from commercial suppliers (Millipore Sigma, VWR, TCI America and Fischer Scientific) and were used without further purification. NMR spectra of chemicals in DMSO-d_6 and $CDCl_3$ were obtained using a Bruker Prodigy 400 MHz spectrometer and were referenced to residual solvent signals. Data for ^1H NMR are reported as follows: chemical shift (δ ppm), multiplicity (s = singlet, d = doublet, t = triplet, q = quartet, hept = heptet, m = multiplet), coupling constant (Hz), and integration. Sonication was performed using a Qsonica Q500 sonicator. High-resolution mass spectra were obtained at the California Institute of Technology Mass Spectral Facility. Optical rotations were measured on a Jasco P-2000 polarimeter using a 100-mm path-length cell at 589 nm. Chemical reactions were monitored using thin layer chromatography (Merck 60 silica gel plates) and a UV lamp for

visualization. Reverse-phase liquid chromatography-mass spectroscopy (LC-MS) for analysis were carried out using Agilent 1200 series instruments, with a C8 (Agilent ZORBAX SB-C8, 4.6 × 50 mm, 3.5 μm) column. Water and acetonitrile containing 0.1% acetic acid were used as eluents. Normal-phase chiral HPLC was performed using Daicel Chiralpak IA and AD-H columns (4.6 × 250 mm, 5 μm) with hexane and isopropanol as the mobile phase.

Cloning, Mutagenesis, and Expression of Enzymes

Expression vector pET22b(+) (Novagen) was used for cloning and expression of all variants described in this paper. Site-saturation mutagenesis was performed using a modified QuikChange™ mutagenesis protocol using the "22-codon trick."[1] Primer sequences are available upon request. The PCR products were digested with *Dpn*I, purified with New England Biolabs gel purification kit, and the gaps were repaired using Gibson Mix™.[2] Without further purification after the Gibson step, 1 μL of the Gibson product was used to transform 50 μL of electrocompetent *Escherichia coli* BL21 *E. cloni*® (Lucigen) cells. BL21 *E. cloni*® cells transformed with pET22b(+) constructs encoding various $P411_{BM3}$ variants were grown overnight in 5 mL Luria-Bertani medium supplemented with 0.1 mg/mL ampicillin (LB_{amp}). Subsequently, 1 mL of this preculture were used to inoculate 49 mL of Hyperbroth medium supplemented with 0.1 mg/mL ampicillin (HB_{amp}). The expression culture was incubated at 37 °C and shaken at 230 rpm for 2 hours. Then, the expression culture was cooled on ice for 1 hour and was induced with 1 mM 5-aminolevulinic acid (ALA) and 0.5 mM isopropyl *β*-D-1-thiogalactopyranoside (IPTG) (final concentrations). Cells were expressed at 22 °C and 140 rpm for 20–22 hours, and the shaking radius was 25 mm. Once expression was finished, the cultures were centrifuged (4,000 × g, 4 minutes, and 4 °C) and the pellets were resuspended to an optical density at 600 nm (OD_{600}) of 40–48 in M9-N minimal medium with pH adjusted to 8.4. Aliquots of the cell suspension (3–4 mL) were used to determine protein concentration after lysis by sonication.

Determination of Hemoprotein Concentration

The concentration of P411 enzymes in whole-cell experiments was determined from ferrous carbon monoxide binding difference spectra using the previously reported extinction coefficient for serine-ligated enzymes ($\varepsilon = 103{,}000\ M^{-1}\bullet cm^{-1}$).[3] Lysate was obtained by sonication (4 minutes,

1 second on, 1 second off, 30% amplitude, on wet ice). The cell debris was removed by centrifugation (14,000 × g, 10 minutes, 4 °C), and 180 µL of the supernatant was then transferred to a well in a 96-well UV-vis flat bottom plate (measurements were performed in quadruplicate). To each well, 20 µL of freshly prepared 0.3 M sodium dithionite aqueous solution was added. Absorbance measurements were performed on a Tecan Spark instrument before and after CO binding. The following formula was used for estimating protein concentration.

$$[Enzyme]\ (\mu M) = 1.1 * \frac{\Delta 411_{CO-red} - \Delta 490_{CO-red}}{0.74\,cm * 0.103\,\mu M^{-1} cm^{-1}}$$

Analytic Reaction Setup and Product Quantification

All the biocatalytic reactions were set up in an anaerobic chamber (oxygen level: <40 ppm). 400 µL of resuspended cells (diluted to OD_{600} = 40 with M9-N minimal buffer, pH = 8.4) were added to 2-mL screw cap vials on an ice bath, followed by D-glucose (60 µL, 500 mM in M9-N buffer), M9-N buffer (312 µL, pH = 8.4), the alkyne substrate (8 µL of 200 mM stock solution in EtOH), and *O*-pivaloylhydroxylamine triflic acid[4] (**2**, 20 µL of 200 mM stock solution in M9-N buffer). Final concentrations were 2.0 mM alkyne, 5.0 mM nitrene precursor **2**, and 37.5 mM D-glucose; final reaction volume was 800 µL. The vials were capped, shaken (250 rpm) inside a shaker (the shaking radius was 25 mm) at 10 ºC for 12–20 hours. After the reaction was completed and the vials removed from the shaker, an internal standard *p*-methyl anisole (400 µL of 1.5 mM stock solution in acetonitrile) was added. The mixture was transferred to a 1.7-mL Eppendorf tube, and then subjected to vortexing (20 s × 2) and centrifugation (14,000 × g, 5 min, 4 °C). A sample of the supernatant (0.2 mL) was transferred to a vial with an insert for LC-MS analysis. Products were identified and quantified based on the corresponding reference compounds (**Section IV** and **V**). To further determine the enantiomeric excess (*ee*), the remaining supernatants of two parallel analytical reactions were combined and transferred to a 2-dram vial and the solvent was removed by blowing air. To the remaining residues were added benzoyl chloride (30 µL of 1 M stock solution in acetonitrile), 100 µL acetonitrile and 50 µL saturated $NaHCO_3$ solution. After shaking the vials for 6 hours, the benzoyl-protected amines were extracted to a solution of hexane and EtOAc mixture (1:1) and subjected to normal-phase HPLC to determine the *ee*.

Reaction Screening in 96-Well Plate in Whole-Cell Format

After a single site-saturation library was generated, 88 single colonies were randomly picked and cultured in 300 μL of LB medium with 0.1 mg/mL ampicillin (LB_{amp}) in a sterilized 96-well culture plate. The plate typically contained six wells inoculated with single colonies expressing the parent enzyme, and two sterile wells. The cells in LB medium were cultured at 37 °C, 230 rpm, and 80% relative humidity for 13–15 hours. A separate sterilized 96-well culture plate was filled with 950 μL of Hyperbroth medium containing 0.1 mg/mL ampicillin (HB_{amp}) in each well. The plate with HB_{amp} was inoculated with the LB preculture (50 μL/well), and incubated at 37 °C, 230 rpm, and 80% relative humidity for 2.5 hours. The plate was cooled on ice for 1 hour, induced with 0.5 mM IPTG and 1 mM 5-aminolevulinic acid (final concentrations), and then expressed at 22 °C and 220 rpm for 20–22 hours. The cells were pelleted (4,000 × g, 4 minutes, and 4 °C) and the 96-well plate was transferred to an anaerobic chamber. Inside the Coy chamber, 312 μL of M9-N (pH 8.4) together with 60 μL of D-glucose solution (500 mM in M9-N, pH 8.4) were added to each well. After cell pellets were fully resuspended by vortexing, 400 μL of M9-N (pH 8.4), alkyne substrate (8 μL of 200 mM stock solution in EtOH) and nitrene precursor **2** (20 μL of 200 mM stock solution in M9-N buffer) were added. The plate was sealed with an aluminum foil and shaken at 250 rpm inside a shaker (the shaking radius was 25 mm) at 10 ºC for 12–20 hours. Once the plate was taken out of the anaerobic chamber and the seal was removed, acetonitrile (400 μL/well) was added. The resulting suspension in the wells was mixed by vortexing, and the plate was left to shake at 700 rpm at room temperature for half an hour for additional mixing. The plate was then centrifuged (4,500 × g, 5 minutes) to precipitate proteins and cell debris. The supernatant (200 μL/well) was filtered through an AcroPrep 96-well filter plate (0.2 μm) into a shallow 96-well plate for LC-MS analysis to determine the yield.

To further determine the enantiomeric excess (*ee*), the remaining supernatants of selected wells were transferred to 2-mL screw cap vials. To each vial were added benzoyl chloride (20 μL of 1 M stock solution in acetonitrile) and 30 μL saturated $NaHCO_3$ solution. After shaking the vials overnight, the benzoyl-protected amines were extracted to a solution of hexane and EtOAc mixture (1:1) and subjected to normal-phase HPLC to determine the *ee*.

2.5 References

(1) Lauder, K.; Toscani, A.; Scalacci, N.; Castagnolo, D. Synthesis and Reactivity of Propargylamines in Organic Chemistry. *Chem. Rev.* **2017**, *117*, 14091–14200.

(2) Zindo, F. T.; Joubert, J.; Malan, S. F. Propargylamine as Functional Moiety in the Design of Multifunctional Drugs for Neurodegenerative Disorders: MAO Inhibition and Beyond. *Future Med. Chem.* **2015**, *7*, 609–629.

(3) (a) Tardif, J.-C.; L'Allier, P. L.; Ibrahim, R.; Grégoire, J. C.; Nozza, A.; Cossette, M.; Kouz, S.; Lavoie, M.-A.; Paquin, J.; Brotz, T. M.; Taub, R.; Pressacco, J. Treatment with 5-Lipoxygenase Inhibitor VIA-2291 (Atreleuton) in Patients with Recent Acute Coronary Syndrome. *Circ. Cardiovasc. Imaging* **2010**, *3*, 298–307. (b) Cossy, J.; Schmitt, A.; Cinquin, C.; Buisson, D.; Belotti, D. A Very Short, Efficient and Inexpensive Synthesis of the Prodrug Form of SC-54701A a Platelet Aggregation Inhibitor. *Bioorg. Med. Chem. Lett.* **1997**, *7*, 1699–1700.

(4) Volkova, Y.; Baranin, S.; Zavarzin, I. A^3 Coupling Reaction in the Synthesis of Heterocyclic Compounds. *Adv. Synth. Catal.* **2021**, *363*, 40–61.

(5) For selected examples, see: (a) Hattori, G.; Matsuzawa, H.; Miyake, Y.; Nishibayashi, Y. Copper-catalyzed Asymmetric Propargylic Substitution Reactions of Propargylic Acetates with Amines. *Angew. Chem. Int. Ed.* **2008**, *47*, 3781–3783. (b) Schmidt, N. G.; Simon, R. C.; Kroutil, W. Biocatalytic Asymmetric Synthesis of Optically Pure Aromatic Propargylic Amines Employing ω-Transaminases. *Adv. Synth. Catal.* **2015**, *357*, 1815–1821. (c) Chen, B.-L.; Wang, B.; Lin, G.-Q. Highly Diastereoselective Addition of Alkynylmagnesium Chlorides to *N-tert*-Butanesulfinyl Aldimines: A Practical and General Access to Chiral α-Branched Amines. *J. Org. Chem.* **2010**, *75*, 941–944.

(6) For selected examples of nitrene propargylic C–H insertion, see: (a) Paradine, S. M.; Griffin, J. R.; Zhao, J.; Petronico, A. L.; Miller, S. M.; White, M. C. A Manganese Catalyst for Highly Reactive Yet Chemoselective Intramolecular C(sp^3)–H Amination. *Nat. Chem.* **2015**, *7*, 987–994. (b) Lu, H.; Li, C.; Jiang, H.; Lizardi, C. L.; Zhang, X. P. Chemoselective Amination of Propargylic C(sp^3)–H Bonds by Cobalt(II)-Based Metalloradical Catalysis. *Angew. Chem. Int. Ed.* **2014**, *53*,

7028–7032. (c) Li, C.; Lang, K.; Lu, H.; Hu, Y.; Cui, X.; Wojtas, L.; Zhang, X. P. Catalytic Radical Process for Enantioselective Amination of C(sp^3)–H Bonds. *Angew. Chem. Int. Ed.* **2018**, *57*, 16837–16841. (d) Lang, K.; Torker, S.; Wojtas, L.; Zhang, X. P. Asymmetric Induction and Enantiodivergence in Catalytic Radical C–H Amination *via* Enantiodifferentiative H-Atom Abstraction and Stereoretentive Radical Substitution. *J. Am. Chem. Soc.* **2019**, *141*, 12388–12396. (e) Park, Y.; Chang, S. Asymmetric Formation of γ-Lactams *via* C–H Amidation Enabled by Chiral Hydrogen-Bond-Donor Catalysts. *Nat. Catal.* **2019**, *2*, 219–227. (f) Xing, Q.; Chan, C.-M.; Yeung, Y.-W.; Yu, W.-Y. Ruthenium(II)-Catalyzed Enantioselective γ-Lactams Formation by Intramolecular C–H Amidation of 1,4,2-dioxazol-5-ones. *J. Am. Chem. Soc.* **2019**, *141*, 3849–3853. (g) Zhou, Z.; Chen, S.; Hong, Y.; Winterling, E.; Tan, Y.; Hemming, M.; Harms, K.; Houk, K. N.; Meggers, E. Non-C_2-Symmetric Chiral-at-Ruthenium Catalyst for Highly Efficient Enantioselective Intramolecular C(sp^3)–H Amidation. *J. Am. Chem. Soc.* **2019**, *141*, 19048–19057. (h) Wang, H.; Park, Y.; Bai, Z.; Chang, S.; He, G.; Chen, G. Iridium-Catalyzed Enantioselective C(sp^3)–H Amidation Controlled by Attractive Noncovalent Interactions. *J. Am. Chem. Soc.* **2019**, *141*, 7194–7201. (i) Ju, M.; Zerull, E. E.; Roberts, J. M.; Huang, M.; Guzei, I. A.; Schomaker, J. M. Silver-Catalyzed Enantioselective Propargylic C–H Bond Amination Through Rational Ligand Design. *J. Am. Chem. Soc.* **2020**, *142*, 12930–12936.

(7) (a) Thornton, A. R.; Blakey, S. B. Catalytic Metallonitrene/Alkyne Metathesis: A Powerful Cascade Process for the Synthesis of Nitrogen-Containing Molecules. *J. Am. Chem. Soc.* **2008**, *130*, 5020–5021. (b) Lai, X.; Liu, J.-B.; Wang, Y.-C.; Qiu, G. Iron-Catalyzed Intramolecular Acyl Nitrene/Alkyne Metalation for the Synthesis of Pyrrolo[2,1-*A*]Isoindol-5-Ones. *Chem. Commun.* **2021**, *57*, 2077–2080.

(8) Jin, L.-M.; Xu, P.; Xie, J.; Zhang, X. P. Enantioselective Intermolecular Radical C–H Amination. *J. Am. Chem. Soc*. **2020**, *142*, 20828–20836. There is an example of intermolecular propargylic C–H amination using a chiral nitrene precursor to achieve diastereoselective control, see: Lebel, H.; Trudel, C.; Spitz, C. Stereoselective Intermolecular C–H Amination Reactions. *Chem. Commun.* **2012**, *48*, 7799–7801.

(9) For a review, see: (a) Liu, Z.; Arnold, F. H. New-To-Nature Chemistry from Old Protein Machinery: Carbene And Nitrene Transferases. *Curr. Opin. Biotechnol*. **2021**, *69*, 43–51. For

selected examples: (b) Prier, C. K.; Zhang, R. K.; Buller, A. R.; Brinkmann-Chen, S.; Arnold, F. H. Enantioselective, Intermolecular Benzylic C–H Amination Catalysed by An Engineered Iron-Haem Enzyme. *Nat. Chem*. **2017**, *9*, 629–634. (c) Singh, R.; Bordeaux, M.; Fasan, R. P450-Catalyzed Intramolecular sp^3 C–H Amination with Arylsulfonyl Azide Substrates. *ACS Catal.* **2014**, *4*, 546–552. (d) Dydio, P.; Key, H. M.; Hayashi, H.; Clark, D. S.; Hartwig, J. F. Chemoselective, Enzymatic C–H Bond Amination Catalyzed by A Cytochrome P450 Containing An Ir(Me)-Pix Cofactor. *J. Am. Chem. Soc*. **2017**, *139*, 1750–1753.

(10) Jia, Z.-J.; Gao, S.; Arnold, F. H. Enzymatic Primary Amination of Benzylic and Allylic C(sp^3)–H Bonds. *J. Am. Chem. Soc*. **2020**, *142*, 10279–10283.

(11) Makai, S.; Falk, E.; Morandi, B. Preparation of *O*-Pivaloyl Hydroxylamine Triflic Acid. *Org. Synth.* **2020**, *97*, 207–216.

(12) Simon, D. Z.; Salvador, R. L.; Champagne, G. Acetylenics. 1. Aromatic Amines Containing the Acetylenic Triple Bond. *J. Med. Chem.* **1970**, *13*, 1249–1250.

(13) Yang, Y.; Arnold, F. H. Navigating the Unnatural Reaction Space: Directed Evolution of Heme Proteins for Selective Carbene and Nitrene Transfer. *Acc. Chem. Res.* **2021**, *54*, 1209–1225.

(14) (a) L'Argentiere, P. C.; Fígoli, N. S. Selective Hydrogenation of Styrene. II. Poisoning of Pd/Al_2O_3 by Thiophene and Pyridine. *J. Chem. Technol. Biotechnol.* **1990**, *48*, 361–368. (b) Temel, B.; Tuxen, A. K.; Kibsgaard, J.; Topsøe, N.-Y.; Hinnemann, B.; Knudsen, K. G.; Topsøe, H.; Lauritsen, J. V.; Besenbacher, F. Atomic-Scale Insight into the Origin of Pyridine Inhibition of Mos_2-Based Hydrotreating Catalysts. *J. Catal.* **2010**, *271*, 280–289.

(15) For low-yielding examples, we only observed remaining alkyne substrates. No side products were detected.

(16) (a) Yang, Y.; Cho, I.; Qi, X.; Liu, P.; Arnold, F. H. An Enzymatic Platform for the Asymmetric Amination of Primary, Secondary and Tertiary C(sp^3)–H Bonds. *Nat. Chem.* **2019**, *11*, 987–993. (b) Athavale, S. V.; Gao, S.; Liu, Z.; Mallojjala, S. C.; Hirschi, J. S.; Arnold, F. H.

Biocatalytic, Intermolecular C–H Bond Functionalization for the Synthesis of Enantioenriched Amides. *Angew. Chem. Int. Ed.* **2021**, *60*, 24864–24869.

(17) Wang, J.; Gao, H.; Yang, L.; Gao, Y. Q. Role of Engineered Iron-Haem Enzyme in Reactivity and Stereoselectivity of Intermolecular Benzylic C–H Bond Amination. *ACS Catal.* **2020**, *10*, 5318–5327.

Appendix A. Supplementary Information for Chapter II

I. Directed Evolution of PA-G8 for Propargylic C(sp^3)–H Amination

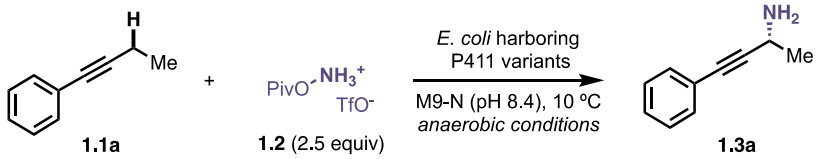

Table A.S1. Detailed information of the evolutionary lineage.

P411-PA variant	**Yield (%)**	***ee* (%)**
P411-b4 (**G0**)	64 ± 1	−1
G0-E267D (**G1**)	103 ± 2	28
G0-E267D N395C (**G2**)	84 ± 3	33
G0-E267D N395C G437Q (**G3**)	56 ± 1	54
G0-E267D N395C G437Q S72T (**G4**)	68 ± 3	61
G0-E267D N395C G437Q S72T S438G (**G5**)	45 ± 3	75
G0-E267D N395C G437Q S72T S438G T269V (**G6**)	51 ± 0.3	82
G0-E267D N395C G437Q S72T S438G T269V H266S (**G7**)	49 ± 1	85
G0-E267D N395C G437Q S72T S438G T269V H266S A74K (**G8**)	79 ± 6	88

Table A.S2. Further information on directed evolution experiments.

Round #	**Parent**	**Sites targeted for SSM**	**Screen for activity or enantioselectivity**	**Beneficial mutations obtained**
1	**PA-G0**	70, 78, 82, 87, 181, 263, **267**, 328, 330, 333	both	**E267D** (~1.5-fold activity improvement, *ee* increased to 28%)
2	**G1**	72, 87, 327, **395**, 409	both	S72F (*ee* increased to 40%, half of the parent activity) **N395C** (*ee* increased to 33%)
3	**G2**	72, 328, 333, **437**	enantioselectivity	G437M (*ee* increased to 41%) **G437Q** (*ee* increased to 54%)
4	**G3**	**72**, 70, 263, 268, 438	enantioselectivity	**S72T** (*ee* increased to 61%) S438G (*ee* increased to 69%)
5	**G4**	**438** (Recombination)	enantioselectivity	**S438G** (*ee* increased to 75%)
6	**G5**	82, 266, **269**, 332, 401, 435	enantioselectivity	**T269V** (*ee* increased to 82%)

7	**G6**	**266**, 332	enantioselectivity	**H266S** (*ee* increased to 85%)
8	**G7**	71, **74**, 86, 177, 188, 331, 332, 439	both	**A74K** (*ee* increased to 88%, yield increased to 79%)

II. Supporting Experimental Figures

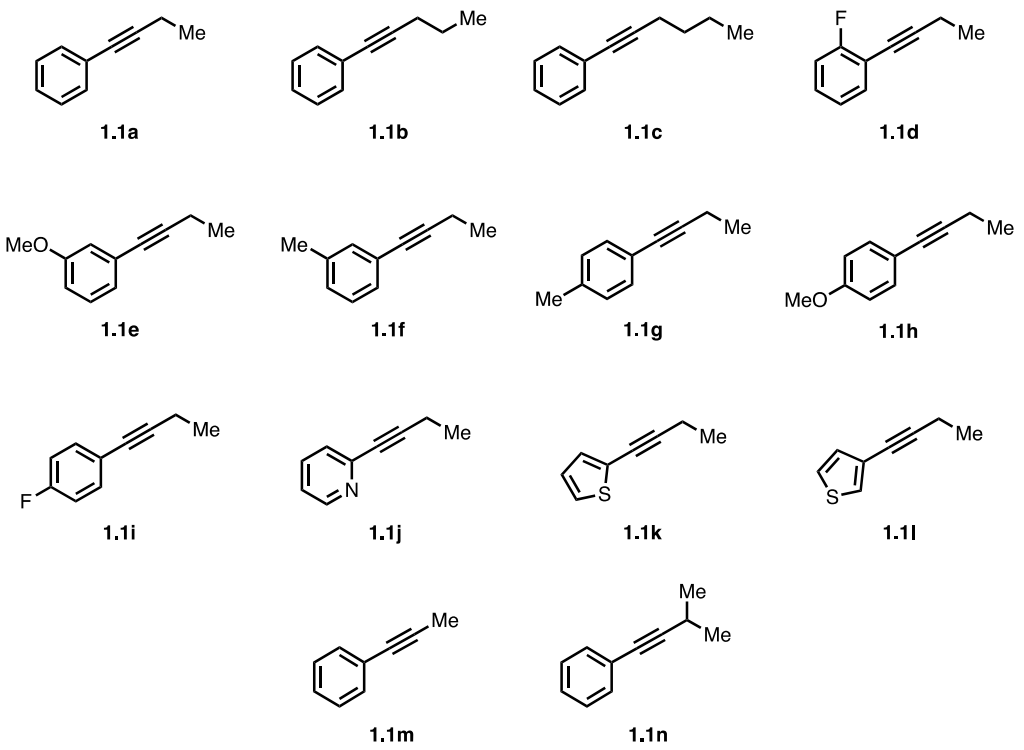

Figure A.S1. Summary of alkyne substrates (**1.1a**–**1.1n**).

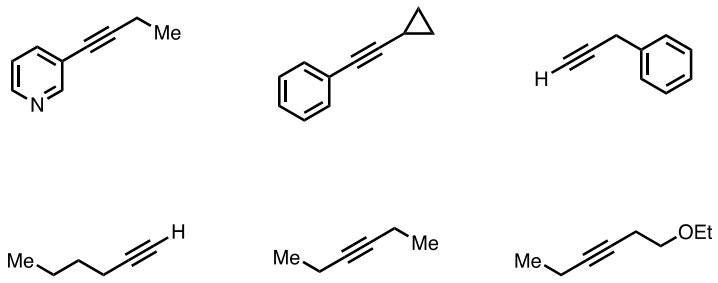

Figure A.S2. Other substrates tested for enzymatic propargylic amination reaction.

Notes: The alkyne substrates listed here have been tested briefly for the propargylic amination chemistry catalyzed by **PA-G8**. However, these substrates only gave low enantioselectivity or reactivity, as preliminarily analyzed by LC-MS and chiral HPLC. These results are noteworthy, but they cannot be used for drawing final conclusions before further validation.

Table A.S3. Investigation of the effect of substrate concentration and cell density (OD_{600}) on the reaction outcome.

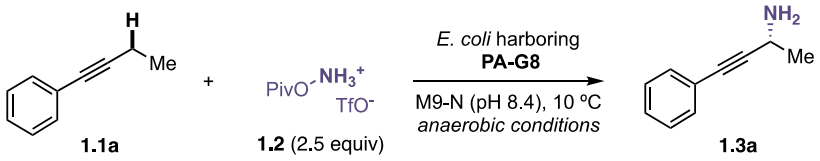

Entry	**1.1a** concentration (mM)	Reaction OD_{600}	Yield (%)	*ee* (%)
1	2	20	79	88
2	4	20	50	88
3	6	20	23	89
4	4	40	74	87
5	6	40	39	88

Notes: Increasing the substrate concentration decreases the reaction yield at OD_{600} = 20. However, increasing the cell density (to OD_{600} = 40) and substrate concentration (to 4 mM) simultaneously result in good yield (74%, Entry 4).

Scheme A.S1. Variants that showed improved activities for low-yielding examples **1.3g** and **1.3n**.

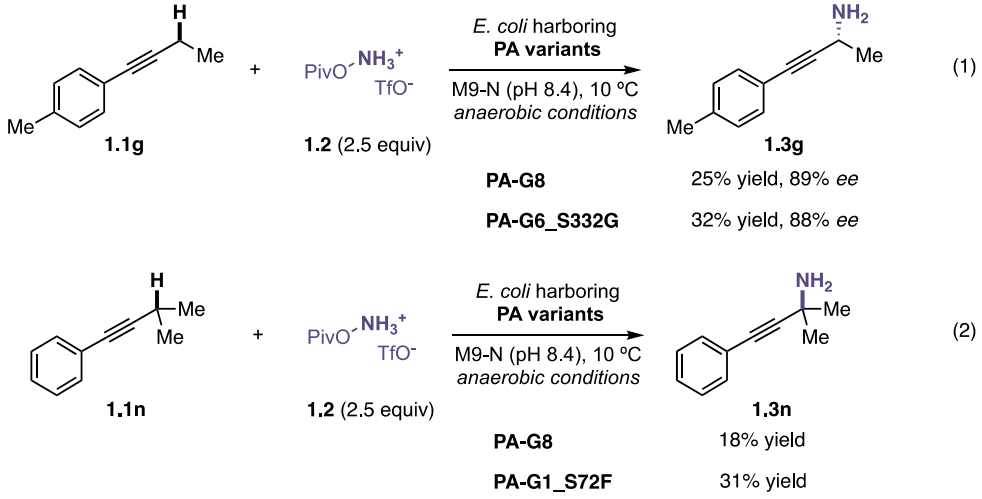

Notes: Variant **PA-G6_S332G** has one mutation (S332G) relative to **PA-G6**. Variant **PA-G1_S72F** has one mutation (S72F) relative to **PA-G1**.

III. Preparation and Characterization of the Alkyne Substrates

General procedure A[5]:

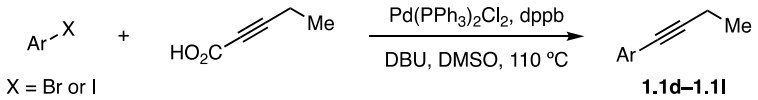

To a 100-mL flask were added aryl halide (5.0 mmol, 1.0 equiv.), 2-pentynoic acid (590.3 mg, 6.0 mmol, 1.2 equiv.), $PdCl_2(PPh_3)_2$ (35 mg, 0.05 mmol, 1 mol%), 1,4- bis(diphenylphosphino)butane (dppb, 43 mg, 0.1 mmol, 2 mol%), and anhydrous DMSO (15 mL). After the mixture was stirred at room temperature for 3 minutes, the flask was capped, degassed, and charged with argon, followed by addition of 1,8-Diazabicyclo[5.4.0]undec-7-ene (DBU, 2.2 mL, 15.0 mmol, 3.0 equiv.) under argon. The reaction was stirred at 110 °C overnight, then cooled to room temperature, quenched by saturated NH_4Cl solution (10 mL), and diluted with water (15 mL). The product was extracted by ether (20 mL × 3), and the combined organic layer was washed with brine (30 mL). The organic phase was further dried over Na_2SO_4 and concentrated to afford a yellow residue. Flash column chromatography was performed to afford pure product in 50% to 90% yield.

Notes: Substrates (**1.1d–1.1l**) were prepared by **General procedure A**.

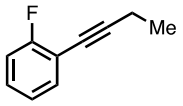

1.1d **1-(but-1-yn-1-yl)-2-fluorobenzene (1.1d): ^{1}H NMR** (400 MHz, $CDCl_3$) δ 7.39 (td, *J* = 7.6, 1.8 Hz, 1H), 7.29–7.19 (m, 1H), 7.10–6.99 (m, 2H), 2.47 (q, *J* = 7.5 Hz, 2H), 1.26 (t, *J* = 7.5 Hz, 3H); **^{13}C NMR** (100 MHz, $CDCl_3$) δ 162.9 (d, *J* = 250.1 Hz), 133.7 (d, *J* = 1.7 Hz), 129.2 (d, *J* = 8.0 Hz), 123.9 (d, *J* = 3.8 Hz), 115.5 (d, *J* = 21.1 Hz), 112.6 (d, *J* = 15.8 Hz), 97.3 (d, *J* = 3.3 Hz), 73.3, 13.9, 13.4; **^{19}F NMR** (376 MHz, $CDCl_3$) δ –111.2.

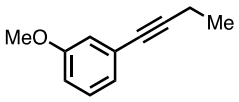

1.1e **1-(but-1-yn-1-yl)-3-methoxybenzene (1.1e): ^{1}H NMR** (400 MHz, $CDCl_3$) δ 7.23–7.14 (m, 1H), 7.00 (dt, *J* = 7.6, 1.2 Hz, 1H), 6.94 (dd, *J* = 2.7, 1.5 Hz, 1H), 6.83 (ddd, *J* = 8.4, 2.6, 1.1 Hz, 1H), 3.79 (s, 3H), 2.42 (q, *J* = 7.5 Hz, 2H), 1.24 (t, *J* = 7.5 Hz, 3H); **^{13}C NMR** (100 MHz, $CDCl_3$) δ 159.4, 129.4, 125.2, 124.2, 116.5, 114.3, 91.7, 79.9, 55.4, 14.0, 13.2.

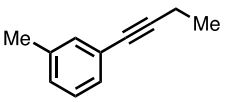

1.1f **1-(but-1-yn-1-yl)-3-methylbenzene (1.1f): ^{1}H NMR** (400 MHz, $CDCl_3$) δ 7.26–7.13 (m, 3H), 7.07 (dtd, *J* = 7.2, 1.7, 0.8 Hz, 1H), 2.41 (q, *J* = 7.5 Hz, 2H), 2.31 (s, 3H), 1.23 (t, *J* = 7.5 Hz, 3H); **^{13}C NMR** (100 MHz, $CDCl_3$) δ 138.0, 132.3, 128.7, 128.5, 128.2, 123.9, 91.4, 80.1, 21.4, 14.1, 13.2.

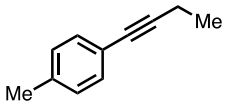

1.1g **1-(but-1-yn-1-yl)-4-methylbenzene (1.1g): ^{1}H NMR** (400 MHz, $CDCl_3$) δ 7.31–7.27 (m, 2H), 7.13–7.04 (m, 2H), 2.41 (q, *J* = 7.5 Hz, 2H), 2.33 (s, 3H), 1.23 (t, *J* = 7.5 Hz, 3H); **^{13}C NMR** (100 MHz, $CDCl_3$) δ 137.6, 131.5, 129.1, 121.0, 91.0, 80.0, 21.5, 14.1, 13.2.

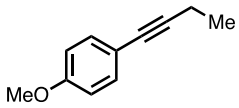

1.1h **1-(but-1-yn-1-yl)-4-methoxybenzene (1.1h): ^{1}H NMR** (400 MHz, $CDCl_3$) δ 7.37–7.29 (m, 2H), 6.85–6.77 (m, 2H), 3.80 (s, 3H), 2.40 (q, *J* = 7.5 Hz, 2H), 1.23 (t, *J* = 7.5 Hz, 3H); **^{13}C NMR** (100 MHz, $CDCl_3$) δ 159.1, 133.0, 116.3, 113.9, 90.2, 79.7, 55.4, 14.2, 13.2.

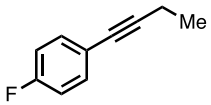

1.1i **1-(but-1-yn-1-yl)-4-fluorobenzene (1.1i): ^{1}H NMR** (400 MHz, $CDCl_3$) δ 7.37 (ddd, *J* = 8.7, 4.9, 2.0 Hz, 2H), 6.97 (ddt, *J* = 10.4, 6.6, 1.4 Hz, 2H), 2.40 (q, *J* = 7.5 Hz, 2H), 1.23 (t, *J* = 7.5 Hz, 3H); **^{13}C NMR** (100 MHz, $CDCl_3$) δ 162.2 (d, *J* = 248.0 Hz), 133.4 (d, *J* = 8.2 Hz), 120.2 (d, *J* = 3.4 Hz), 115.5 (d, *J* = 22.0 Hz), 91.4 (d, *J* = 1.4 Hz), 79.0, 14.0, 13.2; **^{19}F NMR** (376 MHz, $CDCl_3$) δ –112.5.

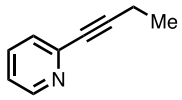

1.1j **2-(but-1-yn-1-yl)pyridine (1.1j): ^{1}H NMR** (400 MHz, $CDCl_3$) δ 8.52 (ddd, *J* = 4.9, 1.8, 0.9 Hz, 1H), 7.59 (td, *J* = 7.7, 1.8 Hz, 1H), 7.35 (dt, *J* = 7.8, 1.1 Hz, 1H), 7.16 (ddd, *J* = 7.6, 4.9, 1.2 Hz, 1H), 2.44 (q, *J* = 7.5 Hz, 2H), 1.24 (t, *J* = 7.5 Hz, 3H); **^{13}C NMR** (100 MHz, $CDCl_3$) δ 149.9, 144.0, 136.1, 126.8, 122.4, 92.4, 79.8, 13.6, 13.1.

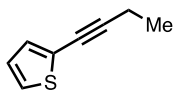

1.1k **2-(but-1-yn-1-yl)thiophene (1.1k): ^{1}H NMR** (400 MHz, $CDCl_3$) δ 7.17 (dd, *J* = 5.2, 1.2 Hz, 1H), 7.12 (dd, *J* = 3.6, 1.2 Hz, 1H), 6.93 (dd, *J* = 5.2, 3.6 Hz, 1H), 2.44 (q, *J* = 7.5 Hz, 2H),

1.23 (t, J = 7.5 Hz, 3H); **^{13}C NMR** (100 MHz, $CDCl_3$) δ 131.0, 126.9, 126.0, 124.3, 95.8, 73.1, 13.8, 13.5.

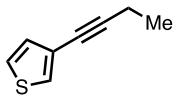

1.1l **3-(but-1-yn-1-yl)thiophene (1.1l): ^{1}H NMR** (400 MHz, $CDCl_3$) δ 7.41–7.32 (m, 1H), 7.23 (dt, J = 4.7, 2.2 Hz, 1H), 7.10–7.04 (m, 1H), 2.40 (q, J = 7.4 Hz, 2H), 1.23 (t, J = 7.5 Hz, 3H); **^{13}C NMR** (100 MHz, $CDCl_3$) δ 130.1, 127.7, 125.1, 123.1, 91.3, 75.0, 14.0, 13.2.

General procedure B[6]:

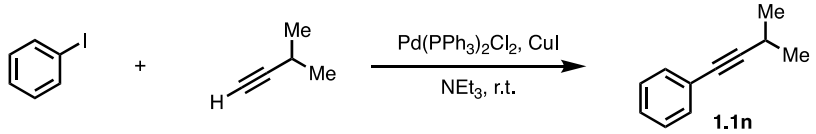

To a 100-mL flask were added iodobenzene (2.04 g, 1.11 mL, 10.0 mmol), $PdCl_2(PPh_3)_2$ (421 mg, 0.6 mol, 6 mol%), CuI (57 mg, 0.3 mmol, 3 mol%) and Et_3N (40 mL). The mixture was stirred at room temperature vigorously, and 3-methylbut-1-yne (1.23 mL, 12.0 mmol, 1.2 equiv.) was added to the reaction. The reaction was further stirred for 42 hours before it was quenched by saturated NH_4Cl solution (150 mL) and extracted with Et_2O (50 mL × 3). The combined organic layer was then washed with brine (100 mL) and dried over Na_2SO_4. The organic player was concentrated and purified through column chromatography to afford product as a colorless liquid in 50% yield.

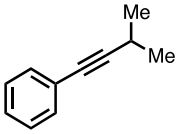

1.1n **(3-methylbut-1-yn-1-yl)benzene (1.1n): ^{1}H NMR** (400 MHz, $CDCl_3$) δ 7.37–7.27 (m, 2H), 7.25–7.13 (m, 3H), 2.70 (hept, J = 6.9 Hz, 1H), 1.19 (d, J = 6.8 Hz, 6H); **^{13}C NMR** (100 MHz, $CDCl_3$) δ 131.7, 128.3, 127.6, 124.1, 95.9, 79.8, 23.2, 21.3

IV. Preparation and Characterization of the Racemic Standards of Products

General procedure C[7]:

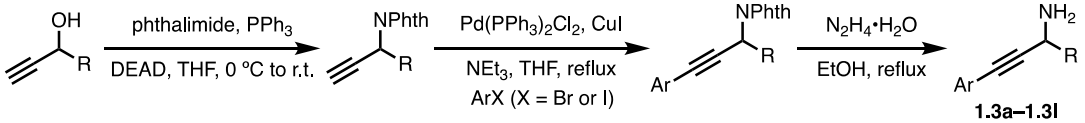

Mitsunobu reaction: To a 250-mL flask were added propargyl alcohol (20.0 mmol, 1.0 equiv.),

phthalimide (2.9 g, 20.0 mmol, 1.0 equiv.), PPh_3 (7.6 g, 30.0 mmol, 1.5 equiv.) and anhydrous THF (50 mL). The mixture was first stirred at 0 °C for 10 minutes. Diethyl azodicarboxylate (DEAD, 7.3 g, 42.0 mmol, 2.1 equiv. in 12.6 mL toluene) was then added dropwise. After stirring at room temperature for 3 hours, the reaction mixture was filtered through a plug of celite. The filtrate was concentrated and purified through column chromatography to afford product as a white solid in 30–50% yield.

Sonogashira coupling: To an 8-dram vial were added the terminal alkyne intermediate (1.0 mmol, 1.0 equiv.), the corresponding aryl halide (1.3 mmol, 1.3 equiv.), $PdCl_2(PPh_3)_2$ (17.6 mg, 0.025 mmol, 2.5 mol%) and CuI (9.5 mg, 0.05 mmol, 5.0 mol%). The vial was then capped, degassed, and charged with argon. A 1:1 mixture of NEt_3 and THF (6 mL) was added to the reaction, which was then stirred at 75 ºC. Upon completion, the reaction was cooled to room temperature, quenched by saturated NH_4Cl solution (10 mL), diluted with water (15 mL), and extracted with EtOAc (20 mL × 3). The combined organic layer was then washed with brine (30 mL), dried over Na_2SO_4, and concentrated to afford a brown residue. Flash column chromatography was performed to afford pure product in 60% to 90% yield.

Amine deprotection: To a 4-dram vial were added all the alkyne intermediate obtained from the previous step, N_2H_4•H_2O (0.3 mL) and EtOH (10 mL). The reaction was stirred at 80 °C for 3 hours. Upon completion, the reaction mixture was filtered through a plug of celite and washed by Et_2O (50 mL). The filtrate was concentrated under reduced pressure and purified through column chromatography to afford pure propargyl amine in 50% to 70% yield.

Notes: Propargyl amines (**1.3a–1.3l**) were prepared by **General procedure C**.

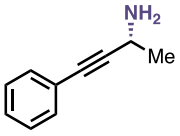

1.3a **4-phenylbut-3-yn-2-amine (1.3a): ^{1}H NMR** (400 MHz, DMSO-d_6) δ 7.42–7.31 (m, 5H), 3.83 (q, J = 6.7 Hz, 1H), 1.30 (d, J = 6.8 Hz, 3H); **^{13}C NMR** (100 MHz, DMSO-d_6) δ 131.2, 128.6, 128.1, 122.9, 95.4, 80.6, 38.6, 24.5; **HRMS** (ESI) Calcd for $C_{10}H_9$ [M–NH_2] 129.0704, found 129.0724.

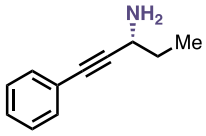

1.3b **1-phenylpent-1-yn-3-amine (1.3b): ^{1}H NMR** (400 MHz, DMSO-d_6) δ 7.42–7.29 (m, 5H), 3.60 (dd, J = 7.3, 6.0 Hz, 1H), 1.95 (s, 2H), 1.68–1.47 (m, 2H), 0.98 (t, J = 7.4 Hz, 3H); **^{13}C NMR** (100 MHz, DMSO-d_6) δ 131.2, 128.6, 128.0, 123.0, 94.5, 81.4, 44.8, 31.0, 10.4; **HRMS** (ESI) Calcd for $C_{11}H_{11}$ [M–NH_2] 143.0861, found 143.0847.

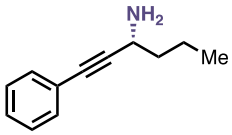

1.3c **1-phenylhex-1-yn-3-amine (1.3c):** **^{1}H NMR** (400 MHz, DMSO-d_6) δ 7.41–7.30 (m, 5H), 3.65 (t, J = 6.7 Hz, 1H), 1.62–1.37 (m, 4H), 0.91 (t, J = 7.2 Hz, 4H); **^{13}C NMR** (100 MHz, DMSO-d_6) δ 131.2, 128.6, 128.0, 123.0, 94.8, 81.3, 43.1, 40.8, 18.9, 13.8; **HRMS** (ESI) Calcd for $C_{12}H_{13}$ [M–NH_2] 157.1017, found 157.1017.

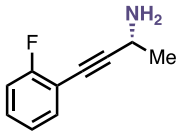

1.3d **4-(2-fluorophenyl)but-3-yn-2-amine (1.3d):** **^{1}H NMR** (400 MHz, $CDCl_3$) δ 7.43–7.34 (m, 1H), 7.31–7.21 (m, 1H), 7.11–7.00 (m, 2H), 3.96 (q, J = 6.8 Hz, 1H), 1.46 (d, J = 6.8 Hz, 3H); **^{13}C NMR** (100 MHz, $CDCl_3$) δ 162.8 (d, J = 250.7 Hz), 133.6 (d, J = 1.5 Hz), 129.8 (d, J = 7.9 Hz), 124.0 (d, J = 3.7 Hz), 115.5 (d, J = 21.0 Hz), 111.8 (d, J = 15.7 Hz), 99.2 (d, J = 3.3 Hz), 75.1, 39.7, 24.4; **^{19}F NMR** (376 MHz, $CDCl_3$) δ –110.7; **HRMS** (ESI) Calcd for $C_{10}H_8F$ [M–NH_2] 147.0610, found 147.0621.

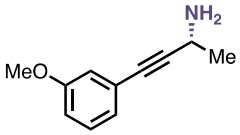

1.3e **4-(3-methoxyphenyl)but-3-yn-2-amine (1.3e):** **^{1}H NMR** (400 MHz, $CDCl_3$) δ 7.24–7.14 (m, 1H), 7.00 (dt, J = 7.6, 1.2 Hz, 1H), 6.93 (dd, J = 2.7, 1.4 Hz, 1H), 6.85 (ddd, J = 8.3, 2.7, 1.0 Hz, 1H), 3.94 (q, J = 6.7 Hz, 1H), 1.45 (d, J = 6.8 Hz, 3H); **^{13}C NMR** (100 MHz, $CDCl_3$) δ 159.4, 129.4, 124.3, 124.2, 116.5, 114.8, 93.6, 81.7, 55.4, 39.6, 24.6; **HRMS** (ESI) Calcd for $C_{11}H_{11}O$ [M–NH_2] 159.0810, found 159.0809.

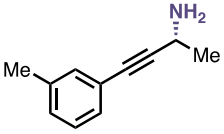

1.3f **4-(*m*-tolyl)but-3-yn-2-amine (1.3f):** **^{1}H NMR** (400 MHz, $CDCl_3$) δ 7.34–6.85 (m, 4H), 3.88 (q, J = 6.4 Hz, 1H), 2.25 (s, 3H), 1.39 (d, J = 6.8 Hz, 3H); **^{13}C NMR** (100 MHz, $CDCl_3$) δ 138.0, 132.3, 129.0, 128.8, 128.3, 123.0, 93.0, 82.2, 39.6, 24.4, 21.4; **HRMS** (ESI) Calcd for $C_{11}H_{11}$ [M–NH_2] 143.0861, found 143.0866.

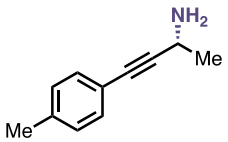

1.3g **4-(*p*-tolyl)but-3-yn-2-amine (1.3g): ^{1}H NMR** (400 MHz, DMSO-d_6) δ 7.29–7.22 (m, 2H), 7.19–7.12 (m, 2H), 3.79 (q, J = 6.7 Hz, 1H), 2.29 (s, 3H), 1.29 (d, J = 6.7 Hz, 3H); **^{13}C NMR** (100 MHz, DMSO-d_6) δ 137.6, 131.0, 129.2, 120.0, 94.9, 80.5, 38.7, 24.7, 21.0; **HRMS** (ESI) Calcd for $C_{11}H_{11}$ [M–NH_2] 143.0861, found 143.0863.

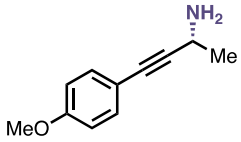

1.3h **4-(4-methoxyphenyl)but-3-yn-2-amine (1.3h): ^{1}H NMR** (400 MHz, DMSO-d_6) δ 7.33–7.27 (m, 2H), 6.95–6.86 (m, 2H), 3.79 (q, J = 6.7 Hz, 1H), 3.75 (s, 3H), 1.28 (d, J = 6.7 Hz, 3H); **^{13}C NMR** (100 MHz, DMSO-d_6) δ 158.9, 132.6, 114.9, 114.2, 93.9, 80.3, 55.2, 38.7, 24.7; **HRMS** (ESI) Calcd for $C_{11}H_{11}O$ [M–NH_2] 159.0810, found 159.0822.

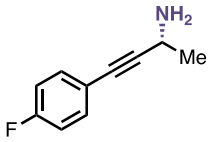

1.3i **4-(thiophen-3-yl)but-3-yn-2-amine (1.3i): ^{1}H NMR** (400 MHz, $CDCl_3$) δ 7.44–7.32 (m, 2H), 7.05–6.90 (m, 2H), 3.94 (q, J = 6.7 Hz, 1H), 1.45 (d, J = 6.8 Hz, 3H); **^{13}C NMR** (100 MHz, $CDCl_3$) δ 162.5 (d, J = 248.9 Hz), 133.6 (d, J = 8.4 Hz), 119.3 (d, J = 3.4 Hz), 115.6 (d, J = 22.0 Hz), 92.9, 81.1, 39.5, 24.4; **^{19}F NMR** (376 MHz, $CDCl_3$) δ –111.5; **HRMS** (ESI) Calcd for $C_{10}H_8F$ [M–NH_2] 147.0610, found 147.0625.

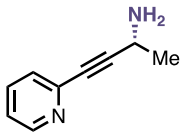

1.3j **4-(pyridin-2-yl)but-3-yn-2-amine (1.3j): ^{1}H NMR** (400 MHz, $CDCl_3$) δ 8.56 (ddt, J = 4.9, 1.6, 0.8 Hz, 1H), 7.69–7.58 (m, 1H), 7.39 (dt, J = 7.9, 1.1 Hz, 1H), 7.25–7.17 (m, 1H), 3.95 (qd, J = 6.9, 1.3 Hz, 1H), 1.47 (d, J = 6.8 Hz, 3H); **^{13}C NMR** (100 MHz, $CDCl_3$) δ 150.0, 143.4, 136.3, 127.0, 122.8, 94.0, 81.4, 39.4, 24.1; **HRMS** (ESI) Calcd for $C_9H_{11}N_2$ [M+H] 147.0922, found 147.0936.

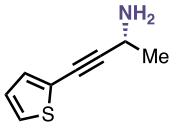

1.3k **4-(thiophen-2-yl)but-3-yn-2-amine (1.3k): ^{1}H NMR** (400 MHz, $CDCl_3$) δ 7.21 (dd, *J* = 5.2, 1.1 Hz, 1H), 7.14 (dd, *J* = 3.6, 1.2 Hz, 1H), 6.95 (dd, *J* = 5.2, 3.6 Hz, 1H), 3.93 (q, *J* = 6.8 Hz, 1H), 1.44 (d, *J* = 6.8 Hz, 3H); **^{13}C NMR** (100 MHz, $CDCl_3$) δ 131.6, 127.0, 126.7, 123.4, 97.7, 75.0, 39.7, 24.4; **HRMS** (ESI) Calcd for C_8H_9NS $[M]^{+\bullet}$ 151.0456, found 151.0457.

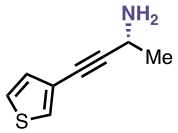

1.3l **4-(thiophen-3-yl)but-3-yn-2-amine (3l): ^{1}H NMR** (400 MHz, $CDCl_3$) δ 7.31 (dd, *J* = 3.0, 1.2 Hz, 1H), 7.18 (dd, *J* = 5.0, 3.0 Hz, 1H), 7.01 (dd, *J* = 5.0, 1.2 Hz, 1H), 3.85 (q, *J* = 6.8 Hz, 1H), 1.37 (d, *J* = 6.8 Hz, 3H); **^{13}C NMR** (100 MHz, $CDCl_3$) δ 129.9, 128.2, 125.2, 122.2, 93.2, 76.8, 39.4, 24.4; **HRMS** (ESI) Calcd for C_8H_7S $[M–NH_2]$ 135.0268, found 135.0279.

General procedure D[8]:

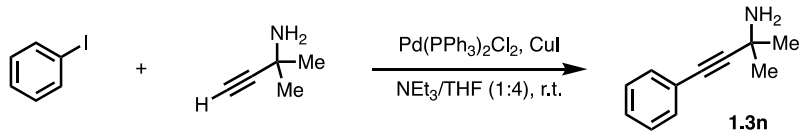

To an 8-dram vial were added iodobenzene (1.12 g, 0.61 mL, 5.5 mmol, 1.1 equiv.), $PdCl_2(PPh_3)_2$ (70.2 mg, 0.10 mmol, 2.0 mol%) and CuI (38.1 mg, 0.20 mmol, 4.0 mol%). The vial was capped, degassed, and charged with argon. NEt_3 (2 mL), 2-methyl-3-butyn-2-amine (416 mg, 5 mmol, 1.0 equiv.) and THF (8 mL) were then added to the reaction. The mixture was stirred at room temperature overnight, before it was quenched by saturated NH_4Cl solution (10 mL), diluted with water (15 mL) and extracted with Et_2O (20 mL × 3). The combined organic layer was then washed with brine (30 mL), dried over Na_2SO_4, and concentrated to afford a brown residue. Flash column chromatography was performed to afford pure product in 60% yield.

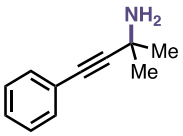

1.3n **2-methyl-4-phenylbut-3-yn-2-amine (1.3n): ^{1}H NMR** (400 MHz, $CDCl_3$) δ 7.36–7.27 (m, 2H), 7.20 (dt, *J* = 4.6, 2.9 Hz, 3H), 1.41 (s, 6H); **^{13}C NMR** (100 MHz, $CDCl_3$) δ 131.6, 128.3, 127.9, 123.4, 97.0, 80.1, 45.8, 31.9; **HRMS** (ESI) Calcd for $C_{11}H_{11}$ $[M–NH_2]$ 143.0861, found 143.0861.

General procedure E[9,10]:

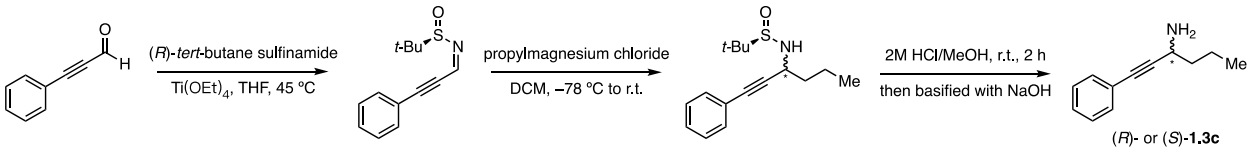

To a solution of (*R*)-*tert*-butanesulfinamide (606.0 mg, 5 mmol, 1.0 equiv.) in anhydrous THF (13 mL) was added phenylpropargyl aldehyde (781.0 mg, 0.74 mL, 6 mmol, 1.2 equiv.) under argon. Subsequently, $Ti(OEt)_4$ (4.56 g, 4.19 mL, 20 mmol, 4.0 equiv.) was added dropwise and the reaction mixture was stirred at 45 ºC for 16 hours. Upon completion, MeOH (5.0 mL) and a solution of saturated $NaHCO_3$ were added until a yellow solid precipitated out. The crude reaction mixture was filtered over celite, dried over Na_2SO_4, and concentrated to afford a brown residue. Flash column chromatography was performed to afford pure product as a brown oil in 85% yield (990.7 mg).[9]

To a cooled (−78 ºC) solution of *N*-sulfinylimine (446.7 mg, 2 mmol, 1.0 equiv.) in anhydrous DCM was added dropwise an ethereal solution of propylmagnesium chloride solution (3.0 mL, 2.0 M in diethyl ether, 6 mmol, 3.0 equiv.) under argon and the reaction mixture was stirred at the same temperature for 2 hours, then gradually warmed up to room temperature stirring overnight. The reaction was quenched by adding saturated NH_4Cl solution, extracted with EtOAc (10 mL × 3) and the combined organic layer was washed with brine, dried over Na_2SO_4, and concentrated to afford a yellow oil. Flash column chromatography was performed to separate two diastereomers as yellow oils in 75% total yield (287.4 mg and 130.2 mg for (*R*,*R*)-, (*R*,*S*)-isomers, respectively).

The pure diastereomer from the previous step was dissolved in a 2M HCl in MeOH solution and stirred at room temperature for 2 hours. Upon completion, the reaction mixture was diluted with EtOAc and extracted with water for three times. The combined aqueous layer was basified with 2M NaOH until pH ≥ 11, back-extracted with EtOAc for three times and the organic layers were combined and concentrated to afford propargylamine **1.3c** as a yellow oil (171.0 mg and 74.5 mg for (*R*)-**1.3c**, (*S*)-**1.3c**, respectively). The ^{1}H NMR and ^{13}C NMR of (*R*)-**1.3c** and (*S*)-**1.3c** are identical to the racemic standard of *rac*-**1.3c**. (*S*)-**1.3c** has a measured optical rotation comparable to the literature value of its HCl salt: $[\alpha]_D^{21}$ = +10.7 ($CHCl_3$, *c* = 0.83, 95% *ee*), Lit.: $[\alpha]_D^{20}$ = +33.0 ($CHCl_3$, *c* = 0.20, HCl salt form).[10]

V. Analytic Scale Enzymatic Reactions and Calibration Curves for Products

All enzymatic reactions for propargylic C–H amination on analytical scale were conducted following the general procedure described in **Section I (D)**. Reactions for every substrate were set up in quadruplicate. Product formation was quantified by LC-MS based on the calibration curve of the corresponding racemic standard compound (**Section IV**). All TTNs for different products were calculated as the concentration of products divided by the concentration of hemoproteins measured by the CO binding assay (**Section I (C)**).

LC-MS calibration curve:

Calibration curves of synthesized reference compounds were created for the determination of yield and TTN. For each substrate, five different concentrations of product (0.30, 0.75, 1.50, 2.25, and 3.00 mM) in 800-µL acetonitrile solutions were mixed each with 400 µL of 1.50 mM internal standard (*p*-methyl anisole) solution. The mixtures were vortexed and then analyzed by LC-MS based on UV absorbance at 270 nm. All data points represent the average of duplicate runs. The calibration curves depict the ratio of product area to internal standard area (y-axis) against product concentration in mM (x-axis).

Notes: Pdt = product area, IS = internal standard area, [Pdt] = product concentration in reaction, [PC] = protein concentration in reaction, Avg. TTN = average total turnover number, SD TTN = standard deviation of TTN, Avg. Yield = average yield, SD Yield = standard deviation of yield.

4-phenylbut-3-yn-2-amine (1.3a)

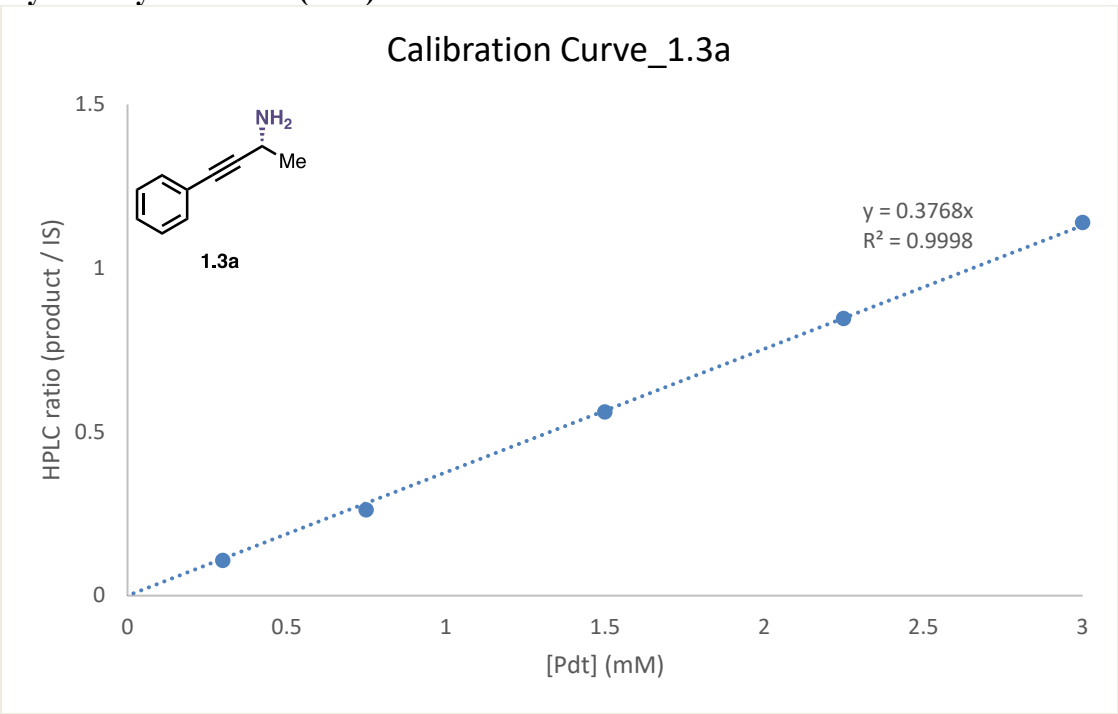

Data analysis for **PA-G0** catalyzed propargylic amination of alkyne **1.1a** (2 mM, OD_{600} = 20):

Entry	Pdt	IS	Pdt/IS	[Pdt]/mM	[PC]/μM	Avg. TTN	SD TTN	Avg. Yield [%]	SD Yield [%]
1	24.9	52.8	0.472	1.25	1.38	929	18	64	1
2	26.6	54.5	0.488	1.30	1.38				
3	26.1	54.9	0.475	1.26	1.38				
4	26.8	54.6	0.491	1.30	1.38				

Data analysis for **PA-G1** catalyzed propargylic amination of alkyne **1.1a** (2 mM, OD_{600} = 20):

Entry	Pdt	IS	Pdt/IS	[Pdt]/mM	[PC]/μM	Avg. TTN	SD TTN	Avg. Yield [%]	SD Yield [%]
1	42.1	54.5	0.772	2.05	1.54	1340	20	103	2
2	42.1	54.7	0.770	2.04	1.54				
3	41.6	53.9	0.772	2.05	1.54				
4	43.0	54.1	0.795	2.11	1.54				

Data analysis for **PA-G2** catalyzed propargylic amination of alkyne **1.1a** (2 mM, OD_{600} = 20):

Entry	Pdt	IS	Pdt/IS	[Pdt]/mM	[PC]/μM	Avg. TTN	SD TTN	Avg. Yield [%]	SD Yield [%]
1	33.6	53.7	0.626	1.66	1.37	1230	40	84	3
2	33.7	55.2	0.611	1.62	1.37				
3	34.4	54.5	0.631	1.68	1.37				
4	36.4	54.8	0.664	1.76	1.37				

Data analysis for **PA-G3** catalyzed propargylic amination of alkyne **1.1a** (2 mM, OD_{600} = 20):

Entry	Pdt	IS	Pdt/IS	[Pdt]/mM	[PC]/μM	Avg. TTN	SD TTN	Avg. Yield [%]	SD Yield [%]
1	23.7	55.2	0.429	1.14	0.456	2440	50	56	1
2	22.6	54.9	0.412	1.09	0.456				
3	23.6	55.3	0.427	1.13	0.456				
4	22.8	55.3	0.412	1.09	0.456				

Data analysis for **PA-G4** catalyzed propargylic amination of alkyne **1.1a** (2 mM, OD_{600} = 20):

Entry	Pdt	IS	Pdt/IS	[Pdt]/mM	[PC]/μM	Avg. TTN	SD TTN	Avg. Yield [%]	SD Yield [%]
1	25.7	50.6	0.508	1.35	0.202	6690	340	68	3
2	26.8	49.3	0.544	1.44	0.202				

3	24.5	50.8	0.482	1.28	0.202				
4	25.4	50.6	0.502	1.33	0.202				

Data analysis for **PA-G5** catalyzed propargylic amination of alkyne **1.1a** (2 mM, OD_{600} = 20):

Entry	Pdt	IS	Pdt/IS	[Pdt]/mM	[PC]/μM	Avg. TTN	SD TTN	Avg. Yield [%]	SD Yield [%]
1	17.8	48.5	0.367	0.974	0.630	1430	80	45	3
2	18.5	55.5	0.333	0.885	0.630				
3	18.4	55.3	0.333	0.883	0.630				
4	17.9	55.3	0.324	0.859	0.630				

Data analysis for **PA-G6** catalyzed propargylic amination of alkyne **1.1a** (2 mM, OD_{600} = 20):

Entry	Pdt	IS	Pdt/IS	[Pdt]/mM	[PC]/μM	Avg. TTN	SD TTN	Avg. Yield [%]	SD Yield [%]
1	19.7	51.5	0.383	1.02	0.740	1380	10	51	0.3
2	19.3	50.6	0.381	1.01	0.740				
3	19.8	51.6	0.384	1.02	0.740				
4	19.7	50.9	0.387	1.03	0.740				

Data analysis for **PA-G7** catalyzed propargylic amination of alkyne **1.1a** (2 mM, OD_{600} = 20):

Entry	Pdt	IS	Pdt/IS	[Pdt]/mM	[PC]/μM	Avg. TTN	SD TTN	Avg. Yield [%]	SD Yield [%]
1	19.4	51.7	0.375	0.996	0.630	1560	40	49	1
2	18.9	51.8	0.365	0.968	0.630				
3	18.7	52.0	0.360	0.954	0.630				
4	19.5	51.5	0.379	1.00	0.630				

Data analysis for **PA-G8** catalyzed propargylic amination of alkyne **1.1a** (2 mM, OD_{600} = 20):

Entry	Pdt	IS	Pdt/IS	[Pdt]/mM	[PC]/μM	Avg. TTN	SD TTN	Avg. Yield [%]	SD Yield [%]
1	28.9	51.4	0.562	1.49	0.870	1820	130	79	6
2	29.5	51.7	0.571	1.51	0.870				
3	30.5	51.3	0.595	1.58	0.870				
4	33.5	50.8	0.659	1.75	0.870				

1-phenylpent-1-yn-3-amine (1.3b)

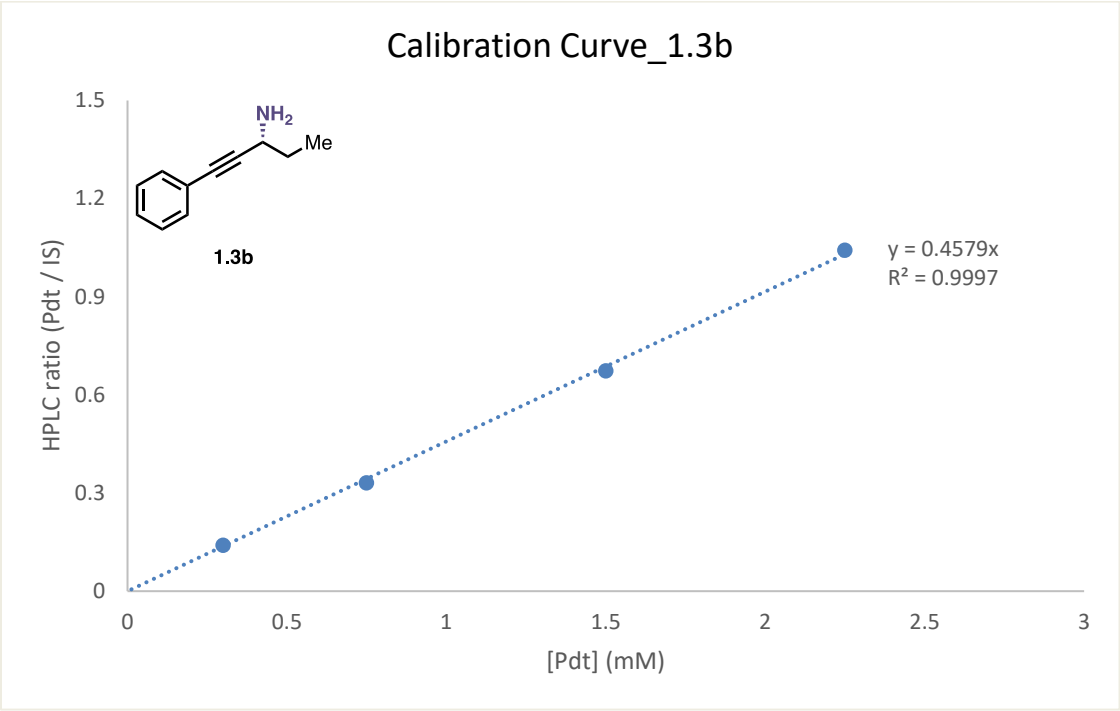

Data analysis for **PA-G8** catalyzed propargylic amination of alkyne **1.1b** (2 mM, OD_{600} = 20):

Entry	Pdt	IS	Pdt/IS	[Pdt]/mM	[PC]/μM	Avg. TTN	SD TTN	Avg. Yield [%]	SD Yield [%]
1	18.6	51.1	0.364	0.795	0.870	919	20	40	1
2	17.8	49.8	0.357	0.781	0.870				
3	19.5	51.8	0.376	0.822	0.870				
4	18.7	51.1	0.366	0.799	0.870				

1-phenylhex-1-yn-3-amine (1.3c)

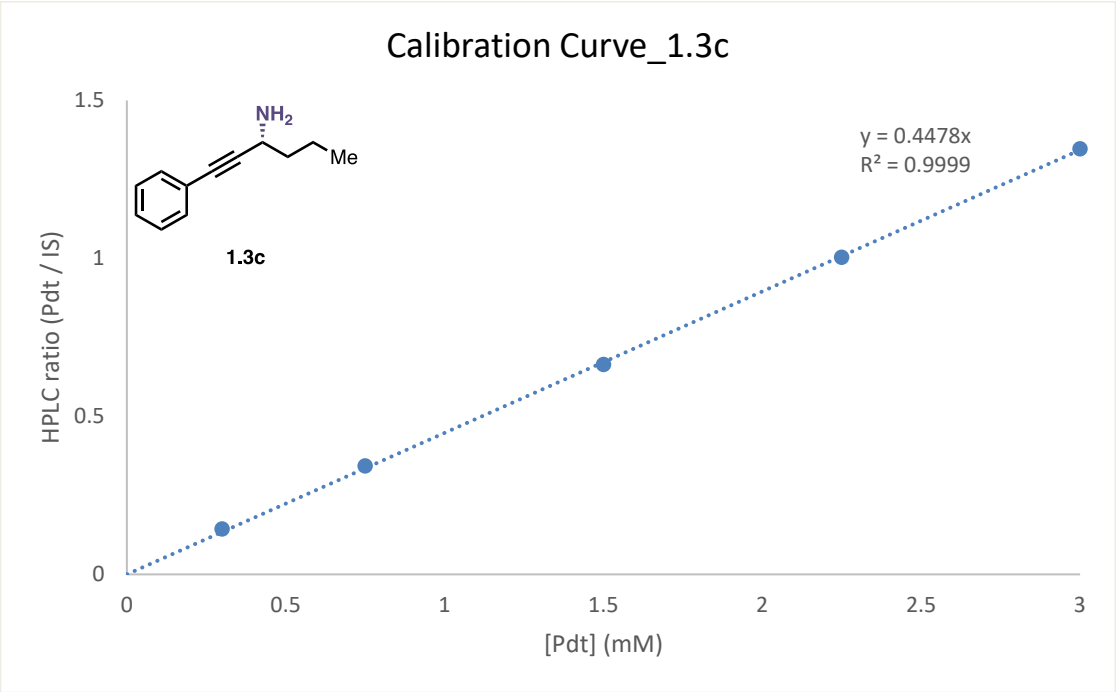

Data analysis for **PA-G8** catalyzed propargylic amination of alkyne **1.1c** (2 mM, OD_{600} = 20):

Entry	Pdt	IS	Pdt/IS	[Pdt]/mM	[PC]/μM	Avg. TTN	SD TTN	Avg. Yield [%]	SD Yield [%]
1	3.09	52.4	0.059	0.132	0.565	219	15	6	0.4
2	2.75	52.1	0.053	0.118	0.565				
3	2.70	52.5	0.051	0.115	0.565				
4	3.02	51.8	0.058	0.130	0.565				

4-(2-fluorophenyl)but-3-yn-2-amine (1.3d)

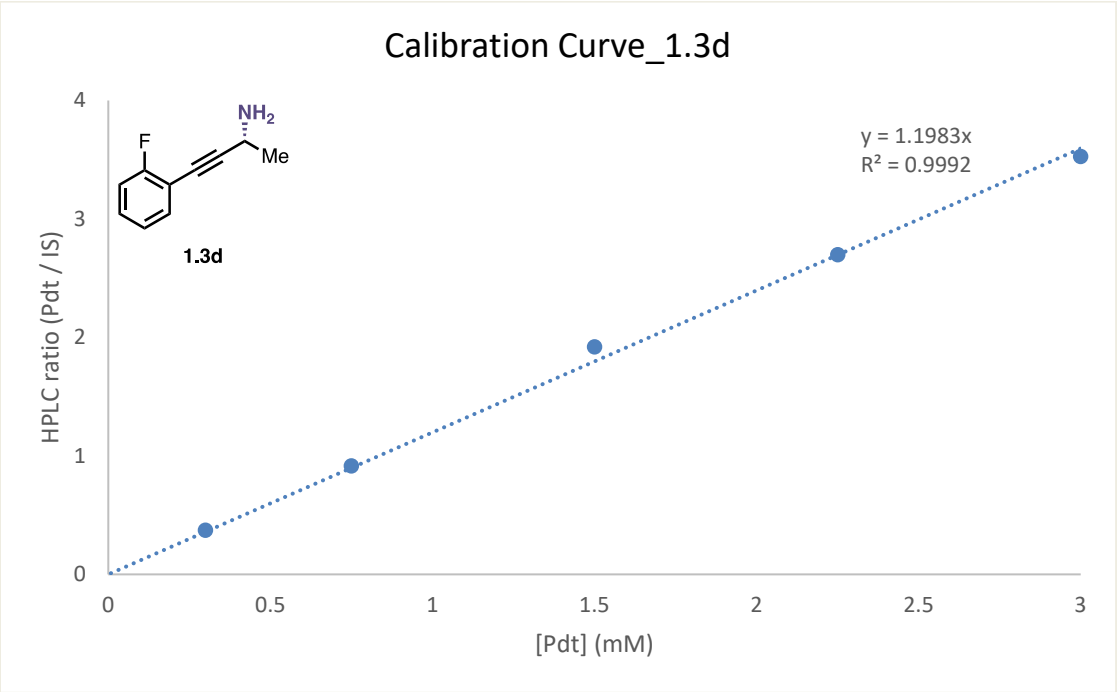

Data analysis for **PA-G8** catalyzed propargylic amination of alkyne **1.1d** (2 mM, OD_{600} = 20):

Entry	Pdt	IS	Pdt/IS	[Pdt]/mM	[PC]/μM	Avg. TTN	SD TTN	Avg. Yield [%]	SD Yield [%]
1	94.7	51.2	1.850	1.54	0.565	2610	80	74	2
2	90.5	52.3	1.730	1.44	0.565				
3	90.9	52.2	1.741	1.45	0.565				
4	92.4	52.8	1.750	1.46	0.565				

4-(3-methoxyphenyl)but-3-yn-2-amine (1.3e)

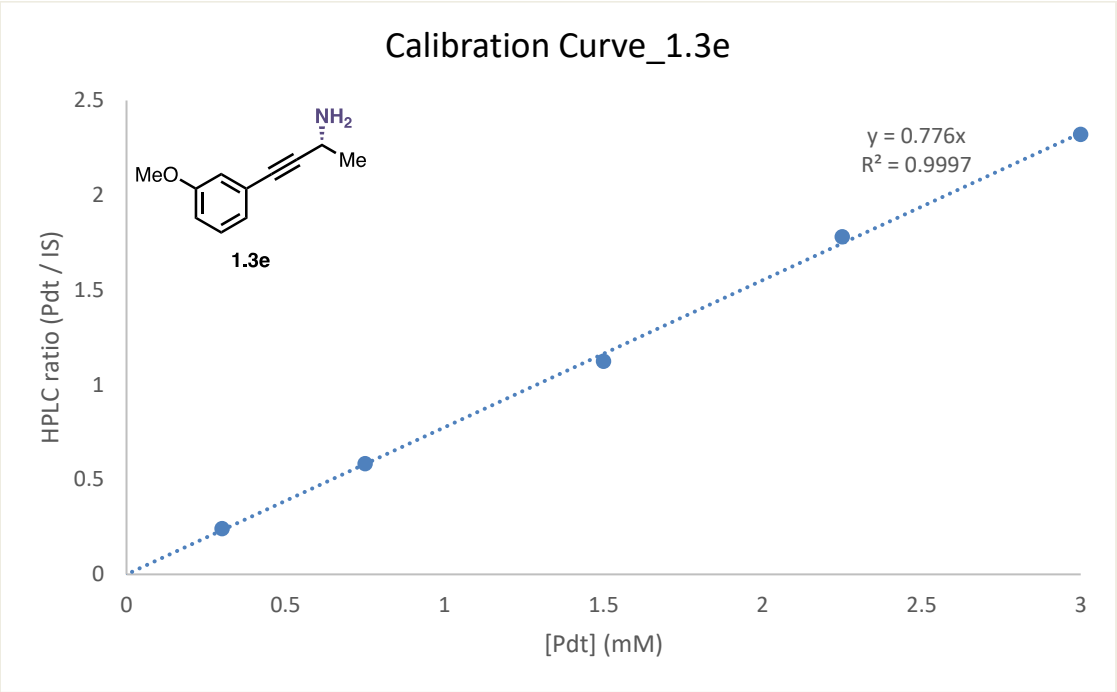

Data analysis for **PA-G8** catalyzed propargylic amination of alkyne **1.1e** (2 mM, OD_{600} = 20):

Entry	Pdt	IS	Pdt/IS	[Pdt]/mM	[PC]/μM	Avg. TTN	SD TTN	Avg. Yield [%]	SD Yield [%]
1	28.3	52.3	0.541	0.697	0.870	901	79	39	3
2	31.7	50.9	0.623	0.803	0.870				
3	32.1	48.0	0.669	0.862	0.870				
4	31.0	51.7	0.600	0.773	0.870				

4-(*m*-tolyl)but-3-yn-2-amine (1.3f)

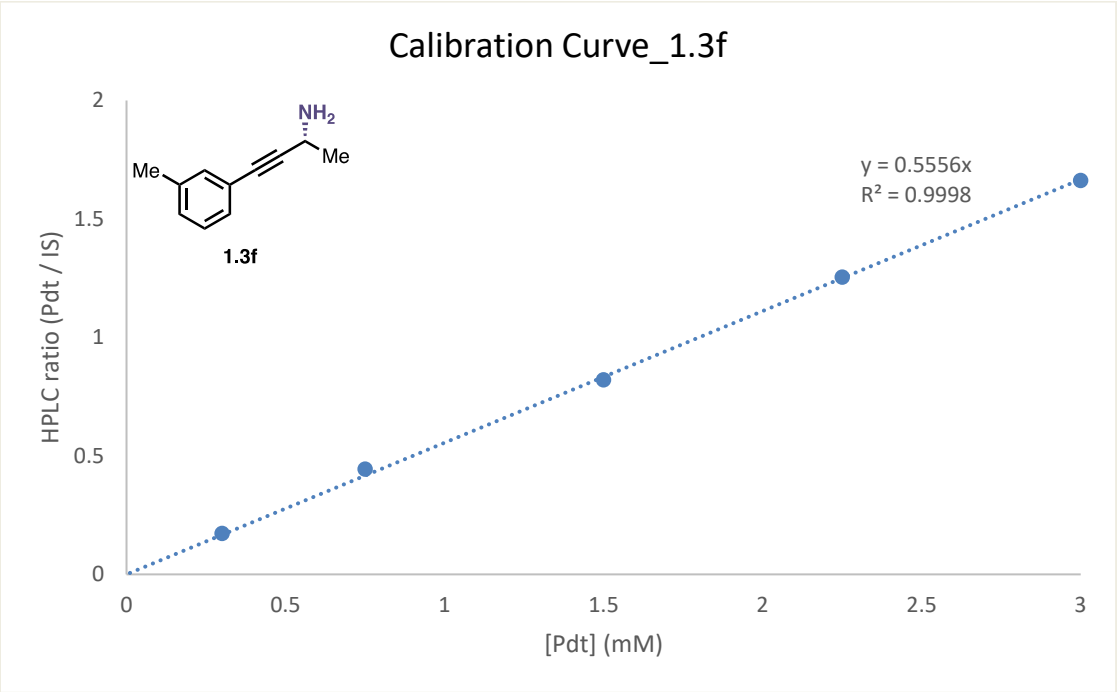

Data analysis for **PA-G8** catalyzed propargylic amination of alkyne **1.1e** (2 mM, OD_{600} = 20):

Entry	Pdt	IS	Pdt/IS	[Pdt]/mM	[PC]/μM	Avg. TTN	SD TTN	Avg. Yield [%]	SD Yield [%]
1	17.9	50.7	0.353	0.635	0.620	1030	70	32	2
2	18.6	50.9	0.365	0.658	0.620				
3	16.8	51.9	0.324	0.583	0.620				
4	19.1	50.8	0.376	0.677	0.620				

4-(*p*-tolyl)but-3-yn-2-amine (1.3g)

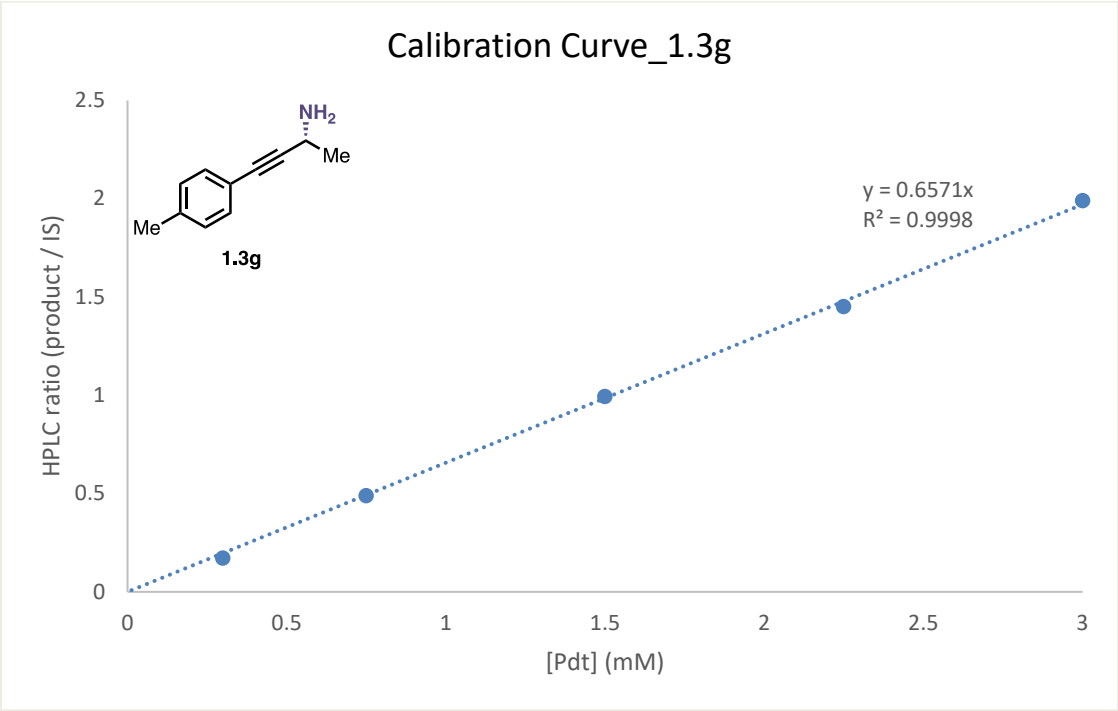

Data analysis for **PA-G8** catalyzed propargylic amination of alkyne **1.1g** (2 mM, OD_{600} = 20):

Entry	Pdt	IS	Pdt/IS	[Pdt]/mM	[PC]/μM	Avg. TTN	SD TTN	Avg. Yield [%]	SD Yield [%]
1	17.7	53.2	0.333	0.506	0.565	884	22	25	0.6
2	16.9	53.4	0.316	0.482	0.565				
3	17.2	52.2	0.330	0.501	0.565				
4	17.7	53.0	0.334	0.508	0.565				

4-(4-methoxyphenyl)but-3-yn-2-amine (1.3h)

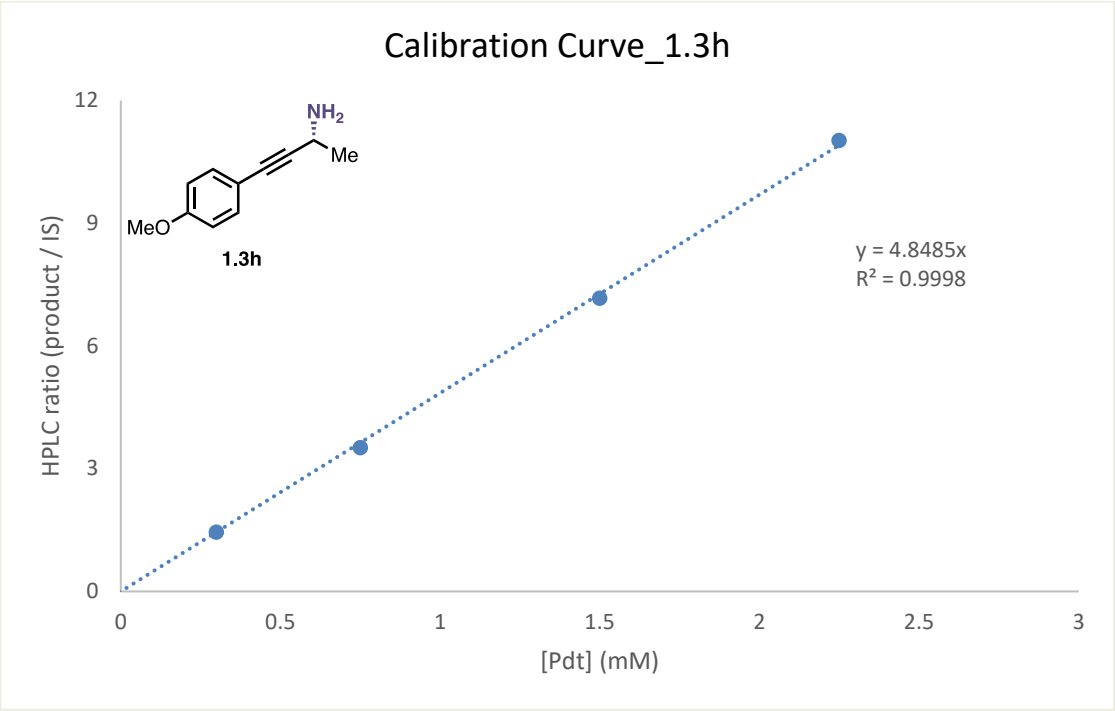

Data analysis for **PA-G8** catalyzed propargylic amination of alkyne **1.1h** (2 mM, OD_{600} = 20):

Entry	Pdt	IS	Pdt/IS	[Pdt]/mM	[PC]/μM	Avg. TTN	SD TTN	Avg. Yield [%]	SD Yield [%]
1	160.0	52.2	3.065	0.632	0.565	1080	70	31	2
2	143.3	52.8	2.714	0.560	0.565				
3	155.0	52.9	2.930	0.604	0.565				
4	162.8	52.1	3.125	0.644	0.565				

4-(thiophen-3-yl)but-3-yn-2-amine (1.3i)

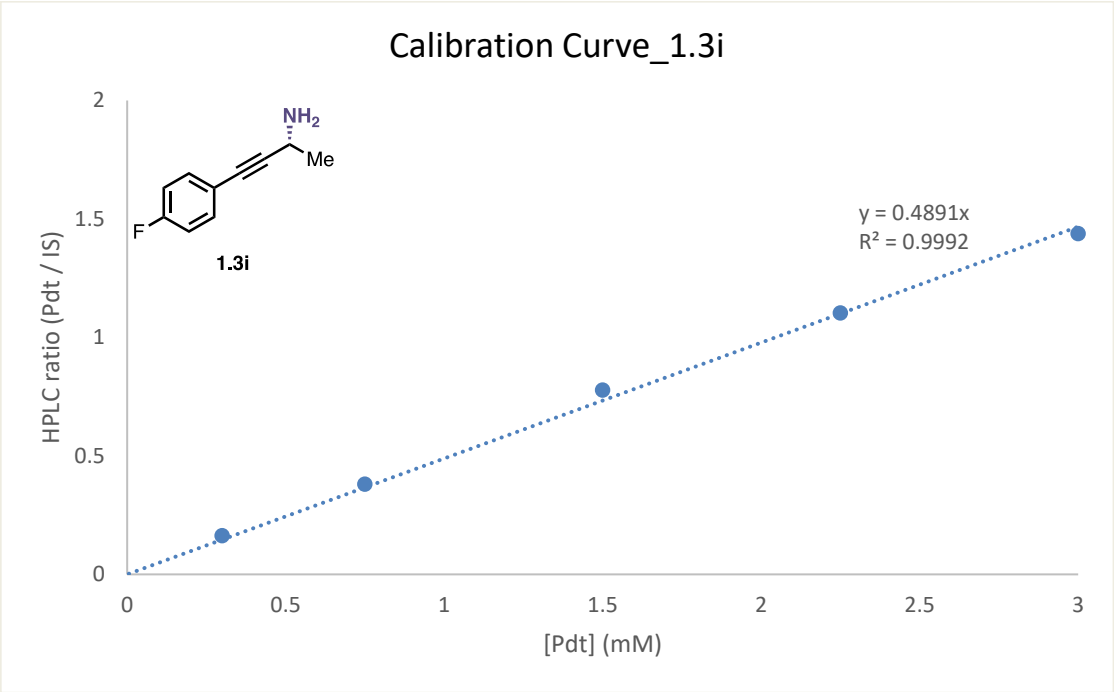

Data analysis for **PA-G8** catalyzed propargylic amination of alkyne **1.1i** (2 mM, OD_{600} = 20):

Entry	Pdt	IS	Pdt/IS	[Pdt]/mM	[PC]/μM	Avg. TTN	SD TTN	Avg. Yield [%]	SD Yield [%]
1	18.5	52.0	0.356	0.727	0.565	1290	10	37	0.4
2	19.3	54.0	0.357	0.731	0.565				
3	18.7	53.0	0.353	0.721	0.565				
4	18.9	52.3	0.361	0.739	0.565				

4-(pyridin-2-yl)but-3-yn-2-amine (1.3j)

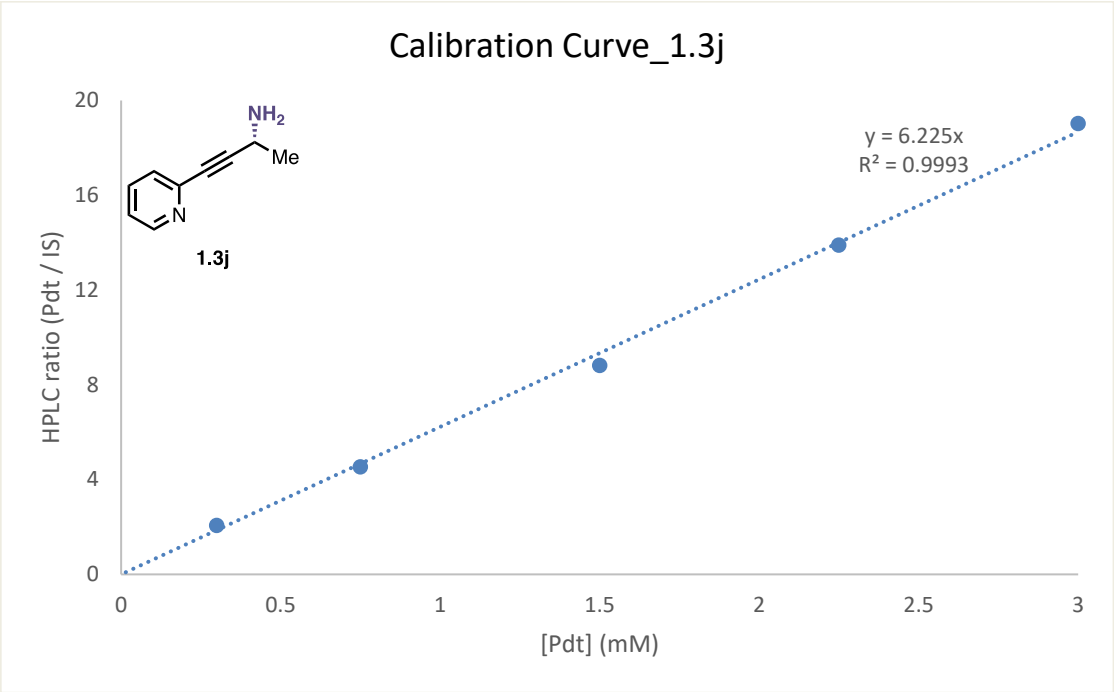

Data analysis for **PA-G8** catalyzed propargylic amination of alkyne **1.1j** (2 mM, OD_{600} = 20):

Entry	Pdt	IS	Pdt/IS	[Pdt]/mM	[PC]/μM	Avg. TTN	SD TTN	Avg. Yield [%]	SD Yield [%]
1	452.1	50.9	8.882	1.43	0.620	2320	30	72	1
2	469.9	51.5	9.124	1.47	0.620				
3	454.7	51.5	8.829	1.42	0.620				
4	462.5	51.5	8.981	1.44	0.620				

4-(thiophen-2-yl)but-3-yn-2-amine (1.3k)

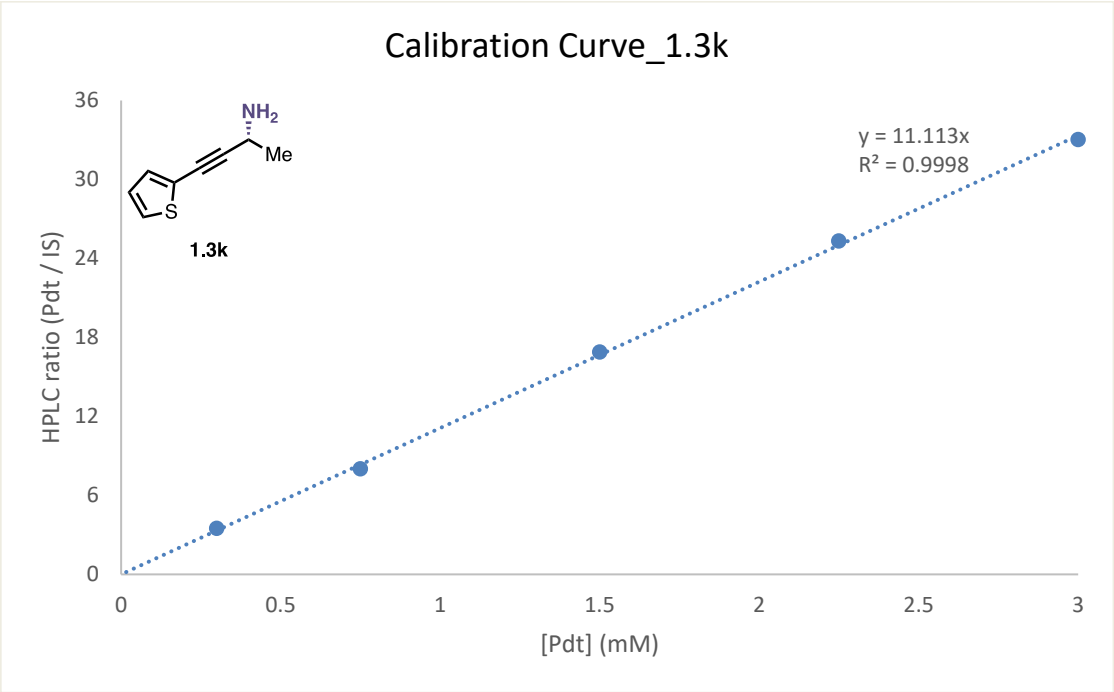

Data analysis for **PA-G8** catalyzed propargylic amination of alkyne **1.1k** (2 mM, OD_{600} = 20):

Entry	Pdt	IS	Pdt/IS	[Pdt]/mM	[PC]/μM	Avg. TTN	SD TTN	Avg. Yield [%]	SD Yield [%]
1	772.8	48.8	15.836	1.43	0.870	1580	50	69	2
2	373.4	25.3	14.759	1.33	0.870				
3	400.3	25.8	15.516	1.40	0.870				
4	381.4	25.7	14.840	1.34	0.870				

4-(thiophen-3-yl)but-3-yn-2-amine (3l)

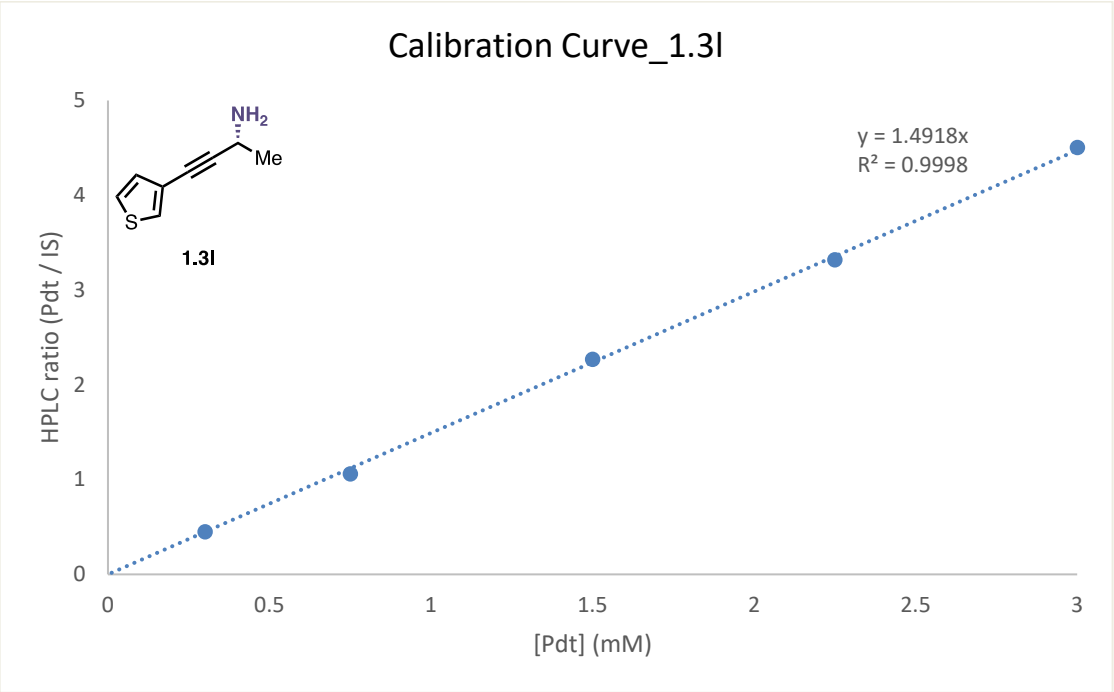

Data analysis for **PA-G8** catalyzed propargylic amination of alkyne **1.1l** (2 mM, OD_{600} = 20):

Entry	Pdt	IS	Pdt/IS	[Pdt]/mM	[PC]/μM	Avg. TTN	SD TTN	Avg. Yield [%]	SD Yield [%]
1	103.8	53.1	1.955	1.31	0.565	2440	80	69	2
2	108.9	52.9	2.059	1.38	0.565				
3	109.9	52.0	2.113	1.42	0.565				
4	110.6	53.1	2.083	1.40	0.565				

3-phenylprop-2-yn-1-amine (1.3m)

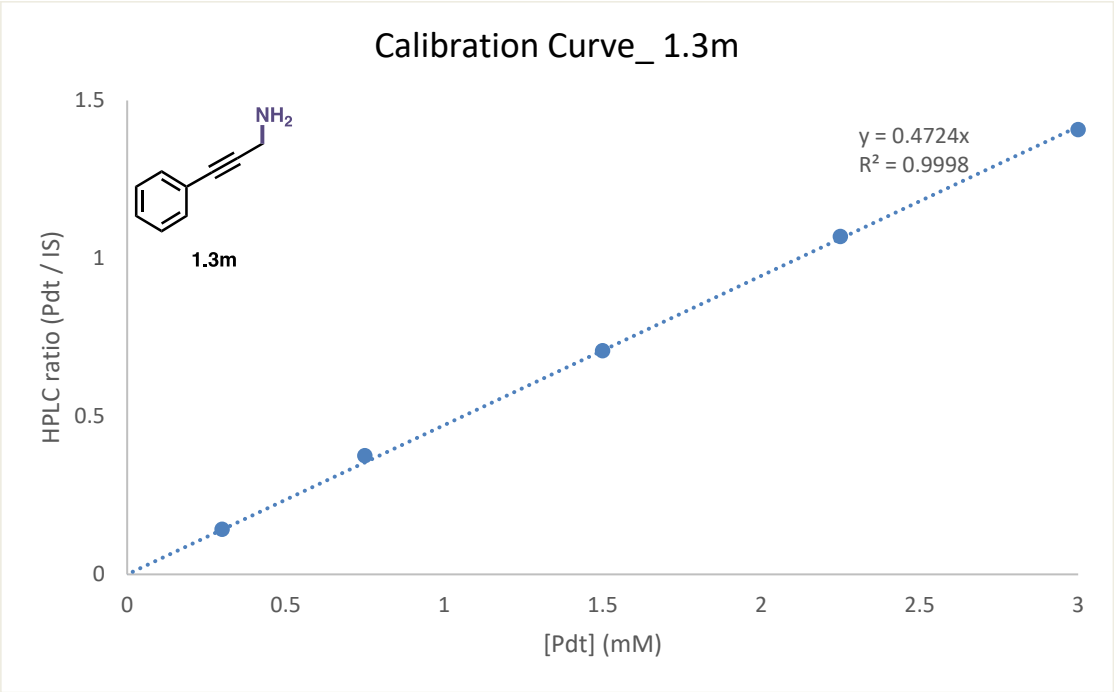

Data analysis for **PA-G8** catalyzed propargylic amination of alkyne **1.1m** (2 mM, OD_{600} = 20):

Entry	Pdt	IS	Pdt/IS	[Pdt]/mM	[PC]/μM	Avg. TTN	SD TTN	Avg. Yield [%]	SD Yield [%]
1	6.2	53.0	0.117	0.248	0.565	442	22	13	0.6
2	6.5	53.2	0.122	0.259	0.565				
3	6.4	52.1	0.123	0.260	0.565				
4	6.0	54.5	0.110	0.233	0.565				

2-methyl-4-phenylbut-3-yn-2-amine (1.3n)

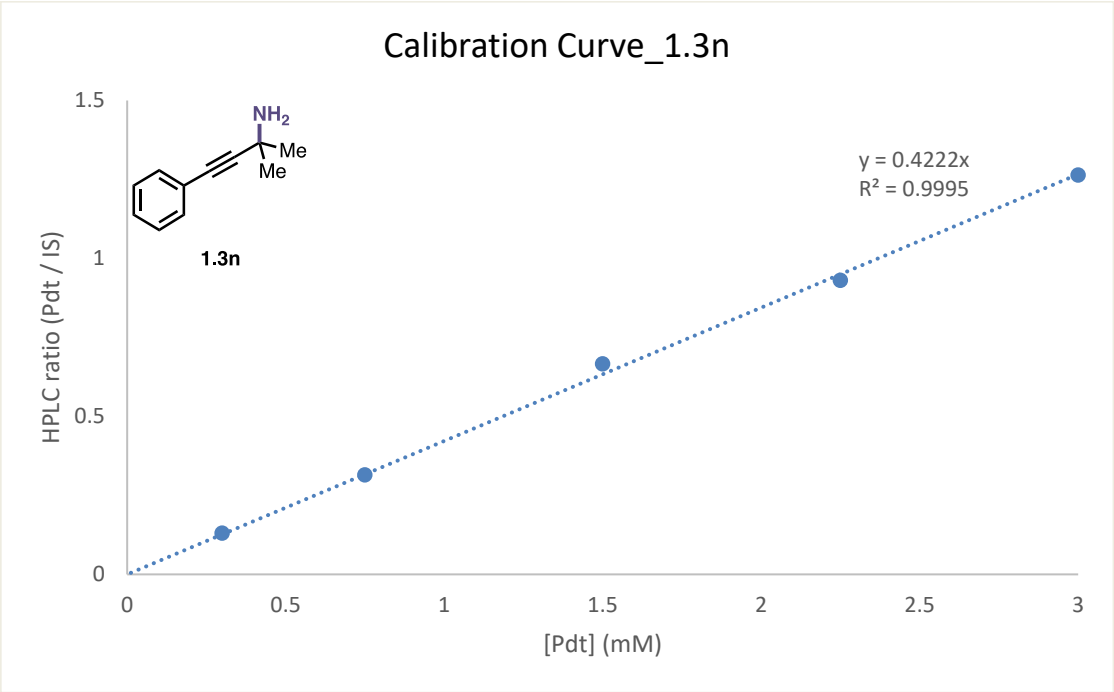

Data analysis for **PA-G8** catalyzed propargylic amination of alkyne **1.1n** (2 mM, OD_{600} = 20):

Entry	Pdt	IS	Pdt/IS	[Pdt]/mM	[PC]/μM	Avg. TTN	SD TTN	Avg. Yield [%]	SD Yield [%]
1	8.5	52.2	0.163	0.386	0.565	649	41	18	1
2	7.6	53.8	0.141	0.335	0.565				
3	8.3	51.5	0.161	0.382	0.565				
4	8.0	52.0	0.154	0.364	0.565				

VI. Preparative-scale Enzymatic Synthesis

General procedure for 1 mmol-scale enzymatic reactions:

To a 1-L flask, a suspension of *E. coli* expressing variant **PA-G8** (OD_{600} = 24), alkyne (1.0 mmol), *O*-pivaloylhydroxylamine triflic acid (666.7 mg, 2.5 mmol, 2.5 equiv.), D-glucose (20 mM), and M9-N buffer/EtOH (50:1 v/v, 500 mL in total) were added under anaerobic conditions. The flask was capped and sealed with parafilm inside the anaerobic chamber. The mixture was shaken at 250 rpm in a shaker outside of anaerobic chamber for 20 h.

After the reaction was completed, the reaction mixture was transferred to two 500-mL centrifuge bottles. The aqueous phase was extracted with organic solvent (hexane/EtOAc = 1:2, 120 mL × 4). The organic layers were combined in an Erlenmeyer flask, dried over Na_2SO_4, and concentrated under reduced pressure. Purification by silica column chromatography with MeOH/DCM as eluents afforded the desired propargyl amine products. TTNs were calculated based on measured protein concentration and isolated product yield.

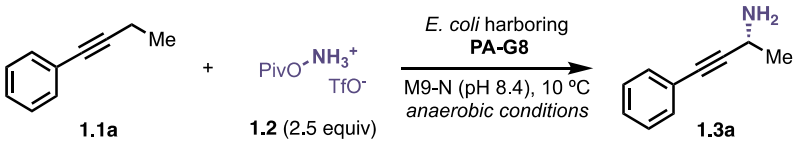

(*R*)-4-phenylbut-3-yn-2-amine

1.3a: 92.9 mg, 64% yield, 1150 TTN, 88% *ee*. The ^{1}H NMR and ^{13}C NMR of **1.3a** are identical to the synthesized racemic standard of *rac*-**1.3a**. **^{1}H NMR** (400 MHz, DMSO-d_6) δ 7.42–7.31 (m, 5H), 3.83 (q, J = 6.7 Hz, 1H), 1.30 (d, J = 6.8 Hz, 3H); **^{13}C NMR** (100 MHz, DMSO-d_6) δ 131.2, 128.6, 128.1, 122.9, 95.4, 80.6, 38.6, 24.5.

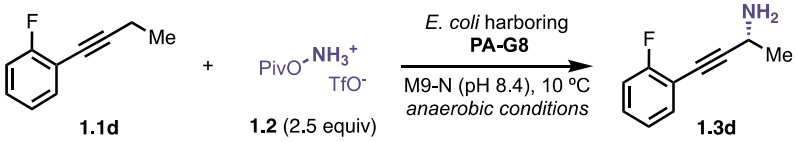

(*R*)-4-(2-fluorophenyl)but-3-yn-2-amine

1.3d: 104.4 mg, 64% yield, 1570 TTN, 91% *ee*. The ^{1}H NMR, ^{13}C NMR and ^{19}F NMR of **1.3d** are identical to the synthesized racemic standard of *rac*-**1.3d**. **^{1}H NMR** (400 MHz, $CDCl_3$) δ 7.43–7.34 (m, 1H), 7.31–7.21 (m, 1H), 7.11–7.00 (m, 2H), 3.96 (q, J = 6.8 Hz, 1H), 1.46 (d, J = 6.8 Hz, 3H); **^{13}C NMR** (100 MHz, $CDCl_3$) δ 162.8 (d, J = 250.7 Hz), 133.6 (d, J = 1.5 Hz), 129.8 (d, J = 7.9 Hz), 124.0 (d, J = 3.7 Hz), 115.5 (d, J = 21.0 Hz), 111.8 (d, J = 15.7 Hz), 99.2 (d, J = 3.3 Hz), 75.1, 39.7, 24.4; **^{19}F NMR** (376 MHz, $CDCl_3$) δ –110.7.

General procedure for benzoylation of propargyl amines 1.3a and 1.3d:

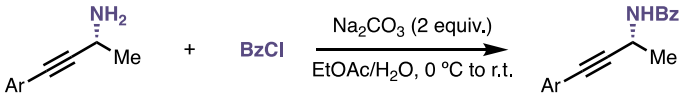

1.3a or **1.3d** **1.4a** or **1.4d**

To a 2-dram vial were added a solution of propargyl amine (0.22 mmol, 1 equiv) in EtOAc (1 mL), Na_2CO_3 (47 mg, 0.44 mmol, 2 equiv.) and water (0.25 mL). The mixture was first stirred at 0 °C, followed by slow addition of benzoyl chloride (64 μL, 0.55 mmol, 2.5 equiv.). The reaction mixture was then stirred vigorously at room temperature for 6 hours. After the reaction was completed, the reaction mixture was diluted with saturated $NaHCO_3$ solution (4 mL) and extracted with Et_2O (5 mL × 3). The organic layers were combined in an Erlenmeyer flask, dried over Na_2SO_4, and concentrated under reduced pressure. Purification by silica column chromatography with hexane/EtOAc as eluents afforded the desired amide product.

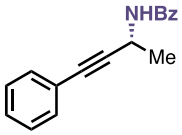

1.4a **(*R*)-N-(4-phenylbut-3-yn-2-yl)benzamide (4a):** 35.4 mg, 65% yield, 88% *ee*. **^{1}H NMR** (400 MHz, $CDCl_3$) δ 7.84–7.77 (m, 2H), 7.55–7.48 (m, 1H), 7.48–7.38 (m, 4H), 7.35–7.28 (m, 3H), 5.27 (dq, *J* = 8.0, 6.9 Hz, 1H), 1.61 (d, *J* = 6.8 Hz, 3H); **^{13}C NMR** (100 MHz, $CDCl_3$) δ 166.4, 134.3, 131.9, 131.8, 128.8, 128.6, 128.4, 127.2, 122.7, 89.5, 82.8, 38.4, 22.9; **HRMS** (FAB) Calcd for $C_{17}H_{16}NO$ [M+H] 250.1232, found 250.1217; $[\alpha]_D^{21}$ = +49.0 ($CHCl_3$, *c* = 0.83), Lit.: $[\alpha]_D^{25}$ = +53.6 ($CHCl_3$, *c* = 0.52, *ee* ≥99% (*R*)).[11]

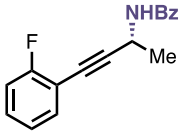

1.4d **(*R*)-N-(4-(2-fluorophenyl)but-3-yn-2-yl)benzamide (4d):** 46.5 mg, 79% yield, 91% *ee*. **^{1}H NMR** (400 MHz, $CDCl_3$) δ 7.84–7.77 (m, 2H), 7.55–7.48 (m, 1H), 7.48–7.38 (m, 3H), 7.30 (dddd, *J* = 8.3, 7.2, 5.3, 1.8 Hz, 1H), 7.13–7.02 (m, 2H), 6.40 (d, *J* = 8.0 Hz, 1H), 5.36–5.26 (m, 1H), 1.62 (d, *J* = 6.8 Hz, 3H); **^{13}C NMR** (100 MHz, $CDCl_3$) δ 166.4, 163.0 (d, *J* = 251.6 Hz), 134.2, 133.8 (d, *J* = 1.4 Hz), 131.8, 130.3 (d, *J* = 8.0 Hz), 128.8, 127.2, 124.1 (d, *J* = 3.7 Hz), 115.6 (d, *J* = 20.9 Hz), 111.2 (d, *J* = 15.6 Hz), 94.7 (d, *J* = 3.3 Hz), 76.2, 38.4, 22.8; **^{19}F NMR** (376 MHz, $CDCl_3$) δ –110.2; **HRMS** (FAB) Calcd for $C_{17}H_{15}NOF$ [M+H] 268.1138, found 268.1149; $[\alpha]_D^{21}$ = +52.2 ($CHCl_3$, *c* = 0.75).

VII. Chiral-phase HPLC Traces

The absolute stereochemistry for enzymatic products **1.3a** and **1.3c** were assigned to be *R* by comparing their optical rotations to the reported value.[10,11] The absolute configuration of enzymatic product **1.3b** was also assigned to be *R* by comparing the elution order of two enantiomers with literature report under same elution conditions using the same column (Chiralpak AD-H).[12] The other products **1.3d–1.3l** were assigned by analogy. Before analysis of *ee*, all amine products were protected by benzoyl group.

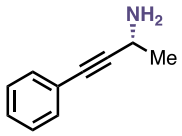

1.3a

(*R*)-4-phenylbut-3-yn-2-amine (1.3a)

Chiral-phase HPLC conditions: Chiralpak IA, 7% *i*-PrOH in hexane, 1.0 mL/min, 25 ºC, 254 nm

Racemic 1.3a:

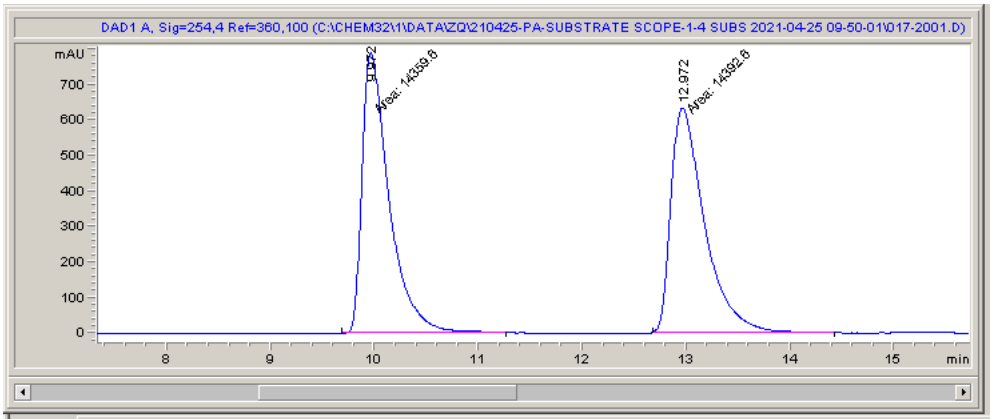

#	Time	Area	Height	Width	Area%	Symmetry
1	9.972	14359.6	788.5	0.3035	49.943	0.466
2	12.972	14392.6	633.9	0.3784	50.057	0.498

Enzymatic preparation of 1.3a with PA-G8: 88% *ee*

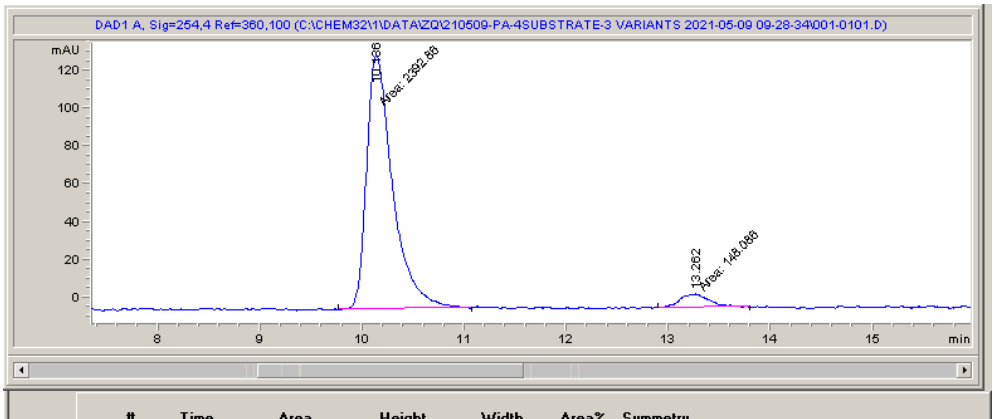

#	Time	Area	Height	Width	Area%	Symmetry
1	10.136	2392.9	134.1	0.2974	94.172	0.559
2	13.262	148.1	7.2	0.3442	5.828	0.996

Preparative-scale enzymatic preparation of 1.3a with PA-G8: 88% *ee*

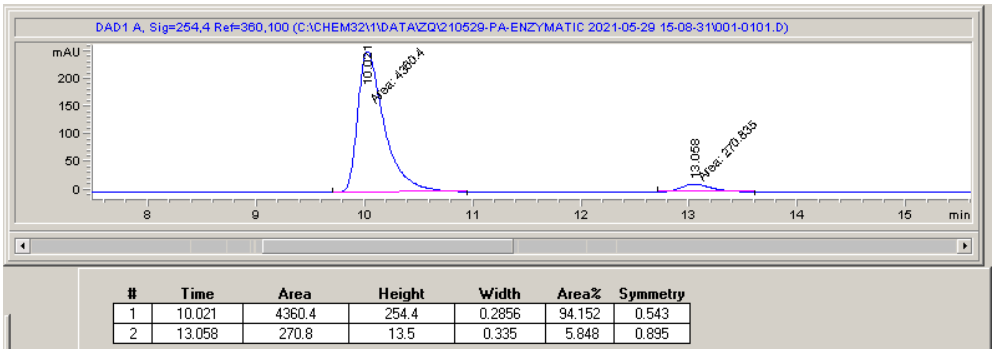

#	Time	Area	Height	Width	Area%	Symmetry
1	10.021	4360.4	254.4	0.2856	94.152	0.543
2	13.058	270.8	13.5	0.335	5.848	0.895

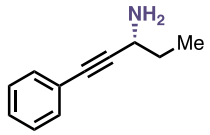

1.3b

(*R*)-1-phenylpent-1-yn-3-amine (1.3b)

Chiral-phase HPLC conditions: Chiralpak AD-H, 5% *i*-PrOH in hexane, 1.0 mL/min, 25 ºC, 254 nm

Racemic 1.3b:

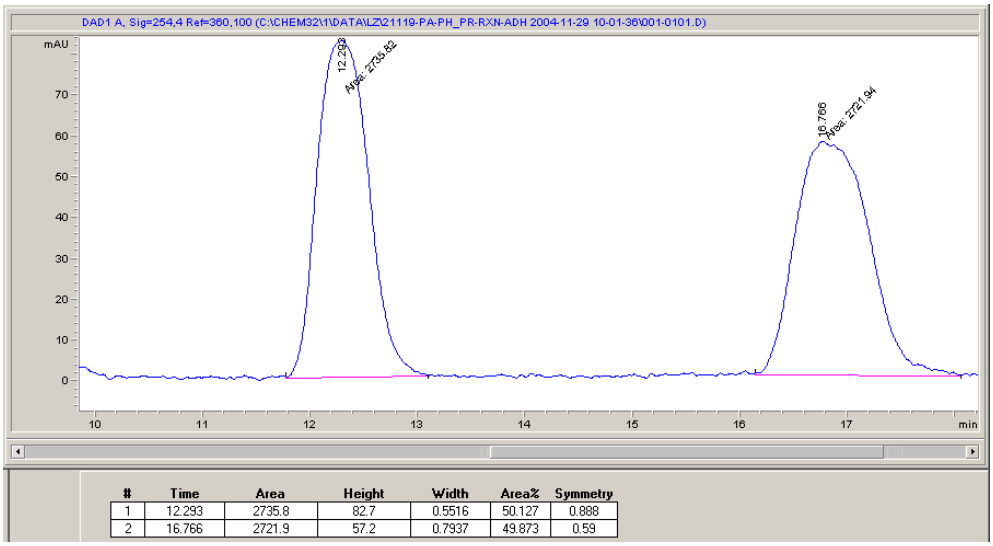

#	Time	Area	Height	Width	Area%	Symmetry
1	12.293	2735.8	82.7	0.5516	50.127	0.888
2	16.766	2721.9	57.2	0.7937	49.873	0.59

Enzymatic preparation of 1.3b with PA-G8: 91% *ee*

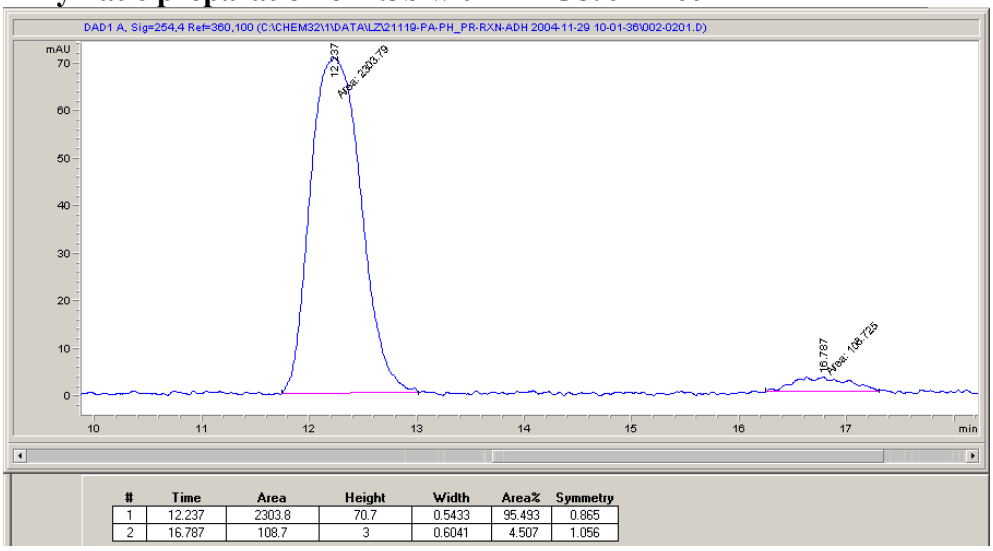

#	Time	Area	Height	Width	Area%	Symmetry
1	12.237	2303.8	70.7	0.5433	95.493	0.865
2	16.787	108.7	3	0.6041	4.507	1.056

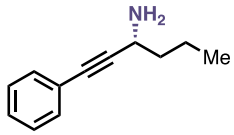

1.3c

(*R*)-1-phenylhex-1-yn-3-amine (1.3c)

Chiral-phase HPLC conditions: Chiralpak IA, 7% *i*-PrOH in hexane, 1.0 mL/min, 25 ºC, 254 nm

Racemic 1.3c:

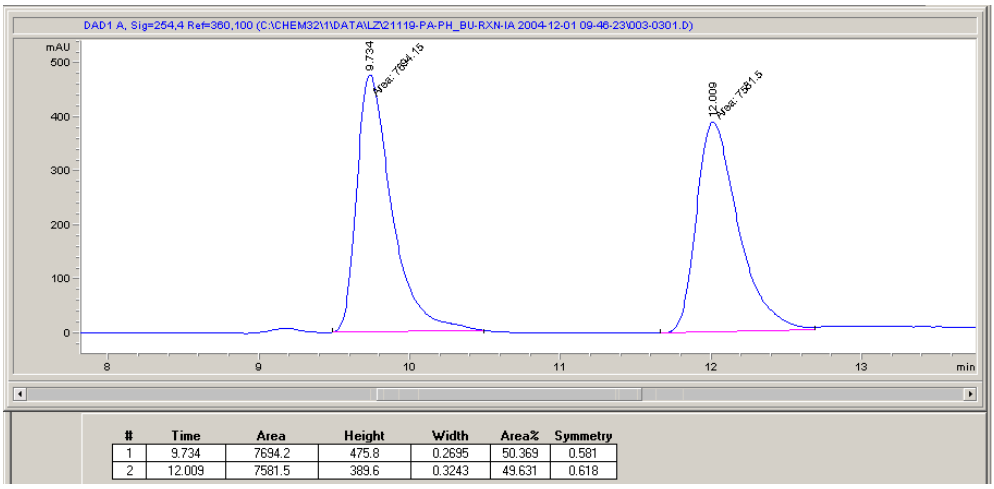

#	Time	Area	Height	Width	Area%	Symmetry
1	9.734	7694.2	475.8	0.2695	50.369	0.581
2	12.009	7581.5	389.6	0.3243	49.631	0.618

(*S*)-1.3c: −95% *ee*

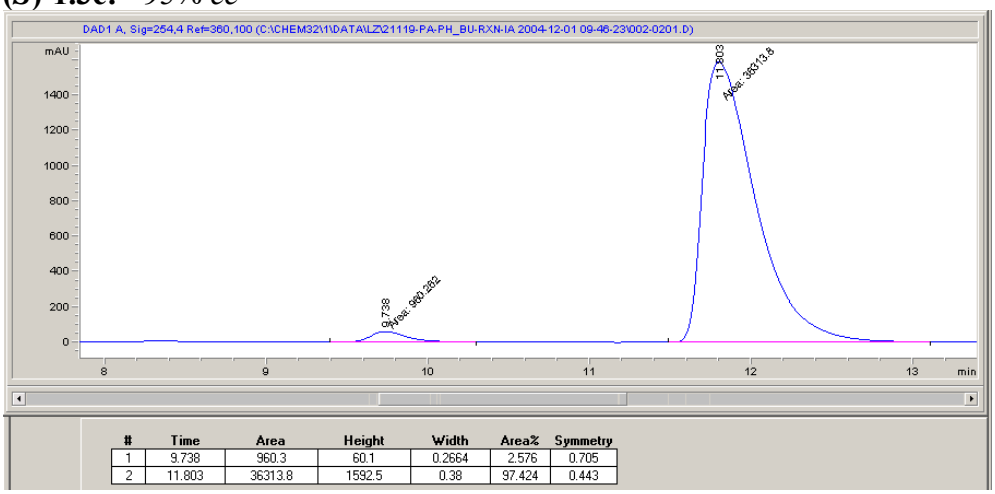

#	Time	Area	Height	Width	Area%	Symmetry
1	9.738	960.3	60.1	0.2664	2.576	0.705
2	11.803	36313.8	1592.5	0.38	97.424	0.443

Enzymatic preparation of 1.3c with PA-G8: 96% *ee*

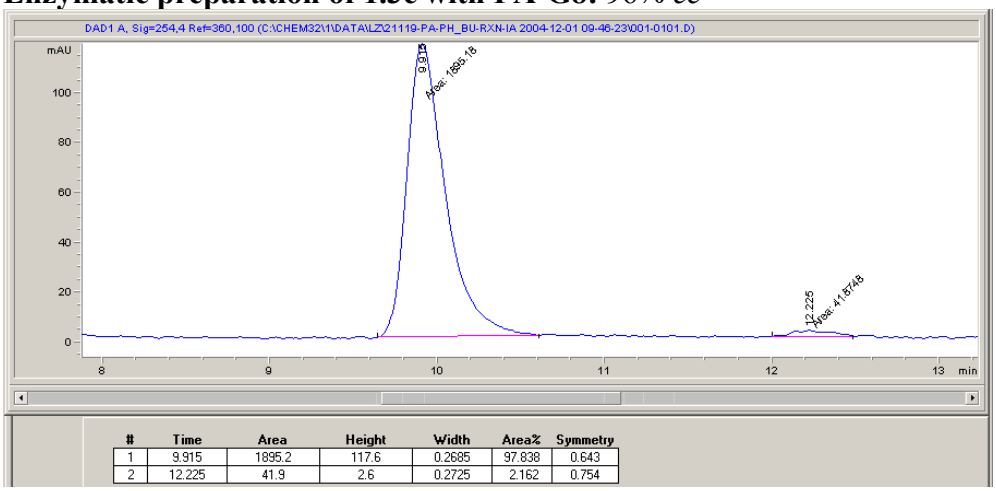

#	Time	Area	Height	Width	Area%	Symmetry
1	9.915	1895.2	117.6	0.2685	97.838	0.643
2	12.225	41.9	2.6	0.2725	2.162	0.754

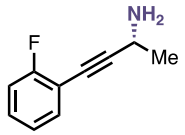

1.3d

(*R*)-4-(2-fluorophenyl)but-3-yn-2-amine (1.3d)

Chiral-phase HPLC conditions: Chiralpak IA, 7% *i*-PrOH in hexane, 1.0 mL/min, 25 ºC, 254 nm

Racemic 1.3d:

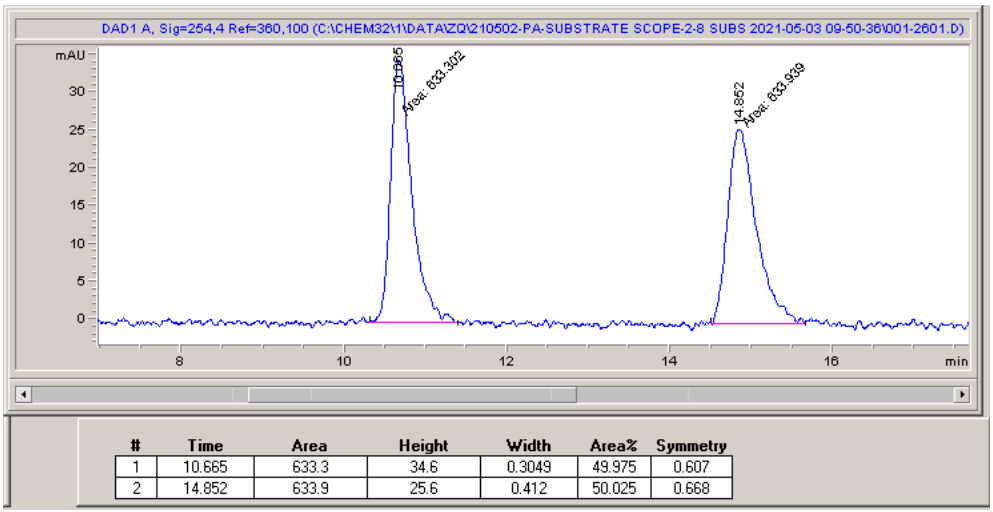

#	Time	Area	Height	Width	Area%	Symmetry
1	10.665	633.3	34.6	0.3049	49.975	0.607
2	14.852	633.9	25.6	0.412	50.025	0.668

Enzymatic preparation of 1.3d with PA-G8: 90% *ee*

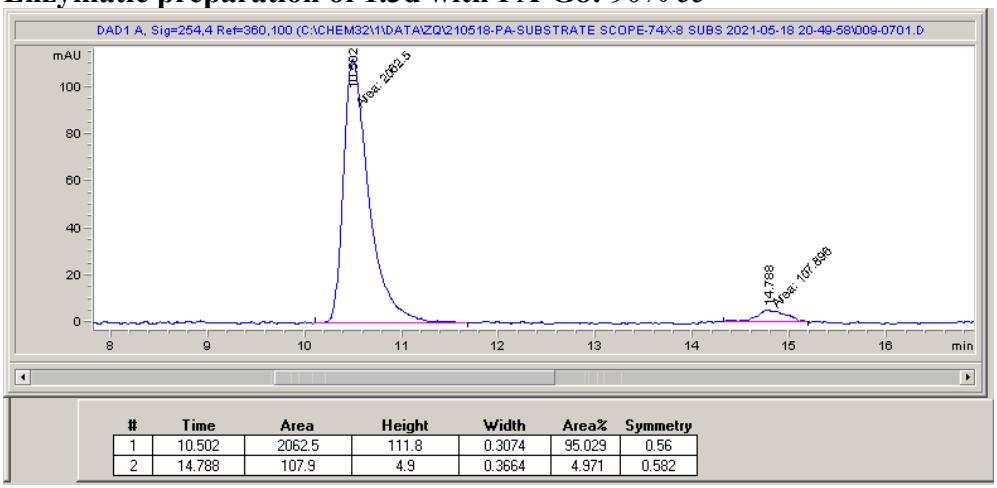

#	Time	Area	Height	Width	Area%	Symmetry
1	10.502	2062.5	111.8	0.3074	95.029	0.56
2	14.788	107.9	4.9	0.3664	4.971	0.582

Preparative-scale enzymatic preparation of 1.3d with PA-G8: 91% *ee*

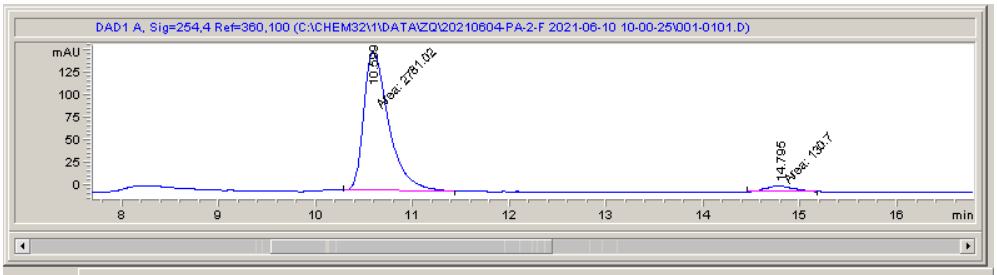

#	Time	Area	Height	Width	Area%	Symmetry
1	10.599	2781	154.4	0.3003	95.511	0.584
2	14.795	130.7	6.4	0.3413	4.489	1.005

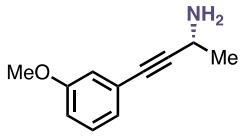

1.3e

(*R*)-4-(3-methoxyphenyl)but-3-yn-2-amine (1.3e)

Chiral-phase HPLC conditions: Chiralpak IA, 10% *i*-PrOH in hexane, 1.0 mL/min, 25 ºC, 254 nm

Racemic 1.3e:

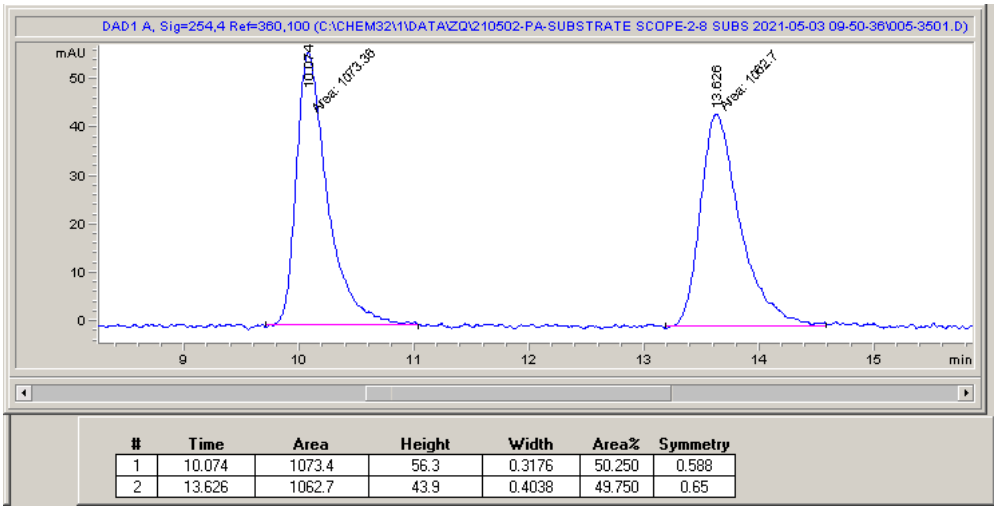

#	Time	Area	Height	Width	Area%	Symmetry
1	10.074	1073.4	56.3	0.3176	50.250	0.588
2	13.626	1062.7	43.9	0.4038	49.750	0.65

Enzymatic preparation of 1.3e with PA-G8: 95% *ee*

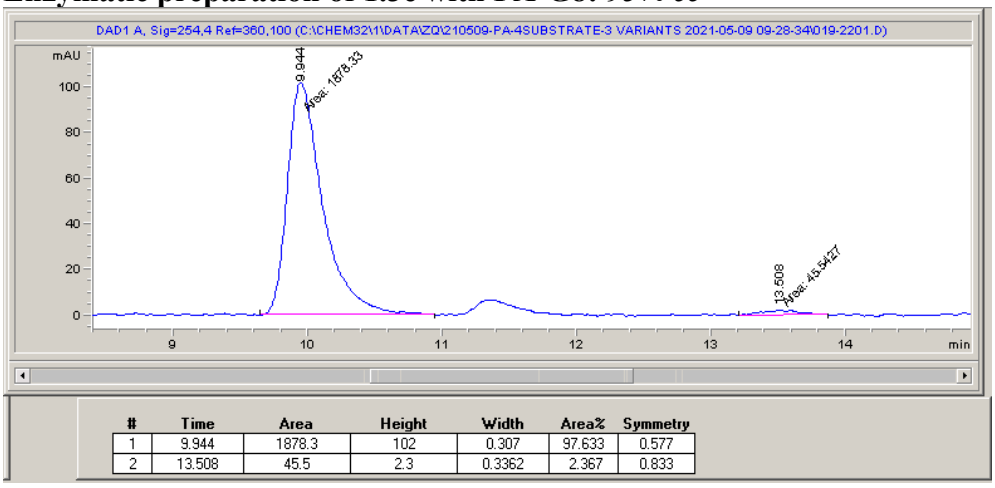

#	Time	Area	Height	Width	Area%	Symmetry
1	9.944	1878.3	102	0.307	97.633	0.577
2	13.508	45.5	2.3	0.3362	2.367	0.833

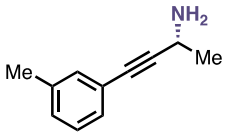

1.3f

(*R*)-4-(*m*-tolyl)but-3-yn-2-amine (1.3f)

Chiral-phase HPLC conditions: Chiralpak IA, 7% *i*-PrOH in hexane, 1.0 mL/min, 25 ºC, 254 nm

Racemic 1.3f:

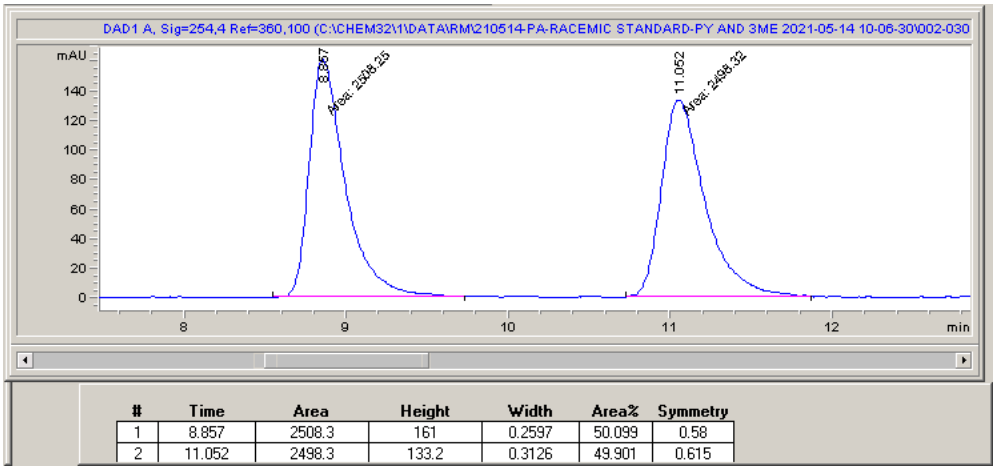

#	Time	Area	Height	Width	Area%	Symmetry
1	8.857	2508.3	161	0.2597	50.099	0.58
2	11.052	2498.3	133.2	0.3126	49.901	0.615

Enzymatic preparation of 1.3f with PA-G8: 89% *ee*

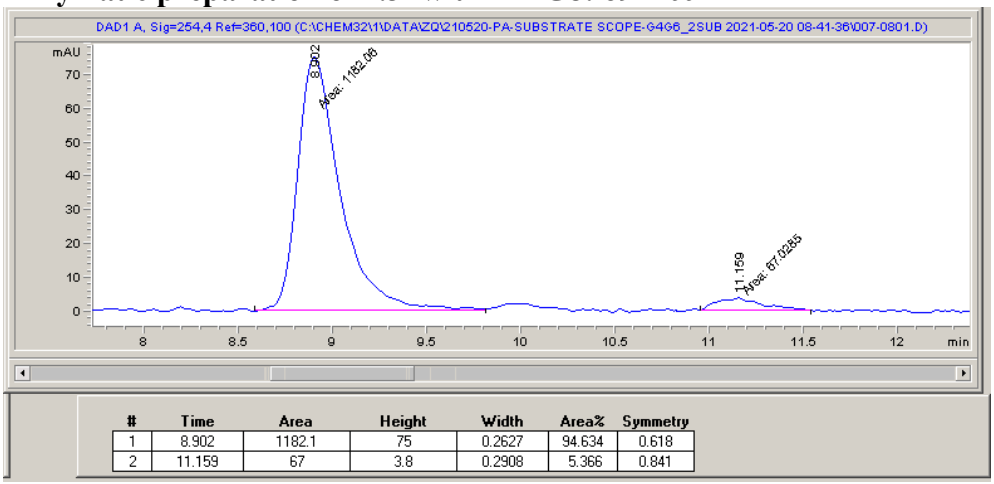

#	Time	Area	Height	Width	Area%	Symmetry
1	8.902	1182.1	75	0.2627	94.634	0.618
2	11.159	67	3.8	0.2908	5.366	0.841

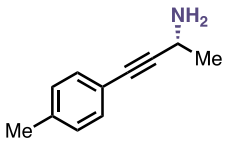

1.3g

(*R*)-4-(*p*-tolyl)but-3-yn-2-amine (1.3g)

Chiral-phase HPLC conditions: Chiralpak IA, 7% *i*-PrOH in hexane, 1.0 mL/min, 25 ºC, 245 nm

Racemic 1.3g:

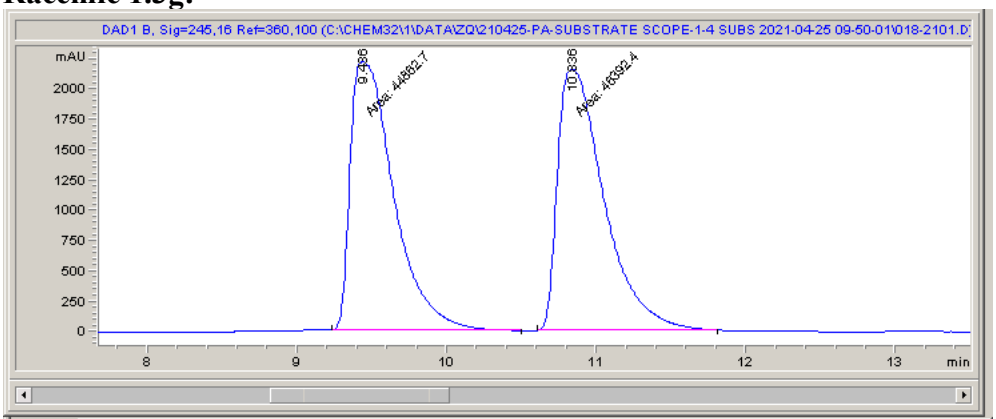

#	Time	Area	Height	Width	Area%	Symmetry
1	9.436	44862.7	2214.6	0.3376	49.162	0.38
2	10.836	46392.4	2152.6	0.3592	50.838	0.431

Enzymatic preparation of 1.3g with PA-G8: 89% *ee*

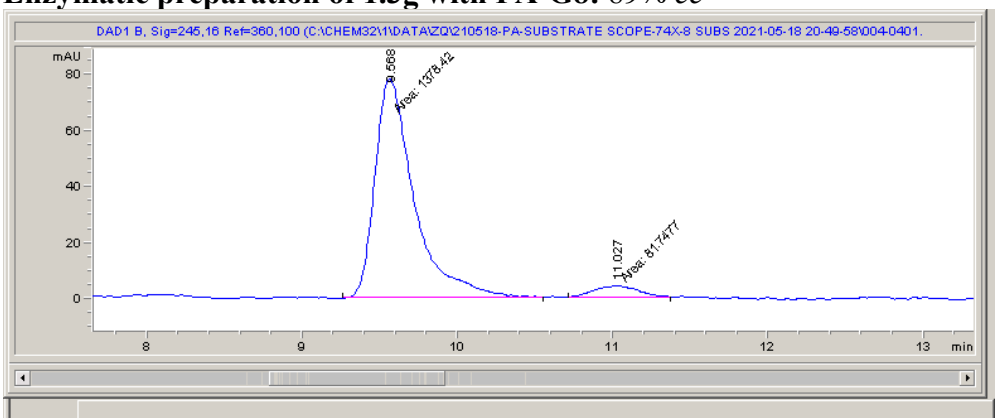

#	Time	Area	Height	Width	Area%	Symmetry
1	9.568	1378.4	78.2	0.2939	94.401	0.58
2	11.027	81.7	4.1	0.3332	5.599	0.978

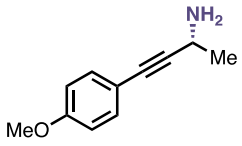

1.3h

(*R*)-4-(4-methoxyphenyl)but-3-yn-2-amine (1.3h)

Chiral-phase HPLC conditions: Chiralpak IA, 10% *i*-PrOH in hexane, 1.0 mL/min, 25 ºC, 254 nm

Racemic 1.3h:

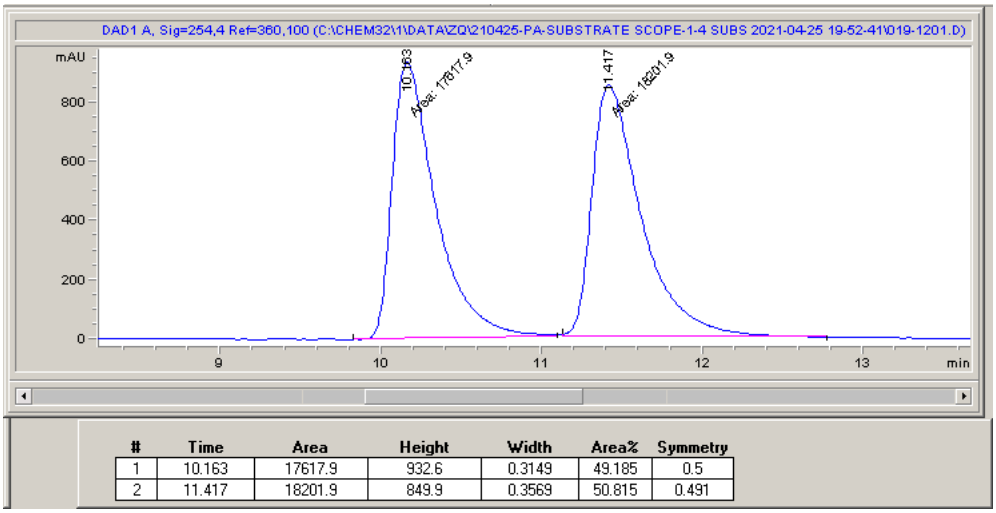

#	Time	Area	Height	Width	Area%	Symmetry
1	10.163	17617.9	932.6	0.3149	49.185	0.5
2	11.417	18201.9	849.9	0.3569	50.815	0.491

Enzymatic preparation of 1.3h with PA-G8: 93% *ee*

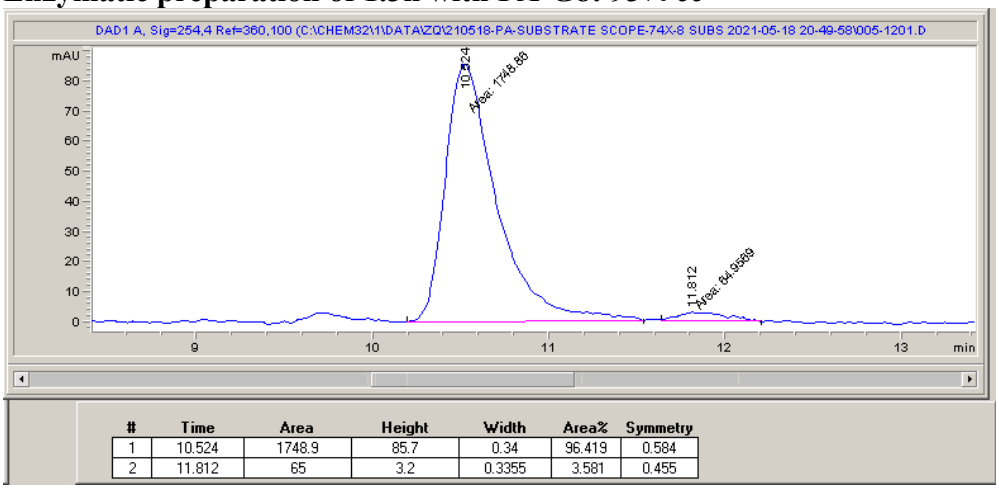

#	Time	Area	Height	Width	Area%	Symmetry
1	10.524	1748.9	85.7	0.34	96.419	0.584
2	11.812	65	3.2	0.3355	3.581	0.455

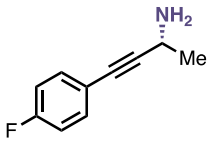

1.3i

(*R*)-4-(4-fluorophenyl)but-3-yn-2-amine (1.3i)

Chiral-phase HPLC conditions: Chiralpak IA, 7% *i*-PrOH in hexane, 1.0 mL/min, 25 ºC, 254 nm

Racemic 1.3i:

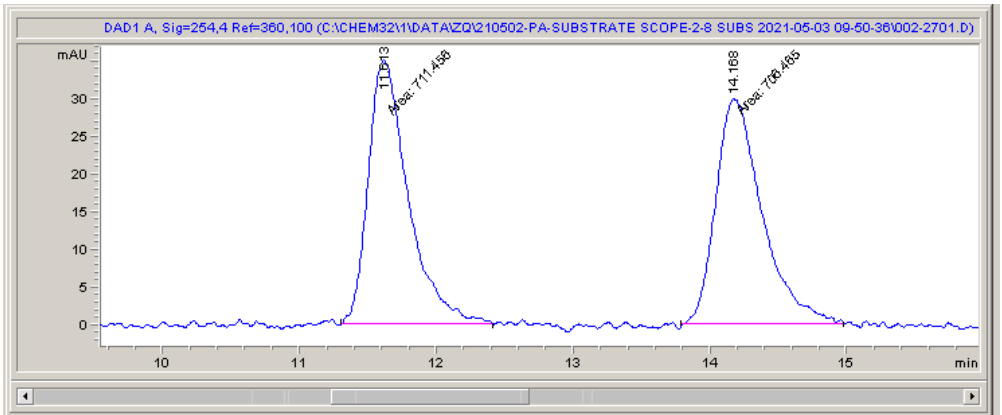

#	Time	Area	Height	Width	Area%	Symmetry
1	11.613	711.5	35	0.3386	50.176	0.631
2	14.168	706.5	29.8	0.3945	49.824	0.605

Enzymatic preparation of 1.3i with PA-G8: 82% *ee*

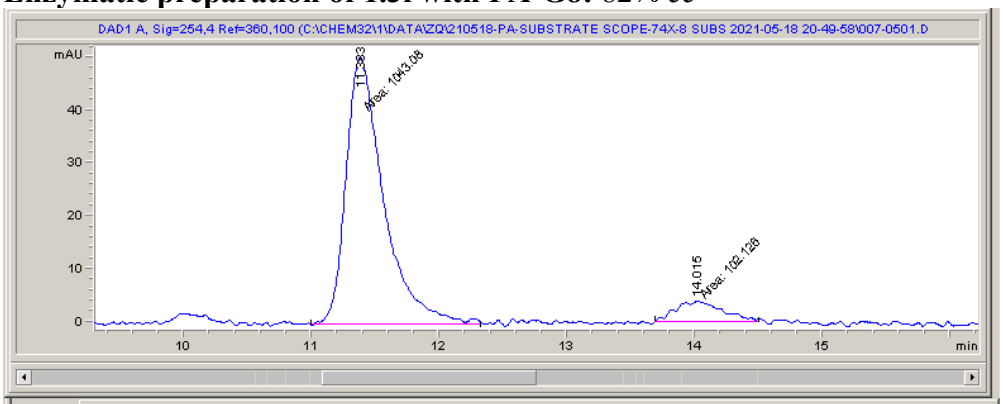

#	Time	Area	Height	Width	Area%	Symmetry
1	11.383	1043.1	50.4	0.3446	91.082	0.6
2	14.015	102.1	3.8	0.4428	8.918	0.806

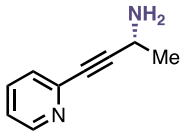

1.3j

(*R*)-4-(pyridin-2-yl)but-3-yn-2-amine (1.3j)

Chiral-phase HPLC conditions: Chiralpak IA, 7% *i*-PrOH in hexane, 1.0 mL/min, 25 ºC, 254 nm

Racemic 1.3j:

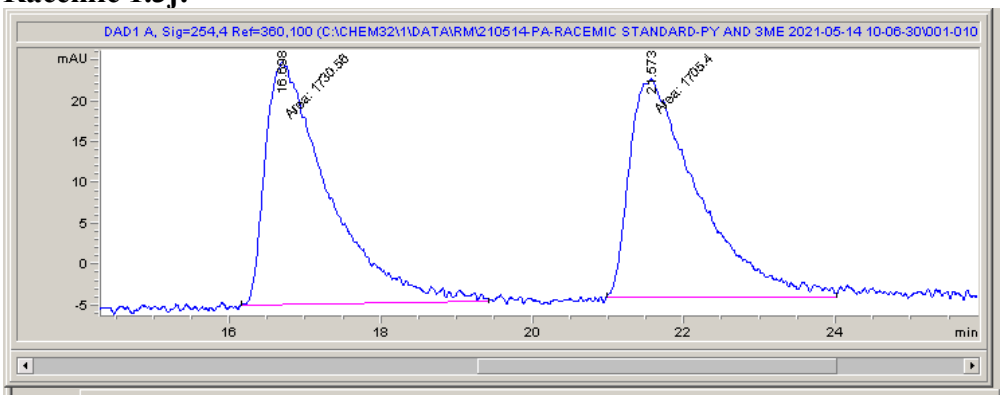

#	Time	Area	Height	Width	Area%	Symmetry
1	16.698	1730.6	29.7	0.9705	50.366	0.338
2	21.573	1705.4	26.8	1.0591	49.634	0.428

Enzymatic preparation of 1.3j with PA-G8: 91% *ee*

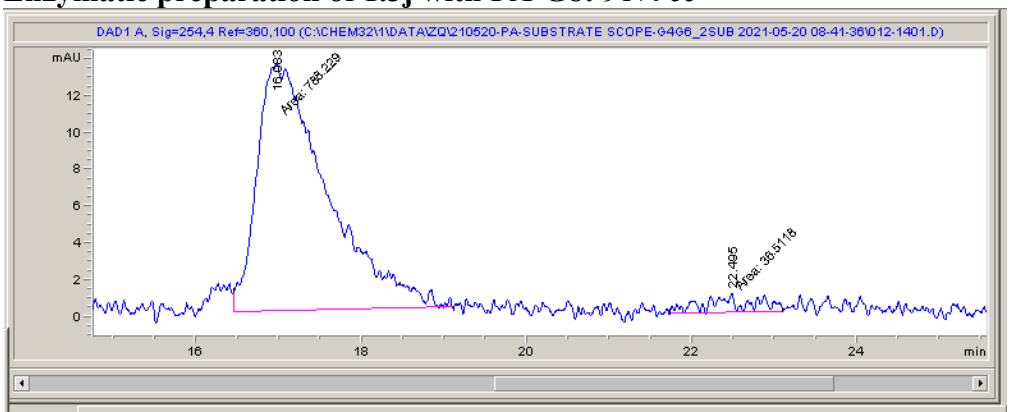

#	Time	Area	Height	Width	Area%	Symmetry
1	16.983	788.2	13.5	0.9744	95.573	0.387
2	22.495	36.5	1	0.583	4.427	1.233

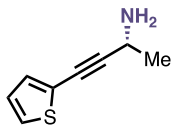

1.3k

(*R*)-4-(thiophen-2-yl)but-3-yn-2-amine (1.3k)

Chiral-phase HPLC conditions: Chiralpak IA, 7% *i*-PrOH in hexane, 1.0 mL/min, 25 ºC, 254 nm

Racemic 1.3k:

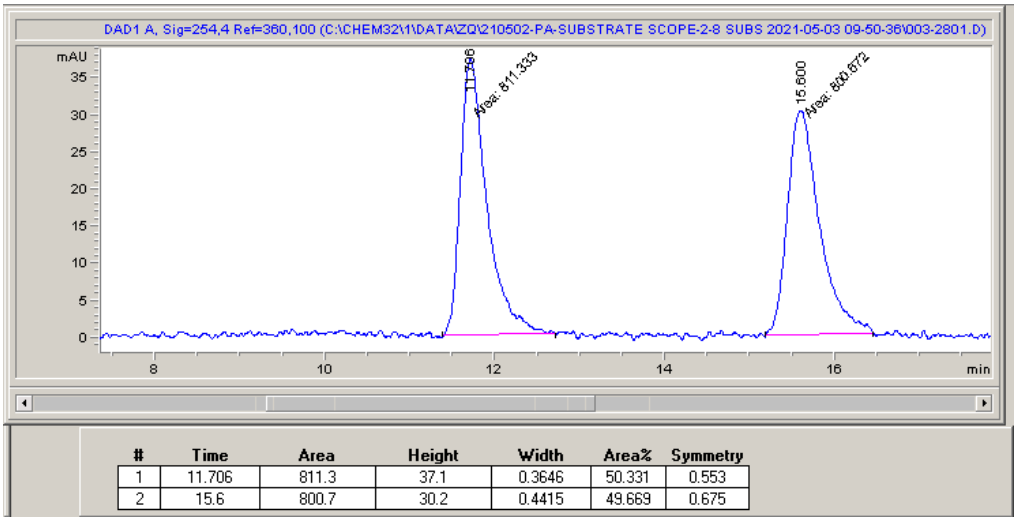

#	Time	Area	Height	Width	Area%	Symmetry
1	11.706	811.3	37.1	0.3646	50.331	0.553
2	15.6	800.7	30.2	0.4415	49.669	0.675

Enzymatic preparation of 1.3k with PA-G8: 92% *ee*

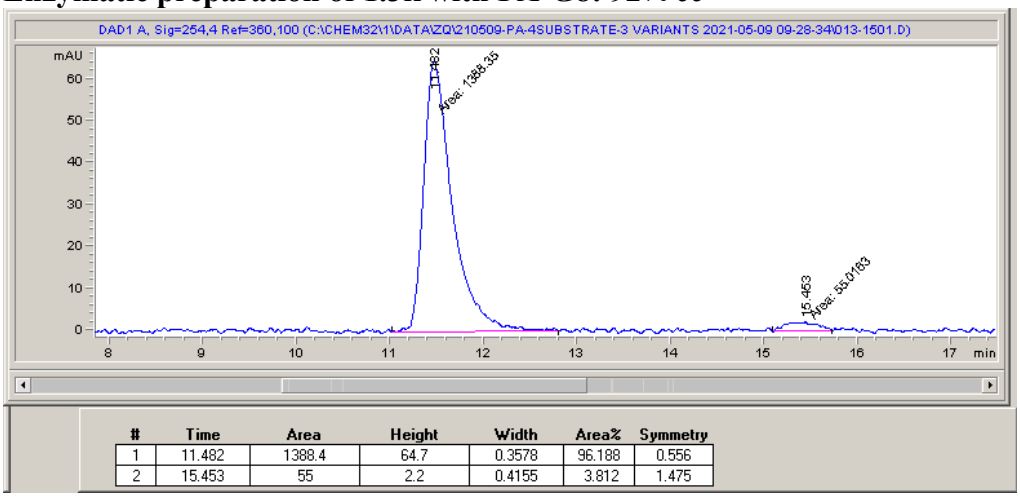

#	Time	Area	Height	Width	Area%	Symmetry
1	11.482	1388.4	64.7	0.3578	96.188	0.556
2	15.453	55	2.2	0.4155	3.812	1.475

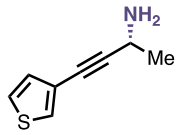

1.3l

(*R*)-4-(thiophen-3-yl)but-3-yn-2-amine (1.3l)

Chiral-phase HPLC conditions: Chiralpak IA, 7% *i*-PrOH in hexane, 1.0 mL/min, 25 ºC, 254 nm

Racemic 1.3l:

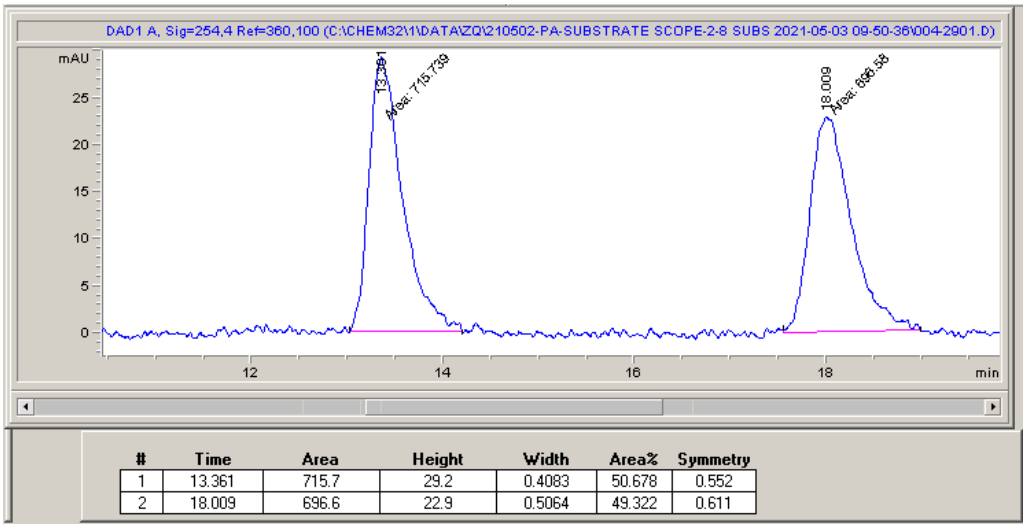

#	Time	Area	Height	Width	Area%	Symmetry
1	13.361	715.7	29.2	0.4083	50.678	0.552
2	18.009	696.6	22.9	0.5064	49.322	0.611

Enzymatic preparation of 1.3k with PA-G8: 91% *ee*

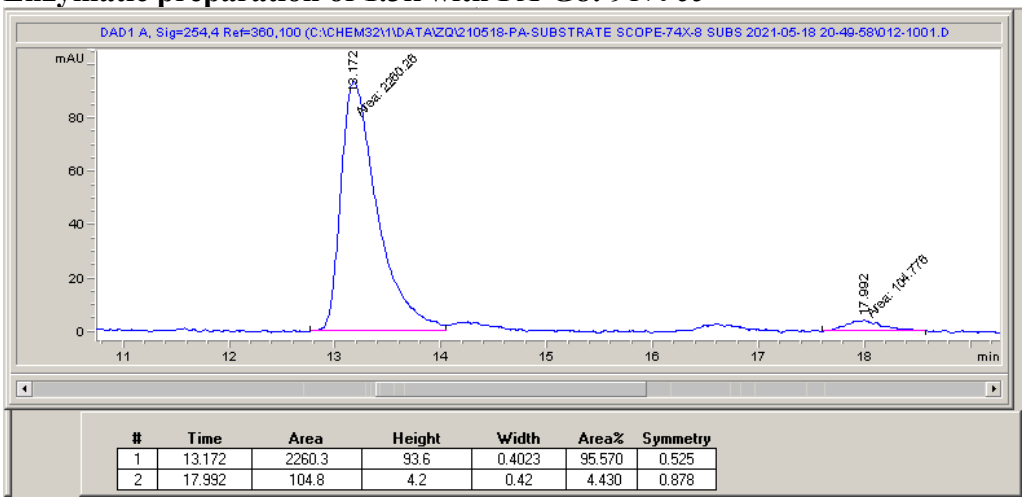

#	Time	Area	Height	Width	Area%	Symmetry
1	13.172	2260.3	93.6	0.4023	95.570	0.525
2	17.992	104.8	4.2	0.42	4.430	0.878

VIII. Sequence Information

Mutations present in P411 variants involved in this study:

P411 variant	Mutations relative to wild-type P450$_{BM3}$
P411-b4 (**PA-G0**)	A78M A82L F87A P142S T175I A184V S226R H236Q E252G I263M T268P A290V A328V L353V I366V C400S L437G T438S E442K
PA-G1	A78M A82L F87A P142S T175I A184V S226R H236Q E252G I263M **E267D** T268P A290V A328V L353V I366V C400S L437G T438S E442K
PA-G2	A78M A82L F87A P142S T175I A184V S226R H236Q E252G I263M **E267D** T268P A290V A328V L353V I366V **N395C** C400S L437G T438S E442K
PA-G3	A78M A82L F87A P142S T175I A184V S226R H236Q E252G I263M **E267D** T268P A290V A328V L353V I366V **N395C** C400S **L437Q** T438S E442K
PA-G4	**S72T** A78M A82L F87A P142S T175I A184V S226R H236Q E252G I263M **E267D** T268P A290V A328V L353V I366V **N395C** C400S **L437Q** T438S E442K
PA-G5	**S72T** A78M A82L F87A P142S T175I A184V S226R H236Q E252G I263M **E267D** T268P A290V A328V L353V I366V **N395C** C400S **L437Q T438G** E442K
PA-G6	**S72T** A78M A82L F87A P142S T175I A184V S226R H236Q E252G I263M **E267D** T268P **T269V** A290V A328V L353V I366V **N395C** C400S **L437Q T438G** E442K
PA-G7	**S72T** A78M A82L F87A P142S T175I A184V S226R H236Q E252G I263M **H266S E267D** T268P **T269V** A290V A328V L353V I366V **N395C** C400S **L437Q T438G** E442K
PA-G8	**S72T A74K** A78M A82L F87A P142S T175I A184V S226R H236Q E252G I263M **H266S E267D** T268P **T269V** A290V A328V L353V I366V **N395C** C400S **L437Q T438G** E442K

Nucleotide and amino acid sequences of P411-b4 (PA-G0):

ATGACAATTAAAGAAATGCCTCAGCCAAAAACGTTTGGAGAGCTTAAAAATTTACCGTTATTAA
ACACAGATAAACCGGTTCAAGCTTTGATGAAAATTGCGGATGAATTAGGAGAAATCTTTAAATT
CGAGGCGCCTGGTCGTGTAACGCGCTACTTATCAAGTCAGCGTCTAATTAAAGAAGCATGCGAT
GAATCACGCTTTGATAAAAACTTAAGTCAAGCGCTTAAATTTATGCGTGATTTTCTTGGAGACG
GGTTAGCCACAAGCTGGACGCATGAAAAAAATTGGAAAAAAGCGCATAATATCTTACTTCCAAG
CTTTAGTCAGCAGGCAATGAAAGGCTATCATGCGATGATGGTCGATATCGCCGTGCAGCTTGTT
CAAAAGTGGGAGCGTCTAAATGCAGATGAGCATATTGAAGTATCGGAAGACATGACACGTTTAA

CGCTTGATACAATTGGTCTTTGCGGCTTTAACTATCGCTTTAACAGCTTTTACCGAGATCAGCC
TCATCCATTTATTATAAGTATGGTCCGTGCACTGGATGAAGTAATGAACAAGCTGCAGCGAGCA
AATCCAGACGACCCAGCTTATGATGAAAACAAGCGCCAGTTTCAAGAAGATATCAAGGTGATGA
ACGACCTAGTAGATAAAATTATTGCAGATCGCAAAGCAAGGGGTGAACAAAGCGATGATTTATT
AACGCAGATGCTAAACGGAAAAGATCCAGAAACGGGTGAGCCGCTTGATGACGGGAACATTCGC
TATCAAATTATTACATTCTTAATGGCGGGACACGAACCGACAAGTGGTCTTTTATCATTTGCGC
TGTATTTCTTAGTGAAAAATCCACATGTATTACAAAAAGTAGCAGAAGAAGCAGCACGAGTTCT
AGTAGATCCTGTTCCAAGCTACAAACAAGTCAAACAGCTTAAATATGTCGGCATGGTCTTAAAC
GAAGCGCTGCGCTTATGGCCAACTGTGCCTGCGTTTTCCCTATATGCAAAAGAAGATACGGTGC
TTGGAGGAGAATATCCTTTAGAAAAAGGCGACGAAGTAATGGTTCTGATTCCTCAGCTTCACCG
TGATAAAACAGTTTGGGGAGACGATGTGGAGGAGTTCCGTCCAGAGCGTTTTGAAAATCCAAGT
GCGATTCCGCAGCATGCGTTTAAACCGTTTGGAAACGGTCAGCGTGCGTCTATCGGTCAGCAGT
TCGCTCTTCATGAAGCAACGCTGGTACTTGGTATGATGCTAAAACACTTTGACTTTGAAGATCA
TACAAACTACGAGCTCGATATTAAAGAAACTGGTAGTTTAAAACCTAAAGGCTTTGTGGTAAAA
GCAAAATCGAAAAAAATTCCGCTTGGCGGTATTCCTTCACCTAGCACTGAACAGTCTGCTAAAA
AAGTACGCAAAAAGGCAGAAAACGCTCATAATACGCCGCTGCTTGTGCTATACGGTTCAAATAT
GGGTACCGCTGAAGGAACGGCGCGTGATTTAGCAGATATTGCAATGAGCAAAGGATTTGCACCG
CAGGTCGCAACGCTTGATTCACACGCCGGAAATCTTCCGCGCGAAGGAGCTGTATTAATTGTAA
CGGCGTCTTATAACGGTCATCCGCCTGATAACGCAAAGCAATTTGTCGACTGGTTAGACCAAGC
GTCTGCTGATGAAGTAAAAGGCGTTCGCTACTCCGTATTTGGATGCGGCGATAAAAACTGGGCT
ACTACGTATCAAAAAGTGCCTGCTTTTATCGATGAAACGCTTGCCGCTAAAGGGGCAGAAAACA
TCGCTGACCGCGGTGAAGCAGATGCAAGCGACGACTTTGAAGGCACATATGAAGAATGGCGTGA
ACATATGTGGAGTGACGTAGCAGCCTACTTTAACCTCGACATTGAAAACAGTGAAGATAATAAA
TCTACTCTTTCACTTCAATTTGTCGACAGCGCCGCGGATATGCCGCTTGCGAAAATGCACGGTG
CGTTTTCAACGAACGTCGTAGCAAGCAAAGAACTTCAACAGCCAGGCAGTGCACGAAGCACGCG
ACATCTTGAAATTGAACTTCCAAAAGAAGCTTCTTATCAAGAAGGAGATCATTTAGGTGTTATT
CCTCGCAACTATGAAGGAATAGTAAACCGTGTAACAGCAAGGTTCGGCCTAGATGCATCACAGC
AAATCCGTCTGGAAGCAGAAGAAGAAAAATTAGCTCATTTGCCACTCGCTAAAACAGTATCCGT
AGAAGAGCTTCTGCAATACGTGGAGCTTCAAGATCCTGTTACGCGCACGCAGCTTCGCGCAATG
GCTGCTAAAACGGTCTGCCCGCCGCATAAAGTAGAGCTTGAAGCCTTGCTTGAAAAGCAAGCCT
ACAAAGAACAAGTGCTGGCAAAACGTTTAACAATGCTTGAACTGCTTGAAAAATACCCGGCGTG
TGAAATGAAATTCAGCGAATTTATCGCCCTTCTGCCAAGCATACGCCCGCGCTATTACTCGATT

TCTTCATCACCTCGTGTCGATGAAAAACAAGCAAGCATCACGGTCAGCGTTGTCTCAGGAGAAG
CGTGGAGCGGATATGGAGAATATAAAGGAATTGCGTCGAACTATCTTGCCGAGCTGCAAGAAGG
AGATACGATTACGTGCTTTATTTCCACACCGCAGTCAGAATTTACGCTGCCAAAAGACCCTGAA
ACGCCGCTTATCATGGTCGGACCGGGAACAGGCGTCGCGCCGTTTAGAGGCTTTGTGCAGGCGC
GCAAACAGCTAAAAGAACAAGGACAGTCACTTGGAGAAGCACATTTATACTTCGGCTGCCGTTC
ACCTCATGAAGACTATCTGTATCAAGAAGAGCTTGAAAACGCCCAAAGCGAAGGCATCATTACG
CTTCATACCGCTTTTTCTCGCATGCCAAATCAGCCGAAAACATACGTTCAGCACGTAATGGAAC
AAGACGGCAAGAAATTGATTGAACTTCTTGATCAAGGAGCGCACTTCTATATTTGCGGAGACGG
AAGCCAAATGGCACCTGCCGTTGAAGCAACGCTTATGAAAAGCTATGCTGACGTTCACCAAGTG
AGTGAAGCAGACGCTCGCTTATGGCTGCAGCAGCTAGAAGAAAAAGGCCGATACGCAAAAGACG
TGTGGGCTGGGCTCGAGCACCACCACCACCACCACTGA

MTIKEMPQPKTFGELKNLPLLNTDKPVQALMKIADELGEIFKFEAPGRVTRYLSSQRLIKEACD
ESRFDKNLSQALKFMRDFLGDGLATSWTHEKNWKKAHNILLPSFSQQAMKGYHAMMVDIAVQLV
QKWERLNADEHIEVSEDMTRLTLDTIGLCGFNYRFNSFYRDQPHPFIISMVRALDEVMNKLQRA
NPDDPAYDENKRQFQEDIKVMNDLVDKIIADRKARGEQSDDLLTQMLNGKDPETGEPLDDGNIR
YQIITFLMAGHEPTSGLLSFALYFLVKNPHVLQKVAEEAARVLVDPVPSYKQVKQLKYVGMVLN
EALRLWPTVPAFSLYAKEDTVLGGEYPLEKGDEVMVLIPQLHRDKTVWGDDVEEFRPERFENPS
AIPQHAFKPFGNGQRASIGQQFALHEATLVLGMMLKHFDFEDHTNYELDIKETGSLKPKGFVVK
AKSKKIPLGGIPSPSTEQSAKKVRKKAENAHNTPLLVLYGSNMGTAEGTARDLADIAMSKGFAP
QVATLDSHAGNLPREGAVLIVTASYNGHPPDNAKQFVDWLDQASADEVKGVRYSVFGCGDKNWA
TTYQKVPAFIDETLAAKGAENIADRGEADASDDFEGTYEEWREHMWSDVAAYFNLDIENSEDNK
STLSLQFVDSAADMPLAKMHGAFSTNVVASKELQQPGSARSTRHLEIELPKEASYQEGDHLGVI
PRNYEGIVNRVTARFGLDASQQIRLEAEEEKLAHLPLAKTVSVEELLQYVELQDPVTRTQLRAM
AAKTVCPPHKVELEALLEKQAYKEQVLAKRLTMLELLEKYPACEMKFSEFIALLPSIRPRYYSI
SSSPRVDEKQASITVSVVSGEAWSGYGEYKGIASNYLAELQEGDTITCFISTPQSEFTLPKDPE
TPLIMVGPGTGVAPFRGFVQARKQLKEQGQSLGEAHLYFGCRSPHEDYLYQEELENAQSEGIIT
LHTAFSRMPNQPKTYVQHVMEQDGKKLIELLDQGAHFYICGDGSQMAPAVEATLMKSYADVHQV
SEADARLWLQQLEEKGRYAKDVWAGLEHHHHHH

Nucleotide and amino acid sequences of P411-PA-G1:

ATGACAATTAAAGAAATGCCTCAGCCAAAAACGTTTGGAGAGCTTAAAAATTTACCGTTATTAA
ACACAGATAAACCGGTTCAAGCTTTGATGAAAATTGCGGATGAATTAGGAGAAATCTTTAAATT
CGAGGCGCCTGGTCGTGTAACGCGCTACTTATCAAGTCAGCGTCTAATTAAAGAAGCATGCGAT
GAATCACGCTTTGATAAAAACTTAAGTCAAGCGCTTAAATTTATGCGTGATTTTCTTGGAGACG
GGTTAGCCACAAGCTGGACGCATGAAAAAAATTGGAAAAAAGCGCATAATATCTTACTTCCAAG
CTTTAGTCAGCAGGCAATGAAAGGCTATCATGCGATGATGGTCGATATCGCCGTGCAGCTTGTT
CAAAAGTGGGAGCGTCTAAATGCAGATGAGCATATTGAAGTATCGGAAGACATGACACGTTTAA
CGCTTGATACAATTGGTCTTTGCGGCTTTAACTATCGCTTTAACAGCTTTTACCGAGATCAGCC
TCATCCATTTATTATAAGTATGGTCCGTGCACTGGATGAAGTAATGAACAAGCTGCAGCGAGCA
AATCCAGACGACCCAGCTTATGATGAAAACAAGCGCCAGTTTCAAGAAGATATCAAGGTGATGA
ACGACCTAGTAGATAAAATTATTGCAGATCGCAAAGCAAGGGGTGAACAAAGCGATGATTTATT
AACGCAGATGCTAAACGGAAAAGATCCAGAAACGGGTGAGCCGCTTGATGACGGGAACATTCGC
TATCAAATTATTACATTCTTAATGGCGGGACACGATCCGACAAGTGGTCTTTTATCATTTGCGC
TGTATTTCTTAGTGAAAAATCCACATGTATTACAAAAAGTAGCAGAAGAAGCAGCACGAGTTCT
AGTAGATCCTGTTCCAAGCTACAAACAAGTCAAACAGCTTAAATATGTCGGCATGGTCTTAAAC
GAAGCGCTGCGCTTATGGCCAACTGTGCCTGCGTTTTCCCTATATGCAAAAGAAGATACGGTGC
TTGGAGGAGAATATCCTTTAGAAAAAGGCGACGAAGTAATGGTTCTGATTCCTCAGCTTCACCG
TGATAAAACAGTTTGGGGAGACGATGTGGAGGAGTTCCGTCCAGAGCGTTTTGAAAATCCAAGT
GCGATTCCGCAGCATGCGTTTAAACCGTTTGGAAACGGTCAGCGTGCGTCTATCGGTCAGCAGT
TCGCTCTTCATGAAGCAACGCTGGTACTTGGTATGATGCTAAAACACTTTGACTTTGAAGATCA
TACAAACTACGAGCTCGATATTAAAGAAACTGGTAGTTTAAAACCTAAAGGCTTTGTGGTAAAA
GCAAAATCGAAAAAAATTCCGCTTGGCGGTATTCCTTCACCTAGCACTGAACAGTCTGCTAAAA
AAGTACGCAAAAAGGCAGAAAACGCTCATAATACGCCGCTGCTTGTGCTATACGGTTCAAATAT
GGGTACCGCTGAAGGAACGGCGCGTGATTTAGCAGATATTGCAATGAGCAAAGGATTTGCACCG
CAGGTCGCAACGCTTGATTCACACGCCGGAAATCTTCCGCGCGAAGGAGCTGTATTAATTGTAA
CGGCGTCTTATAACGGTCATCCGCCTGATAACGCAAAGCAATTTGTCGACTGGTTAGACCAAGC
GTCTGCTGATGAAGTAAAAGGCGTTCGCTACTCCGTATTTGGATGCGGCGATAAAAACTGGGCT
ACTACGTATCAAAAAGTGCCTGCTTTTATCGATGAAACGCTTGCCGCTAAAGGGGCAGAAAACA
TCGCTGACCGCGGTGAAGCAGATGCAAGCGACGACTTTGAAGGCACATATGAAGAATGGCGTGA
ACATATGTGGAGTGACGTAGCAGCCTACTTTAACCTCGACATTGAAAACAGTGAAGATAATAAA

TCTACTCTTTCACTTCAATTTGTCGACAGCGCCGCGGATATGCCGCTTGCGAAAATGCACGGTG
CGTTTTCAACGAACGTCGTAGCAAGCAAAGAACTTCAACAGCCAGGCAGTGCACGAAGCACGCG
ACATCTTGAAATTGAACTTCCAAAAGAAGCTTCTTATCAAGAAGGAGATCATTTAGGTGTTATT
CCTCGCAACTATGAAGGAATAGTAAACCGTGTAACAGCAAGGTTCGGCCTAGATGCATCACAGC
AAATCCGTCTGGAAGCAGAAGAAGAAAAATTAGCTCATTTGCCACTCGCTAAAACAGTATCCGT
AGAAGAGCTTCTGCAATACGTGGAGCTTCAAGATCCTGTTACGCGCACGCAGCTTCGCGCAATG
GCTGCTAAAACGGTCTGCCCGCCGCATAAAGTAGAGCTTGAAGCCTTGCTTGAAAAGCAAGCCT
ACAAAGAACAAGTGCTGGCAAAACGTTTAACAATGCTTGAACTGCTTGAAAAATACCCGGCGTG
TGAAATGAAATTCAGCGAATTTATCGCCCTTCTGCCAAGCATACGCCCGCGCTATTACTCGATT
TCTTCATCACCTCGTGTCGATGAAAAACAAGCAAGCATCACGGTCAGCGTTGTCTCAGGAGAAG
CGTGGAGCGGATATGGAGAATATAAAGGAATTGCGTCGAACTATCTTGCCGAGCTGCAAGAAGG
AGATACGATTACGTGCTTTATTTCCACACCGCAGTCAGAATTTACGCTGCCAAAAGACCCTGAA
ACGCCGCTTATCATGGTCGGACCGGGAACAGGCGTCGCGCCGTTTAGAGGCTTTGTGCAGGCGC
GCAAACAGCTAAAAGAACAAGGACAGTCACTTGGAGAAGCACATTTATACTTCGGCTGCCGTTC
ACCTCATGAAGACTATCTGTATCAAGAAGAGCTTGAAAACGCCCAAAGCGAAGGCATCATTACG
CTTCATACCGCTTTTTCTCGCATGCCAAATCAGCCGAAAACATACGTTCAGCACGTAATGGAAC
AAGACGGCAAGAAATTGATTGAACTTCTTGATCAAGGAGCGCACTTCTATATTTGCGGAGACGG
AAGCCAAATGGCACCTGCCGTTGAAGCAACGCTTATGAAAAGCTATGCTGACGTTCACCAAGTG
AGTGAAGCAGACGCTCGCTTATGGCTGCAGCAGCTAGAAGAAAAAGGCCGATACGCAAAAGACG
TGTGGGCTGGGCTCGAGCACCACCACCACCACCACTGA

MTIKEMPQPKTFGELKNLPLLNTDKPVQALMKIADELGEIFKFEAPGRVTRYLSSQRLIKEACD
ESRFDKNLSQALKFMRDFLGDGLATSWTHEKNWKKAHNILLPSFSQQAMKGYHAMMVDIAVQLV
QKWERLNADEHIEVSEDMTRLTLDTIGLCGFNYRFNSFYRDQPHPFIISMVRALDEVMNKLQRA
NPDDPAYDENKRQFQEDIKVMNDLVDKIIADRKARGEQSDDLLTQMLNGKDPETGEPLDDGNIR
YQIITFLMAGHDPTSGLLSFALYFLVKNPHVLQKVAEEAARVLVDPVPSYKQVKQLKYVGMVLN
EALRLWPTVPAFSLYAKEDTVLGGEYPLEKGDEVMVLIPQLHRDKTVWGDDVEEFRPERFENPS
AIPQHAFKPFGNGQRASIGQQFALHEATLVLGMMLKHFDFEDHTNYELDIKETGSLKPKGFVVK
AKSKKIPLGGIPSPSTEQSAKKVRKKAENAHNTPLLVLYGSNMGTAEGTARDLADIAMSKGFAP
QVATLDSHAGNLPREGAVLIVTASYNGHPPDNAKQFVDWLDQASADEVKGVRYSVFGCGDKNWA

TTYQKVPAFIDETLAAKGAENIADRGEADASDDFEGTYEEWREHMWSDVAAYFNLDIENSEDNK
STLSLQFVDSAADMPLAKMHGAFSTNVVASKELQQPGSARSTRHLEIELPKEASYQEGDHLGVI
PRNYEGIVNRVTARFGLDASQQIRLEAEEEKLAHLPLAKTVSVEELLQYVELQDPVTRTQLRAM
AAKTVCPPHKVELEALLEKQAYKEQVLAKRLTMLELLEKYPACEMKFSEFIALLPSIRPRYYSI
SSSPRVDEKQASITVSVVSGEAWSGYGEYKGIASNYLAELQEGDTITCFISTPQSEFTLPKDPE
TPLIMVGPGTGVAPFRGFVQARKQLKEQGQSLGEAHLYFGCRSPHEDYLYQEELENAQSEGIIT
LHTAFSRMPNQPKTYVQHVMEQDGKKLIELLDQGAHFYICGDGSQMAPAVEATLMKSYADVHQV
SEADARLWLQQLEEKGRYAKDVWAGLEHHHHHH

Nucleotide and amino acid sequences of P411-PA-G2:

ATGACAATTAAAGAAATGCCTCAGCCAAAAACGTTTGGAGAGCTTAAAAATTTACCGTTATTAA
ACACAGATAAACCGGTTCAAGCTTTGATGAAAATTGCGGATGAATTAGGAGAAATCTTTAAATT
CGAGGCGCCTGGTCGTGTAACGCGCTACTTATCAAGTCAGCGTCTAATTAAAGAAGCATGCGAT
GAATCACGCTTTGATAAAAACTTAAGTCAAGCGCTTAAATTTATGCGTGATTTTCTTGGAGACG
GGTTAGCCACAAGCTGGACGCATGAAAAAAATTGGAAAAAAGCGCATAATATCTTACTTCCAAG
CTTTAGTCAGCAGGCAATGAAAGGCTATCATGCGATGATGGTCGATATCGCCGTGCAGCTTGTT
CAAAAGTGGGAGCGTCTAAATGCAGATGAGCATATTGAAGTATCGGAAGACATGACACGTTTAA
CGCTTGATACAATTGGTCTTTGCGGCTTTAACTATCGCTTTAACAGCTTTTACCGAGATCAGCC
TCATCCATTTATTATAAGTATGGTCCGTGCACTGGATGAAGTAATGAACAAGCTGCAGCGAGCA
AATCCAGACGACCCAGCTTATGATGAAAACAAGCGCCAGTTTCAAGAAGATATCAAGGTGATGA
ACGACCTAGTAGATAAAATTATTGCAGATCGCAAAGCAAGGGGTGAACAAAGCGATGATTTATT
AACGCAGATGCTAAACGGAAAAGATCCAGAAACGGGTGAGCCGCTTGATGACGGGAACATTCGC
TATCAAATTATTACATTCTTAATGGCGGGACACGATCCGACAAGTGGTCTTTTATCATTTGCGC
TGTATTTCTTAGTGAAAAATCCACATGTATTACAAAAAGTAGCAGAAGAAGCAGCACGAGTTCT
AGTAGATCCTGTTCCAAGCTACAAACAAGTCAAACAGCTTAAATATGTCGGCATGGTCTTAAAC
GAAGCGCTGCGCTTATGGCCAACTGTGCCTGCGTTTTCCCTATATGCAAAAGAAGATACGGTGC
TTGGAGGAGAATATCCTTTAGAAAAAGGCGACGAAGTAATGGTTCTGATTCCTCAGCTTCACCG
TGATAAAACAGTTTGGGGAGACGATGTGGAGGAGTTCCGTCCAGAGCGTTTTGAAAATCCAAGT
GCGATTCCGCAGCATGCGTTTAAACCGTTTGGATGTGGTCAGCGTGCGTCTATCGGTCAGCAGT
TCGCTCTTCATGAAGCAACGCTGGTACTTGGTATGATGCTAAAACACTTTGACTTTGAAGATCA

TACAAACTACGAGCTCGATATTAAAGAAACTGGTAGTTTAAAACCTAAAGGCTTTGTGGTAAAA
GCAAAATCGAAAAAAATTCCGCTTGGCGGTATTCCTTCACCTAGCACTGAACAGTCTGCTAAAA
AAGTACGCAAAAAGGCAGAAAACGCTCATAATACGCCGCTGCTTGTGCTATACGGTTCAAATAT
GGGTACCGCTGAAGGAACGGCGCGTGATTTAGCAGATATTGCAATGAGCAAAGGATTTGCACCG
CAGGTCGCAACGCTTGATTCACACGCCGGAAATCTTCCGCGCGAAGGAGCTGTATTAATTGTAA
CGGCGTCTTATAACGGTCATCCGCCTGATAACGCAAAGCAATTTGTCGACTGGTTAGACCAAGC
GTCTGCTGATGAAGTAAAAGGCGTTCGCTACTCCGTATTTGGATGCGGCGATAAAAACTGGGCT
ACTACGTATCAAAAAGTGCCTGCTTTTATCGATGAAACGCTTGCCGCTAAAGGGGCAGAAAACA
TCGCTGACCGCGGTGAAGCAGATGCAAGCGACGACTTTGAAGGCACATATGAAGAATGGCGTGA
ACATATGTGGAGTGACGTAGCAGCCTACTTTAACCTCGACATTGAAAACAGTGAAGATAATAAA
TCTACTCTTTCACTTCAATTTGTCGACAGCGCCGCGGATATGCCGCTTGCGAAAATGCACGGTG
CGTTTTCAACGAACGTCGTAGCAAGCAAAGAACTTCAACAGCCAGGCAGTGCACGAAGCACGCG
ACATCTTGAAATTGAACTTCCAAAAGAAGCTTCTTATCAAGAAGGAGATCATTTAGGTGTTATT
CCTCGCAACTATGAAGGAATAGTAAACCGTGTAACAGCAAGGTTCGGCCTAGATGCATCACAGC
AAATCCGTCTGGAAGCAGAAGAAGAAAAATTAGCTCATTTGCCACTCGCTAAAACAGTATCCGT
AGAAGAGCTTCTGCAATACGTGGAGCTTCAAGATCCTGTTACGCGCACGCAGCTTCGCGCAATG
GCTGCTAAAACGGTCTGCCCGCCGCATAAAGTAGAGCTTGAAGCCTTGCTTGAAAAGCAAGCCT
ACAAAGAACAAGTGCTGGCAAAACGTTTAACAATGCTTGAACTGCTTGAAAAATACCCGGCGTG
TGAAATGAAATTCAGCGAATTTATCGCCCTTCTGCCAAGCATACGCCCGCGCTATTACTCGATT
TCTTCATCACCTCGTGTCGATGAAAAACAAGCAAGCATCACGGTCAGCGTTGTCTCAGGAGAAG
CGTGGAGCGGATATGGAGAATATAAAGGAATTGCGTCGAACTATCTTGCCGAGCTGCAAGAAGG
AGATACGATTACGTGCTTTATTTCCACACCGCAGTCAGAATTTACGCTGCCAAAAGACCCTGAA
ACGCCGCTTATCATGGTCGGACCGGGAACAGGCGTCGCGCCGTTTAGAGGCTTTGTGCAGGCGC
GCAAACAGCTAAAAGAACAAGGACAGTCACTTGGAGAAGCACATTTATACTTCGGCTGCCGTTC
ACCTCATGAAGACTATCTGTATCAAGAAGAGCTTGAAAACGCCCAAAGCGAAGGCATCATTACG
CTTCATACCGCTTTTTCTCGCATGCCAAATCAGCCGAAAACATACGTTCAGCACGTAATGGAAC
AAGACGGCAAGAAATTGATTGAACTTCTTGATCAAGGAGCGCACTTCTATATTTGCGGAGACGG
AAGCCAAATGGCACCTGCCGTTGAAGCAACGCTTATGAAAAGCTATGCTGACGTTCACCAAGTG
AGTGAAGCAGACGCTCGCTTATGGCTGCAGCAGCTAGAAGAAAAAGGCCGATACGCAAAAGACG
TGTGGGCTGGGCTCGAGCACCACCACCACCACCACTGA

MTIKEMPQPKTFGELKNLPLLNTDKPVQALMKIADELGEIFKFEAPGRVTRYLSSQRLIKEACD
ESRFDKNLSQALKFMRDFLGDGLATSWTHEKNWKKAHNILLPSFSQQAMKGYHAMMVDIAVQLV
QKWERLNADEHIEVSEDMTRLTLDTIGLCGFNYRFNSFYRDQPHPFIISMVRALDEVMNKLQRA
NPDDPAYDENKRQFQEDIKVMNDLVDKIIADRKARGEQSDDLLTQMLNGKDPETGEPLDDGNIR
YQIITFLMAGHDPTSGLLSFALYFLVKNPHVLQKVAEEAARVLVDPVPSYKQVKQLKYVGMVLN
EALRLWPTVPAFSLYAKEDTVLGGEYPLEKGDEVMVLIPQLHRDKTVWGDDVEEFRPERFENPS
AIPQHAFKPFGCGQRASIGQQFALHEATLVLGMMLKHFDFEDHTNYELDIKETGSLKPKGFVVK
AKSKKIPLGGIPSPSTEQSAKKVRKKAENAHNTPLLVLYGSNMGTAEGTARDLADIAMSKGFAP
QVATLDSHAGNLPREGAVLIVTASYNGHPPDNAKQFVDWLDQASADEVKGVRYSVFGCGDKNWA
TTYQKVPAFIDETLAAKGAENIADRGEADASDDFEGTYEEWREHMWSDVAAYFNLDIENSEDNK
STLSLQFVDSAADMPLAKMHGAFSTNVVASKELQQPGSARSTRHLEIELPKEASYQEGDHLGVI
PRNYEGIVNRVTARFGLDASQQIRLEAEEEKLAHLPLAKTVSVEELLQYVELQDPVTRTQLRAM
AAKTVCPPHKVELEALLEKQAYKEQVLAKRLTMLELLEKYPACEMKFSEFIALLPSIRPRYYSI
SSSPRVDEKQASITVSVVSGEAWSGYGEYKGIASNYLAELQEGDTITCFISTPQSEFTLPKDPE
TPLIMVGPGTGVAPFRGFVQARKQLKEQGQSLGEAHLYFGCRSPHEDYLYQEELENAQSEGIIT
LHTAFSRMPNQPKTYVQHVMEQDGKKLIELLDQGAHFYICGDGSQMAPAVEATLMKSYADVHQV
SEADARLWLQQLEEKGRYAKDVWAGLEHHHHHH

Nucleotide and amino acid sequences of P411-PA-G3:

ATGACAATTAAAGAAATGCCTCAGCCAAAAACGTTTGGAGAGCTTAAAAATTTACCGTTATTAA
ACACAGATAAACCGGTTCAAGCTTTGATGAAAATTGCGGATGAATTAGGAGAAATCTTTAAATT
CGAGGCGCCTGGTCGTGTAACGCGCTACTTATCAAGTCAGCGTCTAATTAAAGAAGCATGCGAT
GAATCACGCTTTGATAAAAACTTAAGTCAAGCGCTTAAATTTATGCGTGATTTTCTTGGAGACG
GGTTAGCCACAAGCTGGACGCATGAAAAAAATTGGAAAAAAGCGCATAATATCTTACTTCCAAG
CTTTAGTCAGCAGGCAATGAAAGGCTATCATGCGATGATGGTCGATATCGCCGTGCAGCTTGTT
CAAAAGTGGGAGCGTCTAAATGCAGATGAGCATATTGAAGTATCGGAAGACATGACACGTTTAA
CGCTTGATACAATTGGTCTTTGCGGCTTTAACTATCGCTTTAACAGCTTTTACCGAGATCAGCC
TCATCCATTTATTATAAGTATGGTCCGTGCACTGGATGAAGTAATGAACAAGCTGCAGCGAGCA
AATCCAGACGACCCAGCTTATGATGAAAACAAGCGCCAGTTTCAAGAAGATATCAAGGTGATGA
ACGACCTAGTAGATAAAATTATTGCAGATCGCAAAGCAAGGGGTGAACAAAGCGATGATTTATT

AACGCAGATGCTAAACGGAAAAGATCCAGAAACGGGTGAGCCGCTTGATGACGGGAACATTCGC
TATCAAATTATTACATTCTTAATGGCGGGACACGATCCGACAAGTGGTCTTTTATCATTTGCGC
TGTATTTCTTAGTGAAAAATCCACATGTATTACAAAAAGTAGCAGAAGAAGCAGCACGAGTTCT
AGTAGATCCTGTTCCAAGCTACAAACAAGTCAAACAGCTTAAATATGTCGGCATGGTCTTAAAC
GAAGCGCTGCGCTTATGGCCAACTGTGCCTGCGTTTTCCCTATATGCAAAAGAAGATACGGTGC
TTGGAGGAGAATATCCTTTAGAAAAAGGCGACGAAGTAATGGTTCTGATTCCTCAGCTTCACCG
TGATAAAACAGTTTGGGGAGACGATGTGGAGGAGTTCCGTCCAGAGCGTTTTGAAAATCCAAGT
GCGATTCCGCAGCATGCGTTTAAACCGTTTGGATGTGGTCAGCGTGCGTCTATCGGTCAGCAGT
TCGCTCTTCATGAAGCAACGCTGGTACTTGGTATGATGCTAAAACACTTTGACTTTGAAGATCA
TACAAACTACGAGCTCGATATTAAAGAAACTCAGAGTTTAAAACCTAAAGGCTTTGTGGTAAAA
GCAAAATCGAAAAAAATTCCGCTTGGCGGTATTCCTTCACCTAGCACTGAACAGTCTGCTAAAA
AAGTACGCAAAAAGGCAGAAAACGCTCATAATACGCCGCTGCTTGTGCTATACGGTTCAAATAT
GGGTACCGCTGAAGGAACGGCGCGTGATTTAGCAGATATTGCAATGAGCAAAGGATTTGCACCG
CAGGTCGCAACGCTTGATTCACACGCCGGAAATCTTCCGCGCGAAGGAGCTGTATTAATTGTAA
CGGCGTCTTATAACGGTCATCCGCCTGATAACGCAAAGCAATTTGTCGACTGGTTAGACCAAGC
GTCTGCTGATGAAGTAAAAGGCGTTCGCTACTCCGTATTTGGATGCGGCGATAAAAACTGGGCT
ACTACGTATCAAAAAGTGCCTGCTTTTATCGATGAAACGCTTGCCGCTAAAGGGGCAGAAAACA
TCGCTGACCGCGGTGAAGCAGATGCAAGCGACGACTTTGAAGGCACATATGAAGAATGGCGTGA
ACATATGTGGAGTGACGTAGCAGCCTACTTTAACCTCGACATTGAAAACAGTGAAGATAATAAA
TCTACTCTTTCACTTCAATTTGTCGACAGCGCCGCGGATATGCCGCTTGCGAAAATGCACGGTG
CGTTTTCAACGAACGTCGTAGCAAGCAAAGAACTTCAACAGCCAGGCAGTGCACGAAGCACGCG
ACATCTTGAAATTGAACTTCCAAAAGAAGCTTCTTATCAAGAAGGAGATCATTTAGGTGTTATT
CCTCGCAACTATGAAGGAATAGTAAACCGTGTAACAGCAAGGTTCGGCCTAGATGCATCACAGC
AAATCCGTCTGGAAGCAGAAGAAGAAAAATTAGCTCATTTGCCACTCGCTAAAACAGTATCCGT
AGAAGAGCTTCTGCAATACGTGGAGCTTCAAGATCCTGTTACGCGCACGCAGCTTCGCGCAATG
GCTGCTAAAACGGTCTGCCCGCCGCATAAAGTAGAGCTTGAAGCCTTGCTTGAAAAGCAAGCCT
ACAAAGAACAAGTGCTGGCAAAACGTTTAACAATGCTTGAACTGCTTGAAAAATACCCGGCGTG
TGAAATGAAATTCAGCGAATTTATCGCCCTTCTGCCAAGCATACGCCCGCGCTATTACTCGATT
TCTTCATCACCTCGTGTCGATGAAAAACAAGCAAGCATCACGGTCAGCGTTGTCTCAGGAGAAG
CGTGGAGCGGATATGGAGAATATAAAGGAATTGCGTCGAACTATCTTGCCGAGCTGCAAGAAGG
AGATACGATTACGTGCTTTATTTCCACACCGCAGTCAGAATTTACGCTGCCAAAAGACCCTGAA
ACGCCGCTTATCATGGTCGGACCGGGAACAGGCGTCGCGCCGTTTAGAGGCTTTGTGCAGGCGC

GCAAACAGCTAAAAGAACAAGGACAGTCACTTGGAGAAGCACATTTATACTTCGGCTGCCGTTC
ACCTCATGAAGACTATCTGTATCAAGAAGAGCTTGAAAACGCCCAAAGCGAAGGCATCATTACG
CTTCATACCGCTTTTTCTCGCATGCCAAATCAGCCGAAAACATACGTTCAGCACGTAATGGAAC
AAGACGGCAAGAAATTGATTGAACTTCTTGATCAAGGAGCGCACTTCTATATTTGCGGAGACGG
AAGCCAAATGGCACCTGCCGTTGAAGCAACGCTTATGAAAAGCTATGCTGACGTTCACCAAGTG
AGTGAAGCAGACGCTCGCTTATGGCTGCAGCAGCTAGAAGAAAAAGGCCGATACGCAAAAGACG
TGTGGGCTGGGCTCGAGCACCACCACCACCACCACTGA

MTIKEMPQPKTFGELKNLPLLNTDKPVQALMKIADELGEIFKFEAPGRVTRYLSSQRLIKEACD
ESRFDKNLSQALKFMRDFLGDGLATSWTHEKNWKKAHNILLPSFSQQAMKGYHAMMVDIAVQLV
QKWERLNADEHIEVSEDMTRLTLDTIGLCGFNYRFNSFYRDQPHPFIISMVRALDEVMNKLQRA
NPDDPAYDENKRQFQEDIKVMNDLVDKIIADRKARGEQSDDLLTQMLNGKDPETGEPLDDGNIR
YQIITFLMAGHDPTSGLLSFALYFLVKNPHVLQKVAEEAARVLVDPVPSYKQVKQLKYVGMVLN
EALRLWPTVPAFSLYAKEDTVLGGEYPLEKGDEVMVLIPQLHRDKTVWGDDVEEFRPERFENPS
AIPQHAFKPFGCGQRASIGQQFALHEATLVLGMMLKHFDFEDHTNYELDIKETQSLKPKGFVVK
AKSKKIPLGGIPSPSTEQSAKKVRKKAENAHNTPLLVLYGSNMGTAEGTARDLADIAMSKGFAP
QVATLDSHAGNLPREGAVLIVTASYNGHPPDNAKQFVDWLDQASADEVKGVRYSVFGCGDKNWA
TTYQKVPAFIDETLAAKGAENIADRGEADASDDFEGTYEEWREHMWSDVAAYFNLDIENSEDNK
STLSLQFVDSAADMPLAKMHGAFSTNVVASKELQQPGSARSTRHLEIELPKEASYQEGDHLGVI
PRNYEGIVNRVTARFGLDASQQIRLEAEEEKLAHLPLAKTVSVEELLQYVELQDPVTRTQLRAM
AAKTVCPPHKVELEALLEKQAYKEQVLAKRLTMLELLEKYPACEMKFSEFIALLPSIRPRYYSI
SSSPRVDEKQASITVSVVSGEAWSGYGEYKGIASNYLAELQEGDTITCFISTPQSEFTLPKDPE
TPLIMVGPGTGVAPFRGFVQARKQLKEQGQSLGEAHLYFGCRSPHEDYLYQEELENAQSEGIIT
LHTAFSRMPNQPKTYVQHVMEQDGKKLIELLDQGAHFYICGDGSQMAPAVEATLMKSYADVHQV
SEADARLWLQQLEEKGRYAKDVWAGLEHHHHHH

Nucleotide and amino acid sequences of P411-PA-G4:

ATGACAATTAAAGAAATGCCTCAGCCAAAAACGTTTGGAGAGCTTAAAAATTTACCGTTATTAA
ACACAGATAAACCGGTTCAAGCTTTGATGAAAATTGCGGATGAATTAGGAGAAATCTTTAAATT
CGAGGCGCCTGGTCGTGTAACGCGCTACTTATCAAGTCAGCGTCTAATTAAAGAAGCATGCGAT
GAATCACGCTTTGATAAAAACTTAACGCAAGCGCTGAAATTTATGCGTGATTTTCTTGGAGACG
GGTTAGCCACAAGCTGGACGCATGAAAAAAATTGGAAAAAAGCGCATAATATCTTACTTCCAAG
CTTTAGTCAGCAGGCAATGAAAGGCTATCATGCGATGATGGTCGATATCGCCGTGCAGCTTGTT
CAAAAGTGGGAGCGTCTAAATGCAGATGAGCATATTGAAGTATCGGAAGACATGACACGTTTAA
CGCTTGATACAATTGGTCTTTGCGGCTTTAACTATCGCTTTAACAGCTTTTACCGAGATCAGCC
TCATCCATTTATTATAAGTATGGTCCGTGCACTGGATGAAGTAATGAACAAGCTGCAGCGAGCA
AATCCAGACGACCCAGCTTATGATGAAAACAAGCGCCAGTTTCAAGAAGATATCAAGGTGATGA
ACGACCTAGTAGATAAAATTATTGCAGATCGCAAAGCAAGGGGTGAACAAAGCGATGATTTATT
AACGCAGATGCTAAACGGAAAAGATCCAGAAACGGGTGAGCCGCTTGATGACGGGAACATTCGC
TATCAAATTATTACATTCTTAATGGCGGGACACGATCCGACAAGTGGTCTTTTATCATTTGCGC
TGTATTTCTTAGTGAAAAATCCACATGTATTACAAAAAGTAGCAGAAGAAGCAGCACGAGTTCT
AGTAGATCCTGTTCCAAGCTACAAACAAGTCAAACAGCTTAAATATGTCGGCATGGTCTTAAAC
GAAGCGCTGCGCTTATGGCCAACTGTGCCTGCGTTTTCCCTATATGCAAAAGAAGATACGGTGC
TTGGAGGAGAATATCCTTTAGAAAAAGGCGACGAAGTAATGGTTCTGATTCCTCAGCTTCACCG
TGATAAAACAGTTTGGGGAGACGATGTGGAGGAGTTCCGTCCAGAGCGTTTTGAAAATCCAAGT
GCGATTCCGCAGCATGCGTTTAAACCGTTTGGATGTGGTCAGCGTGCGTCTATCGGTCAGCAGT
TCGCTCTTCATGAAGCAACGCTGGTACTTGGTATGATGCTAAAACACTTTGACTTTGAAGATCA
TACAAACTACGAGCTCGATATTAAAGAAACTCAGAGTTTAAAACCTAAAGGCTTTGTGGTAAAA
GCAAAATCGAAAAAAATTCCGCTTGGCGGTATTCCTTCACCTAGCACTGAACAGTCTGCTAAAA
AAGTACGCAAAAAGGCAGAAAACGCTCATAATACGCCGCTGCTTGTGCTATACGGTTCAAATAT
GGGTACCGCTGAAGGAACGGCGCGTGATTTAGCAGATATTGCAATGAGCAAAGGATTTGCACCG
CAGGTCGCAACGCTTGATTCACACGCCGGAAATCTTCCGCGCGAAGGAGCTGTATTAATTGTAA
CGGCGTCTTATAACGGTCATCCGCCTGATAACGCAAAGCAATTTGTCGACTGGTTAGACCAAGC
GTCTGCTGATGAAGTAAAAGGCGTTCGCTACTCCGTATTTGGATGCGGCGATAAAAACTGGGCT
ACTACGTATCAAAAAGTGCCTGCTTTTATCGATGAAACGCTTGCCGCTAAAGGGGCAGAAAACA
TCGCTGACCGCGGTGAAGCAGATGCAAGCGACGACTTTGAAGGCACATATGAAGAATGGCGTGA
ACATATGTGGAGTGACGTAGCAGCCTACTTTAACCTCGACATTGAAAACAGTGAAGATAATAAA
TCTACTCTTTCACTTCAATTTGTCGACAGCGCCGCGGATATGCCGCTTGCGAAAATGCACGGTG
CGTTTTCAACGAACGTCGTAGCAAGCAAAGAACTTCAACAGCCAGGCAGTGCACGAAGCACGCG

ACATCTTGAAATTGAACTTCCAAAAGAAGCTTCTTATCAAGAAGGAGATCATTTAGGTGTTATT
CCTCGCAACTATGAAGGAATAGTAAACCGTGTAACAGCAAGGTTCGGCCTAGATGCATCACAGC
AAATCCGTCTGGAAGCAGAAGAAGAAAAATTAGCTCATTTGCCACTCGCTAAAACAGTATCCGT
AGAAGAGCTTCTGCAATACGTGGAGCTTCAAGATCCTGTTACGCGCACGCAGCTTCGCGCAATG
GCTGCTAAAACGGTCTGCCCGCCGCATAAAGTAGAGCTTGAAGCCTTGCTTGAAAAGCAAGCCT
ACAAAGAACAAGTGCTGGCAAAACGTTTAACAATGCTTGAACTGCTTGAAAAATACCCGGCGTG
TGAAATGAAATTCAGCGAATTTATCGCCCTTCTGCCAAGCATACGCCCGCGCTATTACTCGATT
TCTTCATCACCTCGTGTCGATGAAAAACAAGCAAGCATCACGGTCAGCGTTGTCTCAGGAGAAG
CGTGGAGCGGATATGGAGAATATAAAGGAATTGCGTCGAACTATCTTGCCGAGCTGCAAGAAGG
AGATACGATTACGTGCTTTATTTCCACACCGCAGTCAGAATTTACGCTGCCAAAAGACCCTGAA
ACGCCGCTTATCATGGTCGGACCGGGAACAGGCGTCGCGCCGTTTAGAGGCTTTGTGCAGGCGC
GCAAACAGCTAAAAGAACAAGGACAGTCACTTGGAGAAGCACATTTATACTTCGGCTGCCGTTC
ACCTCATGAAGACTATCTGTATCAAGAAGAGCTTGAAAACGCCCAAAGCGAAGGCATCATTACG
CTTCATACCGCTTTTTCTCGCATGCCAAATCAGCCGAAAACATACGTTCAGCACGTAATGGAAC
AAGACGGCAAGAAATTGATTGAACTTCTTGATCAAGGAGCGCACTTCTATATTTGCGGAGACGG
AAGCCAAATGGCACCTGCCGTTGAAGCAACGCTTATGAAAAGCTATGCTGACGTTCACCAAGTG
AGTGAAGCAGACGCTCGCTTATGGCTGCAGCAGCTAGAAGAAAAAGGCCGATACGCAAAAGACG
TGTGGGCTGGGCTCGAGCACCACCACCACCACCACTGA

MTIKEMPQPKTFGELKNLPLLNTDKPVQALMKIADELGEIFKFEAPGRVTRYLSSQRLIKEACD
ESRFDKNLTQALKFMRDFLGDGLATSWTHEKNWKKAHNILLPSFSQQAMKGYHAMMVDIAVQLV
QKWERLNADEHIEVSEDMTRLTLDTIGLCGFNYRFNSFYRDQPHPFIISMVRALDEVMNKLQRA
NPDDPAYDENKRQFQEDIKVMNDLVDKIIADRKARGEQSDDLLTQMLNGKDPETGEPLDDGNIR
YQIITFLMAGHDPTSGLLSFALYFLVKNPHVLQKVAEEAARVLVDPVPSYKQVKQLKYVGMVLN
EALRLWPTVPAFSLYAKEDTVLGGEYPLEKGDEVMVLIPQLHRDKTVWGDDVEEFRPERFENPS
AIPQHAFKPFGCGQRASIGQQFALHEATLVLGMMLKHFDFEDHTNYELDIKETQSLKPKGFVVK
AKSKKIPLGGIPSPSTEQSAKKVRKKAENAHNTPLLVLYGSNMGTAEGTARDLADIAMSKGFAP
QVATLDSHAGNLPREGAVLIVTASYNGHPPDNAKQFVDWLDQASADEVKGVRYSVFGCGDKNWA
TTYQKVPAFIDETLAAKGAENIADRGEADASDDFEGTYEEWREHMWSDVAAYFNLDIENSEDNK
STLSLQFVDSAADMPLAKMHGAFSTNVVASKELQQPGSARSTRHLEIELPKEASYQEGDHLGVI

PRNYEGIVNRVTARFGLDASQQIRLEAEEEKLAHLPLAKTVSVEELLQYVELQDPVTRTQLRAM
AAKTVCPPHKVELEALLEKQAYKEQVLAKRLTMLELLEKYPACEMKFSEFIALLPSIRPRYYSI
SSSPRVDEKQASITVSVVSGEAWSGYGEYKGIASNYLAELQEGDTITCFISTPQSEFTLPKDPE
TPLIMVGPGTGVAPFRGFVQARKQLKEQGQSLGEAHLYFGCRSPHEDYLYQEELENAQSEGIIT
LHTAFSRMPNQPKTYVQHVMEQDGKKLIELLDQGAHFYICGDGSQMAPAVEATLMKSYADVHQV
SEADARLWLQQLEEKGRYAKDVWAGLEHHHHHH

Nucleotide and amino acid sequences of P411-PA-G5:

ATGACAATTAAAGAAATGCCTCAGCCAAAAACGTTTGGAGAGCTTAAAAATTTACCGTTATTAA
ACACAGATAAACCGGTTCAAGCTTTGATGAAAATTGCGGATGAATTAGGAGAAATCTTTAAATT
CGAGGCGCCTGGTCGTGTAACGCGCTACTTATCAAGTCAGCGTCTAATTAAAGAAGCATGCGAT
GAATCACGCTTTGATAAAAACTTAACGCAAGCGCTGAAATTTATGCGTGATTTTCTTGGAGACG
GGTTAGCCACAAGCTGGACGCATGAAAAAAATTGGAAAAAAGCGCATAATATCTTACTTCCAAG
CTTTAGTCAGCAGGCAATGAAAGGCTATCATGCGATGATGGTCGATATCGCCGTGCAGCTTGTT
CAAAAGTGGGAGCGTCTAAATGCAGATGAGCATATTGAAGTATCGGAAGACATGACACGTTTAA
CGCTTGATACAATTGGTCTTTGCGGCTTTAACTATCGCTTTAACAGCTTTTACCGAGATCAGCC
TCATCCATTTATTATAAGTATGGTCCGTGCACTGGATGAAGTAATGAACAAGCTGCAGCGAGCA
AATCCAGACGACCCAGCTTATGATGAAAACAAGCGCCAGTTTCAAGAAGATATCAAGGTGATGA
ACGACCTAGTAGATAAAATTATTGCAGATCGCAAAGCAAGGGGTGAACAAAGCGATGATTTATT
AACGCAGATGCTAAACGGAAAAGATCCAGAAACGGGTGAGCCGCTTGATGACGGGAACATTCGC
TATCAAATTATTACATTCTTAATGGCGGGACACGATCCGACAAGTGGTCTTTTATCATTTGCGC
TGTATTTCTTAGTGAAAAATCCACATGTATTACAAAAAGTAGCAGAAGAAGCAGCACGAGTTCT
AGTAGATCCTGTTCCAAGCTACAAACAAGTCAAACAGCTTAAATATGTCGGCATGGTCTTAAAC
GAAGCGCTGCGCTTATGGCCAACTGTGCCTGCGTTTTCCCTATATGCAAAAGAAGATACGGTGC
TTGGAGGAGAATATCCTTTAGAAAAAGGCGACGAAGTAATGGTTCTGATTCCTCAGCTTCACCG
TGATAAAACAGTTTGGGGAGACGATGTGGAGGAGTTCCGTCCAGAGCGTTTTGAAAATCCAAGT
GCGATTCCGCAGCATGCGTTTAAACCGTTTGGATGTGGTCAGCGTGCGTCTATCGGTCAGCAGT
TCGCTCTTCATGAAGCAACGCTGGTACTTGGTATGATGCTAAAACACTTTGACTTTGAAGATCA
TACAAACTACGAGCTCGATATTAAAGAAACTCAGGGTTTAAAACCTAAAGGCTTTGTGGTAAAA
GCAAAATCGAAAAAAATTCCGCTTGGCGGTATTCCTTCACCTAGCACTGAACAGTCTGCTAAAA

AAGTACGCAAAAAGGCAGAAAACGCTCATAATACGCCGCTGCTTGTGCTATACGGTTCAAATAT
GGGTACCGCTGAAGGAACGGCGCGTGATTTAGCAGATATTGCAATGAGCAAAGGATTTGCACCG
CAGGTCGCAACGCTTGATTCACACGCCGGAAATCTTCCGCGCGAAGGAGCTGTATTAATTGTAA
CGGCGTCTTATAACGGTCATCCGCCTGATAACGCAAAGCAATTTGTCGACTGGTTAGACCAAGC
GTCTGCTGATGAAGTAAAAGGCGTTCGCTACTCCGTATTTGGATGCGGCGATAAAAACTGGGCT
ACTACGTATCAAAAAGTGCCTGCTTTTATCGATGAAACGCTTGCCGCTAAAGGGGCAGAAAACA
TCGCTGACCGCGGTGAAGCAGATGCAAGCGACGACTTTGAAGGCACATATGAAGAATGGCGTGA
ACATATGTGGAGTGACGTAGCAGCCTACTTTAACCTCGACATTGAAAACAGTGAAGATAATAAA
TCTACTCTTTCACTTCAATTTGTCGACAGCGCCGCGGATATGCCGCTTGCGAAAATGCACGGTG
CGTTTTCAACGAACGTCGTAGCAAGCAAAGAACTTCAACAGCCAGGCAGTGCACGAAGCACGCG
ACATCTTGAAATTGAACTTCCAAAAGAAGCTTCTTATCAAGAAGGAGATCATTTAGGTGTTATT
CCTCGCAACTATGAAGGAATAGTAAACCGTGTAACAGCAAGGTTCGGCCTAGATGCATCACAGC
AAATCCGTCTGGAAGCAGAAGAAGAAAAATTAGCTCATTTGCCACTCGCTAAAACAGTATCCGT
AGAAGAGCTTCTGCAATACGTGGAGCTTCAAGATCCTGTTACGCGCACGCAGCTTCGCGCAATG
GCTGCTAAAACGGTCTGCCCGCCGCATAAAGTAGAGCTTGAAGCCTTGCTTGAAAAGCAAGCCT
ACAAAGAACAAGTGCTGGCAAAACGTTTAACAATGCTTGAACTGCTTGAAAAATACCCGGCGTG
TGAAATGAAATTCAGCGAATTTATCGCCCTTCTGCCAAGCATACGCCCGCGCTATTACTCGATT
TCTTCATCACCTCGTGTCGATGAAAAACAAGCAAGCATCACGGTCAGCGTTGTCTCAGGAGAAG
CGTGGAGCGGATATGGAGAATATAAAGGAATTGCGTCGAACTATCTTGCCGAGCTGCAAGAAGG
AGATACGATTACGTGCTTTATTTCCACACCGCAGTCAGAATTTACGCTGCCAAAAGACCCTGAA
ACGCCGCTTATCATGGTCGGACCGGGAACAGGCGTCGCGCCGTTTAGAGGCTTTGTGCAGGCGC
GCAAACAGCTAAAAGAACAAGGACAGTCACTTGGAGAAGCACATTTATACTTCGGCTGCCGTTC
ACCTCATGAAGACTATCTGTATCAAGAAGAGCTTGAAAACGCCCAAAGCGAAGGCATCATTACG
CTTCATACCGCTTTTTCTCGCATGCCAAATCAGCCGAAAACATACGTTCAGCACGTAATGGAAC
AAGACGGCAAGAAATTGATTGAACTTCTTGATCAAGGAGCGCACTTCTATATTTGCGGAGACGG
AAGCCAAATGGCACCTGCCGTTGAAGCAACGCTTATGAAAAGCTATGCTGACGTTCACCAAGTG
AGTGAAGCAGACGCTCGCTTATGGCTGCAGCAGCTAGAAGAAAAAGGCCGATACGCAAAAGACG
TGTGGGCTGGGCTCGAGCACCACCACCACCACTGA

MTIKEMPQPKTFGELKNLPLLNTDKPVQALMKIADELGEIFKFEAPGRVTRYLSSQRLIKEACD

ESRFDKNLTQALKFMRDFLGDGLATSWTHEKNWKKAHNILLPSFSQQAMKGYHAMMVDIAVQLV
QKWERLNADEHIEVSEDMTRLTLDTIGLCGFNYRFNSFYRDQPHPFIISMVRALDEVMNKLQRA
NPDDPAYDENKRQFQEDIKVMNDLVDKIIADRKARGEQSDDLLTQMLNGKDPETGEPLDDGNIR
YQIITFLMAGHDPTSGLLSFALYFLVKNPHVLQKVAEEAARVLVDPVPSYKQVKQLKYVGMVLN
EALRLWPTVPAFSLYAKEDTVLGGEYPLEKGDEVMVLIPQLHRDKTVWGDDVEEFRPERFENPS
AIPQHAFKPFGCGQRASIGQQFALHEATLVLGMMLKHFDFEDHTNYELDIKETQGLKPKGFVVK
AKSKKIPLGGIPSPSTEQSAKKVRKKAENAHNTPLLVLYGSNMGTAEGTARDLADIAMSKGFAP
QVATLDSHAGNLPREGAVLIVTASYNGHPPDNAKQFVDWLDQASADEVKGVRYSVFGCGDKNWA
TTYQKVPAFIDETLAAKGAENIADRGEADASDDFEGTYEEWREHMWSDVAAYFNLDIENSEDNK
STLSLQFVDSAADMPLAKMHGAFSTNVVASKELQQPGSARSTRHLEIELPKEASYQEGDHLGVI
PRNYEGIVNRVTARFGLDASQQIRLEAEEEKLAHLPLAKTVSVEELLQYVELQDPVTRTQLRAM
AAKTVCPPHKVELEALLEKQAYKEQVLAKRLTMLELLEKYPACEMKFSEFIALLPSIRPRYYSI
SSSPRVDEKQASITVSVVSGEAWSGYGEYKGIASNYLAELQEGDTITCFISTPQSEFTLPKDPE
TPLIMVGPGTGVAPFRGFVQARKQLKEQGQSLGEAHLYFGCRSPHEDYLYQEELENAQSEGIIT
LHTAFSRMPNQPKTYVQHVMEQDGKKLIELLDQGAHFYICGDGSQMAPAVEATLMKSYADVHQV
SEADARLWLQQLEEKGRYAKDVWAGLEHHHHHH

Nucleotide and amino acid sequences of P411-PA-G6:

ATGACAATTAAAGAAATGCCTCAGCCAAAAACGTTTGGAGAGCTTAAAAATTTACCGTTATTAA
ACACAGATAAACCGGTTCAAGCTTTGATGAAAATTGCGGATGAATTAGGAGAAATCTTTAAATT
CGAGGCGCCTGGTCGTGTAACGCGCTACTTATCAAGTCAGCGTCTAATTAAAGAAGCATGCGAT
GAATCACGCTTTGATAAAAACTTAACGCAAGCGCTGAAATTTATGCGTGATTTTCTTGGAGACG
GGTTAGCCACAAGCTGGACGCATGAAAAAAATTGGAAAAAAGCGCATAATATCTTACTTCCAAG
CTTTAGTCAGCAGGCAATGAAAGGCTATCATGCGATGATGGTCGATATCGCCGTGCAGCTTGTT
CAAAAGTGGGAGCGTCTAAATGCAGATGAGCATATTGAAGTATCGGAAGACATGACACGTTTAA
CGCTTGATACAATTGGTCTTTGCGGCTTTAACTATCGCTTTAACAGCTTTTACCGAGATCAGCC
TCATCCATTTATTATAAGTATGGTCCGTGCACTGGATGAAGTAATGAACAAGCTGCAGCGAGCA
AATCCAGACGACCCAGCTTATGATGAAAACAAGCGCCAGTTTCAAGAAGATATCAAGGTGATGA
ACGACCTAGTAGATAAAATTATTGCAGATCGCAAAGCAAGGGGTGAACAAAGCGATGATTTATT
AACGCAGATGCTAAACGGAAAAGATCCAGAAACGGGTGAGCCGCTTGATGACGGGAACATTCGC

TATCAAATTATTACATTCTTAATGGCGGGACACGATCCGGTTAGTGGTCTTTTATCATTTGCGC
TGTATTTCTTAGTGAAAAATCCACATGTATTACAAAAAGTAGCAGAAGAAGCAGCACGAGTTCT
AGTAGATCCTGTTCCAAGCTACAAACAAGTCAAACAGCTTAAATATGTCGGCATGGTCTTAAAC
GAAGCGCTGCGCTTATGGCCAACTGTGCCTGCGTTTTCCCTATATGCAAAAGAAGATACGGTGC
TTGGAGGAGAATATCCTTTAGAAAAAGGCGACGAAGTAATGGTTCTGATTCCTCAGCTTCACCG
TGATAAAACAGTTTGGGGAGACGATGTGGAGGAGTTCCGTCCAGAGCGTTTTGAAAATCCAAGT
GCGATTCCGCAGCATGCGTTTAAACCGTTTGGATGTGGTCAGCGTGCGTCTATCGGTCAGCAGT
TCGCTCTTCATGAAGCAACGCTGGTACTTGGTATGATGCTAAAACACTTTGACTTTGAAGATCA
TACAAACTACGAGCTCGATATTAAAGAAACTCAGGGTTTAAAACCTAAAGGCTTTGTGGTAAAA
GCAAAATCGAAAAAAATTCCGCTTGGCGGTATTCCTTCACCTAGCACTGAACAGTCTGCTAAAA
AAGTACGCAAAAAGGCAGAAAACGCTCATAATACGCCGCTGCTTGTGCTATACGGTTCAAATAT
GGGTACCGCTGAAGGAACGGCGCGTGATTTAGCAGATATTGCAATGAGCAAAGGATTTGCACCG
CAGGTCGCAACGCTTGATTCACACGCCGGAAATCTTCCGCGCGAAGGAGCTGTATTAATTGTAA
CGGCGTCTTATAACGGTCATCCGCCTGATAACGCAAAGCAATTTGTCGACTGGTTAGACCAAGC
GTCTGCTGATGAAGTAAAAGGCGTTCGCTACTCCGTATTTGGATGCGGCGATAAAAACTGGGCT
ACTACGTATCAAAAAGTGCCTGCTTTTATCGATGAAACGCTTGCCGCTAAAGGGGCAGAAAACA
TCGCTGACCGCGGTGAAGCAGATGCAAGCGACGACTTTGAAGGCACATATGAAGAATGGCGTGA
ACATATGTGGAGTGACGTAGCAGCCTACTTTAACCTCGACATTGAAAACAGTGAAGATAATAAA
TCTACTCTTTCACTTCAATTTGTCGACAGCGCCGCGGATATGCCGCTTGCGAAAATGCACGGTG
CGTTTTCAACGAACGTCGTAGCAAGCAAAGAACTTCAACAGCCAGGCAGTGCACGAAGCACGCG
ACATCTTGAAATTGAACTTCCAAAAGAAGCTTCTTATCAAGAAGGAGATCATTTAGGTGTTATT
CCTCGCAACTATGAAGGAATAGTAAACCGTGTAACAGCAAGGTTCGGCCTAGATGCATCACAGC
AAATCCGTCTGGAAGCAGAAGAAGAAAAATTAGCTCATTTGCCACTCGCTAAAACAGTATCCGT
AGAAGAGCTTCTGCAATACGTGGAGCTTCAAGATCCTGTTACGCGCACGCAGCTTCGCGCAATG
GCTGCTAAAACGGTCTGCCCGCCGCATAAAGTAGAGCTTGAAGCCTTGCTTGAAAAGCAAGCCT
ACAAAGAACAAGTGCTGGCAAAACGTTTAACAATGCTTGAACTGCTTGAAAAATACCCGGCGTG
TGAAATGAAATTCAGCGAATTTATCGCCCTTCTGCCAAGCATACGCCCGCGCTATTACTCGATT
TCTTCATCACCTCGTGTCGATGAAAAACAAGCAAGCATCACGGTCAGCGTTGTCTCAGGAGAAG
CGTGGAGCGGATATGGAGAATATAAAGGAATTGCGTCGAACTATCTTGCCGAGCTGCAAGAAGG
AGATACGATTACGTGCTTTATTTCCACACCGCAGTCAGAATTTACGCTGCCAAAAGACCCTGAA
ACGCCGCTTATCATGGTCGGACCGGGAACAGGCGTCGCGCCGTTTAGAGGCTTTGTGCAGGCGC
GCAAACAGCTAAAAGAACAAGGACAGTCACTTGGAGAAGCACATTTATACTTCGGCTGCCGTTC

ACCTCATGAAGACTATCTGTATCAAGAAGAGCTTGAAAACGCCCAAAGCGAAGGCATCATTACG
CTTCATACCGCTTTTTCTCGCATGCCAAATCAGCCGAAAACATACGTTCAGCACGTAATGGAAC
AAGACGGCAAGAAATTGATTGAACTTCTTGATCAAGGAGCGCACTTCTATATTTGCGGAGACGG
AAGCCAAATGGCACCTGCCGTTGAAGCAACGCTTATGAAAAGCTATGCTGACGTTCACCAAGTG
AGTGAAGCAGACGCTCGCTTATGGCTGCAGCAGCTAGAAGAAAAAGGCCGATACGCAAAAGACG
TGTGGGCTGGGCTCGAGCACCACCACCACCACCACTGA

MTIKEMPQPKTFGELKNLPLLNTDKPVQALMKIADELGEIFKFEAPGRVTRYLSSQRLIKEACD
ESRFDKNLTQALKFMRDFLGDGLATSWTHEKNWKKAHNILLPSFSQQAMKGYHAMMVDIAVQLV
QKWERLNADEHIEVSEDMTRLTLDTIGLCGFNYRFNSFYRDQPHPFIISMVRALDEVMNKLQRA
NPDDPAYDENKRQFQEDIKVMNDLVDKIIADRKARGEQSDDLLTQMLNGKDPETGEPLDDGNIR
YQIITFLMAGHDPVSGLLSFALYFLVKNPHVLQKVAEEAARVLVDPVPSYKQVKQLKYVGMVLN
EALRLWPTVPAFSLYAKEDTVLGGEYPLEKGDEVMVLIPQLHRDKTVWGDDVEEFRPERFENPS
AIPQHAFKPFGCGQRASIGQQFALHEATLVLGMMLKHFDFEDHTNYELDIKETQGLKPKGFVVK
AKSKKIPLGGIPSPSTEQSAKKVRKKAENAHNTPLLVLYGSNMGTAEGTARDLADIAMSKGFAP
QVATLDSHAGNLPREGAVLIVTASYNGHPPDNAKQFVDWLDQASADEVKGVRYSVFGCGDKNWA
TTYQKVPAFIDETLAAKGAENIADRGEADASDDFEGTYEEWREHMWSDVAAYFNLDIENSEDNK
STLSLQFVDSAADMPLAKMHGAFSTNVVASKELQQPGSARSTRHLEIELPKEASYQEGDHLGVI
PRNYEGIVNRVTARFGLDASQQIRLEAEEEKLAHLPLAKTVSVEELLQYVELQDPVTRTQLRAM
AAKTVCPPHKVELEALLEKQAYKEQVLAKRLTMLELLEKYPACEMKFSEFIALLPSIRPRYYSI
SSSPRVDEKQASITVSVVSGEAWSGYGEYKGIASNYLAELQEGDTITCFISTPQSEFTLPKDPE
TPLIMVGPGTGVAPFRGFVQARKQLKEQGQSLGEAHLYFGCRSPHEDYLYQEELENAQSEGIIT
LHTAFSRMPNQPKTYVQHVMEQDGKKLIELLDQGAHFYICGDGSQMAPAVEATLMKSYADVHQV
SEADARLWLQQLEEKGRYAKDVWAGLEHHHHHH

Nucleotide and amino acid sequences of P411-PA-G7:

ATGACAATTAAAGAAATGCCTCAGCCAAAAACGTTTGGAGAGCTTAAAAATTTACCGTTATTAA
ACACAGATAAACCGGTTCAAGCTTTGATGAAAATTGCGGATGAATTAGGAGAAATCTTTAAATT

CGAGGCGCCTGGTCGTGTAACGCGCTACTTATCAAGTCAGCGTCTAATTAAAGAAGCATGCGAT
GAATCACGCTTTGATAAAAACTTAACGCAAGCGCTGAAATTTATGCGTGATTTTCTTGGAGACG
GGTTAGCCACAAGCTGGACGCATGAAAAAAATTGGAAAAAAGCGCATAATATCTTACTTCCAAG
CTTTAGTCAGCAGGCAATGAAAGGCTATCATGCGATGATGGTCGATATCGCCGTGCAGCTTGTT
CAAAAGTGGGAGCGTCTAAATGCAGATGAGCATATTGAAGTATCGGAAGACATGACACGTTTAA
CGCTTGATACAATTGGTCTTTGCGGCTTTAACTATCGCTTTAACAGCTTTTACCGAGATCAGCC
TCATCCATTTATTATAAGTATGGTCCGTGCACTGGATGAAGTAATGAACAAGCTGCAGCGAGCA
AATCCAGACGACCCAGCTTATGATGAAAACAAGCGCCAGTTTCAAGAAGATATCAAGGTGATGA
ACGACCTAGTAGATAAAATTATTGCAGATCGCAAAGCAAGGGGTGAACAAAGCGATGATTTATT
AACGCAGATGCTAAACGGAAAAGATCCAGAAACGGGTGAGCCGCTTGATGACGGGAACATTCGC
TATCAAATTATTACATTCTTAATGGCGGGAAGTGATCCGGTTAGTGGTCTTTTATCATTTGCGC
TGTATTTCTTAGTGAAAAATCCACATGTATTACAAAAAGTAGCAGAAGAAGCAGCACGAGTTCT
AGTAGATCCTGTTCCAAGCTACAAACAAGTCAAACAGCTTAAATATGTCGGCATGGTCTTAAAC
GAAGCGCTGCGCTTATGGCCAACTGTGCCTGCGTTTTCCCTATATGCAAAAGAAGATACGGTGC
TTGGAGGAGAATATCCTTTAGAAAAAGGCGACGAAGTAATGGTTCTGATTCCTCAGCTTCACCG
TGATAAAACAGTTTGGGGAGACGATGTGGAGGAGTTCCGTCCAGAGCGTTTTGAAAATCCAAGT
GCGATTCCGCAGCATGCGTTTAAACCGTTTGGATGTGGTCAGCGTGCGTCTATCGGTCAGCAGT
TCGCTCTTCATGAAGCAACGCTGGTACTTGGTATGATGCTAAAACACTTTGACTTTGAAGATCA
TACAAACTACGAGCTCGATATTAAAGAAACTCAGGGTTTAAAACCTAAAGGCTTTGTGGTAAAA
GCAAAATCGAAAAAAATTCCGCTTGGCGGTATTCCTTCACCTAGCACTGAACAGTCTGCTAAAA
AAGTACGCAAAAAGGCAGAAAACGCTCATAATACGCCGCTGCTTGTGCTATACGGTTCAAATAT
GGGTACCGCTGAAGGAACGGCGCGTGATTTAGCAGATATTGCAATGAGCAAAGGATTTGCACCG
CAGGTCGCAACGCTTGATTCACACGCCGGAAATCTTCCGCGCGAAGGAGCTGTATTAATTGTAA
CGGCGTCTTATAACGGTCATCCGCCTGATAACGCAAAGCAATTTGTCGACTGGTTAGACCAAGC
GTCTGCTGATGAAGTAAAAGGCGTTCGCTACTCCGTATTTGGATGCGGCGATAAAAACTGGGCT
ACTACGTATCAAAAAGTGCCTGCTTTTATCGATGAAACGCTTGCCGCTAAAGGGGCAGAAAACA
TCGCTGACCGCGGTGAAGCAGATGCAAGCGACGACTTTGAAGGCACATATGAAGAATGGCGTGA
ACATATGTGGAGTGACGTAGCAGCCTACTTTAACCTCGACATTGAAAACAGTGAAGATAATAAA
TCTACTCTTTCACTTCAATTTGTCGACAGCGCCGCGGATATGCCGCTTGCGAAAATGCACGGTG
CGTTTTCAACGAACGTCGTAGCAAGCAAAGAACTTCAACAGCCAGGCAGTGCACGAAGCACGCG
ACATCTTGAAATTGAACTTCCAAAAGAAGCTTCTTATCAAGAAGGAGATCATTTAGGTGTTATT
CCTCGCAACTATGAAGGAATAGTAAACCGTGTAACAGCAAGGTTCGGCCTAGATGCATCACAGC

AAATCCGTCTGGAAGCAGAAGAAGAAAAATTAGCTCATTTGCCACTCGCTAAAACAGTATCCGT
AGAAGAGCTTCTGCAATACGTGGAGCTTCAAGATCCTGTTACGCGCACGCAGCTTCGCGCAATG
GCTGCTAAAACGGTCTGCCCGCCGCATAAAGTAGAGCTTGAAGCCTTGCTTGAAAAGCAAGCCT
ACAAAGAACAAGTGCTGGCAAAACGTTTAACAATGCTTGAACTGCTTGAAAAATACCCGGCGTG
TGAAATGAAATTCAGCGAATTTATCGCCCTTCTGCCAAGCATACGCCCGCGCTATTACTCGATT
TCTTCATCACCTCGTGTCGATGAAAAACAAGCAAGCATCACGGTCAGCGTTGTCTCAGGAGAAG
CGTGGAGCGGATATGGAGAATATAAAGGAATTGCGTCGAACTATCTTGCCGAGCTGCAAGAAGG
AGATACGATTACGTGCTTTATTTCCACACCGCAGTCAGAATTTACGCTGCCAAAAGACCCTGAA
ACGCCGCTTATCATGGTCGGACCGGGAACAGGCGTCGCGCCGTTTAGAGGCTTTGTGCAGGCGC
GCAAACAGCTAAAAGAACAAGGACAGTCACTTGGAGAAGCACATTTATACTTCGGCTGCCGTTC
ACCTCATGAAGACTATCTGTATCAAGAAGAGCTTGAAAACGCCCAAAGCGAAGGCATCATTACG
CTTCATACCGCTTTTTCTCGCATGCCAAATCAGCCGAAAACATACGTTCAGCACGTAATGGAAC
AAGACGGCAAGAAATTGATTGAACTTCTTGATCAAGGAGCGCACTTCTATATTTGCGGAGACGG
AAGCCAAATGGCACCTGCCGTTGAAGCAACGCTTATGAAAAGCTATGCTGACGTTCACCAAGTG
AGTGAAGCAGACGCTCGCTTATGGCTGCAGCAGCTAGAAGAAAAAGGCCGATACGCAAAAGACG
TGTGGGCTGGGCTCGAGCACCACCACCACCACTGA

MTIKEMPQPKTFGELKNLPLLNTDKPVQALMKIADELGEIFKFEAPGRVTRYLSSQRLIKEACD
ESRFDKNLTQALKFMRDFLGDGLATSWTHEKNWKKAHNILLPSFSQQAMKGYHAMMVDIAVQLV
QKWERLNADEHIEVSEDMTRLTLDTIGLCGFNYRFNSFYRDQPHPFIISMVRALDEVMNKLQRA
NPDDPAYDENKRQFQEDIKVMNDLVDKIIADRKARGEQSDDLLTQMLNGKDPETGEPLDDGNIR
YQIITFLMAGSDPVSGLLSFALYFLVKNPHVLQKVAEEAARVLVDPVPSYKQVKQLKYVGMVLN
EALRLWPTVPAFSLYAKEDTVLGGEYPLEKGDEVMVLIPQLHRDKTVWGDDVEEFRPERFENPS
AIPQHAFKPFGCGQRASIGQQFALHEATLVLGMMLKHFDFEDHTNYELDIKETQGLKPKGFVVK
AKSKKIPLGGIPSPSTEQSAKKVRKKAENAHNTPLLVLYGSNMGTAEGTARDLADIAMSKGFAP
QVATLDSHAGNLPREGAVLIVTASYNGHPPDNAKQFVDWLDQASADEVKGVRYSVFGCGDKNWA
TTYQKVPAFIDETLAAKGAENIADRGEADASDDFEGTYEEWREHMWSDVAAYFNLDIENSEDNK
STLSLQFVDSAADMPLAKMHGAFSTNVVASKELQQPGSARSTRHLEIELPKEASYQEGDHLGVI
PRNYEGIVNRVTARFGLDASQQIRLEAEEEKLAHLPLAKTVSVEELLQYVELQDPVTRTQLRAM
AAKTVCPPHKVELEALLEKQAYKEQVLAKRLTMLELLEKYPACEMKFSEFIALLPSIRPRYYSI

SSSPRVDEKQASITVSVVSGEAWSGYGEYKGIASNYLAELQEGDTITCFISTPQSEFTLPKDPE
TPLIMVGPGTGVAPFRGFVQARKQLKEQGQSLGEAHLYFGCRSPHEDYLYQEELENAQSEGIIT
LHTAFSRMPNQPKTYVQHVMEQDGKKLIELLDQGAHFYICGDGSQMAPAVEATLMKSYADVHQV
SEADARLWLQQLEEKGRYAKDVWAGLEHHHHHH

Nucleotide and amino acid sequences of P411-PA-G8:

ATGACAATTAAAGAAATGCCTCAGCCAAAAACGTTTGGAGAGCTTAAAAATTTACCGTTATTAA
ACACAGATAAACCGGTTCAAGCTTTGATGAAAATTGCGGATGAATTAGGAGAAATCTTTAAATT
CGAGGCGCCTGGTCGTGTAACGCGCTACTTATCAAGTCAGCGTCTAATTAAAGAAGCATGCGAT
GAATCACGCTTTGATAAAAACTTAACGCAAAAGCTGAAATTTATGCGTGATTTTCTTGGAGACG
GGTTAGCCACAAGCTGGACGCATGAAAAAAATTGGAAAAAAGCGCATAATATCTTACTTCCAAG
CTTTAGTCAGCAGGCAATGAAAGGCTATCATGCGATGATGGTCGATATCGCCGTGCAGCTTGTT
CAAAAGTGGGAGCGTCTAAATGCAGATGAGCATATTGAAGTATCGGAAGACATGACACGTTTAA
CGCTTGATACAATTGGTCTTTGCGGCTTTAACTATCGCTTTAACAGCTTTTACCGAGATCAGCC
TCATCCATTTATTATAAGTATGGTCCGTGCACTGGATGAAGTAATGAACAAGCTGCAGCGAGCA
AATCCAGACGACCCAGCTTATGATGAAAACAAGCGCCAGTTTCAAGAAGATATCAAGGTGATGA
ACGACCTAGTAGATAAAATTATTGCAGATCGCAAAGCAAGGGGTGAACAAAGCGATGATTTATT
AACGCAGATGCTAAACGGAAAAGATCCAGAAACGGGTGAGCCGCTTGATGACGGGAACATTCGC
TATCAAATTATTACATTCTTAATGGCGGGAAGTGATCCGGTTAGTGGTCTTTTATCATTTGCGC
TGTATTTCTTAGTGAAAAATCCACATGTATTACAAAAAGTAGCAGAAGAAGCAGCACGAGTTCT
AGTAGATCCTGTTCCAAGCTACAAACAAGTCAAACAGCTTAAATATGTCGGCATGGTCTTAAAC
GAAGCGCTGCGCTTATGGCCAACTGTGCCTGCGTTTTCCCTATATGCAAAAGAAGATACGGTGC
TTGGAGGAGAATATCCTTTAGAAAAAGGCGACGAAGTAATGGTTCTGATTCCTCAGCTTCACCG
TGATAAAACAGTTTGGGGAGACGATGTGGAGGAGTTCCGTCCAGAGCGTTTTGAAAATCCAAGT
GCGATTCCGCAGCATGCGTTTAAACCGTTTGGATGTGGTCAGCGTGCGTCTATCGGTCAGCAGT
TCGCTCTTCATGAAGCAACGCTGGTACTTGGTATGATGCTAAAACACTTTGACTTTGAAGATCA
TACAAACTACGAGCTCGATATTAAAGAAACTCAGGGTTTAAAACCTAAAGGCTTTGTGGTAAAA
GCAAAATCGAAAAAAATTCCGCTTGGCGGTATTCCTTCACCTAGCACTGAACAGTCTGCTAAAA
AAGTACGCAAAAAGGCAGAAAACGCTCATAATACGCCGCTGCTTGTGCTATACGGTTCAAATAT
GGGTACCGCTGAAGGAACGGCGCGTGATTTAGCAGATATTGCAATGAGCAAAGGATTTGCACCG

CAGGTCGCAACGCTTGATTCACACGCCGGAAATCTTCCGCGCGAAGGAGCTGTATTAATTGTAA
CGGCGTCTTATAACGGTCATCCGCCTGATAACGCAAAGCAATTTGTCGACTGGTTAGACCAAGC
GTCTGCTGATGAAGTAAAAGGCGTTCGCTACTCCGTATTTGGATGCGGCGATAAAAACTGGGCT
ACTACGTATCAAAAAGTGCCTGCTTTTATCGATGAAACGCTTGCCGCTAAAGGGGCAGAAAACA
TCGCTGACCGCGGTGAAGCAGATGCAAGCGACGACTTTGAAGGCACATATGAAGAATGGCGTGA
ACATATGTGGAGTGACGTAGCAGCCTACTTTAACCTCGACATTGAAAACAGTGAAGATAATAAA
TCTACTCTTTCACTTCAATTTGTCGACAGCGCCGCGGATATGCCGCTTGCGAAAATGCACGGTG
CGTTTTCAACGAACGTCGTAGCAAGCAAAGAACTTCAACAGCCAGGCAGTGCACGAAGCACGCG
ACATCTTGAAATTGAACTTCCAAAAGAAGCTTCTTATCAAGAAGGAGATCATTTAGGTGTTATT
CCTCGCAACTATGAAGGAATAGTAAACCGTGTAACAGCAAGGTTCGGCCTAGATGCATCACAGC
AAATCCGTCTGGAAGCAGAAGAAGAAAAATTAGCTCATTTGCCACTCGCTAAAACAGTATCCGT
AGAAGAGCTTCTGCAATACGTGGAGCTTCAAGATCCTGTTACGCGCACGCAGCTTCGCGCAATG
GCTGCTAAAACGGTCTGCCCGCCGCATAAAGTAGAGCTTGAAGCCTTGCTTGAAAAGCAAGCCT
ACAAAGAACAAGTGCTGGCAAAACGTTTAACAATGCTTGAACTGCTTGAAAAATACCCGGCGTG
TGAAATGAAATTCAGCGAATTTATCGCCCTTCTGCCAAGCATACGCCCGCGCTATTACTCGATT
TCTTCATCACCTCGTGTCGATGAAAAACAAGCAAGCATCACGGTCAGCGTTGTCTCAGGAGAAG
CGTGGAGCGGATATGGAGAATATAAAGGAATTGCGTCGAACTATCTTGCCGAGCTGCAAGAAGG
AGATACGATTACGTGCTTTATTTCCACACCGCAGTCAGAATTTACGCTGCCAAAAGACCCTGAA
ACGCCGCTTATCATGGTCGGACCGGGAACAGGCGTCGCGCCGTTTAGAGGCTTTGTGCAGGCGC
GCAAACAGCTAAAAGAACAAGGACAGTCACTTGGAGAAGCACATTTATACTTCGGCTGCCGTTC
ACCTCATGAAGACTATCTGTATCAAGAAGAGCTTGAAAACGCCCAAAGCGAAGGCATCATTACG
CTTCATACCGCTTTTTCTCGCATGCCAAATCAGCCGAAAACATACGTTCAGCACGTAATGGAAC
AAGACGGCAAGAAATTGATTGAACTTCTTGATCAAGGAGCGCACTTCTATATTTGCGGAGACGG
AAGCCAAATGGCACCTGCCGTTGAAGCAACGCTTATGAAAAGCTATGCTGACGTTCACCAAGTG
AGTGAAGCAGACGCTCGCTTATGGCTGCAGCAGCTAGAAGAAAAAGGCCGATACGCAAAAGACG
TGTGGGCTGGGCTCGAGCACCACCACCACCACTGA

MTIKEMPQPKTFGELKNLPLLNTDKPVQALMKIADELGEIFKFEAPGRVTRYLSSQRLI
KEACDESRFDKNLTQKLKFMRDFLGDGLATSWTHEKNWKKAHNILLPSFSQQAMKGYHAMMVDI
AVQLVQKWERLNADEHIEVSEDMTRLTLDTIGLCGFNYRFNSFYRDQPHPFIISMVRALDEVMN

KLQRANPDDPAYDENKRQFQEDIKVMNDLVDKIIADRKARGEQSDDLLTQMLNGKDPETGEPLD
DGNIRYQIITFLMAGSDPVSGLLSFALYFLVKNPHVLQKVAEEAARVLVDPVPSYKQVKQLKYV
GMVLNEALRLWPTVPAFSLYAKEDTVLGGEYPLEKGDEVMVLIPQLHRDKTVWGDDVEEFRPER
FENPSAIPQHAFKPFGCGQRASIGQQFALHEATLVLGMMLKHFDFEDHTNYELDIKETQGLKPK
GFVVKAKSKKIPLGGIPSPSTEQSAKKVRKKAENAHNTPLLVLYGSNMGTAEGTARDLADIAMS
KGFAPQVATLDSHAGNLPREGAVLIVTASYNGHPPDNAKQFVDWLDQASADEVKGVRYSVFGCG
DKNWATTYQKVPAFIDETLAAKGAENIADRGEADASDDFEGTYEEWREHMWSDVAAYFNLDIEN
SEDNKSTLSLQFVDSAADMPLAKMHGAFSTNVVASKELQQPGSARSTRHLEIELPKEASYQEGD
HLGVIPRNYEGIVNRVTARFGLDASQQIRLEAEEEKLAHLPLAKTVSVEELLQYVELQDPVTRT
QLRAMAAKTVCPPHKVELEALLEKQAYKEQVLAKRLTMLELLEKYPACEMKFSEFIALLPSIRP
RYYSISSSPRVDEKQASITVSVVSGEAWSGYGEYKGIASNYLAELQEGDTITCFISTPQSEFTL
PKDPETPLIMVGPGTGVAPFRGFVQARKQLKEQGQSLGEAHLYFGCRSPHEDYLYQEELENAQS
EGIITLHTAFSRMPNQPKTYVQHVMEQDGKKLIELLDQGAHFYICGDGSQMAPAVEATLMKSYA
DVHQVSEADARLWLQQLEEKGRYAKDVWAGLEHHHHHH

IX. Computational methods

All DFT calculations were performed using the Gaussian16 software[13] on the Hoffman2 Cluster at UCLA. A truncated computational model has been used, which includes the porphyrin pyrrole core, the Fe(II) center and a methanol molecule to mimic the axial serine. This model is similar to those used in previous computational mechanistic studies of heme-dependent enzymatic reactions.[14,15] Two protonation states for the axial serine have been modelled, using a methanol (protonated state) or a methoxy (deprotonated state) molecule. Geometry optimizations were performed using dispersion corrected (U)B3LYP-D3(BJ)[16–19] density functional in combination with the SDD basis set for Fe and 6-31G(d) for other atoms. All the optimized transition states were confirmed by the intrinsic reaction coordinate (IRC) calculations, which connect the corresponding reactants and intermediates (or intermediates and products). Single-point energy calculations were carried out at Def2TZVP level, using SMD solvation model[20] with diethyl ether (ε=4) solvent to simulate the dielectric permittivity in the enzyme active site.[21–23] A quasi-harmonic corrections to entropy using Grimme's method[24] with a frequency cut-off value of 100 cm^{-1} was applied to the entropy calculations using the Goodvibes software.[25] Therefore, all energies are reported at the B3LYP-D3(BJ)/Def2TZVP (SMD, ε=4)//B3LYP-D3(BJ)/6-31G(d)+SDD(Fe) level of theory. This methodology is similar to the previously used to investigate the mechanism of iron porphyrin-catalyzed carbene and oxo transfer reactions.[15,25–28] The open-shell electronic state was modelled by using a Gaussian16 "stable = opt" calculation[29–31] to generate a singlet open-shell orbital guess from the triplet optimized geometry, followed by a full optimization of the system starting from this guess. Optimized DFT structures are illustrated with CYLView.[32]

Computational modelling of the Fe-heme catalyzed amination of propargylic C(sp^3)–H bonds.

Similar to previously studied iron porphyrin-catalyzed C–H amination reactions,[15,33] the propargylic amination reaction first proceeds through a hydrogen atom transfer (HAT) step, and then undergoes a radical rebound to form the propargyl amine product. Figures S3 and S4 report the calculated energy profiles in the singlet closed-shell (CSS), singlet open-shell (OSS), triplet and quintet electronic states in green, blue, black, and red, respectively.

DFT calculations carried out for the deprotonated axial serine model (**Figure A.S3**), described that the electronic ground state of iron-nitrenoid **0** is the triplet state. Calculations revealed that the corresponding CSS, singlet OSS, and quintet are 11.1 kcal/mol, 8.6 kcal/mol, and 8.4 kcal/mol higher in energy than the triplet. The propargyl radical intermediate **2** is generated via a hydrogen atom transfer (HAT) transition state **TS1** ($\Delta G^{\ddagger}$ = 14.7 kcal/mol, triplet lowest in energy). The CSS, OSS and quintet HAT **TS1** are higher in energy than the triplet. The second step corresponds to the new C–N bond formation through rebound **TS2**. Our calculations describe that the triplet rebound transition state **TS2** is the lowest in energy, with an energy barrier of $\Delta G^{\ddagger}$ = 8.2 kcal/mol, and it is 19.8 kcal/mol and 8.5 kcal/mol lower in energy than the OSS and quintet states, respectively. The higher in energy CSS electronic state is found to directly lead to the final product via **TS1**.

For the protonated axial serine model (**Figure A.S4**), the triplet state of the iron-nitrenoid **4** is also found to be the electronic ground state, being 8.1 kcal/mol, 5.7 kcal/mol and 8.0 kcal/mol lower in energy than the CSS, OSS and quintet, respectively. Calculations indicate that protonation of the axial serine would slightly increase the HAT barrier. The iron-nitrenoid **4** undergoes a HAT step via a lowest in energy quintet transition state **TS3** ($\Delta G^{\ddagger}$ = 18.9 kcal/mol), involving a two-state reactivity. In this case, the quintet HAT **TS3** is 1.8, 2.9 and 7.1 kcal/mol lower in energy than the triplet, the OSS and the CSS **TS3**, respectively. The HAT step generates a radical intermediate **6** with a quintet ground state, which undergoes a radical rebound through **TS4** with a barrier of $\Delta G^{\ddagger}$ = 5.4 kcal/mol (quintet lowest in energy). The quintet **TS4** is 6.2 kcal/mol and 9.2 kcal/mol lower in energy than the triplet and the OSS **TS4**, respectively.

Taken together, our DFT calculations revealed a stepwise mechanism in the propargylic C–H amination reaction involving nitrenoid **0** (or **4**), preferentially occurring on the triplet potential energy surface in the deprotonated axial serine model (**Figure A.S3**) and the quintet potential energy surface in the protonated axial serine model (**Figure A.S4**). Calculations suggest a change on the preferred nitrenoid spin state due to axial serine protonation, which also affects to the HAT (**TS1**, **TS3**) and rebound (**TS2**, **TS4**) energy barriers.

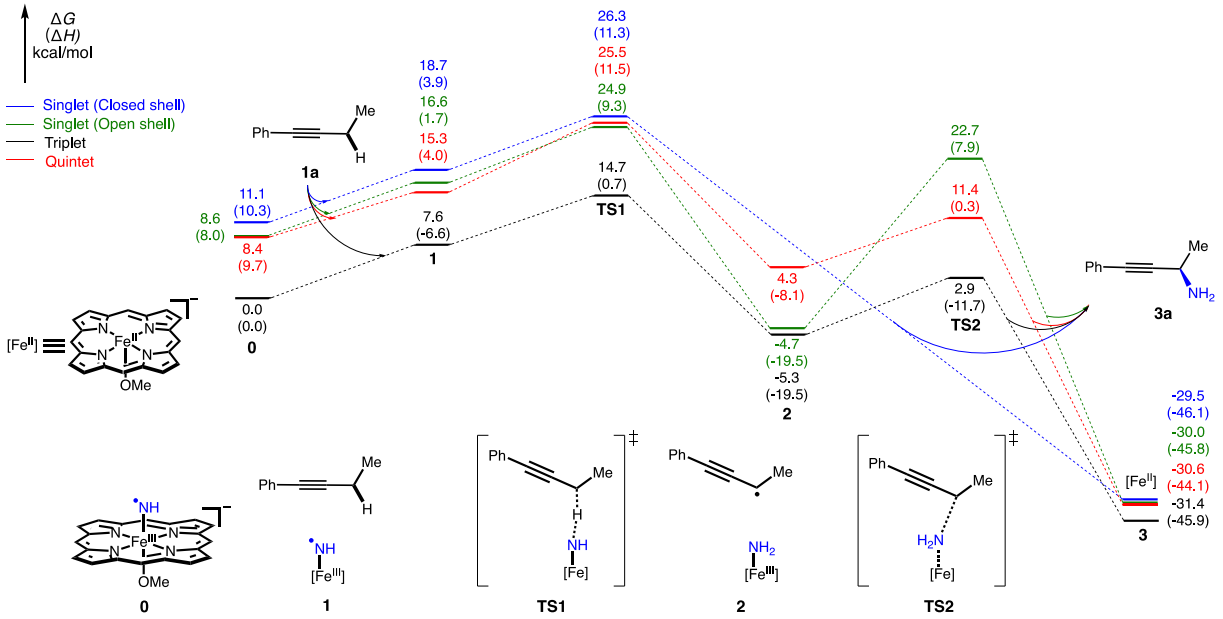

Figure A.S3. Singlet, triplet, and quintet free energy profiles of the iron porphyrin-catalyzed (deprotonated model) C–H amination.

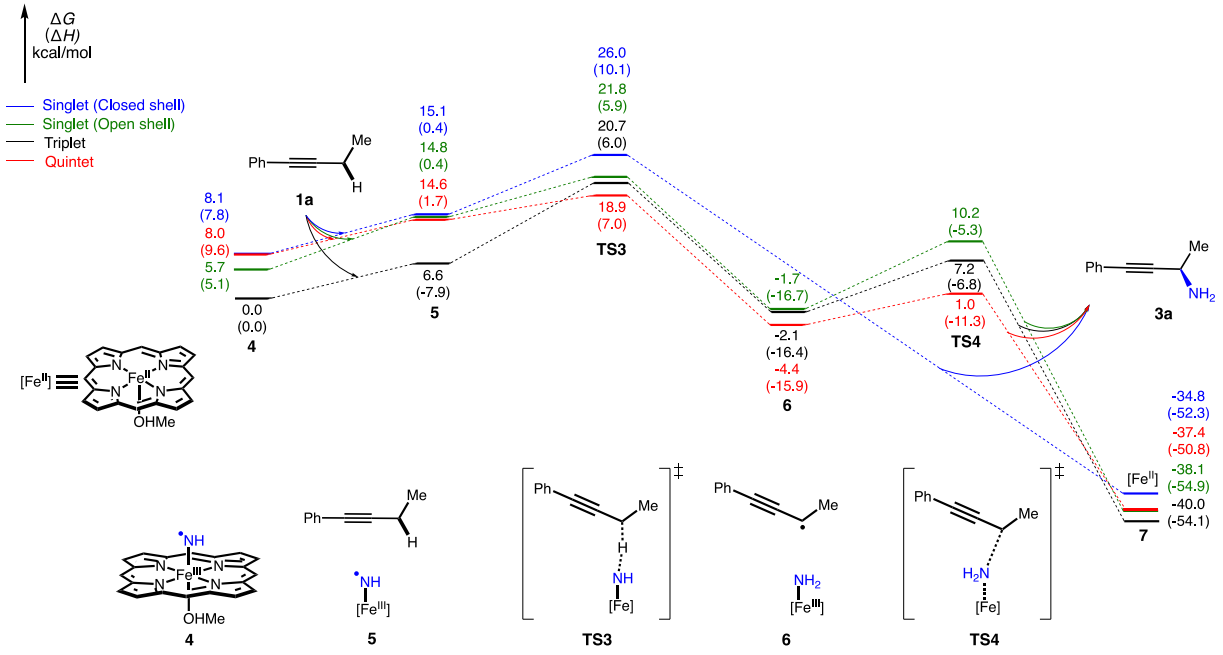

Figure A.S4. Singlet, triplet, and quintet free energy profiles of the iron porphyrin-catalyzed (protonated model) C–H amination.

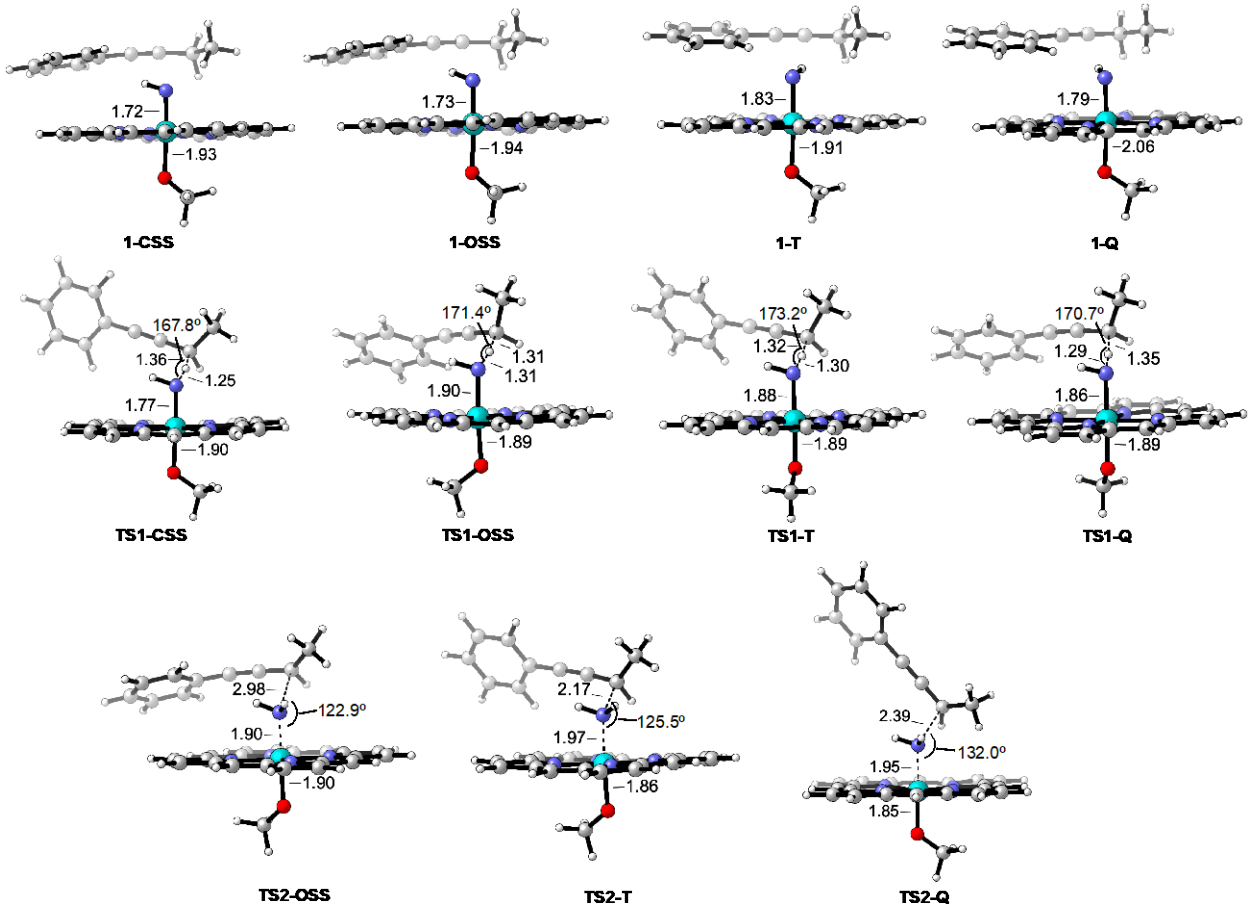

Figure A.S5. Optimized structures of iron porphyrin nitrenoid **1**, HAT transition states **TS1**, and radical rebound transition states **TS2** with deprotonated model in closed-shell singlet (CSS), open-shell singlet (OSS), triplet (T), and quintet (Q) states.

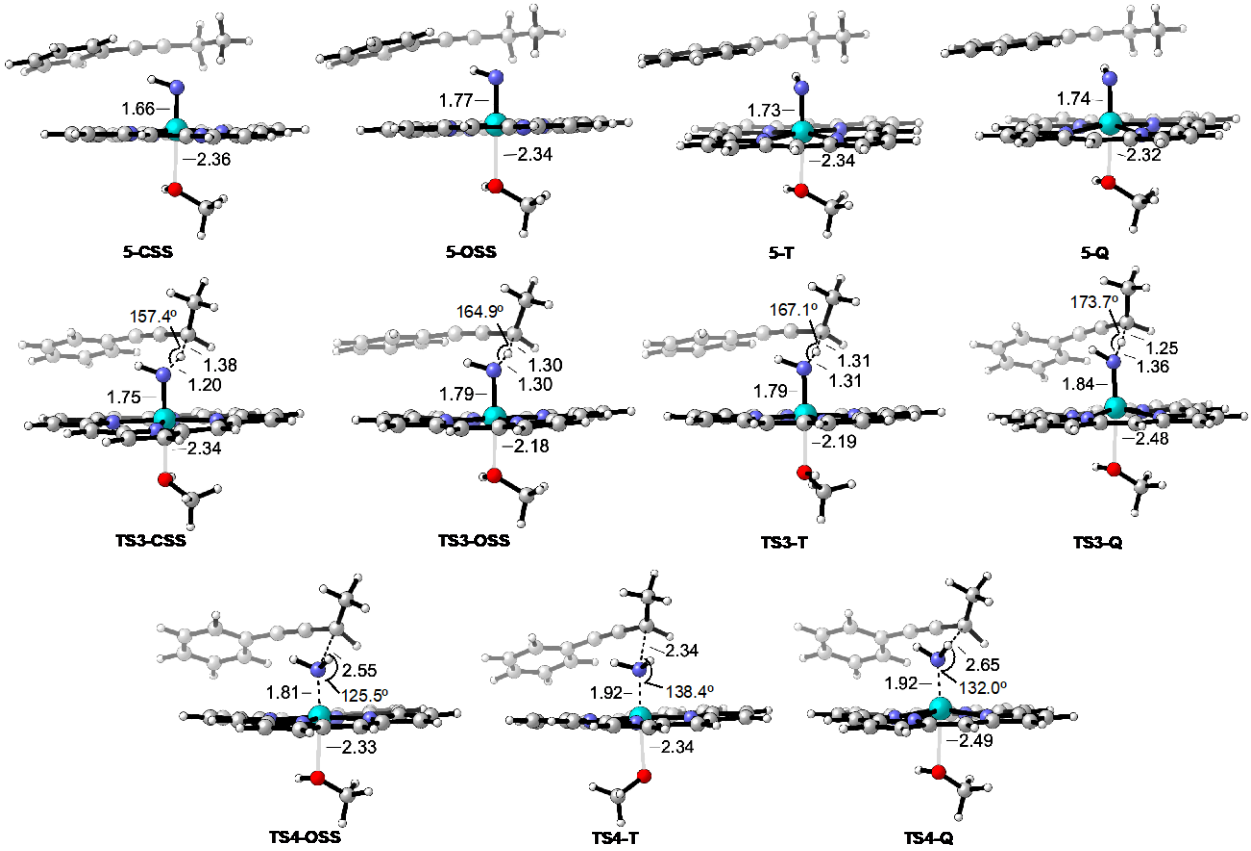

Figure A.S6. Optimized structures of iron porphyrin nitrenoid **4**, HAT transition states **TS3**, and radical rebound transition states **TS4** with protonated model in closed-shell singlet (CSS), open-shell singlet (OSS), triplet (T), and quintet (Q) states.

Table A.S4. **DFT optimized deprotonated model geometries**. Energies and thermochemistry parameters (at T = 298.15 K and P = 1 atm) of all computationally characterized stationary points: Electronic energies (E), Zero point energy (ZPE), enthalpy (H), entropic term (T.S), quasi harmonic corrected entropic term (T.qh-S), free energy (G(T)), quasi harmonic corrected free energy (qh-G(T)). All energies are given in a.u.

	E	ZPE	H	T.S	T.qh-S	G(T)	qh-G(T)
1a	-387.06652	0.167431	-386.88861	0.049506	0.046515	-386.93812	-386.93513
0-CSS	-1282.9095	0.32904	-1282.5574	0.072465	0.070186	-1282.6298	-1282.6275
0-OSS	-1282.9122	0.328513	-1282.5604	0.072759	0.070409	-1282.6332	-1282.6309
0-T	-1282.9255	0.328041	-1282.5741	0.073656	0.07151	-1282.6478	-1282.6456
0-Q	-1282.9124	0.325976	-1282.5625	0.07578	0.073364	-1282.6383	-1282.6359
1-CSS	-1669.993	0.497766	-1669.4609	0.099612	0.092913	-1669.5605	-1669.5538
1-OSS	-1669.9957	0.497362	-1669.4639	0.099379	0.092885	-1669.5633	-1669.5568
1-T	-1670.011	0.497226	-1669.4793	0.100624	0.094084	-1669.5799	-1669.5734
1-Q	-1669.9978	0.496935	-1669.4652	0.105145	0.097843	-1669.5703	-1669.563
TS1-CSS	-1669.9756	0.492606	-1669.4492	0.099202	0.092143	-1669.5484	-1669.5414
TS1-OSS	-1669.9934	0.491726	-1669.4677	0.098291	0.091833	-1669.566	-1669.5596
TS1-T	-1669.9924	0.491587	-1669.4668	0.100896	0.093754	-1669.5677	-1669.5605
TS1-Q	-1669.9777	0.489562	-1669.4537	0.100886	0.09451	-1669.5546	-1669.5483
2-OSS	-1670.0301	0.496181	-1669.4993	0.099606	0.093194	-1669.5989	-1669.5924
2-T	-1670.0301	0.496175	-1669.4993	0.100561	0.094189	-1669.5998	-1669.5934
2-Q	-1670.0165	0.493449	-1669.4876	0.103413	0.096676	-1669.591	-1669.5843
TS2-OSS	-1670.0224	0.495503	-1669.4926	0.099467	0.092772	-1669.592	-1669.5853
TS2-T	-1670.0203	0.496794	-1669.4896	0.099838	0.093048	-1669.5894	-1669.5826
TS2-Q	-1670.0069	0.493558	-1669.4784	0.105501	0.097143	-1669.5839	-1669.5755
3-3a CSS	-1670.0753	0.502285	-1669.5397	0.096645	0.090463	-1669.6364	-1669.6302
3-3a OSS	-1670.0749	0.502308	-1669.5392	0.097926	0.091086	-1669.6371	-1669.6303
3-3a T	-1670.0761	0.499662	-1669.5421	0.100092	0.093693	-1669.6422	-1669.6358
3-3a Q	-1670.0883	0.498384	-1669.5553	0.101681	0.095045	-1669.657	-1669.6503

Table A.S5. **DFT optimized protonated model geometries**. Energies and thermochemistry parameters (at T = 298.15 K and P = 1 atm) of all computationally characterized stationary points:

Electronic energies (E), Zero point energy (ZPE), enthalpy (H), entropic term (T.S), quasi harmonic corrected entropic term (T.qh-S), free energy (G(T)), quasi harmonic corrected free energy (qh-G(T)). All energies are given in a.u.

	E	ZPE	H	T.S	T.qh-S	G(T)	qh-G(T)
1a	-387.06652	0.167431	-386.88861	0.049506	0.046515	-386.93812	-386.93513
4-CSS	-1283.485	0.344429	-1283.1167	0.074774	0.072076	-1283.1915	-1283.1888
4-OSS	-1283.4889	0.344273	-1283.1208	0.074235	0.07171	-1283.1951	-1283.1925
4-T	-1283.4965	0.343728	-1283.1289	0.075287	0.072897	-1283.2041	-1283.2018
4-Q	-1283.4829	0.340277	-1283.1178	0.07775	0.075316	-1283.1956	-1283.1931
5-CSS	-1670.5693	0.513756	-1670.0205	0.101384	0.09436	-1670.1219	-1670.1149
5-OSS	-1670.5787	0.512688	-1670.0306	0.101876	0.094933	-1670.1325	-1670.1256
5-T	-1670.5817	0.512889	-1670.0338	0.101767	0.095108	-1670.1356	-1670.1289
5-Q	-1670.5679	0.509557	-1670.0225	0.104236	0.097432	-1670.1267	-1670.1199
TS3-CSS	-1670.5453	0.508933	-1670.0021	0.099523	0.092704	-1670.1017	-1670.0948
TS3-OSS	-1670.5516	0.507058	-1670.0102	0.099471	0.092881	-1670.1097	-1670.1031
TS3-T	-1670.5497	0.506517	-1670.0086	0.101448	0.094514	-1670.1101	-1670.1032
TS3-Q	-1670.5497	0.502751	-1670.0111	0.105854	0.098151	-1670.1169	-1670.1092
6-OSS	-1670.5932	0.510967	-1670.0468	0.100913	0.094624	-1670.1477	-1670.1415
6-T	-1670.5936	0.511102	-1670.0471	0.10204	0.095594	-1670.1492	-1670.1427
6-Q	-1670.5945	0.507062	-1670.0507	0.106367	0.099347	-1670.1571	-1670.1501
TS4-OSS	-1670.5906	0.512557	-1670.0436	0.100003	0.093192	-1670.1436	-1670.1368
TS4-T	-1670.5815	0.511193	-1670.0354	0.102443	0.095161	-1670.1379	-1670.1306
TS4-Q	-1670.5842	0.506884	-1670.0412	0.105087	0.09793	-1670.1463	-1670.1391
7-3a CSS	-1670.6595	0.518698	-1670.1074	0.097003	0.090808	-1670.2044	-1670.1982
7-3a OSS	-1670.6648	0.519324	-1670.1118	0.098057	0.09154	-1670.2098	-1670.2033
7-3a T	-1670.6598	0.51557	-1670.1094	0.102353	0.09507	-1670.2117	-1670.2044
7-3a Q	-1670.6643	0.514096	-1670.1151	0.103349	0.096187	-1670.2184	-1670.2113

Cartesian coordinates and energies of optimized structures
Deprotonated Model:

1a
B3LYP-D3(BJ) SCF energy in solution: -387.224406476 a.u.
B3LYP-D3(BJ) enthalpy: -387.0464965 a.u.
B3LYP-D3(BJ) free energy: -387.0960025 a.u.

Cartesian coordinates

ATOM	X	Y	Z
C	-0.59085800	-0.07689500	-0.09737100
C	-1.21859000	1.18071700	-0.16924600
C	-1.38536100	-1.22257800	0.09509500
C	-2.60161700	1.28561700	-0.05154000
H	-0.60848000	2.06601500	-0.31760100
C	-2.76786600	-1.10971200	0.21140800
H	-0.90420300	-2.19382200	0.15113600
C	-3.38114600	0.14277100	0.13886900
H	-3.07323100	2.26267600	-0.10880900
H	-3.36928800	-2.00230400	0.35944600
H	-4.46021500	0.22769200	0.23017500
C	0.82753100	-0.18788000	-0.21670700
C	2.03100700	-0.28775600	-0.32359200
C	4.20815500	0.49124800	0.62565600
H	5.29391300	0.39555800	0.51798200
H	3.93928000	1.54505500	0.50397000
H	3.93163900	0.18692900	1.63974200
C	3.48688000	-0.37901500	-0.42007800
H	3.80631200	-0.08025700	-1.42818600
H	3.79547000	-1.42664000	-0.30281700

0-CSS
B3LYP-D3(BJ) SCF energy in solution: -2810.50927729 a.u.
B3LYP-D3(BJ) enthalpy: -2809.977093 a.u.
B3LYP-D3(BJ) free energy: -2810.076705 a.u.

Cartesian coordinates

ATOM	X	Y	Z
Fe	-0.04399300	0.00001800	-0.18442800
C	-3.48149700	0.00011100	-0.04685000
C	-0.04138200	3.40321500	-0.08794900
C	3.39321000	-0.00010900	-0.23475500
C	-0.04159400	-3.40320700	-0.08788400
N	-1.48963500	1.42205400	-0.10457500
C	-2.84181900	1.23420100	-0.05651000
C	-3.52012600	2.51400400	-0.00261000
C	-2.54979800	3.46972600	-0.01028800
C	-1.28013500	2.77257700	-0.07256200
N	1.40416600	1.42354400	-0.15290300
C	1.19743300	2.77324000	-0.12814100
C	2.46868500	3.47044800	-0.15775800
C	3.43662800	2.51372200	-0.20789400
C	2.75524100	1.23408800	-0.20529500
N	1.40409000	-1.42363600	-0.15287000
C	2.75517200	-1.23427300	-0.20531300
C	3.43647300	-2.51395600	-0.20795200
C	2.46846600	-3.47061400	-0.15779000
C	1.19726300	-2.77331600	-0.12811700
N	-1.48973700	-1.42196100	-0.10453600
C	-1.28031000	-2.77249500	-0.07249200
C	-2.55001400	-3.46956700	-0.01018700
C	-3.52028700	-2.51378800	-0.00252300
C	-2.84190700	-1.23402600	-0.05646600
H	-4.56751800	0.00015100	-0.00747200
H	-0.04142500	4.48993800	-0.06443100
H	4.47925200	-0.00013800	-0.27364600
H	-0.04170700	-4.48993000	-0.06435600
C	1.01011100	0.00010200	2.55598300
H	1.65994200	-0.88667500	2.40714800
H	1.65975400	0.88704800	2.40728600
N	-0.04317700	-0.00018300	-1.90168300
H	-1.04205900	-0.00015600	-2.19260200
O	-0.11004300	0.00001600	1.74878400
H	0.72239600	-0.00001300	3.62701700
H	-2.66102200	-4.54678300	0.02757100
H	-4.59534100	-2.64115800	0.04485700
H	-4.59517300	2.64143700	0.04476000
H	-2.66074200	4.54694900	0.02744200
H	2.58237400	4.54794400	-0.14216000
H	4.51233800	2.64043700	-0.23907400
H	4.51217300	-2.64074600	-0.23917500
H	2.58208100	-4.54811800	-0.14220700

0-OSS
B3LYP-D3(BJ) SCF energy in solution: -2423.2758872 a.u.
B3LYP-D3(BJ) enthalpy: -2422.924129 a.u.
B3LYP-D3(BJ) free energy: -2422.996888 a.u.

Cartesian coordinates

ATOM	X	Y	Z
Fe	-0.04366500	0.00003900	-0.18352600
C	-3.47423800	-0.00282900	-0.04462900
C	-0.04073600	3.40689100	-0.08878400
C	3.39325400	0.00293000	-0.23107100
C	-0.03504700	-3.40679400	-0.08915100
N	-1.48459800	1.42315400	-0.10338800
C	-2.83643900	1.23201600	-0.05504300
C	-3.51730400	2.51042500	-0.00302500
C	-2.54913800	3.46821200	-0.01206100
C	-1.27795400	2.77385500	-0.07290200
N	1.40317900	1.42663400	-0.14977800
C	1.19749200	2.77680800	-0.12875100
C	2.46865200	3.47329700	-0.16254900

C	3.43621900	2.51602600	-0.21049500
C	2.75462500	1.23676400	-0.20277600
N	1.40554100	-1.42410400	-0.15001400
C	2.75667100	-1.23195900	-0.20291700
C	3.44040800	-2.51007300	-0.21072000
C	2.47444800	-3.46897400	-0.16291300
C	1.20212100	-2.77462400	-0.12911000
N	-1.48222400	-1.42548300	-0.10347100
C	-1.27332300	-2.77583800	-0.07316500
C	-2.54334900	-3.47232300	-0.01238500
C	-3.51311100	-2.51615600	-0.00323800
C	-2.83438300	-1.23660300	-0.05512400
H	-4.56023800	-0.00373600	-0.00484900
H	-0.04192400	4.49360200	-0.06732600
H	4.47926700	0.00383000	-0.27058100
H	-0.03440600	-4.49350800	-0.06780400
C	0.99572400	-0.00108200	2.56252400
H	1.64495500	-0.88980200	2.41833300
H	1.64850100	0.88467400	2.41620600
N	-0.08442200	-0.00001000	-1.90860200
H	-1.06642300	0.00019300	-2.24102600
O	-0.12424000	0.00017300	1.75564600
H	0.70596100	0.00077300	3.63327400
H	-2.65456100	-4.54954000	0.02398200
H	-4.58823300	-2.64290500	0.04397400
H	-4.59263600	2.63537400	0.04420300
H	-2.66215000	4.54523700	0.02443100
H	2.58266900	4.55079800	-0.15072600
H	4.51192600	2.64222300	-0.24386000
H	4.51632700	-2.63446100	-0.24405900
H	2.59027600	-4.54628200	-0.15118000

0-T

B3LYP-D3(BJ) SCF energy in solution: -2423.28828272 a.u.
B3LYP-D3(BJ) enthalpy: -2422.936875 a.u.
B3LYP-D3(BJ) free energy: -2423.010531 a.u.

Cartesian coordinates

ATOM	X	Y	Z
Fe	-0.04573800	0.00547300	-0.13840400
C	-0.03498800	-3.40236200	-0.06101200
C	-3.47728500	-0.00316500	-0.07566400
C	-0.05948200	3.41592400	-0.06540500
C	3.38272300	0.02180400	-0.26460000
N	-1.48209000	-1.42346600	-0.09654600
C	-1.27464300	-2.77421000	-0.05222100
C	-2.54498300	-3.47087500	-0.00677400
C	-3.51445700	-2.51464300	-0.02286800
C	-2.83463100	-1.23546000	-0.07359700
N	-1.49239200	1.42872800	-0.08040600
C	-2.84361600	1.23235900	-0.07214700
C	-3.53320400	2.50776400	-0.04119400
C	-2.56973700	3.46925800	-0.02789400
C	-1.29427400	2.77876900	-0.05546500
N	1.38668000	1.43614400	-0.14951600
C	1.17832200	2.78623000	-0.11926600
C	2.44662800	3.48568300	-0.16820100
C	3.41728300	2.53272800	-0.23541800
C	2.74035200	1.25199200	-0.22335300
N	1.39666100	-1.41108300	-0.16820700
C	2.74969700	-1.21529700	-0.22707500
C	3.43609700	-2.48970000	-0.21946700
C	2.47314600	-3.45167800	-0.14903000
C	1.19923200	-2.76489000	-0.11777000
H	-0.02929900	-4.48863400	-0.02636000
H	-4.56393200	-0.00750900	-0.06006100
H	-0.06160900	4.50257400	-0.04559500
H	4.46825000	0.02554500	-0.31355100
C	1.04172000	0.00293200	2.56110800
H	1.74583300	-0.83114600	2.36565700
H	1.62364200	0.93802900	2.43107100
N	-0.10092900	-0.01619100	-1.96749500
H	-0.05685900	-1.00305400	-2.27293500
O	-0.09756100	-0.04640900	1.77894300
H	0.77524100	-0.05682600	3.63504500
H	4.51211400	-2.61094400	-0.25697400
H	2.59397500	-4.52803700	-0.11785200
H	-2.65690000	-4.54784800	0.03520800
H	-4.59028000	-2.64080500	0.00392100
H	-4.61004700	2.62736500	-0.02778200
H	-2.68801900	4.54608700	-0.00245500
H	2.55692800	4.56355600	-0.15441500
H	4.49173100	2.66271800	-0.28688600

0-Q

B3LYP-D3(BJ) SCF energy in solution: -2423.27129641 a.u.
B3LYP-D3(BJ) enthalpy: -2422.921384 a.u.
B3LYP-D3(BJ) free energy: -2422.997165 a.u.

Cartesian coordinates

ATOM	X	Y	Z
Fe	-0.04606100	0.00176700	-0.14749800
C	0.08326900	-3.43802200	-0.08238800
C	-3.47438000	-0.12395000	-0.05816400
C	-0.17740700	3.44130700	-0.08511800
C	3.38329200	0.13445600	-0.23677000
N	-1.46049600	-1.53154700	-0.10625600
C	-1.19587500	-2.86701900	-0.06696400
C	-2.45375600	-3.59516800	-0.00966900
C	-3.45100200	-2.66278400	-0.00964000
C	-2.81051100	-1.35764800	-0.06604200
N	-1.57550500	1.42856500	-0.07873500
C	-2.90786700	1.15662900	-0.06231900
C	-3.64613100	2.41162800	-0.03659600
C	-2.72022000	3.41399100	-0.03932500
C	-1.41067300	2.77768300	-0.06700800

N	1.36908100	1.53429900	-0.13655000
C	1.10056300	2.86892700	-0.12755100
C	2.35554000	3.60199200	-0.18398100
C	3.35613300	2.67440300	-0.23302700
C	2.71970600	1.36697100	-0.20600700
N	1.47916800	-1.41839100	-0.16636100
C	2.81503800	-1.14616300	-0.21104400
C	3.54933000	-2.39996400	-0.20591500
C	2.62331000	-3.40325700	-0.15382600
C	1.31523800	-2.77185500	-0.12826900
H	0.12583900	-4.52438700	-0.05407900
H	-4.56092800	-0.16700400	-0.03144700
H	-0.21576600	4.52827800	-0.07927800
H	4.46930000	0.17503000	-0.27829100
C	1.02989000	0.06535900	2.56727000
H	1.78561900	-0.71753800	2.36009900
H	1.54741400	1.03897500	2.46013400
N	-0.09824600	-0.00583400	-1.95509100
H	-0.02271400	-0.99712300	-2.24013800
O	-0.09950900	-0.04123700	1.77342400
H	0.75579700	-0.03367000	3.63579800
H	4.62918000	-2.48845900	-0.23275100
H	2.79847000	-4.47265000	-0.13089600
H	-2.54743100	-4.67419300	0.03214000
H	-4.52122500	-2.82903600	0.03170200
H	-4.72631900	2.49901900	-0.01779500
H	-2.89312400	4.48389200	-0.02172400
H	2.44551200	4.68215500	-0.18691000
H	4.42509400	2.84592500	-0.28395000

1-CSS

B3LYP-D3(BJ) SCF energy in solution: -2810.50927729 a.u.
B3LYP-D3(BJ) enthalpy: -2809.977093 a.u.
B3LYP-D3(BJ) free energy: -2810.076705 a.u.

Cartesian coordinates

ATOM	X	Y	Z
Fe	-0.93362200	0.29042100	-0.32008500
C	-0.70803400	-2.96284100	-1.29907400
C	-4.10117200	-0.28663700	0.87984900
C	-1.22194600	3.58145900	0.49626200
C	2.24439100	0.86397800	-1.50805300
N	-2.18123700	-1.30887100	-0.24550200
C	-1.89446600	-2.56898600	-0.68885700
C	-3.00097300	-3.45945000	-0.39971200
C	-3.94963500	-2.71132200	0.23093300
C	-3.42481300	-1.36382600	0.32001800
N	-2.40120200	1.43149000	0.49772900
C	-3.61979400	1.01564200	0.94971700
C	-4.34913600	2.13503100	1.51288600
C	-3.54165200	3.22539500	1.39355500
C	-2.31833200	2.76849900	0.76257700
N	0.28432000	1.90728100	-0.47991200
C	-0.01933900	3.17642400	-0.07178900
C	1.10765300	4.05631000	-0.31618900
C	2.08636200	3.29162000	-0.87617000
C	1.55459700	1.94763700	-0.97984300
N	0.49957600	-0.82921600	-1.21730500
C	1.74083900	-0.42467400	-1.62161600
C	2.46382200	-1.53949300	-2.20044900
C	1.62917300	-2.61359100	-2.14992300
C	0.39876200	-2.15454000	-1.53345300
H	-0.63479100	-4.00206300	-1.60990200
H	-5.09073700	-0.47599200	1.28711200
H	-1.30856700	4.63009300	0.76912700
H	3.26313200	1.03415000	-1.84201400
C	-2.88220700	0.85356800	-2.42610500
H	-3.50114600	-0.01797300	-2.13119000
H	-3.00640500	0.97110600	-3.52158000
N	-0.33595000	-0.03389300	1.25715600
H	0.69679300	-0.04967200	1.17861300
H	-3.73437500	4.24665900	1.70019200
H	-5.34500800	2.07386400	1.93558000
H	1.12516700	5.11469300	-0.08438800
H	3.07787800	3.58645600	-1.19728600
H	-4.91947000	-3.02189300	0.60109600
H	-3.02732600	-4.51316100	-0.65096600
H	1.80883000	-3.62726100	-2.48788000
H	3.47426800	-1.48255500	-2.58594500
H	-3.35705900	1.74194000	-1.96075500
C	3.65228900	-0.73831000	1.22795000
C	3.38298600	0.55874800	1.70487200
C	4.81065500	-0.94976800	0.45678300
C	4.23938400	1.61316600	1.40226400
H	2.47729600	0.73166000	2.27630000
C	5.66636800	0.10854300	0.16356300
H	5.00949700	-1.94570600	0.07409300
C	5.38352600	1.39480100	0.63181500
H	3.99414500	2.61377300	1.74566100
H	6.55268400	-0.06798400	-0.44125500
H	6.04609100	2.22204300	0.39029100
O	-1.54785700	0.71450000	-2.09795400
C	2.73484600	-1.79994300	1.47774100
C	1.89848100	-2.65972300	1.65295300
C	-0.38928800	-3.05582700	2.57773200
H	-1.21824100	-3.77278100	2.55913200
H	-0.71567200	-2.11648400	2.11826600
H	-0.12712700	-2.84618400	3.62113000
C	0.82064200	-3.63223700	1.81839500
H	0.49431300	-3.94722800	0.81948100
H	1.20037300	-4.53190700	2.32596700

1-OSS

B3LYP-D3(BJ) SCF energy in solution: -2810.51245969 a.u.
B3LYP-D3(BJ) enthalpy: -2809.980644 a.u.
B3LYP-D3(BJ) free energy: -2810.080023 a.u.

Cartesian coordinates

ATOM	X	Y	Z
Fe	-0.95337100	0.28513300	-0.30861100
C	-0.77707200	-2.98718700	-1.25711900
C	-4.12466700	-0.23994900	0.90111000
C	-1.19500900	3.58777400	0.48399500
C	2.21783500	0.80341100	-1.52001700
N	-2.22429400	-1.30057500	-0.22126400
C	-1.95604100	-2.57012000	-0.64955600
C	-3.07401700	-3.44164500	-0.34713600
C	-4.01094700	-2.67282700	0.27572300
C	-3.46692000	-1.33181400	0.34775600
N	-2.39936700	1.45236800	0.50368900
C	-3.62239900	1.05473700	0.96281800
C	-4.33286500	2.18550400	1.52610300
C	-3.51121100	3.26450700	1.39964000
C	-2.29828500	2.78968200	0.76348900
N	0.27788100	1.88426000	-0.48960600
C	-0.00380600	3.16122000	-0.09126400
C	1.13273400	4.02277300	-0.35531300
C	2.09476100	3.23913700	-0.91763000
C	1.54427000	1.90143700	-1.00168000
N	0.45672200	-0.86793500	-1.19961400
C	1.70051500	-0.48131500	-1.61401500
C	2.40824800	-1.61019200	-2.18334100
C	1.56130800	-2.67400200	-2.11886400
C	0.33864300	-2.19460600	-1.50275600
H	-0.71753600	-4.03067000	-1.55615900
H	-5.11562800	-0.41077700	1.31309000
H	-1.26568100	4.63920700	0.75027000
H	3.23629800	0.95835700	-1.86239700
C	-2.88387600	0.89374500	-2.41764700
H	-3.55435400	0.07372200	-2.08747500
H	-3.01710600	0.98235600	-3.51505900
N	-0.31692000	-0.05129500	1.25928600
H	0.70774200	-0.16834100	1.20643900
H	-3.68845400	4.28924300	1.70392700
H	-5.32711800	2.13890100	1.95439200
H	1.16667500	5.08309400	-0.13459200
H	3.08731600	3.51626400	-1.25079900
H	-4.98399200	-2.96537200	0.65211400
H	-3.11531300	-4.49787500	-0.58543100
H	1.72757700	-3.69291600	-2.44777000
H	3.41781300	-1.56888200	-2.57321100
H	-3.29582400	1.82614700	-1.97773700
C	3.70450400	-0.70216300	1.20346700
C	3.40057600	0.59536200	1.65760800
C	4.87899200	-0.90013300	0.45333100
C	4.24137100	1.66244400	1.35606700
H	2.47982700	0.75943000	2.20723400
C	5.71790900	0.17150000	0.15952200
H	5.10521900	-1.89712400	0.08867200
C	5.40229400	1.45737200	0.60733300
H	3.96956800	2.66218000	1.68116800
H	6.61721700	0.00520300	-0.42876700
H	6.05231100	2.29460400	0.36615600
O	-1.55634300	0.67816400	-2.10480900
C	2.80596000	-1.78000000	1.45377600
C	1.98631600	-2.65631800	1.62620900
C	-0.29967000	-3.10192200	2.53432100
H	-1.10808100	-3.84203300	2.52065700
H	-0.65102800	-2.17806200	2.06230700
H	-0.04865700	-2.87325500	3.57636000
C	0.92976900	-3.65285700	1.78753700
H	0.61959400	-3.98076100	0.78763000
H	1.32650000	-4.54052000	2.30308600

1-T

B3LYP-D3(BJ) SCF energy in solution: -2810.52552609 a.u.
B3LYP-D3(BJ) enthalpy: -2809.993833 a.u.
B3LYP-D3(BJ) free energy: -2810.094457 a.u.

Cartesian coordinates

ATOM	X	Y	Z
Fe	0.93917200	-0.34723000	-0.34328200
C	-0.16683600	2.61371100	-1.62702000
C	3.79839400	1.19190300	0.76431300
C	2.06768800	-3.32601700	0.86598200
C	-1.94769800	-1.87489600	-1.40509900
N	1.67465600	1.53759500	-0.41105700
C	1.07611500	2.61737300	-1.00283500
C	1.91454300	3.78785900	-0.85613100
C	3.02339700	3.39373800	-0.16643400
C	2.86518700	1.98099800	0.10206700
N	2.62262400	-0.95098800	0.59995900
C	3.67854500	-0.17332300	0.98941500
C	4.66588800	-0.98231100	1.67436500
C	4.18003300	-2.25452900	1.69427800
C	2.89594000	-2.22118600	1.02360200
N	0.20157300	-2.23699500	-0.29038100
C	0.81550300	-3.32383000	0.26310900
C	-0.03403300	-4.49215300	0.13710100
C	-1.16562700	-4.08413800	-0.50246700
C	-1.00309900	-2.66826300	-0.76720600
N	-0.74321800	0.25382600	-1.30371100
C	-1.81884700	-0.51538400	-1.64891400
C	-2.81739500	0.29436900	-2.31830400
C	-2.31357000	1.55643000	-2.38547000
C	-1.00962700	1.51738500	-1.75249400
H	-0.51267500	3.55493300	-2.04609600
H	4.69932000	1.68103400	1.12447200
H	2.42501800	-4.27251200	1.26296600
H	-2.87206600	-2.35096600	-1.71778400
C	2.96912100	-0.43801100	-2.41763700
H	3.21374000	0.64012500	-2.33627200
H	3.16277500	-0.72636400	-3.46938400

N	0.15378300	0.01095600	1.27063000
H	-0.27162800	0.94811400	1.20796000
H	4.63001000	-3.14349400	2.12007200
H	5.59801300	-0.60696700	2.07949900
H	0.22130700	-5.48245800	0.49512300
H	-2.03471200	-4.66790700	-0.78140100
H	3.87817100	3.98715400	0.13502900
H	1.67024400	4.77256300	-1.23660600
H	-2.76615500	2.44482900	-2.80899100
H	-3.77376500	-0.07405500	-2.66770800
H	3.71546000	-0.97503200	-1.79816100
C	-3.56270900	0.69087600	1.20192100
C	-2.96431900	-0.55116500	1.48779700
C	-4.91395800	0.72977200	0.80930300
C	-3.71280400	-1.72107800	1.38287700
H	-1.90358500	-0.58691800	1.73512400
C	-5.65152900	-0.44671100	0.70663300
H	-5.36842400	1.68863600	0.57768600
C	-5.05387200	-1.67684500	0.99582200
H	-3.22851100	-2.67431200	1.57508600
H	-6.69333100	-0.40481100	0.39707400
H	-5.62927000	-2.59565600	0.90894200
O	1.66146600	-0.72969600	-2.07249500
C	-2.79757700	1.89327800	1.29308500
C	-2.11983800	2.89531800	1.37131500
C	0.04912800	3.73756000	2.27572600
H	0.70657900	4.61385200	2.29640900
H	0.60022400	2.90776000	1.82785700
H	-0.20638500	3.46163500	3.30410500
C	-1.22215100	4.04534400	1.46261200
H	-0.92856800	4.34721500	0.44897500
H	-1.75186600	4.90194400	1.90537700

1-Q

B3LYP-D3(BJ) SCF energy in solution: -2810.50963434 a.u.
B3LYP-D3(BJ) enthalpy: -2809.976959 a.u.
B3LYP-D3(BJ) free energy: -2810.082105 a.u.

Cartesian coordinates

ATOM	X	Y	Z
Fe	0.91491200	-0.33350500	-0.27516400
C	-1.22271800	1.83798800	-1.88573300
C	3.20797400	2.21614100	0.13402300
C	3.15478900	-2.55758600	1.15644900
C	-1.27993200	-2.92545200	-0.82692100
N	0.97125500	1.73580500	-0.77745900
C	-0.00722600	2.40076900	-1.44972600
C	0.43125600	3.77630800	-1.62847600
C	1.67154200	3.88437200	-1.05357600
C	2.01222900	2.57515100	-0.51999700
N	2.89609600	-0.19592800	0.50941100
C	3.61457800	0.95595000	0.60840200
C	4.87281900	0.64587600	1.27470600
C	4.85817600	-0.69181300	1.55717600
C	3.59128900	-1.22106900	1.06754900
N	0.93937700	-2.44381600	0.10781800
C	1.94258000	-3.12252000	0.71844900
C	1.53689000	-4.51972700	0.83249800
C	0.29115300	-4.62174600	0.27855900
C	-0.08246000	-3.28846200	-0.18198300
N	-0.98161000	-0.50737000	-1.18882200
C	-1.68710000	-1.66382900	-1.30079700
C	-2.93380300	-1.36415300	-1.99447500
C	-2.92524300	-0.02912100	-2.28116000
C	-1.66938100	0.51043000	-1.77492700
H	-1.90373500	2.52235400	-2.38623000
H	3.92244700	3.02393200	0.27730100
H	3.84969100	-3.24571200	1.63327100
H	-1.98701300	-3.73513400	-0.99501800
C	2.81649900	-0.17631400	-2.62793700
H	2.77048700	0.93184700	-2.66901500
H	3.01681700	-0.51770900	-3.66426200
N	0.16482500	0.01807200	1.30960700
H	-0.47088700	0.82363500	1.19041900
H	5.62964300	-1.27379500	2.04813600
H	5.65751100	1.36122900	1.49228200
H	2.13295400	-5.31063600	1.27309200
H	-0.32060200	-5.51141700	0.18245000
H	2.30438100	4.76289500	-1.00572000
H	-0.13229600	4.55064800	-2.13620300
H	-3.69258400	0.54568500	-2.78547800
H	-3.71336900	-2.08371500	-2.21229100
H	3.71954500	-0.42801700	-2.03440300
O	1.65875200	-0.75724800	-2.14506500
C	-2.04232200	2.81178100	1.50873900
C	0.15433600	3.46679400	2.50136000
H	0.87619000	4.29000500	2.55175200
H	0.64740700	2.60143400	2.05245500
H	-0.14425000	3.19805100	3.52032200
C	-1.06860400	3.89049500	1.66541600
H	-0.72489700	4.20458800	0.67174600
H	-1.55192400	4.76580600	2.12426000
C	-2.78981600	1.86681900	1.37157500
C	-3.62518900	0.72031500	1.21014900
C	-4.97111400	0.85895100	0.82168400
C	-3.10451100	-0.56892400	1.43210500
C	-5.77822300	-0.26414800	0.66299500
H	-5.36804900	1.85405600	0.64314400
C	-3.92075800	-1.68466100	1.26851100
H	-2.05473500	-0.68278800	1.68899600
C	-5.25650800	-1.54045500	0.88807900
H	-6.81534600	-0.14394000	0.35873300
H	-3.49590600	-2.67305800	1.41729800
H	-5.88599000	-2.41743900	0.75756200

TS1-CSS

B3LYP-D3(BJ) SCF energy in solution: -2810.49179345 a.u.
B3LYP-D3(BJ) enthalpy: -2809.965399 a.u.
B3LYP-D3(BJ) free energy: -2810.064601 a.u.

Cartesian coordinates

ATOM	X	Y	Z
Fe	-1.30019800	0.24293700	-0.29261000
C	-3.47738400	-2.21047900	0.72311700
C	-3.21072800	2.58418100	1.28416100
C	0.96696500	2.67610300	-1.15319100
C	0.44272300	-2.03661500	-2.11536600
N	-3.03871000	0.19280500	0.76842200
C	-3.76697300	-0.90830400	1.11368400
C	-4.90201600	-0.51906300	1.92737500
C	-4.83831200	0.83492200	2.06033600
C	-3.65693600	1.26849600	1.33885700
N	-1.13668600	2.24478500	0.01714500
C	-2.03998800	3.02802300	0.67980100
C	-1.59102700	4.40686000	0.68356900
C	-0.40375700	4.43317800	0.01680600
C	-0.13550300	3.07226600	-0.40386200
N	0.38615000	0.30865500	-1.40212400
C	1.19030800	1.39072200	-1.63062100
C	2.30003500	1.01396300	-2.48337900
C	2.13978400	-0.30774400	-2.77127600
C	0.93879500	-0.73948600	-2.08386800
N	-1.49128300	-1.73316500	-0.63620600
C	-0.67785000	-2.49449000	-1.43147100
C	-1.11176100	-3.87552700	-1.40668200
C	-2.19011600	-3.93209800	-0.57440800
C	-2.42575000	-2.58329700	-0.10580500
H	-4.14273300	-2.99704200	1.06854100
H	-3.82028600	3.33207900	1.78458100
H	1.69462900	3.43901500	-1.41528700
H	0.99793400	-2.76503000	-2.69972600
C	-3.38163600	-0.02522800	-2.28582800
H	-3.13984600	-1.08039900	-2.52212800
H	-3.79819700	0.42380500	-3.20754200
N	-0.42625800	-0.03192100	1.22540400
H	0.32870000	0.66780800	1.30920200
H	0.19082100	-1.10189500	1.41466000
H	0.23725200	5.28157700	-0.19062000
H	-2.12699900	5.22900600	1.14253100
H	3.08228200	1.68796000	-2.81070300
H	2.76391100	-0.94785900	-3.38301000
H	-5.50970000	1.49381000	2.59793000
H	-5.64022900	-1.20408800	2.32701700
H	-2.78862100	-4.79316000	-0.30222900
H	-0.63437500	-4.68189500	-1.95017900
H	-4.20247700	-0.05176800	-1.54339900
C	4.75166800	-0.49407200	0.98998800
C	5.66499100	-0.32410000	2.05521900
C	5.13505300	-0.04108800	-0.29399000
C	6.90530900	0.26986000	1.84257300
H	5.37994300	-0.66516300	3.04600300
C	6.37834600	0.54900900	-0.49485800
H	4.42974800	-0.14744400	-1.11126900
C	7.27383200	0.70910000	0.56762000
H	7.59106300	0.39142500	2.67822300
H	6.65029800	0.89396700	-1.49004800
H	8.24317500	1.17344800	0.40528700
C	1.07936600	-2.13326800	1.48310300
H	0.74833000	-2.73288800	0.63398800
O	-2.28352600	0.69770600	-1.85431600
C	3.48752200	-1.09710400	1.19224100
C	2.38730400	-1.61387700	1.32558000
C	0.71128200	-2.73027300	2.83452100
H	-0.36239600	-2.94860000	2.85944000
H	0.93144600	-2.02351600	3.64296800
H	1.25591100	-3.66271300	3.04598900

TS1-OSS

B3LYP-D3(BJ) SCF energy in solution: -2810.49425918 a.u.
B3LYP-D3(BJ) enthalpy: -2809.968626 a.u.
B3LYP-D3(BJ) free energy: -2810.066918 a.u.

Cartesian coordinates

ATOM	X	Y	Z
Fe	1.26748400	0.12974000	0.30093800
C	2.26551500	-3.15326500	0.46813500
C	4.38509700	1.02024600	-0.73911600
C	0.19961800	3.37183400	-0.10638100
C	-1.78259600	-0.72686100	1.53283200
N	2.99676700	-0.87836300	-0.05064700
C	3.21067300	-2.22161900	0.05734300
C	4.57913100	-2.53911400	-0.30181600
C	5.17986500	-1.35961400	-0.62115900
C	4.17312000	-0.32657800	-0.46741700
N	2.12211000	1.86569800	-0.29575400
C	3.42849800	2.02649800	-0.67094300
C	3.67386000	3.40953100	-1.02177800
C	2.49296700	4.07158500	-0.86290100
C	1.52871900	3.09445800	-0.40519100
N	-0.45475700	1.12960100	0.63462600
C	-0.71701000	2.45209300	0.38922500
C	-2.08346500	2.76236400	0.75439100
C	-2.63155700	1.61297100	1.23810400
C	-1.60269600	0.59732100	1.15890600
N	0.41090000	-1.60665600	0.88036000
C	-0.85250000	-1.74755300	1.38147200
C	-1.11193900	-3.13851500	1.69056800
C	0.01714100	-3.82841100	1.36454000
C	0.96878200	-2.85422800	0.86895900
H	2.57309100	-4.19473800	0.50821800
H	5.38167100	1.30891000	-1.06262300
H	-0.14243100	4.39357700	-0.24596500

H	-2.75689000	-0.99657700	1.92742700
C	1.80481800	1.59094800	2.71690800
H	2.48093000	2.33532600	2.25324300
H	2.12301900	1.48306200	3.77107700
N	0.82624000	-0.17053700	-1.51760800
H	0.25114300	0.63489300	-1.81438400
H	0.02647700	-1.16830700	-1.78664900
H	2.27758500	5.12016000	-1.02997200
H	4.62913100	3.80183100	-1.34963800
H	-2.54514800	3.73636400	0.64607800
H	-3.64149700	1.43938600	1.58671500
H	6.20119900	-1.18424000	-0.93764000
H	5.00404600	-3.53580400	-0.29671000
H	0.21014400	-4.89085900	1.45265800
H	-2.04296800	-3.51654700	2.09529900
H	0.79569200	2.04599900	2.73229700
C	-4.40143500	-0.41774200	-0.92173600
C	-4.88281300	0.80139500	-1.44564000
C	-5.08739400	-0.98575700	0.17510200
C	-5.99205900	1.42786800	-0.88692200
H	-4.35313300	1.25500800	-2.27711900
C	-6.19288400	-0.34990300	0.73185300
H	-4.72339900	-1.92272400	0.58449600
C	-6.65344600	0.86147500	0.20698800
H	-6.33693600	2.37311000	-1.29937700
H	-6.69858500	-0.80085100	1.58257200
H	-7.51490100	1.35808600	0.64566200
C	-0.89365600	-2.03410000	-2.13617400
H	-0.60551400	-2.90761100	-1.54257500
O	1.83713000	0.35615900	2.08621200
C	-3.23718100	-1.03357000	-1.44034900
C	-2.17694400	-1.53290000	-1.78168200
C	-0.60534900	-2.19692000	-3.62553900
H	0.45915600	-2.41031800	-3.77261700
H	-0.83944600	-1.27207700	-4.16457100
H	-1.19014000	-3.00939100	-4.08031000

TS1-T

B3LYP-D3(BJ) SCF energy in solution: -2810.50787749 a.u.
B3LYP-D3(BJ) enthalpy: -2809.982284 a.u.
B3LYP-D3(BJ) free energy: -2810.08318 a.u.

Cartesian coordinates

ATOM	X	Y	Z
Fe	1.34608800	0.13979100	0.30104500
C	3.84599900	-1.96218600	-0.67134700
C	3.08727600	2.80540200	-0.98977700
C	-1.20813900	2.21955500	1.16957700
C	-0.33173100	-2.50498900	1.70784200
N	3.13455900	0.38443900	-0.61821300
C	4.01299400	-0.61019300	-0.94478400
C	5.16160200	-0.05287000	-1.63002900
C	4.95461000	1.29058300	-1.71266200
C	3.67652300	1.55187400	-1.08334100
N	1.01264500	2.12821300	0.12551100
C	1.84214000	3.06568600	-0.42880500
C	1.22816800	4.37372100	-0.35763300
C	0.01528100	4.20476800	0.24135400
C	-0.10871700	2.79505800	0.54250800
N	-0.43547700	-0.10664000	1.23195900
C	-1.34445900	0.87796400	1.50196800
C	-2.47324400	0.32893600	2.22688100
C	-2.21859500	-0.99704700	2.39614400
C	-0.94007500	-1.25817700	1.76553900
N	1.67367200	-1.85144700	0.46249200
C	0.88251300	-2.77399200	1.08905300
C	1.48381600	-4.08832200	0.99921400
C	2.64947300	-3.93705400	0.31056800
C	2.76261900	-2.52896800	-0.01094100
H	4.63775700	-2.63395600	-0.99173000
H	3.63609400	3.64844000	-1.40020100
H	-2.02540300	2.88168200	1.44120300
H	-0.85393800	-3.33821700	2.16949100
C	3.08585800	1.28868600	2.29921000
H	4.02631800	1.08974600	1.75000700
H	3.33183000	1.26739200	3.37754800
N	0.55664900	-0.08918100	-1.38529800
H	-0.11280900	0.68193300	-1.52350600
H	-0.24683300	-1.10961200	-1.50280900
H	-0.73563200	4.95140900	0.46975500
H	1.67939000	5.28758400	-0.72484700
H	-3.33811900	0.89839700	2.54267700
H	-2.82665200	-1.74629500	2.88856300
H	5.58894200	2.04729700	-2.15840600
H	6.00353300	-0.63095000	-1.99170400
H	3.38106400	-4.69085900	0.04539600
H	1.05403600	-4.99277600	1.41250500
H	2.79312700	2.32877700	2.05854100
C	-4.75668500	-0.35032800	-0.90295400
C	-5.44760300	0.38392200	-1.89369300
C	-5.34965300	-0.45589000	0.37625900
C	-6.67150200	0.98402500	-1.61422500
H	-5.00107800	0.47529500	-2.87916400
C	-6.57292300	0.14879700	0.64603700
H	-4.82047700	-1.00670100	1.14511300
C	-7.24480500	0.87258000	-0.34408600
H	-7.18189700	1.54632600	-2.39301100
H	-7.00705200	0.05621500	1.63917200
H	-8.19985800	1.34462200	-0.12837400
C	-1.15712200	-2.04517900	-1.69522400
H	-0.84782000	-2.80001100	-0.96823200
O	2.08914400	0.36566900	2.02386100
C	-3.51202800	-0.96316400	-1.18340500
C	-2.43931400	-1.50007600	-1.41619700
C	-0.88345300	-2.45141500	-3.13979000
H	0.17544000	-2.70801200	-3.25415600
H	-1.10215800	-1.62068100	-3.82019500

H	-1.48651600	-3.31489600	-3.45642600

TS1-Q

B3LYP-D3(BJ) SCF energy in solution: -2810.48901022 a.u.
B3LYP-D3(BJ) enthalpy: -2809.965017 a.u.
B3LYP-D3(BJ) free energy: -2810.065903 a.u.

Cartesian coordinates

ATOM	X	Y	Z
Fe	1.31588000	0.17500200	0.31618400
C	4.37553100	1.24099600	-0.80132800
C	0.14124200	3.40897500	0.22463700
C	-1.76016300	-0.89948500	1.40550900
C	2.46474200	-3.07275400	0.32781700
N	2.11717300	2.01616400	-0.21004000
C	3.39710300	2.22806400	-0.62575700
C	3.58525200	3.65147300	-0.85769200
C	2.39877000	4.26198300	-0.56984800
C	1.47581300	3.21703700	-0.15672700
N	-0.51162400	1.10350600	0.75190100
C	-0.77733000	2.43638600	0.63881600
C	-2.16404600	2.67109400	1.00744300
C	-2.70071500	1.46037800	1.33999800
C	-1.64426200	0.47577200	1.17766200
N	0.50839900	-1.66130200	0.82458000
C	-0.78085700	-1.88105500	1.22301600
C	-0.98263900	-3.30677100	1.39818700
C	0.20021800	-3.91767900	1.09034900
C	1.13718800	-2.86969600	0.72653200
N	3.14073900	-0.76691400	-0.12391300
C	3.39191000	-2.10122300	-0.06771400
C	4.75924200	-2.34430000	-0.50206100
C	5.29448500	-1.12840500	-0.81712100
C	4.25621000	-0.13633300	-0.58116200
H	5.34342000	1.58753100	-1.15625600
H	-0.22374000	4.43291300	0.19527700
H	-2.73786400	-1.24939700	1.72265300
H	2.80659900	-4.10489200	0.30935800
C	1.31935200	0.02035700	3.19121200
H	1.39011400	-1.08131700	3.25465000
H	0.24619000	0.27879200	3.25079500
N	0.83636300	-0.02440000	-1.46569500
H	0.29984500	0.81550400	-1.72693800
H	-0.00210500	-0.96362700	-1.73900200
H	-3.71727500	1.23766200	1.63810400
H	-2.65508900	3.63704800	0.99955800
H	-1.91398100	-3.76787600	1.70449200
H	0.42780600	-4.97714600	1.10206200
H	2.15946700	5.31761100	-0.62310700
H	4.50834200	4.10927600	-1.19352200
H	6.29242400	-0.91173000	-1.18015700
H	5.23393100	-3.31724700	-0.55418700
H	1.80171200	0.43046600	4.09771900
C	-4.46387400	-0.38182700	-0.99724400
C	-4.97265200	0.85004900	-1.46489400
C	-5.15002200	-1.02276100	0.05980900
C	-6.10490000	1.41762900	-0.89027400
H	-4.44618600	1.35907600	-2.26587600
C	-6.27884900	-0.44516900	0.63257300
H	-4.76902100	-1.97142400	0.42464000
C	-6.76518500	0.77934500	0.16433800
H	-6.46997100	2.37322700	-1.25941200
H	-6.78335400	-0.95286800	1.45152000
H	-7.64508500	1.23022800	0.61553400
C	-0.89969900	-1.84649500	-2.21955100
H	-0.60591600	-2.75459000	-1.68348900
O	1.93784100	0.54052300	2.06177200
C	-3.27876700	-0.94012400	-1.52962200
C	-2.20063100	-1.39971700	-1.87671400
C	-0.53668600	-1.87323400	-3.70028000
H	0.54121500	-2.03359800	-3.81230200
H	-0.78369500	-0.91646400	-4.17426600
H	-1.06542600	-2.66583800	-4.25011300

2-OSS

B3LYP-D3(BJ) SCF energy in solution: -2810.54527542 a.u.
B3LYP-D3(BJ) enthalpy: -2810.014471 a.u.
B3LYP-D3(BJ) free energy: -2810.114077 a.u.

Cartesian coordinates

ATOM	X	Y	Z
Fe	1.02420200	-0.23324100	-0.33479900
C	2.10290000	-3.24940100	0.90915400
C	-1.88044200	-1.68440100	-1.35685900
C	-0.11049200	2.81212800	-1.46759500
C	3.96587000	1.20669200	0.57896700
N	0.26518400	-2.10860200	-0.24059000
C	0.84467100	-3.21721800	0.31532000
C	-0.03874200	-4.35611900	0.18659900
C	-1.15289500	-3.91406400	-0.46513100
C	-0.95065100	-2.50512900	-0.72821500
N	-0.67686000	0.44583800	-1.20934300
C	-1.75293200	-0.31829000	-1.56756500
C	-2.77077200	0.50930700	-2.18524700
C	-2.28217000	1.77943800	-2.19871100
C	-0.96303300	1.72334600	-1.59870100
N	1.78464300	1.64744700	-0.44853200
C	1.17619100	2.76317000	-0.94520600
C	2.06275300	3.90552900	-0.83442900
C	3.21131800	3.45134500	-0.25905300
C	3.02142300	2.03343500	-0.01795500
N	2.70873600	-0.90205200	0.55629000
C	3.80979700	-0.14805900	0.85226800
C	4.80864800	-0.96575600	1.51118600
C	4.28492500	-2.21932500	1.61246700
C	2.96821000	-2.16706300	1.01090200

H	2.44055300	-4.19986800	1.31350800
H	-2.80931000	-2.14677000	-1.67725800
H	-0.47259000	3.77513800	-1.81655400
H	4.90663400	1.66383700	0.87464600
C	2.52948200	-1.59603900	-2.37206900
H	3.52083900	-1.48807400	-1.88821900
H	2.71280600	-1.65323700	-3.46263700
N	0.32355900	0.16017900	1.39552400
H	-0.63702200	0.49474100	1.33742300
H	0.31852500	-0.67261200	1.98786600
H	-2.75187000	2.68145300	-2.57197300
H	-3.73160800	0.14822100	-2.53023100
H	1.81947300	4.91011600	-1.15964300
H	4.10942200	4.00519200	-0.01243700
H	-2.03527200	-4.47386500	-0.75185600
H	0.18335400	-5.35421300	0.54515400
H	4.73089700	-3.10592000	2.04737200
H	5.77490400	-0.60806300	1.84666900
H	2.13589600	-2.58549000	-2.06559000
C	-3.79419100	0.63230800	1.14557700
C	-3.32769100	-0.68817400	1.35723500
C	-5.12663800	0.81220600	0.70121100
C	-4.16536700	-1.77457400	1.13873000
H	-2.29371700	-0.83825000	1.64726100
C	-5.95337500	-0.28320600	0.48540100
H	-5.48585700	1.82095000	0.52194300
C	-5.48093700	-1.58293200	0.70513300
H	-3.77400600	-2.77831000	1.27977900
H	-6.97257500	-0.12700600	0.13956600
H	-6.13015200	-2.43687900	0.52958600
C	-1.21356700	3.63376200	1.73359400
H	-1.51217900	4.66208800	1.52743300
O	1.66420400	-0.55163900	-2.09104800
C	-2.94003700	1.72896900	1.35440800
C	-2.13286900	2.64874500	1.53821600
C	0.17725700	3.38126600	2.23924400
H	0.46489400	2.33030500	2.09868200
H	0.24980700	3.62544600	3.31271200
H	0.89855900	4.01739400	1.71325500

2-T

B3LYP-D3(BJ) SCF energy in solution: -2810.5452672 a.u.
B3LYP-D3(BJ) enthalpy: -2810.014471 a.u.
B3LYP-D3(BJ) free energy: -2810.115032 a.u.

Cartesian coordinates

ATOM	X	Y	Z
Fe	1.02430900	-0.23280200	-0.33347400
C	3.91960000	1.32361400	0.53434200
C	2.21808700	-3.18968700	0.94752000
C	-1.83101500	-1.80236200	-1.31737300
C	-0.22646500	2.75351200	-1.50252500
N	2.73773900	-0.82833800	0.55456000
C	3.81353400	-0.03125700	0.82988500
C	4.84552500	-0.80264300	1.49357800
C	4.36721200	-2.07212100	1.61862400
C	3.04514100	-2.07586800	1.02654400
N	0.33382600	-2.13191300	-0.20621800
C	0.95594900	-3.21086800	0.36188500
C	0.11350400	-4.38272300	0.25457200
C	-1.01925400	-3.99075100	-0.39668500
C	-0.86971500	-2.57916300	-0.68093700
N	-0.70514100	0.37209100	-1.20725200
C	-1.75410400	-0.43547300	-1.54915500
C	-2.80441400	0.34554200	-2.17298400
C	-2.36295800	1.63247100	-2.20611700
C	-1.03976200	1.63317500	-1.61260000
N	1.71553600	1.67236600	-0.47973200
C	1.06442400	2.75836100	-0.98800300
C	1.91164700	3.93229000	-0.90331100
C	3.08058000	3.52714300	-0.33224200
C	2.94202400	2.10751100	-0.06708700
H	4.84622500	1.81789000	0.81454200
H	2.59194800	-4.12140500	1.36345400
H	-2.74349400	-2.30281900	-1.62764300
H	-0.62522500	3.69779000	-1.86246800
C	2.55390700	-1.57943500	-2.36418600
H	3.54288000	-1.44922900	-1.88095100
H	2.73845900	-1.63839000	-3.45444100
N	0.32220200	0.16213400	1.39606400
H	0.32505100	-0.66688300	1.99359900
H	-0.64074700	0.49000900	1.33919100
H	-1.88213500	-4.58638300	-0.67035300
H	0.37354900	-5.36685500	0.62597500
H	-3.75353000	-0.05476000	-2.50689900
H	-2.86752600	2.51143000	-2.58871900
H	4.84748000	-2.93543100	2.06373200
H	5.80094500	-0.40580500	1.81581800
H	3.96121400	4.11547000	-0.10306600
H	1.63060100	4.92262400	-1.24148100
H	2.18026000	-2.57503500	-2.05273000
C	-3.79874100	0.62805500	1.14454500
C	-3.32804700	-0.69186400	1.35015600
C	-5.13386200	0.80604300	0.70748200
C	-4.16432700	-1.77952300	1.13251900
H	-2.29252700	-0.84048600	1.63535600
C	-5.95903700	-0.29058300	0.49236900
H	-5.49650200	1.81447200	0.53331800
C	-5.48236700	-1.58983800	0.70571800
H	-3.77036200	-2.78274600	1.27003200
H	-6.98032500	-0.13578200	0.15211300
H	-6.13041100	-2.44482600	0.53090500
C	-1.22481400	3.63484000	1.73426700
H	-1.52707600	4.66304500	1.53272600
O	1.66788400	-0.55111700	-2.08845000
C	-2.94645700	1.72623100	1.35285700
C	-2.14152000	2.64781500	1.53783900

C	0.16865100	3.38494500	2.23378100
H	0.45612600	2.33364000	2.09591800
H	0.24686800	3.63432500	3.30564000
H	0.88647300	4.01922100	1.70072900

2-Q

B3LYP-D3(BJ) SCF energy in solution: -2810.52522925 a.u.
B3LYP-D3(BJ) enthalpy: -2809.996266 a.u.
B3LYP-D3(BJ) free energy: -2810.099679 a.u.

Cartesian coordinates

ATOM	X	Y	Z
Fe	1.03360600	0.33797600	0.37738800
C	4.20943000	-0.19133500	-0.81135600
C	1.26257600	3.67085900	-0.45883800
C	-2.17843600	0.85005400	1.48536100
C	0.73997900	-3.02539200	1.05410300
N	2.48888200	1.53880200	-0.49626800
C	3.72658200	1.12460300	-0.88399700
C	4.46728400	2.26792100	-1.39493500
C	3.64131600	3.35199800	-1.29653200
C	2.39017000	2.87850300	-0.72519300
N	-0.25799000	1.99838500	0.48664200
C	0.04193600	3.26868800	0.10373500
C	-1.10388900	4.12661500	0.37442700
C	-2.06915800	3.33239600	0.92795200
C	-1.51748500	1.98677300	0.99695100
N	-0.46354300	-0.88179300	1.13786200
C	-1.69847600	-0.46387600	1.54444000
C	-2.44646800	-1.61103200	2.03147600
C	-1.63102000	-2.69934200	1.90560900
C	-0.37714600	-2.22575500	1.34208000
N	2.30073200	-1.33570100	0.21609800
C	1.97166100	-2.61782700	0.52388400
C	3.08675500	-3.48947200	0.17944100
C	4.06180100	-2.69070900	-0.34877600
C	3.54640900	-1.32839200	-0.32789800
H	5.21526400	-0.35038000	-1.19455900
H	1.35070700	4.72557400	-0.71096700
H	-3.19908000	0.99935200	1.82803000
H	0.63072300	-4.08818000	1.25786300
C	2.09575300	-0.18471800	2.99214500
H	3.03252400	-0.67697300	2.67479400
H	1.35782800	-0.98422200	3.18534300
N	0.39216300	-0.01399100	-1.39685200
H	0.48202900	0.87097400	-1.90172200
H	-0.61067700	-0.18150500	-1.29828100
H	-3.06047500	3.61796200	1.26005900
H	-1.15233600	5.19030500	0.17015500
H	-3.46487200	-1.57636800	2.39941900
H	-1.84968600	-3.73003900	2.15986400
H	3.85027700	4.37749400	-1.57931000
H	5.48312500	2.23571200	-1.77208800
H	5.03405000	-2.98696200	-0.72600400
H	3.10772300	-4.56461700	0.31774800
H	2.29689900	0.31162800	3.95915100
C	-3.73807100	-0.73013400	-1.21292000
C	-3.46210600	0.62724600	-1.50755400
C	-4.97154900	-1.04438000	-0.59202900
C	-4.38088000	1.62014700	-1.19271500
H	-2.50327900	0.88402900	-1.94412100
C	-5.88165900	-0.04190500	-0.28057000
H	-5.18235500	-2.08070100	-0.34732400
C	-5.59504000	1.29566100	-0.57941100
H	-4.13045400	2.65706000	-1.39664200
H	-6.82020600	-0.30077500	0.20407300
H	-6.30707400	2.07691300	-0.32665200
C	-0.91194800	-3.47118800	-1.92513300
H	-1.10210900	-4.51421100	-1.67209900
O	1.64155000	0.75601800	2.07662300
C	-2.79225500	-1.72984100	-1.49607400
C	-1.90911400	-2.57011700	-1.70648600
C	0.42451600	-3.09816900	-2.49753600
H	0.66202000	-2.05038100	-2.26210200
H	0.43103300	-3.22277900	-3.59385500
H	1.21171800	-3.74162400	-2.09011900

TS2-OSS

B3LYP-D3(BJ) SCF energy in solution: -2810.50061996 a.u.
B3LYP-D3(BJ) enthalpy: -2809.970828 a.u.
B3LYP-D3(BJ) free energy: -2810.070294 a.u.

Cartesian coordinates

ATOM	X	Y	Z
Fe	1.15503100	0.22648000	0.34164300
C	4.42744100	0.08572700	-0.71258900
C	1.07761700	3.55839000	-0.34707600
C	-2.11513500	0.36579800	1.39835900
C	1.21741100	-3.11764700	0.96744700
N	2.49717000	1.55814900	-0.39547200
C	3.79532300	1.32409800	-0.74976600
C	4.42282000	2.55545600	-1.18712100
C	3.47776600	3.53137000	-1.08602400
C	2.27543000	2.89410000	-0.58571300
N	-0.24900900	1.67631200	0.50427500
C	-0.08970400	2.98825200	0.14862600
C	-1.32838100	3.71111900	0.35721000
C	-2.23005800	2.81330400	0.84560900
C	-1.54015200	1.54409900	0.93866700
N	-0.18377900	-1.10398900	1.06786700
C	-1.47491100	-0.86446700	1.45450500
C	-2.09488100	-2.09217300	1.90753900
C	-1.15823800	-3.07267100	1.77692900
C	0.03533800	-2.44083400	1.24922300
N	2.55886300	-1.23056000	0.16171300
C	2.38094800	-2.55074900	0.45984800

C	3.59662700	-3.29218700	0.18095600
C	4.50427000	-2.39065200	-0.28555500
C	3.83990000	-1.10128300	-0.29331500
H	5.46311600	0.04337600	-1.03940300
H	1.05121500	4.62270400	-0.56668600
H	-3.15512600	0.40492500	1.70499000
H	1.23298400	-4.18658600	1.16476400
C	1.05676300	0.67962900	3.18560100
H	0.21403800	1.39350300	3.10099400
H	1.65603200	0.99958100	4.06021000
N	0.55854700	-0.14531700	-1.42387800
H	-0.42554000	0.09138600	-1.54842500
H	1.08963800	0.38535900	-2.11740000
H	-3.26857600	2.96702200	1.11097700
H	-1.46919600	4.76520500	0.14890700
H	-3.11356500	-2.17028400	2.26620900
H	-1.24682700	-4.12748800	2.00865800
H	3.56714500	4.58616300	-1.31765800
H	5.45047600	2.64089500	-1.52009400
H	5.52786800	-2.56049600	-0.59804800
H	3.71880200	-4.35803500	0.33395600
H	0.61299300	-0.30174000	3.44638800
C	-4.01293400	-0.60150200	-1.14847400
C	-4.21689200	0.70277200	-1.65873500
C	-4.89353100	-1.06925500	-0.14243300
C	-5.23983200	1.50445300	-1.16690300
H	-3.53395000	1.07955900	-2.41298500
C	-5.91527000	-0.25989600	0.33894000
H	-4.73592300	-2.06404800	0.26067000
C	-6.09571100	1.03335400	-0.16525900
H	-5.36258100	2.51188300	-1.55646900
H	-6.57402400	-0.63501500	1.11876000
H	-6.89057100	1.66643200	0.21987400
C	-0.77326800	-2.70466700	-2.17564900
H	-0.41704200	-3.42729200	-1.44524100
O	1.85497600	0.63823200	2.05448800
C	-2.93803100	-1.39396200	-1.58942300
C	-1.92065100	-2.02832100	-1.88819700
C	0.04394700	-2.51310400	-3.41742600
H	1.08788900	-2.33323000	-3.14415400
H	-0.31000900	-1.65488700	-3.99472700
H	0.00344200	-3.40669100	-4.06303900

TS2-T

B3LYP-D3(BJ) SCF energy in solution: -2810.53275238 a.u.
B3LYP-D3(BJ) enthalpy: -2810.002078 a.u.
B3LYP-D3(BJ) free energy: -2810.101916 a.u.

Cartesian coordinates

ATOM	X	Y	Z
Fe	1.30313500	0.18144600	0.37051100
C	4.31859400	-0.40917200	-1.17896200
C	1.60929300	3.50564500	-0.29833800
C	-1.83614000	0.72092900	1.66004700
C	1.04884000	-3.12898900	1.12886500
N	2.69387500	1.32084700	-0.56578100
C	3.87655000	0.90800700	-1.11877700
C	4.60685600	2.04474100	-1.63441700
C	3.84959700	3.14822200	-1.37365000
C	2.65296100	2.68210200	-0.70553600
N	0.11718700	1.79122100	0.63196500
C	0.42737900	3.08410200	0.29869200
C	-0.67858700	3.95835900	0.62760100
C	-1.65955500	3.17160300	1.15267900
C	-1.14917400	1.81891100	1.15972700
N	-0.10745400	-0.96630300	1.25674500
C	-1.33352200	-0.57139100	1.72383200
C	-2.02813900	-1.69719300	2.30712100
C	-1.20474500	-2.77540900	2.17480100
C	-0.00902200	-2.30742500	1.50657600
N	2.45276600	-1.45304200	0.01568000
C	2.17724000	-2.72831700	0.42140900
C	3.23525200	-3.62377400	-0.00289100
C	4.14925100	-2.86265300	-0.66712000
C	3.65253900	-1.50259700	-0.64141500
H	5.27410200	-0.59353400	-1.66243300
H	1.71335200	4.56976900	-0.49201800
H	-2.84273400	0.88629900	2.03087600
H	0.97158700	-4.18232700	1.38355100
C	1.56223200	0.80092300	3.13965200
H	1.06304800	1.78417600	3.05979700
H	2.29274200	0.87176400	3.96565800
N	0.43927600	-0.11495000	-1.37283300
H	-0.31680300	0.55630100	-1.50828200
H	1.09978100	0.02539000	-2.14036500
H	-2.64156900	3.45921500	1.50715200
H	-0.68773600	5.02879500	0.46143200
H	-3.01071200	-1.64857600	2.75923100
H	-1.37821700	-3.79935500	2.48242500
H	4.06292800	4.18490300	-1.60475700
H	5.57235000	1.98764500	-2.12270900
H	5.07967300	-3.17168000	-1.12822500
H	3.25632800	-4.68922900	0.19225900
H	0.79030600	0.07318300	3.44966000
C	-4.43661400	-0.46276300	-1.13028800
C	-5.22761000	0.24006200	-2.08359100
C	-4.97923600	-0.61801200	0.17872800
C	-6.46958000	0.75576200	-1.74160800
H	-4.83393400	0.37213400	-3.08736700
C	-6.22082200	-0.09302300	0.50473900
H	-4.39326100	-1.15902600	0.91352800
C	-6.98411000	0.60029500	-0.44637600
H	-7.04845800	1.29119500	-2.49199800
H	-6.60611000	-0.22541900	1.51423500
H	-7.95658100	1.00877800	-0.18473300
C	-0.75683200	-1.84252100	-1.90575500
H	-0.28122300	-2.42914700	-1.12794900

O	2.21900100	0.43047800	1.97175900
C	-3.17681400	-0.97668900	-1.45060600
C	-2.05922300	-1.45010200	-1.68705000
C	-0.23656700	-2.06243300	-3.30580700
H	0.85770300	-2.10866400	-3.30191700
H	-0.55092500	-1.25483300	-3.97706000
H	-0.61044600	-3.00679000	-3.73149200

TS2-Q

B3LYP-D3(BJ) SCF energy in solution: -2810.51146613 a.u.
B3LYP-D3(BJ) enthalpy: -2809.982879 a.u.
B3LYP-D3(BJ) free energy: -2810.08838 a.u.

Cartesian coordinates

ATOM	X	Y	Z
Fe	-1.53652500	0.29299900	-0.29645500
C	-2.61471300	2.05742400	2.44072800
C	-0.08780500	3.13991200	-1.57049700
C	-0.28584800	-1.51951900	-2.94666500
C	-2.80544700	-2.60765100	1.06533500
N	-1.35705700	2.27032800	0.34291700
C	-1.91298300	2.78990700	1.47221800
C	-1.65283900	4.22130500	1.51124800
C	-0.94188600	4.52487000	0.38518600
C	-0.76327600	3.28116000	-0.34924900
N	-0.36670700	0.73566200	-1.97805600
C	0.09414600	1.96988200	-2.32250700
C	0.80579500	1.87283100	-3.58834300
C	0.75197200	0.56324200	-3.97232700
C	0.00359800	-0.14686200	-2.94550800
N	-1.59702500	-1.72626100	-0.88034800
C	-1.00761800	-2.24942500	-1.99020300
C	-1.21431100	-3.69071800	-2.00126800
C	-1.92277300	-3.99699600	-0.87400600
C	-2.15160900	-2.74518900	-0.16788900
N	-2.52951600	-0.19907100	1.47204400
C	-2.98288800	-1.43650400	1.81923600
C	-3.67850400	-1.34315900	3.09252900
C	-3.62855500	-0.03231500	3.47725500
C	-2.89930900	0.68349500	2.44325100
H	-2.98723700	2.62361300	3.29153600
H	0.34121700	4.04820300	-1.98756000
H	0.10979600	-2.09007000	-3.78394500
H	-3.20954200	-3.52009800	1.49796900
C	-4.18034700	-0.17216600	-1.31401300
H	-3.93954000	-1.05954900	-1.92554800
H	-5.01740200	0.35178200	-1.80956900
N	0.14513000	-0.08564700	0.62323900
H	0.84708800	0.53744500	0.21903400
H	0.05105800	0.20419100	1.60057600
H	1.17208000	0.11210400	-4.86377600
H	1.28107800	2.69960000	-4.10332900
H	-0.85230800	-4.36839900	-2.76574600
H	-2.25217400	-4.97367100	-0.53870500
H	-0.57153800	5.49403300	0.07163500
H	-1.97759200	4.89430800	2.29637400
H	-4.04280600	0.41500100	4.37345300
H	-4.14395800	-2.17262400	3.61237100
H	-4.55475300	-0.53791200	-0.34114500
C	5.29114200	-0.53395700	0.78558500
C	6.01524100	-0.46447200	2.00637300
C	5.93706300	-0.06108600	-0.38888600
C	7.30636600	0.04536600	2.04240800
H	5.53601400	-0.81837000	2.91420500
C	7.22832400	0.44644900	-0.33718500
H	5.39601700	-0.10158800	-1.32926400
C	7.92806600	0.50527400	0.87482500
H	7.83729900	0.08748800	2.99108100
H	7.69786100	0.80352900	-1.25121100
H	8.93816000	0.90457300	0.90910300
C	1.56529400	-2.00408900	0.63181900
H	1.10780000	-2.15677400	-0.33886400
O	-3.10517600	0.69827500	-1.18165400
C	3.98911700	-1.05092200	0.73862100
C	2.84517900	-1.51758100	0.68300800
C	0.91948500	-2.68571100	1.80639500
H	-0.16151800	-2.53360300	1.77964300
H	1.31231300	-2.29822200	2.75275600
H	1.10939500	-3.77100500	1.78660200

3a-3-CSS

B3LYP-D3(BJ) SCF energy in solution: -2810.59240241 a.u.
B3LYP-D3(BJ) enthalpy: -2810.056837 a.u.
B3LYP-D3(BJ) free energy: -2810.153482 a.u.

Cartesian coordinates

ATOM	X	Y	Z
Fe	1.12220000	0.13544200	0.40709900
C	4.39398200	-0.03250200	-0.57820400
C	1.15964900	3.52855700	-0.05289500
C	-2.07402600	0.31278500	1.56185400
C	0.94841100	-3.28742300	0.42630400
N	2.51284700	1.48828100	-0.18004800
C	3.81890700	1.23343600	-0.50801100
C	4.50535100	2.46841800	-0.83170000
C	3.58799400	3.46918100	-0.70582100
C	2.34694200	2.84565800	-0.29384100
N	-0.21267700	1.62417600	0.65760100
C	-0.02604000	2.95893100	0.40336600
C	-1.22346000	3.70533400	0.73487000
C	-2.12083500	2.80252100	1.22571200
C	-1.47524400	1.50591500	1.17323200
N	-0.27906200	-1.22019800	0.90328500
C	-1.52493100	-0.95255000	1.40813600
C	-2.24079900	-2.18647800	1.66365300

C	-1.41206400	-3.20310900	1.29340000
C	-0.18155200	-2.58849100	0.83611900
N	2.41904600	-1.36561000	0.01327300
C	2.16594900	-2.71496000	0.06762200
C	3.35740900	-3.46157600	-0.27473900
C	4.33600400	-2.54506300	-0.52577300
C	3.73616300	-1.23814000	-0.35365600
H	5.44156900	-0.08617400	-0.86461700
H	1.16901700	4.60649100	-0.19663800
H	-3.08669200	0.36998000	1.95124100
H	0.88980800	-4.37319200	0.42388400
C	2.14663200	-0.70337700	2.93744900
H	1.47419300	-1.58964500	2.95473000
H	2.31987800	-0.43119300	4.00052000
N	0.66628800	0.09208900	-1.66438000
H	0.28173800	1.01127500	-1.88195300
H	1.60803800	0.05139900	-2.05129500
H	-3.12607200	2.97615300	1.59124800
H	-1.33532700	4.77785300	0.62422700
H	-3.24993800	-2.24271100	2.05399100
H	-1.59085700	-4.27138800	1.33656200
H	3.72390100	4.53309100	-0.86281900
H	5.54813200	2.54013200	-1.11873100
H	5.36780900	-2.71958200	-0.80818700
H	3.42339400	-4.54323300	-0.30034100
H	3.12505600	-1.07067400	2.55187300
C	-4.00970000	-0.21736200	-1.08468700
C	-4.42710700	1.11339700	-0.89311600
C	-4.88892500	-1.26321000	-0.74904500
C	-5.69318200	1.38443800	-0.38225700
H	-3.73301200	1.91816600	-1.10898100
C	-6.15473400	-0.98256300	-0.24031400
H	-4.55187700	-2.28759400	-0.86806500
C	-6.56371200	0.34052300	-0.05684800
H	-5.99798100	2.41617700	-0.22710600
H	-6.82146800	-1.79996500	0.02258900
H	-7.54992700	0.55665200	0.34573100
C	-0.16584400	-0.97238100	-2.26353100
H	0.17073500	-1.91095100	-1.80952000
O	1.63682300	0.37243600	2.24674800
C	-2.70078000	-0.49909800	-1.56853600
C	-1.56232300	-0.74754400	-1.89581700
C	0.00014700	-1.06985500	-3.79151600
H	1.05023300	-1.26296400	-4.04073200
H	-0.30927000	-0.13545800	-4.27369600
H	-0.60765700	-1.88526800	-4.19902800

3a-3-OSS

B3LYP-D3(BJ) SCF energy in solution: -2810.59203094 a.u.

B3LYP-D3(BJ) enthalpy: -2810.056389 a.u.

B3LYP-D3(BJ) free energy: -2810.154315 a.u.

Cartesian coordinates

ATOM	X	Y	Z
Fe	1.14331900	0.14814200	0.41076600
C	4.27728100	-0.32086400	-0.91208800
C	1.40023200	3.50394700	-0.19223600
C	-2.01254200	0.59740200	1.62781300
C	0.83687800	-3.23382800	0.86208700
N	2.57508100	1.35733000	-0.36215000
C	3.80682800	0.98646800	-0.84420400
C	4.54079000	2.15086000	-1.29565000
C	3.73276500	3.22805100	-1.08351000
C	2.50421400	2.72026000	-0.50707000
N	-0.08850600	1.73267100	0.62141500
C	0.19501100	3.04140800	0.32950900
C	-0.93212500	3.88746100	0.66556500
C	-1.89083800	3.06886200	1.18769400
C	-1.34684400	1.72601800	1.16238600
N	-0.30362400	-1.07576200	1.09466600
C	-1.52522500	-0.70070200	1.59045400
C	-2.27137800	-1.86307300	2.02959000
C	-1.47790900	-2.94518100	1.79946700
C	-0.24495100	-2.43912600	1.22557600
N	2.33008200	-1.45914600	0.05969800
C	2.03387400	-2.77464900	0.32120200
C	3.14082500	-3.62436600	-0.06429500
C	4.10730500	-2.80406600	-0.56727000
C	3.59069300	-1.45432800	-0.48624000
H	5.27162700	-0.47004000	-1.32592300
H	1.48565500	4.57360500	-0.36858700
H	-3.01007700	0.74120700	2.03376600
H	0.74070300	-4.30589200	1.01595100
C	2.90911800	-0.07150200	2.64276000
H	2.91431000	-1.18506600	2.67914200
H	3.14463600	0.26840800	3.67411500
N	0.54769800	-0.04895800	-1.61149300
H	0.12210500	0.83799300	-1.87952100
H	1.46307500	-0.09943800	-2.05632200
H	-2.86917100	3.33229900	1.57319500
H	-0.96172500	4.96246000	0.53016200
H	-3.27075400	-1.83211300	2.44718300
H	-1.68391700	-3.99062600	1.99810400
H	3.93132000	4.27268000	-1.29379200
H	5.54130500	2.12833500	-1.71203800
H	5.08372700	-3.07015200	-0.95550400
H	3.15953700	-4.70262200	0.04436700
H	3.78604600	0.21560300	2.01969100
C	-4.15486200	-0.29202400	-1.05825300
C	-4.45268500	1.02925700	-0.67016300
C	-5.18145000	-1.25383700	-1.04277900
C	-5.74444700	1.37022700	-0.27989000
H	-3.65532700	1.76410000	-0.65279400
C	-6.47130800	-0.90303200	-0.65042100
H	-4.94918500	-2.27431300	-1.33069500
C	-6.75933900	0.40915500	-0.26892800
H	-5.95816300	2.39152600	0.02471100

H	-7.25335300	-1.65809000	-0.63820000
H	-7.76567000	0.67990300	0.03998000
C	-0.28749200	-1.18385800	-2.06145100
H	0.05808500	-2.05752800	-1.49837400
O	1.71864900	0.47427000	2.22075200
C	-2.82939500	-0.64129400	-1.44457400
C	-1.68309700	-0.91977700	-1.71695000
C	-0.13442300	-1.47284100	-3.56655600
H	0.91457800	-1.69341400	-3.79646000
H	-0.45131200	-0.60819300	-4.16085600
H	-0.74167400	-2.33561300	-3.86163600

3a-3-T

B3LYP-D3(BJ) SCF energy in solution: -2810.5905353 a.u.
B3LYP-D3(BJ) enthalpy: -2810.056539 a.u.
B3LYP-D3(BJ) free energy: -2810.156631 a.u.

Cartesian coordinates

ATOM	X	Y	Z
Fe	1.11577300	0.11484300	0.54427200
C	4.32708100	-0.01340000	-0.71488300
C	1.04739000	3.49960000	-0.05878300
C	-2.16081400	0.22352100	1.55161200
C	1.00238300	-3.32203900	0.56725600
N	2.45898800	1.50603100	-0.25426500
C	3.74917700	1.26799900	-0.65034400
C	4.38340800	2.49485400	-1.02421000
C	3.44397300	3.49287400	-0.85037900
C	2.25796000	2.85983900	-0.36833700
N	-0.25863200	1.53971200	0.70022400
C	-0.08880700	2.88922100	0.42664000
C	-1.31291600	3.60349200	0.73296400
C	-2.20367400	2.69246000	1.20435100
C	-1.54524500	1.39967100	1.18187000
N	-0.32992600	-1.29549200	0.95662200
C	-1.59536400	-1.05213300	1.42444700
C	-2.26594900	-2.28595500	1.70015200
C	-1.37773600	-3.29556100	1.39025700
C	-0.17683700	-2.66286300	0.94381400
N	2.39552800	-1.34505200	0.06779500
C	2.17459400	-2.71074200	0.17698600
C	3.37051100	-3.42851500	-0.20980100
C	4.30344700	-2.50281200	-0.55582500
C	3.69253600	-1.19667400	-0.39749800
H	5.35449400	-0.07900800	-1.06260500
H	1.00447800	4.57581000	-0.20638600
H	-3.18571200	0.28385500	1.90384100
H	0.99511500	-4.40859300	0.59673500
C	3.04002400	0.08571300	2.74499100
H	3.32919000	-0.97104200	2.58060300
H	3.17012400	0.29090100	3.82578200
N	0.63216000	-0.01240300	-1.83531500
H	0.30722800	0.90679600	-2.12711700
H	1.59547000	-0.12929400	-2.14112500
H	-3.22516600	2.84671600	1.52998100
H	-1.44432000	4.67119600	0.60000400
H	-3.27920000	-2.36838400	2.07409200
H	-1.52082100	-4.36677800	1.47363200
H	3.55428200	4.55653200	-1.02751400
H	5.40475400	2.58660600	-1.37490000
H	5.31759400	-2.66278600	-0.90277300
H	3.45993100	-4.50873500	-0.20899700
H	3.78759300	0.70394200	2.20991000
C	-4.01237700	-0.19506000	-1.07574300
C	-4.45166800	1.14069800	-1.02283400
C	-4.84478900	-1.20818500	-0.56432700
C	-5.69165400	1.45110500	-0.47178100
H	-3.79225800	1.92468300	-1.37898300
C	-6.08432900	-0.88881100	-0.01584600
H	-4.48593400	-2.23165500	-0.57355400
C	-6.51457000	0.43962000	0.03168200
H	-6.01271700	2.48854000	-0.42459000
H	-6.71357100	-1.67917800	0.38569600
H	-7.48010900	0.68610600	0.46577200
C	-0.22610700	-1.08757900	-2.34750800
H	0.09801400	-2.00264300	-1.83546100
O	1.74283800	0.35852300	2.34656500
C	-2.72609000	-0.51579000	-1.59461000
C	-1.60758800	-0.80820500	-1.95303000
C	-0.11230700	-1.30619700	-3.86939800
H	0.92674000	-1.53394100	-4.13495200
H	-0.42199200	-0.40470100	-4.41046500
H	-0.74481700	-2.13950000	-4.19696500

3a-3-Q

B3LYP-D3(BJ) SCF energy in solution: -2810.5866193 a.u.
B3LYP-D3(BJ) enthalpy: -2810.053583 a.u.
B3LYP-D3(BJ) free energy: -2810.155265 a.u.

Cartesian coordinates

ATOM	X	Y	Z
Fe	1.17077400	0.13765800	0.64764300
C	4.29431000	-0.26467700	-0.82231000
C	1.26232300	3.49234200	-0.23915300
C	-2.14642000	0.48121500	1.53888200
C	0.81427600	-3.29554000	0.77125100
N	2.55819400	1.40058000	-0.29019600
C	3.79357000	1.03272300	-0.77068900
C	4.47308900	2.21653900	-1.27807100
C	3.62013400	3.26791700	-1.12215600
C	2.40559900	2.75138600	-0.51223900
N	-0.21930800	1.72261800	0.63270900
C	0.03900100	3.02536700	0.28926400
C	-1.13009000	3.82055600	0.54409300
C	-2.08903800	2.97201100	1.05776600

C	-1.50109200	1.65972200	1.10770900
N	-0.37335900	-1.16247800	1.10399000
C	-1.63731000	-0.80944800	1.50618800
C	-2.38887800	-2.01525100	1.82500200
C	-1.56412200	-3.07373600	1.59553900
C	-0.28947500	-2.53633800	1.14002400
N	2.36385600	-1.51642200	0.06043500
C	2.05397600	-2.83443600	0.27339800
C	3.17371300	-3.64810200	-0.10833800
C	4.16227400	-2.79139900	-0.54868500
C	3.63716700	-1.45729500	-0.43789000
H	5.29637200	-0.37995100	-1.22881800
H	1.30794100	4.55406100	-0.47162400
H	-3.17434100	0.59066500	1.87241300
H	0.70951200	-4.37426000	0.86479600
C	3.18458600	0.59795800	2.70438000
H	3.90326600	-0.14634700	2.30920100
H	3.35068300	0.65562300	3.79735700
N	0.59730600	-0.07988300	-1.72343900
H	0.24682900	0.82342200	-2.03503800
H	1.55685900	-0.18586400	-2.04400500
H	-3.09852700	3.21368500	1.36908800
H	-1.21224100	4.88625400	0.36268000
H	-3.42118300	-2.02739800	2.15393100
H	-1.78266700	-4.12924400	1.71204900
H	3.78058700	4.30368500	-1.39963500
H	5.46694700	2.22121600	-1.71100100
H	5.15030300	-3.04672200	-0.91422400
H	3.21122600	-4.72972300	-0.04514300
H	3.47727600	1.57701300	2.27907000
C	-4.06536000	-0.26588700	-1.07110400
C	-4.42588200	1.08794800	-0.92819200
C	-4.99725000	-1.25977700	-0.71974100
C	-5.68624100	1.43105000	-0.44793500
H	-3.69246400	1.85380800	-1.15514900
C	-6.25695300	-0.90704000	-0.24112900
H	-4.70783900	-2.30200600	-0.80614400
C	-6.60843300	0.43803900	-0.10500600
H	-5.94616700	2.47989500	-0.33002200
H	-6.96457300	-1.68523900	0.03389500
H	-7.59025200	0.71067400	0.27335700
C	-0.24033800	-1.18669700	-2.20110700
H	0.09010600	-2.07589300	-1.64966200
O	1.86917700	0.26081800	2.42234400
C	-2.76348800	-0.61799100	-1.52702400
C	-1.63184900	-0.91046600	-1.84207800
C	-0.10068600	-1.46683400	-3.71107700
H	0.94512100	-1.69330300	-3.94933600
H	-0.41205400	-0.59262900	-4.29438900
H	-0.71778100	-2.32112900	-4.01304500

4-CSS

B3LYP-D3(BJ) SCF energy in solution: -2423.7939593 a.u.

B3LYP-D3(BJ) enthalpy: -2423.425635 a.u.

B3LYP-D3(BJ) free energy: -2423.500409 a.u.

Cartesian coordinates

ATOM	X	Y	Z
Fe	-0.05411000	0.00543700	-0.31566800
C	1.81658400	2.87928100	-0.10421400
C	2.82503700	-1.83357300	-0.30042400
C	-1.90866000	-2.85806700	-0.03193700
C	-2.92758000	1.86061600	-0.07396600
N	1.93716800	0.44137400	-0.24592400
C	2.51150300	1.68435100	-0.22466800
C	3.95209000	1.57253000	-0.31025400
C	4.23649200	0.24311000	-0.38026000
C	2.96962900	-0.45464700	-0.33138400
N	0.37088600	-1.93593700	-0.09945000
C	1.62053300	-2.51080200	-0.17526300
C	1.50533400	-3.94761000	-0.11129000
C	0.17734700	-4.23585800	-0.01960000
C	-0.52685700	-2.97687700	-0.03320600
N	-2.03095500	-0.41731100	-0.15609200
C	-2.60674300	-1.66176800	-0.09531500
C	-4.04743300	-1.54648400	-0.06340700
C	-4.33436600	-0.21596200	-0.08813100
C	-3.06844800	0.48147400	-0.12885500
N	-0.46842000	1.95777400	-0.00440200
C	-1.72007500	2.53990000	-0.01056200
C	-1.59554300	3.97448700	0.03452100
C	-0.26235600	4.25861300	0.03684900
C	0.43754500	2.99999600	-0.01350700
H	2.39514000	3.79774900	-0.09943000
H	3.72703100	-2.43454000	-0.36007100
H	-2.48705400	-3.77519800	0.01757900
H	-3.83433500	2.45716300	-0.06233600
C	1.12000300	-0.35937000	2.75067300
H	2.01431000	0.14735900	2.37363400
H	1.01021600	-0.17848300	3.82705700
N	-0.06072800	0.04606600	-1.97550600
H	-1.00039200	-0.28428900	-2.28437700
H	-0.30076200	-5.20487500	0.04209500
H	2.34423800	-4.63098100	-0.13838100
H	-4.73134600	-2.38395500	-0.01344500
H	-5.30283500	0.26666800	-0.06084900
H	5.20393700	-0.23778400	-0.44729700
H	4.63722600	2.41056000	-0.30945800
H	0.22031700	5.22721100	0.05595800
H	-2.43125300	4.66202300	0.05326400
H	1.22107500	-1.43056800	2.57310900
O	-0.05413100	0.05308500	2.04772400
H	-0.12548100	1.02210200	2.07334000

4-OSS

B3LYP-D3(BJ) SCF energy in solution: -2423.79793754 a.u.

B3LYP-D3(BJ) enthalpy: -2423.429879 a.u.
B3LYP-D3(BJ) free energy: -2423.504114 a.u.

Cartesian coordinates

ATOM	X	Y	Z
Fe	-0.05341800	-0.01021600	-0.30486300
C	0.88893800	3.30209000	-0.07236200
C	3.23710100	-0.92070600	-0.32233200
C	-0.97809300	-3.29138900	-0.01384700
C	-3.33488700	0.93641900	-0.10329300
N	1.71343800	0.99358800	-0.18664200
C	1.89864700	2.35302600	-0.15145400
C	3.30874900	2.66477500	-0.21856400
C	3.97000700	1.47780100	-0.30896000
C	2.96520600	0.43921700	-0.28884400
N	0.92843500	-1.75188800	-0.15309800
C	2.29020100	-1.93177100	-0.24273700
C	2.60440900	-3.34017100	-0.20633200
C	1.42156100	-4.00739900	-0.09818200
C	0.37875400	-3.00987000	-0.07606700
N	-1.80192700	-0.98456100	-0.10330200
C	-1.98970100	-2.34281700	-0.03357900
C	-3.40118500	-2.64789900	0.01173200
C	-4.06192300	-1.45856100	-0.03299000
C	-3.05604000	-0.42290000	-0.09737400
N	-1.02701300	1.76690200	-0.04693800
C	-2.38999400	1.95174100	-0.07589800
C	-2.69957500	3.36130900	-0.06103100
C	-1.51049700	4.02652700	-0.03585300
C	-0.47053100	3.02540000	-0.04417300
H	1.18543900	4.34626200	-0.06051700
H	4.27803900	-1.22014800	-0.39389900
H	-1.27048300	-4.33518900	0.04088200
H	-4.38020400	1.22904600	-0.10892500
C	1.13446700	-0.13212400	2.76123000
H	1.91983500	0.53935100	2.39990000
H	0.97460500	0.01738600	3.83590400
N	-0.11321500	-0.01317800	-1.97633800
H	-0.48186800	-0.91414700	-2.33672800
H	1.25159100	-5.07474400	-0.03996600
H	3.60650300	-3.74665500	-0.25268500
H	-3.81223200	-3.64718600	0.07475800
H	-5.12885400	-1.27766600	-0.01187200
H	5.03585800	1.30251900	-0.37888000
H	3.71893800	3.66633000	-0.20105200
H	-1.33566900	5.09465200	-0.02165100
H	-3.70123200	3.77146900	-0.06950900
H	1.44076300	-1.16309400	2.58104600
O	-0.08669200	0.05226100	2.04060200
H	-0.35033600	0.98710300	2.07448200

4-T

B3LYP-D3(BJ) SCF energy in solution: -2423.80564054 a.u.

B3LYP-D3(BJ) enthalpy: -2423.43799 a.u.
B3LYP-D3(BJ) free energy: -2423.513277 a.u.

Cartesian coordinates

ATOM	X	Y	Z
Fe	-0.05101500	-0.01712000	-0.27710800
C	0.57053400	3.36114000	-0.13938600
C	3.32444900	-0.61754900	-0.27046400
C	-0.66275700	-3.36234700	-0.05494200
C	-3.41898100	0.62025600	-0.05939200
N	1.61769700	1.13917200	-0.18528500
C	1.66743000	2.51154500	-0.18860800
C	3.04060100	2.95833700	-0.24906700
C	3.81733800	1.84040500	-0.29456800
C	2.92029900	0.70912200	-0.25807000
N	1.10093200	-1.65607900	-0.14982800
C	2.47438600	-1.71255000	-0.21384600
C	2.91313400	-3.08746600	-0.19527500
C	1.79248600	-3.85916400	-0.12541800
C	0.66419800	-2.95898200	-0.10429100
N	-1.70706300	-1.14169900	-0.08441400
C	-1.76022800	-2.51367700	-0.04685700
C	-3.13502500	-2.95504300	0.00335000
C	-3.90904500	-1.83511400	-0.00709800
C	-3.00989700	-0.70556400	-0.05928300
N	-1.19716700	1.65792300	-0.05686300
C	-2.57213000	1.71868800	-0.06415800
C	-3.00844300	3.09383500	-0.07630000
C	-1.88414500	3.86409400	-0.09167000
C	-0.75761400	2.96154500	-0.09363400
H	0.76791600	4.42847300	-0.15663000
H	4.39029900	-0.81599400	-0.32338500
H	-0.85778700	-4.42964200	-0.02344300
H	-4.48726500	0.81232900	-0.05194100
C	1.14347700	0.09401700	2.77524000
H	1.75549700	0.93677300	2.43910800
H	0.95824000	0.16665500	3.85360900
N	-0.12242400	-0.08838000	-2.00711200
H	-0.31508700	-1.03991900	-2.35705500
H	1.71787100	-4.93841500	-0.09023000
H	3.94820100	-3.40221100	-0.22811600
H	-3.44659800	-3.99076900	0.04515700
H	-4.98824100	-1.75972200	0.02584400
H	4.89612700	1.76966600	-0.34737500
H	3.34996300	3.99560000	-0.25872400
H	-1.80725100	4.94368900	-0.10869100
H	-4.04317800	3.41145700	-0.07562800
H	1.67275400	-0.83468700	2.55957600
O	-0.09256500	0.02275400	2.05839300
H	-0.54878400	0.88007400	2.10251100

4-Q

B3LYP-D3(BJ) SCF energy in solution: -2423.78782011 a.u.

B3LYP-D3(BJ) enthalpy: -2423.422728 a.u.
B3LYP-D3(BJ) free energy: -2423.500479 a.u.

Cartesian coordinates

ATOM	X	Y	Z
Fe	-0.04984300	-0.01056500	-0.34592200
C	0.86645700	3.33186500	-0.10056600
C	3.25893000	-0.89582200	-0.25136400
C	-0.95027600	-3.31569100	-0.03007800
C	-3.34745400	0.91422700	-0.04480800
N	1.74433800	1.03813900	-0.14816800
C	1.90465400	2.39792400	-0.15100100
C	3.31702800	2.71270000	-0.22307700
C	3.98765900	1.52502900	-0.27532200
C	2.99108500	0.47483900	-0.23313800
N	0.97311900	-1.79380200	-0.12219400
C	2.33448000	-1.94125400	-0.19808300
C	2.65829700	-3.35268500	-0.18993400
C	1.47745900	-4.03387100	-0.11558000
C	0.41921100	-3.04587000	-0.08138700
N	-1.83062400	-1.02279400	-0.06257900
C	-1.98927800	-2.38272200	-0.02396900
C	-3.40349700	-2.69417800	0.02130100
C	-4.07474900	-1.50641900	0.00540900
C	-3.07802100	-0.45619000	-0.04460500
N	-1.05758100	1.80804700	-0.00680500
C	-2.42193400	1.95979900	-0.04252500
C	-2.74413500	3.36994600	-0.08055000
C	-1.56026900	4.05069100	-0.08753400
C	-0.50316300	3.06272400	-0.05767500
H	1.15459700	4.37881000	-0.12571700
H	4.30515800	-1.18157900	-0.31177300
H	-1.23814600	-4.36250000	-0.00094400
H	-4.39587400	1.19820500	-0.04918400
C	1.10552400	-0.04971100	2.74661200
H	1.83417500	0.70788100	2.44163200
H	0.88087300	0.04980300	3.81529000
N	-0.14580800	-0.10002700	-2.08534400
H	-0.49772600	-1.02455300	-2.38461700
H	1.32557400	-5.10534300	-0.08600900
H	3.66142000	-3.75770300	-0.23060200
H	-3.81578300	-3.69424800	0.06420900
H	-5.14441200	-1.34283800	0.03591200
H	5.05632800	1.36355900	-0.33769800
H	3.72928600	3.71367900	-0.23536200
H	-1.40682500	5.12188900	-0.12036200
H	-3.74734800	3.77614500	-0.10433500
H	1.52207400	-1.03901300	2.55454700
O	-0.09377000	0.03427600	1.97338500
H	-0.44944100	0.93936300	2.00476200

5-CSS

B3LYP-D3(BJ) SCF energy in solution: -2811.03267255 a.u.

B3LYP-D3(BJ) enthalpy: -2810.483894 a.u.
B3LYP-D3(BJ) free energy: -2810.585278 a.u.

Cartesian coordinates

ATOM	X	Y	Z
Fe	0.82935700	0.31774900	0.20178500
C	0.78071200	-2.94545300	1.24242700
C	4.07494000	-0.08705100	-0.84608200
C	0.98721200	3.63429000	-0.57466100
C	-2.28857100	0.79546000	1.57023700
N	2.17142700	-1.21568000	0.20313400
C	1.93917200	-2.50297600	0.61686300
C	3.08659500	-3.33316800	0.32711500
C	4.01257600	-2.52857500	-0.26619300
C	3.43241400	-1.20665500	-0.33736400
N	2.27794700	1.54720100	-0.47978700
C	3.53426700	1.18968600	-0.90444700
C	4.21545500	2.33923600	-1.45475500
C	3.34691700	3.38532700	-1.38009600
C	2.13282400	2.87847600	-0.78265900
N	-0.41393300	1.89344900	0.43860900
C	-0.19194900	3.17359500	-0.00752000
C	-1.35763400	3.99360300	0.23964900
C	-2.27765100	3.19635300	0.84882600
C	-1.67654100	1.88826500	0.97652200
N	-0.45630500	-0.81593900	1.27219000
C	-1.71888500	-0.46146200	1.69882800
C	-2.38390200	-1.60403700	2.27285700
C	-1.52511700	-2.65724700	2.17128900
C	-0.32754300	-2.16437700	1.53655900
H	0.73578200	-3.99326100	1.52372100
H	5.07973400	-0.22043800	-1.23473300
H	1.02031500	4.67728000	-0.87407500
H	-3.30436400	0.92226100	1.92696900
C	2.95997300	0.56597300	2.71546300
H	3.21206700	-0.48066500	2.51704800
H	3.14342100	0.80438600	3.77039900
N	0.24931200	-0.06525600	-1.30673600
H	-0.76580000	0.15450800	-1.31451600
H	3.49433200	4.40919300	-1.69879800
H	5.22401700	2.32575000	-1.84756200
H	-1.43706900	5.04212400	-0.01738700
H	-3.27286900	3.44846500	1.19025200
H	5.00155500	-2.78740000	-0.62211000
H	3.15797400	-4.38862000	0.55684700
H	-1.67477900	-3.68203300	2.48604700
H	-3.38433100	-1.58539500	2.68424300
H	3.58302200	1.20321500	2.08690800
C	-3.48757700	-0.83538100	-1.23350600
C	-3.39161400	0.44745700	-1.80546900
C	-4.54950800	-1.10459900	-0.34922100
C	-4.31386300	1.43799100	-1.47788800
H	-2.58486300	0.65867600	-2.50019600
C	-5.47287300	-0.11243500	-0.03263800

H	-4.62347700	-2.09209000	0.09370800
C	-5.35521700	1.16471100	-0.58885400
H	-4.21270000	2.42805700	-1.91223600
H	-6.28674500	-0.33418600	0.65260900
H	-6.07420800	1.93876400	-0.33556900
O	1.60655300	0.85886200	2.36085300
H	1.01010500	0.22635600	2.79533200
C	-2.50500600	-1.83108700	-1.51124100
C	-1.64275400	-2.65888500	-1.71765700
C	0.60200900	-3.06875900	-2.75353500
H	1.38833800	-3.82612000	-2.84485100
H	1.00465000	-2.18674800	-2.25014000
H	0.28849200	-2.76782900	-3.75853600
C	-0.58806400	-3.64051200	-1.96182400
H	-0.23051500	-4.01344800	-0.99379000
H	-1.01173300	-4.50618800	-2.49083400

5-OSS

B3LYP-D3(BJ) SCF energy in solution: -2811.03185771 a.u.
B3LYP-D3(BJ) enthalpy: -2810.48383 a.u.
B3LYP-D3(BJ) free energy: -2810.585707 a.u.

Cartesian coordinates

ATOM	X	Y	Z
Fe	0.88991400	0.31608100	0.22459200
C	0.77276300	-2.97335300	1.18709200
C	4.10368000	-0.13452700	-0.89484200
C	1.07069900	3.62106500	-0.56515200
C	-2.24346300	0.80088800	1.56393200
N	2.19347100	-1.23749300	0.18353800
C	1.94313100	-2.52799000	0.58471700
C	3.08114900	-3.36625400	0.28904500
C	4.01598600	-2.56912900	-0.30206100
C	3.45322800	-1.24156300	-0.36769500
N	2.33374500	1.51950000	-0.51641700
C	3.57710400	1.14785700	-0.96332700
C	4.25990600	2.28697400	-1.53429300
C	3.40481100	3.34305000	-1.44300200
C	2.19898900	2.85100500	-0.81473700
N	-0.33853000	1.89240100	0.46759600
C	-0.10054100	3.17280600	0.02980000
C	-1.24987400	4.00728200	0.29982100
C	-2.17902400	3.21691600	0.90518700
C	-1.60190100	1.89701900	1.00724600
N	-0.44998400	-0.84113100	1.22353000
C	-1.70735100	-0.47455900	1.65427600
C	-2.39501000	-1.61789100	2.19997800
C	-1.54928600	-2.68101100	2.08754800
C	-0.33875000	-2.19218000	1.47272600
H	0.72126600	-4.02490500	1.45269400
H	5.10133900	-0.28676100	-1.29480500
H	1.10811000	4.66565900	-0.85849100
H	-3.25819500	0.94298600	1.91839500
C	3.03367400	0.51707600	2.70009000
H	3.30322900	-0.51857700	2.47070200
H	3.23260300	0.73509300	3.75627700
N	0.26155700	-0.05015200	-1.39153400
H	-0.73914000	-0.28293900	-1.25703000
H	3.55705800	4.36407600	-1.76867600
H	5.25886400	2.26145400	-1.95035200
H	-1.31546300	5.05969000	0.05503500
H	-3.16909700	3.47987000	1.25305500
H	4.99951000	-2.83914600	-0.66457300
H	3.13997400	-4.42443700	0.50955500
H	-1.71664900	-3.70881200	2.38318300
H	-3.39903300	-1.59353000	2.60219300
H	3.62742100	1.18335500	2.07346600
C	-3.60824300	-0.74657400	-1.18546600
C	-3.37247600	0.53091600	-1.72778700
C	-4.71873700	-0.93268800	-0.34086900
C	-4.21473700	1.59458400	-1.41562200
H	-2.51609600	0.68165700	-2.37704300
C	-5.55918900	0.13470900	-0.03700600
H	-4.89876100	-1.91668300	0.07953000
C	-5.30828800	1.40303200	-0.56858500
H	-4.00701400	2.57861300	-1.82473800
H	-6.41278100	-0.02188600	0.61711100
H	-5.96372100	2.23506500	-0.32673800
O	1.66547800	0.78808100	2.38108500
H	1.09050300	0.13680500	2.81664800
C	-2.70756800	-1.82056500	-1.45099500
C	-1.90382600	-2.70705600	-1.64762000
C	0.35369600	-3.19286400	-2.60785900
H	1.10616000	-3.98335400	-2.70293700
H	0.79148300	-2.35286300	-2.06255600
H	0.09059900	-2.83779600	-3.60907400
C	-0.89012500	-3.73393100	-1.87855700
H	-0.58896900	-4.15296800	-0.90983900
H	-1.32918600	-4.56256200	-2.45196500

5-T

B3LYP-D3(BJ) SCF energy in solution: -2811.04491548 a.u.
B3LYP-D3(BJ) enthalpy: -2810.497023 a.u.
B3LYP-D3(BJ) free energy: -2810.59879 a.u.

Cartesian coordinates

ATOM	X	Y	Z
Fe	0.84107400	0.35111500	0.20657600
C	0.25486700	-2.79293500	1.45177400
C	3.95297400	-0.64627300	-0.82351900
C	1.54030300	3.55115600	-0.74547400
C	-2.18901900	1.39360800	1.45179900
N	1.89730800	-1.37432100	0.30281400
C	1.47218500	-2.57467300	0.81978800
C	2.47897800	-3.58877600	0.60825700
C	3.51272200	-2.98852800	-0.04656400

C	3.14470400	-1.60468400	-0.23078800
N	2.46106500	1.28303800	-0.54812100
C	3.63029300	0.69592900	-0.96830700
C	4.48074000	1.67862900	-1.59697900
C	3.80255800	2.86012700	-1.56920400
C	2.53639700	2.60085500	-0.92497900
N	-0.12723800	2.12260500	0.34530700
C	0.30406600	3.32218300	-0.16040700
C	-0.71701700	4.33247100	0.01701800
C	-1.76550700	3.72568900	0.63748900
C	-1.38582500	2.34522600	0.84096900
N	-0.64283300	-0.50995800	1.28501300
C	-1.84325000	0.06695300	1.64754000
C	-2.69518400	-0.91731800	2.26549800
C	-2.00776300	-2.09414800	2.26847000
C	-0.73133800	-1.83766800	1.64898900
H	0.05208000	-3.79757700	1.80964200
H	4.91620200	-0.97190400	-1.20374500
H	1.74422500	4.55649400	-1.10082500
H	-3.17797300	1.70229700	1.77183400
C	2.94043300	0.36858500	2.72836900
H	3.02570700	-0.71435400	2.59395000
H	3.16030100	0.63866900	3.76828400
N	0.16409400	-0.07338600	-1.32774400
H	-0.39754000	-0.93681400	-1.27822600
H	4.11229600	3.82450400	-1.95094800
H	5.46182700	1.47288100	-2.00535200
H	-0.62161100	5.36468600	-0.29474700
H	-2.71266100	4.15277100	0.94042300
H	4.44693800	-3.42534100	-0.37523100
H	2.38912300	-4.62004300	0.92489700
H	-2.32550400	-3.05934900	2.64118600
H	-3.69392900	-0.71753900	2.62961700
H	3.65190800	0.86333800	2.06645000
C	-3.44488700	-0.78881800	-1.20836800
C	-3.03654900	0.46384200	-1.70363500
C	-4.67090800	-0.88828900	-0.52475000
C	-3.83776200	1.58606900	-1.51191900
H	-2.07348800	0.55285100	-2.19475600
C	-5.46537000	0.23967600	-0.33774500
H	-4.98096600	-1.85330400	-0.13704000
C	-5.05208300	1.48065000	-0.83040500
H	-3.49891900	2.55055500	-1.87824100
H	-6.40987900	0.15083700	0.19235700
H	-5.67323700	2.35982900	-0.68204100
O	1.64701800	0.84742300	2.34901200
H	0.95957800	0.34549800	2.81813600
C	-2.61154300	-1.93682900	-1.37217500
C	-1.87976000	-2.89564000	-1.50201500
C	0.31784200	-3.60596300	-2.45619800
H	0.99496000	-4.46207800	-2.54437200
H	0.85125400	-2.79786800	-1.94953200
H	0.05591100	-3.26171500	-3.46141200
C	-0.94580100	-4.00767700	-1.67236700
H	-0.65305500	-4.38268500	-0.68290600
H	-1.45136900	-4.83942800	-2.18232800

5-Q

B3LYP-D3(BJ) SCF energy in solution: -2811.0271424 a.u.
B3LYP-D3(BJ) enthalpy: -2810.481763 a.u.
B3LYP-D3(BJ) free energy: -2810.585999 a.u.

Cartesian coordinates

ATOM	X	Y	Z
Fe	0.84282200	0.32654500	0.14703800
C	0.25797200	-2.83460000	1.45401000
C	3.97810400	-0.66215700	-0.80133500
C	1.59406700	3.56882700	-0.68757200
C	-2.17382200	1.38021300	1.45116600
N	1.93493500	-1.43355200	0.33552400
C	1.49255100	-2.63104700	0.83166900
C	2.49971900	-3.64517900	0.59594800
C	3.53577200	-3.03565300	-0.05181200
C	3.17617300	-1.64205400	-0.21342500
N	2.53580600	1.30649700	-0.52702000
C	3.68555900	0.69637200	-0.95270000
C	4.53954900	1.67989300	-1.58508700
C	3.87200700	2.87083700	-1.54498700
C	2.60434400	2.62403500	-0.88969000
N	-0.11032100	2.16168800	0.38110500
C	0.34133900	3.35570700	-0.10940400
C	-0.68804500	4.36411900	0.06823200
C	-1.74789600	3.74862200	0.66631900
C	-1.37343000	2.36076700	0.86164700
N	-0.64964700	-0.55212700	1.32709300
C	-1.85069400	0.03927800	1.65212700
C	-2.72375500	-0.95404600	2.23414500
C	-2.04227900	-2.13751200	2.24050400
C	-0.74323600	-1.88401700	1.65968400
H	0.04439900	-3.84449500	1.79213500
H	4.93681600	-0.99493400	-1.18888500
H	1.80106500	4.57744400	-1.03389700
H	-3.17040700	1.68439200	1.75397700
C	2.92370800	0.39183500	2.69607800
H	3.04376800	-0.69075700	2.58879600
H	3.10250900	0.69078200	3.73586100
N	0.15263100	-0.10479000	-1.38902000
H	-0.46278000	-0.92658600	-1.27165200
H	4.19597500	3.83030700	-1.92782800
H	5.51597700	1.47568700	-2.00574400
H	-0.59642400	5.40170500	-0.22708600
H	-2.69690000	4.18020000	0.95759500
H	4.46474500	-3.47787500	-0.38872700
H	2.41415700	-4.68364600	0.88999300
H	-2.38433600	-3.10262700	2.59183300
H	-3.73274600	-0.76160600	2.57364500

H	3.64063600	0.89362500	2.04557800
O	1.62985700	0.82362800	2.26773400
H	0.93985100	0.31335500	2.72565300
C	-1.93305100	-2.85323400	-1.50961500
C	0.26643800	-3.58759200	-2.44735900
H	0.93340500	-4.45226800	-2.52887100
H	0.80531200	-2.78535000	-1.93722100
H	0.01765800	-3.24128800	-3.45523600
C	-1.00881500	-3.97439300	-1.67471000
H	-0.72920100	-4.35349700	-0.68308100
H	-1.51992800	-4.79953600	-2.18980200
C	-2.66040900	-1.89067100	-1.38067900
C	-3.49188200	-0.74196400	-1.21121600
C	-4.71936100	-0.84509400	-0.53065800
C	-3.08003600	0.51459400	-1.69311400
C	-5.51080300	0.28313100	-0.33264900
H	-5.03256100	-1.81323200	-0.15345200
C	-3.87784200	1.63727600	-1.49031800
H	-2.11654400	0.60634700	-2.18267200
C	-5.09309500	1.52823100	-0.81102300
H	-6.45620300	0.19135900	0.19528100
H	-3.53575100	2.60451600	-1.84620400
H	-5.71166400	2.40761600	-0.65368400

TS3-CSS

B3LYP-D3(BJ) SCF energy in solution: -2811.0114757 a.u.
B3LYP-D3(BJ) enthalpy: -2810.468344 a.u.
B3LYP-D3(BJ) free energy: -2810.567866 a.u.

Cartesian coordinates

ATOM	X	Y	Z
Fe	1.08869500	0.17484000	0.16908300
C	4.37546600	-0.12693400	-0.74932100
C	1.27342000	3.56459800	-0.28813300
C	-2.11003100	0.52517400	1.34835100
C	0.99162200	-3.17911500	0.86888400
N	2.56770300	1.47767700	-0.31437400
C	3.84533300	1.15695400	-0.69811700
C	4.56200500	2.35544800	-1.07537600
C	3.69121800	3.39404100	-0.94070300
C	2.43966800	2.83379200	-0.48054500
N	-0.19144100	1.72959900	0.41814000
C	0.05045300	3.04800700	0.12145800
C	-1.14426900	3.83455000	0.34616600
C	-2.09945300	2.97727300	0.80268400
C	-1.48832000	1.66735800	0.86064500
N	-0.24877300	-1.05431600	1.02431100
C	-1.52902600	-0.73132000	1.43070300
C	-2.20825800	-1.91257800	1.89936000
C	-1.34438100	-2.95706700	1.74950200
C	-0.12542200	-2.41986400	1.19559100
N	2.41521600	-1.36340700	0.05188400
C	2.17467900	-2.68414600	0.33176900
C	3.34468100	-3.47953200	0.02679400
C	4.29480700	-2.61747300	-0.43178500
C	3.70687400	-1.29530400	-0.40786400
H	5.40357700	-0.22374200	-1.08517100
H	1.32343300	4.63321900	-0.47430900
H	-3.14141800	0.61689000	1.67164800
H	0.93551300	-4.24744500	1.05513200
C	3.05640700	0.17828500	2.77762900
H	3.29945800	-0.84757300	2.48330500
H	3.19219000	0.30413200	3.85878800
N	0.66546200	-0.02581000	-1.51627100
H	-0.13674600	0.59216000	-1.72682400
H	0.24031200	-1.08658100	-1.86791900
H	-3.12205100	3.18980600	1.08624800
H	-1.21858400	4.90234700	0.18377600
H	-3.22344100	-1.92398700	2.27316300
H	-1.50379400	-4.00180500	1.98426700
H	3.85969800	4.44507300	-1.13766200
H	5.59283200	2.37818600	-1.40522300
H	5.30563800	-2.83742400	-0.75103200
H	3.41541200	-4.55149800	0.16095100
H	3.71757700	0.86327800	2.24621000
C	-4.21190500	-0.45090400	-0.97327800
C	-4.50934500	0.89334000	-1.27384500
C	-5.05364900	-1.15234800	-0.08695000
C	-5.60675000	1.51845300	-0.68946400
H	-3.85424000	1.44016500	-1.94378100
C	-6.15035500	-0.51980800	0.49149000
H	-4.82271100	-2.18642100	0.14609900
C	-6.42960500	0.81774200	0.19689600
H	-5.81851800	2.55832500	-0.92212600
H	-6.78963900	-1.07053500	1.17597900
H	-7.28371800	1.30969800	0.65317200
C	-0.70607600	-2.02327400	-2.23483300
H	-0.33956800	-2.85660300	-1.63014900
C	-3.04240900	-1.06309400	-1.49583100
C	-1.98722500	-1.55278000	-1.85981900
C	-0.36777200	-2.10632700	-3.71237900
H	0.70173500	-2.29692200	-3.84776700
H	-0.62190400	-1.17182800	-4.22250400
H	-0.92628000	-2.91837000	-4.19747100
O	1.72448000	0.53361700	2.39512000
H	1.10186300	-0.13241100	2.73219000

TS3-OSS

B3LYP-D3(BJ) SCF energy in solution: -2811.01653065 a.u.
B3LYP-D3(BJ) enthalpy: -2810.475127 a.u.
B3LYP-D3(BJ) free energy: -2810.574598 a.u.

Cartesian coordinates

ATOM	X	Y	Z
Fe	1.16309000	0.20587800	0.19879700
C	3.98736800	-1.55762900	-0.59921300

C	2.74132000	3.11808500	-0.60313900
C	-1.69327600	1.95985700	0.94267400
C	-0.27613400	-2.65179300	1.40826500
N	3.02905700	0.68925700	-0.38526300
C	4.04005000	-0.17591000	-0.72154700
C	5.17737500	0.55957200	-1.22366500
C	4.83332900	1.87743300	-1.20036700
C	3.48116100	1.94676900	-0.69537700
N	0.62362400	2.14927500	0.16885000
C	1.41045400	3.20408900	-0.22122200
C	0.64801900	4.43287900	-0.18905700
C	-0.60906400	4.10522300	0.21795000
C	-0.61110100	2.67805500	0.45046600
N	-0.59316600	-0.23406500	1.07529600
C	-1.67125800	0.60959200	1.25590000
C	-2.77713700	-0.11456700	1.82894900
C	-2.36745200	-1.40463400	1.98408700
C	-1.01507100	-1.48084300	1.49088300
N	1.73198500	-1.72371900	0.34871100
C	0.99327300	-2.76397500	0.85516300
C	1.72271300	-4.00509000	0.72323000
C	2.90977400	-3.70086400	0.12743700
C	2.91296600	-2.27242300	-0.09014900
H	4.86324100	-2.12078800	-0.90613700
H	3.23694800	4.04111600	-0.88779600
H	-2.62025700	2.49608200	1.11740400
H	-0.74427400	-3.56080000	1.77288600
C	2.87709600	-0.24395100	2.82303400
H	2.61661900	-1.30629000	2.80900300
H	3.08099500	0.08655600	3.84760000
N	0.62070100	0.00608200	-1.50045600
H	-0.20325900	0.61946900	-1.61730200
H	0.03950300	-1.13485300	-1.73935600
H	-1.46149100	4.75497300	0.36926900
H	1.04101800	5.40763000	-0.44819800
H	-3.74528300	0.31579500	2.04675000
H	-2.93003700	-2.24713800	2.36490200
H	5.42027900	2.73361100	-1.50724500
H	6.10667700	0.10994400	-1.54919400
H	3.72358800	-4.36544200	-0.13300000
H	1.35805100	-4.97159700	1.04693700
H	3.75946000	-0.08421100	2.20387600
C	-4.34399700	-0.44795400	-0.96618400
C	-4.51325000	0.93828700	-1.15286900
C	-5.33683600	-1.16413100	-0.27053500
C	-5.63506100	1.58668100	-0.64393100
H	-3.74396000	1.49413300	-1.67886700
C	-6.45692300	-0.50925400	0.23390500
H	-5.20597900	-2.23093500	-0.12066500
C	-6.60984500	0.86815100	0.05382700
H	-5.74926300	2.65737700	-0.79020100
H	-7.21296900	-1.07415200	0.77236700
H	-7.48339400	1.37697400	0.45124400
C	-0.79540400	-2.07011000	-2.08358200
H	-0.46519300	-2.90827600	-1.46371900
O	1.83838100	0.55892700	2.24634900
H	0.99384000	0.38124200	2.69466600
C	-3.15728400	-1.08985300	-1.41664400
C	-2.09767200	-1.59465100	-1.74093200
C	-0.48471000	-2.24426800	-3.56477700
H	0.57768600	-2.47078200	-3.69943800
H	-0.71305700	-1.32749400	-4.11742900
H	-1.07283300	-3.06084600	-4.00332000

TS3-T

B3LYP-D3(BJ) SCF energy in solution: -2811.0159044 a.u.
B3LYP-D3(BJ) enthalpy: -2810.474853 a.u.
B3LYP-D3(BJ) free energy: -2810.5763 a.u.

Cartesian coordinates

ATOM	X	Y	Z
Fe	1.19079900	0.19078500	0.19845200
C	4.16264400	-1.30560600	-0.57069400
C	2.55421500	3.25928400	-0.54282900
C	-1.74432500	1.69891600	1.04596200
C	-0.07249800	-2.83962700	1.20729100
N	3.02995400	0.86097600	-0.33572300
C	4.11008300	0.07700600	-0.67273500
C	5.18508400	0.90179200	-1.16949300
C	4.73663900	2.18882800	-1.15333000
C	3.38485000	2.15379900	-0.65078800
N	0.53850700	2.09633300	0.23675800
C	1.22716300	3.22379900	-0.13756800
C	0.36923100	4.38330600	-0.04861200
C	-0.84428100	3.94184000	0.38356200
C	-0.72799000	2.51303800	0.56651000
N	-0.53418800	-0.43811800	1.01271200
C	-1.63953400	0.33539200	1.27438400
C	-2.69890600	-0.47719600	1.82585000
C	-2.22861900	-1.75289000	1.87800100
C	-0.88200900	-1.72384000	1.35648900
N	1.89624600	-1.69393400	0.29894700
C	1.21670200	-2.82205700	0.69379400
C	2.04420800	-3.99084600	0.51489600
C	3.23175600	-3.55703900	0.00575200
C	3.13305800	-2.12186800	-0.12205400
H	5.08589800	-1.79121700	-0.87128100
H	2.96678600	4.22422500	-0.82020300
H	-2.69848600	2.16550100	1.26765100
H	-0.48384900	-3.80042300	1.50028400
C	1.99199900	-0.47645400	3.19988900
H	0.96190400	-0.78685000	3.37274700
H	2.42402300	-0.09789000	4.13289000
N	0.63493300	0.02169600	-1.49751500
H	-0.09647600	0.70912400	-1.72197300
H	-0.00369300	-1.08530200	-1.77808500

H	-1.74160700	4.51504400	0.57832900
H	0.67511100	5.39411000	-0.28593300
H	-3.67709700	-0.10576300	2.09914100
H	-2.73675400	-2.64645400	2.21665100
H	5.25545600	3.08743000	-1.46153200
H	6.14776700	0.52772800	-1.49372600
H	4.10498700	-4.13954300	-0.25874800
H	1.74114800	-5.00238000	0.75301000
H	2.56703800	-1.33115400	2.83154600
C	-4.33955100	-0.39130000	-0.98731400
C	-4.51287100	0.99883100	-1.14076900
C	-5.31924300	-1.12098800	-0.28593200
C	-5.62550300	1.63616900	-0.59867400
H	-3.75417800	1.56583500	-1.67038100
C	-6.43012400	-0.47709800	0.25222300
H	-5.18499900	-2.19038800	-0.15996600
C	-6.58757700	0.90331200	0.10182400
H	-5.74242300	2.70959900	-0.72111700
H	-7.17573700	-1.05335800	0.79328400
H	-7.45401600	1.40348300	0.52496900
C	-0.82485400	-2.01184200	-2.20297900
H	-0.50508400	-2.88427600	-1.62547200
C	-3.16635800	-1.02668000	-1.47875500
C	-2.12118500	-1.53992700	-1.83710000
C	-0.51501500	-2.12027600	-3.69114600
H	0.54750800	-2.34009600	-3.83718000
H	-0.74366900	-1.18035800	-4.20397100
H	-1.10167100	-2.91588700	-4.16906700
O	1.93336800	0.57214400	2.22450500
H	2.83310600	0.82437700	1.95217700

TS3-Q

B3LYP-D3(BJ) SCF energy in solution: -2811.01191099 a.u.
B3LYP-D3(BJ) enthalpy: -2810.473255 a.u.
B3LYP-D3(BJ) free energy: -2810.57911 a.u.

Cartesian coordinates

ATOM	X	Y	Z
Fe	1.21019600	0.13620600	-0.03253200
C	4.39722200	1.20067300	-0.71318100
C	0.17669700	3.43595300	0.20541600
C	-1.79428600	-0.83388900	1.42148300
C	2.37675500	-3.08867300	0.33211500
N	2.11546000	1.98950500	-0.23402200
C	3.42335100	2.19394400	-0.59075400
C	3.64258900	3.61068300	-0.79180500
C	2.45651300	4.23897000	-0.54154600
C	1.50163800	3.21259000	-0.17962700
N	-0.47511900	1.14042100	0.78845800
C	-0.74128400	2.48000600	0.64524600
C	-2.11724500	2.73512500	1.01680200
C	-2.66857700	1.53582700	1.36720300
C	-1.63459800	0.53550700	1.21013700
N	0.43473500	-1.63930600	0.75745300
C	-0.84741300	-1.83743300	1.20367300
C	-1.06344400	-3.25078600	1.41838400
C	0.10415100	-3.88732300	1.10117200
C	1.04487700	-2.86709200	0.69310400
N	3.08081300	-0.77885000	-0.09805200
C	3.32227900	-2.12327300	-0.02100400
C	4.70791700	-2.37908300	-0.36077400
C	5.27617400	-1.17174800	-0.64732300
C	4.24132600	-0.16932000	-0.48931100
H	5.38742000	1.53172900	-1.01268000
H	-0.17114000	4.46435400	0.17140800
H	-2.77387500	-1.15595200	1.75835900
H	2.71541700	-4.12070200	0.34041600
C	2.19487800	-0.50688400	3.18738400
H	3.15175000	-0.89688200	2.83603000
H	1.45041900	-1.30884000	3.13728100
N	0.71949000	-0.02771000	-1.80001600
H	0.45168500	0.78948900	-2.36412800
H	-0.20323200	-0.96583400	-2.16065600
H	-3.68480400	1.33182600	1.67746800
H	-2.59352200	3.70729700	1.00013500
H	-1.98841100	-3.68967200	1.77047200
H	0.31945900	-4.94749600	1.14546100
H	2.24166000	5.29942000	-0.57820200
H	4.58750100	4.05640400	-1.07544500
H	6.29811200	-0.96709800	-0.94020000
H	5.17363700	-3.35638900	-0.37238400
H	2.30465200	-0.16559500	4.22528800
C	-4.46480200	-0.33659300	-0.86170400
C	-4.93423600	0.95633800	-1.16418200
C	-5.11011000	-1.07289400	0.15202900
C	-6.00573300	1.49933600	-0.46144900
H	-4.43296700	1.52873900	-1.93749600
C	-6.17900200	-0.52179600	0.85311000
H	-4.75450000	-2.07252800	0.38081200
C	-6.62907200	0.76714400	0.55256900
H	-6.35216100	2.50096400	-0.70001800
H	-6.66427600	-1.09871100	1.63546800
H	-7.46221700	1.19563600	1.10209700
C	-1.07430900	-1.74461300	-2.59899700
H	-0.72831100	-2.68905300	-2.16271400
O	1.86307000	0.57723000	2.32371300
H	0.95059300	0.86773000	2.49323300
C	-3.32593800	-0.86690300	-1.52582200
C	-2.31788800	-1.31235700	-2.04245100
C	-0.95187000	-1.71134800	-4.11960400
H	0.08084200	-1.91851600	-4.41641200
H	-1.23551700	-0.72885100	-4.51030800
H	-1.60490500	-2.45960600	-4.58567600

6-OSS

B3LYP-D3(BJ) SCF energy in solution: -2811.05738472 a.u.

B3LYP-D3(BJ) enthalpy: -2810.51106 a.u.
B3LYP-D3(BJ) free energy: -2810.611974 a.u.

Cartesian coordinates

ATOM	X	Y	Z
Fe	0.95270900	0.23593000	0.23203900
C	3.20024400	2.43375800	-1.15927800
C	-1.23518100	2.78868200	0.75260800
C	-1.23419100	-1.94382700	1.76323100
C	3.23416200	-2.28437100	-0.07108000
N	0.98742000	2.21610400	-0.12191700
C	1.97921600	2.94268000	-0.73808100
C	1.57182400	4.32172200	-0.87716400
C	0.32398700	4.41893200	-0.33892200
C	-0.03429000	3.09949100	0.12881300
N	-0.86146300	0.38726000	1.09656000
C	-1.60873800	1.53328100	1.20819200
C	-2.86676500	1.24713300	1.86220800
C	-2.87352000	-0.08487700	2.13439600
C	-1.61522300	-0.61495700	1.65738300
N	1.00106800	-1.71721300	0.78326800
C	-0.01464600	-2.45646400	1.34533800
C	0.37954300	-3.84012800	1.45362500
C	1.64454400	-3.93070900	0.95214300
C	2.02143200	-2.60385100	0.52408500
N	2.85485100	0.11648100	-0.44097300
C	3.61092000	-1.02664900	-0.52399500
C	4.87844400	-0.73850200	-1.15694500
C	4.87174100	0.58807800	-1.46656500
C	3.60145200	1.11221200	-1.02055700
H	3.89197700	3.12100700	-1.63644100
H	-1.94447600	3.59800700	0.89570100
H	-1.94665200	-2.63620700	2.19973800
H	3.94565500	-3.09291400	-0.20897300
C	2.96824500	1.26824400	2.42204000
H	3.79390400	0.74558800	1.93099400
H	3.16135700	1.36938200	3.49560400
N	0.26384700	-0.12483700	-1.40494200
H	-0.66206900	-0.54751000	-1.38840000
H	0.27854800	0.66261400	-2.05183100
H	-3.65093700	-0.67396000	2.60237800
H	-3.64204000	1.97746900	2.04956200
H	-0.24042900	-4.62592800	1.86554400
H	2.27379700	-4.80742600	0.86528300
H	-0.30755600	5.29411500	-0.25423300
H	2.17574700	5.09971100	-1.32647000
H	5.64297400	1.17171800	-1.95280500
H	5.65633100	-1.46941200	-1.33757700
H	2.85297400	2.25511600	1.97470800
C	-3.76399900	-0.59955300	-1.12861700
C	-3.37550900	0.71653500	-1.47397400
C	-5.03803600	-0.79602800	-0.54327100
C	-4.22920700	1.78649200	-1.23848800
H	-2.39222300	0.88144300	-1.89960000
C	-5.88174100	0.28277100	-0.31267500
H	-5.34112400	-1.80309900	-0.27488100
C	-5.48417500	1.57923200	-0.65792200
H	-3.90835700	2.79100800	-1.49964300
H	-6.85585200	0.11579600	0.13894000
H	-6.14789700	2.41974200	-0.47621300
C	-1.24385700	-3.65403000	-1.72881200
H	-1.56854400	-4.66264700	-1.47632700
O	1.72196900	0.59027900	2.21294000
H	1.79246300	-0.33707100	2.49847800
C	-2.89736900	-1.68576100	-1.34729200
C	-2.11925600	-2.63049600	-1.53228900
C	0.13097400	-3.48006600	-2.30386100
H	0.44961400	-2.43421800	-2.26818300
H	0.16492900	-3.82601900	-3.34896600
H	0.85547700	-4.08112700	-1.74251800

6-T

B3LYP-D3(BJ) SCF energy in solution: -2811.05707159 a.u.
B3LYP-D3(BJ) enthalpy: -2810.510645 a.u.
B3LYP-D3(BJ) free energy: -2810.612685 a.u.

Cartesian coordinates

ATOM	X	Y	Z
Fe	0.93508800	0.23132800	0.24705500
C	4.06632900	-0.71648500	-0.72913800
C	1.60191500	3.45030100	-0.73134900
C	-2.11423100	1.19804600	1.41431200
C	0.32044900	-2.97861200	1.34545700
N	2.51982300	1.18564000	-0.55613800
C	3.71264100	0.61282400	-0.92255400
C	4.57142300	1.60159500	-1.53578100
C	3.88042300	2.77545800	-1.54017400
C	2.59990200	2.50569600	-0.92744200
N	-0.03196300	1.98458000	0.36963500
C	0.37592100	3.20054300	-0.12904700
C	-0.66326200	4.18536400	0.05635600
C	-1.70422500	3.54905500	0.66485700
C	-1.30480500	2.17497300	0.85140900
N	-0.59216100	-0.70942000	1.17620400
C	-1.77872200	-0.13739900	1.56264400
C	-2.64534500	-1.13279100	2.15542100
C	-1.96574300	-2.31029300	2.12590700
C	-0.67995800	-2.03376800	1.52209500
N	2.01539500	-1.48678400	0.38643700
C	1.57376000	-2.72014500	0.80899000
C	2.59282600	-3.71586700	0.58256500
C	3.64544600	-3.07740600	-0.00495400
C	3.27225700	-1.68988400	-0.13873400
H	5.04429300	-1.02518400	-1.08582200
H	1.79215100	4.46116800	-1.07851400
H	-3.10600100	1.49959300	1.73393500
H	0.10492000	-3.99889600	1.64637900

C	2.54778900	1.72523500	2.49720800
H	3.43095400	1.73290300	1.85203700
H	2.84308500	1.73284300	3.55218700
N	0.28069200	-0.13737400	-1.40041700
H	0.25426000	0.67146900	-2.02061000
H	-0.62503600	-0.60193900	-1.39405900
H	-2.66324900	3.95341000	0.96169800
H	-0.58917500	5.22221200	-0.24596700
H	-3.64226400	-0.93375500	2.52517500
H	-2.28312900	-3.28386800	2.47657200
H	4.19254800	3.74108800	-1.91703400
H	5.56818600	1.40434000	-1.90925300
H	4.58906200	-3.49529500	-0.33188600
H	2.49765700	-4.76345700	0.83857900
H	1.93874000	2.60236300	2.27998100
C	-3.67636200	-0.65505900	-1.17972400
C	-3.33414500	0.64187800	-1.63076800
C	-4.88219700	-0.82206100	-0.45775700
C	-4.16170100	1.72428700	-1.36044600
H	-2.40085900	0.78417300	-2.16394400
C	-5.70039800	0.26886000	-0.19143300
H	-5.14607100	-1.81287500	-0.10298400
C	-5.34632800	1.54725200	-0.63889700
H	-3.87087300	2.71477900	-1.69779800
H	-6.62068000	0.12549400	0.36837900
H	-5.98963000	2.39655900	-0.42731200
C	-1.11234000	-3.68054700	-1.73063900
H	-1.39991000	-4.68719000	-1.42988100
O	1.71513500	0.58830200	2.23190100
H	2.23859100	-0.23007500	2.29343500
C	-2.81589700	-1.74447800	-1.40753800
C	-2.01945900	-2.67805100	-1.56796400
C	0.25118900	-3.48061800	-2.32662400
H	0.55291800	-2.42962500	-2.28302600
H	0.27298600	-3.80909900	-3.37777900
H	0.99773700	-4.07600900	-1.78871200

6-Q

B3LYP-D3(BJ) SCF energy in solution: -2811.05365034 a.u.
B3LYP-D3(BJ) enthalpy: -2810.509851 a.u.
B3LYP-D3(BJ) free energy: -2810.616218 a.u.

Cartesian coordinates

ATOM	X	Y	Z
Fe	0.84975700	0.26495800	-0.01949900
C	4.12503100	-0.56380800	-0.67890700
C	1.60353200	3.59445700	-0.61758200
C	-2.13289100	1.27659100	1.45238800
C	0.34732500	-2.90433000	1.27494400
N	2.55873800	1.33062500	-0.55393300
C	3.77375900	0.77712300	-0.86016300
C	4.64808400	1.80790400	-1.37795000
C	3.93955700	2.97576500	-1.36640400
C	2.62784100	2.66846000	-0.83736800
N	-0.06137700	2.12940600	0.44360400
C	0.35995800	3.34718600	-0.03246100
C	-0.68635700	4.32575300	0.17154300
C	-1.73356200	3.67545400	0.76172800
C	-1.33794000	2.29375100	0.92127500
N	-0.62833800	-0.64812100	1.13966800
C	-1.80480100	-0.07526800	1.55799700
C	-2.64654300	-1.09147500	2.14734500
C	-1.95480700	-2.26787100	2.08731700
C	-0.68229900	-1.98087600	1.46463300
N	2.04174100	-1.43306900	0.28980200
C	1.61675800	-2.64669600	0.75276900
C	2.68942800	-3.61281000	0.61673600
C	3.74970100	-2.95331800	0.06457500
C	3.33341100	-1.57953900	-0.13902200
H	5.13273100	-0.84167600	-0.97430600
H	1.80219900	4.61828100	-0.92102200
H	-3.12488700	1.55987100	1.78894600
H	0.14738500	-3.92373200	1.59094700
C	1.54854000	0.05143400	3.37703700
H	2.13367700	-0.85826100	3.22964400
H	0.49164200	-0.22332000	3.46372800
N	0.23941500	-0.03214400	-1.79692100
H	0.72773600	0.31204300	-2.62031000
H	-0.48752700	-0.69385300	-2.05660500
H	-2.69040800	4.08335300	1.06173300
H	-0.61923800	5.37107000	-0.10254500
H	-3.63766000	-0.91626900	2.54449300
H	-2.26659000	-3.24457800	2.43475000
H	4.27050200	3.96054400	-1.67105200
H	5.67113400	1.65098800	-1.69553100
H	4.72860200	-3.34713100	-0.17787500
H	2.63034900	-4.65189600	0.91545200
H	1.87951500	0.54519400	4.30060800
C	-3.52662500	-0.72744400	-1.23877400
C	-3.16313400	0.59560200	-1.58560400
C	-4.78705300	-0.94816300	-0.63288100
C	-4.03379100	1.64947100	-1.33639700
H	-2.17943900	0.78088800	-2.00315800
C	-5.64468600	0.11603300	-0.38445400
H	-5.06515300	-1.96005600	-0.35661900
C	-5.27546700	1.41977600	-0.73636300
H	-3.72915200	2.66059100	-1.59036700
H	-6.60760700	-0.06826400	0.08423700
H	-5.95038600	2.24843800	-0.54136700
C	-0.98888700	-3.78047300	-1.77676700
H	-1.32298700	-4.78412100	-1.51673500
O	1.79144200	0.87351200	2.23932000
H	1.16605800	1.61838000	2.23147800
C	-2.64711800	-1.80381200	-1.46026700
C	-1.86645300	-2.75145000	-1.61946700
C	0.40221200	-3.62444300	-2.31907000
H	1.11735800	-4.21042900	-1.73021200

H	0.72409800	-2.58004000	-2.29713100
H	0.46521800	-3.98780300	-3.35660100

TS4-OSS

B3LYP-D3(BJ) SCF energy in solution: -2811.04003809 a.u.
B3LYP-D3(BJ) enthalpy: -2810.493005 a.u.
B3LYP-D3(BJ) free energy: -2810.593008 a.u.

Cartesian coordinates

ATOM	X	Y	Z
Fe	1.12657900	0.19607700	0.21087500
C	4.27189200	1.15250300	-0.75674300
C	0.09825000	3.45099300	0.13773800
C	-1.88963500	-0.71029700	1.60801500
C	2.12034500	-3.06847900	0.24502200
N	2.02460200	1.95650800	-0.18272800
C	3.32583500	2.15352400	-0.57520000
C	3.55866700	3.55878000	-0.82217900
C	2.37947600	4.20033600	-0.59144900
C	1.42398200	3.19130100	-0.19143400
N	-0.56567200	1.17743100	0.77384800
C	-0.82541000	2.51506000	0.58616200
C	-2.18837100	2.81109800	0.96951000
C	-2.74124000	1.64433500	1.40484000
C	-1.72103800	0.62819100	1.28007600
N	0.30511600	-1.53512700	0.87526600
C	-0.95769600	-1.71620100	1.38767100
C	-1.20615800	-3.12243400	1.60311600
C	-0.09071300	-3.78919500	1.19038000
C	0.84993900	-2.79057400	0.73521000
N	2.86050900	-0.76698100	-0.17889100
C	3.05829300	-2.12586500	-0.16040000
C	4.40908500	-2.43445000	-0.57449300
C	5.02415300	-1.24572000	-0.83172100
C	4.04697600	-0.20855000	-0.58765700
H	5.26218500	1.45739400	-1.08117900
H	-0.23714000	4.48084600	0.06036300
H	-2.85484700	-1.00252100	2.00558300
H	2.41614300	-4.11243400	0.20136000
C	2.43499400	-0.50389300	3.09693300
H	1.85742300	-1.42984500	3.01715500
H	2.60013100	-0.24792900	4.15028700
N	0.54624000	0.02843000	-1.49260200
H	-0.31324600	0.53459300	-1.70070700
H	1.24580700	0.22400700	-2.20934900
H	-3.75109600	1.46222600	1.74772500
H	-2.64707300	3.78972400	0.90798600
H	-2.12491900	-3.53116800	2.00404900
H	0.09350700	-4.85600500	1.18797100
H	2.16006300	5.25722800	-0.67323500
H	4.50525400	3.98007600	-1.13575900
H	6.04156400	-1.07040700	-1.15743700
H	4.82015000	-3.43370500	-0.64214800
H	3.39578800	-0.64113700	2.60034700
C	-4.17068900	-0.45051500	-1.03917500
C	-4.66710700	0.78898900	-1.50070300
C	-4.84758700	-1.09248500	0.02373800
C	-5.78017500	1.37067700	-0.90417300
H	-4.15143300	1.28970700	-2.31371600
C	-5.95968100	-0.50233100	0.61341600
H	-4.47816800	-2.05137800	0.37218600
C	-6.42981600	0.73435000	0.15809200
H	-6.14144300	2.32988700	-1.26469100
H	-6.46687700	-1.00871100	1.43039000
H	-7.29795100	1.19341900	0.62203300
C	-0.73066900	-1.98029800	-2.42019600
H	-0.20243800	-2.67032800	-1.76966200
O	1.78756000	0.57648100	2.41560100
H	0.88545900	0.68591600	2.75927100
C	-3.00208700	-1.01785100	-1.59026000
C	-1.95073700	-1.50759400	-2.00390600
C	-0.20794700	-1.78755900	-3.81425100
H	0.88697400	-1.77628000	-3.81683400
H	-0.57307300	-0.85311000	-4.25323100
H	-0.52861400	-2.60682300	-4.47644200

TS4-T

B3LYP-D3(BJ) SCF energy in solution: -2811.04139793 a.u.
B3LYP-D3(BJ) enthalpy: -2810.495347 a.u.
B3LYP-D3(BJ) free energy: -2810.59779 a.u.

Cartesian coordinates

ATOM	X	Y	Z
Fe	1.16605300	0.08078400	0.23633000
C	4.50139200	-0.01969500	-0.53005300
C	1.08782300	3.42228400	-0.41465600
C	-2.07567400	0.24252600	1.41778500
C	1.18225500	-3.28263700	0.79823700
N	2.53254200	1.43478000	-0.31662100
C	3.86316100	1.21179100	-0.59320900
C	4.49227400	2.44093800	-1.01035300
C	3.52564900	3.40300000	-1.00233100
C	2.30420600	2.76799800	-0.56924300
N	-0.21967500	1.53445900	0.45046800
C	-0.08198100	2.84792100	0.06488400
C	-1.31873200	3.56250300	0.28805900
C	-2.19842200	2.67178500	0.82635100
C	-1.50599400	1.40776300	0.92544200
N	-0.16040300	-1.24299200	1.05049300
C	-1.45475600	-0.99911000	1.44599100
C	-2.09858300	-2.23420700	1.82446100
C	-1.19218200	-3.23113500	1.61306000
C	0.01443900	-2.60447000	1.12487200
N	2.56925800	-1.36037900	0.15004500
C	2.36862700	-2.69952900	0.36895100
C	3.59752500	-3.42884500	0.13911700

C	4.54223600	-2.51086500	-0.20566100
C	3.88781400	-1.22121100	-0.20141500
H	5.55594200	-0.04862300	-0.78619800
H	1.05745900	4.47830400	-0.66497100
H	-3.10989600	0.29240600	1.73977200
H	1.17748600	-4.36182900	0.91861700
C	1.75612800	1.69126700	2.99911700
H	2.55159000	2.23373200	2.48650900
H	1.95467900	1.68740200	4.07779400
N	0.61625200	-0.29548500	-1.56133300
H	-0.04921000	0.44005700	-1.81386900
H	1.41775700	-0.17369800	-2.19041500
H	-3.22819000	2.82757900	1.11908200
H	-1.47329900	4.61011600	0.06289600
H	-3.11593600	-2.31090900	2.18372900
H	-1.31463100	-4.29557900	1.76812100
H	3.61666200	4.45062300	-1.25956200
H	5.53654900	2.53767900	-1.27841300
H	5.58547800	-2.67280700	-0.44467300
H	3.70662900	-4.50058200	0.24621300
H	0.80119000	2.18520700	2.79313200
C	-4.14961900	-0.40010400	-1.03330500
C	-4.55788300	0.93106700	-1.27127800
C	-4.87499800	-1.16908900	-0.09483400
C	-5.63403500	1.47467100	-0.57754100
H	-4.00008500	1.53092600	-1.98280700
C	-5.94908100	-0.61595400	0.59368000
H	-4.56745000	-2.19333200	0.08654300
C	-6.33242700	0.70950200	0.36195100
H	-5.92808300	2.50373200	-0.76626000
H	-6.49362100	-1.22021100	1.31450300
H	-7.17048000	1.13897300	0.90312900
C	-0.77215800	-1.80925400	-2.68683400
H	-0.27946600	-2.63311100	-2.17964600
C	-3.01040900	-0.93397000	-1.67496200
C	-1.98175900	-1.37954200	-2.17820300
C	-0.34620200	-1.50355700	-4.09718000
H	0.74041600	-1.58481200	-4.20352700
H	-0.65599800	-0.49726500	-4.39828300
H	-0.79879100	-2.21053300	-4.80983400
O	1.78215900	0.35961200	2.47676100
H	1.01101300	-0.13447000	2.80299100

TS4-Q

B3LYP-D3(BJ) SCF energy in solution: -2811.04546929 a.u.

B3LYP-D3(BJ) enthalpy: -2810.50253 a.u.

B3LYP-D3(BJ) free energy: -2810.607616 a.u.

Cartesian coordinates

ATOM	X	Y	Z
Fe	1.11104600	0.17003800	-0.00442000
C	4.32272000	1.16283600	-0.80002300
C	0.16491100	3.49101500	0.12116100
C	-1.84971300	-0.68880900	1.59420900
C	2.21763700	-3.06029300	0.39554400
N	2.08472800	2.01500800	-0.27056200
C	3.38565500	2.18757800	-0.65049700
C	3.63240600	3.59967000	-0.88320100
C	2.46082900	4.25255700	-0.63741900
C	1.49153500	3.24497700	-0.24476300
N	-0.52478500	1.22265500	0.79240500
C	-0.76984200	2.56077800	0.58571700
C	-2.13754800	2.85208400	0.95323200
C	-2.70100800	1.68137100	1.37892600
C	-1.68396000	0.66024100	1.27348100
N	0.33347100	-1.56212100	0.89063300
C	-0.92341000	-1.71744800	1.40874200
C	-1.14874600	-3.11830100	1.70343400
C	-0.01254500	-3.78819600	1.34919700
C	0.91903800	-2.80003400	0.84078800
N	2.94773300	-0.77925400	-0.17021600
C	3.16200400	-2.12841000	-0.04891500
C	4.53147100	-2.42397200	-0.40777500
C	5.12601100	-1.23542800	-0.72967100
C	4.12347900	-0.20410700	-0.57734800
H	5.31867500	1.45883300	-1.11705800
H	-0.17352900	4.52109700	0.05438600
H	-2.81955400	-0.97144700	1.98846000
H	2.54160500	-4.09669000	0.42817100
C	2.20059900	-0.39705600	3.19792100
H	1.41077200	-1.15524400	3.22171100
H	2.38804700	-0.02262700	4.21305600
N	0.45637100	-0.05556200	-1.80018800
H	-0.43892700	0.33873500	-2.08045400
H	1.07606200	-0.08938300	-2.60799300
H	-3.71843400	1.50935700	1.70456800
H	-2.60244600	3.82762800	0.88665900
H	-2.05951700	-3.52530600	2.12428300
H	0.18822100	-4.84937100	1.42622100
H	2.26192900	5.31506200	-0.69852400
H	4.58123000	4.02174600	-1.18958300
H	6.15020700	-1.06437300	-1.03634200
H	4.97658300	-3.41092500	-0.39793300
H	3.11283200	-0.85608100	2.81228300
C	-4.26141000	-0.44612700	-0.96066100
C	-4.71164700	0.78195300	-1.49264500
C	-4.93694700	-0.98361200	0.15868100
C	-5.77983500	1.45480800	-0.90955000
H	-4.19624600	1.20235800	-2.35008800
C	-6.00516800	-0.30398400	0.73356800
H	-4.60446000	-1.93487200	0.56102300
C	-6.42920000	0.92099400	0.20762700
H	-6.10580400	2.40451200	-1.32447500
H	-6.51311700	-0.73085600	1.59415600
H	-7.26219500	1.45074800	0.66046100
C	-0.94345200	-2.23660800	-2.33338700
H	-0.38242000	-2.83328500	-1.62002900

O	1.88378300	0.67069900	2.30804100
H	0.99408400	1.00964500	2.50480600
C	-3.13574400	-1.10520000	-1.50269300
C	-2.12090100	-1.67055900	-1.91109500
C	-0.51350900	-2.26590700	-3.77129100
H	0.57873500	-2.27339600	-3.84914500
H	-0.90294100	-1.40535100	-4.32480200
H	-0.88176200	-3.17303600	-4.27549100

3a-7-CSS

B3LYP-D3(BJ) SCF energy in solution: -2811.11997914 a.u.
B3LYP-D3(BJ) enthalpy: -2810.567809 a.u.
B3LYP-D3(BJ) free energy: -2810.664812 a.u.

Cartesian coordinates

ATOM	X	Y	Z
Fe	1.07724700	0.11915900	0.31432900
C	4.32484300	-0.19004900	-0.72347300
C	1.26243500	3.50577000	-0.08238100
C	-2.12259600	0.42807700	1.49798400
C	0.85789100	-3.29073700	0.64046700
N	2.52634700	1.40890100	-0.23889500
C	3.80733500	1.09850000	-0.63199800
C	4.53213100	2.30468100	-0.96883700
C	3.66868700	3.34388500	-0.79129700
C	2.41644600	2.77502800	-0.34273100
N	-0.19329200	1.65324400	0.60306300
C	0.05224800	2.98217900	0.35938700
C	-1.12039900	3.77487400	0.67060700
C	-2.06596400	2.90931000	1.12932600
C	-1.47463100	1.58740700	1.09044800
N	-0.33929700	-1.17295700	0.97186900
C	-1.59827100	-0.85515500	1.42983300
C	-2.32488900	-2.05689100	1.76924800
C	-1.49760500	-3.10704900	1.50220200
C	-0.25782700	-2.54742800	1.01079200
N	2.34018700	-1.43231900	0.01810000
C	2.06633600	-2.76981300	0.18789700
C	3.22405900	-3.56483800	-0.16067700
C	4.20029200	-2.69327400	-0.54026600
C	3.64014900	-1.36399800	-0.42798100
H	5.35237100	-0.28804200	-1.06171400
H	1.31575400	4.58175000	-0.22133200
H	-3.14102600	0.52933900	1.85885200
H	0.78347400	-4.37133400	0.72145800
C	2.95608100	0.02098800	2.73740500
H	3.30252700	-0.96187500	2.40575800
H	3.04235600	0.11238800	3.82595100
N	0.60630700	0.03626300	-1.65823200
H	0.18200800	0.93406400	-1.89621700
H	1.52507300	0.01653600	-2.10221500
H	-3.07183400	3.12251800	1.46805400
H	-1.18607900	4.84999700	0.55987600
H	-3.34047800	-2.07508900	2.14310000
H	-1.69059500	-4.16533800	1.62602000
H	3.84610300	4.40059500	-0.94712600
H	5.56233400	2.33396900	-1.30089900
H	5.20888000	-2.91287900	-0.86740200
H	3.26824600	-4.64562600	-0.11145700
H	3.55381800	0.79308800	2.25438800
C	-4.06239200	-0.24456200	-1.07622800
C	-4.48049400	1.09605600	-0.98717400
C	-4.92503300	-1.26317300	-0.63281200
C	-5.73213400	1.40586200	-0.46239600
H	-3.80429600	1.88203600	-1.30617400
C	-6.17644400	-0.94430700	-0.11134600
H	-4.59223000	-2.29440000	-0.68656600
C	-6.58420000	0.38898000	-0.02345500
H	-6.04286900	2.44454700	-0.39230100
H	-6.83423100	-1.73813000	0.23141500
H	-7.55959600	0.63446000	0.38673500
C	-0.22302600	-1.06700600	-2.21925600
H	0.12153100	-1.98285800	-1.72818500
O	1.60031500	0.25829400	2.33536000
H	1.02900700	-0.45905800	2.66107200
C	-2.75666100	-0.55945100	-1.55227000
C	-1.62028700	-0.82928000	-1.86956200
C	-0.03155500	-1.20996500	-3.73820200
H	1.02122800	-1.41118000	-3.96846400
H	-0.33859100	-0.29451000	-4.25553000
H	-0.63273600	-2.03912200	-4.12338500

3a-7-OSS

B3LYP-D3(BJ) SCF energy in solution: -2811.12502664 a.u.
B3LYP-D3(BJ) enthalpy: -2810.572 a.u.
B3LYP-D3(BJ) free energy: -2810.670057 a.u.

Cartesian coordinates

ATOM	X	Y	Z
Fe	1.06832900	0.12441800	0.29584900
C	4.33013000	-0.15149400	-0.72268000
C	1.22330700	3.51581300	-0.08992100
C	-2.13070200	0.40167400	1.49587000
C	0.88951000	-3.29008000	0.63238500
N	2.51197100	1.43237900	-0.25243300
C	3.79751000	1.13251400	-0.63758800
C	4.50964500	2.34763500	-0.97300400
C	3.63416300	3.37766400	-0.80000600
C	2.38529900	2.79687900	-0.35467500
N	-0.21993100	1.65519800	0.60050700
C	0.01656900	2.98508500	0.35826600
C	-1.16198900	3.76541500	0.67785600
C	-2.09898700	2.88959300	1.13788700
C	-1.49761800	1.57261000	1.09258600
N	-0.33429100	-1.18573800	0.96601100

C	-1.59489800	-0.87790800	1.42418400
C	-2.30820400	-2.08869700	1.76408700
C	-1.47025800	-3.13023100	1.49624100
C	-0.23547900	-2.55856400	1.00291300
N	2.36167500	-1.42331300	0.01155400
C	2.09780600	-2.76156100	0.18260400
C	3.26646600	-3.54311800	-0.15920100
C	4.23619900	-2.66059800	-0.53444400
C	3.66189500	-1.33707200	-0.42754200
H	5.36069600	-0.23628900	-1.05540200
H	1.26796900	4.59241800	-0.22757500
H	-3.14960400	0.49064600	1.85881200
H	0.82424000	-4.37127100	0.71432900
C	3.00442000	0.00712500	2.81276300
H	3.35041400	-0.94793800	2.40624900
H	3.13702500	0.02862800	3.90114100
N	0.59569300	0.02155000	-1.74253300
H	0.18344900	0.92142400	-1.99158300
H	1.51968600	-0.01508200	-2.17385700
H	-3.10497800	3.09475500	1.48107200
H	-1.23908700	4.84029000	0.57209000
H	-3.32262700	-2.11846400	2.14030100
H	-1.65309800	-4.19020600	1.62109800
H	3.80252900	4.43597200	-0.95510000
H	5.54106900	2.38920400	-1.29990600
H	5.24875700	-2.87145000	-0.85501200
H	3.32428000	-4.62322700	-0.10875100
H	3.57976200	0.81411300	2.35851800
C	-4.05950800	-0.25106300	-1.06997500
C	-4.47855600	1.08944500	-0.98544500
C	-4.91103500	-1.26708100	-0.59996600
C	-5.71974900	1.40195900	-0.43793300
H	-3.81059800	1.87369100	-1.32526900
C	-6.15202500	-0.94562600	-0.05574200
H	-4.57709400	-2.29807400	-0.65058300
C	-6.56041200	0.38775800	0.02832000
H	-6.03101400	2.44070200	-0.37122900
H	-6.80109400	-1.73737000	0.30781700
H	-7.52752300	0.63535100	0.45645300
C	-0.24234600	-1.08327400	-2.28053300
H	0.10932000	-1.99517600	-1.78565600
O	1.63594200	0.25558100	2.47316300
H	1.08872300	-0.50298500	2.73900700
C	-2.76228900	-0.56833700	-1.56728200
C	-1.63245400	-0.84063200	-1.90506100
C	-0.08133200	-1.24417200	-3.80130600
H	0.96706900	-1.44582100	-4.05032100
H	-0.40023300	-0.33504500	-4.32252400
H	-0.68842500	-2.07879600	-4.16519000

3a-7-T

B3LYP-D3(BJ) SCF energy in solution: -2811.12112941 a.u.

B3LYP-D3(BJ) enthalpy: -2810.570663 a.u.

B3LYP-D3(BJ) free energy: -2810.673017 a.u.

Cartesian coordinates

ATOM	X	Y	Z
Fe	1.06779800	0.14252200	0.30000900
C	4.35130300	-0.03982100	-0.69044300
C	1.12657000	3.52622900	-0.10021100
C	-2.13903200	0.33480400	1.51236700
C	0.96851900	-3.26675200	0.59329100
N	2.47341400	1.47951400	-0.25263000
C	3.77475500	1.22320400	-0.61821800
C	4.45018600	2.45645500	-0.95473900
C	3.53741700	3.45696600	-0.80106000
C	2.30599500	2.83873300	-0.36359700
N	-0.25592800	1.62681500	0.61347000
C	-0.05749500	2.96199400	0.36123300
C	-1.25113500	3.71253500	0.68619000
C	-2.16330200	2.81716500	1.15884700
C	-1.53053900	1.51774800	1.11406700
N	-0.30001000	-1.19387600	0.95805600
C	-1.57137500	-0.92717500	1.41793200
C	-2.25482000	-2.15843500	1.73651700
C	-1.39070400	-3.17375400	1.45106800
C	-0.17084200	-2.56534500	0.97061600
N	2.39803300	-1.35548000	0.00535800
C	2.16449500	-2.70219400	0.15953400
C	3.35452700	-3.45230300	-0.16926800
C	4.31210900	-2.54484500	-0.51636800
C	3.70569100	-1.23839500	-0.40885200
H	5.38924900	-0.09590600	-1.00472800
H	1.13891900	4.60274700	-0.24343300
H	-3.15919500	0.39665600	1.87624300
H	0.92829500	-4.34998200	0.66034600
C	3.00637000	-0.18864300	2.96303000
H	3.24316600	-1.16041800	2.51631400
H	3.14735700	-0.23438700	4.05110500
N	0.57948200	-0.01697400	-1.98571400
H	0.21646600	0.88325300	-2.29741000
H	1.51597700	-0.12234200	-2.37400300
H	-3.17245700	2.99691900	1.50591200
H	-1.35543200	4.78440100	0.57335200
H	-3.26864100	-2.21789900	2.11005200
H	-1.54800700	-4.24015600	1.55419000
H	3.67094700	4.51934900	-0.96216500
H	5.48346400	2.52896200	-1.26955400
H	5.33480800	-2.72837800	-0.82049100
H	3.43474200	-4.53140200	-0.12863100
H	3.68256200	0.55948600	2.54514600
C	-4.04065300	-0.25675200	-1.05154400
C	-4.45988500	1.08341100	-0.96389000
C	-4.86619600	-1.26817200	-0.52782200
C	-5.67232300	1.40059700	-0.35756700
H	-3.81254100	1.86472400	-1.34730900
C	-6.07830000	-0.94249000	0.07573200

H	-4.53311800	-2.29917400	-0.58334200
C	-6.48504200	0.39118300	0.16512400
H	-5.98262800	2.43955500	-0.28892700
H	-6.70629100	-1.73104700	0.48099700
H	-7.42937500	0.64234800	0.63953700
C	-0.29160200	-1.11398700	-2.45699000
H	0.07509600	-2.02258900	-1.96235800
O	1.68550400	0.23774300	2.63153300
H	1.05603800	-0.47500700	2.82982300
C	-2.76771100	-0.57814200	-1.60607000
C	-1.65600900	-0.85299800	-1.99843300
C	-0.24121800	-1.32703800	-3.98091600
H	0.78680800	-1.54031500	-4.29632000
H	-0.59090700	-0.43107300	-4.50534500
H	-0.87554300	-2.16853900	-4.27865500

3a-7-Q

B3LYP-D3(BJ) SCF energy in solution: -2811.11470871 a.u.
B3LYP-D3(BJ) enthalpy: -2810.565473 a.u.
B3LYP-D3(BJ) free energy: -2810.668822 a.u.

Cartesian coordinates

ATOM	X	Y	Z
Fe	1.04708900	0.14201900	0.30737600
C	4.31813700	-0.09326100	-0.73874500
C	1.16800200	3.54985800	-0.08409100
C	-2.16388000	0.36539400	1.49802400
C	0.93438800	-3.29596600	0.70921000
N	2.50944000	1.50406300	-0.28059200
C	3.78451100	1.19969500	-0.67648800
C	4.47598200	2.42832700	-1.03507900
C	3.59117100	3.45055100	-0.85218300
C	2.34920200	2.85972200	-0.37925700
N	-0.28186900	1.69093200	0.62364100
C	-0.04427700	3.01672800	0.38267100
C	-1.23568800	3.77375800	0.70971000
C	-2.16776900	2.87861500	1.16012500
C	-1.55465800	1.56750700	1.11005300
N	-0.35725700	-1.23190300	1.02475600
C	-1.62478600	-0.92205600	1.44532200
C	-2.32796800	-2.14879700	1.77847000
C	-1.46697200	-3.18062900	1.54193800
C	-0.22298200	-2.59567300	1.06797900
N	2.40026500	-1.43109000	0.04490100
C	2.14856100	-2.76326700	0.24394100
C	3.33262700	-3.52081200	-0.09938000
C	4.28312100	-2.62070400	-0.50181900
C	3.68731200	-1.30496400	-0.41125500
H	5.34582500	-0.17110100	-1.08365400
H	1.19477000	4.62786200	-0.21940400
H	-3.19050600	0.44139100	1.84325600
H	0.89173000	-4.37779300	0.80314400
C	3.05812900	0.08273400	2.86450900
H	3.47726100	-0.83098000	2.43042300
H	3.20731500	0.08708000	3.95142100
N	0.61092100	-0.07151600	-1.92550600
H	0.25173900	0.82188200	-2.26204400
H	1.55228300	-0.18024100	-2.30257900
H	-3.17678700	3.07827600	1.49782100
H	-1.33714200	4.84772400	0.61382300
H	-3.35017700	-2.19867700	2.13117100
H	-1.64536100	-4.24078400	1.67324700
H	3.75339400	4.50833800	-1.01859400
H	5.50089800	2.48833500	-1.37973200
H	5.29430300	-2.82575400	-0.83098700
H	3.42325300	-4.59823800	-0.03696400
H	3.56378000	0.94393600	2.42572800
C	-4.02277100	-0.25952000	-1.09176300
C	-4.42334700	1.08764600	-1.02868300
C	-4.87487700	-1.25295700	-0.57654200
C	-5.64505200	1.42930900	-0.45531500
H	-3.75533600	1.85520400	-1.40437000
C	-6.09613600	-0.90270400	-0.00618400
H	-4.55543400	-2.28915200	-0.61169500
C	-6.48500700	0.43770100	0.05829800
H	-5.94108400	2.47342500	-0.40496400
H	-6.74509000	-1.67724000	0.39298200
H	-7.43656500	0.70799800	0.50707000
C	-0.25229800	-1.18120300	-2.39147200
H	0.09947300	-2.07571200	-1.86240400
O	1.67362300	0.22886800	2.53998100
H	1.18606600	-0.57091300	2.79827000
C	-2.74194900	-0.60562600	-1.61228200
C	-1.62623100	-0.90176600	-1.97660400
C	-0.15521100	-1.42996800	-3.90675000
H	0.88098600	-1.65468800	-4.18526400
H	-0.48579900	-0.54646200	-4.46366600
H	-0.78331800	-2.27659700	-4.20221100

Chapter III

BIOCATALYTIC, ENANTIOENRICHED PRIMARY AMINATION OF TERTIARY C(SP^3)–H BONDS

3.1 Introduction

Direct enantioselective functionalization of C(sp^3)–H bonds is an ideal approach to synthesize high value-added chiral molecules from the viewpoint of atom- and step-economy.[1-5] In recent years, many powerful catalytic methods have been developed toward this goal, with significant advances made for enantioselective functionalization of secondary C–H bonds (**Figure 3.1a**).[1-10] In contrast, intermolecular asymmetric functionalization of racemic tertiary C–H bonds, particularly those with a $pK_a > 25$ and in the absence of directing groups, toward the formation of fully substituted sp^3-carbon stereocenters remains unexplored in synthetic chemistry (**Figure 3.1b**). The challenges of this transformation include: First, the difficulty of precisely recognizing three different substituents attached to a tertiary carbon center (**Figure 3.1b**), especially when those substituents have only subtle steric and/or electronic differences; Second, the lack of an intermolecular counterpart to recent breakthroughs in intramolecular enantioselective tertiary C–H functionalizations;[11-15] and last, potential steric clash between the catalyst and the tertiary carbon. Chemists often achieve precise facial recognition by strategically incorporating bulky substituents or functional groups into a chiral catalyst. However, when it comes to the functionalization of a tertiary C–H bond, the steric clash between the bulky catalyst and the crowded surrounding of a tertiary carbon inhibits the approach of the catalyst to the tertiary C–H bond. Consequently, a tradeoff arises between increasing the catalyst's steric bulk to better control stereoselectivity and decreasing it to avoid a steric clash with the tertiary sp^3-carbon surroundings (**Figure 3.1b**).

Unlike small-molecule catalysts, enzymes have large, three-dimensional (3D) structures determined by the folding of their polypeptide chain(s). With precisely sculpted 3D structures, enzymes can differentiate steric and electronic nuances as subtle as those between methane and ethane molecules.[16] With precise adjustments of their folded structures, enzymes can also achieve excellent stereoselectivity while maintaining high activity by avoiding severe steric clashes with

bulky substrates.[17] We thus consider enzyme catalysis to be a promising approach to tackle existing challenges in the enantioselective functionalization of tertiary C–H bonds.

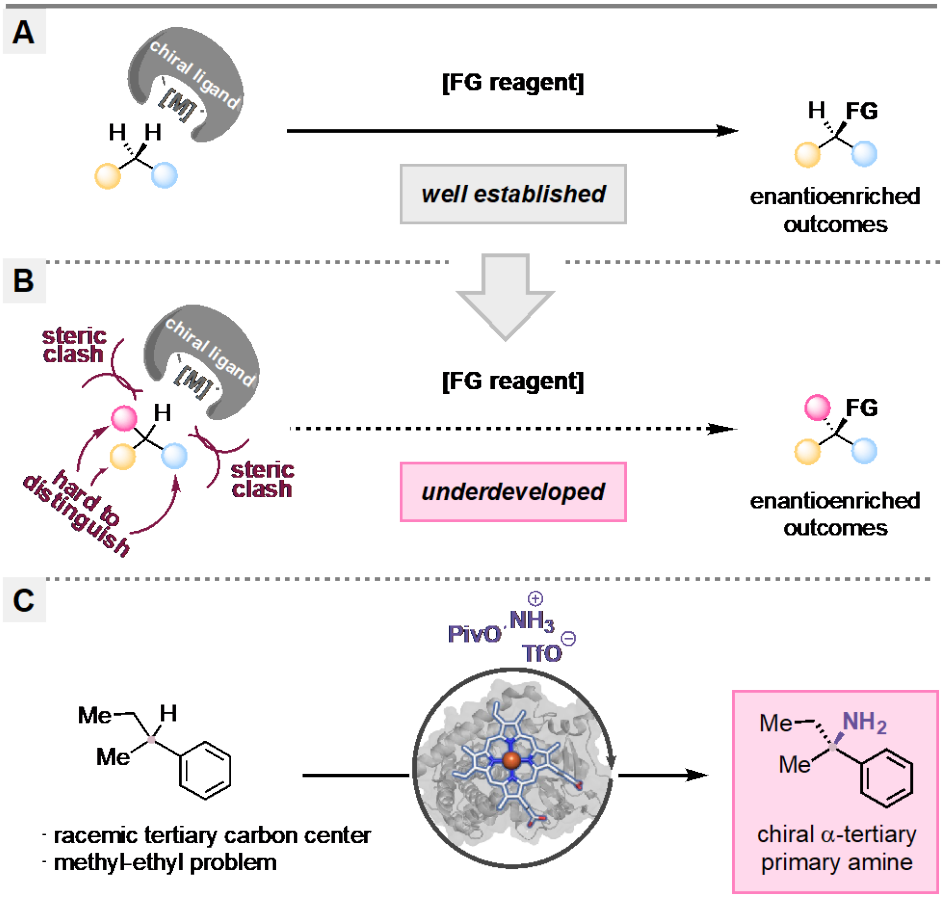

Figure 3.1. Background and project synopsis. (A) A general scenario for intermolecular enantioselective functionalization of secondary carbon centers. Secondary carbons possess smaller steric hindrance, which facilitates the construction of chirality. (B) A general scenario for intermolecular enantioselective functionalization of tertiary carbon centers. Tertiary carbons that possess chiral centers make catalyst approach and substrate recognition difficult. This type of transformation is rarely reported. (C) This work: biocatalytic, enantioselective primary amination of tertiary C–H bonds. M, metal catalysts; FG, functional groups; Piv, pivaloyl.

Cytochromes P450 represent nature's most prevalent catalysts for C–H functionalization,[10] with enzymes from this vast family directly activating C–H bonds for a wide range of oxidative transformations.[18] Furthermore, cytochromes P450 are excellent candidates for directed evolution and discovery of non-natural activities due to their structural flexibility and remarkable promiscuity.[19] Several reports have demonstrated abiological C–H functionalizations achieved by expanding the catalytic repertoire of the iron-heme-containing cytochrome P450 family.[8,9,20] The

activity and selectivity of these biocatalytic C–H functionalizations frequently complement state-of-the-art methodologies based on small-molecule catalysts, making them valuable additions to the synthetic chemist's toolbox.[8,21] Motivated by these precedents, we sought to leverage these enzymes for enantioselective intermolecular functionalization of tertiary C–H bonds.

Given the widespread presence of α-tertiary amines in bioactive compounds,[22] the initial focus was on the primary amination of tertiary C–H bonds. Despite the existence of many methods for synthesizing chiral α-tertiary amines with *stoichiometric* amounts of auxiliary reagents, such as Ellman's sulfinamides,[23,24] *catalytic* strategies for enantioselective conversion of substrates into chiral α-tertiary amines are rare,[11-13,22,25] because classical methods for synthesizing chiral α-secondary amines, including asymmetric reduction of imines,[26] biocatalytic transamination,[27] and reductive amination,[28] are not applicable to the synthesis of chiral α-tertiary amines due to the absence of protons in the fully substituted carbon center. From a retrosynthetic perspective, intermolecular amination of tertiary C–H bonds provides an ideal and straightforward method for the assembly of chiral α-tertiary amines (Figure 3.1c). The Arnold group recently reported primary amination of these tertiary C–H bonds, but all the products were non-chiral.[29,30] Here we present a biocatalytic system that exhibits remarkable ability to aminate tertiary C–H bonds, providing high-value chiral α-tertiary primary amines with exceptional efficiency and selectivity.

3.2 Results and Discussions

Initial Discovery and Evolution of Tertiary C–H Primary Aminase P411-TEA-5274.

We initiated the study by testing the coupling of *sec*-butylbenzene **2.1a** and hydroxylamine ester **2.2a** (**Figure 3.2a**) catalysed by an in-house collection of engineered cytochromes P411 (serine-ligated cytochrome P450 variants). These reagents were chosen for several reasons: First, compared to the elaborated starting materials used for many other tertiary C–H functionalizations, **2.1a** is simple, inexpensive, and readily available.[11-15] Second, the tertiary carbon center of **2.1a** is racemic and attaches to a methyl and an ethyl substituent; distinguishing these is notoriously difficult in asymmetric catalysis.[11,31,32] Last, hydroxylamine ester **2.2a** has recently been shown to serve as a nitrene precursor for hemoprotein-catalysed secondary C–H primary amination;[29] we wanted to expand that demonstration to primary amination of tertiary C–H bonds.

A panel of 48 cytochromes P411 previously engineered for nitrene transformations was screened in whole *Escherichia coli* cells against **2.1a** and **2.2a** under anaerobic conditions (**Figure 3.2**). The resulting reaction mixtures were monitored and analyzed after 20 h for the formation of *α*-tertiary primary amine **2.3a**. Variant P411-TEA-5267 (***TE****rtiary C–H Primary* ***A****minase*), which has three mutations (C324L, N395R, and G438V) with respect to $P411_{BPA}$ (previously engineered for benzylic C–H primary amination),[29] produced the desired product **2.3a** with a total turnover number (TTN) of 20 (Figure 3.2b; 1% yield, Supplementary Table B.S1). The primary amine **2.3a** synthesized by P411-TEA-5267 was determined to have excellent stereopurity, with 90% *e.e.*.

P411-TEA-5267 served as the starting point for directed evolution. Sequential rounds of site-saturation mutagenesis (SSM)[33,34] and screening were performed to improve catalytic activity toward synthesis of **2.3a**. We referred to the crystal structure of related P411 variant **E10**[35] (heme domain only) and mainly targeted for mutagenesis amino acid residues proximal to the heme cofactor and/or residing on flexible loops, or those distal sites that have shown to play an important role in enhancing abiological carbene and nitrene transfer activities (**Figure 3.2c**).[8] During each round of SSM, enzyme libraries were generated and screened for product formation in 96-well plates in the form of bacterial whole-cell catalysts. Three rounds of SSM and screening introduced mutations M354E, R395S, and A327V, leading to a three-fold improvement of the TTN from 20 to 64 (**Figures 3.2b** and **3.2d**). Subsequent rounds of evolution introduced the M177Y and S72T mutations on the *α*-helices above the heme cofactor, as well as the A399G mutation on the loop directly below the heme cofactor. These mutations boosted the activity more than two-fold, reaching 140 TTN (**Figure 3.2**). The Q403A mutation located on the *α*-helix below the heme cofactor doubled the enzyme activity to 270 TTN (**Figure 3.2**). Interestingly, upon re-evaluation of position 395 in the loop beneath the heme cofactor, we found the S395V mutation increased the enzyme's activity almost four-fold to 970 TTN (26% yield, **Supplementary Table B.S2**), culminating in the final variant, P411-TEA-5274 (**Figure 3.2**). In the standard conditions, an oxygen depletion system (catalase and glucose oxidase) was introduced to ensure a strict anaerobic environment. However, in the absence of this oxygen depletion system the yield and TTN only decrease slightly (entries 8 and 10, **Supplementary Table B.S2**), demonstrating the synthetic utility of this biotransformation. Notably, the enzyme's enantioselectivity toward the formation of

2.3a also improved slightly during the evolution campaign, increasing from 90% *e.e.* (P411-TEA-5267, Figure 3.2d) to 92% *e.e.* (P411-TEA-5274, **Figure 3.2d**).

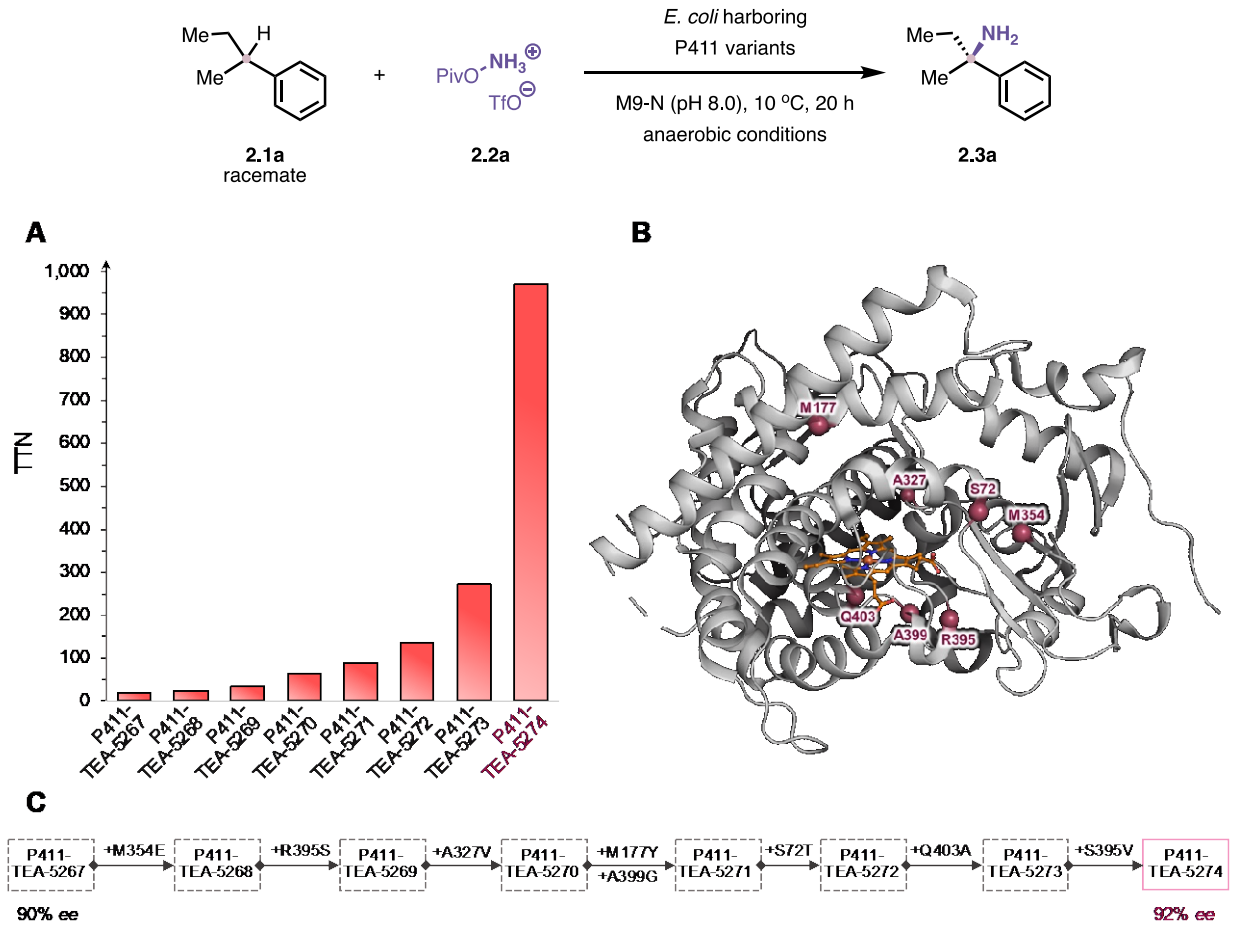

Figure 3.2. Directed evolution for enzymatic primary amination of tertiary C–H bonds. Reaction conditions: 5 mM **2.1a**, 10 mM **2.2a**, *E. coli* whole cells harboring P411 variants (OD_{600} = 30) in M9-N aqueous buffer (pH 8.0), 5% (v/v) EtOH (co-solvent), 10 ºC, anaerobic conditions, 20 h. (A) Evolution trajectory of *tertiary C−H primary aminase* (P411-TEA) for the synthesis of *α*-tertiary primary amine **2.3a**. (B) The mutations (S72, M177, A327, M354, R395, A399, and Q403) that enhance activity or enantioselectivity are highlighted in the active site of closely related P411 variant **E10** (PDB ID: 5UCW).[31] (C) Summary of beneficial mutations leading to P411-TEA-5274. TTN is defined as the amount of indicated product divided by heme protein as measured by the hemochrome assay (see Supplementary Information for more details).

Substrate Scope Study of Tertiary C–H Primary Aminase P411-TEA-5274.

With C–H primary aminase P411-TEA-5274 in hand, we proceeded to explore its performance on various substrates (**Figure 3.3**). Representative substrates were designed with

mixed kinds of C–H bonds (**2.1a**, **Figure 3.3**) and with diverse spatial hindrances (**2.1a** and **2.1c**–**2.1e**, **Figure 3.3**), electronic effects (**2.1f**–**2.1g**, **Figure 3.3**), structures (**2.1i**–**2.1j**, **Figure 3.3**), and two different types of tertiary C–H bonds (**2.1k**–**2.1l**, **Figure 3.3**) to examine the impact of these factors on the activity and selectivity of the enzyme, as well as the enzyme's regional selectivity. Importantly, we incorporated both methyl and ethyl groups at the tertiary carbon centers of most substrates (**2.1a**, **2.1c**–**2.1g** and **2.1i**–**2.1l** , **Figure 3.3**).[11,31,32] These substrates allow us to assess the selectivity of the enzyme in conditions that present significant challenges for other systems.

To investigate enzyme regioselectivity, we tested substrate **2.1a** (**Figure 3.3**). **2.1a** has both an sp^3 tertiary C–H bond and sp^2 C–H bonds. Existing reports have demonstrated iron catalysts can efficiently catalyse primary amination of sp^2 C–H bonds.[36-38] In contrast, this enzyme exclusively catalysed the amination of the sp^3 tertiary C–H bond of **2.1a**, giving **2.3a** with high efficiency (970 TTN, **Figure 3.3**) and exclusive regioselectivity (>99:1 regioselectivity ratio (r.r.), **Figure 3.3**) and enantioselectivity (92% *e.e.*, **Figure 3.3**). A 1.0-mmol reaction was performed under the standard conditions, and primary amine **2.3a** could be isolated in 17% isolated yield and with 92% *e.e.* by using simple acid−base extraction (**Figure 3.3**). Substrates (**2.1b**–**2.1d**) possess both an sp^3 tertiary C–H bond and sp^3 primary C–H bonds. Although the former has a smaller bond-dissociation energy (BDE) than the latter,[39] the latter is kinetically more favorable for activation. This enzyme aminated the tertiary C–H bond of **2.1b**–**2.1d**, delivering **2.3b**–**2.3d** with high efficiency (up to 860 TTN). We next installed a methyl group (**2.1c**) and a methoxy group (**2.1f**) at the *para*-position of the phenyl ring. Interestingly, the enzyme's activity toward the construction of **2.3c** and **2.3f** dropped to 310 TTN and 110 TTN, respectively. However, the enantioselectivities for both compounds were >99% *e.e.* (**Figure 3.3**). Conversely, when a methyl group was introduced at the *meta*-position of the phenyl ring, the enantioselectivity decreased to 60% e.e., but the enzyme's activity was high (**2.3d**, 860 TTN, **Figure 3.3**). When a methyl group was introduced at the *ortho*-position, the enzyme struggled to convert **2.1e** to **2.3e** (**Figure 3.3**). When a fluoro-substituent was introduced at the *para*-position, the enzyme maintained high enantioselectivity, albeit with decreased activity (**2.3g**, 95% *e.e.*, 73 TTN, **Figure 3.3**). When aminating an achiral tertiary carbon center, we found the efficiency was also good (**2.3h**, 300 TTN, **Figure 3.3**). In addition, when the aryl moiety was replaced with heteroaryl moieties, such as a pyridyl (**2.1i**) or a thienyl (**2.1j**) substituent, the enzyme retained satisfactory catalytic activity and

good enantioselectivity (**2.3i** (52 TTN, 82% *e.e.*) and **2.3j** (420 TTN, 92% *e.e.*)). Moreover, the biocatalytic system is not only applicable to benzylic tertiary C–H bonds but also to allylic (**2.3k**, 70 TTN, 90% *e.e.*) and propargylic tertiary C–H bonds (**2.3l**, 120 TTN, 67% *e.e.*). The absolute stereochemistry for enzymatic product **2.3f** was assigned as *S* by comparing the elution order of the two enantiomers with a literature report[40] and through X-ray crystallography (see Supplementary Table B.S8 and Supplementary Figure B.S21). The other *α*-tertiary primary amines **3** were assigned by analogy.

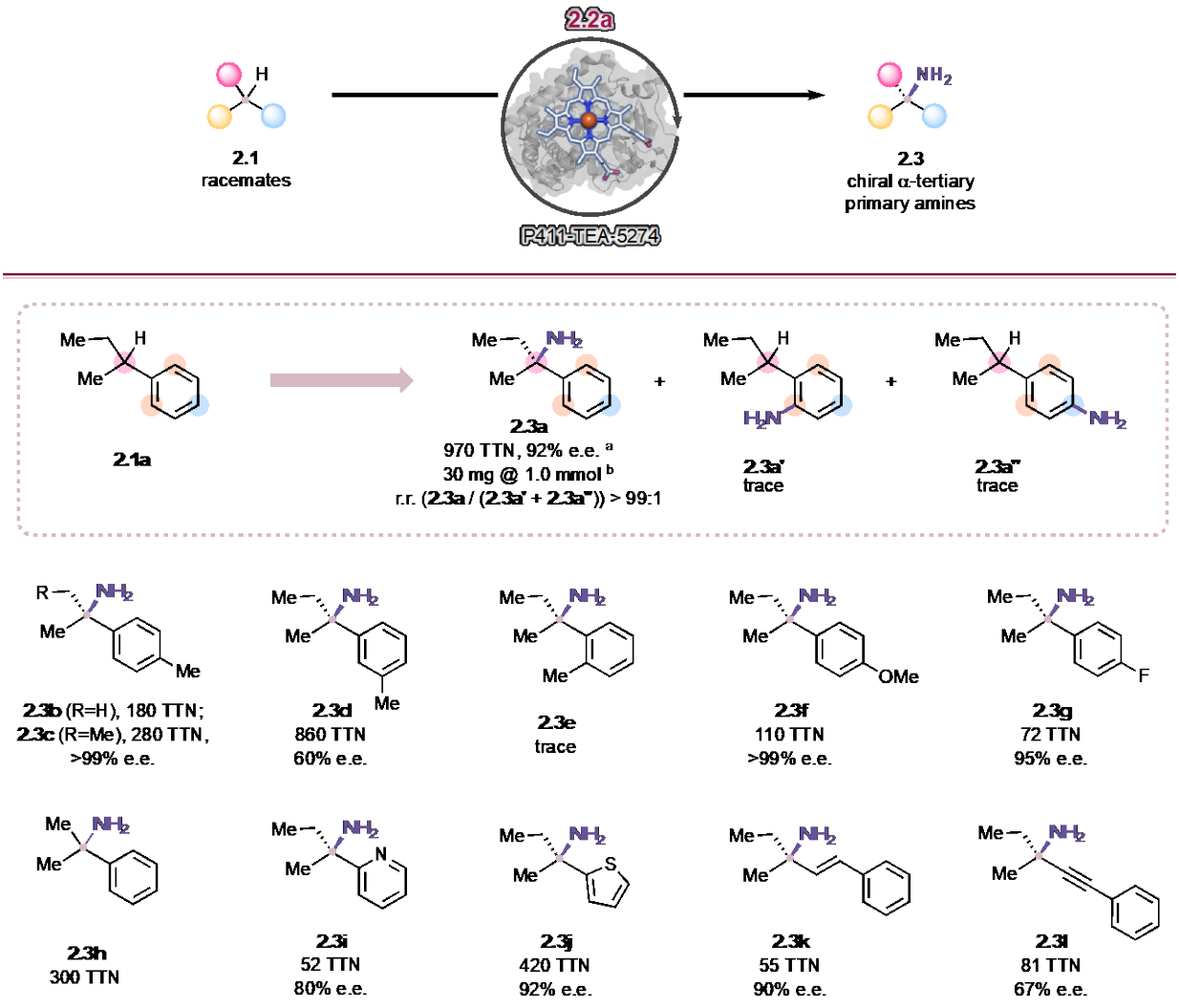

Figure 3.3. Substrate scope study. Reaction conditions: 5 mM **3.1a**, 10 mM **3.2a**, *E. coli* whole cells harboring P411-TEA-5274 (OD_{600} = 30) in M9-N aqueous buffer (pH 8.0), 5% (v/v) EtOH (co-solvent), 10 ºC, anaerobic conditions, 20 h. [a]20% isolated yield (see the Supplementary Information for further details of the scale-up reaction). TTN is defined as the amount of indicated product

divided by heme protein as measured by the hemochrome assay (see Supplementary Information for more details). e.e., enantiomeric excess. r.r., regioisomeric ratio.

Combined Experimental and Computational Study of P411-TEA-5274.

To better understand the mechanism of this biotransformation, we designed a series of substrate probes (Figure 3.4). First, enantiopure substrates (*R*)-**2.1f** and (*S*)-**2.1f** were synthesized (see SI for more details) and used to react with **2.2a** under standard conditions catalysed by P411-TEA-5274 (Figures 4a and 4b). Experimental results showed that the efficiency of (*R*)-**2.1f** transforming into **2.3f** (420 TTN, Figure 3.4a) was significantly higher (more than 16-fold difference) than that of (*S*)-**2.1f** transforming into **2.3f** (26 TTN, Figure 3.4b), indicating the enzyme prefers the (*R*)-enantiomer. Moreover, we observed that (*R*)-**2.1f** was converted to (*S*)-**2.3f** (>99% e.e.), and (*S*)-**2.1f** was converted to (*R*)-**2.3f** (-85% e.e.), indicating that the enzyme achieves enantioselectivity via kinetic resolution and maintains the stereoconfiguration of the favored enantiomer.

Next, we synthesized substrates that incorporate a stereodefined olefin moiety ((*E*)-**2.1m** and (*Z*)-**2.1m**, Figures 4C and 4D), and subjected them to enzymatic reactions. Interestingly, scrambling of the olefin geometry was observed in the (Z)-substrate, with the (*Z*)-substrate yielding a significant proportion of the scrambled product that harbors a thermodynamically more stable product (*E*)-**2.3m** (*E*/*Z* > 99:1, Figure 3.4d). In line with established literature on related iron-based catalysts,[11,41-43] this observed erosion of C=C stereochemistry supports the generation of a carbon-centered radical at the allylic position and a stepwise pathway, contradicting a concerted C–H insertion mechanism.

To understand the rate-determining step of this enzyme-catalysed reaction, the kinetic isotope effect (KIE) between cumene **2.1b** and cumene-d_7 **2.1b'** was measured (Figures 4e and 4f). The non-competitive KIE was 9.5, while the competitive KIE was 22.9. These results contrast with previously measured KIEs for the benzylic C–H amidation of ethyl benzene,[35] while aligning with those for the nitrogen insertion into unactivated C–H bonds,[44] suggesting that the hydrogen atom transfer (HAT) is the rate-limiting step and a higher degree of tunneling than previously observed in these systems.[44]

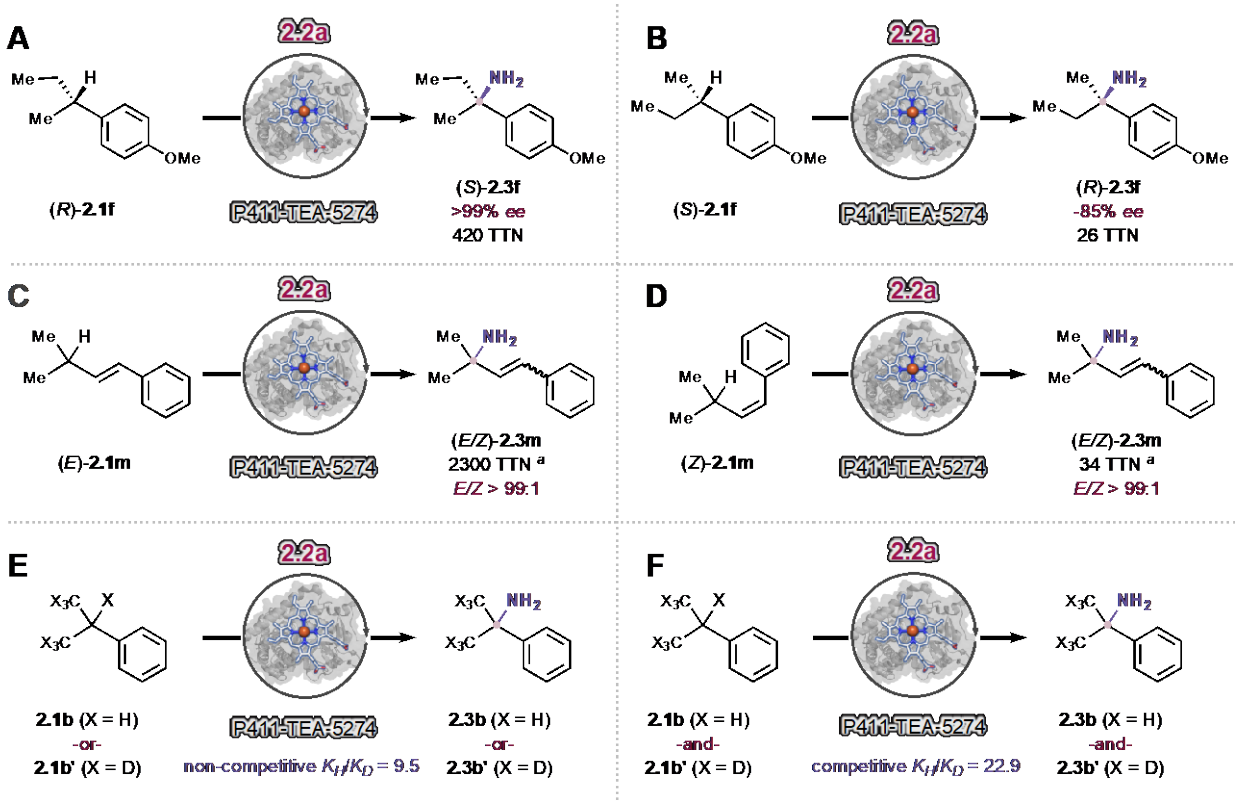

Figure 3.4. Mechanistic studies of enantioenriched enzymatic primary amination of tertiary C–H bonds. (A) and (B) Nitrene transfer reactions catalyzed by P411-TEA-5274 using (*R*)- or (*S*)-**1e**. Reaction conditions: 5 mM (*R*)- or (*S*)-**3.1f**, 10 mM **3.2a**, *E. coli* whole cells harboring P411-TEA-5274 (OD_{600} = 30) in M9-N aqueous buffer (pH 8.0), 5% (v/v) EtOH (co-solvent), 10 ºC, anaerobic conditions, 20 h. (C) and (D) Nitrene transfer reactions catalyzed by P411-TEA-5274 using (*E*)- or (*Z*)- **3.1m**. Reaction conditions: 5 mM (*E*)- or (*Z*)- **3.1m**, 10 mM **3.2a**, *E. coli* whole cells harboring P411-TEA-5274 (OD_{600} = 30) in M9-N aqueous buffer (pH 8.0), 5% (v/v) EtOH (co-solvent), 10 ºC, anaerobic conditions, 20 h. *E/Z* ratios were determined by ^{1}H NMR. (E) and (F) Nitrene transfer reactions catalyzed by P411-TEA-5274 using **3.1b** or **3.1b'** (d_7-**3.1b**). Reaction conditions: 5 mM **3.1b** or **3.1b'**, 10 mM **3.2a**, *E. coli* whole cells harboring P411-TEA-5274 (OD_{600} = 30) in M9-N aqueous buffer (pH 8.0), 5% (v/v) EtOH (co-solvent), 10 ºC, anaerobic conditions, 20 h. TTN is defined as the amount of indicated product divided by heme protein as measured by the hemochrome assay (see Supplementary Information for more details). [a]TTNs were calculated based on all stereoisomers.

To gain further insight into the reaction of **2.1a** with the iron-nitrene intermediate in the active site of the enzyme, molecular dynamics (MD) simulations were performed on a mimic of the enantioselectivity-determining HAT transition state, employing the closely-related P411 enzyme **E10**[35] as the starting point (beneficial mutations were introduced manually and a restraint

was applied to the $N_{nitrene}$--H–$C_{tertiary}$ distance; see Supplementary Figures 22–26). Simulations on the hydrogen atom transfer with substrate (*R*)-**2.1a**, which in the experiment delivers the major enantiomer (*S*)-**2.3a**, and the other enantiomer (*S*)-**2.1a** revealed that with both substrates the phenyl-substituent is preferentially oriented toward the left-hand side of the active site, corresponding to an N1-Fe-$N_{nitrene}$-C_{phenyl} dihedral angle of approximately 20° (Figure 3.5). In this orientation, the phenyl substituent is tightly positioned between a number of surrounding hydrophobic residues, with minimum C–C distances as close as 3.5 Å, 3.9 Å, and 3.9 Å between **2.1a** and A87, A264, and M263, respectively, indicating the possibility of stabilizing C–H-π interactions (see Supplementary Figures 22 and 23 for details). This tight fit prevents significant movement of the carbon-centered radical species after hydrogen-atom transfer, precluding reorientation and rotation around the C_{phenyl}–$C_{tertiary}$ bond, thus avoiding an interconversion of the radical intermediates formed from (*R*)-**2.1a** and (*S*)-**2.1a** and ablation of enantioselectivity. In addition, for substrate (*R*)-**2.1a**, the ethyl substituent is placed in a sterically accessible area between residues P268 and V328, while the methyl group is oriented toward the outward-facing side of the active site (see Supplementary Figures 22–26 for details). In contrast, for the other enantiomer, (*S*)-**2.1a**, the ethyl substituent mostly rotates upwards to avoid an otherwise close contact of the CH_3 group of the ethyl substituent with the heme ring system. However, the rotation of the ethyl group causes a significant movement of F437 and the respective open-loop protein backbone, which results in exclusion of (*S*)-**2.1a** from the enzyme pocket or a destabilization of the HAT transition state, thereby disfavoring reaction with (*S*)-**2.1a** (see Supplementary Figures 22–26 for details). The computational results are consistent with the experimental findings based on the biotransformation of enantiomers (*R*)-**2.1f** (Figure 3.4a) and (*S*)-**2.1f** (Figure 3.4b).

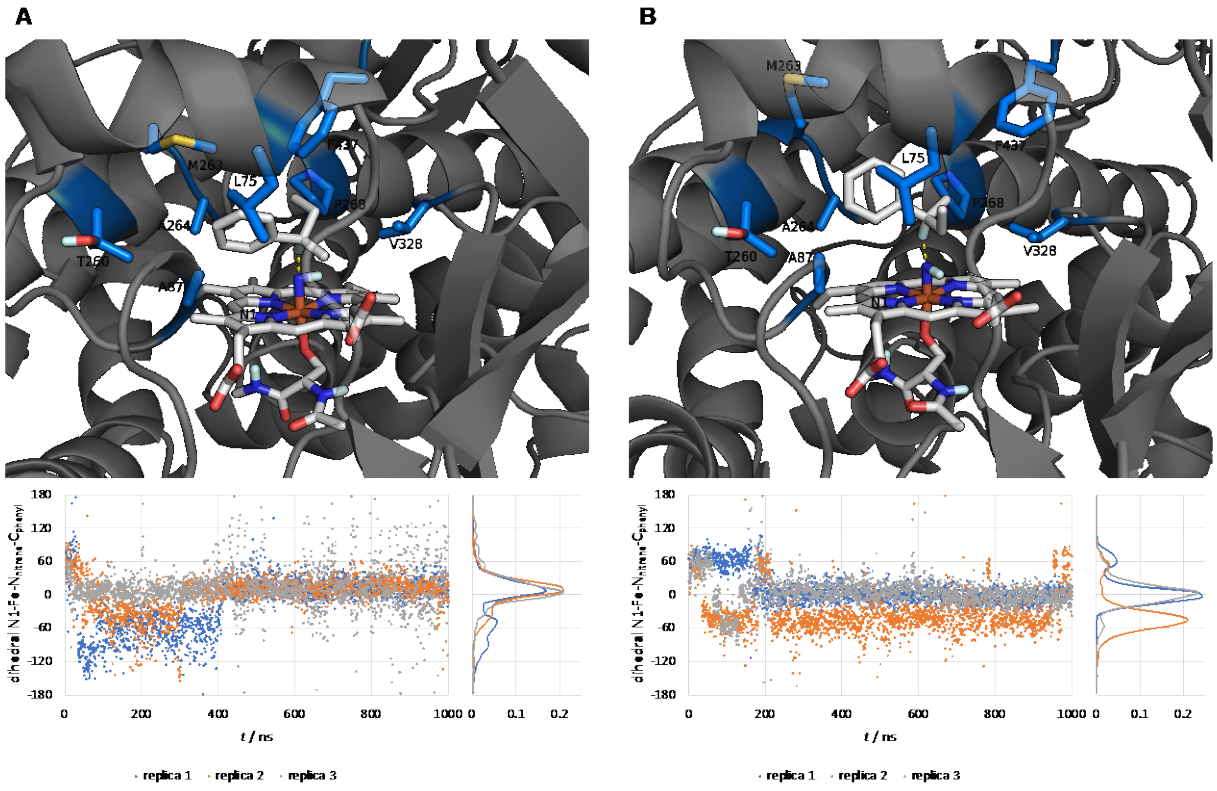

Figure 3.5. Molecular dynamics simulations on iron heme-catalyzed tertiary C–H amination. (A) and (B) Molecular dynamics simulations on HAT transition state mimics with (*R*)- **3.1a** (A) and (*S*)- **3.1a** (B). Plot of the N1-Fe-$N_{nitrene}$-C_{phenyl} dihedral angle over time and respective probability density plot. During the simulations, the $N_{nitrene}$--H–$C_{tertiary}$ distance (dashed yellow line) was restrained. Structures correspond to representative structures of the most populated cluster. Non-relevant, non-polar hydrogens are omitted for clarity.

3.3 Conclusion

We have developed an engineered enzyme, P411-TEA-5274, that can directly aminate tertiary C–H bonds, efficiently and selectively producing high-value chiral *α*-tertiary primary amines. This biocatalyst provides an alternative to small-molecule catalysts that struggle to functionalize tertiary C–H bonds and demonstrates remarkable enantioselectivity and activity. The substrate scope study demonstrated the compatibility of this biotransformation toward various substrates, the exclusive regioselectivity to tertiary C–H bonds, and the broad applicability against different tertiary C–H bonds. Experimental and computational investigations indicate that the enzyme's excellent enantioselectivity arises from its enantiomeric substrate specificity. Given the prevalence of *α*-tertiary amines in bioactive molecules, this work provides a straightforward

disconnection strategy to construct these fragments. Leveraging this work in the future, we hope to expand the limited repertoire of catalysts for asymmetric intermolecular functionalization of tertiary C–H bonds.

3.4 Experimental Methods

General Procedure

Unless otherwise noted, all chemicals and reagents were obtained from commercial suppliers (Sigma-Aldrich, VWR, TCI America, Fischer Scientific, Alfa Aesar, Acros, and Combi Blocks) and used without further purification. Silica gel chromatography was carried out using AMD Silica Gel 60, 230–400 mesh. ^{1}H and ^{13}C NMR spectra were recorded on a Bruker Prodigy 400 MHz instrument (400 MHz for ^{1}H and 101 MHz for ^{13}C NMR) or a Varian 300 MHz Spectrometer (300 MHz for ^{1}H NMR). Chemical shifts (δ) are reported in ppm downfield from tetramethylsilane, using the solvent resonance as the internal standard (^{1}H NMR: δ = 7.26, ^{13}C NMR: δ = 77.16 for $CDCl_3$). Data for ^{1}H NMR are reported as follows: chemical shift (δ ppm), multiplicity (s = singlet, d = doublet, t = triplet, q = quartet, p = pentet, sext = sextet, m = multiplet, dd = doublet of doublets, dt = doublet of triplets, ddd = doublet of doublet of doublets), coupling constant (Hz), integration. Sonication was performed using a Qsonica Q500 sonicator. High-resolution mass spectra were obtained at the California Institute of Technology Mass Spectral Facility. Samples were analyzed by field ionization (FI) using a JEOL AccuTOF GC-Alpha (JMS-T2000GC) mass spectrometer interfaced with an Agilent 8890 GC system. Ions detected by FI are radical cations.

Chemical reactions were monitored using thin layer chromatography (Merck 60 silica gel plates) and a UV lamp for visualization. Analytical reverse-phase high-performance liquid chromatography-mass spectroscopy (HPLC-MS) was carried out using an Agilent 1200 series instrument and a Kromasil 100 C18 column (4.6 mm × 50 mm, 3 μm) or an Agilent C18 column (InfinityLab Poroshell 120 EC-C18, 4.6 x 50 mm, 2.7 μm; Part Number: 699975-902T) with water and acetonitrile, both containing 0.1% acetic acid, as the mobile phase. Analytical chiral normal-phase HPLC was conducted using either an Agilent 1200 series instrument with *n*-hexane and isopropanol as the mobile phase or a JASCO SF-2000 integrated analytical supercritical fluid

chromatography (SFC) system with supercritical CO_2 and isopropanol as the mobile phase. Enantiomers were separated using one of the following chiral columns: Chiralpak IA, Chiralpak IB, Chiralpak IC, Chiralpak AD-H, and Daicel CHIRALCEL OJ-H (all 4.6 mm × 250 mm, 5 μm).

Escherichia coli cells were grown using Luria-Bertani medium or HyperBroth (AthenaES) with 100 μg/mL ampicillin (LB_{amp} or HB_{amp}). Primer sequences are available upon request. T5 exonuclease, Phusion polymerase, and *Taq* ligase were purchased from New England Biolabs (NEB, Ipswich, MA). M9-N minimal media (abbreviated as M9-N buffer, pH = 8.0) were used as buffering systems for whole cells, unless otherwise specified. M9-N buffer was used without a carbon source; it contains 47.7 mM Na_2HPO_4, 22.0 mM KH_2PO_4, 8.6 mM NaCl, 2.0 mM $MgSO_4$, and 0.1 mM $CaCl_2$.

Substrates **2.1a**, **2.1b**, **2.1b'**, **2.1f**, **2.1g**, **2.1h**, **2.1i**, (*Z*)- **2.1m**, **2.3b**, and **2.3f**–**2.3h** were purchased from commercial suppliers (Sigma-Aldrich, VWR, TCI America, Fischer Scientific, Alfa Aesar, Acros, and Combi Blocks) and used without further purification. Other substrates were synthesized as described in **Appendix B**.

Cloning, Mutagenesis, and Expression of Enzymes

The genes encoding all enzymes described in this study were cloned using Gibson assembly[1] into vector pET22b(+) (Novagen) between restriction sites *Nde*I and *Xho*I in frame with a *C*-terminal 6×His-tag. Site-saturation mutagenesis was performed using the "22c-trick"[2] or "NNK" as degenerative codons. The PCR products were digested with *Dpn*I, gel purified, and ligated using Gibson Mix™.[1] Without further purification after the Gibson step, 1 μL of the Gibson product was used to transform 50 μL of electrocompetent *E. coli* BL21 E. cloni® (Lucigen) cells.

E. coli (E. cloni BL21(DE3)) cells carrying plasmid encoding the appropriate P411 variant were grown overnight in 5 mL Luria-Bertani medium supplemented with 0.1 mg/mL ampicillin (LB_{amp}). The preculture (1 mL) was used to inoculate 50 mL of Hyperbroth medium supplemented with 0.1 mg/mL ampicillin (HB_{amp}) in a 125-mL Erlenmeyer flask. This culture was incubated at 37 ºC and 220 rpm for 2.5 hours. The culture was then cooled on ice for 30 min and induced with 0.5 mM IPTG and 1.0 mM ALA (final concentrations). Expression was conducted at 22 ºC and 140 rpm for 20–22 hours. Subsequently, the *E. coli* cells were pelleted by centrifugation (4,000 g,

3 min, and 4 ºC). Media were removed, and the pellets were resuspended to an optical density at 600 nm (OD_{600}) of 38 in M9-N minimal medium with pH adjusted to 8.0. Aliquots of the cell suspension (3 mL) were used to determine protein concentration after lysis by sonication.

Hemochrome Assay for the Determination of Hemoprotein Concentration

Protein concentration in the cell was determined using the hemochrome assay on cell lysate.[3] Lysate was obtained by sonication using using a Qsonica Q500 sonicator (4 minutes, 1 second on, 1 seconds off, 30% amplitude, on wet ice). The cell debris was removed by centrifugation (14,000 g, 10 minutes, 4 °C). To a cuvette, 500 µL of the lysate and 500 µL of solution I [0.2 M NaOH, 40% (v/v) pyridine, 0.5 mM $K_3Fe(CN)_6$] were added. The UV-Vis spectrum (380–620 nm) of the oxidized state Fe(III) was recorded immediately. Sodium dithionite (10 µL of 0.5 M solution in water) was added, and the UV-Vis spectrum of the reduced state Fe(II) was recorded immediately. The protein concentration was calculated using the extinction coefficient and dilution factor (2× dilution in volume): $\varepsilon\_[557_{reduced} - 540_{oxidized}] = 23.98\ mM^{-1}cm^{-1}$. The hemochrome assay detects total heme level, which is a good approximation of over-expressed heme enzyme.

Analytic Reaction Setup and Product Quantification

All the biocatalytic reactions were set up in an anaerobic chamber (oxygen level: <40 ppm). M9-N medium (pH 8.0) and D-glucose solution (500 mM in M9-N, pH 8.0) were placed in the anaerobic chamber for at least 24 hours. Harvested cells were resuspended with M9-N buffer (pH 8.0) to OD_{600} = 38, and 320 µL of resuspended cells were aliquoted to 2-mL screw cap vials. The screw-cap vials with cells were precooled to 0 ℃ on an ice bath. Unless otherwise specified, 30 µL of the precooled glucose solution, 10 µL of a stock solution containing glucose oxidase (from *Aspergillus niger*, 1,000 U/mL) and catalase (from bovine liver, 14,000 U/mL) in double-distilled water were added to make the total volume to 360 µL. The resulting mixtures stayed on the ice bath for another 2 minutes, and then the hydrocarbon substrate **2.1** (20 µL, 0.1 M stock in ethanol) and the nitrene precursor **2.2a** (20 µL, 0.2 M stock in water) were added in a sequential manner. Unless otherwise noted, the reactions were then shaken at 10 ℃ for 20 hours at 250 rpm.

After the reaction was completed and the vials removed from the shaker, an internal standard (400 μL ethanol containing 2 mM 1,2,3-trimethoxybenzene) was added. The mixture was transferred to a 1.7-mL Eppendorf tube and then subjected to vortexing (20 s × 2) and centrifugation (14,000 × g, 5 min, 4 °C). A sample of the supernatant (0.2 mL) was transferred to a vial with an insert for reverse-phase HPLC-MS analysis. Products were identified and quantified based on the corresponding reference compounds (XII).

To further determine the enantiomeric excess (*ee*), the remaining supernatants of three parallel analytical reactions were combined and transferred to a 2-dram vial. The solvent was evaporated by blowing air. To the remaining residues, 100 μL EtOAc, 2 mg Na_2CO_3, and 10 μL water were added. The 2-dram vial was cooled to 0 °C prior to adding 2 μL benzoyl chloride. After overnight shaking, 100 μL of 1 M NaOH solution and 1 mL of saturated $NaHCO_3$ solution were added. The benzoyl-protected amines were then extracted into a solution of hexane and EtOAc (1:1) mixture and subjected to normal-phase HPLC to determine the *ee* (XII).

Reaction Screening in 96-Well Plate in Whole-Cell Format

Single colonies from LB_{amp} agar plates were picked using sterile toothpicks and cultured in deep-well 96-well plates containing LB_{amp} (300 μL/well) at 37 ºC, 80% humidity, and 220 rpm shaking overnight. Subsequently, HB_{amp} (1000 μL/well) in a deep-well plate was inoculated with an aliquot (50 μL/well) of these overnight cultures and allowed to shake for 2.5 hours at 37 ºC, 80% humidity, and 220 rpm. The plates were then cooled on ice for 30 minutes, and the cultures were induced with 0.5 mM isopropyl *β*-D-1-thiogalactopyranoside (IPTG) and 1.0 mM 5-aminolevulinic acid (ALA) (final concentrations). Expression was then conducted at 20 ºC, and 220 rpm for 20–22 hours.

E. coli cells harboring P411 variants in deep-well 96-well plates were pelleted (4,000 g, 3 min, 4 ºC) and resuspended in M9-N buffer (300 μL, pH 8.0) and D-glucose solution (60 μL, 500 mM in M9-N buffer (pH 8.0)) by gently vortexing. The 96-well plates were then transferred to an anaerobic chamber. To deep-well plates of cell suspensions were added *sec*-butylbenzene **2.1a** (20 μL/well, 100 mM in EtOH) and the nitrene precursor **2.2a** (20 μL/well, 200 mM in water). The plates were sealed with aluminum sealing foil immediately after the addition and shaken in the

anaerobic chamber at room temperature and 600 rpm. After 20 hours, the seals were removed, and ethanol (800 μL/well) was added. The plates were tightly sealed with silicone mats, vigorously vortexed, and centrifuged (4,500 g, 5 min) to precipitate proteins and cell debris. The supernatant (200 μL/well) was filtered through an AcroPrep 96-well filter plate (0.2 μm) into a shallow 96-well plate for reverse-phase HPLC-MS analysis to determine the yield.

3.5 References

(1) Chu, J. C. K. & Rovis, T. Complementary Strategies for Directed C(Sp^3)–H Functionalization: A Comparison of Transition-Metalcatalyzed Activation, Hydrogen Atom Transfer, and Carbene/Nitrene Transfer. *Angew. Chem. Int. Ed.* **2018**, *57*, 62–101.

(2) Dalton, T., Faber, T. & Glorius, F. C–H Activation: Toward Sustainability and Applications. *ACS Cent. Sci.* **2021**, *7*, 245–261.

(3) Newton, C. G., Wang, S. G., Oliveira, C. C. & Cramer, N. Catalytic Enantioselective Transformations Involving C–H Bond Cleavage by Transition-Metal Complexes. *Chem. Rev.* **2017**, *117*, 8908–8976.

(4) Saint-Denis, T. G., Zhu, R. Y., Chen, G., Wu, Q. F. & Yu, J. Q. Enantioselective C(Sp^3)–H Bond Activation by Chiral Transition Metal Catalysts. *Science* **2018**, *359*, eaao4798.

(5) Rogge, T. et al. C–H Activation. *Nat. Rev. Methods Primers* **2021**, *1*, 43.

(6) Davies, H. M. L. & Beckwith, R. E. J. Catalytic Enantioselective C–H Activation by Means of Metal-Carbenoid-Induced C–H Insertion. *Chem. Rev.* **2003**, *103*, 2861–2904.

(7) Zhang, C., Li, Z. L., Gu, Q. S. & Liu, X. Y. Catalytic Enantioselective C(sp^3)–H Functionalization Involving Radical Intermediates. *Nat. Commun.* **2021**, *12*, 475.

(8) Yang, Y. & Arnold, F. H. Navigating the Unnatural Reaction Space: Directed Evolution of Heme Proteins for Selective Carbene and Nitrene Transfer. *Acc. Chem. Res.* **2021**, *54*, 1209–1225.

(9) Zhang, R. K., Huang, X. & Arnold, F. H. Selective C–H Bond Functionalization With Engineered Heme Proteins: New Tools To Generate Complexity. *Curr. Opin. Chem. Biol.* **2019**, *49*, 67–75.

(10) Lewis, J. C., Coelho, P. S. & Arnold, F. H. Enzymatic Functionalization of Carbon–Hydrogen Bonds. *Chem. Soc. Rev.* **2011**, *40*, 2003–2021.

(11) Yang, Y., Cho, I., Qi, X., Liu, P. & Arnold, F. H. An Enzymatic Platform for the Asymmetric Amination of Primary, Secondary and Tertiary C(sp^3)–H Bonds. *Nat. Chem.* **2019**, *11*, 987–993.

(12) Yang, C.-J. et al. Cu-Catalysed Intramolecular Radical Enantioconvergent Tertiary B-C(Sp^3)–H Amination of Racemic Ketones. *Nat. Catal.* **2020**, *3*, 539–546.

(13) Lang, K., Li, C., Kim, I. & Zhang, X. P. Enantioconvergent Amination of Racemic Tertiary C–H Bonds. *J. Am. Chem. Soc.* **2020**, *142*, 20902–20911.

(14) Ye, C. X., Shen, X., Chen, S. & Meggers, E. Stereocontrolled 1,3-Nitrogen Migration to Access Chiral α-Amino Acids. *Nat. Chem.* **2022**, *14*, 566–573.

(15) Ye, C.-X., Dansby, D. R., Chen, S. & Meggers, E. Expedited Synthesis of α-Amino Acids by Single-Step Enantioselective α-Amination of Carboxylic Acids. *Nat. Synth.* **2023**, *2*, 645–652.

(16) Hahn, C. J. et al. Crystal Structure of a Key Enzyme for Anaerobic Ethane Activation. *Science* **2021**, *373*, 118–121.

(17) Zanger, U. M. & Schwab, M. Cytochrome P450 Enzymes in Drug Metabolism: Regulation of Gene Expression, Enzyme Activities, And Impact of Genetic Variation. *Pharmacol. Ther.* **2013**, *138*, 103–141.

(18) Huang, X. & Groves, J. T. Oxygen Activation and Radical Transformations in Heme Proteins and Metalloporphyrins. *Chem. Rev.* **2018**, 118, 2491–2553.

(19) Poulos, T. L. Cytochrome P450 Flexibility. *Proc. Natl Acad. Sci. USA* **2003**, *100*, 13121–13122.

(20) Brandenberg, O. F., Fasan, R. & Arnold, F. H. Exploiting and Engineering Hemoproteins for Abiological Carbene and Nitrene Transfer Reactions. *Curr. Opin. Biotechnol.* **2017**, *47*, 102–111.

(21) Chen, K. & Arnold, F. H. Engineering New Catalytic Activities in Enzymes. *Nat. Catal.* **2020**, 3, 203–213.

(22) Hager, A., Vrielink, N., Hager, D., Lefranc, J. & Trauner, D. Synthetic Approaches Towards Alkaloids Bearing α-Tertiary Amines. *Nat. Prod. Rep.* **2016**, *33*, 491–522.

(23) Liu, G., Cogan, D. A. & Ellman, J. A. Catalytic Asymmetric Synthesis of tert-Butanesulfinamide. Application to the Asymmetric Synthesis of Amines. *J. Am. Chem. Soc.* **1997**, *119*, 9913–9914.

(24) Ellman, J. A., Owens, T. D. & Tang, T. P. *N*-tert-Butanesulfinyl Imines: Versatile Intermediates for the Asymmetric Synthesis of Amines. *Acc. Chem. Res.* **2002**, *35*, 984–995.

(25) Gao, X., Turek-Herman, J. R., Choi, Y. J., Cohen, R. D. & Hyster, T. K. Photoenzymatic Synthesis of α-Tertiary Amines by Engineered Flavin-Dependent 'Ene'-Reductases. *J. Am. Chem. Soc.* **2021**, 143, 19643–19647.

(26) Barrios-Rivera, J., Xu, Y., Wills, M. & Vyas, V. K. A Diversity of Recently Reported Methodology for Asymmetric Imine Reduction. *Org. Chem. Front.* **2020**, *7*, 3312–3342.

(27) Slabu, I., Galman, J. L., Lloyd, R. C. & Turner, N. J. Discovery, Engineering, and Synthetic Application of Transaminase Biocatalysts. *ACS Catal.* **2017**, *7*, 8263–8284.

(28) Afanasyev, O. I., Kuchuk, E., Usanov, D. L. & Chusov, D. Reductive Amination in the Synthesis of Pharmaceuticals. *Chem. Rev.* **2019**, *119*, 11857–11911.

(29) Jia, Z. J., Gao, S. & Arnold, F. H. Enzymatic Primary Amination of Benzylic and Allylic C(sp^3)–H Bonds. *J. Am. Chem. Soc.* **2020**, *142*, 10279–10283.

(30) Liu, Z. et al. An Enzymatic Platform for Primary Amination of 1-Aryl 2-Alkyl Alkynes. *J. Am. Chem. Soc.* **2022**, *144*, 80–85.

(31) Yang, Y., Shi, S.-L., Niu, D., Liu, P. & Buchwald, S. L. Catalytic Asymmetric Hydroamination of Unactivated Internal Olefins to Aliphatic Amines. *Science* **2015**, *349*, 62–66.

(32) Fandrick, K. R. et al. A General Copper-BINAP-Catalyzed Asymmetric Propargylation of Ketones with Propargyl Boronates. *J. Am. Chem. Soc.* **2011**, *133*, 10332–10335.

(33) Kille, S. et al. Reducing Codon Redundancy and Screening Effort of Combinatorial Protein Libraries Created by Saturation Mutagenesis. *ACS Synth. Biol.* **2013**, *2*, 83–92.

(34) Reetz, M. T. & Carballeira, J. D. Iterative Saturation Mutagenesis (ISM) for Rapid Directed Evolution of Functional Enzymes. *Nat. Protoc.* **2007**, *2*, 891–903.

(35) Prier, C. K., Zhang, R. K., Buller, A. R., Brinkmann-Chen, S. & Arnold, F. H. Enantioselective, Intermolecular Benzylic C–H Amination Catalysed by an Engineered Iron-Haem Enzyme. *Nat. Chem.* **2017**, *9*, 629–634.

(36) D'Amato, E. M., Borgel, J. & Ritter, T. Aromatic C–H Amination in Hexafluoroisopropanol. *Chem. Sci.* **2019**, *10*, 2424–2428.

(37) Legnani, L., Prina Cerai, G. & Morandi, B. Direct and Practical Synthesis of Primary Anilines Through Iron-Catalyzed C–H Bond Amination. *ACS Catal.* **2016**, *6*, 8162–8165.

(38) Liu, J. et al. Fe-Catalyzed Amination of (Hetero)Arenes with a Redox-Active Aminating Reagent Under Mild Conditions. *Eur. J. Chem.* **2017**, *23*, 563–567.

(39) Luo, Y.-R. Comprehensive Handbook of Chemical Bond Energies (Taylor & Francis, 2007).

(40) Pan, Y. et al. Kinetic Resolution of α-tertiary Propargylic Amines Through Asymmetric Remote Aminations of Anilines. *ACS Catal.* **2021**, *11*, 8443–8448.

(41) Hennessy, E. T., Liu, R. Y., Iovan, D. A., Duncan, R. A. & Betley, T. A. Iron-Mediated Intermolecular *N*-Group Transfer Chemistry with Olefinic Substrates. *Chem. Sci.* **2014**, *5*, 1526–1532.

(42) Jacobs, B. P., Wolczanski, P. T., Jiang, Q., Cundari, T. R. & MacMillan, S. N. Rare Examples of Fe(IV) Alkyl-Imide Migratory Insertions: Impact of Fe–C Covalency in (Me2IPr) Fe(=NAd)R2 (R=neoPe, 1-nor). *J. Am. Chem. Soc.* **2017**, *139*, 12145–12148.

(43) Singh, R., Kolev, J. N., Sutera, P. A. & Fasan, R. Enzymatic C(sp^3)–H Amination: P450-Catalyzed Conversion of Carbonazidates into Oxazolidinones. *ACS Catal.* **2015**, *5*, 1685–1691.

(44) Athavale, S. V. et al. Enzymatic Nitrogen Insertion into Unactivated C–H Bonds. *J. Am. Chem. Soc.* **2022**, *144*, 19097–19105.

Appendix B. Supplementary Information for Chapter III

I. Initial activity screening with engineered P411s.[a]

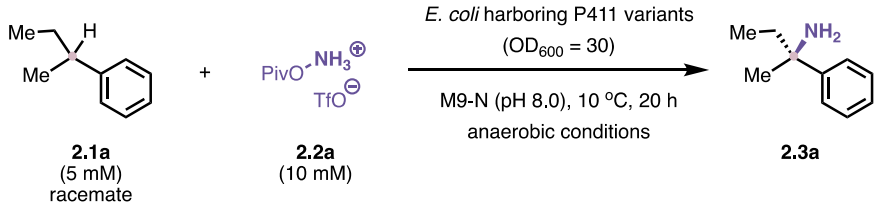

A panel of 48 cytochromes P411 previously engineered for nitrene transformations[40] was screened in whole *Escherichia coli* cells against **2.1a** and **2.2a** under anaerobic conditions. Among these, P411-TEA-5267 demonstrated the highest activity for synthesis of α-tertiary primary amine compound **2.3a**.

Table B.S1. Initial activity screening and control experiments.

Entry	Variant / Catalyst	Yield of 2.3a[a]	Standard deviation of yield	TTN	Standard deviation of TTN
1	P411-TEA-5267	1.0%	0.2%	20	4
2	hemin (20 μM) [b]	N.D.	-	N.D.	-
3	hemin (20 μM) + $Na_2S_2O_4$ [c]	N.D.	-	N.D.	-
4	cellular background [d]	N.D.	-	N.D.	-

[a] Experiments were performed using whole *E. coli* cells according to the protocol described in **Experimental Methods E**. The yields of 2.3a were calculated based on comparing the signal integration ratio of the products and an added internal standard compound (see XII for more details). All reactions were performed in triplicate, with the reported yields representing the average of three experiments. The signal calibration curves correlating the products and the internal standard compound can be found in XII. To enhance systematic management of different enzyme variants within the Arnold lab, we recently implemented a nomenclature system in which

variants are named as follows: family name-chemistry abbreviation-entry code. All enzyme variants in this study follow this nomenclature.

[b] Negative control experiments (with free hemin) were performed without the addition of $Na_2S_2O_4$. Under this condition, the resting oxidation state of hemin in aqueous buffer should be Fe(III).

[c] Negative control experiments using free hemin under reduced conditions (Fe(II)) were performed using an excess amount of $Na_2S_2O_4$ (20 mM).

[d] Cellular background control experiments were performed in whole-cell format, using *E. coli* (*E. cloni* BL21(DE3)) cells harboring an engineered tryptophan synthase *β*-subunit (Tm9D8*). The gene of this enzyme was also cloned into the pET22b(+) vector (Novagen) between restriction sites *Nde*I and *Xho*I. The protein expression protocol for this experiment followed the standard P411 expression conditions as described in **Experimental Methods B, C,** and **D**.

N.D. – no product was detected.

II. Directed evolution of P411-TEA-5274 for primary amination of tertiary C–H bonds.[a]

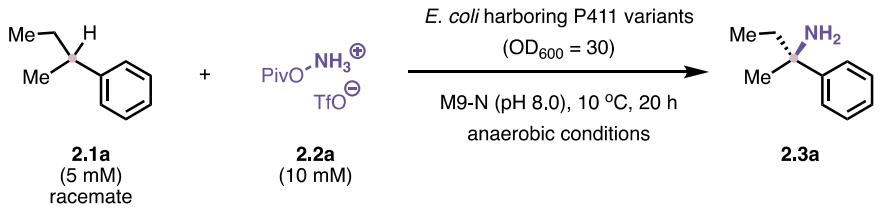

Table B.S2. Detailed information of the evolutionary lineage

Entry	Round #	Variant	Yield of 2.3a[a]	Standard deviation of yield	TTN	Standard deviation of TTN
1	0	P411-TEA-5267	1.0%	0.2%	20	4
2	1	P411-TEA-5268	1.7%	0.3%	24	5
3	2	P411-TEA-5269	2.3%	0.3%	35	4
4	3	P411-TEA-5270	3.0%	0.6%	64	13
5	4	P411-TEA-5271	5.8%	0.1%	89	1
6	5	P411-TEA-5272	6.7%	0.5%	140	10
7	6	P411-TEA-5273	17%	0.5%	270	8
8	7	P411-TEA-5274	26%	0.5%	970	18
9[b]	7	P411-TEA-5274	34%	1.1%	537	17
10[c]	7	P411-TEA-5274	24%	0.4%	879	15

[a] Experiments were performed using a suspension of *E. coli* cells harboring enzyme variants prepared according to the protocol described in **Experimental Methods B, C,** and **D**. Yields were calculated from HPLC calibration curves and the average of triplicate experiments (n = 3).

[b] OD_{600} = 40.

[c] In the absence of catalase and glucose oxidase.

Table B.S3. Mutations of the P411 variants in this study.

Name	**Mutations relative to the wild type P450$_{BM3}$**	**Mutations relative to P411-TEA-5267**
P411-TEA-5267	V78M, A82L, F87A, P142S, T175I, A184V, S226R, H236Q, E252G, I263M, E267D, T268P, A290V, T327A, A328V, L353V, I366V, N395R, C400S, L437F, T438V, E442K	-
P411-TEA-5268	V78M, A82L, F87A, P142S, T175I, A184V, S226R, H236Q, E252G, I263M, E267D, T268P, A290V, T327A, A328V, L353V, **M354E**, I366V, N395R, C400S, L437F, T438V, E442K	M354E
P411-TEA-5269	V78M, A82L, F87A, P142S, T175I, A184V, S226R, H236Q, E252G, I263M, E267D, T268P, A290V, T327A, A328V, L353V, **M354E**, I366V, **N395S**, C400S, L437F, T438V, E442K	M354E, R395S

P411-TEA-5270	V78M, A82L, F87A, P142S, T175I, A184V, S226R, H236Q, E252G, I263M, E267D, T268P, A290V, **T327V**, A328V, L353V, **M354E**, I366V, **N395S**, C400S, L437F, T438V, E442K	A327V, M354E, R395S
P411-TEA-5271	V78M, A82L, F87A, P142S, T175I, **M177Y**, A184V, S226R, H236Q, E252G, I263M, E267D, T268P, A290V, **T327V**, A328V, L353V, **M354E**, I366V, **N395S**, **A399G**, C400S, L437F, T438V, E442K	M177Y, A327V, M354E, R395S, A399G
P411-TEA-5272	**S72T**, V78M, A82L, F87A, P142S, T175I, **M177Y**, A184V, S226R, H236Q, E252G, I263M, E267D, T268P, A290V, **T327V**, A328V, L353V, **M354E**, I366V, **N395S**, **A399G**, C400S, L437F, T438V, E442K	S72T, M177Y, A327V, M354E, R395S, A399G
P411-TEA-5273	**S72T**, V78M, A82L, F87A, P142S, T175I, **M177Y**, A184V, S226R, H236Q, E252G, I263M, E267D, T268P, A290V, **T327V**, A328V, L353V, **M354E**, I366V, **N395S**, **A399G**, C400S, **Q403A**, L437F, T438V, E442K	S72T, M177Y, A327V, M354E, R395S, A399G, Q403A
P411-TEA-5274	**S72T**, V78M, A82L, F87A, P142S, T175I, **M177Y**, A184V, S226R, H236Q, E252G, I263M, E267D, T268P, A290V, **T327V**, A328V, L353V, **M354E**, I366V, **N395V**, **A399G**, C400S, **Q403A**, L437F, T438V, E442K	S72T, M177Y, A327V, M354E, R395V, A399G, Q403A

Variants are named as follows: family name-chemistry abbreviation-entry code. All enzyme variants in this study follow this nomenclature.

The genes encoding the heme proteins shown below were cloned using Gibson assembly[1] into vector pET-22b(+) (Novagen) between restriction sites *Nde*I and *Xho*I in frame with a *C*-terminal 6×His-tag.

III. Preparation of *sec*-butylarenes

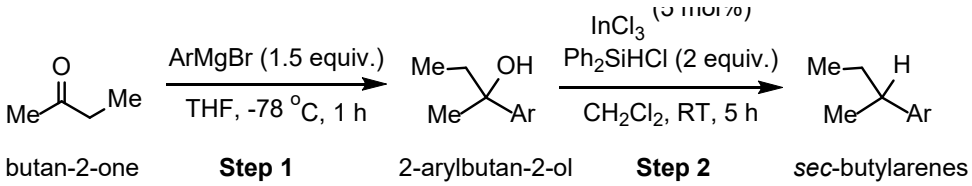

Step 1: In a 50-mL, oven-dried round-bottom flask under nitrogen was prepared a solution of butan-2-one (3.0 mmol) in dry THF (10 mL). The solution was cooled to -78 °C, and the Grignard reagent ArMgBr (4.5 mmol, solution in THF) was added dropwise. The mixture was stirred at -78 °C for 1 hour, and then quenched with saturated ammonium chloride solution (3 mL) and water (3 mL). The phases were separated, and the aqueous phase was extracted with Et_2O (3 x 15 mL). The combined organic phases were dried over sodium sulfate, filtered, and the solvent removed under reduced pressure. The crude product was used directly in the next step without further purification.

Step 2: This step was based on a reported method and implemented with minor modifications. [4] To a mixture of $InCl_3$ (0.05 mmol) and the 2-arylbutan-2-ol (1.0 mmol) in dry dichloromethane (1 mL) was added chlorodiphenylsilane (2.0 mmol) under nitrogen. The reaction mixture was stirred at room temperature for 5 h. The resulting mixture was poured into Et_2O (20 mL) and water (20 mL). The phases were separated, and the aqueous phase was extracted with Et_2O (3 x 15 mL). The combined organic phases were dried over sodium sulfate, filtered, and the solvent removed under reduced pressure. The residue was purified by flash column chromatography, with pure pentane as the eluent, to afford the corresponding *sec*-butylarenes **2.1c**–**2.1e**.

1-(*sec*-Butyl)-4-methylbenzene (2.1c)

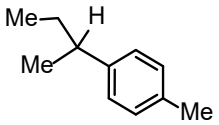

^{1}H NMR (400 MHz, Chloroform-*d*) δ 7.15 – 7.04 (m, 4H), 2.56 (h, *J* = 7.1 Hz, 1H), 2.32 (s, 3H), 1.61 – 1.55 (m, 2H), 1.22 (d, *J* = 6.9 Hz, 3H), 0.82 (t, *J* = 7.4 Hz, 3H).

^{13}C NMR (101 MHz, Chloroform-*d*) δ 144.81 , 135.28 , 129.06 , 127.05 , 41.40 , 31.35 , 22.10 , 21.14 , 12.43 .

Spectral data were in accordance with literature values.[5]

1-(*sec*-Butyl)-3-methylbenzene (2.1d)

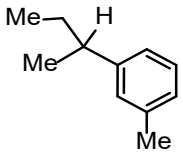

^{1}H NMR (400 MHz, Chloroform-*d*) δ 7.18 (t, *J* = 7.7 Hz, 1H), 7.04 – 6.94 (m, 3H), 2.55 (h, *J* = 7.0 Hz, 1H), 2.34 (s, 3H), 1.58 (td, *J* = 7.3, 2.1 Hz, 2H), 1.22 (dd, *J* = 6.9, 0.8 Hz, 3H), 0.85 – 0.80 (m, 3H).

^{13}C NMR (101 MHz, Chloroform-*d*) δ 147.82 , 137.83 , 128.25 , 128.00 , 126.64 , 124.18 , 41.77 , 31.30 , 22.00 , 21.66 , 12.46 .

Spectral data were in accordance with literature values.[5]

1-(*sec*-Butyl)-2-methylbenzene (2.1e)

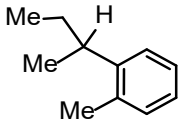

^{1}H NMR (400 MHz, Chloroform-*d*) δ 7.25 – 6.98 (m, 4H), 2.88 (h, *J* = 7.0 Hz, 1H), 2.33 (s, 3H), 1.62 (ddt, *J* = 20.7, 13.6, 7.0 Hz, 2H), 1.20 (d, *J* = 6.9 Hz, 3H), 0.86 (t, *J* = 7.4 Hz, 3H).

^{13}C NMR (101 MHz, Chloroform-*d*) δ 146.00 , 135.58 , 130.24 , 126.23 , 125.49 , 125.36 , 36.30 , 30.68 , 21.31 , 19.74 , 12.44 .

Spectral data were in accordance with literature values.[6]

IV. Preparation of (R)- and (S)-4-(*sec*-butyl)phenol

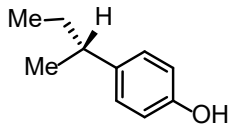

(*R*)-4-(*sec*-butyl)phenol

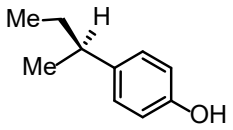

(*S*)-4-(*sec*-butyl)phenol

Chiral chromatographic separations of the enantiomers of (*R*)-4-(sec-butyl)phenol and (*S*)-4-(sec-butyl)phenol were conducted using a Thar analytical SFC system using a Mettler-Toledo column compartment and an Agilent 1200 series G1315B diode-array detector using 20% isopropanol in CO_2 on 4.6 x 250 mm Chiralcel® AD-H column at 3.5 mL/min.

(*rac*)-4-(sec-butyl)phenol:

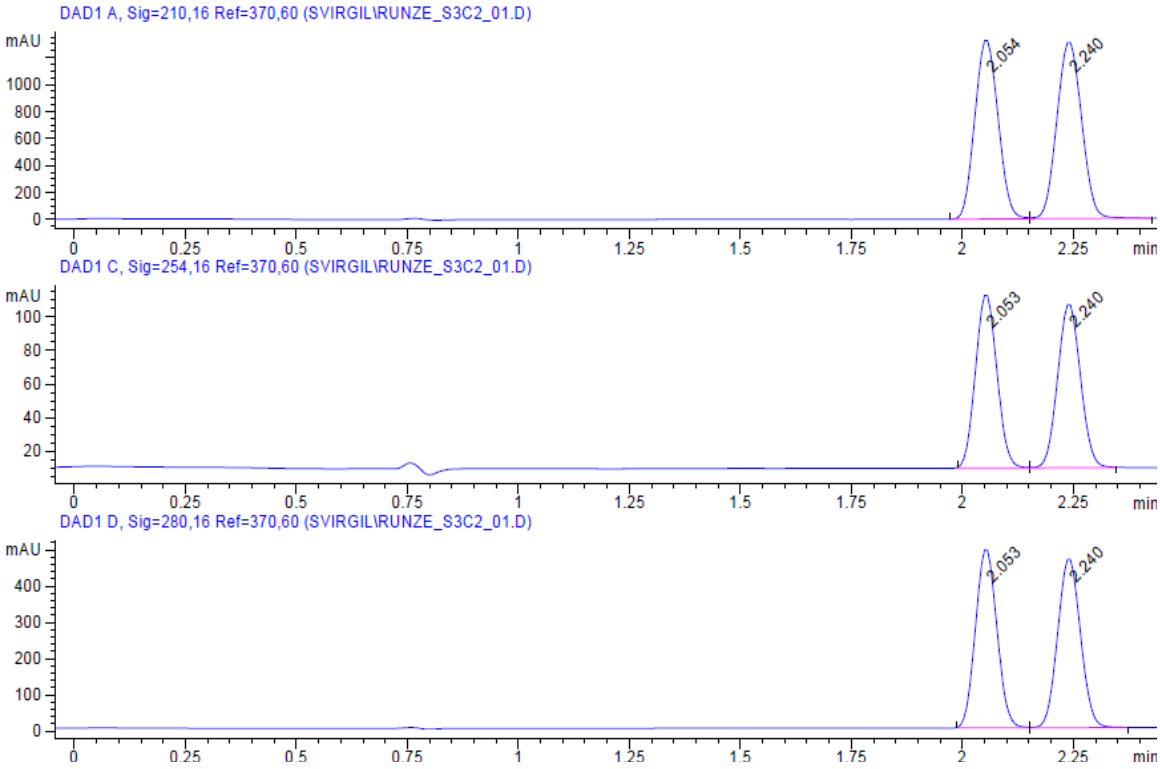

(*S*)-4-(*sec*-butyl)phenol (>99% *ee*):

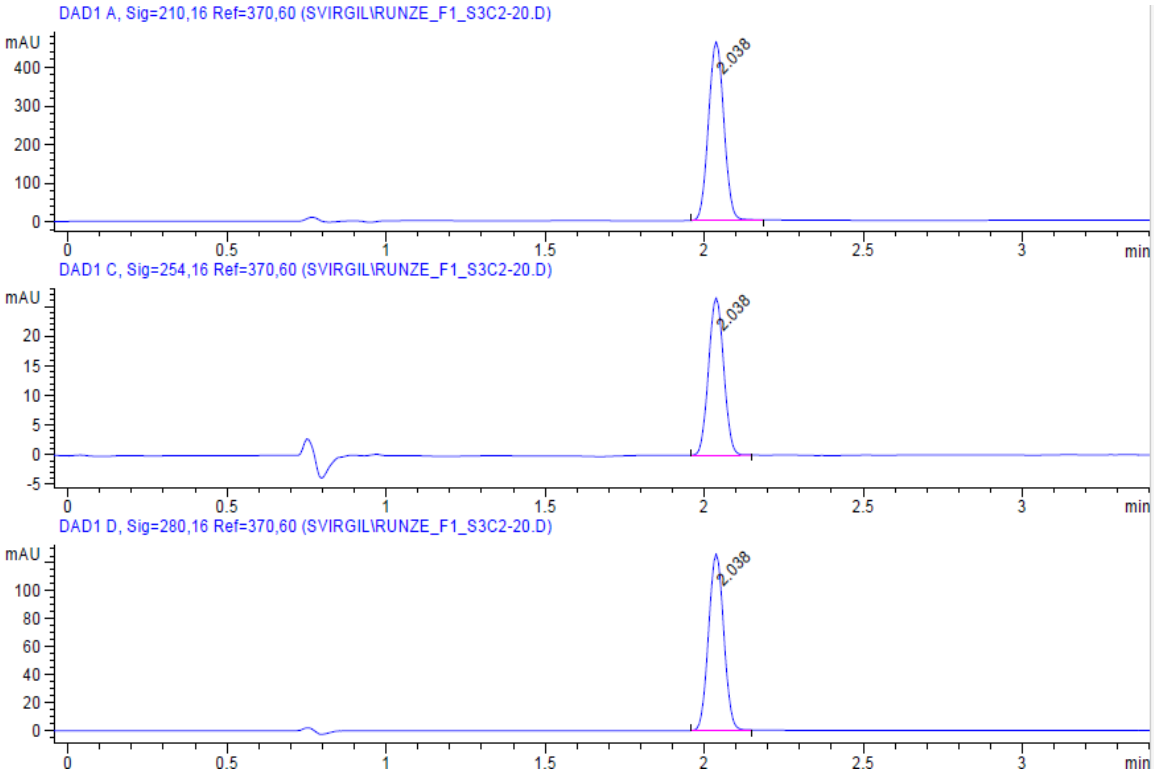

(*R*)-4-(*sec*-butyl)phenol (>99% *ee*):

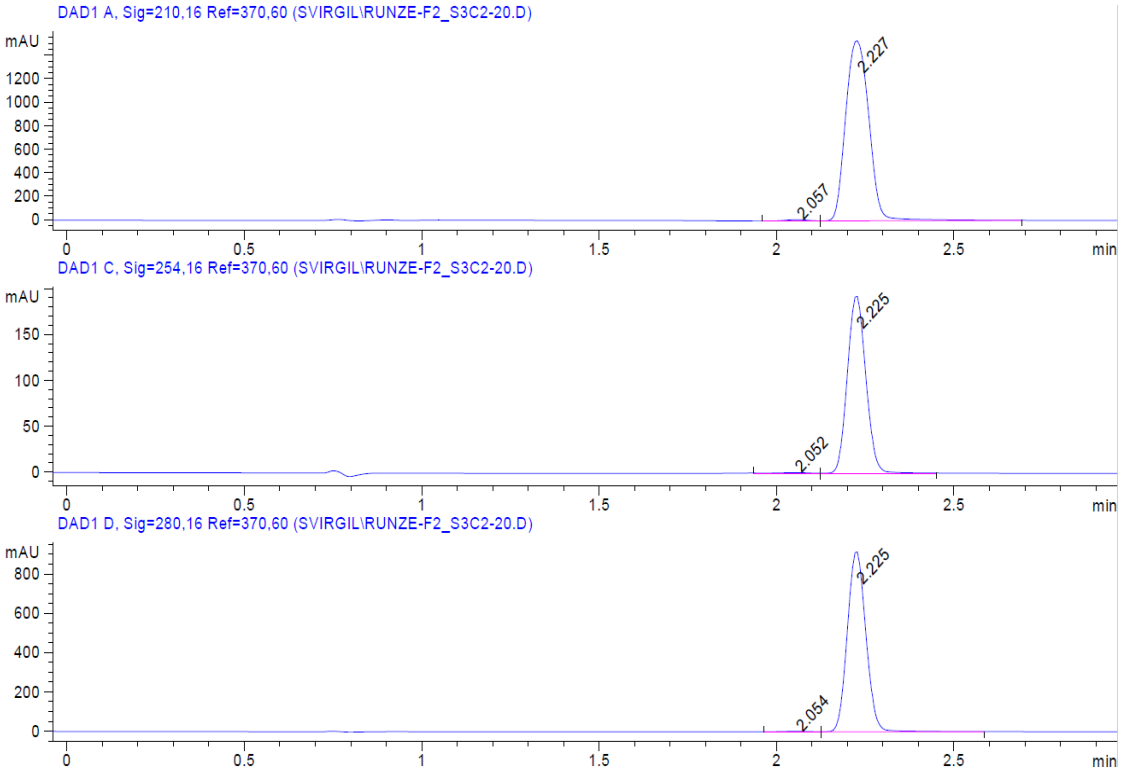

V. Preparation of (*R*)- and (*S*)-1-(*sec*-butyl)-4-methoxybenzene (2.1f)

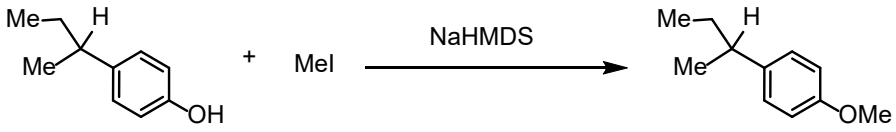

This step was based on a reported method and implemented with minor modifications.[7]

Iodomethane (0.05 mL) was added to a solution of (*R*)- or (*S*)-4-(sec-butyl)phenol (0.4 mmol) in dry THF (4 mL) via syringe followed by NaHMDS (1 M, 0.6 mL, 0.6 mmol) under Ar. The mixture was stirred at room temperature overnight and then poured into ice water. The aqueous solution was extracted with CH_2Cl_2 (10 mL x 3), and the combined extracts were washed with brine, dried over Na_2SO_4, filtered, and concentrated under reduced pressure. The residue was purified by column chromatography on silica gel (pure pentane).

Chiral-phase HPLC conditions: Chiralpak OJH, 1% *i*-PrOH in hexane, 1.0 mL/min, 25 ºC, 235 nm

(*rac*)-1-(*sec*-butyl)-4-methoxybenzene ((*rac*)-2.1f)

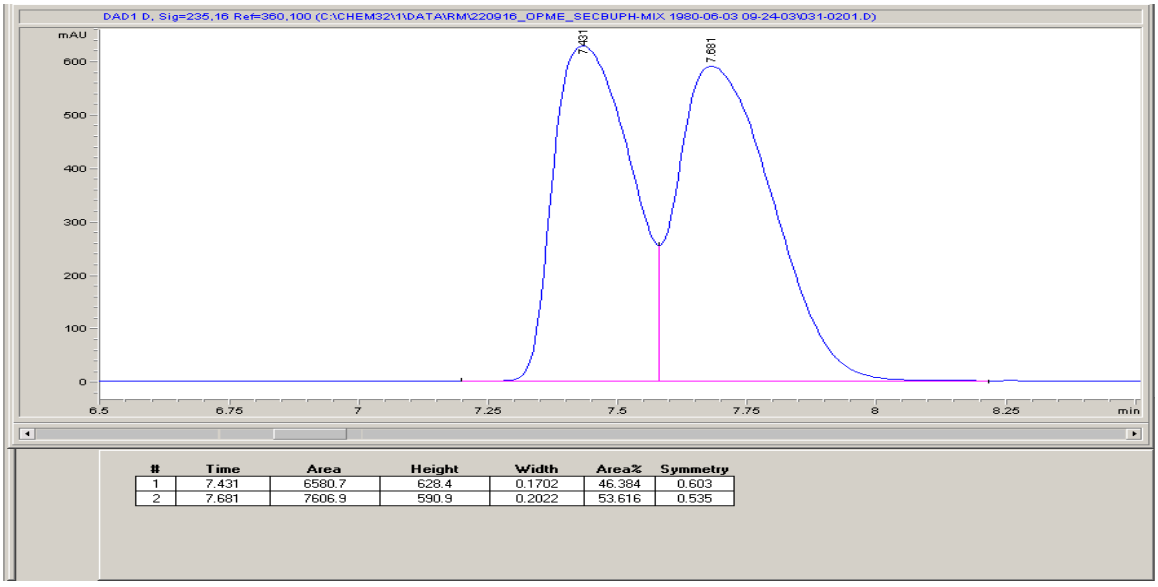

#	Time	Area	Height	Width	Area%	Symmetry
1	7.431	6580.7	628.4	0.1702	46.384	0.603
2	7.681	7606.9	590.9	0.2022	53.616	0.535

(*R*)-1-(*sec*-butyl)-4-methoxybenzene ((*R*)-2.1f; >99% *ee*)

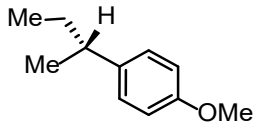

^{1}H NMR (400 MHz, Chloroform-*d*) δ 7.23 – 7.04 (m, 2H), 6.98 – 6.63 (m, 2H), 3.79 (s, 3H), 2.54 (p, *J* = 7.0 Hz, 1H), 1.58 – 1.54 (m, 2H), 1.21 (d, *J* = 6.9 Hz, 3H), 0.81 (t, *J* = 7.4 Hz, 3H).

$[\alpha]^{25}_{D}$ = -24.6 (*c* = 0.530 g / 100 mL, $CHCl_3$), >99% *ee*

Spectral data were in accordance with literature values.[8]

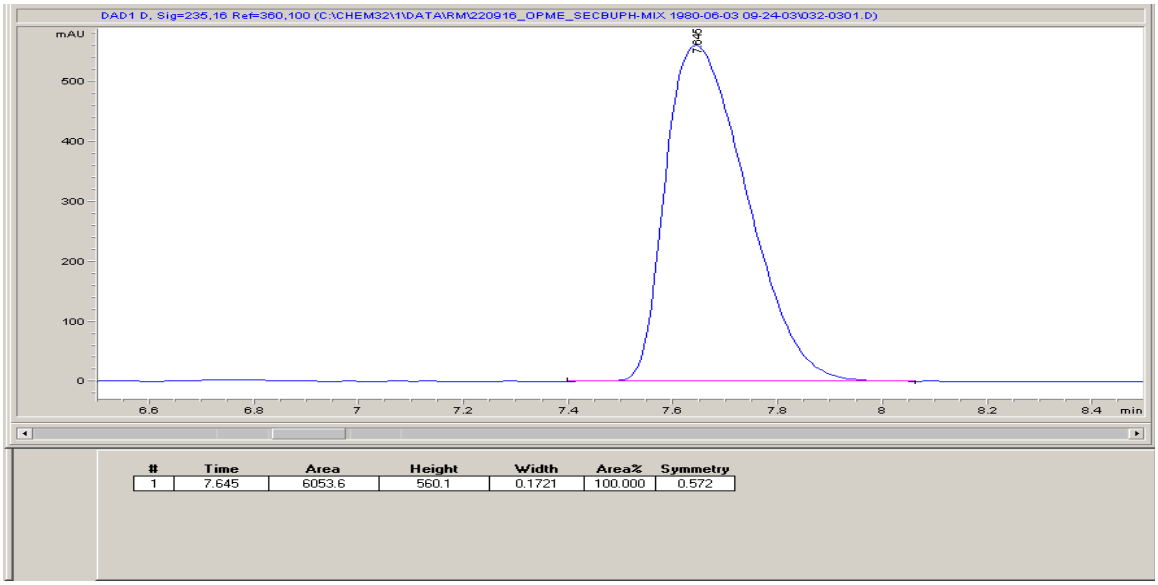

(*S*)-1-(*sec*-butyl)-4-methoxybenzene ((*S*)-2.1f; >99% *ee*)

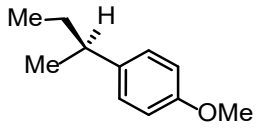

^{1}H NMR (400 MHz, Chloroform-*d*) δ 7.10 (d, *J* = 8.8 Hz, 2H), 6.84 (d, *J* = 8.6 Hz, 2H), 3.80 (s, 3H), 2.55 (h, *J* = 7.0 Hz, 1H), 1.58 – 1.53 (m, 2H), 1.21 (d, *J* = 6.9 Hz, 3H), 0.82 (t, *J* = 7.4 Hz, 3H).

$[\alpha]^{25}_{D}$ = +26.7 (*c* = 0.375 g / 100 mL, $CHCl_3$), >99% *ee*

Spectral data were in accordance with literature values.[8]

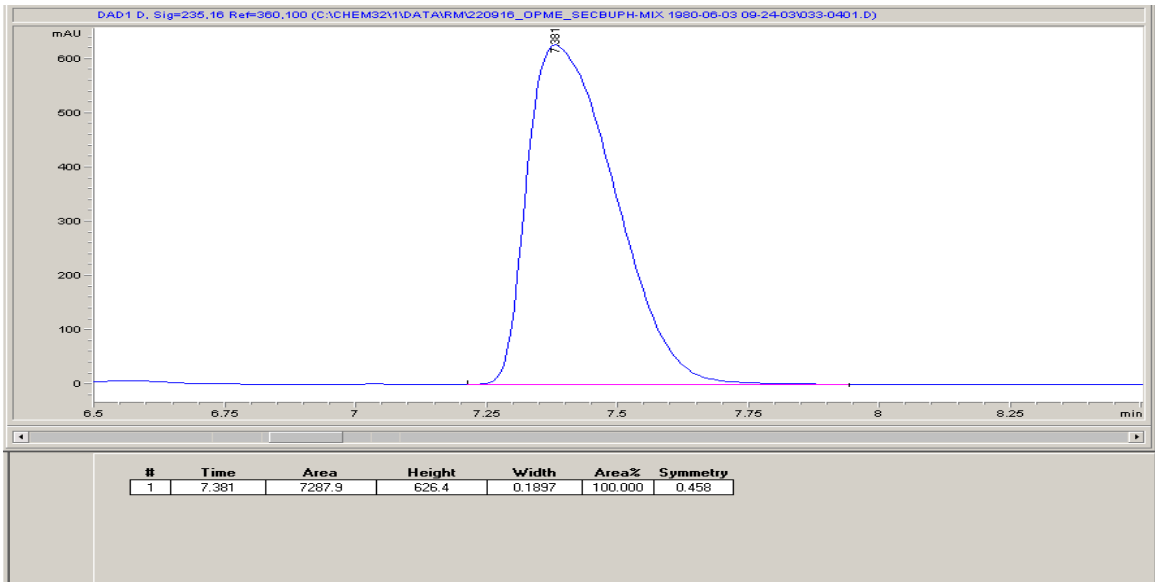

VI. Preparation of 2-(*sec*-butyl)thiophene 2.1j

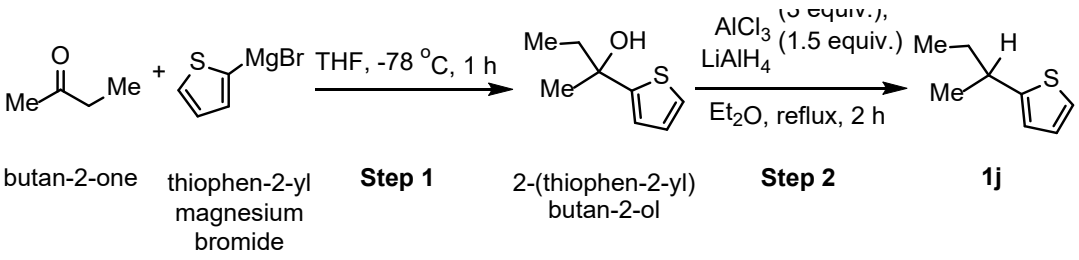

Step 1: In a 50-mL, oven-dried round-bottom flask under nitrogen was prepared a solution of butan-2-one (3.0 mmol) in dry THF (10 mL). The solution was cooled to -78 °C, and the 2-thienylmagnesium bromide (4.5 mmol; solution in THF or Et_2O) was added dropwise. The mixture was stirred at -78 °C for 1 hour and then quenched with saturated ammonium chloride solution (3 mL) and water (3 mL). The phases were separated, and the aqueous phase was extracted with Et_2O (3 x 15 mL). The combined organic phases were dried over sodium sulfate, filtered, and the solvent removed under reduced pressure. The crude product was used directly in the next step without further purification.

Step 2: This step was based on a reported method and implemented with minor modifications.[9] Dry diethyl ether (1.5 mL) was added into a flask containing $AlCl_3$ (3 mmol) under argon atmosphere at 0 °C, and $LiAlH_4$ (1.5 mmol) was added to the solution. To the reaction mixture was slowly added 2-(thiophen-2-yl)butan-2-ol (1 mmol) in dry diethyl ether (1.5 mL). After reflux for 2 h, the solution was quenched with water. The phases were separated, and the aqueous phase was extracted with Et_2O (3 x 15 mL). The combined organic phases were dried over sodium sulfate, filtered, and the solvent removed under reduced pressure. The residue was purified by flash column chromatography, with pure pentane as the eluent, to afford **2.1j**.

2-(*sec*-butyl)thiophene (2.1j)

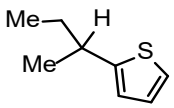

^{1}H NMR (400 MHz, Chloroform-*d*) δ 7.14 (dd, *J* = 5.1, 1.3 Hz, 1H), 6.95 (dd, *J* = 5.1, 3.5 Hz, 1H), 6.81 (dt, *J* = 3.5, 1.1 Hz, 1H), 2.96 (q, *J* = 6.9 Hz, 1H), 1.67 (q, *J* = 7.1 Hz, 2H), 1.34 (d, *J* = 7.0 Hz, 3H), 0.91 (t, *J* = 7.4 Hz, 3H). Spectral data were in accordance with literature values.[9]

VII. Preparation of Substrate 2.1k ((*E*)-(3-methylpent-1-en-1-yl)benzene)

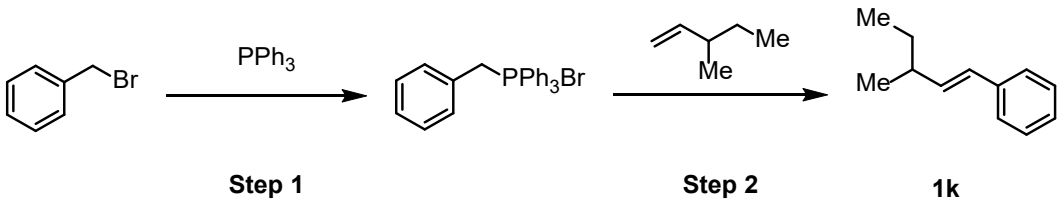

This protocol was based on a reported method and implemented with minor modifications.[10]

Step 1: To a 100-mL round-bottomed flask containing a magnetic bar was added triphenylphosphine (2.62 g, 10.0 mmol) and toluene (25 ml). To the mixture was then added benzyl bromide (1.2 mL, 10.0 mmol) via syringe, the flask was fitted with a condenser, and the reaction was heated at 90 °C for 15 h. The mixture was then cooled to room temperature, and the solid formed was isolated by suction filtration, washed with diethyl ether (3 x 10 mL), and dried *in vacuo* to give the Wittig reagent as a white solid.

Step 2: To a 50-mL round-bottomed flask containing a magnetic stirring bar under argon atmosphere was added the Wittig reagent (0.44 g, 1.0 mmol). Anhydrous THF (10 mL) was then added via syringe, and the solution was cooled to 0 °C. A solution of *n*-butyl lithium (2.5 M in hexanes, 0.4 mL, 1.0 mmol) was added dropwise via syringe, and the reaction was allowed to stir for 1 h. A solution of 2-methylbutyraldehyde (0.11 mL, 1.0 mmol) in dry THF (10 ml) was added dropwise via syringe over 30 min at 0 °C, and the resulting solution was allowed to stir at room temperature for 15 h. The reaction mixture was then poured into a saturated solution of NH_4Cl (10 mL) at 0 °C and extracted with dichloromethane (3 x 10 mL). The combined organic layers were dried over anhydrous Na_2SO_4, filtered, concentrated *in vacuo*, and purified by flash column chromatography to afford desired product **2.1k** as a colorless oil.

(*E*)-(3-methylpent-1-en-1-yl)benzene (2.1k)

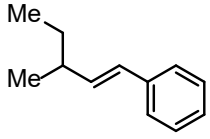

^{1}H NMR (400 MHz, Chloroform-*d*) δ 7.40 – 7.32 (m, 5H), 7.33 – 7.26 (m, 3H), 7.18 (t, *J* = 7.2 Hz, 1H), 6.34 (d, *J* = 16.1 Hz, 1H), 6.10 (dd, *J* = 15.9, 7.9 Hz, 1H), 2.20 (hept, *J* = 7.0 Hz, 1H), 1.41 (p, *J* = 7.2 Hz, 2H), 1.08 (d, *J* = 6.7 Hz, 3H), 0.91 (t, *J* = 7.4 Hz, 3H).

Spectral data were in accordance with literature values.[11]

VIII. Preparation of Substrate 2.1l ((3-methylpent-1-yn-1-yl)benzene)

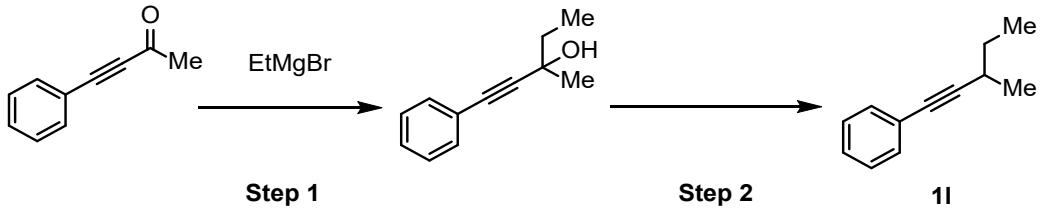

Step 1: In a 50-mL, oven-dried round-bottom flask under nitrogen was prepared a solution of 4-phenyl-3-butyn-2-one (3.0 mmol) in dry THF (10 mL). The solution was cooled to -78 °C, and ethylmagnesium bromide (4.5 mmol; 3.0 M in diethyl ether solution) was added dropwise. The mixture was stirred at -78 °C for 1 hour and then quenched with saturated ammonium chloride solution (3 mL) and water (3 mL). The phases were separated, and the aqueous phase was extracted with Et_2O (3 x 15 mL). The combined organic phases were dried over sodium sulfate, filtered, and the solvent removed under reduced pressure. The crude product was used directly in the next step without further purification.

Step 2: This step was based on a reported method and implemented with minor modifications.[12] 3-Methyl-1-phenylpent-1-yn-3-ol (0.5 mmol) and triethylsilane (1.5 mmol) were dissolved in dichloromethane (1 mL). Next, Bu_4NPF_6 (5 mol %) and $Ca(NTf_2)_2$ (5 mol %) were added at room temperature and stirred until conversion of the alcohol was complete (monitored by TLC). The product was isolated by adding sat. $NaHCO_3$ solution (5 mL), extracting the aqueous phase with dichloromethane (3 x 15 mL), and the combined organic phases were then dried over Na_2SO_4 and concentrated *in vacuo*. The crude product was purified by column chromatography, with pure pentane as the eluent, to afford **2.1l**.

(3-methylpent-1-yn-1-yl)benzene (2.1l)

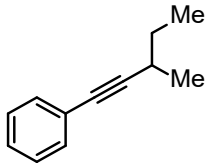

^{1}H NMR (400 MHz, Chloroform-*d*) δ 7.43 – 7.37 (m, 2H), 7.33 – 7.24 (m, 3H), 2.59 (h, *J* = 6.9 Hz, 1H), 1.58 – 1.52 (m, 2H), 1.25 (d, *J* = 6.9 Hz, 3H), 1.06 (t, *J* = 7.4 Hz, 3H).

Spectral data were in accordance with literature values.[13]

IX. Preparation of 2-arylbutan-2-amines

Step 1: In a 50-mL, oven-dried round-bottom flask under nitrogen was prepared a solution of butan-2-one (3.0 mmol) in dry THF (10 mL). The solution was cooled to -78 °C, and the Grignard reagent ArMgBr (4.5 mmol; solution in THF or Et_2O) was added dropwise. The mixture was stirred at -78 °C for 1 hour and then quenched with saturated ammonium chloride solution (3 mL) and water (3 mL). The phases were separated, and the aqueous phase was extracted with Et_2O (3 x 15 mL). The combined organic phases were dried over sodium sulfate, filtered, and the solvent removed under reduced pressure. The crude product was used directly in the next step without further purification.

Step 2: This step was based on a reported method and implemented with minor modifications.[14] A solution of the 2-arylbutan-2-ol (1 mmol) in dry CH_2Cl_2 (5 mL) and $TMSN_3$ (1.5 mmol) were placed in a 25-mL, oven-dried round-bottom flask under nitrogen. $InBr_3$ (0.1 mmol) was added to this reaction mixture. The contents were stirred at room temperature for 1 h. The reaction then was quenched with water. The product was extracted with CH_2Cl_2 (3×15 mL), washed with 10% Na_2CO_3 (20 mL), and water (20 mL). The combined organic phases were dried over sodium sulfate, filtered, and the solvent removed under reduced pressure. The crude product was used directly in the next step without further purification.

Step 3: This step was based on a reported method and implemented with minor modifications.[15] $LiAlH_4$ (2 mmol) was added at room temperature to a solution of the 2-arylbutan-2-azide (0.5 mmol) in Et_2O (2 mL). After 5 h reflux, the reaction mixture was carefully quenched with 15% aq. NaOH (0.1 mL), and water (0.1 mL). After dilution of the residue with 5 mL ethyl acetate, the mixture was filtered through Celite and anhydrous sodium sulfate. To the filtrate was added HCl solution (1 M) until pH < 2. After washing three times with ethyl acetate, the aqueous phase was treated with NaOH solution (1M) to pH > 12 and extracted three times with 20 mL ethyl

acetate. The combined organic layer was washed with brine, dried by Na_2SO_4, and concentrated to afford the corresponding racemic 2-arylbutan-2-amines **2.3a**, **2.3c, 2.3d, 2.3e**, **2.3g**, **2.3j,** and **2.3k**.

2-phenylbutan-2-amine (2.3a)

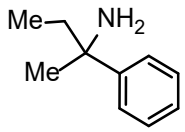

^{1}H NMR (400 MHz, Chloroform-*d*) δ 7.45 (d, *J* = 7.8 Hz, 2H), 7.36 – 7.30 (m, 2H), 7.22 (t, *J* = 7.3 Hz, 1H), 2.28 (br s, 2H), 1.87 – 1.73 (m, 2H), 1.50 (s, 3H), 0.75 (t, *J* = 7.4 Hz, 3H).

^{13}C NMR (101 MHz, Chloroform-*d*) δ 128.31 , 126.40 , 125.44 , 56.00 , 37.37 , 29.86 , 8.78 .

Spectral data were in accordance with literature values.[15]

2-(*p*-tolyl)butan-2-amine (2.3c)

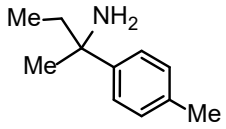

^{1}H NMR (400 MHz, Chloroform-*d*) δ 7.37 – 7.30 (m, 2H), 7.17 – 7.11 (m, 2H), 2.33 (s, 3H), 1.83 – 1.72 (m, 2H), 1.70 – 1.65 (br s, 2H), 1.44 (s, 3H), 0.74 (t, *J* = 7.4 Hz, 3H).

^{13}C NMR (101 MHz, Chloroform-*d*) δ 145.88 , 135.61 , 128.90 , 125.33 , 55.12 , 37.73 , 30.76 , 21.02 , 8.84 .

Physical State: yellowish oil.

HRMS (FD): calcd for $C_{11}H_{18}N$ $[M+H]^+$ 164.14392; found 164.14310.

2-(*m*-tolyl)butan-2-amine (2.3d)

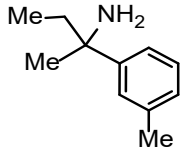

^{1}H NMR (400 MHz, Chloroform-*d*) δ 7.29 – 7.17 (m, 3H), 7.08 – 6.98 (m, 1H), 2.36 (s, 3H), 1.82 – 1.69 (m, 4H), 1.44 (s, 3H), 0.75 (t, *J* = 7.4 Hz, 3H).

^{13}C NMR (101 MHz, Chloroform-*d*) δ 148.60 , 137.57 , 127.98 , 126.78 , 126.05 , 122.33 , 55.18 , 37.59 , 30.57 , 21.70 , 8.71 .

Physical State: yellowish oil.

HRMS (FD): calcd for $C_{11}H_{18}N$ $[M+H]^+$ 164.14392; found 164.14501.

2-(*o*-tolyl)butan-2-amine (2.3e)

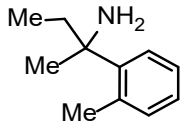

^{1}H NMR (400 MHz, Chloroform-*d*) δ 7.47 (d, *J* = 6.6 Hz, 1H), 7.17 – 7.12 (m, 3H), 2.57 (s, 3H), 2.00 – 1.72 (m, 4H), 1.53 (s, 3H), 0.74 (t, *J* = 7.5 Hz, 3H).

^{13}C NMR (101 MHz, Chloroform-*d*) δ 145.61 , 135.83 , 132.89 , 126.74 , 126.55 , 125.76 , 56.74 , 35.43 , 30.45 , 23.17 , 9.14 .

Spectral data were in accordance with literature values.[5]

2-phenylpropan-2-amine (2.3h)

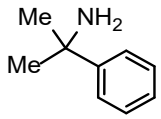

^{1}H NMR (400 MHz, Chloroform-*d*) δ 7.58 – 7.46 (m, 2H), 7.36 – 7.31 (m, 2H), 7.26 – 7.21 (m, 1H), 2.94 (br, 2H), 1.56 (s, 6H).

^{13}C NMR (101 MHz, Chloroform-*d*) δ 148.84, 128.56, 128.50, 126.79, 124.93, 53.47, 32.05, 29.94.

Physical State: pale yellowish oil.

2-(pyridin-2-yl)butan-2-amine (2.3i)

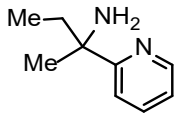

^{1}H NMR (400 MHz, Chloroform-*d*) δ 8.55 (ddd, *J* = 4.8, 1.9, 1.0 Hz, 1H), 7.63 (ddd, *J* = 8.0, 7.5, 1.9 Hz, 1H), 7.40 (dt, *J* = 8.0, 1.0 Hz, 1H), 7.11 (ddd, *J* = 7.5, 4.9, 1.1 Hz, 1H), 2.60 (s, 2H), 1.88 – 1.78 (m, 2H), 1.48 (s, 3H), 0.73 (t, *J* = 7.5 Hz, 3H).

Spectral data were in accordance with literature values.[16]

2-(thiophen-2-yl)butan-2-amine (2.3j)

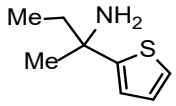

^{1}H NMR (400 MHz, Chloroform-*d*) δ 7.17 (dd, *J* = 5.0, 1.3 Hz, 1H), 6.95 – 6.91 (m, 2H), 1.95 (br s, 2H), 1.87 – 1.82 (m, 2H), 1.55 (s, 3H), 0.86 (t, *J* = 7.4 Hz, 3H).

Spectral data were in accordance with literature values.[17]

(*E*)-3-methyl-1-phenylpent-1-en-3-amine (2.3k)

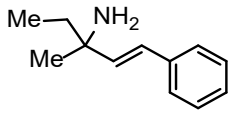

In the first step shown in IX, benzylideneacetone and ethylmagnesium bromide (3.0 M in diethyl

ether solution) were used as reactants, while keeping the other conditions unchanged.

^{1}H NMR (400 MHz, Chloroform-*d*) δ 7.40 – 7.34 (m, 2H), 7.26 – 7.21 (m, 3H), 6.77 (d, *J* = 16.4 Hz, 1H), 6.22 (d, *J* = 16.4 Hz, 1H), 2.03 – 1.81 (m, 2H), 1.58 (s, 3H), 0.95 (t, *J* = 7.5 Hz, 3H).

^{13}C NMR (101 MHz, Chloroform-*d*) δ 136.08 , 131.79 , 129.62 , 128.67 , 128.20 , 126.89 , 58.46 , 33.21 , 23.97 , 8.38 .

Spectral data were in accordance with literature values.[18]

X. Preparation of 2.3l (3-methyl-1-phenylpent-1-yn-3-amine)

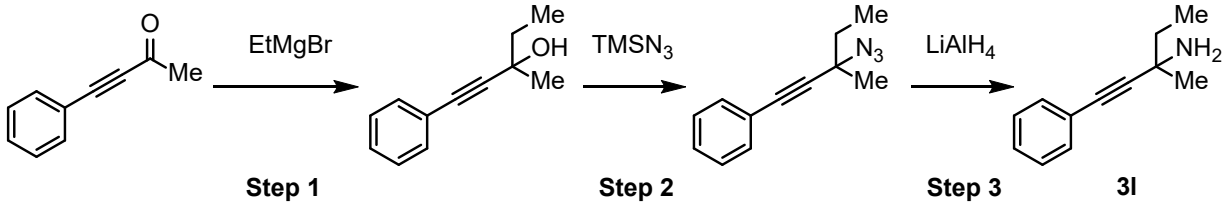

Step 1: In a 50-mL, oven-dried round-bottom flask under nitrogen was prepared a solution of 4-phenylbut-3-yn-2-one (3.0 mmol) in dry THF (10 mL). The solution was cooled to -78 °C, and the Grignard reagent EtMgBr (4.5 mmol; solution in THF or Et_2O) was added dropwise. The mixture was stirred at -78 °C for 1 hour and then quenched with saturated ammonium chloride solution (3 mL) and water (3 mL). The phases were separated, and the aqueous phase was extracted with Et_2O (3 x 15 mL). The combined organic phases were dried over sodium sulfate, filtered, and the solvent removed under reduced pressure. The crude product was used directly in the next step without further purification.

Step 2: This step was based on a reported method and implemented with minor modifications. [14] A solution of the 3-methyl-1-phenylpent-1-yn-3-ol (1 mmol) in dry CH_2Cl_2 (5 mL) and $TMSN_3$ (1.5 mmol) were placed in a 25-mL oven-dried round-bottom flask under nitrogen. $InBr_3$ (0.1 mmol) was added to this reaction mixture. The contents were stirred at room temperature for 1 h. The reaction then was quenched with water. The product was extracted with CH_2Cl_2 (3×15 mL), washed with 10% Na_2CO_3 (20 mL) and water (20 mL). The combined organic phases were dried over sodium sulfate, filtered, and the solvent removed under reduced pressure. The crude product was used directly in the next step without further purification.

Step 3: This step was based on a reported method and implemented with minor modifications.[15] $LiAlH_4$ (2 mmol) was added at room temperature to a solution of the (3-azido-3-methylpent-1-yn-1-yl)benzene (0.5 mmol) in Et_2O (2 mL). After 5 h reflux, the reaction mixture was carefully quenched with water (0.1 mL), 15% aq. NaOH (0.1 mL), and water (0.1 mL). After dilution of the residue with 5 mL ethyl acetate, the mixture was filtered through Celite and anhydrous sodium sulfate. To the filtrate was added HCl solution (1 M) until pH < 2. After washing three times with ethyl acetate, the aqueous phase was treated with NaOH solution (1 M) to pH >

12 and extracted three times with 20 mL ethyl acetate. The combined organic layer was washed with brine, dried by Na_2SO_4, and concentrated to afford the corresponding racemic amine **2.3l**.

3-methyl-1-phenylpent-1-yn-3-amine (2.3l)

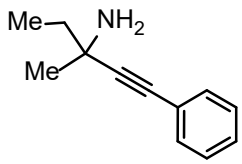

^{1}H NMR ^{1}H NMR (400 MHz, Chloroform-*d*) δ 7.43 – 7.36 (m, 2H), 7.34 – 7.26 (m, 3H), 2.50 (br, 2H), 1.71 (d, *J* = 7.5 Hz, 2H), 1.47 (s, 3H), 1.10 (t, *J* = 7.5 Hz, 3H).

Spectral data were in accordance with literature values.[19]

XI. 0.6-mmol Scale biosynthesis of amine 2.3m from (*E*)- or (*Z*)-2.1m

Protein expression: BL21 *E. coli* cells transformed with pET22b(+) plasmid encoding P411-TEA-5274 variant were grown in 30 mL LB_{amp} (37 °C, 230 rpm) in a 125-mL Erlenmeyer flask for 14–16 hours. HB_{amp} medium (1,000 mL) in a 2,800-mL flask was inoculated with 20 mL of the overnight culture. The HB culture was shaken at 37 °C and 140 rpm for about 2.5 hours in an incubator with a 25 mm shaking radius until the OD_{600} was between 0.8 and 0.9. The culture was cooled on an ice bath for 1 hour and then treated with 0.5 mM IPTG and 1 mM 5-aminolevulinic acid (final concentrations). The culture was allowed to shake for 22 hours in the same incubator at 90 rpm and with the temperature reduced to 22 °C.

Reaction setup: While harvesting cells, M9-N buffer (pH 8.0), D-glucose solution (0.5 M), and the substrates (0.1 M in ethanol or water) were precooled on an ice bath. Cells were pelleted by centrifugation (4,500 g, 5 minutes, and 4 °C), resuspended in approximately 250 mL precooled M9-N buffer, and adjusted to OD_{600} = 40. Depending on the substrates, a specific volume of cell suspension, precooled M9-N buffer, and precooled D-glucose solution (0.5 M, 9 mL) were then poured into a 250-mL Erlenmeyer flask with screw cap on an ice bath to make a final volume of 96 mL. Subsequently, the flask with cells, substrate (*E*)- or (*Z*)-**2.1m** (100 mM in ethanol, 6 mL, 0.6 mmol), substrate **2.2a** (100 mM in water, 12 mL, 1.2 mmol), and a precooled stock solution for oxygen depletion (6 mL, 14,000 U/mL catalase and 1,000 U/mL glucose oxidase in M9-N buffer) were quickly transferred into an anaerobic chamber without the ice bath. In the anaerobic chamber, to the flask with cells was added the solution for oxygen depletion and the mixture was gently swirled by hand for around 5 minutes. Then, substrate (*E*)- or (*Z*)-**2.1m** and substrate **2.2a** were added sequentially. The final reaction volume was 120 mL, and the final OD_{600} = 30. The flask was sealed tightly, and the reaction proceeded outside the anaerobic chamber at 10 °C for 12 hours with shaking at 250 rpm with a 25 mm shaking radius. The leftover cell suspension was lysed to determine the hemoprotein concentration using the hemochrome assay (see **Experimental Methods C**).

Reaction work-up: To the resulting mixture was added 120 mL ethanol and mixed vigorously by shaking. The cell debris was removed by centrifugation (5,000 g, 10 minutes, 4 °C). Then ethanol and the majority of the water in the supernatant were removed by rotary evaporation

until a final volume of approximately 30 mL was achieved, and the remaining aqueous layer was treated with HCl solution (1M) to pH < 2 in an ice bath. After washing three times with diethyl ether (20 mL each time), the aqueous phase was treated with NaOH solution (1 M) to pH > 12 on an ice bath and extracted with ethyl acetate for four times (30 mL each time). During the extraction, centrifugation was used for phase separation (5,000 g, 5 minutes, and 4 °C). The combined organic layer was washed with brine (30 mL), dried by Na_2SO_4, and concentrated *in vacuo* to give the final products without further purification.

2-methyl-4-phenylbut-3-en-2-amine (2.3m)

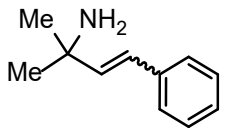

^{1}H NMR (400 MHz, Chloroform-*d*) δ 7.37 (d, *J* = 7.5 Hz, 2H), 7.29 (t, *J* = 7.5 Hz, 2H), 7.22 (t, *J* = 7.2 Hz, 1H), 6.50 (d, *J* = 16.2 Hz, 1H; same from (*E*)- or (*Z*)-**2.1m**), 6.31 (d, *J* = 16.2 Hz, 1H; same from (*E*)- or (*Z*)-**2.1m**), 3.86 (br s, 2H), 1.37 (s, 6H).

From (*E*)-**2.1m**, (*E*)-**2.3m** was obtained in >99:1 stereopurity (from ^{1}H NMR).

From (*Z*)-**2.1m**, (*E*)-**2.3m** was obtained in >99:1 stereopurity (from ^{1}H NMR).

Spectral data were in accordance with literature values.[20]

XII. HPLC Calibration Curves

Calibration curves of synthesized reference compounds were created for the determination of yield and TTN. For each substrate, five different concentrations of product (0.5, 1, 1.5, 2, and 2.5 mM) were prepared in 400 µL M9-N (pH = 8.0) buffer. Internal standard solution (1 mM of 3,4-dimethoxylacetophenon e) was prepared in acetonitrile. The mixtures of standard product and 400-µL internal standard acetonitrile solution were vortexed and centrifuged to pellet down all the solids. The supernatant was analyzed by HPLC based on UV absorbance at 210 nm. The calibration curves depict the ratio of concentration in mM (x-axis) against product area to internal standard area (y-axis). Notes: Pdt = product area, IS = internal standard area, [Pdt] = product concentration in reaction, [PC] = protein concentration in reaction, Avg. TTN = average total turnover number, SD TTN = standard deviation of TTN, Avg. Yield = average yield, SD Yield = standard deviation of yield.

2-phenylbutan-2-amine (2.3a)

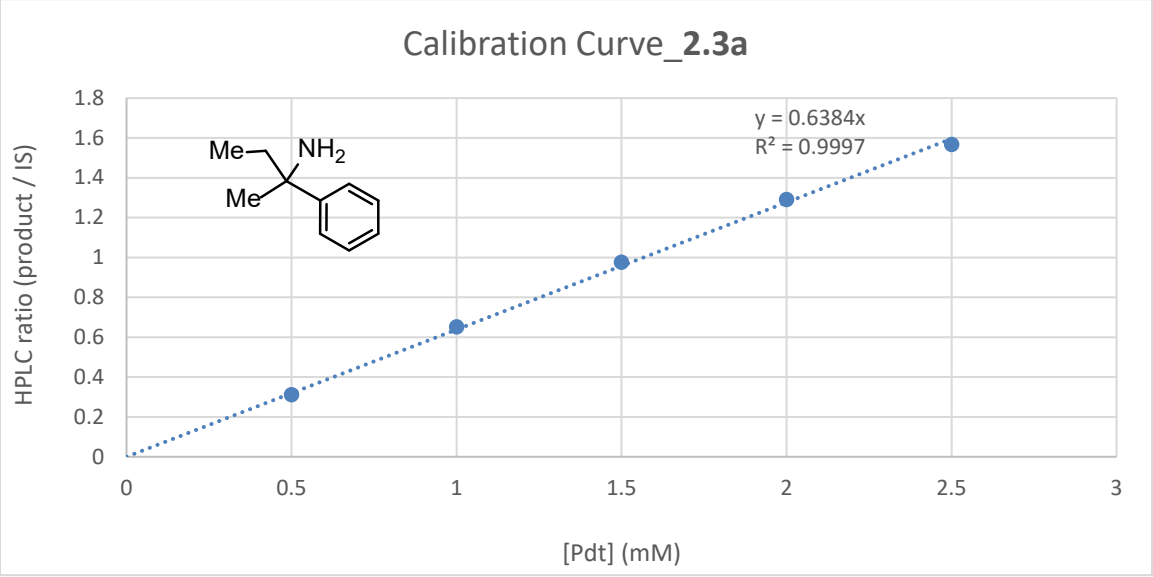

Data analysis for P411-TEA-5267-catalyzed amination of **2.1a** (5 mM), OD_{600} = 30; Table B.S1, entry 1 and Table B.S2, entry 1:

Entry	Pdt	IS	Pdt/IS	[Pdt]/mM	[PC]/μM	Avg. TTN	SD TTN	Avg. Yield [%]	SD Yield [%]
1	34.0	1003.6	0.034	0.053	2.4	20	4	1.0	0.2
2	25.2	1003.7	0.025	0.039	2.4				
3	35.6	1012.8	0.035	0.055	2.4				

Data analysis for P411-TEA-5268-catalyzed amination of **2.1a** (5 mM), OD_{600} = 30; Table B.S2, entry 2:

Entry	Pdt	IS	Pdt/IS	[Pdt]/mM	[PC]/μM	Avg. TTN	SD TTN	Avg. Yield [%]	SD Yield [%]
1	64.6	1016.6	0.064	0.100	3.4	24	5	1.7	0.3
2	41.9	982.0	0.043	0.067	3.4				
3	52.5	1005.2	0.052	0.082	3.4				

Data analysis for P411-TEA-5269-catalyzed amination of **2.1a** (5 mM), OD_{600} = 30; Table B.S2, entry 3:

Entry	Pdt	IS	Pdt/IS	[Pdt]/mM	[PC]/μM	Avg. TTN	SD TTN	Avg. Yield [%]	SD Yield [%]
1	80.0	1002.2	0.080	0.125	3.3	35	4	2.3	0.3

2	80.9	1005.8	0.080	0.126	3.3				
3	63.0	983.9	0.064	0.101	3.3				

Data analysis for P411-TEA-5270-catalyzed amination of **2.1a** (5 mM), OD_{600} = 30; Table B.S2, entry 4:

Entry	Pdt	IS	Pdt/IS	[Pdt]/mM	[PC]/μM	Avg. TTN	SD TTN	Avg. Yield [%]	SD Yield [%]
1	113.3	996.3	0.114	0.179	2.3	64	13	3.0	0.6
2	92.3	948.0	0.097	0.153	2.3				
3	74.2	985.9	0.075	0.118	2.3				

Data analysis for P411-TEA-5271-catalyzed amination of **2.1a** (5 mM), OD_{600} = 30; Table B.S2, entry 5:

Entry	Pdt	IS	Pdt/IS	[Pdt]/mM	[PC]/μM	Avg. TTN	SD TTN	Avg. Yield [%]	SD Yield [%]
1	192.0	1048.9	0.183	0.288	3.3	89	1	5.8	0.1
2	196.7	1069.5	0.184	0.289	3.3				
3	178.7	957.8	0.187	0.293	3.3				

Data analysis for P411-TEA-5272-catalyzed amination of **2.1a** (5 mM), OD_{600} = 30; Table B.S2, entry 6:

Entry	Pdt	IS	Pdt/IS	[Pdt]/mM	[PC]/μM	Avg. TTN	SD TTN	Avg. Yield [%]	SD Yield [%]
1	228.5	985.4	0.232	0.364	2.5	140	10	6.7	0.5
2	207.8	1013.0	0.205	0.322	2.5				
3	206.9	1024.2	0.202	0.317	2.5				

Data analysis for P411-TEA-5273-catalyzed amination of **2.1a** (5 mM), OD_{600} = 30; Table B.S2, entry 7:

Entry	Pdt	IS	Pdt/IS	[Pdt]/mM	[PC]/μM	Avg. TTN	SD TTN	Avg. Yield [%]	SD Yield [%]
1	563.5	1022.7	0.551	0.866	3.1	270	8	17	0.5
2	564.4	1032.5	0.547	0.859	3.1				
3	527.4	1007.5	0.523	0.822	3.1				

Data analysis for P411-TEA-5274-catalyzed amination of **2.1a** (5 mM), OD_{600} = 30; Table B.S2, entry 8:

Entry	Pdt	IS	Pdt/IS	[Pdt]/mM	[PC]/μM	Avg. TTN	SD TTN	Avg. Yield [%]	SD Yield [%]
1	867.9	1032.7	0.840	1.320	1.3	970	18	26	0.5
2	822.6	976.7	0.842	1.323	1.3				
3	842.4	1034.3	0.814	1.280	1.3				

Selectivity analysis for P411-TEA-5274-catalyzed amination of **2.1a** (5 mM), OD_{600} = 30 (HPLC-MS was used to identify the retention time of products based on the single ion mass peak (M + 1)):

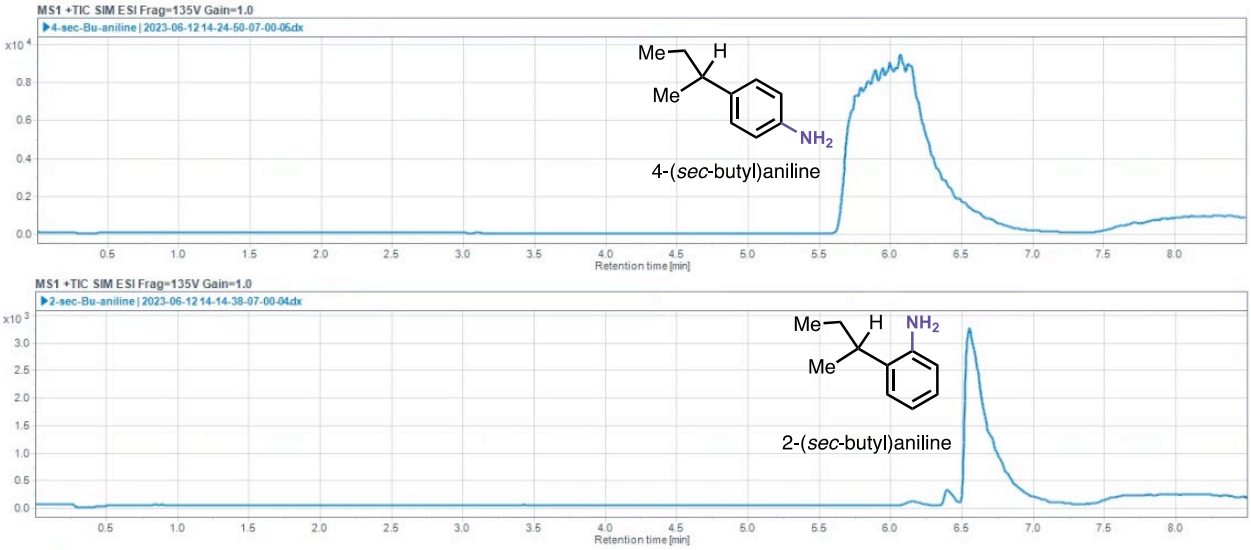

P411-TEA-5274-catalyzed amination (regioselectivity (**2.3a**: others) >99:1):

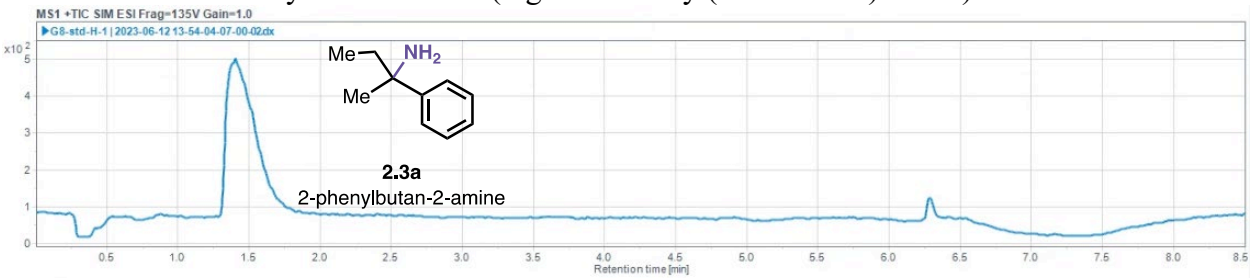

2-(*p*-tolyl)propan-2-amine (2.3b)

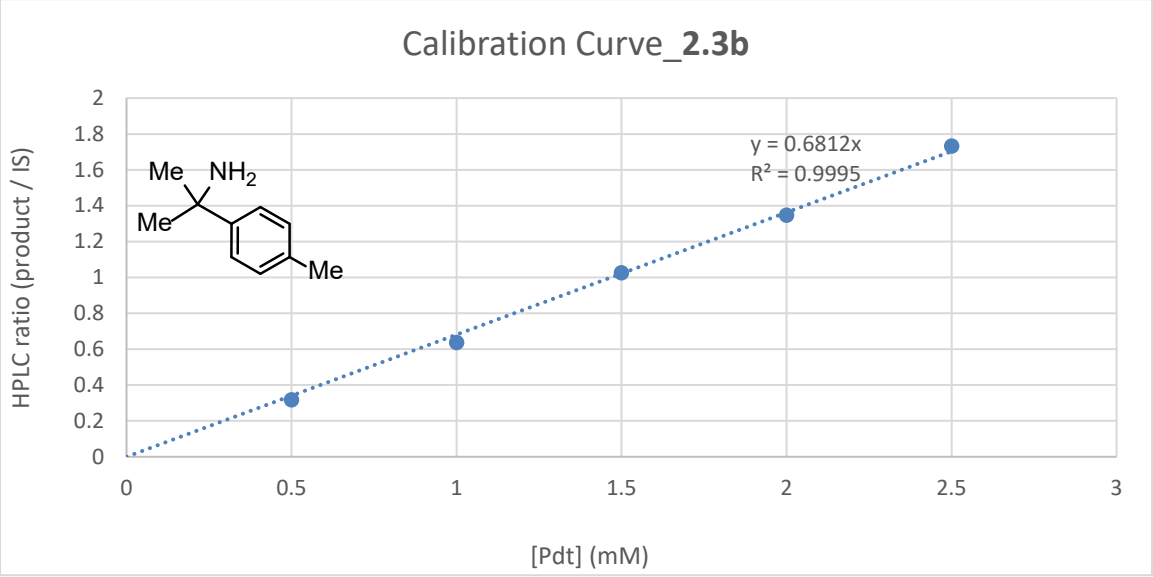

Data analysis for P411-TEA-5274-catalyzed amination of **2.1b** (5 mM), OD_{600} = 30.

Entry	Pdt	IS	Pdt/IS	[Pdt]/mM	[PC]/μM	Avg. TTN	SD TTN	Avg. Yield [%]	SD Yield [%]
1	222.5	1036.3	0.215	0.315	1.9	180	12	6.8	0.4
2	242.7	1027.4	0.236	0.347	1.9				
3	254.7	1044.9	0.244	0.358	1.9				

2-(*p*-tolyl)butan-2-amine (2.3c)

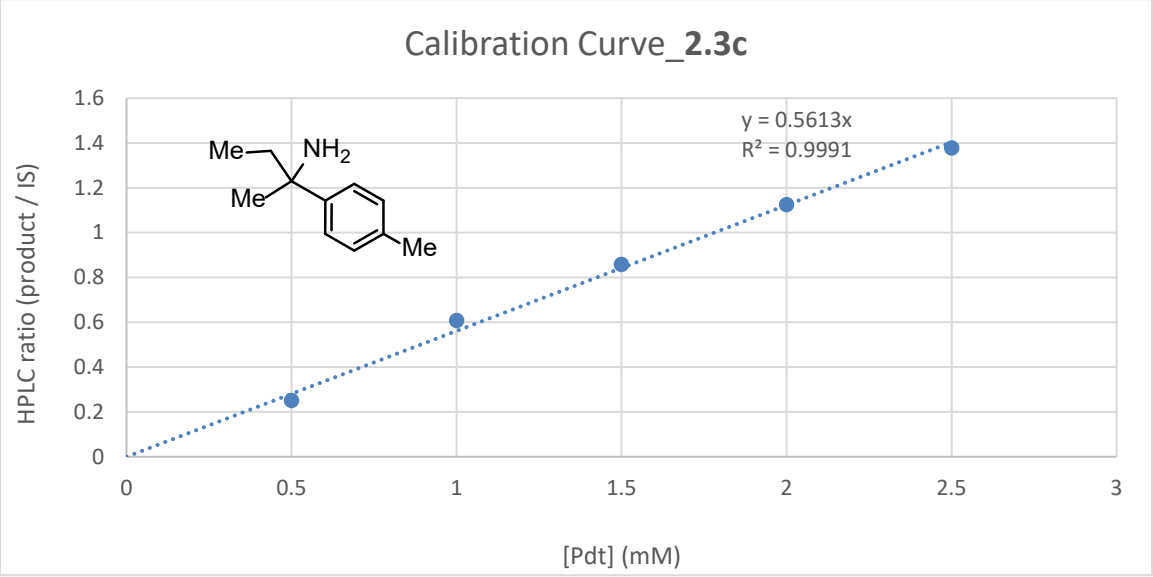

Data analysis for P411-TEA-5274-catalyzed amination of **2.1c** (5 mM), OD_{600} = 30.

Entry	Pdt	IS	Pdt/IS	[Pdt]/mM	[PC]/µM	Avg. TTN	SD TTN	Avg. Yield [%]	SD Yield [%]
1	242.0	986.2	0.245	0.437	1.3	310	10	8.4	0.3
2	229.0	990.7	0.231	0.412	1.3				
3	226.5	965.3	0.235	0.418	1.3				

2-(*m*-tolyl)butan-2-amine (2.3d)

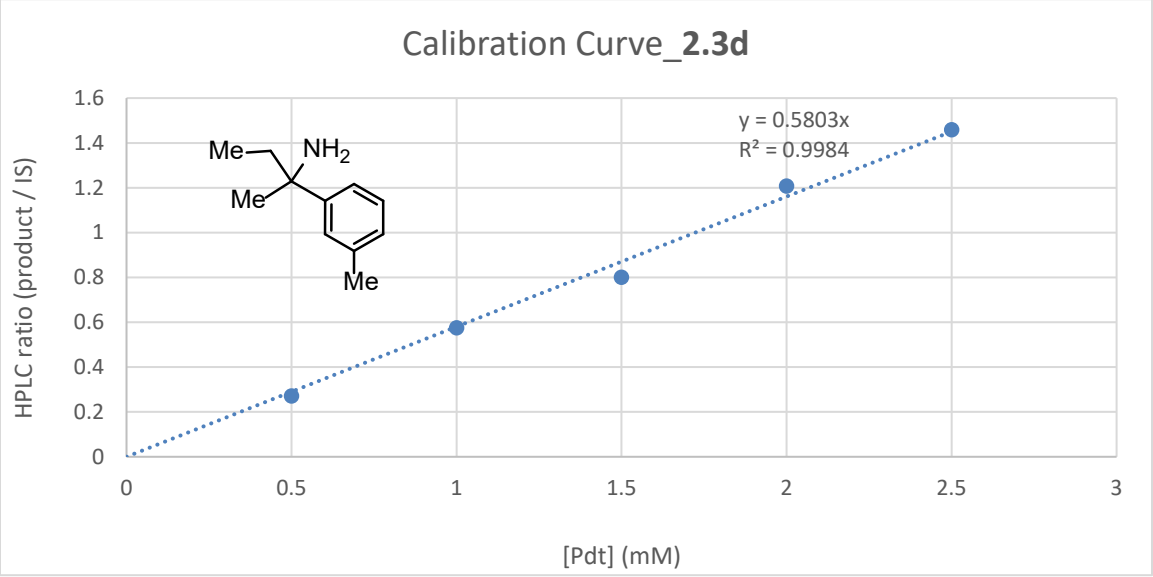

Data analysis for P411-TEA-5274-catalyzed amination of **2.1d** (5 mM), OD_{600} = 30.

Entry	Pdt	IS	Pdt/IS	[Pdt]/mM	[PC]/μM	Avg. TTN	SD TTN	Avg. Yield [%]	SD Yield [%]
1	657.7	920.5	0.715	1.231	1.3	860	57	23	1.5
2	639.0	962.1	0.664	1.145	1.3				
3	601.4	960.8	0.626	1.079	1.3				

2-(4-methoxyphenyl)butan-2-amine (2.3f)

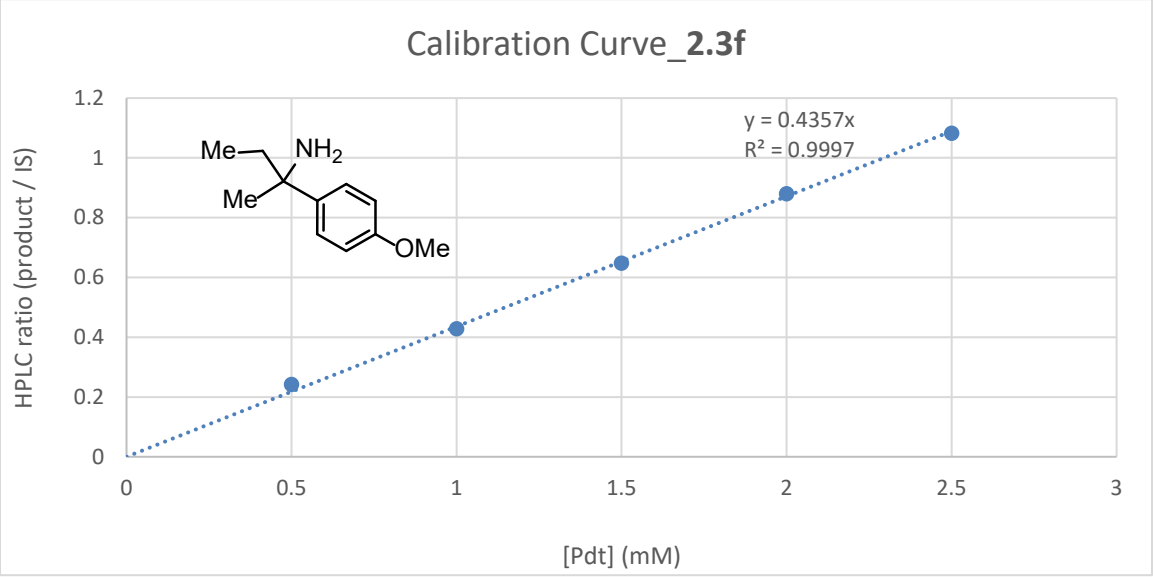

Data analysis for P411-TEA-5274-catalyzed amination of (*rac*)-**2.1f** (5 mM), OD_{600} = 30.

Entry	Pdt	IS	Pdt/IS	[Pdt]/mM	[PC]/μM	Avg. TTN	SD TTN	Avg. Yield [%]	SD Yield [%]
1	76.9	961.2	0.080	0.184	1.3	110	30	2.9	0.8
2	64.0	996.6	0.064	0.147	1.3				
3	41.4	913.1	0.045	0.104	1.3				

Data analysis for P411-TEA-5274-catalyzed amination of (*S*)-**2.1f** (5 mM), OD_{600} = 30.

Entry	Pdt	IS	Pdt/IS	[Pdt]/mM	[PC]/μM	Avg. TTN	SD TTN	Avg. Yield [%]	SD Yield [%]
1	14.6	1023.8	0.014	0.033	1.3	26	2	0.7	0.0
2	15.5	1043.1	0.015	0.034	1.3				
3	16.4	1006.9	0.016	0.037	1.3				

Data analysis for P411-TEA-5274-catalyzed amination of (*R*)-**2.1f** (5 mM), OD_{600} = 30.

Entry	Pdt	IS	Pdt/IS	[Pdt]/mM	[PC]/μM	Avg. TTN	SD TTN	Avg. Yield [%]	SD Yield [%]
1	250.2	1052.8	0.238	0.545	1.3	420	29	11	0.8
2	261.4	990.0	0.264	0.606	1.3				
3	227.9	980.0	0.233	0.534	1.3				

2-(4-fluorophenyl)butan-2-amine (2.3g)

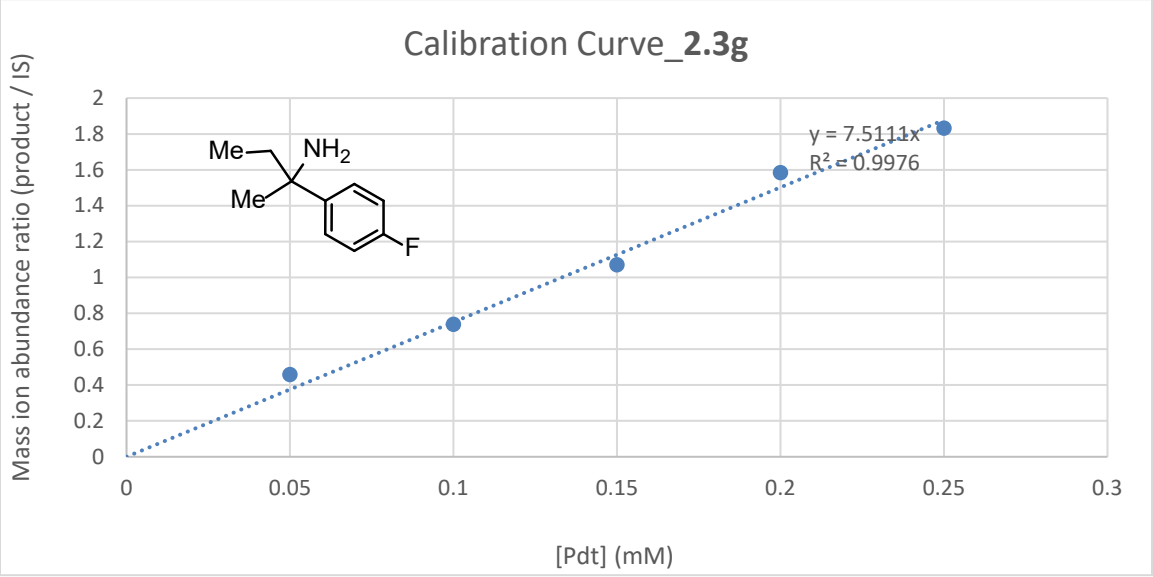

Data analysis for P411-TEA-5274-catalyzed amination of **2.1g** (5 mM), OD_{600} = 30.

Entry	Pdt	IS	Pdt/IS	[Pdt]/mM	[PC]/μM	Avg. TTN	SD TTN	Avg. Yield [%]	SD Yield [%]
1	815.0	1002.7	0.813	0.108	1.5	73	1	2.1	0.0
2	826.4	1028.1	0.804	0.107	1.5				
3	803.5	1025.0	0.784	0.104	1.5				

2-phenylpropan-2-amine (2.3h)

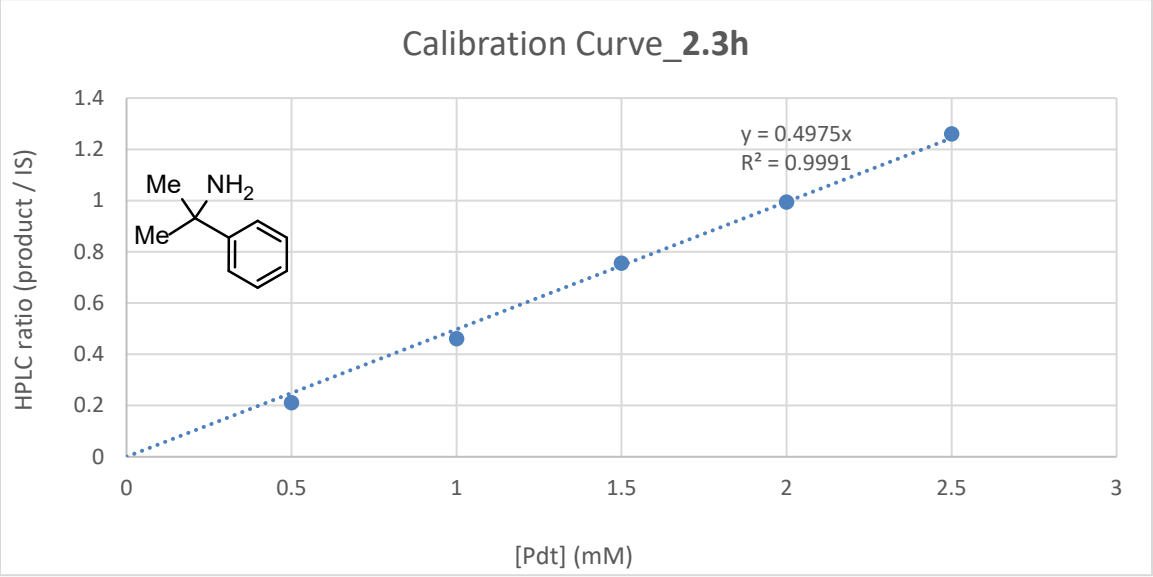

Data analysis for P411-TEA-5274-catalyzed amination of **2.1h** (5 mM), OD_{600} = 30.

Entry	Pdt	IS	Pdt/IS	[Pdt]/mM	[PC]/μM	Avg. TTN	SD TTN	Avg. Yield [%]	SD Yield [%]
1	306.8	1017.8	0.301	0.606	1.9	300	18	11	0.7
2	280.6	1033.8	0.271	0.546	1.9				
3	280.1	1025.1	0.273	0.549	1.9				

2-(pyridin-2-yl)butan-2-amine (2.3i)

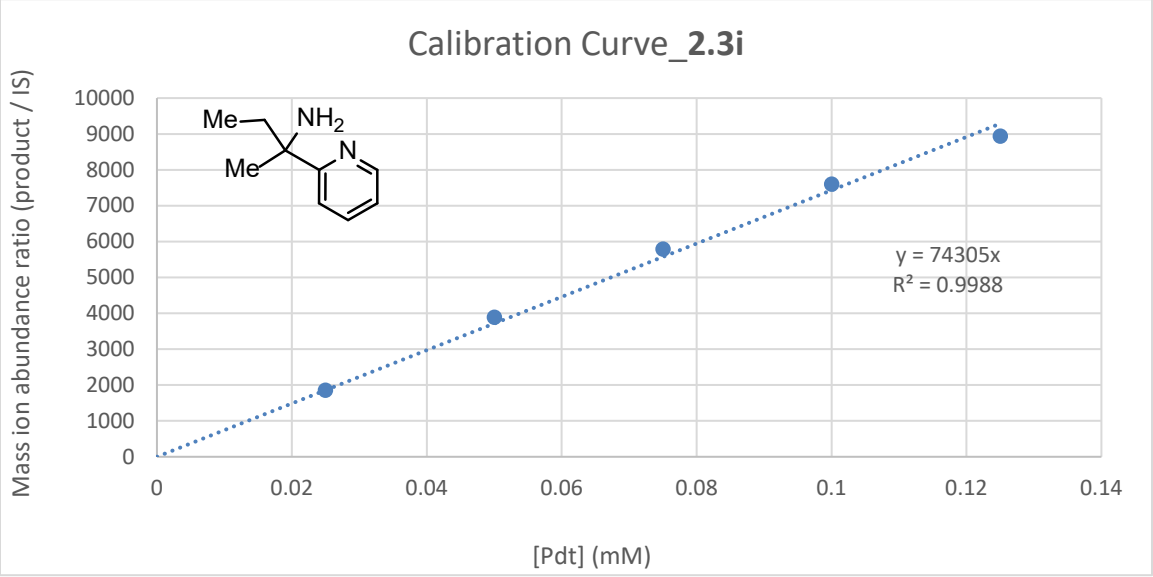

Data analysis for P411-TEA-5274-catalyzed amination of **2.1i** (5 mM), OD_{600} = 30.

Entry	Pdt	IS	Pdt/IS	[Pdt]/mM	[PC]/μM	Avg. TTN	SD TTN	Avg. Yield [%]	SD Yield [%]
1	2240663	395.5	5665.39	0.076	1.3	52	4	1.4	0.1
2	1955600	397.0	4925.95	0.066	1.3				
3	1943657	396.3	4904.51	0.066	1.3				

2-(thiophen-2-yl)butan-2-amine (2.3j)

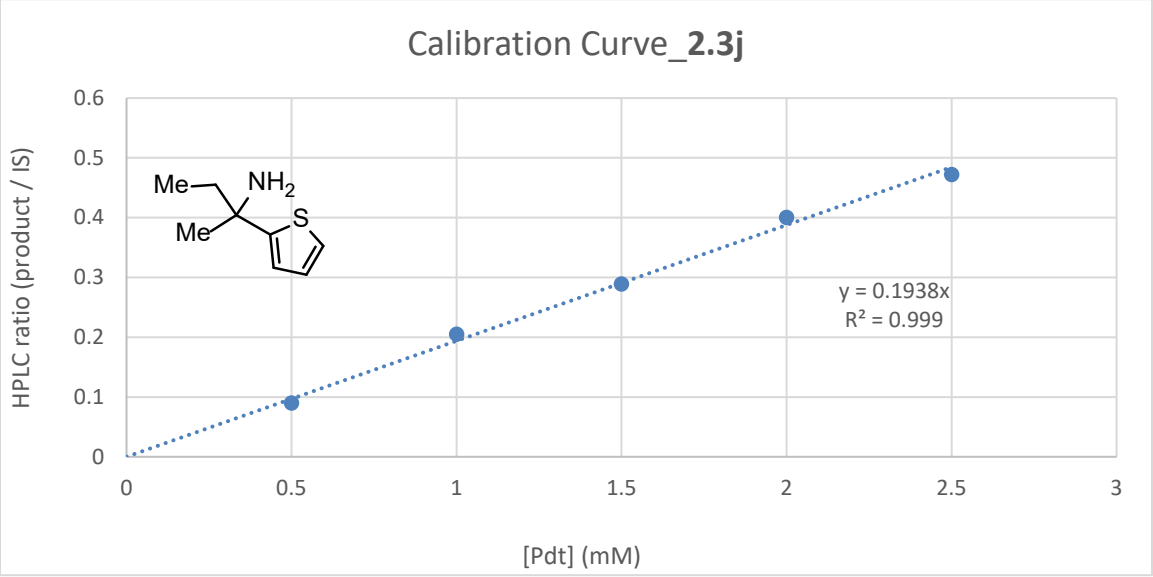

Data analysis for P411-TEA-5274-catalyzed amination of **2.1j** (5 mM), OD_{600} = 30.

Entry	Pdt	IS	Pdt/IS	[Pdt]/mM	[PC]/μM	Avg. TTN	SD TTN	Avg. Yield [%]	SD Yield [%]
1	122.4	1025.3	0.119	0.616	1.5	420	21	12	0.6
2	108.2	960.3	0.110	0.581	1.5				
3	122.8	988.9	0.124	0.641	1.5				

(*E*)-3-methyl-1-phenylpent-1-en-3-amine (2.3k)

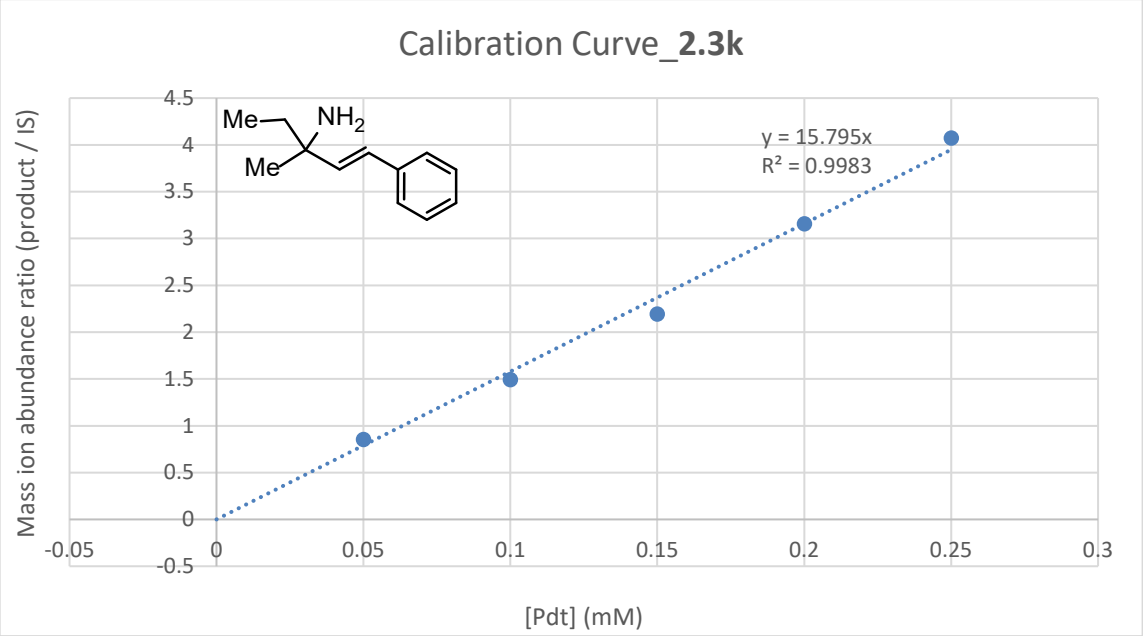

Data analysis for P411-TEA-5274-catalyzed amination of **2.1k** (5 mM), OD_{600} = 30.

Entry	Pdt	IS	Pdt/IS	[Pdt]/mM	[PC]/μM	Avg. TTN	SD TTN	Avg. Yield [%]	SD Yield [%]
1	1349.5	1072.8	1.258	0.080	1.3	70	14	1.9	0.4
2	1463.2	1059.1	1.382	0.087	1.3				
3	1844.5	1006.9	1.832	0.116	1.3				

3-methyl-1-phenylpent-1-yn-3-amine (2.3l)

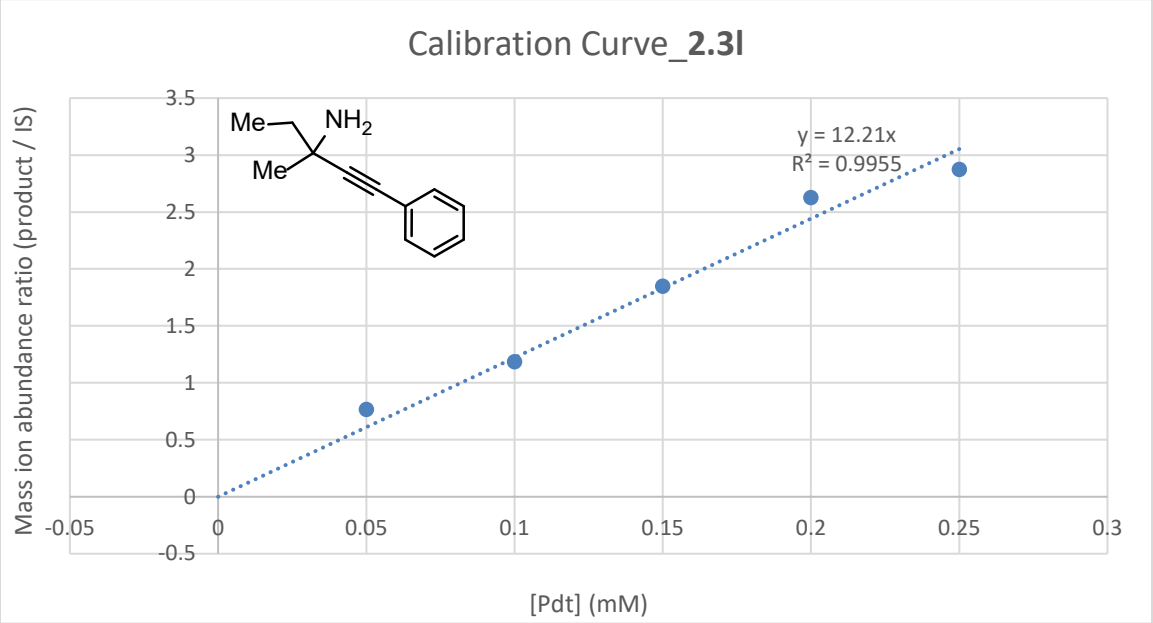

Data analysis for P411-TEA-5274-catalyzed amination of **2.1l** (5 mM), OD_{600} = 30.

Entry	Pdt	IS	Pdt/IS	[Pdt]/mM	[PC]/μM	Avg. TTN	SD TTN	Avg. Yield [%]	SD Yield [%]
1	2367.8	986.2	2.401	0.197	1.3	120	22	3.3	0.6
2	1812.7	1021.5	1.775	0.145	1.3				
3	1875.2	1043.6	1.797	0.147	1.3				

2-methyl-4-phenylbut-3-en-2-amine (2.3m)

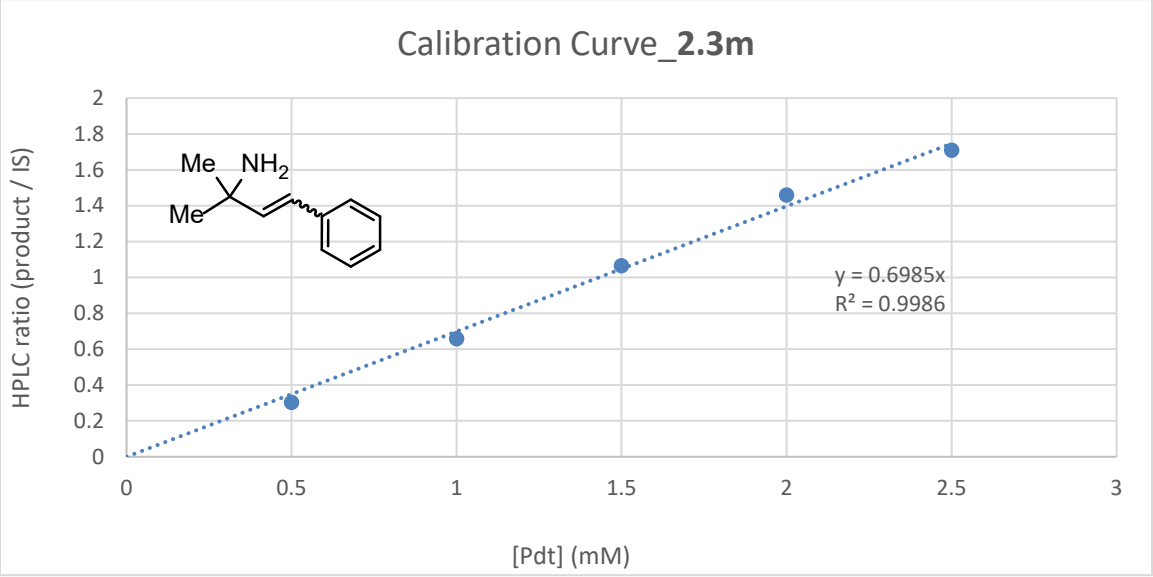

Data analysis for P411-TEA-5274-catalyzed amination of (*E*)-**2.1m** (5 mM), OD_{600} = 30.

Entry	Pdt	IS	Pdt/IS	[Pdt]/mM	[PC]/μM	Avg. TTN	SD TTN	Avg. Yield [%]	SD Yield [%]
1	2339.9	1004.4	2.330	3.335	1.5	2300	76	66	2.2
2	2419.5	1028.4	2.353	3.368	1.5				
3	2327.6	1053.7	2.209	3.162	1.5				

E/*Z* ratio (>99:1) was determined by ^{1}H NMR.

2-methyl-4-phenylbut-3-en-2-amine (2.3m)

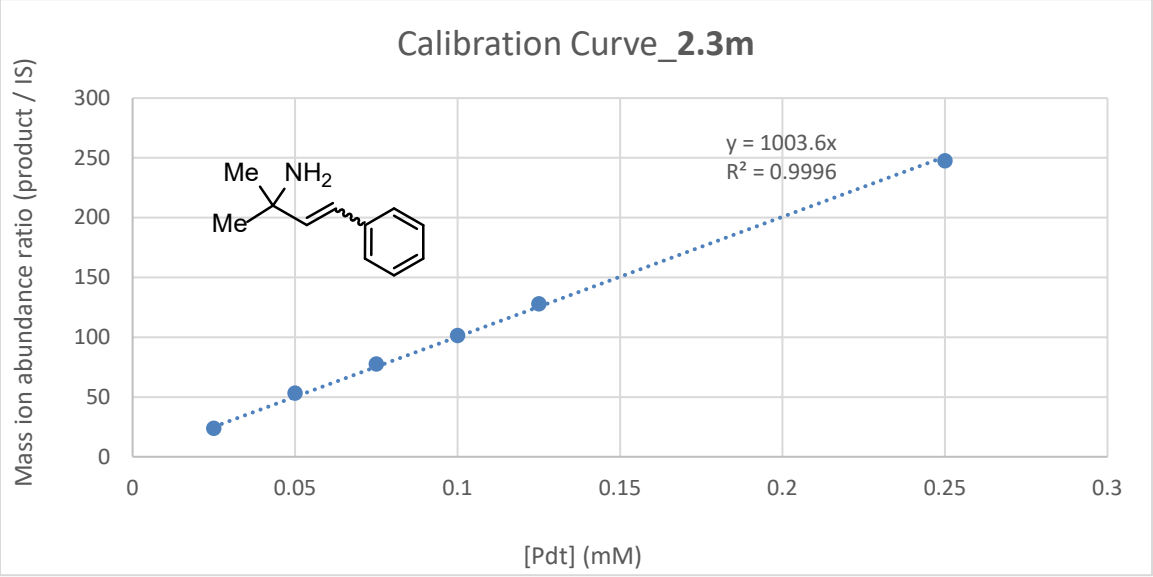

Data analysis for P411-TEA-5274-catalyzed amination of (*Z*)-**2.1m** (5 mM), OD_{600} = 30.

Entry	Pdt	IS	Pdt/IS	[Pdt]/mM	[PC]/μM	Avg. TTN	SD TTN	Avg. Yield [%]	SD Yield [%]
1	49129.3	1007.9	48.744	0.049	1.5	34	1	1.0	0.0
2	51477.0	1005.6	51.190	0.051	1.5				
3	48664.6	1017.4	47.832	0.048	1.5				

E/*Z* ratio (>99:1) was determined by ^{1}H NMR.

XIII. Enantioselectivity Determinations of *α*-Tertiary Primary Amines 3

To determine the enantiomeric excess (*ee*), primary amines were converted into benzoyl-protected amines (refer to **Experimental Methods D** for details) and subsequently analyzed using normal-phase HPLC to determine the *ee*. The absolute configuration of enzymatic product **2.3a** was determined to be *S* by comparing the elution order of the two enantiomers with a literature report, using the same elution conditions and column (Chiralpak IA),[21] and through X-ray crystallography (**2.3f**, see XVI). The assignment of the other products, **2.3c**, **2.3d**, **2.3g**, **2.3i**, **2.3j**, **2.3k**, and **2.3l**, was made by analogy. It should be noted that some of the samples exhibited retention time drifts during normal-phase HPLC analysis.

(*S*)-2-phenylbutan-2-amine (2.3a)

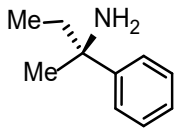

Chiral-phase HPLC conditions: Chiralpak IA, 10% *i*-PrOH in hexane, 1.0 mL/min, 25 ºC, 210 nm

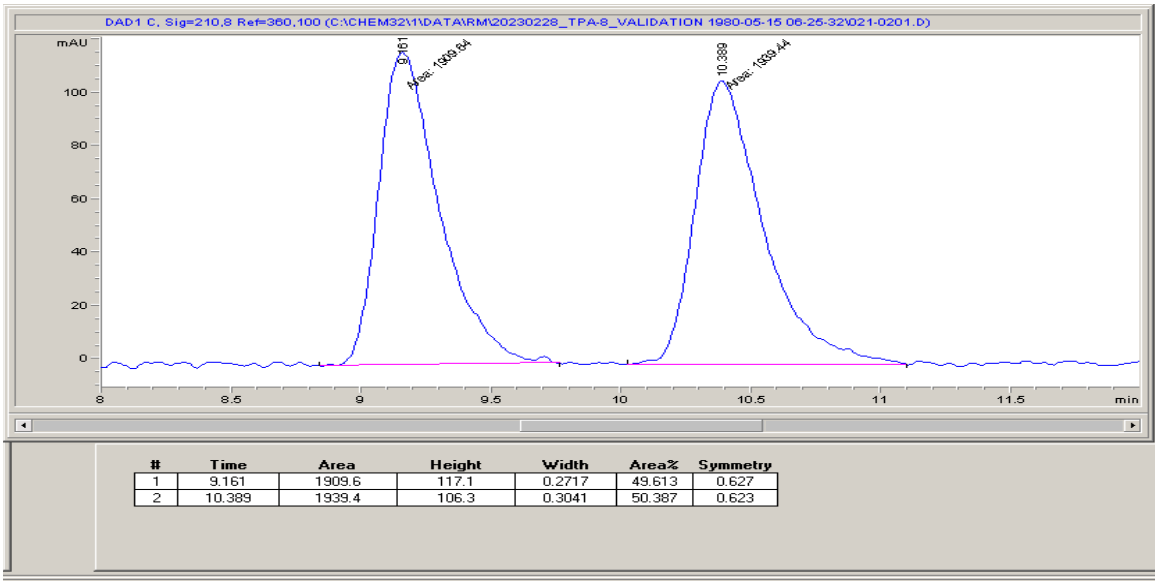

#	Time	Area	Height	Width	Area%	Symmetry
1	9.161	1909.6	117.1	0.2717	49.613	0.627
2	10.389	1939.4	106.3	0.3041	50.387	0.623

Enzymatic preparation of 2.3a with P411-TEA-5267**:** 90% *ee*

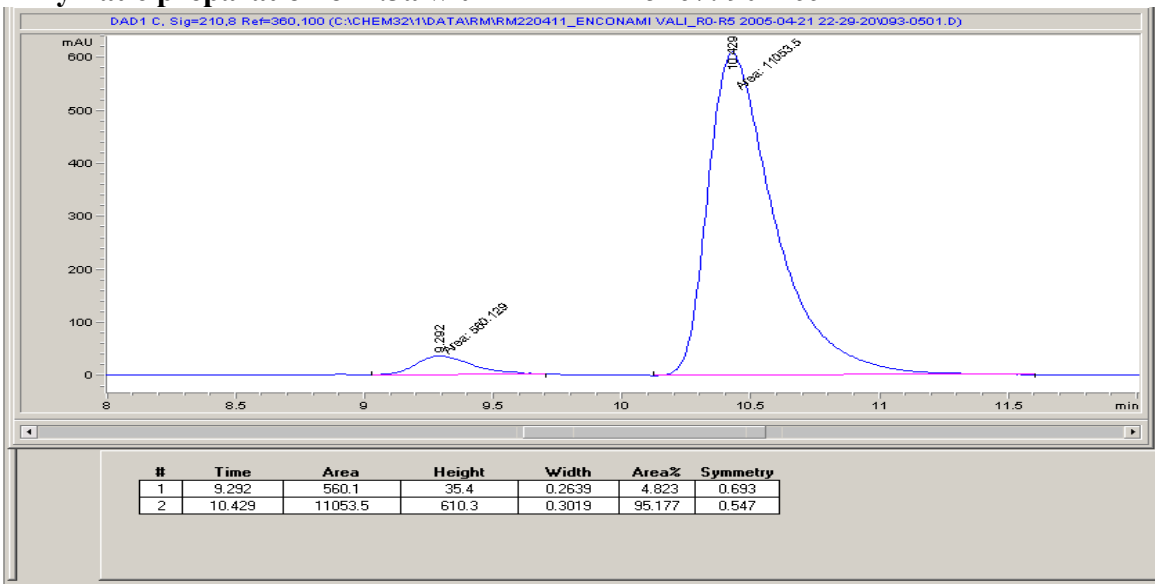

#	Time	Area	Height	Width	Area%	Symmetry
1	9.292	560.1	35.4	0.2639	4.823	0.693
2	10.429	11053.5	610.3	0.3019	95.177	0.547

Enzymatic preparation of 2.3a with P411-TEA-5274**:** 92% *ee*

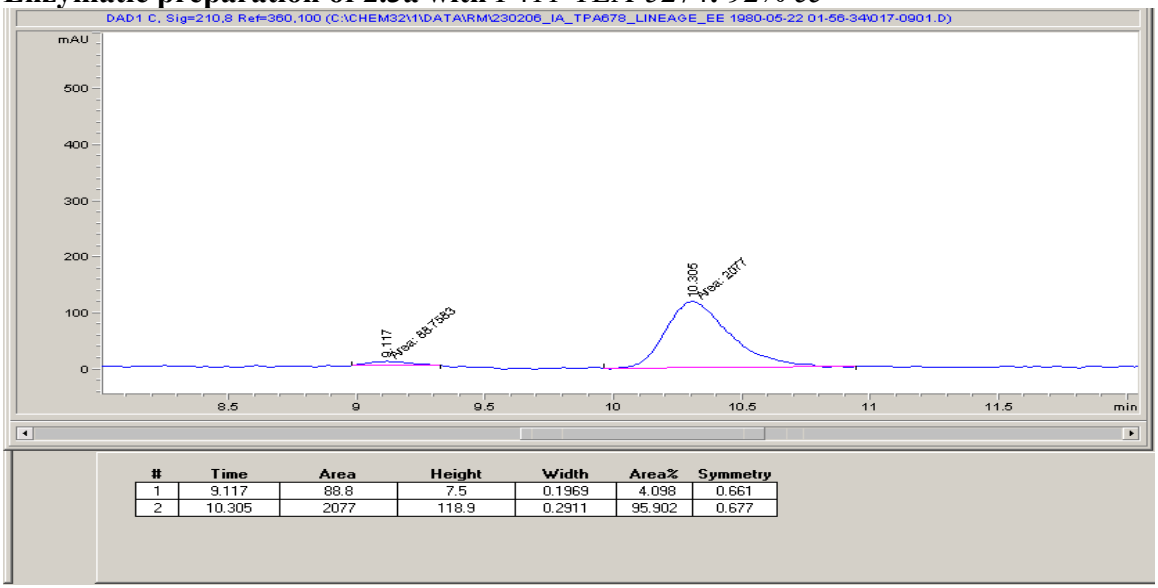

#	Time	Area	Height	Width	Area%	Symmetry
1	9.117	88.8	7.5	0.1969	4.098	0.661
2	10.305	2077	118.9	0.2911	95.902	0.677

(*S*)-2-(*p*-tolyl)butan-2-amine (2.3c)

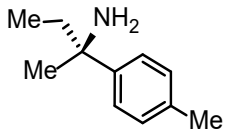

Chiral-phase HPLC conditions: Chiralpak IA, 5% *i*-PrOH in hexane, 1.0 mL/min, 25 ºC, 245 nm

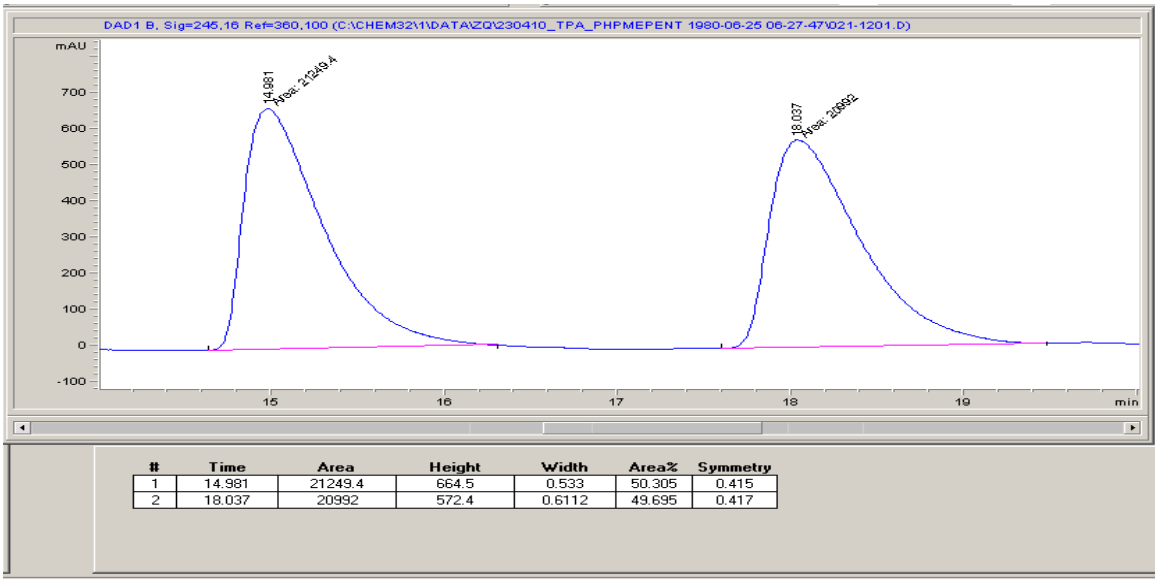

#	Time	Area	Height	Width	Area%	Symmetry
1	14.981	21249.4	664.5	0.533	50.305	0.415
2	18.037	20992	572.4	0.6112	49.695	0.417

Enzymatic preparation of 2.3c with P411-TEA-5274**:** >99% *ee*

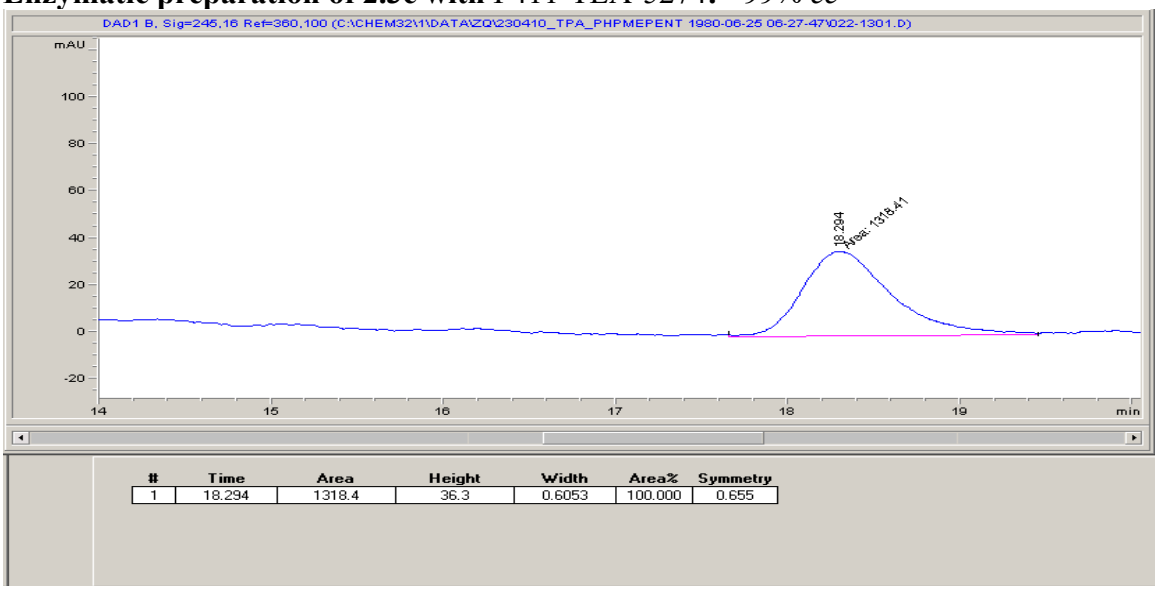

#	Time	Area	Height	Width	Area%	Symmetry
1	18.294	1318.4	36.3	0.6053	100.000	0.655

(*S*)-2-(*m*-tolyl)butan-2-amine (2.3d)

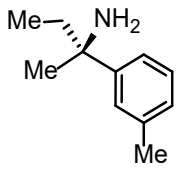

Chiral-phase HPLC conditions: Chiralpak IA, 5% *i*-PrOH in hexane, 1.0 mL/min, 25 ºC, 254 nm

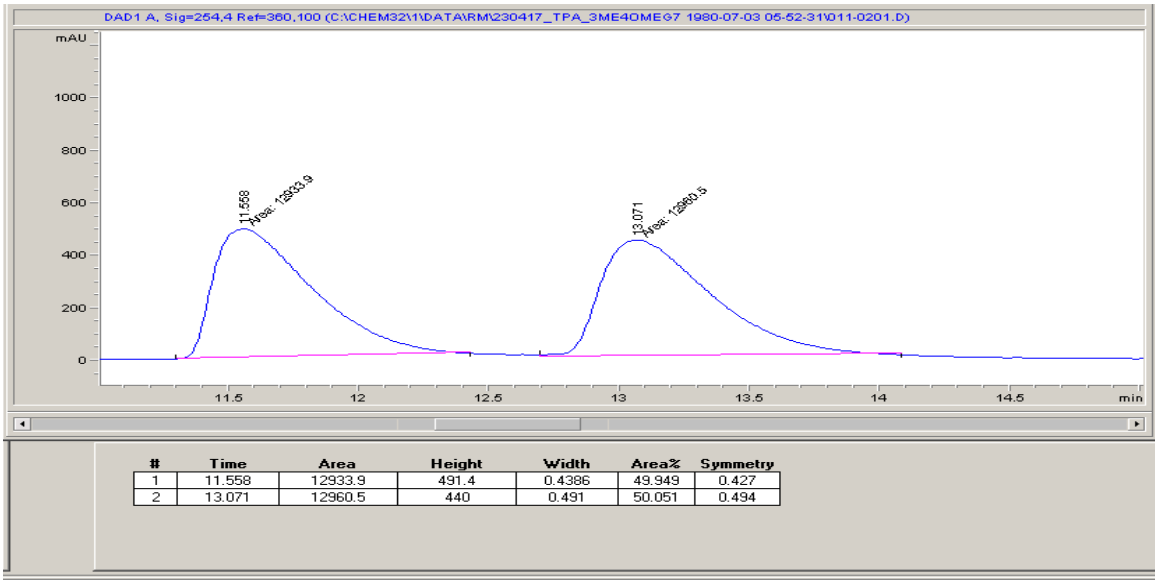

#	Time	Area	Height	Width	Area%	Symmetry
1	11.558	12933.9	491.4	0.4386	49.949	0.427
2	13.071	12960.5	440	0.491	50.051	0.494

Enzymatic preparation of 2.3d with P411-TEA-5274**:** 60% *ee*

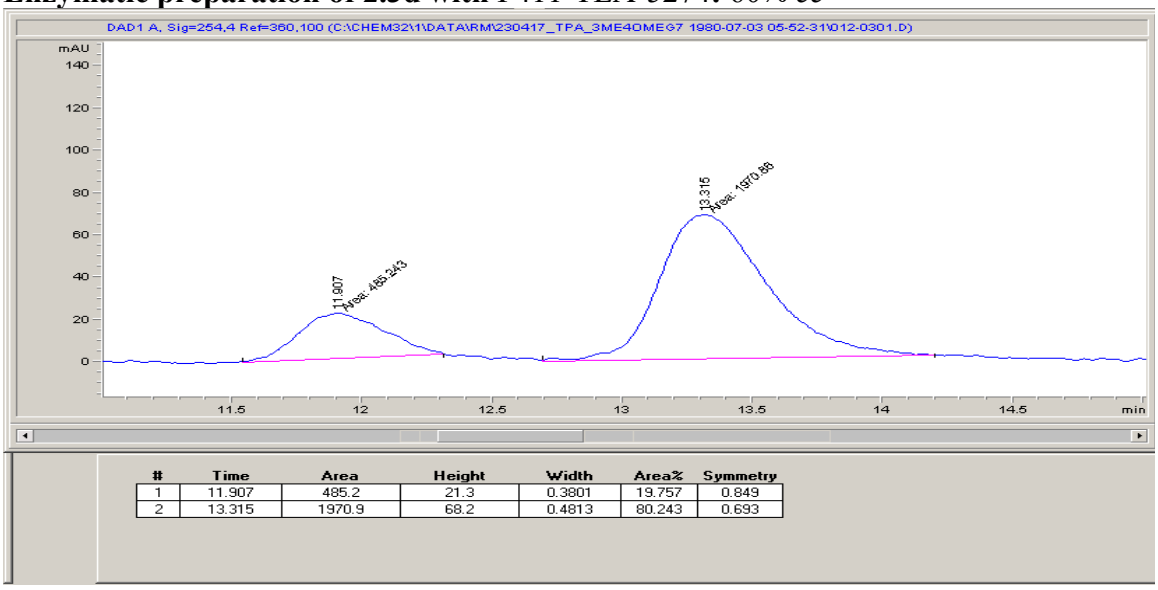

#	Time	Area	Height	Width	Area%	Symmetry
1	11.907	485.2	21.3	0.3801	19.757	0.849
2	13.315	1970.9	68.2	0.4813	80.243	0.693

(*S*)-2-(4-methoxyphenyl)butan-2-amine ((*S*)-2.3f)

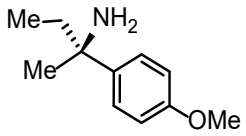

Chiral-phase HPLC conditions: Chiralpak IA, 5% *i*-PrOH in hexane, 1.0 mL/min, 25 ºC, 220 nm

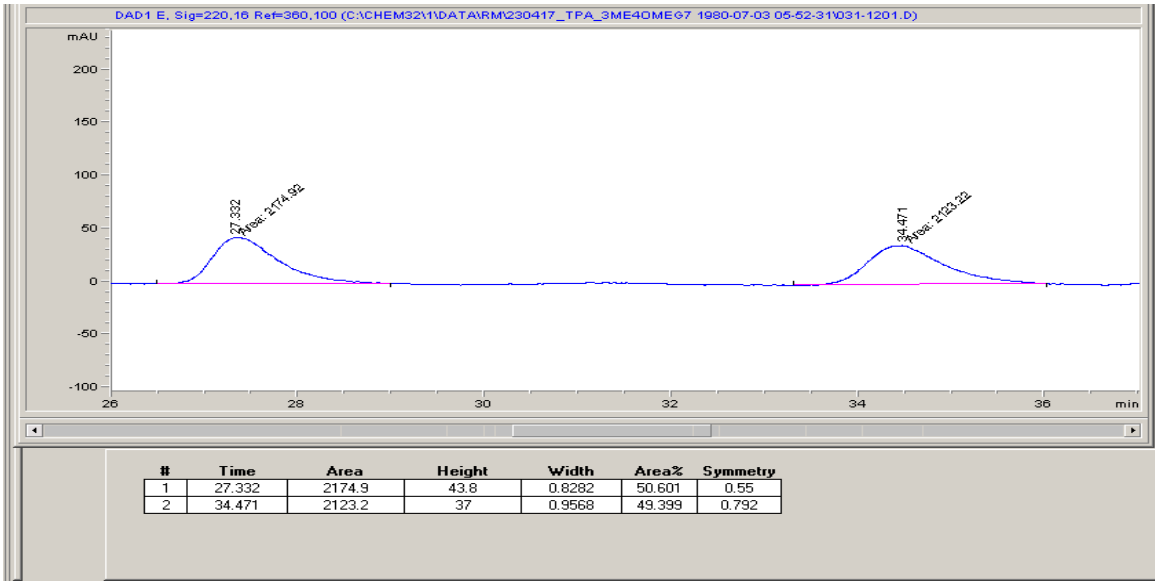

#	Time	Area	Height	Width	Area%	Symmetry
1	27.332	2174.9	43.8	0.8282	50.601	0.55
2	34.471	2123.2	37	0.9568	49.399	0.792

Enzymatic preparation of (*S*)-2.3f with P411-TEA-5274**:** >99% *ee*

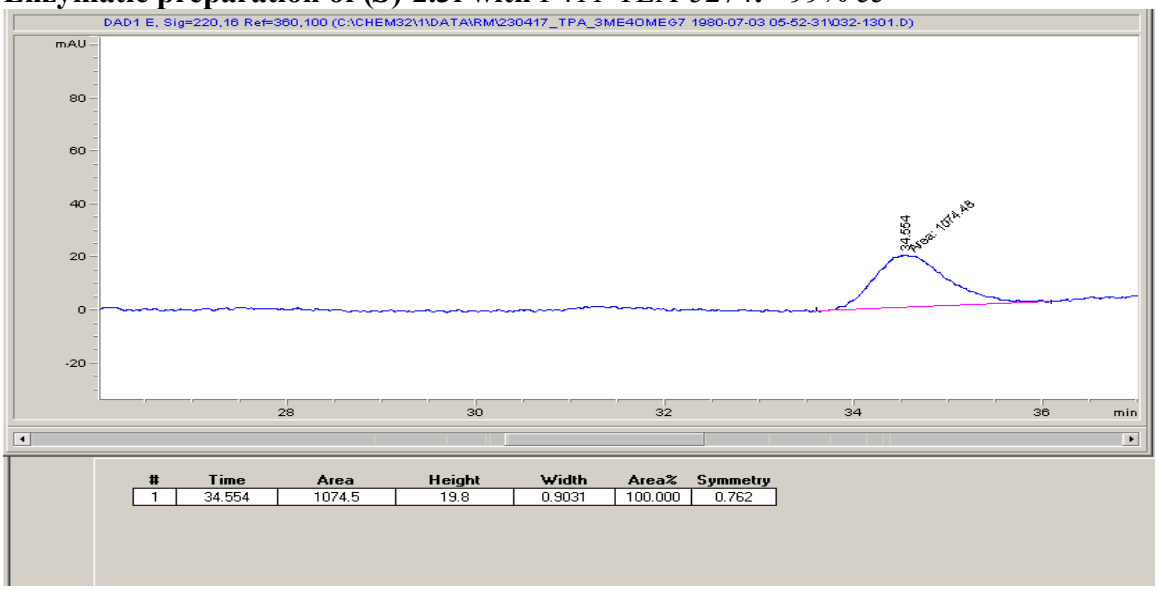

#	Time	Area	Height	Width	Area%	Symmetry
1	34.554	1074.5	19.8	0.9031	100.000	0.762

(*R*)-2-(4-methoxyphenyl)butan-2-amine ((*R*)-2.3f)

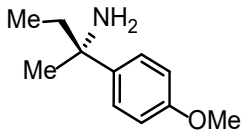

Chiral-phase HPLC conditions: Chiralpak IA, 20% *i*-PrOH in hexane, 1.0 mL/min, 25 ºC, 235 nm

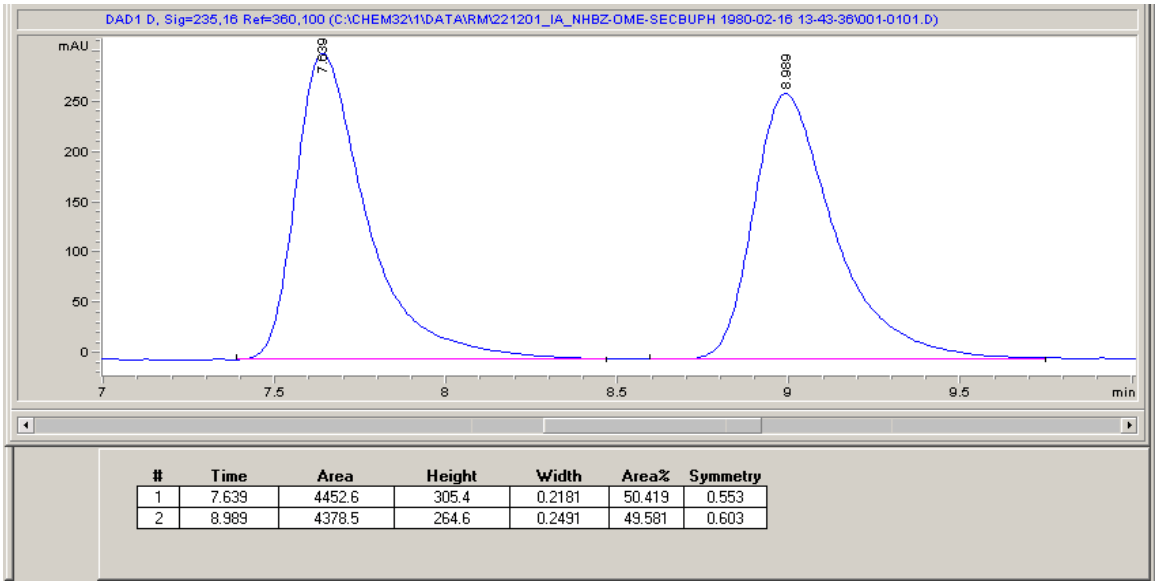

#	Time	Area	Height	Width	Area%	Symmetry
1	7.639	4452.6	305.4	0.2181	50.419	0.553
2	8.989	4378.5	264.6	0.2491	49.581	0.603

Enzymatic preparation of (*R*)-2.3f with P411-TEA-5274**: -**85% *ee*

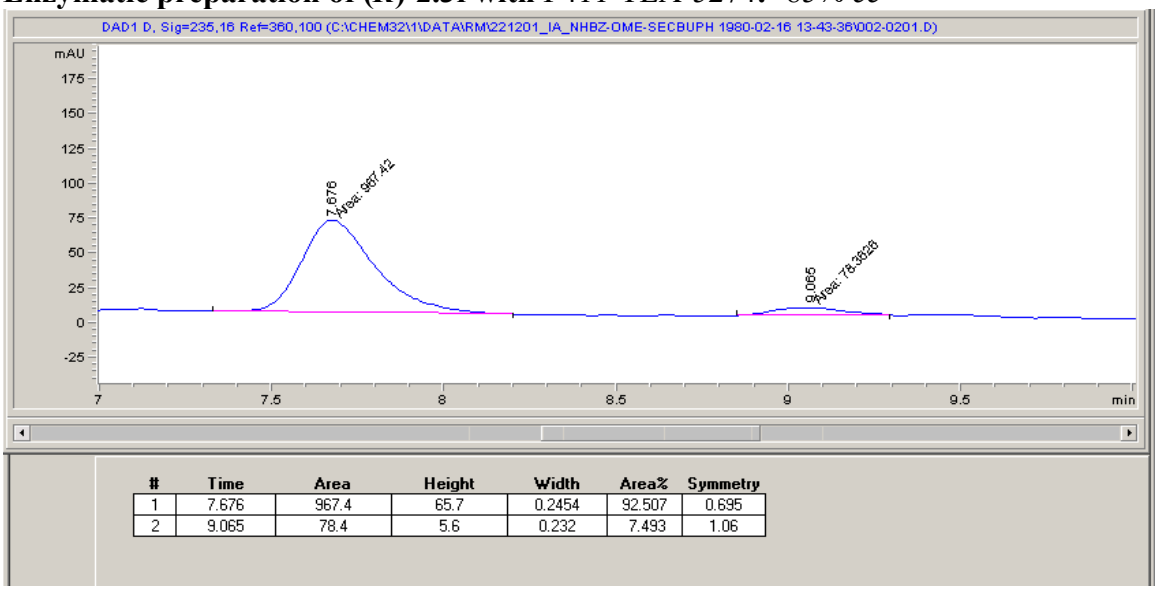

#	Time	Area	Height	Width	Area%	Symmetry
1	7.676	967.4	65.7	0.2454	92.507	0.695
2	9.065	78.4	5.6	0.232	7.493	1.06

(*S*)-2-(4-fluorophenyl)butan-2-amine (2.3g)

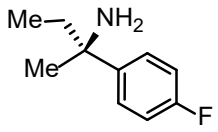

Chiral-phase HPLC conditions: Chiralpak IA, 7% *i*-PrOH in hexane, 1.0 mL/min, 25 ºC, 235 nm

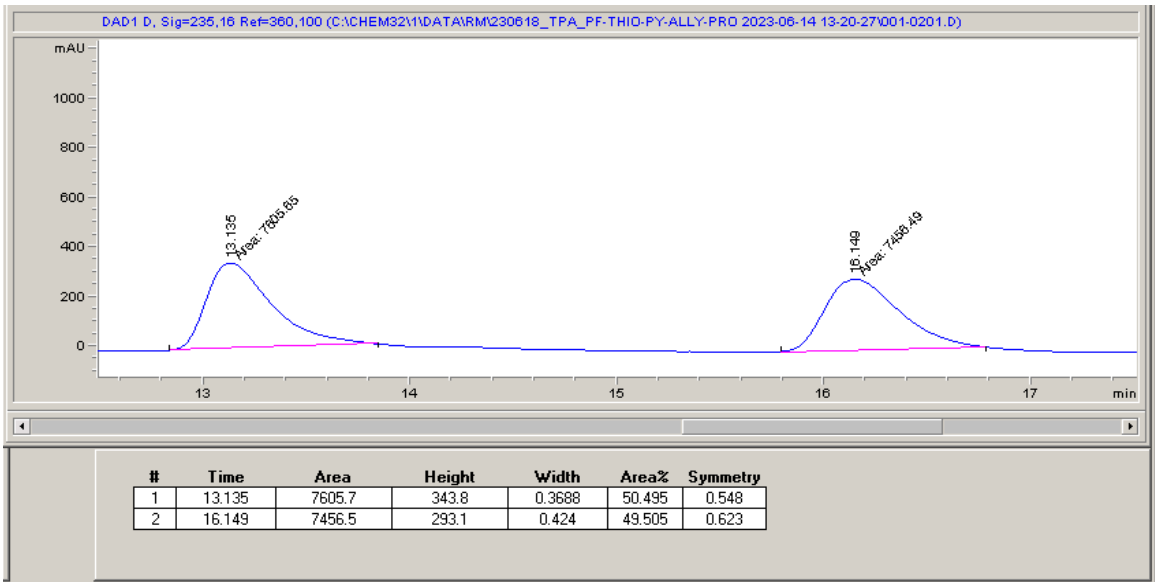

#	Time	Area	Height	Width	Area%	Symmetry
1	13.135	7605.7	343.8	0.3688	50.495	0.548
2	16.149	7456.5	293.1	0.424	49.505	0.623

Enzymatic preparation of 2.3g with P411-TEA-5274**:** >99% *ee*

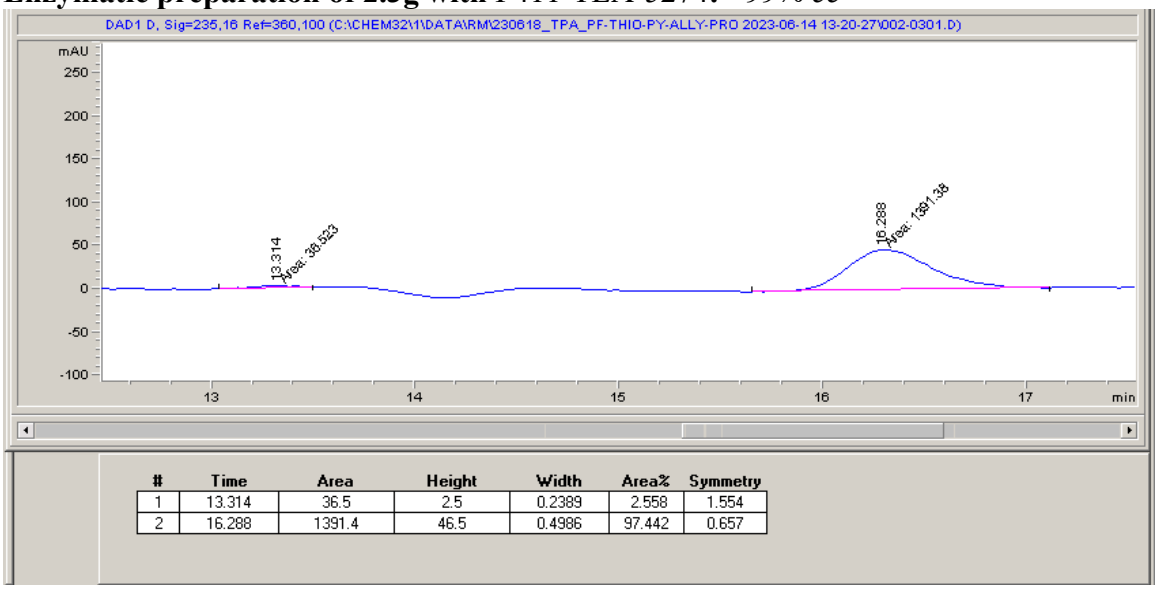

#	Time	Area	Height	Width	Area%	Symmetry
1	13.314	36.5	2.5	0.2389	2.558	1.554
2	16.288	1391.4	46.5	0.4986	97.442	0.657

(*S*)-2-(pyridin-2-yl)butan-2-amine (2.3i)

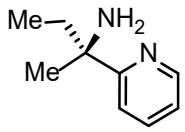

Chiral GC conditions: Agilent J&W CycloSil-B column. Ramp from 50 ºC to 150 ºC at 10 ºC / min, hold at 150 ºC for 12 min. Then ramp to 200 ºC at 10 ºC / min, and hold at 200 ºC for 8 min.

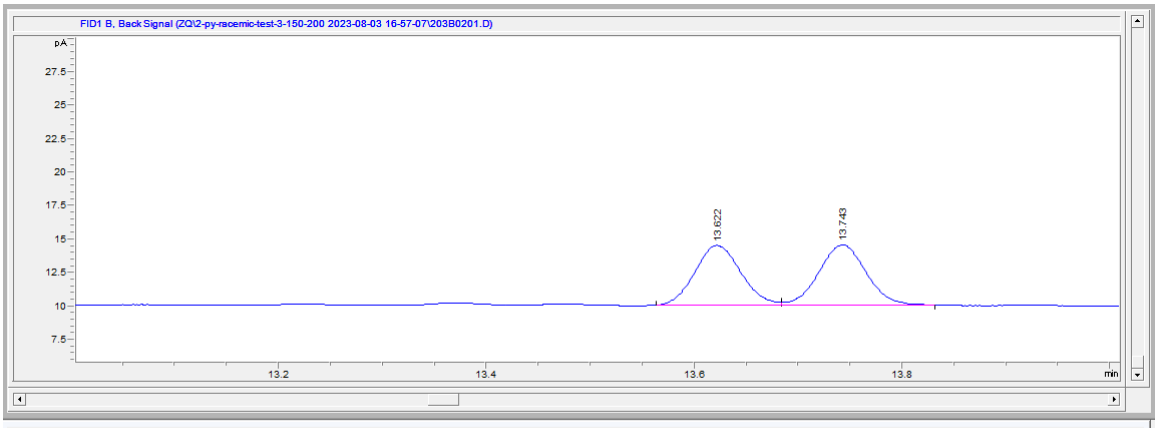

#	Time	Area	Height	Width	Area%	Symmetry
1	13.622	13.8	4.5	0.048	48.920	0.885
2	13.743	14.4	4.5	0.0502	51.080	0.959

Enzymatic preparation of 2.3i with P411-TEA-5274**:** 82% *ee*

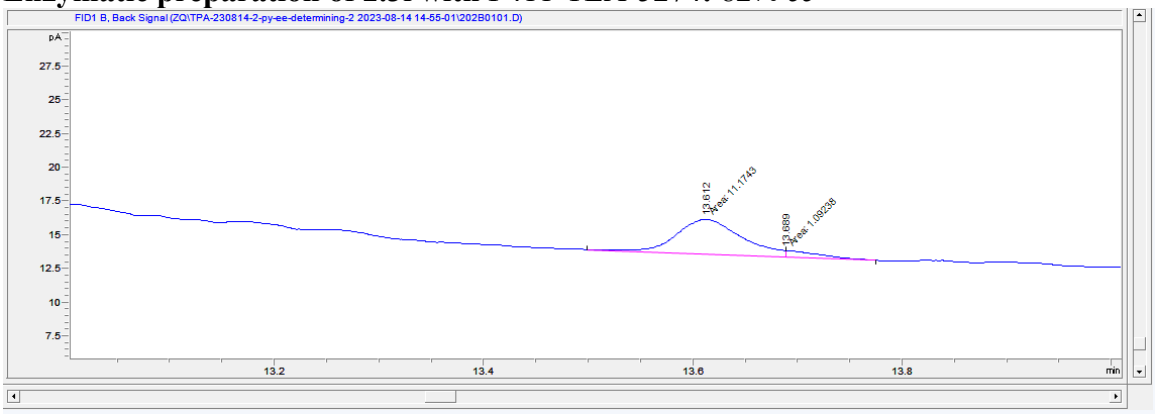

#	Time	Area	Height	Width	Area%	Symmetry
1	13.612	11.2	2.6	0.0728	91.095	0
2	13.689	1.1	4.8E-1	0.0382	8.905	0

(*S*)-2-(thiophen-2-yl)butan-2-amine (2.3j)

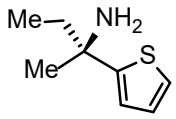

Chiral-phase HPLC conditions: Chiralpak IA, 5% *i*-PrOH in hexane, 1.0 mL/min, 25 ºC, 254 nm

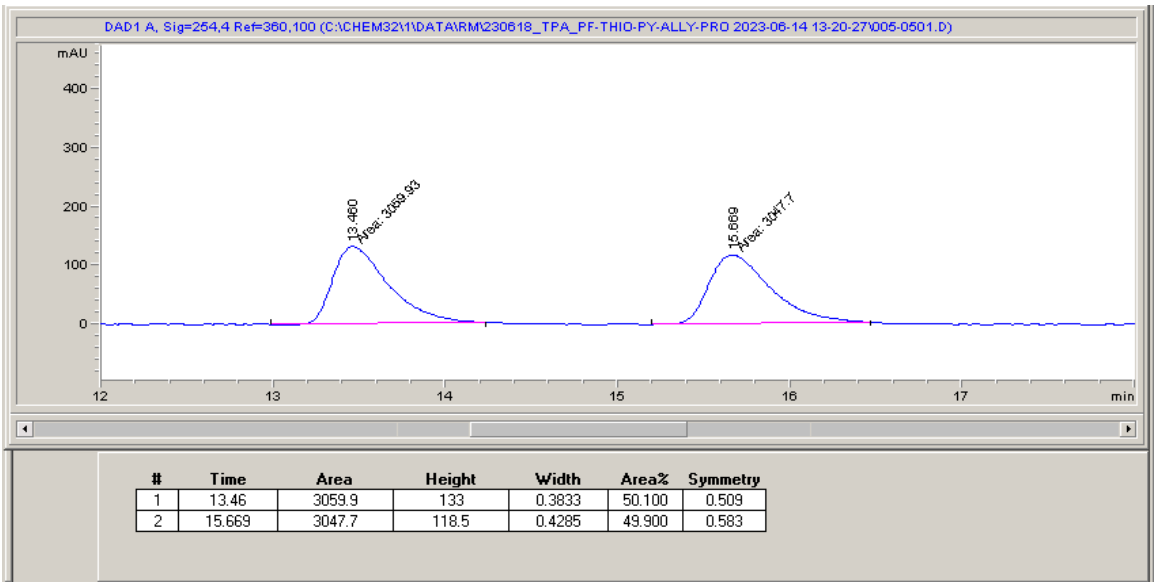

#	Time	Area	Height	Width	Area%	Symmetry
1	13.46	3059.9	133	0.3833	50.100	0.509
2	15.669	3047.7	118.5	0.4285	49.900	0.583

Enzymatic preparation of 2.3j with P411-TEA-5274**:** 92% *ee*

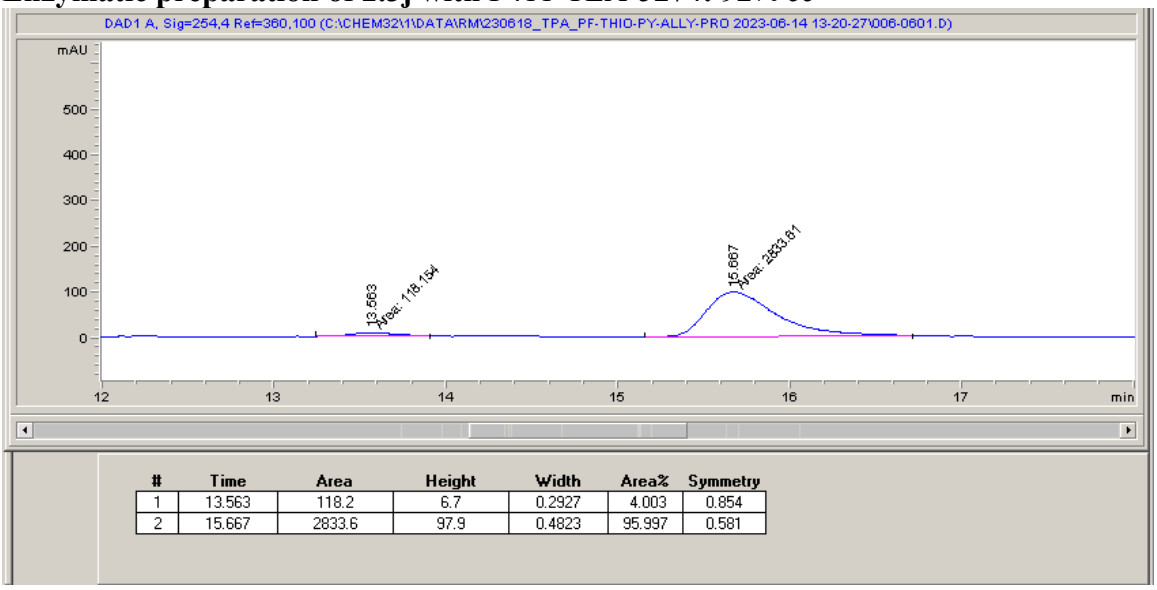

#	Time	Area	Height	Width	Area%	Symmetry
1	13.563	118.2	6.7	0.2927	4.003	0.854
2	15.667	2833.6	97.9	0.4823	95.997	0.581

(*S*,*E*)-3-methyl-1-phenylpent-1-en-3-amine (2.3k)

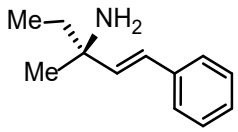

Chiral-phase HPLC conditions: Chiralpak IA, 5% *i*-PrOH in hexane, 1.0 mL/min, 25 ºC, 254 nm

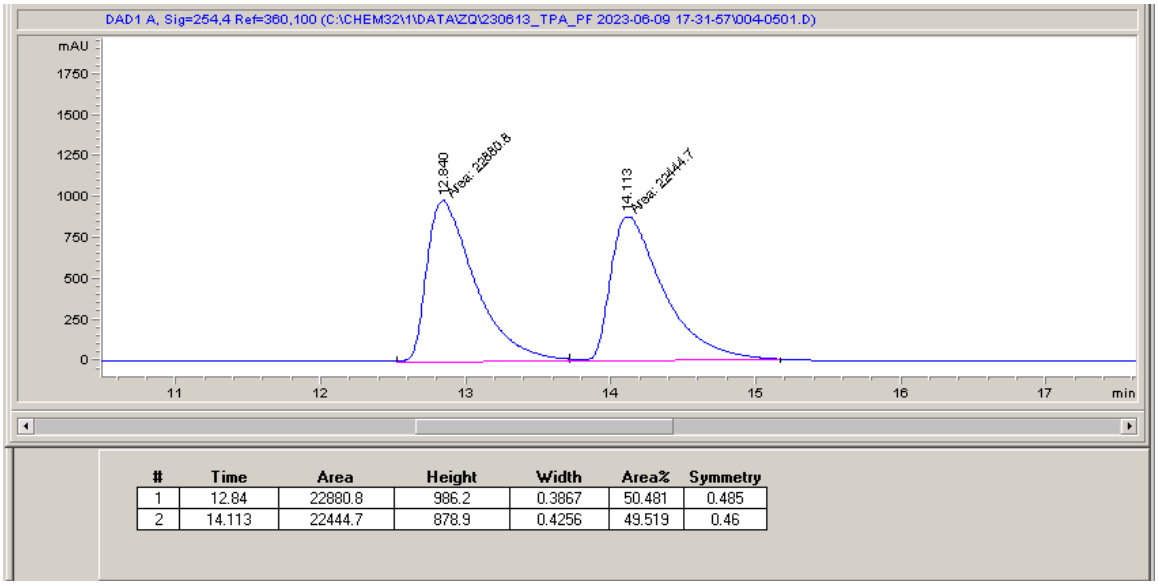

#	Time	Area	Height	Width	Area%	Symmetry
1	12.84	22880.8	986.2	0.3867	50.481	0.485
2	14.113	22444.7	878.9	0.4256	49.519	0.46

Enzymatic preparation of 2.3k with P411-TEA-5274**:** 90% *ee*

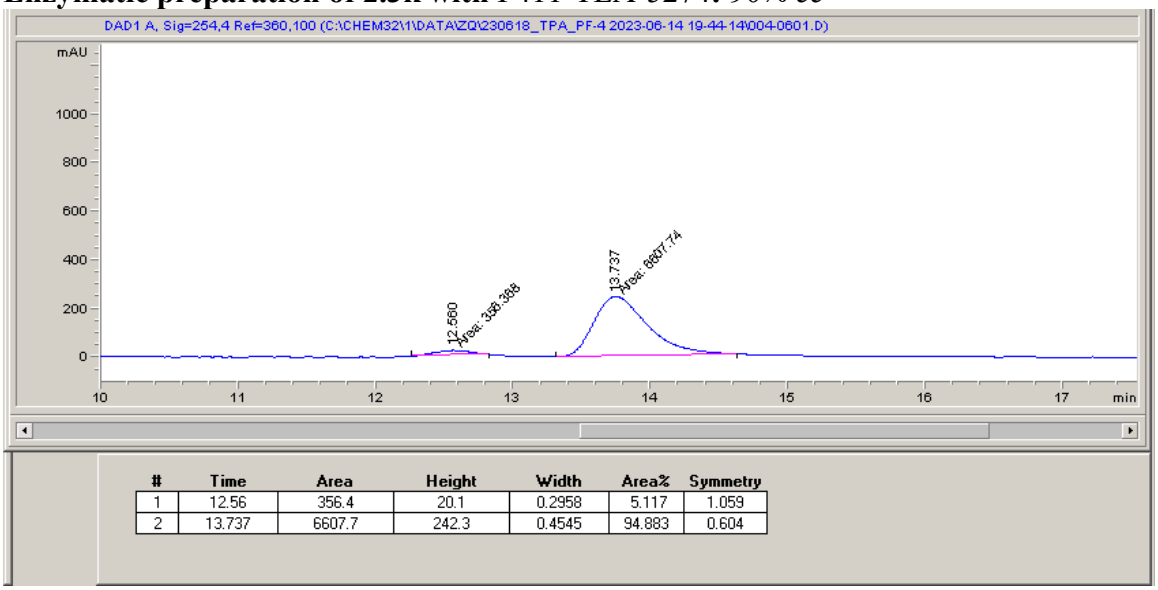

#	Time	Area	Height	Width	Area%	Symmetry
1	12.56	356.4	20.1	0.2958	5.117	1.059
2	13.737	6607.7	242.3	0.4545	94.883	0.604

(*S*)-3-methyl-1-phenylpent-1-yn-3-amine (2.3l)

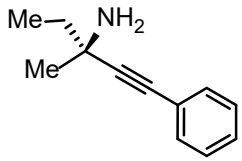

Chiral-phase HPLC conditions: Chiralpak OJH, 2% *i*-PrOH in hexane, 1.0 mL/min, 25 ºC, 245 nm

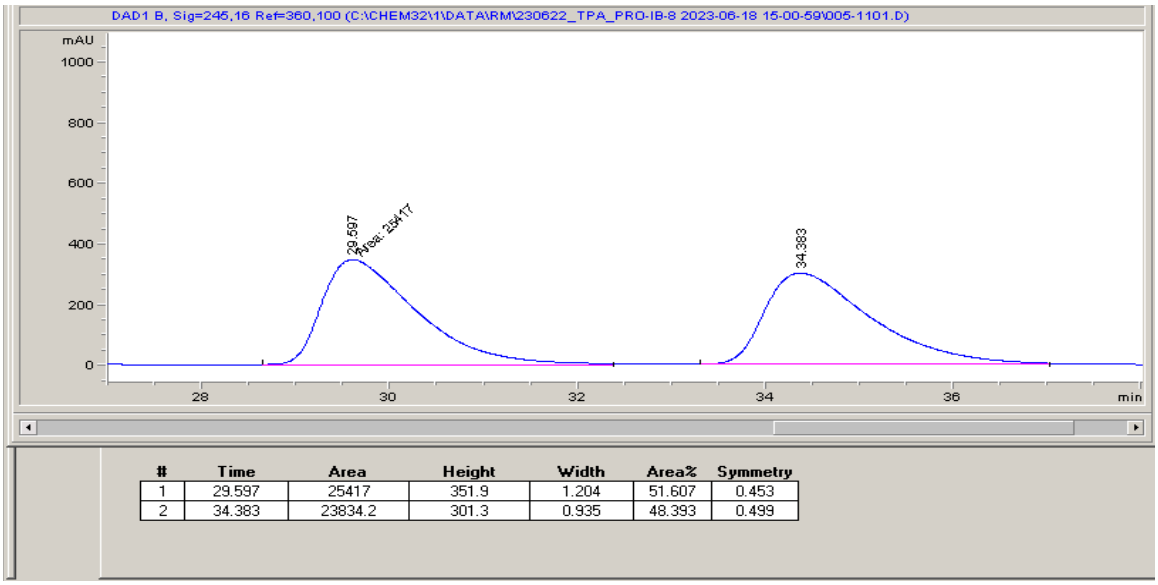

#	Time	Area	Height	Width	Area%	Symmetry
1	29.597	25417	351.9	1.204	51.607	0.453
2	34.383	23834.2	301.3	0.935	48.393	0.499

Enzymatic preparation of 2.3l with P411-TEA-5274**:** 67% *ee*

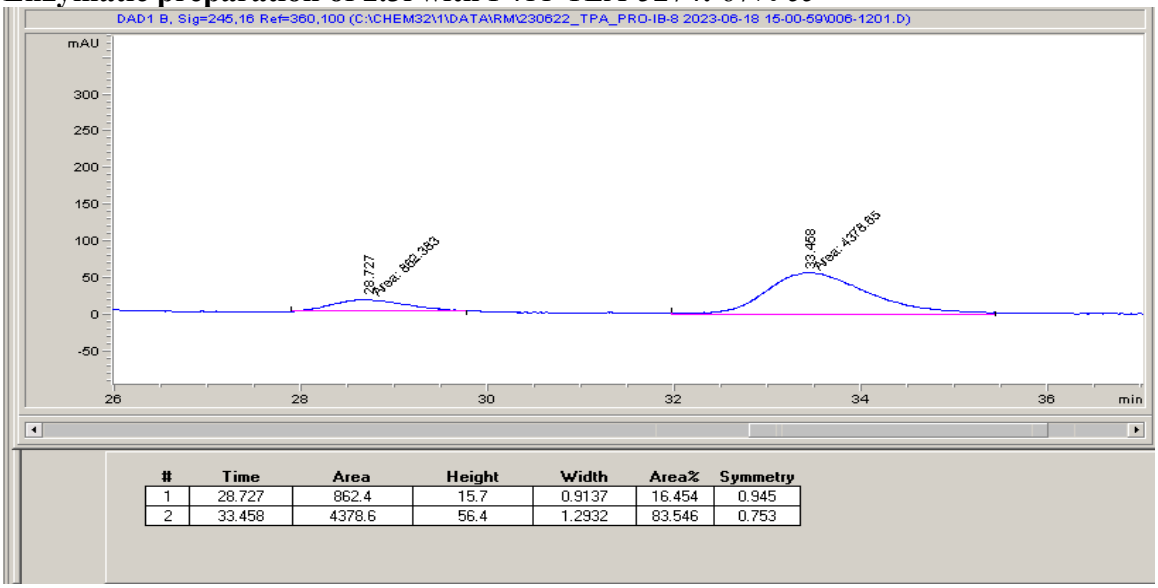

#	Time	Area	Height	Width	Area%	Symmetry
1	28.727	862.4	15.7	0.9137	16.454	0.945
2	33.458	4378.6	56.4	1.2932	83.546	0.753

XIV. Non-Competitive KIE

Experiments were performed using a suspension of *E. coli* cells harboring P411-TEA-5274 variant prepared according to the protocol described in **Experimental Methods B** and **Experimental Methods D**.

The non-competitive KIE reactions (triplicate experiments) were set up in an anaerobic chamber (oxygen level: <40 ppm). M9-N medium (pH 8.0) and D-glucose solution (500 mM in M9-N, pH 8.0) were placed in the anaerobic chamber for at least 24 hours. Harvested cells were resuspended with M9-N buffer (pH 8.0) in to OD_{600} = 39, and 1.55 mL of resuspended cells were aliquoted to 2-mL screw cap vials. The screw cap vials with cells were precooled to 0 ℃ on an ice bath. Unless otherwise specified, 150 μL of the precooled glucose solution, 100 μL of a stock solution containing glucose oxidase (from *Aspergillus niger*, 1,000 U/mL), and catalase (from bovine liver, 14,000 U/mL) in double-distilled water were added to make the total volume to 1.8 mL. The resulting mixtures stayed on the ice bath for another 2 minutes, and then isopropylbenzene **2.1b** (100 μL, 0.1 M stock in ethanol) or d_7-isopropylbenzene **2.1b** (100 μL, 0.1 M stock in ethanol), and the nitrene precursor **2.2a** (100 μL, 0.2 M stock in water; designated as t = 0) were added in a sequential manner. The vials were then capped and shaken in the anaerobic chamber at room temperature and 600 rpm. At regular intervals, 200 μL of the reaction mixture were transferred to an Eppendorf tube with 200 μL EtOH. The Eppendorf tube was vortexed and centrifuged (14,000 g, 4 °C, and 10 min), and the supernatant was analyzed by HPLC-MS to quantify product formation based on single ion mass peak for the non-deuterated and deuterated product.

The non-competitive KIE values 9.8, 9.7, and 9.0 are collected from Table B.S4, Table B.S5, Table B.S6, giving an average value of 9.5.

Table B.S4. Non-competitive KIE experiment 1.

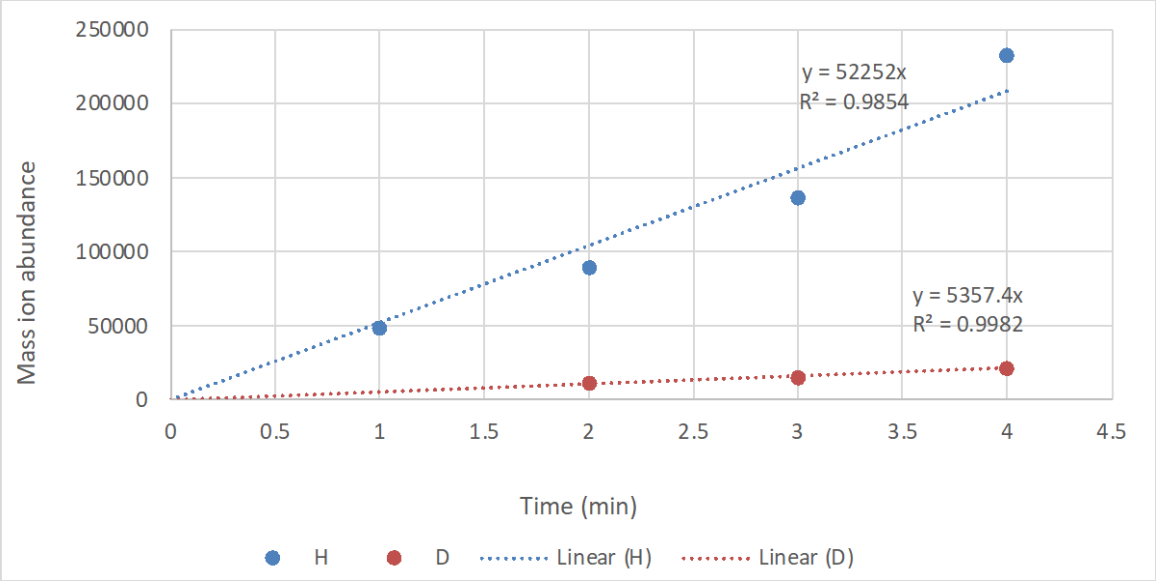

Time (min)	Ion count (**2.3b**; in blue)	Ion count (**2.3b'**; in red)
0	0	0
1	48108.3	-
2	89223.6	11638.2
3	136749.4	15285.7
4	232692.2	21558.1

KIE from the initial rates of the curve = 52252/5357.4 = 9.8

Table B.S5. Non-competitive KIE experiment 2.

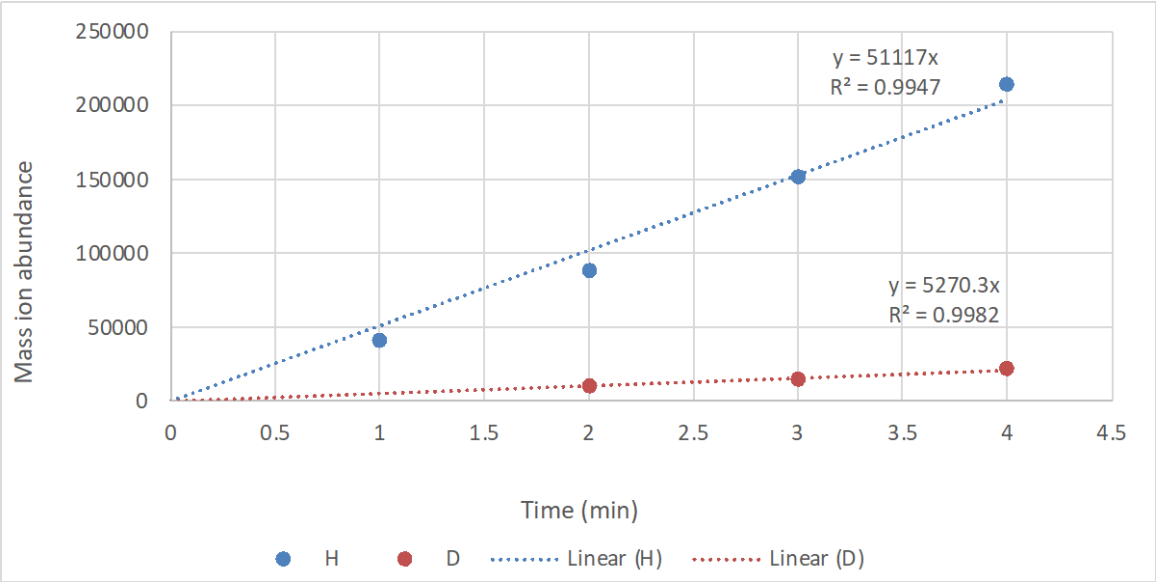

Time (min)	Ion count (**2.3b**; in blue)	Ion count (**2.3b'**; in red)
0	0	0
1	40816.4	-
2	88054	10420.7
3	152418.4	14879.5
4	214835.5	21839.5

KIE from the initial rates of the curve = 51117/5270.3 = 9.7

Table B.S6. Non-competitive KIE experiment 3.

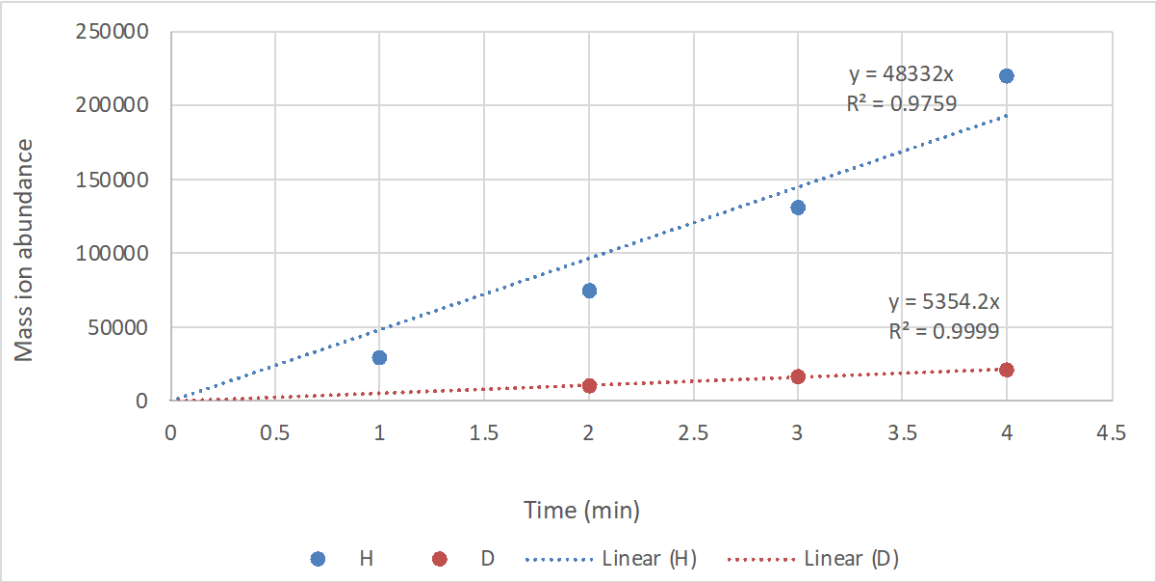

Time (min)	Ion count (**2.3b**; in blue)	Ion count (**2.3b'**; in red)
0	0	0
1	29713.1	-
2	74581.3	10591.1
3	130760.3	16304.4
4	219698	21294

KIE from the initial rates of the curve = 48332/5354.2 = 9.0

XV. Competitive KIE

Experiments were performed using a suspension of *E. coli* cells harboring P411-TEA-5274 variant prepared according to the protocol described in **Experimental Methods B** and **Experimental Methods D**.

The competitive KIE reaction was set up in an anaerobic chamber (oxygen level: <40 ppm). M9-N medium (pH 8.0) and D-glucose solution (500 mM in M9-N, pH 8.0) were placed in the anaerobic chamber for at least 24 hours. Harvested cells were resuspended with M9-N buffer (pH 8.0) to OD_{600} = 39, and 325 µL of resuspended cells were aliquoted to 2-mL screw cap vials. The reactions were carried out in triplicate, and the screw cap vials with cells were precooled to 0 °C on an ice bath. Unless otherwise specified, 30 µL of the precooled glucose solution, 20 µL of a stock solution containing glucose oxidase (from *Aspergillus niger*, 1,000 U/mL), and catalase (from bovine liver, 14,000 U/mL) in double-distilled water were added to make the total volume to 375 µL. The resulting mixtures stayed on the ice bath for another 2 minutes, and then the 1:1 mixture of isopropylbenzene **2.1b** and d_7-isopropylbenzene **2.1b** (20 µL, 0.2 M stock in ethanol), and the nitrene precursor **2.2a** (5 µL, 0.2 M stock in water; designated as t = 0) were added in a sequential manner. The vial was then capped, taken out of anaerobic chamber, and shaken in an Innova Shaker at 10 °C and 250 rpm. After 16 hours, 400 µL EtOH were added into the reaction mixture and the whole mixture was transferred to an Eppendorf tube. The Eppendorf tube was vortexed and centrifuged (14,000 g, 4 °C, and 10 min), and the supernatant was analyzed by HPLC-MS to quantify product formation based on single ion mass peak for the non-deuterated and deuterated product.

The competitive KIE values 22.9 is collected from Table B.S7.

Table B.S7. Competitive KIE experiment.

Time (min)	Ion count (**2.3b**)	Ion count (**2.3b'**)	Ratio (**2.3b**/**2.3b'**)	Avg. Ratio	SD ratio
1	1244699	55265.1	22.5	22.9	0.7
2	1253376	52984.3	23.7		
3	811441.6	36172.1	22.4		

XVI. X-Ray Crystallography

Low-temperature diffraction data (ϕ-and ω-scans) were collected on a Bruker AXS D8 VENTURE KAPPA diffractometer coupled to a PHOTON II CPAD detector with Cu K_α radiation (λ = 1.54178 Å) from an IμS micro-source for the structure of compound V23249. The structure was solved by direct methods using SHELXS[22] and refined against F^2 on all data by full-matrix least squares with SHELXL-2019[23] using established refinement techniques.[24] All non-hydrogen atoms were refined anisotropically. Unless otherwise noted, all hydrogen atoms were included into the model at geometrically calculated positions and refined using a riding model. The isotropic displacement parameters of all hydrogen atoms were fixed to 1.2 times the U value of the atoms they are linked to (1.5 times for methyl groups).

See Table B.S8 and Figure B.S1.

Table B.S8. X-ray experimental details of the **2.3f** derivative (S)-*N*-(2-(4-methoxyphenyl)butan-2-yl)benzamide (**CCDC 2287786**).

Crystal data	
Chemical formula	$C_{18}H_{21}NO_2$
M_r	283.36
Crystal system, space group	Triclinic, P_1
Temperature (K)	100(2)
a, *b*, *c* (Å)	7.3435 (6), 10.1398 (8), 10.9086 (12)
a, b, g (°)	82.154 (5), 79.776 (4), 84.245 (3)
V (Å^3)	789.48 (13)
Z	2
Radiation type	Cu *Ka*
m (mm^{-1})	0.61
Crystal size (mm)	0.20 × 0.10 × 0.10
Data collection	
Diffractometer	Bruker D8 VENTURE Kappa Duo PHOTON II CPAD
Absorption correction	Multi-scan *SADABS2016*/2 (Sheldrick, 2014)
T_{min}, T_{max}	0.711, 0.754
No. of measured, independent and observed [I > 2s(I)] reflections	29538, 6193, 6051
R_{int}	0.036
(sin q/l)$_{max}$ (Å^{-1})	0.625
Refinement	
$R[F^2 > 2s(F^2)]$, $wR(F^2)$, S	0.029, 0.073, 1.02
No. of reflections	6193
No. of parameters	393
No. of restraints	5
H-atom treatment	H atoms treated by a mixture of independent and constrained refinement
Γ_{max}, Γ_{min} (e Å^{-3})	0.22, -0.17
Absolute structure	Flack x determined using 2813 quotients [(I+)-(I-)]/[(I+)+(I-)] (Parsons, Flack and Wagner, Acta Cryst. B69 (2013) 249-259).
Absolute structure parameter	0.07 (7)

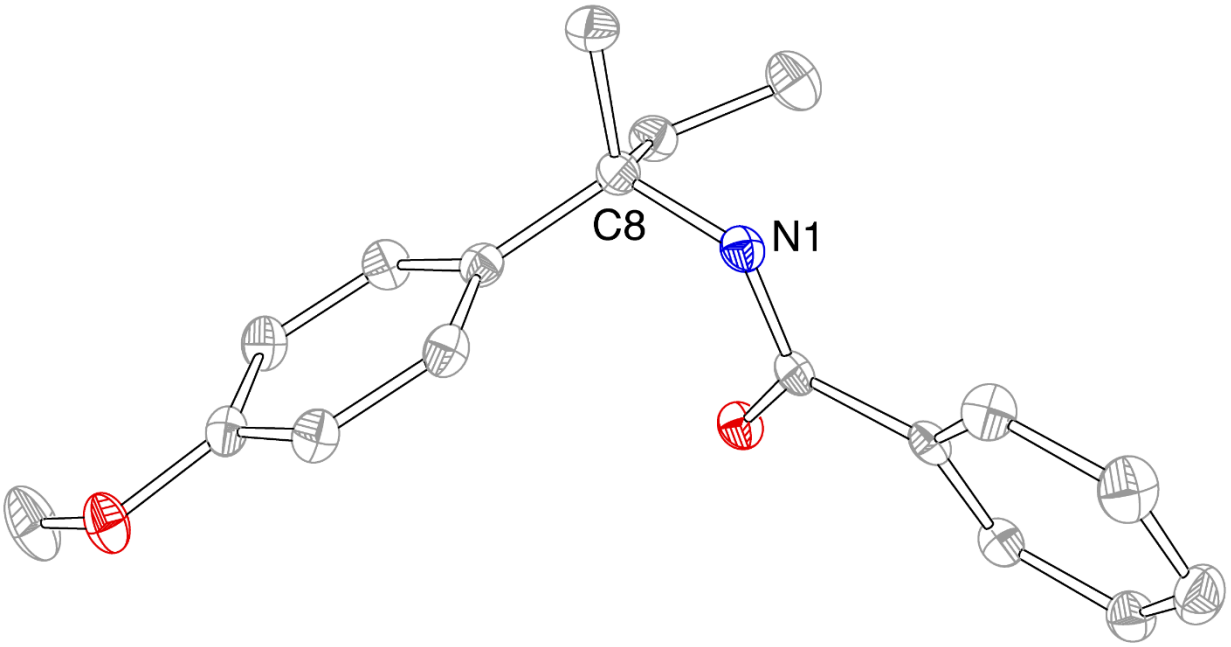

Figure B.S1. Displacement ellipsoid plot for the **2.3f** (CCDC 2287786) derivative (S)-*N*-(2-(4-methoxyphenyl)butan-2-yl)benzamide plotted at 50% probability. Single crystals were obtained from slow evaporation of the **2.3f** derivative dissolved in $CHCl_3$ at 4 °C. The compound crystallizes in the triclinic space group *P*1 with two molecules in the asymmetric unit. The coordinates for the hydrogen atoms bound to N1 and N21 were located in the difference Fourier synthesis and refined semi-freely with the help of a restraint on the N-H distance (0.88(4) Å).

XVII. Sequence Information

DNA and amino acid sequences of P411-TEA-5267:

ATGACAATTAAAGAAATGCCTCAGCCAAAAACGTTTGGAGAGCTTAAAAATTTACCGTTATTAA
ACACAGATAAACCGGTTCAAGCTTTGATGAAAATTGCGGATGAATTAGGAGAAATCTTTAAATT
CGAGGCGCCTGGTCGTGTAACGCGCTACTTATCAAGTCAGCGTCTAATTAAAGAAGCATGCGAT
GAATCACGCTTTGATAAAAACTTAAGTCAAGCGCTTAAATTTATGCGTGATTTTCTTGGAGACG
GGTTAGCCACAAGCTGGACGCATGAAAAAAATTGGAAAAAAGCGCATAATATCTTACTTCCAAG
CTTTAGTCAGCAGGCAATGAAAGGCTATCATGCGATGATGGTCGATATCGCCGTGCAGCTTGTT
CAAAAGTGGGAGCGTCTAAATGCAGATGAGCATATTGAAGTATCGGAAGACATGACACGTTTAA
CGCTTGATACAATTGGTCTTTGCGGCTTTAACTATCGCTTTAACAGCTTTTACCGAGATCAGCC
TCATCCATTTATTATAAGTATGGTCCGTGCACTGGATGAAGTAATGAACAAGCTGCAGCGAGCA
AATCCAGACGACCCAGCTTATGATGAAAACAAGCGCCAGTTTCAAGAAGATATCAAGGTGATGA
ACGACCTAGTAGATAAAATTATTGCAGATCGCAAAGCAAGGGGTGAACAAAGCGATGATTTATT
AACGCAGATGCTAAACGGAAAAGATCCAGAAACGGGTGAGCCGCTTGATGACGGGAACATTCGC
TATCAAATTATTACATTCTTAATGGCGGGACACGATCCGACAAGTGGTCTTTTATCATTTGCGC
TGTATTTCTTAGTGAAAAATCCACATGTATTACAAAAAGTAGCAGAAGAAGCAGCACGAGTTCT
AGTAGATCCTGTTCCAAGCTACAAACAAGTCAAACAGCTTAAATATGTCGGCATGGTCTTAAAC
GAAGCGCTGCGCTTATGGCCAGCGGTGCCTGCGTTTTCCCTATATGCAAAAGAAGATACGGTGC
TTGGAGGAGAATATCCTTTAGAAAAAGGCGACGAAGTAATGGTTCTGATTCCTCAGCTTCACCG
TGATAAAACAGTTTGGGGAGACGATGTGGAGGAGTTCCGTCCAGAGCGTTTTGAAAATCCAAGT
GCGATTCCGCAGCATGCGTTTAAACCGTTTGGACGTGGTCAGCGTGCGTCTATCGGTCAGCAGT
TCGCTCTTCATGAAGCAACGCTGGTACTTGGTATGATGCTAAAACACTTTGACTTTGAAGATCA
TACAAACTACGAGCTCGATATTAAAGAAACTTTTGTGTTAAAACCTAAAGGCTTTGTGGTAAAA
GCAAAATCGAAAAAAATTCCGCTTGGCGGTATTCCTTCACCTAGCACTGAACAGTCTGCTAAAA
AAGTACGCAAAAAGGCAGAAAACGCTCATAATACGCCGCTGCTTGTGCTATACGGTTCAAATAT
GGGTACCGCTGAAGGAACGGCGCGTGATTTAGCAGATATTGCAATGAGCAAAGGATTTGCACCG
CAGGTCGCAACGCTTGATTCACACGCCGGAAATCTTCCGCGCGAAGGAGCTGTATTAATTGTAA
CGGCGTCTTATAACGGTCATCCGCCTGATAACGCAAAGCAATTTGTCGACTGGTTAGACCAAGC
GTCTGCTGATGAAGTAAAAGGCGTTCGCTACTCCGTATTTGGATGCGGCGATAAAAACTGGGCT
ACTACGTATCAAAAAGTGCCTGCTTTTATCGATGAAACGCTTGCCGCTAAAGGGGCAGAAAACA

TCGCTGACCGCGGTGAAGCAGATGCAAGCGACGACTTTGAAGGCACATATGAAGAATGGCGTGA
ACATATGTGGAGTGACGTAGCAGCCTACTTTAACCTCGACATTGAAAACAGTGAAGATAATAAA
TCTACTCTTTCACTTCAATTTGTCGACAGCGCCGCGGATATGCCGCTTGCGAAAATGCACGGTG
CGTTTTCAACGAACGTCGTAGCAAGCAAAGAACTTCAACAGCCAGGCAGTGCACGAAGCACGCG
ACATCTTGAAATTGAACTTCCAAAAGAAGCTTCTTATCAAGAAGGAGATCATTTAGGTGTTATT
CCTCGCAACTATGAAGGAATAGTAAACCGTGTAACAGCAAGGTTCGGCCTAGATGCATCACAGC
AAATCCGTCTGGAAGCAGAAGAAGAAAAATTAGCTCATTTGCCACTCGCTAAAACAGTATCCGT
AGAAGAGCTTCTGCAATACGTGGAGCTTCAAGATCCTGTTACGCGCACGCAGCTTCGCGCAATG
GCTGCTAAAACGGTCTGCCCGCCGCATAAAGTAGAGCTTGAAGCCTTGCTTGAAAAGCAAGCCT
ACAAAGAACAAGTGCTGGCAAAACGTTTAACAATGCTTGAACTGCTTGAAAAATACCCGGCGTG
TGAAATGAAATTCAGCGAATTTATCGCCCTTCTGCCAAGCATACGCCCGCGCTATTACTCGATT
TCTTCATCACCTCGTGTCGATGAAAAACAAGCAAGCATCACGGTCAGCGTTGTCTCAGGAGAAG
CGTGGAGCGGATATGGAGAATATAAAGGAATTGCGTCGAACTATCTTGCCGAGCTGCAAGAAGG
AGATACGATTACGTGCTTTATTTCCACACCGCAGTCAGAATTTACGCTGCCAAAAGACCCTGAA
ACGCCGCTTATCATGGTCGGACCGGGAACAGGCGTCGCGCCGTTTAGAGGCTTTGTGCAGGCGC
GCAAACAGCTAAAAGAACAAGGACAGTCACTTGGAGAAGCACATTTATACTTCGGCTGCCGTTC
ACCTCATGAAGACTATCTGTATCAAGAAGAGCTTGAAAACGCCCAAAGCGAAGGCATCATTACG
CTTCATACCGCTTTTTCTCGCATGCCAAATCAGCCGAAAACATACGTTCAGCACGTAATGGAAC
AAGACGGCAAGAAATTGATTGAACTTCTTGATCAAGGAGCGCACTTCTATATTTGCGGAGACGG
AAGCCAAATGGCACCTGCCGTTGAAGCAACGCTTATGAAAAGCTATGCTGACGTTCACCAAGTG
AGTGAAGCAGACGCTCGCTTATGGCTGCAGCAGCTAGAAGAAAAAGGCCGATACGCAAAAGACG
TGTGGGCTGGGCTCGAGCACCACCACCACCACCACTGA

MTIKEMPQPKTFGELKNLPLLNTDKPVQALMKIADELGEIFKFEAPGRVTRYLSSQRLIKEACD
ESRFDKNLSQALKFMRDFLGDGLATSWTHEKNWKKAHNILLPSFSQQAMKGYHAMMVDIAVQLV
QKWERLNADEHIEVSEDMTRLTLDTIGLCGFNYRFNSFYRDQPHPFIISMVRALDEVMNKLQRA
NPDDPAYDENKRQFQEDIKVMNDLVDKIIADRKARGEQSDDLLTQMLNGKDPETGEPLDDGNIR
YQIITFLMAGHDPTSGLLSFALYFLVKNPHVLQKVAEEAARVLVDPVPSYKQVKQLKYVGMVLN
EALRLWPAVPAFSLYAKEDTVLGGEYPLEKGDEVMVLIPQLHRDKTVWGDDVEEFRPERFENPS
AIPQHAFKPFGRGQRASIGQQFALHEATLVLGMMLKHFDFEDHTNYELDIKETFVLKPKGFVVK
AKSKKIPLGGIPSPSTEQSAKKVRKKAENAHNTPLLVLYGSNMGTAEGTARDLADIAMSKGFAP
QVATLDSHAGNLPREGAVLIVTASYNGHPPDNAKQFVDWLDQASADEVKGVRYSVFGCGDKNWA

TTYQKVPAFIDETLAAKGAENIADRGEADASDDFEGTYEEWREHMWSDVAAYFNLDIENSEDNK
STLSLQFVDSAADMPLAKMHGAFSTNVVASKELQQPGSARSTRHLEIELPKEASYQEGDHLGVI
PRNYEGIVNRVTARFGLDASQQIRLEAEEEKLAHLPLAKTVSVEELLQYVELQDPVTRTQLRAM
AAKTVCPPHKVELEALLEKQAYKEQVLAKRLTMLELLEKYPACEMKFSEFIALLPSIRPRYYSI
SSSPRVDEKQASITVSVVSGEAWSGYGEYKGIASNYLAELQEGDTITCFISTPQSEFTLPKDPE
TPLIMVGPGTGVAPFRGFVQARKQLKEQGQSLGEAHLYFGCRSPHEDYLYQEELENAQSEGIIT
LHTAFSRMPNQPKTYVQHVMEQDGKKLIELLDQGAHFYICGDGSQMAPAVEATLMKSYADVHQV
SEADARLWLQQLEEKGRYAKDVWAGLEHHHHHH*

DNA and amino acid sequences of P411-TEA-5274:

ATGACAATTAAAGAAATGCCTCAGCCAAAAACGTTTGGAGAGCTTAAAAATTTACCGTTATTAA
ACACAGATAAACCGGTTCAAGCTTTGATGAAAATTGCGGATGAATTAGGAGAAATCTTTAAATT
CGAGGCGCCTGGTCGTGTAACGCGCTACTTATCAAGTCAGCGTCTAATTAAAGAAGCATGCGAT
GAATCACGCTTTGATAAAAACTTAACGCAAGCGCTTAAATTTATGCGTGATTTTCTTGGAGACG
GGTTAGCCACAAGCTGGACGCATGAAAAAAATTGGAAAAAAGCGCATAATATCTTACTTCCAAG
CTTTAGTCAGCAGGCAATGAAAGGCTATCATGCGATGATGGTCGATATCGCCGTGCAGCTTGTT
CAAAAGTGGGAGCGTCTAAATGCAGATGAGCATATTGAAGTATCGGAAGACATGACACGTTTAA
CGCTTGATACAATTGGTCTTTGCGGCTTTAACTATCGCTTTAACAGCTTTTACCGAGATCAGCC
TCATCCATTTATTATAAGTTATGTCCGTGCACTGGATGAAGTAATGAACAAGCTGCAGCGAGCA
AATCCAGACGACCCAGCTTATGATGAAAACAAGCGCCAGTTTCAAGAAGATATCAAGGTGATGA
ACGACCTAGTAGATAAAATTATTGCAGATCGCAAAGCAAGGGGTGAACAAAGCGATGATTTATT
AACGCAGATGCTAAACGGAAAAGATCCAGAAACGGGTGAGCCGCTTGATGACGGGAACATTCGC
TATCAAATTATTACATTCTTAATGGCGGGACACGATCCGACAAGTGGTCTTTTATCATTTGCGC
TGTATTTCTTAGTGAAAAATCCACATGTATTACAAAAAGTAGCAGAAGAAGCAGCACGAGTTCT
AGTAGATCCTGTTCCAAGCTACAAACAAGTCAAACAGCTTAAATATGTCGGCATGGTCTTAAAC
GAAGCGCTGCGCTTATGGCCAGTGGTGCCTGCGTTTTCCCTATATGCAAAAGAAGATACGGTGC
TTGGAGGAGAATATCCTTTAGAAAAAGGCGACGAAGTAGAGGTTCTGATTCCTCAGCTTCACCG
TGATAAAACAGTTTGGGGAGACGATGTGGAGGAGTTCCGTCCAGAGCGTTTTGAAAATCCAAGT
GCGATTCCGCAGCATGCGTTTAAACCGTTTGGAGTGGGTCAGCGTGGTTCTATCGGTGCGCAGT
TCGCTCTTCATGAAGCAACGCTGGTACTTGGTATGATGCTAAAACACTTTGACTTTGAAGATCA
TACAAACTACGAGCTCGATATTAAAGAAACTTTTGTGTTAAAACCTAAAGGCTTTGTGGTAAAA
GCAAAATCGAAAAAAATTCCGCTTGGCGGTATTCCTTCACCTAGCACTGAACAGTCTGCTAAAA
AAGTACGCAAAAAGGCAGAAAACGCTCATAATACGCCGCTGCTTGTGCTATACGGTTCAAATAT
GGGTACCGCTGAAGGAACGGCGCGTGATTTAGCAGATATTGCAATGAGCAAAGGATTTGCACCG
CAGGTCGCAACGCTTGATTCACACGCCGGAAATCTTCCGCGCGAAGGAGCTGTATTAATTGTAA
CGGCGTCTTATAACGGTCATCCGCCTGATAACGCAAAGCAATTTGTCGACTGGTTAGACCAAGC
GTCTGCTGATGAAGTAAAAGGCGTTCGCTACTCCGTATTTGGATGCGGCGATAAAAACTGGGCT
ACTACGTATCAAAAAGTGCCTGCTTTTATCGATGAAACGCTTGCCGCTAAAGGGGCAGAAAACA
TCGCTGACCGCGGTGAAGCAGATGCAAGCGACGACTTTGAAGGCACATATGAAGAATGGCGTGA
ACATATGTGGAGTGACGTAGCAGCCTACTTTAACCTCGACATTGAAAACAGTGAAGATAATAAA

TCTACTCTTTCACTTCAATTTGTCGACAGCGCCGCGGATATGCCGCTTGCGAAAATGCACGGTG
CGTTTTCAACGAACGTCGTAGCAAGCAAAGAACTTCAACAGCCAGGCAGTGCACGAAGCACGCG
ACATCTTGAAATTGAACTTCCAAAAGAAGCTTCTTATCAAGAAGGAGATCATTTAGGTGTTATT
CCTCGCAACTATGAAGGAATAGTAAACCGTGTAACAGCAAGGTTCGGCCTAGATGCATCACAGC
AAATCCGTCTGGAAGCAGAAGAAGAAAAATTAGCTCATTTGCCACTCGCTAAAACAGTATCCGT
AGAAGAGCTTCTGCAATACGTGGAGCTTCAAGATCCTGTTACGCGCACGCAGCTTCGCGCAATG
GCTGCTAAAACGGTCTGCCCGCCGCATAAAGTAGAGCTTGAAGCCTTGCTTGAAAAGCAAGCCT
ACAAAGAACAAGTGCTGGCAAAACGTTTAACAATGCTTGAACTGCTTGAAAAATACCCGGCGTG
TGAAATGAAATTCAGCGAATTTATCGCCCTTCTGCCAAGCATACGCCCGCGCTATTACTCGATT
TCTTCATCACCTCGTGTCGATGAAAAACAAGCAAGCATCACGGTCAGCGTTGTCTCAGGAGAAG
CGTGGAGCGGATATGGAGAATATAAAGGAATTGCGTCGAACTATCTTGCCGAGCTGCAAGAAGG
AGATACGATTACGTGCTTTATTTCCACACCGCAGTCAGAATTTACGCTGCCAAAAGACCCTGAA
ACGCCGCTTATCATGGTCGGACCGGGAACAGGCGTCGCGCCGTTTAGAGGCTTTGTGCAGGCGC
GCAAACAGCTAAAAGAACAAGGACAGTCACTTGGAGAAGCACATTTATACTTCGGCTGCCGTTC
ACCTCATGAAGACTATCTGTATCAAGAAGAGCTTGAAAACGCCCAAAGCGAAGGCATCATTACG
CTTCATACCGCTTTTTCTCGCATGCCAAATCAGCCGAAAACATACGTTCAGCACGTAATGGAAC
AAGACGGCAAGAAATTGATTGAACTTCTTGATCAAGGAGCGCACTTCTATATTTGCGGAGACGG
AAGCCAAATGGCACCTGCCGTTGAAGCAACGCTTATGAAAAGCTATGCTGACGTTCACCAAGTG
AGTGAAGCAGACGCTCGCTTATGGCTGCAGCAGCTAGAAGAAAAAGGCCGATACGCAAAAGACG
TGTGGGCTGGGCTCGAGCACCACCACCACCACCACTGA

MTIKEMPQPKTFGELKNLPLLNTDKPVQALMKIADELGEIFKFEAPGRVTRYLSSQRLIKEACD
ESRFDKNLTQALKFMRDFLGDGLATSWTHEKNWKKAHNILLPSFSQQAMKGYHAMMVDIAVQLV
QKWERLNADEHIEVSEDMTRLTLDTIGLCGFNYRFNSFYRDQPHPFIISYVRALDEVMNKLQRA
NPDDPAYDENKRQFQEDIKVMNDLVDKIIADRKARGEQSDDLLTQMLNGKDPETGEPLDDGNIR
YQIITFLMAGHDPTSGLLSFALYFLVKNPHVLQKVAEEAARVLVDPVPSYKQVKQLKYVGMVLN
EALRLWPVVPAFSLYAKEDTVLGGEYPLEKGDEVEVLIPQLHRDKTVWGDDVEEFRPERFENPS
AIPQHAFKPFGVGQRGSIGAQFALHEATLVLGMMLKHFDFEDHTNYELDIKETFVLKPKGFVVK
AKSKKIPLGGIPSPSTEQSAKKVRKKAENAHNTPLLVLYGSNMGTAEGTARDLADIAMSKGFAP
QVATLDSHAGNLPREGAVLIVTASYNGHPPDNAKQFVDWLDQASADEVKGVRYSVFGCGDKNWA
TTYQKVPAFIDETLAAKGAENIADRGEADASDDFEGTYEEWREHMWSDVAAYFNLDIENSEDNK
STLSLQFVDSAADMPLAKMHGAFSTNVVASKELQQPGSARSTRHLEIELPKEASYQEGDHLGVI

PRNYEGIVNRVTARFGLDASQQIRLEAEEEKLAHLPLAKTVSVEELLQYVELQDPVTRTQLRAM
AAKTVCPPHKVELEALLEKQAYKEQVLAKRLTMLELLEKYPACEMKFSEFIALLPSIRPRYYSI
SSSPRVDEKQASITVSVVSGEAWSGYGEYKGIASNYLAELQEGDTITCFISTPQSEFTLPKDPE
TPLIMVGPGTGVAPFRGFVQARKQLKEQGQSLGEAHLYFGCRSPHEDYLYQEELENAQSEGIIT
LHTAFSRMPNQPKTYVQHVMEQDGKKLIELLDQGAHFYICGDGSQMAPAVEATLMKSYADVHQV
SEADARLWLQQLEEKGRYAKDVWAGLEHHHHHH*

XIX. Molecular Dynamics Simulations

Molecular dynamics (MD) simulations were prepared with the Amber 16 package[25] and the AmberTools 21 package.[26] The structure of the A-chain of the structurally strongly related P411 **E10** variant (PDB ID: 5UCW) was used as the starting point for the preparation of the MD simulations.[27] The S72T, V78M, M177Y, L262.3m, E267D, G268P, T327V, M354E, N395V, A399G, Q403A, L437F, and S438V mutations were manually introduced using Pymol v.1.8.2.[28] Hydrogen atoms were added using the *reduce* tool from the AmberTools 21 package. For the deprotonated serine residue coordinated to iron (named SEO), the residue was capped with an acyl group (N-terminus) and a methylamidate group (C-terminus) and restrained electrostatic potential (RESP) atomic charges[29] were calculated at the B3LYP/6-31G(d)[30,31] level of theory in Gaussian 09, Rev. D.01,[32] according to the Merz–Singh–Kollman scheme.[33,34] A combination of the ff14SB force field for proteins, the General Amber Force Field (gaff)[35] for **2.1a** and TIP3P parameters[36] for water molecules was employed.[37] For substrate **2.1a**, RESP atomic charges were calculated at the B3LYP/6-31G(d) level of theory according to the Merz–Singh–Kollman scheme. Force field parameters and charges for the iron heme-nitrene complex were generating using the MCPB.py program[38] with geometry optimizations, force constant and Merz–Singh–Kollman RESP charge calculations at the B3LYP/6-31G(d) level of theory. For the bond between Fe and the side-chain oxygen from SEO, r_{eq} was set to 1.883 Å and *k* to 100.0 kcal mol^{-1} Å^{-2} using *parmed*. The system was solvated in a 10-Å buffer water box and neutralized by addition of sodium ions.

Employing the GPU-accelerated pmemd[39] code implemented in Amber 16, the energy was minimized over 5,000 steps with positional restraints (500 kcal mol^{-1} Å^{-2}) applied to all atoms except water molecules and sodium ions, followed by an energy minimization over 5,000 steps with positional restraints (2.0 kcal mol^{-1} Å^{-2}) on all peptide backbone atoms (C, Cα, N) as well as all non-hydrogen atoms of the iron heme-nitrene complex and **2.1a**. Subsequently, the temperature was raised from 0 K to 300 K within 300 ps in an NVT ensemble with positional restraints (30 kcal mol^{-1} Å^{-2}) on all peptide backbone atoms (C, Cα, N) as well as all non-hydrogen atoms of the iron heme-nitrene complex and **2.1a**. Afterwards, the system was equilibrated at 300 K and 1 atm for 2 ns in an NPT ensemble with high positional restraints (30 kcal mol^{-1} Å^{-2}) on all peptide backbone atoms (C, Cα, N) as well as all non-hydrogen atoms of the iron heme-nitrene complex and **2.1a**, followed by an equilibration at 300 K and 1 atm for 2 ns in an NPT ensemble with low positional restraints (0.5 kcal mol^{-1} Å^{-2}) on all peptide backbone atoms (C, Cα, N) as well as all

non-hydrogen atoms of the iron heme-nitrene complex and **2.1a**. Production runs were performed in an NPT ensemble for 1,000 ns. For each system, three independent replicas were simulated. For the HAT transition state mimics (Figure 3.5), a harmonic potential with $k = 150$ kcal mol^{-1} Å^{-2} and a distance of 1.30 Å and 1.33 Å were added between the nitrene nitrogen and the hydrogen on the tertiary carbon of the substrate (N–H) and the C–H bond, respectively. *k*-Means clustering was performed using *cpptraj* to analyze each MD trajectory and obtain representative structures for the most populated clusters. Distances were measured between the closest carbon atoms of **2.1a** and the respective amino acid residues. Probability density plots were prepared with Excel 2016 with bin sizes of 0.2 Å for distances and 10° for dihedral angles. Structures were visualized using Pymol v.1.8.2.[28]

See Supplementary Figure B.S2, Supplementary Figure B.S3, Supplementary Figure B.S4, Supplementary Figure B.S5 and Supplementary Figure B.S6.

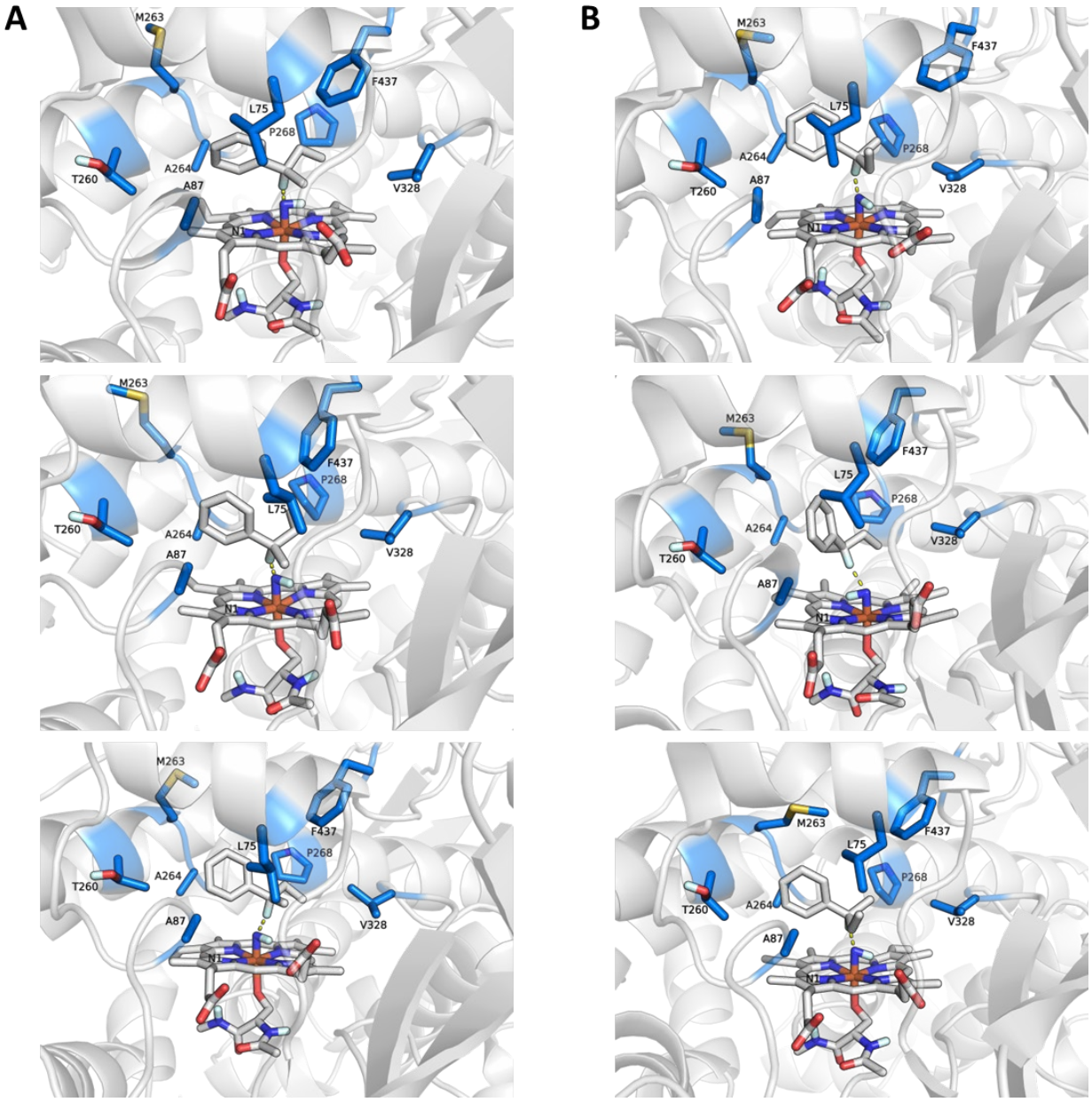

Figure B.S2. Molecular dynamics simulations on HAT transition state mimics. (A) with substrate (*R*)-**2.1a** and (B) with substrate (*S*)-**2.1a.** Representative structures of the most populated cluster of each independent replica. Non-relevant, non-polar hydrogens are omitted for clarity.

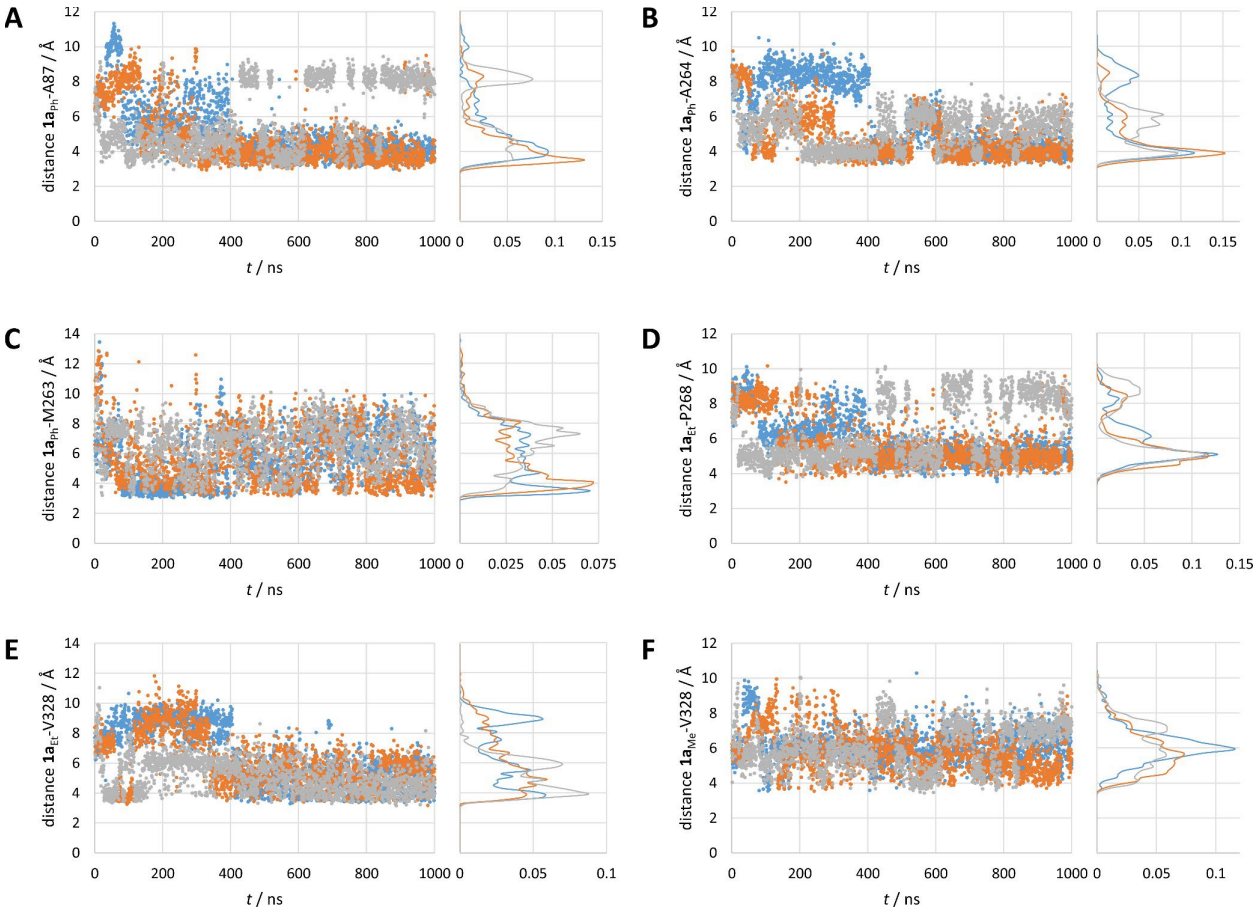

Figure B.S3. Distances between (*R*)-2.1a and key residues. Plot of distances (in Å) over time and probability density plot between the closest carbon atoms of **2.1a** and (A) A87, (B) A264, (C) M263, (D) P268, (E), and (F) V328 from MD simulations of three independent replicas.

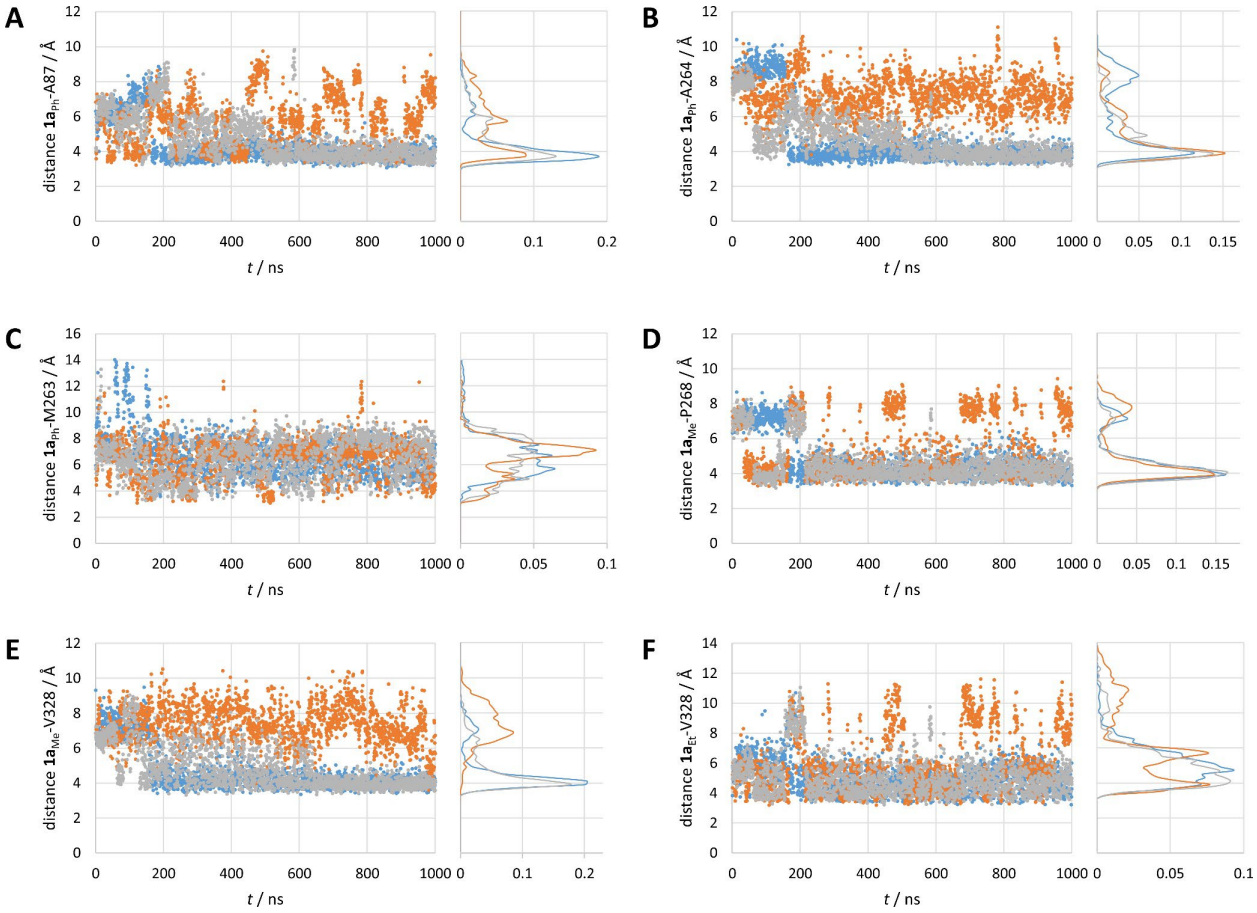

Figure B.S4. Distances between (*S*)-2.1a and key residues. Plot of distances (in Å) over time and probability density plot between the closest carbon atoms of **2.1a** and (A) A87, (B) A264, (C) M263, (D) P268, (E), and (F) V328 from MD simulations of three independent replicas.

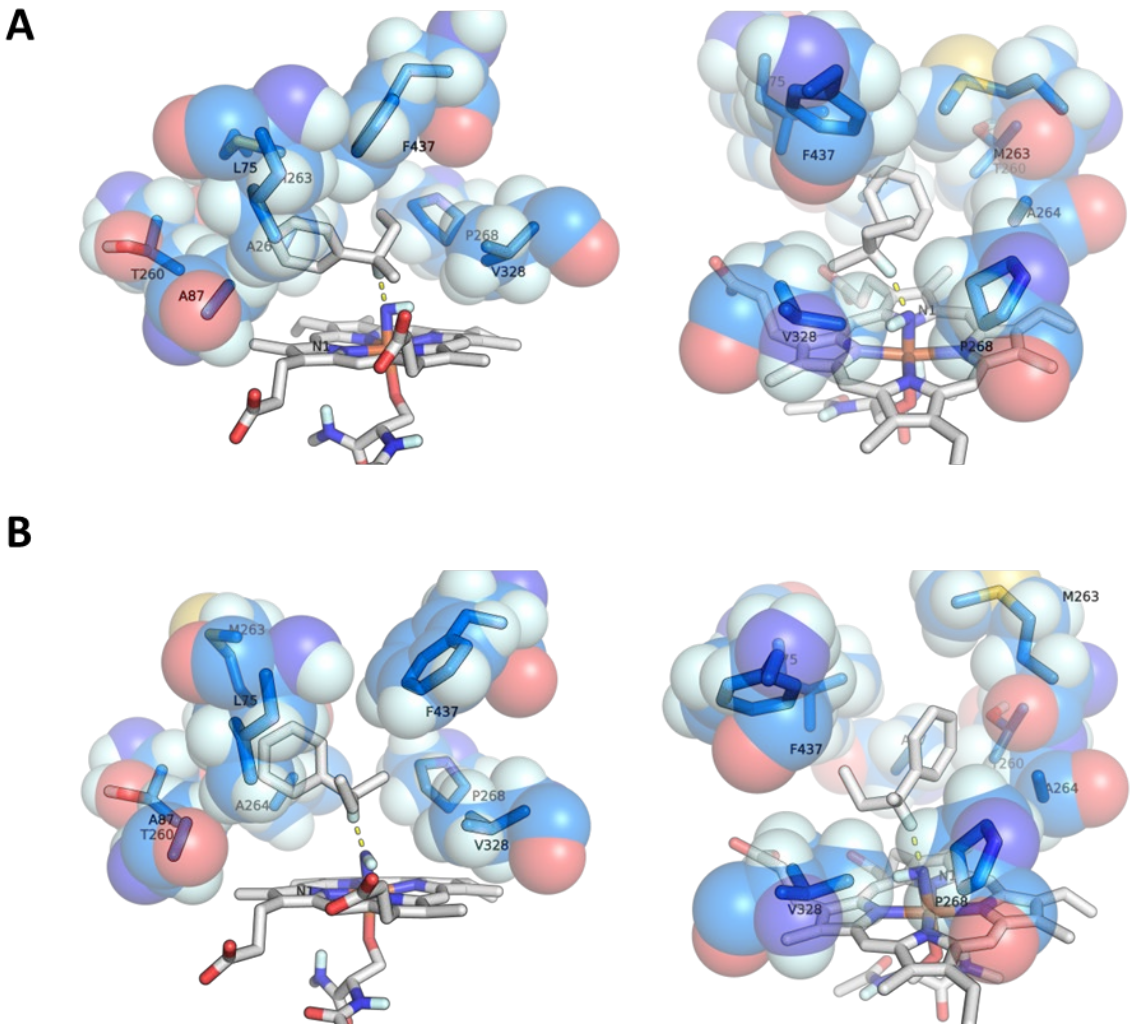

Figure B.S5. Key residues in MD simulations on HAT transition state mimics. (A) with substrate (*R*)-**2.1a** and (B) with substrate (*S*)-**2.1a.** Representative structures of the most populated cluster with key residues shown as space-filling model.

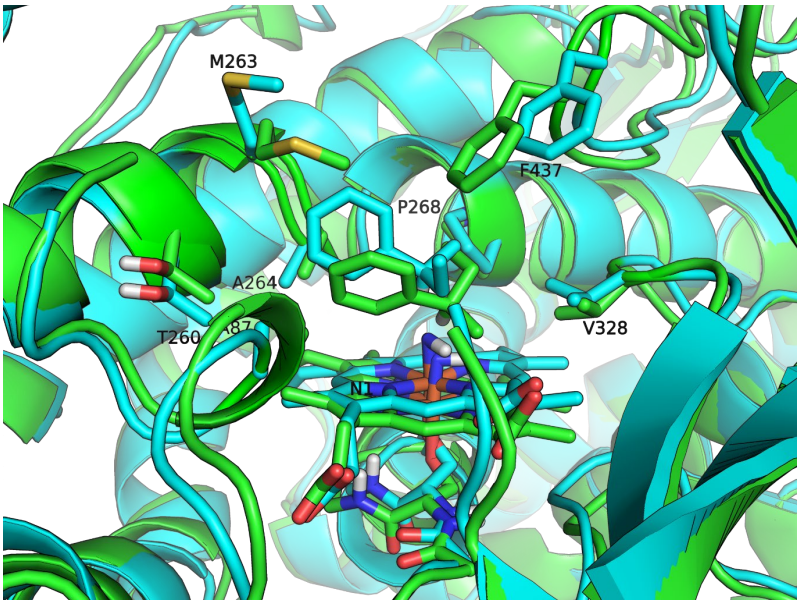

Figure B.S6. Overlay of most populated structures from MD simulations. HAT transition state mimic for substrate (*R*)-**2.1a** (green color) and substrate (*S*)-**2.1a** (blue color). Non-relevant, non-polar hydrogens, and part of the peptide backbone located in front are omitted for clarity.

Chapter IV

BIOCATALYTIC CONSTRUCTION OF CHIRAL PYRROLIDINES AND INDOLINES VIA INTRAMOLECULAR C(SP^3)–H AMINATION

4.1 Introduction

N-Heterocycles are ubiquitous in functional materials, bioactive natural products, and pharmaceutical compounds (Scheme 4.1a).[1,2] Especially privileged are saturated cyclic amines such as pyrrolidines, whose desirable structural and pharmacokinetic/pharmacodynamic (PK/PD) properties help make them one of the most common *N*-heterocyclic moieties in drug molecules.[3–5] A prevalent biosynthetic and biocatalytic approach to forging chiral cyclic amines is intramolecular condensation of aminoketones or aminoaldehydes followed by reduction using imine reductases.[6–15] This route requires pre-oxidation at a given position and preinstalled carbonyl/amino functionality on the substrates. Very recently, Hyster and coworkers demonstrated new-to-nature photoenzymatic hydroamination of olefins to synthesize cyclic amines.[16] Chemists have been seeking catalytic C–H functionalization methodologies for the synthesis of cyclic amines in order to maximize atom and step economy (Scheme 4.1b);[17] transition-metal-catalyzed alkyl nitrene C–H insertion reactions are attractive in this context. Compared to well-established metallonitrenes with electron-withdrawing substituents on the nitrogen, C(sp^3)–H insertion with alkyl nitrenes is less developed due to lower reactivity and propensity to undergo an unproductive 1,2-hydride shift leading to the irreversible formation of undesired imines.[18] In addition, another major challenge is to achieve high stereoselectivity;[18,19] stereoselective examples with an environmentally benign 3d transition metal are even rarer.[20,21] We posited that importing this human-invented chemistry into metalloenzymes could leverage the remarkable selectivity and sustainability of enzymes to streamline construction of chiral cyclic amines.

Cytochrome P450 heme monooxygenases utilize molecular oxygen and NAD(P)H to generate a high-valent iron-oxo species[22] to perform selective C–H functionalization transformations that are challenging for small-molecule catalysts. With tunable protein–substrate interactions in the chiral environment of the active site, these biocatalysts use an earth-abundant metal (iron) and exert exquisite control over develop an array of non-natural functions based on

transfer of oxidation chemistries. Over the past decade, our lab and others have ventured beyond the native oxidation activities of P450s to reactive carbene and nitrene-like intermediates.[23,24] Enzymatic nitrene transfer reactions have expanded the biocatalytic repertoire to include transformations ranging from C–H sulfamidation to C–H amination/amidation.[25–31] However, heme enzymes have not been demonstrated to employ more challenging nitrene species bearing electron-donating substitutions in asymmetric C–H functionalization processes. We thus set out to tackle this challenge by a heme enzyme to perform cyclic amine synthesis.

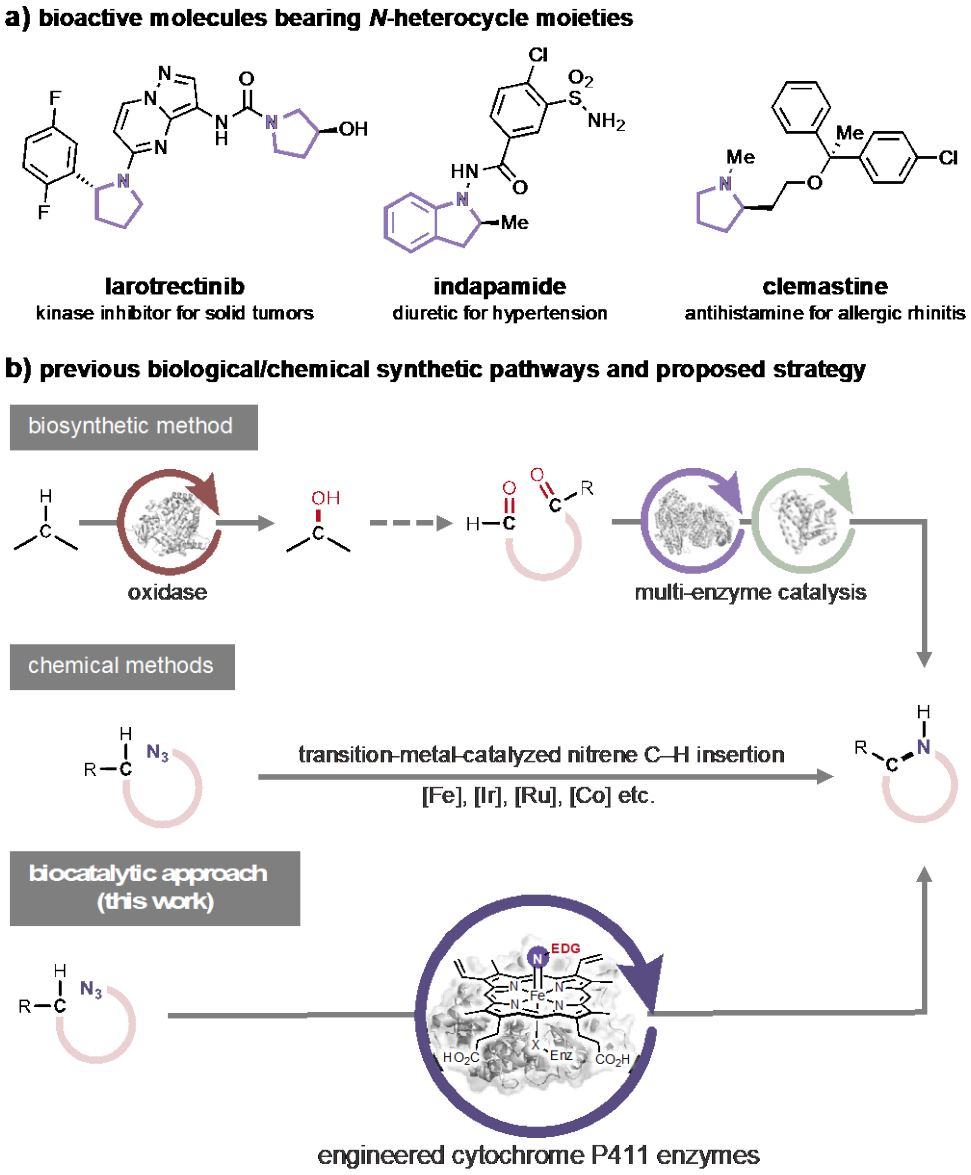

Scheme 4.1. Background and project synopsis

4.2 Results and Discussions

Azides, readily prepared from alcohols and bromides, serve as atom-economical nitrene precursors for making the corresponding pyrrolidines, because they eliminate only nitrogen gas.[32] We commenced this investigation with model substrate (4-azidobutyl)benzene **3.1a**. A panel of hemoproteins previously engineered for other nitrene and carbene transfer reactions was screened for activity on **3.1a** as whole *Escherichia coli* (*E. coli*) cell catalysts. To our delight, a P411 (cytochrome P450 having a Ser in place of Cys as the heme axial ligand) variant engineered for carbene C–H insertion was able to catalyze the desired transformation with 4% yield and moderate enantioselectivity (82:18 er). Control studies showed that free heme had no activity for this reaction. This variant, renamed P411-PYS-5141 (See Section IX for sequence details), was subjected to four rounds of site-saturation mutagenesis (SSM) and screening to accumulate beneficial mutations L75E, Q437L, A330Q, and M118V, which improved the yield to 29% and the enantioselectivity to 94:6 er Four additional rounds of evolution led to variant P411-PYS-5149 with 74% yield and slightly decreased enantioselectivity (91:9 er) (**Figure 4.1a–b**). The absolute configuration of the pyrrolidine product **3.2a** was confirmed as *R* by comparing the enzymatically produced product with the commercially available enantiomer (*S*)-**3.2a** after benzoyl protection. (See Section VIII in supporting information).

Evaluating the substrate scope of **P411-PYS-5149** for pyrrolidine synthesis (**Figure 4.1c**), we found that substrates *para*-fluoro **3.1b**, *para*-methyl **3.1c**, and *para*-methoxyl **3.1d** generally afforded corresponding pyrrolidine products in moderate to good yield and enantioselectivity (up to 67% yield and 99:1 er). The *ortho*-methyl substrate was not well tolerated in this system, however, presumably due to steric hindrance between ortho substituents and the porphyrin. (**Figure C.S2** and **Figure C.S7**) Variant **P411-PYS-5149** also showed promising initial activity (3% yield, 85:15 er) with 2,5-difluoro substrate **3.1e**, which serves as a building block for the drug molecule larotrectinib;[33,34] further evolution for activity on **3.1e** could improve this activity. Other substrates bearing different aromatic rings like naphthalene (**3.1f**), thiophene (**3.1g**), and indole (**3.1h**) were also compatible. Surprisingly, variant **P411-PYS-5149** failed to provide high enantioselectivity (bonds indicate uncertainty regarding the absolute configuration) for thiophene

3.1g and the indole substrate **3.1h,** even though the yields were low-moderate (32% and 41%, respectively). We also investigated more challenging substrates with unactivated C(sp^3)–H bonds. Azidobutylcyclohexane **3.1i** and azido-4-methylpentane **3.1j** afforded small amounts (2–3% yield) of product cyclized at the tertiary C–H position. It is likely that these promising activities can be improved to synthetically useful levels by further enzyme engineering, as has been demonstrated many times.[35–37]

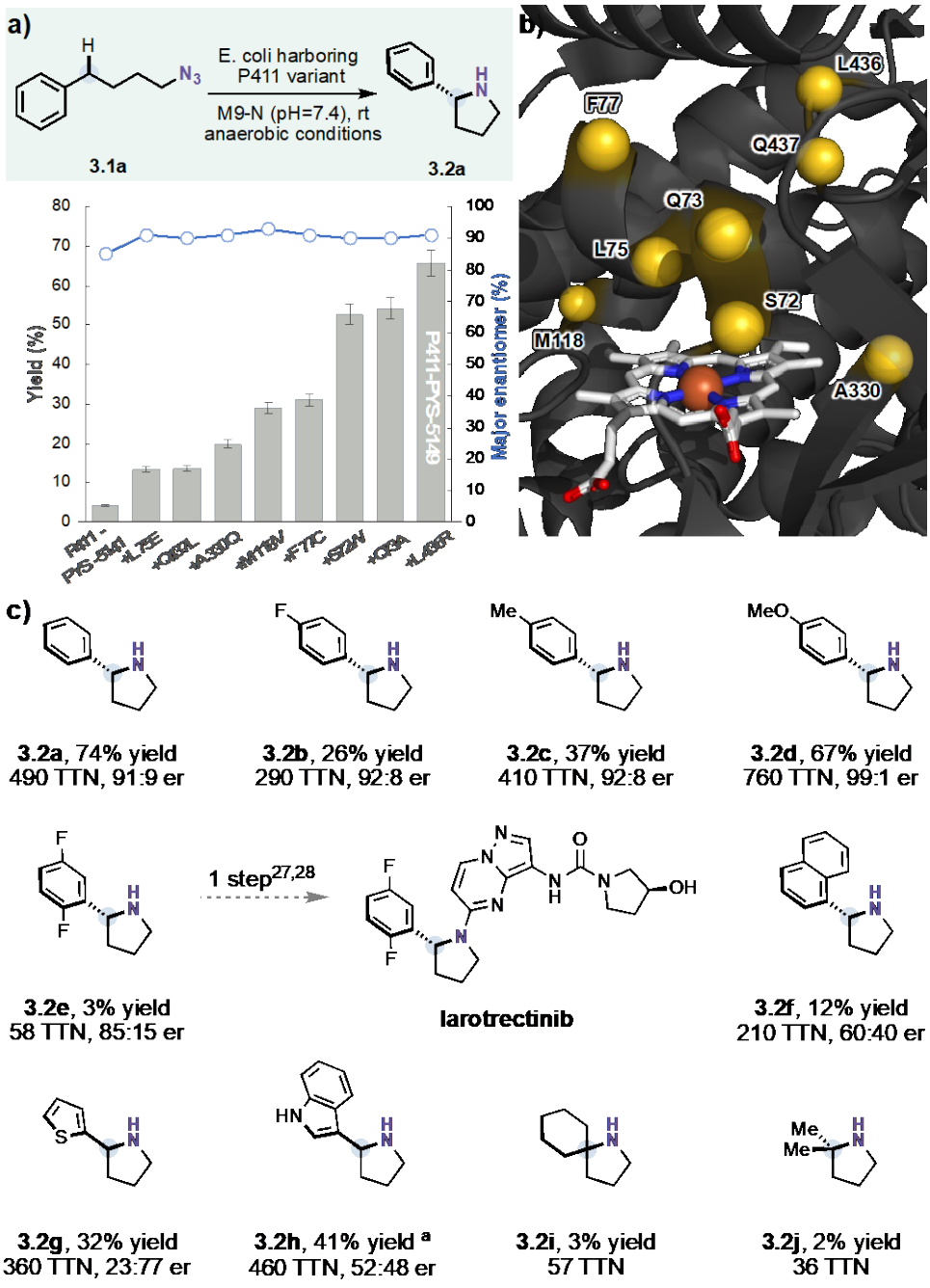

Figure 4.1. Directed evolution and substrate scope study for enantioselective alkyl nitrene transfer to make pyrrolidines. a) Cytochrome P411 variant **P411-PYS-5149** was obtained after eight rounds of site-saturation mutagenesis and screening from **P411-PYS-5141** (See **Section IX** for sequences). Indicated mutations are relative to **P411-PYS-5141**. Experiments were performed using *E. coli* (OD_{600} = 30) expressing P411 enzymes with 2.5 mM substrate **3.1a** in M9-N buffer (pH = 7.4) at room temperature under anaerobic conditions for 16 h. Yields were quantified by LC-MS based on the calibration curve of **3.2a**. Enantioselectivities were measured by HPLC on a chiral phase after benzoyl protection. b) Mutated residues (S72, Q73, L75, F77, M118, A330, L436 and Q437) are highlighted in the active site of P411 variant **E10** (PDB ID: 5UCW). c) Substrate scope of enantioselective alkyl nitrene transfer. Experiments were performed at analytical scale using *E. coli* (OD_{600} = 30) that expressed the **P411-PYS-5149** variant with 2.5 mM substrate (**3.1a–j**) and in M9-N buffer (pH = 8.4) at room temperature under anaerobic conditions for 16 h. Yields were quantified by LC-MS based on the calibration curves of the corresponding reference products. Enantioselectivities were measured by HPLC on a chiral phase after benzoyl protection of the pyrrolidine products. a **3.2h** was obtained in 60% yield, 51:49 er with variant **P411-PYS-5148**.

While evolving the cyclic amine synthases, we also investigated the ability of the evolved enzymes to forge indolines, another important class of bioactive *N*-heterocycles.[38,39] Aryl azides have been used as nitrene precursors to synthesize indolines *via* nitrene C–H insertion, but rarely in an asymmetric manner.[40] We utilized 1-azido-2-propylbenzene **3.3a** as the starting material for initial enzyme screening. In contrast to pyrrolidine synthesis *via* alkyl metallonitrene insertion into activated benzylic C–H bonds, indoline synthesis requires aryl metallonitrene insertion into unactivated aliphatic C–H bonds.

Upon testing the lineage of "pyrrolidine synthases," we found that variant **P411-PYS-5148** afforded the best yield (46%), although with negligible enantio selectivity (48:52 er) for indoline synthesis from **3.3a**. **P411-PYS-5148**, was used for directed evolution of an "indoline synthase." Mutations L437P and L181N introduced during two rounds of mutagenesis and screening generated **P411-INS-5151**, with improved activity and enantioselectivity for indoline formation (64% analytical yield, 60% isolated yield, and 92:8 er) (**Figure 4.2a**). The absolute configuration of the methylindoline product **3.4a** was confirmed as *S* by comparing the enzymatic product with the commercially available enantiomer (*R*)-**3.4a** (See **Section VIII** in supporting information). We proceeded to probe the scope of enzymatic indoline synthesis (**Figure 4.2b**). Cyclization of 1-azido-2-butylbenzene **3.3b** using evolved enzyme generated **P411-INS-5151**, predominantly afforded a five-membered heterocycle, ethylindoline **3.4b**, with 13% yield and good selectivity (91:9 er). A plausible six-membered tetrahydroquinoline product (**3.4ba**) through C–H insertion at

the subterminal site was not detected. A substrate bearing a longer carbon chain (1-azido-2-pentylbenzene) also showed initial activity (See **Figure C.S4**). Substitutions on phenyl groups such as **3.3c** and **3.3d** yielded the corresponding indoline products with good enantioselectivities. Finally, a 1.0-mmol scale enzymatic reaction using substrate 1-azido-2-isobutylbenzene **3.3e** bearing a tertiary C–H bond gave **3.4e** in 40% isolated yield.

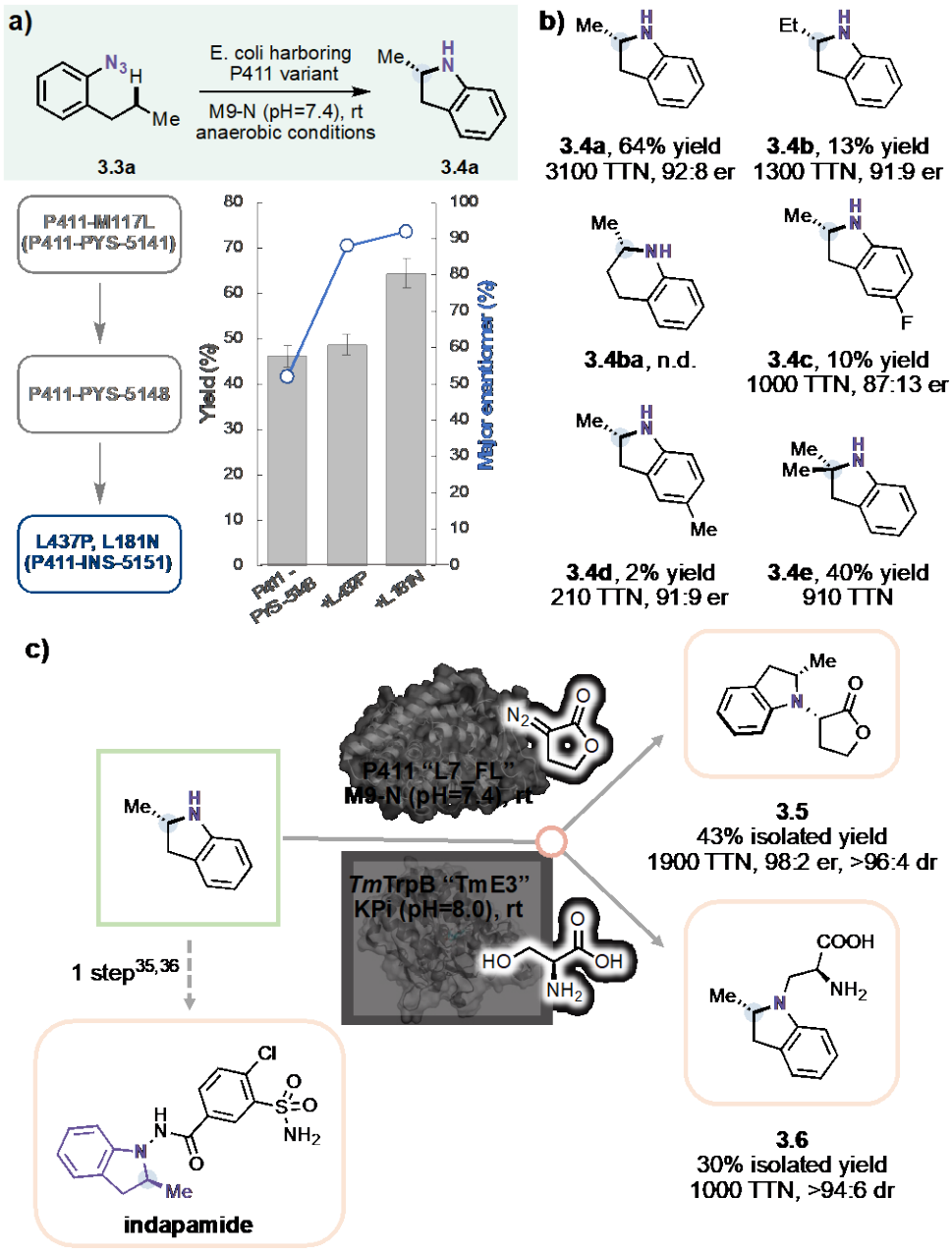

Figure 4.2. Directed evolution and substrate scope study for enantioselective aryl nitrene transfer: evolutionary trajectory for synthesis of methylindolines. a) **P411-INS-5151** was obtained after two

rounds of site-saturation mutagenesis and screening starting from **P411-PYS-5148** (See **Table C.S2** for sequence details). Indicated mutations are relative to **P411-PYS-5148**. Experiments were performed using *E. coli* (OD_{600} = 40) expressing enzymes with 5.0 mM substrate **3.3a** in M9-N buffer (pH = 7.4) at room temperature under anaerobic conditions overnight. Buffer was switched to M9-N (pH = 8.4) after condition optimization on **P411-INS-5151**. Yields were quantified by LC-MS based on the calibration curve of **3.4a**. Enantioselectivities were measured by HPLC on a chiral phase. b) Substrate scope of enantioselective aryl nitrene transfer reaction. Experiments were performed at analytical scale using *E. coli* (OD_{600} = 40) that expressed **P411-INS-5151** with 5 mM substrate (**3.3a–d**) and in M9-N buffer (pH = 8.4) at room temperature under anaerobic conditions for 16 h. Yields were quantified by LC-MS based on the calibration curves of the corresponding reference products. Enantioselectivities were measured by HPLC on a chiral phase. Reactions with **3.3e** were performed at 1-mmol scale using same condition as analytical scale reaction and yield was isolated yield. c) Further enzymatic elaboration of enzymatically produced methylindoline. Experiments were performed using *E. coli* (OD_{600} = 30) expressing P411 enzyme with 10 mM substrate **3.4a** in M9-N buffer (pH = 7.4) at room temperature under anaerobic conditions overnight. The experiment with tryptophan synthase was performed using purified enzyme with 10 mM **3.4a** in phosphate buffer (0.1 M, pH = 8.0) at room temperature overnight.

Versatile synthetic intermediates, *N*-heterocycles can be converted into various high-value-added compounds (for example, methylindoline product **3.4a** can be used in the synthesis of indapamide (**Figure 4.2c**)).[41,42] To demonstrate the utility of the engineered enzymes in constructing synthetically challenging molecules, we conducted two biocatalytic derivatization reactions, one to synthesize an α-amino ester and another to make a noncanonical amino acid, both bearing two chiral centers. Cytochrome P411 variant **L7_FL** from a carbene N−H insertion lineage[43] accepted methylindoline **3.4a** and a lactone-based diazo substrate in the form of whole-cell catalysts to provide the enantioenriched α-amino ester **5** in good yield with excellent enantioselectivity and diastereoselectivity (47% yield, 98:2 er and >96:4 dr). In a preparative scale reaction, the enzyme afforded α-amino ester **5** as a white solid with 43% yield and identical selectivities. In another demonstration, *Thermotoga maritima* tryptophan synthase (*Tm*TrpB) variant **TmE3** from a ketone alkylation lineage[44] coupled **3.4a** and L-serine to provide *N*-alkylated noncanonical amino acid **6** in 30% isolated yield with excellent diastereoselectivity (>94:6 dr). These biocatalytic derivatization reactions using engineered enzymes demonstrate how complexity can be built rapidly and under mild conditions for asymmetric synthesis of *N*-heterocycle-containing molecules.

To better understand the alkyl/aryl nitrene C(sp^3)–H insertion processes, density functional theory (DFT) calculations were carried out on a model iron-porphyrin system using substrates **3.1a** (**Figure C.S8**) and **3.3b** (**Figure C.S9**).[45] In agreement with previous results for enzymatic nitrene insertion reactions, transformations for both **3.1a** and **3.3b** proceed *via* three general steps (see **Figure C.S8** and **S9** for the full energy profiles): (1) nitrene formation and nitrogen extrusion, (2) hydrogen atom abstraction to initially generate a carbon-centered radical, and (3) radical rebound to form corresponding products **3.2a** and **3.4b**.[25,46] Interestingly, for alkyl azide substrate **3.1a**, the nitrogen extrusion step is computed to have a high energy barrier, reflecting the difficulty of activating alkyl azides to eliminate nitrogen at room temperature in a truncated system (**Figure 4.3b**, 24.6 kcal/mol vs. the subsequent HAT transition state of 13.5 kcal/mol).[26,46] Experimental observation reveals a non-competitive kinetic isotopic effect (KIE) of 1.4 and a competitive KIE of 3.2 (**Figure 4.3a**), which also indicates the HAT step might not be involved in the rate-determining step.

For the aryl azide substrate, this is reversed (**Figure 4.3b**). The HAT step (20.8 kcal/mol) has a higher barrier than the nitrogen extrusion step (18.0 kcal/mol); this is due to the 10 kcal/mol greater stability of the iron-arylnitrene intermediate verse the iron- alkynitrene intermediate. Thus, the arylnitrene species is both easier to form and less reactive. There is no significant barrier to cyclization of the diradical intermediate to cyclic amine in either case. We docked each transition state with the iron porphyrin coenzyme into the enzyme structure and performed 1 μs molecular dynamics simulations with the whole enzyme and a water box to obtain an equilibrium structure of the transition state and catalytic active site. These simulations indicate that no single residue contributes strong stabilizing interactions; the preferred enantiomeric transition state shape is complementary to the active site, while the antipodal transition state experiences significant destabilizing steric clashes (See **Figure C.S10**).

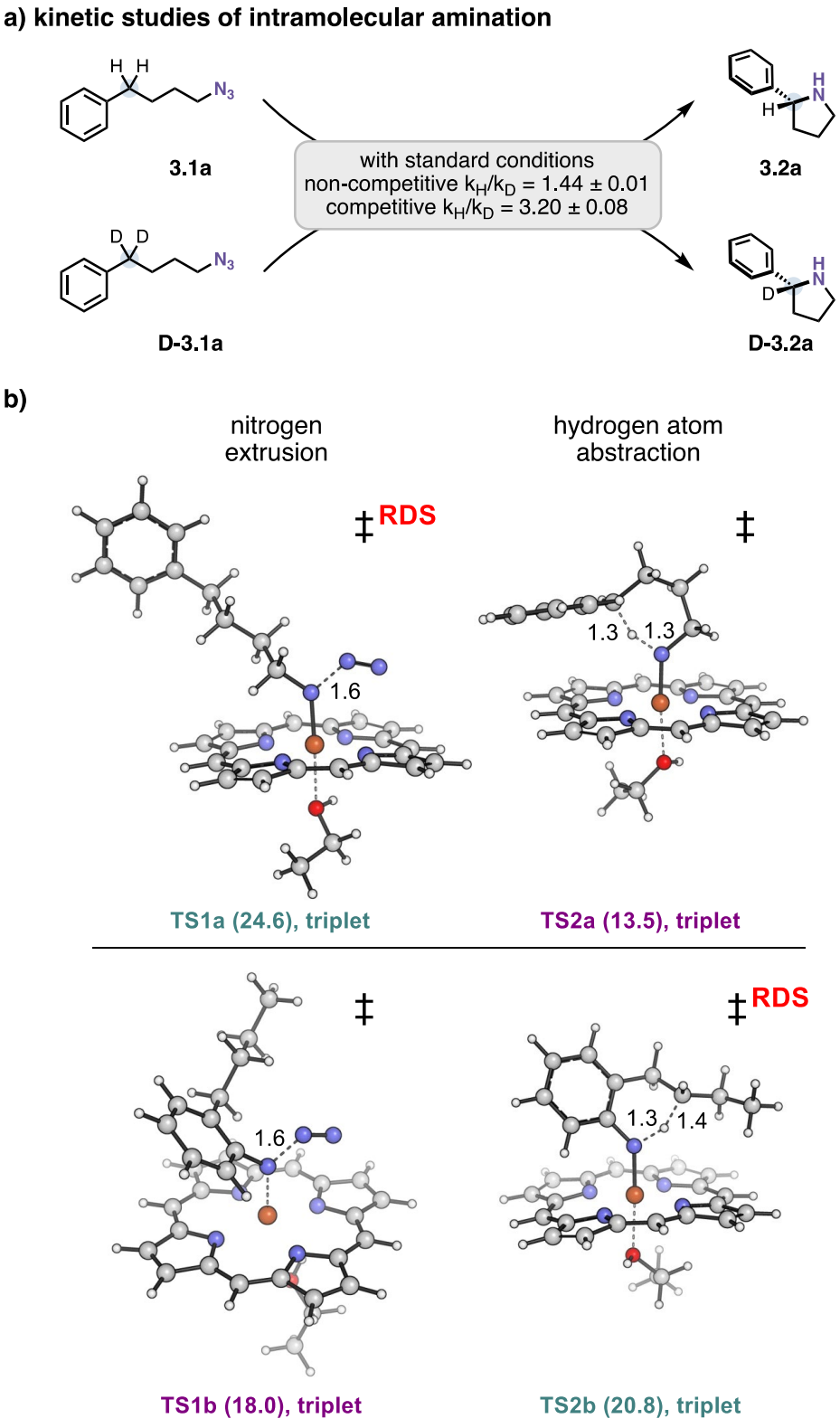

Figure 4.3. DFT-computed transition states for iron(II)-porphyrin-catalyzed intramolecular alkyl nitrene C(sp^3)–H amination using substrates **3.2a** and **3.4b**. Gibbs free energies are obtained at the

B3LYP(D3)/def2tzvp/CPCM(Et_2O)//B3LYP/6-31G(d),SDD(Fe)/ CPCM(Et_2O) level of theory, all in triplet state, and are given in kcal·mol^{-1}. Key distances are given in Å.

4.3 Conclusion

In conclusion, we have demonstrated new-to-nature enzyme-catalyzed intramolecular C(sp^3)–H amination *via* alkyl and aryl nitrene intermediates to forge two key classes of chiral *N*-heterocycles from simple azide precursors. This work represents the first example of enzymatic intramolecular alkyl/aryl nitrene C(sp^3)–H insertion reactions. Using directed evolution, we engineered two P411 variants, **P411-PYS-5149** and **P411-INS-5151**, which can catalyze pyrrolidine and indoline synthesis, respectively, in moderate to good efficiency and selectivity (up to 74% yield and 99:1 er). These new biocatalysts can be coupled with other biocatalytic transformations to construct complex molecules. DFT calculations suggest the selectivity is controlled by the binding pose of substrate inside the enzymes' active sites. This biocatalytic platform provides a general and concise route for the preparation of chiral *N*-heterocycles. More importantly, it lays a foundation for future work toward biocatalytic construction of *N*-heterocycles of different sizes and intermolecular alkyl and aryl nitrene C–H insertion reactions. We envision this alkyl/aryl nitrene C–H insertion system can be used to prepare chiral *N*-heterocyclic building blocks for synthetic chemistry and drug discovery.

4.4 Experimental Methods

General Procedure

Unless otherwise noted, all chemicals and reagents were obtained from commercial suppliers (Millipore Sigma, VWR, Alfa Aesar, Ambeed, Combi-Blocks, TCI America, and Fisher Scientific) and used without further purification. Silica-gel chromatography was carried out using AMD Silica Gel 60, 230–400 mesh. ^1H and ^{13}C NMR spectra were recorded on a Varian Inova 300 MHz or Bruker 400 MHz instrument in $CDCl_3$. Data for ^1H NMR are reported as follows: chemical shift (δ ppm), multiplicity (s = singlet, d = doublet, t = triplet, q = quartet, hept = heptet, m = multiplet), coupling constant (Hz), and integration. Chemical reactions were monitored using thin-layer chromatography (Merck 60 silica gel plates) and a UV lamp for visualization. Sonication was performed using a Qsonica Q500 sonicator. High-resolution mass spectra HRMS were

acquired from the Caltech Mass Spectral Facility using Field Desorption (FD-MS) with a JEOL AccuTOF GC-Alpha (JMS-T2000GC) mass spectrometer (enabled by funds from DOW next generation instrumentation). High-performance liquid-chromatography mass spectroscopy (HPLC-MS) for analysis was carried out using Agilent 1200 series instruments, with C18 (Kromasil®, 4.6 × 50 mm, 5 μm) columns. Water and acetonitrile containing 0.1% acetic acid were used as eluents. Normal-phase chiral HPLC was performed using Daicel Chiralpak IC column (4.6 × 250 mm, 5 μm) with hexane and isopropanol as the mobile phase. Distilled water was utilized for growth media while double-distilled water was employed for all buffer preparations.

The M9-N buffer described in this study was prepared as follows:

A 5X stock solution was prepared by dissolving Na_2HPO_4 (34 g), KH_2PO_4 (15 g) and NaCl (2.5 g) in 1 L of water followed by sterilization by autoclaving. A 1X stock was then prepared by diluting 200 mL of the 5X solution to 1 L, followed by addition of 1 mL $CaCl_2$ (0.1 M), 2 mL $MgSO_4$ (1.0 M), and adjusting the pH to 7.4 or 8.4 by the addition of 6.0 M aqueous NaOH.

In all cases, commercially available cyclic amines (Sigma, Enamine, Ambeed, Combi-Blocks) were utilized as amine standards without further purification. These were acetylated with benzoyl chloride to give the corresponding acetyl amides for use as amide standards for enantioselectivity.

Cloning, Mutagenesis, and Expression of Enzymes

Expression vector pET22b(+) (Novagen) was used for cloning and expression of all variants described in this paper. Site-saturation mutagenesis was performed using a modified QuikChangeTM mutagenesis protocol using the 22-codon trick.[1] The PCR products were purified with New England Biolabs gel purification kit, and the gaps were repaired using Gibson Mix™.[2] Without further purification, 1 μL of the Gibson product was used to transform 50 μL of electrocompetent *Escherichia coli* cells. Electrocompetent *E. coli* BL21 *E. cloni*® (Lucigen) cells were utilized for all experiments. Luria-Bertani (LB) media were used for growth.

E. coli transformed with pET22b(+) constructs encoding various P411 variants were grown overnight (14 h to 16 h) in 5-mL LB medium supplemented with ampicillin (LB_{amp}). Subsequently, 1 mL of this preculture was used to inoculate 49 mL of Hyper-Broth™ (HB, AthenaES) medium in a 150-mL Erlenmeyer flask, supplemented with ampicillin (HB_{amp}) and Glucose Mix for expression. The expression culture was incubated at 37 °C and shaken at 220 rpm for 2 hours until the optical cell density at 600 nm (OD_{600}) was ~0.9–1.1. Then, the expression culture was cooled in an ice bath for 45–60 minutes and was treated with 1 mM 5-aminolevulinic acid (ALA) and 0.5 mM isopropyl *β*-D-1-thiogalactopyranoside (IPTG) (final concentrations). Cells were grown at 22 °C and 140 rpm for 20–24 hours, and the shaking radius was 25 mm. Once expression was finished, the cultures were centrifuged (4,000*g*, 6 minutes, 4 °C) and the pellets were resuspended to an OD_{600} of 30–40 (or other appropriate OD as necessary) in M9-N buffer with pH adjusted to 8.4. This cell suspension was utilized to setup whole-cell reactions. Aliquots of the cell suspension (3–4 mL) were used to determine protein concentration after lysis by sonication.

Determination of Hemoprotein Concentration

The concentration of P411 enzymes in whole-cell experiments was determined from ferrous carbon monoxide binding difference spectra using the previously reported extinction coefficient for serine-ligated enzymes ($\varepsilon = 103{,}000\ M^{-1}\bullet cm^{-1}$).[3] Lysate was obtained by sonication (2 minutes, 1 second on, 1 second off, 30% amplitude, on wet ice). The cell debris was removed by centrifugation (14,000 × g, 10 minutes, 4 °C), and 180 µL of the supernatant were then transferred to a well in a 96-well UV-vis flat bottom plate (measurements were performed in quadruplicate). To each well, 20 µL of freshly prepared 0.5 M sodium dithionite aqueous solution were added. Absorbance measurements were performed on a Tecan Spark instrument before and after CO binding. The following formula was used for estimating protein concentration.

$$[Enzyme]\ (\mu M) = 1.1 * \frac{\Delta 411_{CO-red} - \Delta 490_{CO-red}}{0.74\,cm * 0.103\,\mu M^{-1} cm^{-1}}$$

Analytic Reaction Setup and Product Quantification

All biocatalytic reactions were set up in an anaerobic chamber (oxygen level: <40 ppm).

For pyrrolidine construction, 300 μL of resuspended cells (diluted to OD_{600} = 40 with M9-N minimal buffer, pH = 8.4) were added to 2-mL screw cap vials, followed by addition of D-glucose (90 μL, 500 mM in M9-N buffer), M9-N buffer, and the azide substrate (10 μL of 100 mM stock solution in EtOH). Final concentrations were 2.5 mM alkyl azide and 112.5 mM D-glucose; final reaction volume was 400 μL. The vials were capped and then shaken inside coy chamber (600 rpm) at room temperature for 12–20 hours (overnight). After the reaction was completed and the vials were removed from the shaker, 400 μL of 2.5 mM internal standard (ethyl benzoate) acetonitrile solution were added. The mixture was transferred to a 2.0-mL Eppendorf tube and then subjected to vortexing (20 s × 2) and centrifugation (14,000 × g, 5 min, 4 °C). A sample of the supernatant (0.2 mL) was transferred to a vial with an insert for LC-MS analysis. Products were identified and quantified based on the corresponding reference compounds (**Section V** and **VI**). To further determine the enantiomeric excess (*ee*), the remaining supernatants of three parallel analytical reactions were combined and transferred to a 2-dram vial and the solvent was removed by blowing air. To the remaining residues from air blowing were added benzoyl chloride (60 μL of 1 M stock solution in acetonitrile) and 60 μL saturated $NaHCO_3$ solution. After shaking the vials overnight, the benzoyl-protected pyrrolidines were extracted to a solution of hexane and EtOAc mixture (1:1) and subjected to normal-phase HPLC to determine the *ee*.

For indoline construction, 360 μL of resuspended cells (diluted to OD_{600} = 45 with M9-N minimal buffer, pH = 8.4) were added to 2-mL screw cap vials, followed by D-glucose (30 μL, 500 mM in M9-N buffer), M9-N buffer the azide substrate (10 μL of 200 mM stock solution in EtOH). Final concentrations were 5.0 mM alkyl azide and 37.5 mM D-glucose; final reaction volume was 400 μL. The vials were capped and then shaken inside coy chamber (600 rpm) at room temperature for 12–20 hours (overnight). After the reaction was completed and the vials were removed from the shaker, 400 μL of 5.0 mM internal standard (1,2,3-trimethoxylbenzene) acetonitrile solution were added. The mixture was transferred to a 2.0-mL Eppendorf tube and then subjected to vortexing (20 s × 2) and centrifugation (14,000 × g, 5 min, 4 °C). A sample of the supernatant (0.2 mL) was transferred to a vial with an insert for LC-MS analysis. Products were

identified and quantified based on the corresponding reference compounds (**Section V** and **VI**). To further determine the enantiomeric excess (*ee*), the remaining supernatants of three parallel analytical reactions were combined and transferred to a 2-dram vial and the solvent was removed by blowing air. After shaking the vials for 1 hour, the indolines were extracted to a solution of hexane and EtOAc mixture (1:1) and subjected to normal-phase HPLC to determine the *ee*.

Reaction Screening in 96-Well Plate in Whole-Cell Format

After a single-site saturation mutagenesis (SSM) library was generated, 88 single colonies were randomly picked and cultured in 300 μL of LB medium with 0.1 mg/mL ampicillin (LB_{amp}) in a sterilized 96-well culture plate. The plate typically contained six wells inoculated with single colonies expressing the parent enzyme and two sterile wells. The cultures were grown at 37 °C, 250 rpm, and 80% relative humidity for 13–15 hours. A separate, sterilized 96-well culture plate was filled with 950 μL of Hyperbroth medium containing 0.1 mg/mL ampicillin (HB_{amp}) in each well. Likewise, a glycerol stock replica plate of the preculture (50 μL of preculture added to 50 μL of 50% glycerol per well) was also prepared and stored at -80 °C for future reference. The plate with HB_{amp} was inoculated with the LB preculture (50 μL/well), and incubated at 37 °C, 250 rpm, and 80% relative humidity for 2.5 hours. The plate was cooled on ice for 1 hour, induced with 0.5 mM IPTG and 1 mM ALA (final concentrations), and then expressed at 22 °C and 220 rpm for 21–23 hours. The cells were pelleted (4,000*g*, 6 minutes), and after removal of the supernatant, 390 μL of M9-N (pH 7.4, 20 mM D-glucose) were added to each well. After the cell pellets were fully resuspended by shaking at 500 rpm, the 96-well plate was transferred to an anaerobic chamber. Inside the anaerobic chamber, to each well were added 10 μL of a reactant stock solution in ethanol (100 or 200 mM stock solution, 2.5 or 5.0 mM final concentration). The plate was sealed with aluminum foil tape and shaken at 600 rpm in the anaerobic chamber at room temperature overnight.

Once the plate was taken out of the anaerobic chamber and the seal was removed, ethanol (400 μL/well) was added. The resulting suspension in the wells was mixed by vortexing and shaking. The plate was then centrifuged (5,000*g*, 5 minutes) to precipitate proteins and cell debris. The supernatant (200 μL/well) was transferred to a shallow 96-well plate for reverse-phase HPLC-MS analysis. The MS product signals from each well were compared, and wells showing signals higher than the parent wells were identified. These ‘hits’ were recultured using the wells from the

frozen replica glycerol stock plate and then sequenced. Among these, the activities of candidates showing mutations at the targeted site were revalidated in analytical scale reactions. In this way, the best variant was selected as the final hit and was used as the parent for the next round of site-saturation mutagenesis.

4.5 References

(1) O'Hagan, D. Pyrrole, Pyrrolidine, Pyridine, Piperidine and Tropane Alkaloids. *Nat. Prod. Rep.* **2000**, *17*, 435–446.

(2) Nakamura, I.; Yamamoto, Y. Transition-Metal-Catalyzed Reactions in Heterocyclic Synthesis. *Chem. Rev.* **2004**, *104*, 2127–2198.

(3) Vitaku, E.; Smith, D. T.; Njardarson, J. T. Analysis of the Structural Diversity, Substitution Patterns, and Frequency of Nitrogen Heterocycles Among U.S. FDA Approved Pharmaceuticals. *J. Med. Chem.* **2014**, *57*, 10257–10274.

(4) Goldberg, F. W.; Kettle, J. G.; Kogej, T.; Perry, M. W. D.; Tomkinson, N. P. Designing Novel Building Blocks Is an Overlooked Strategy to Improve Compound Quality. *Drug Discov. Today* **2015**, *20*, 11–17.

(5) Li Petri, G.; Raimondi, M. V.; Spanò, V.; Holl, R.; Barraja, P.; Montalbano, A. Pyrrolidine in Drug Discovery: A Versatile Scaffold for Novel Biologically Active Compounds. *Top. Curr. Chem.* **2021**, *379*, 1–46.

(6) Katoh, A.; Hashimoto, T. Molecular Biology of Pyridine Nucleotide and Nicotine Biosynthesis. *Front. Biosci.* **2004**, *9*, 1577–1586.

(7) Hotti, H.; Seppänen-Laasko, T.; Arvas, M.; Teeri, T. H.; Rischer, H. Polyketide Synthases from Poison Hemlock (*Conium Maculatum L.*). *FEBS J.* **2015**, *16*, 4141–4156.

(8) Hameed, A.; Javed, S.; Noreen, R.; Huma, T.; Iqbal, S.; Umbreen, H.; Gulzar, T.; Farooq, T. Facile and Green Synthesis of Saturated Cyclic Amines. *Molecules* **2017**, *22*, 1691–1713.

(9) Iizaka, Y.; Sherman, D. H.; Anzai, Y. An Overview of the Cytochrome P450 Enzymes that Catalyze the Same-Site Multistep Oxidation Reactions in Biotechnologically Relevant Selected Actinomycete Strains. *Appl. Microbiol. Biotechnol.* **2021**, *105*, 2647–2661.

(10) Berglund, P.; Guo, F. Transaminase Biocatalysis: Optimization and Application. *Green Chem.* **2017**, *19*, 333–360.

(11) Schrittwieser, J. H.; Velikogne, S.; Kroutil, W. Biocatalytic Imine Reduction And Reductive Amination of Ketones. *Adv. Synth. Catal.* **2015**, *357*, 1655–1685.

(12) Mangas-Sanchez, J.; France, S. P.; Montgomery, S. L.; Aleku, G. A.; Man, H.; Sharma, M.; Ramsden, J. I.; Grogan, G.; Turner, N. Imine Reductases (IREDs) *Curr. Opin. in Chem. Biol.* **2017**, *37*, 19–25.

(13) Gilio, A. K.; Thorpe, T. W.; Heyam, A.; Petchey, M. R.; Pogrányi, B.; France, S. P.; Howard, R. M.; Karmilowicz, M. J.; Lewis, R.; Turner, N.; Grogan, G. A Reductive Aminase Switches to Imine Reductase Mode for a Bulky Amine Substrate. *ACS Catal.* **2023**, *13*, 1669–1677.

(14) Zhang, Y.-H.; Chen, F.-F.; Li, B.-B.; Zhou, X.-Y.; Chen, Q.; Xu, J.-H.; Zheng, G.-W. Stereocomplementary Synthesis of Pharmaceutically Relevant Chiral 2-Aryl-Substituted Pyrrolidines Using Imine Reductases. *Org. Lett.* **2020**, *22*, 3367–3372.

(15) Mitsukura, K.; Suzuki, M.; Tada, K.; Yoshida, T.; Nagasawa, T. Asymmetric Synthesis of Chiral Cyclic Amine from Cyclic Imine by Bacterial Whole-Cell Catalyst of Enantioselective Imine Reductase. *Org. Biomol. Chem.* **2010**, *8*, 4533–4535.

(16) Ye, Y.; Cao, J.; Oblinsky, D. G.; Verma, D.; Prier, C. K.; Scholes, G. D.; Hyster, T. K. Using Enzymes to Tame Nitrogen-Centred Radicals for Enantioselective Hydroamination. *Nat. Chem.* **2023**, *15*, 206–212.

(17) Gandeepan, P.; Müller, T.; Zell, D.; Cera, G.; Warratz, S.; Ackermann, L. 3d Transition Metals for C−H Activation. *Chem. Rev.* **2019**, *119*, 2192−2452.

(18) Munnuri, S.; Adebesin, A. M.; Paudyal, M. P.; Yousufuddin, M.; Dalipe, A.; Falck, J. R. Catalyst-Controlled Diastereoselective Synthesis of Cyclic Amines *via* C–H Functionalization. *J. Am. Chem. Soc.* **2017**, *139*, 18288–18294.

(19) Qin, J.; Zhou, Z.; Cui, T.; Hemming, M.; Meggers, E. Enantioselective Intramolecular C–H Amination of Aliphatic Azides by Dual Ruthenium and Phosphine Catalysis. *Chem. Sci.* **2019**, *10*, 3202–3207.

(20) Iovan, D. A.; Wilding, M. J. T.; Baek, Y.; Hennessy, E. T.; Betley, T. A. Diastereoselective C–H Bond Amination for Disubstituted Pyrrolidines. *Angew. Chem. Int. Ed.* **2017**, *56*, 15599–15602.

(21) Dong, Y.; Lund, C. J.; Porter, G. P.; Clarke, R. M.; Zheng, S.-L.; Cundari, T. R.; Betley, T. A. Enantioselective C–H Amination Catalyzed by Nickel Iminyl Complexes Supported by Anionic Bisoxazoline. *J. Am. Chem. Soc.* **2021**, *2*, 817–829.

(22) Meunier, B.; de Visser, S. P.; Shaik, S. Mechanism of Oxidation Reactions Catalyzed by Cytochrome P450 Enzymes. *Chem. Rev.* **2004**, *104*, 3947–3980.

(23) Liu, Z.; Arnold, F. H. New-to-Nature Chemistry from Old Protein Machinery: Carbene and Nitrene Transferases. *Curr. Opin. in Biotech.* **2021**, *69*, 43–51.

(24) Yang, Y.; Arnold, F. H. Navigating the Unnatural Reaction Space: Directed Evolution of Heme Proteins for Selective Carbene and Nitrene Transfer. *Acc. Chem. Res.* **2021**, *54*, 1209–1225.

(25) Yang, Y.; Cho, I.; Qi, X.; Liu, P.; Arnold, F. H. An Enzymatic Platform for the Asymmetric Amination of Primary, Secondary and Tertiary C(Sp^3)–H Bonds. *Nat. Chem.* **2019**, *11*, 987–993.

(26) Athavale, S. V.; Gao, S.; Liu, Z.; Mallojjala, S. C.; Hirschi, J. S.; Arnold, F. H. Biocatalytic Intermolecular C–H Bond Functionalization for the Synthesis of Enantioenriched Amides. *Angew. Chem. Int. Ed.* **2021**, *60*, 24864–24869.

(27) Liu, Z.; Qin, Z.-Y.; Zhu, L.; Athavale, S. V.; Sengupta, A.; Jia, Z.-J.; Garcia-Borràs, M.; Houk, K. N.; Arnold, F. H. An Enzymatic Platform for Primary Amination of 1-Aryl-2-Alkyl Alkynes. *J. Am. Chem. Soc.* **2022**, *144*, 80–85.

(28) Athavale, S. V.; Gao, S.; Das, A.; Mallojjala, S. C.; Alfonzo, E.; Long, Y.; Hirschi, J. S.; Arnold, F. H. Enzymatic Nitrogen Insertion into Unactivated C–H Bonds. *J. Am. Chem. Soc.* **2022**, *144*, 19097–19105.

(29) Singh, R.; Kolev, J. N.; Sutera, P. A.; Fasan, R. Enzymatic C(sp^3)–H Amination: P450-Catalyzed Conversion of Carbonazidates into Oxazolidinones. *ACS Catal.* **2015**, *5*, 1685–1691.

(30) Dydio, P.; Key, H. M.; Hayashi, H.; Clark, D. S.; Hartwig, J. F. Chemoselective, Enzymatic C–H Bond Amination Catalyzed by a Cytochrome P450 Containing an Ir(Me)-PIX Cofactor. *J. Am. Chem. Soc.* **2017**, *139*, 1750–1753.

(31) Steck, V.; Kolev, J. N.; Ren, X.; Fasan, R. Mechanism-Guided Design and Discovery of Efficient Cytochrome P450-Derived C–H Amination Biocatalysts. *J. Am. Chem. Soc.* **2020**, *142*, 10343–10357.

(32) Stroek, W.; Keilwerth, M.; Pividori, D. M.; Meyer, K.; Arecht, M. An Iron–Mesoionic Carbene Complex for Catalytic Intramolecular C–H Amination Utilizing Organic Azides. *J. Am. Chem. Soc.* **2021**, *143*, 20157–20165.

(33) Wang, S.; Yuan, X.-H.; Wang, S.-Q.; Zhao, W.; Chen, X.-B.; Yu, B. FDA-Approved Pyrimidine-Fused Bicyclic Heterocycles for Cancer Therapy: Synthesis and Clinical Application. *Eur. J. Med. Chem.* **2021**, *214*, 113218–113239.

(34) Ji, M.; Liu, H.; Zong, X.; Li, R.; Wan, G.; Wang, D.; Yang, S.; Yu, W.; Zhang, Y.; Hu, H. Preparation Method of larotrectinib and Intermediate of larotrectinib. CN107987082A, May 4, **2018**.

(35) Arnold, F. H. Directed Evolution: Bringing New Chemistry to Life. *Angew. Chem., Int. Ed.* **2018**, *57*, 4143−4148.

(36) Zhang, R. K.; Chen, K.; Huang, X.; Wohlschlager, L.; Renata, H.; Arnold, F. H. Enzymatic Assembly of Carbon−Carbon Bonds *via* Iron-Catalysed sp^3 C−H Functionalization. *Nature* **2019**, *565*, 67−72.

(37) Röthlisberger, D.; Khersonsky, O.; Wollacott, A. M.; Jiang, L.; DeChancie, J.; Betker, J.; Gallaher, J. L.; Althoff, E. A.; Zanghellini, A.; Dym, O.; Albeck, S.; Houk, K. N.; Tawfik, D. S.; Baker, D. Kemp Elimination Catalysts by Computational Enzyme Design. *Nature* **2008**, *453*, 190−195.

(38) Zeeli, S.; Weill, T.; Finkin-Groner, E.; Bejar, C.; Melamed, M.; Furman, S.; Zhenin, M.; Nudelman, A.; Weinstock, M. Synthesis And Biological Evaluation of Derivatives of Indoline As Highly Potent Antioxidant and Anti-Inflammatory Agents. *J. Med. Chem.* **2018**, *9*, 4004–4019.

(39) Blunt, J. W.; Copp, B. R.; Keyzers, R. A.; Munro, M. H. G.; Prinsep, M. R. Marine Natural Products. *Nat. Prod. Rep.* **2017**, *34*, 235–294.

(40) Alt, I. T.; Guttroff, C.; Plietker, B. Iron-Catalyzed Intramolecular Aminations of C(sp^3)–H Bonds in Alkyl Aryl Azides. *Angew. Chem. Int. Ed.* **2017**, *56*, 10582–10586.

(41) Bataillard, A.; Schiavi, P.; Sassard, J. Pharmacological Properties of indapamide. *Clinical Pharmacokinetics*, **1999**, *37*, 7–12.

(42) Cai, Z. Synthesis Method of indapamide. CN112142643, October 10, **2020**.

(43) Liu, Z.; Calvó-Tusell, C.; Zhou, A. Z.; Chen, K.; Garcia-Borràs, M.; Arnold, F. H. Dual-Function Enzyme Catalysis for Enantioselective Carbon–Nitrogen Bond Formation. *Nat. Chem.* **2021**, *13*, 1166–1172.

(44) Watkins-Dulaney, E. J.; Dunham, N. P.; Straathof, S.; Turi, S.; Arnold, F. H.; Buller, A. R. Asymmetric Alkylation of Ketones Catalyzed by Engineered TrpB. *Angew. Chem. Int. Ed.* **2021**, *60*, 21412–21417.

(45) Shaw, D. E.; Grossman, J. P.; Bank, J. A.; Baston B.; Butts, J. A.; Chao, J. C.; Deneroff, M. M.; Dror, R. O.; Even, A.; Fenton, C. H.; Forte, A.; Gagliardo, J.; Gill, G.; Greskamp, B.; Ho, C. R.; Ierardi, D. J.; Iserovich, L.; Kuskin, J. S.; Larson, R. H.; Layman, T.; Lee, L.-S.; Lerer, A. K.; Li, C.; Killebrew, D.; Mackenzie, K. M.; Mok, S. Y.-H.; Moraes, M. A.; Mueller, R.; Nociolo L. J.; Peticolas, J. L.; Quan, T.; Ramot, D.; Salmon, J. K.; Scarpazza, D. P.; Schafer, U. B.; Siddique, N.; Snyder, C. W.; Spengler, J.; Tang, P. T. P.; Theobald, M.; Toma, H.; Towles, B.; Vitale, B.; Wang, S. C.; Young, C. Anton 2: Raising the Bar for Performance and Programmability in a Special-Purpose Molecular Dynamic Supercomputer. In *SC14: International Conferene for High Performance Computing, Networking, Storage and Analysis; IEEE*: New Orleans, LA, USA, **2014**, 41–53.

(46) Wang, J.; Gao, H.; Yang, L.; Gao Y. Q. Role of Engineered Iron-Haem Enzyme in Reactivity and Stereoselectivity of Intermolecular Benzylic C–H Bond Amination. *ACS Catal.* **2020**, *10*, 5318–5327.

Appendix C. Supplementary Information for Chapter IV

I. Directed Evolution of P411-PYS-5149 and P411-INS-5151 for Intramolecular C(sp^3)–H Amination

Discovery of Initial Activity

The Arnold lab collection of heme enzymes (including P450s, P411s, protoglobins, and cytochromes *c*) was screened in 96-well-plate whole-cell reactions for product formation (see Section I.E.). The collection consisted of nearly 400 distinct variants accumulated from prior directed evolution campaigns. For pyrrolidine synthesis, one variant from a previous carbene transferring lineage showed the highest product formation as assayed by LCMS. For indoline synthesis, the pyrrolidine synthase lineage showed the most promising results, and the 7th generation showed highest activity as assayed by LCMS. No product was detected in control reactions with free heme.

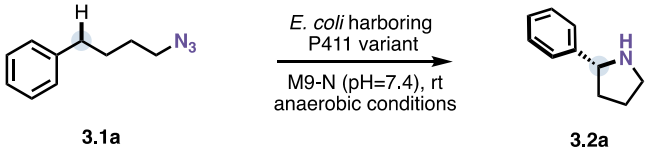

3.1a **3.2a**

Pyrrolidine synthesis variants showing product formation:

Variant	Ion Count
P450-BM3 (WT)	0
P411-A330Y	2786747
P411-M177L	4420892

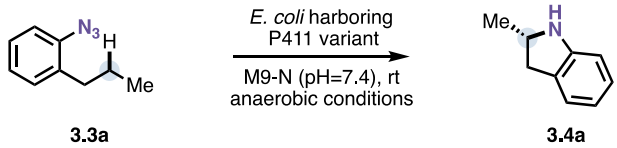

3.3a **3.4a**

Indoline synthesis variants showing product formation:

Variant	Ion Count
P450-BM3 (WT)	0
P411-PYS-5146	2027686
P411-PYS-5148	8380970

Table C.S1. Detailed information of the evolutionary lineage for **PY**rrolidine **S**ynthase (**PYS**).

P411-PYS variant	**Yield (%)**	***er***
P411-M177L (**P411-PYS-5141**)	4 ± 0.8	84:16
P411-PYS-5141- L75E (**P411-PYS-5142**)	13 ± 0.2	91:9
P411-PYS-5141- L75E Q437L (**P411-PYS-5143**)	13 ± 1.0	90:10
P411-PYS-5141- L75E Q437L A330Q (**P411-PYS-5144**)	20 ± 0.9	91:9
P411-PYS-5141- L75E Q437L A330Q M118V(**P411-PYS-5145**)	29 ± 1.6	93:7
P411-PYS-5141- L75E Q437L A330Q M118V F77C (**P411-PYS-5146**)	31 ± 1.0	91:9
P411-PYS-5141- L75E Q437L A330Q M118V F77C S72W (**P411-PYS-5147**)	53 ± 0.6	90:10
P411-PYS-5141- L75E Q437L A330Q M118V F77C S72W Q73A (**P411-PYS-5148**)	54 ± 1.6	91:9
P411-PYS-5141- L75E Q437L A330Q M118V F77C S72W Q73A L436R (**P411-PYS-5149**)	66 ± 3.5	91:9

Table C.S2. Detailed information of the evolutionary lineage for **IN**doline **S**ynthase (**INS**).

P411-INS variant	**Yield (%)**	***er***
P411-PYS-5148	46 ± 3.2	51:49
P411-PYS-5148- L437P (**P411-INS-5150**)	49 ± 1.7	88:12
P411-PYS-5148- L437P L181N (**P411-INS-5151**)	52 ± 1.0	91:9

Table C.S3. Further information on directed evolution experiments.

Round #	**Parent**	**Sites targeted for SSM**	**Screen for activity or enantioselectivity**
1	**P411-PYS-5141**	75X	**activity**
2	**P411-PYS-5142**	78X, 87X, 263X, 268X, 327X, 328X, **437X**	**activity**
3	**P411-PYS-5143**	86X, 267X, **330X**, 400X	**activity**
4	**P411-PYS-5144**	82X, **118X**, 181X, 395X, 438X, 401X	**activity**
5	**P411-PYS-5145**	**77X**, 177X 266X, 326X, 409X, 436X	**activity**
6	**P411-PYS-**	**72X**, 88X, 162X,	**activity**

	5146	264X, 333X, 435X	
7	**P411-PYS-5147**	70X, 71X, **73X**, 74X, 76X, 178X, 269X, 331X, 332X	**activity**
8	**P411-PYS-5148**	87X, 267X, 268X, 327X, **436X**, 437X	**activity**
9	**P411-PYS-5148 (for indoline synthesis)**	87X, 267X, 268X, 327X, 436X, **437X**	**both**
10	**P411-INS-5149**	72X, 78X, 82X, **181X**, 188X, 438X	**both**

II. Supporting Experimental Figures and Miscellaneous Experiments

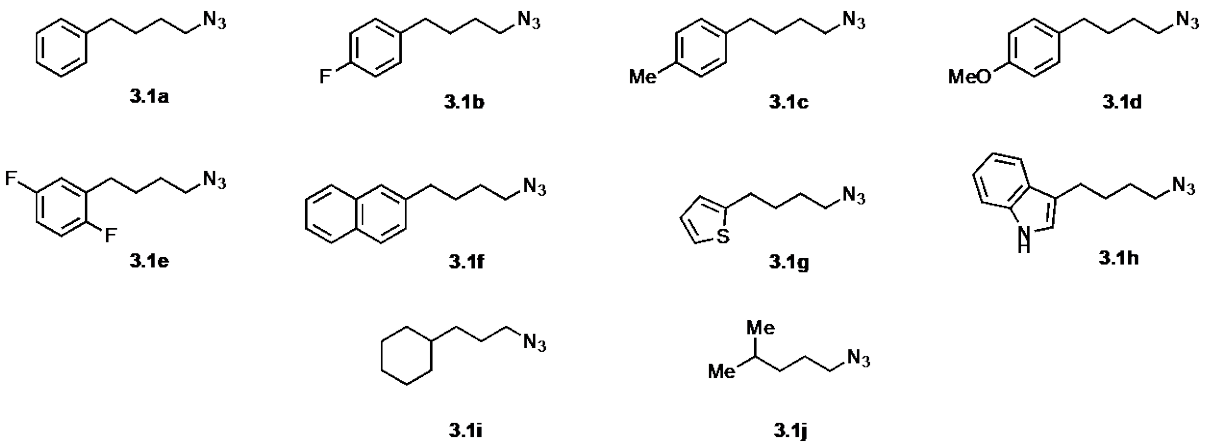

Figure C.S1. Summary of alkyl azide substrates (**3.1a**–**3.1j**).

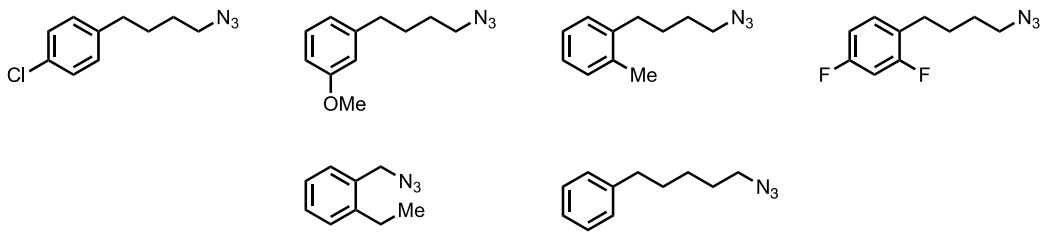

Figure C.S2. Other substrates tested for intramolecular alkyl nitrene C(sp^3)–H amination reaction.

Notes: The alkyl azide substrates listed here have been tested briefly for the intramolecular C(sp^3)–H amination chemistry catalyzed by **P411-PYS-5149**. However, these substrates only gave low activity, as preliminarily analyzed by LC-MS and chiral HPLC. These results are noteworthy, but they cannot be used for drawing final conclusions before further validation.

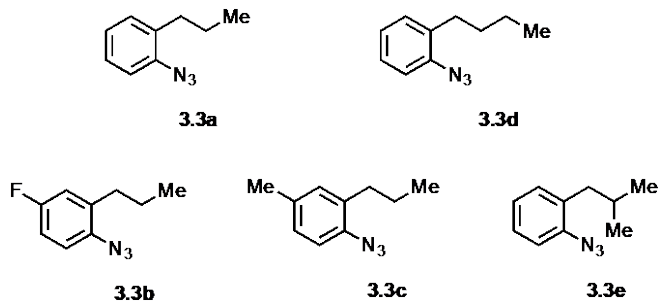

Figure C.S3. Summary of aryl azide substrates (**3.3a**–**3.3j**).

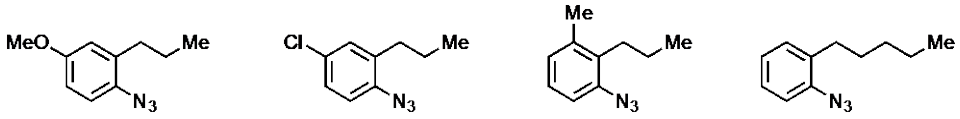

Figure C.S4. Other substrates tested for intramolecular aryl nitrene C(sp^3)–H amination reaction.

Notes: The aryl azide substrates listed here have been tested briefly for the intramolecular C(sp^3)–H amination chemistry catalyzed by **P411-INS-5151**. However, these substrates only gave low activity, as preliminarily analyzed by LC-MS and chiral HPLC. These results are noteworthy, but they cannot be used for drawing final conclusions before further validation.

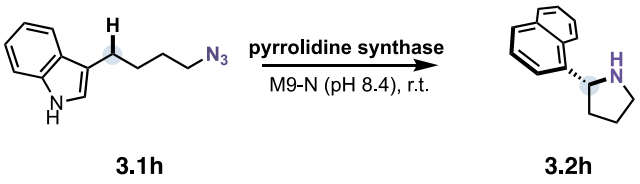

3.1h **3.2h**

P411-PYS-5149	41% yield, 52:48 er
P411-PYS-5148	60% yield, 51:49 er

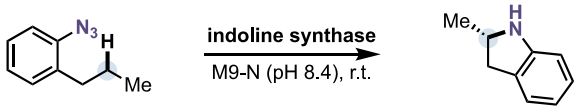

3.3a **3.4a**

P411-INS-5151 (OD 40)	64% yield, 3100 TTN, 92:8 er
P411-INS-5151_V184M (OD 60)	40% yield, 3200 TTN, 95:5 er

Figure C.S5. Variants that showed improved activity or selectivity for examples **3.1h** and **3.3a**.

Notes: Variant **P411-PYS-5148 (CA-G7)** is the seventh generation of 'pyrrolidine synthase' lineage. Variant **P411-INS-5151_V184M** has one mutation (V184M) relative to **P411-INS-5151 (AN-G2)**.

III. Kinetic Isotope Effect (KIE) Studies

From a freshly streaked plate of *E. coli.* cells with the **P411-PYS-5149** plasmid, two single colonies were inoculated into two separate, 4-mL LB media tubes for ~14 h at 37 ºC. These were utilized for duplicate experiments. After growing the overnight culture for ~14 h, 1 mL of the starter culture was transferred to 49 mL HB media (supplemented with Ampicillin and Glucose Mix) in a 150-mL Erlenmeyer flask and grown with vigorous shaking at 37 ºC (230 rpm) for 2 h, by which time the cell optical density (OD_{600}) was 0.8 to 1.0. The flask was chilled on ice for 45 min. ALA (1 mM) and IPTG (0.5 mM) were supplemented, and the flask shaken at 22 ºC (140 rpm) for 22 h. The culture was centrifuged (4,000g, 6 min), and the cell pellets were resuspended in 12 mL of M9-N buffer (pH 8.4) to give a suspension with OD_{600}~40. All manipulations were done on ice. Reaction setup follows the standard procedure mentioned in **Section I (D)**.

• Calibration curve of non-deuterated product **3.2a** at low yields (using ion count in single-mass channel to quantify)

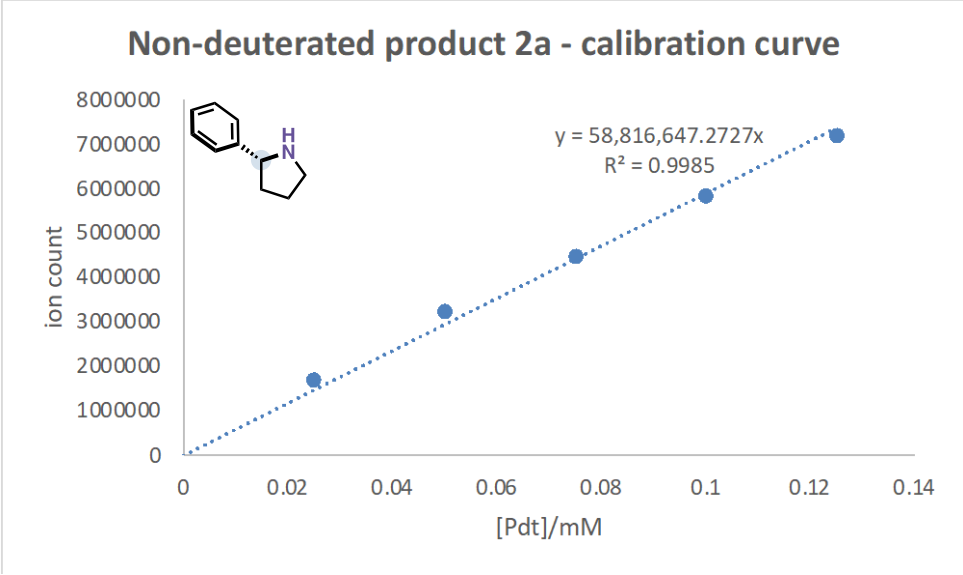

• Non-competitive KIE Experiments

Entry	Subs	Ion Count			Yield (%)			$K_{H/D}$	KIE (K_H/K_D)
		30 s	60 s	90 s	30 s	60 s	90 s		

1	H-**3.1a**	146156	247766	176056	0.099	0.169	0.220	0.00261	1.43
	D-**3.1a**	100606	176056	224437	0.068	0.120	0.153	0.00182	
2	H-**3.1a**	161435	267685	353785	0.110	0.182	0.241	0.00285	1.45
	D-**3.1a**	105536	190294	240509	0.072	0.129	0.164	0.00196	

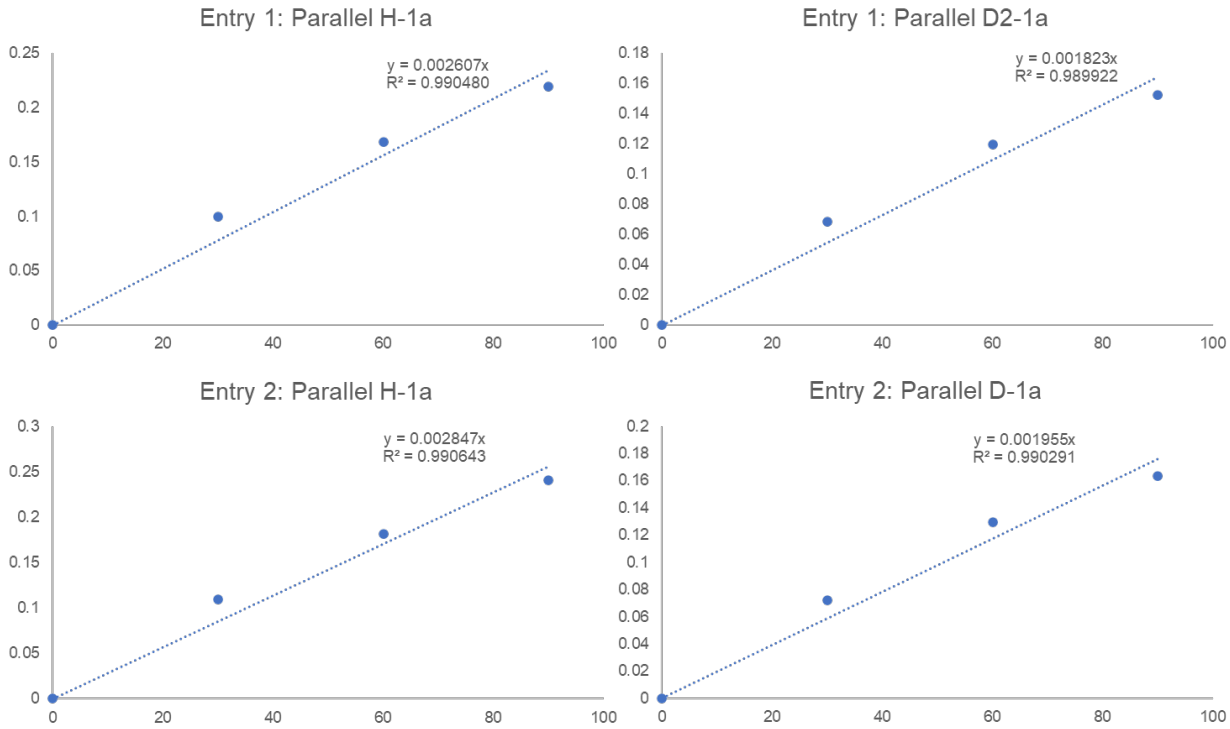

Figure C.S6. Duplicate of non-competitive kinetic isotope effect (KIE) experiments.

• Competitive KIE Experiments

Entry	Subs	Ion Count			Yield (%)			$K_{H/D}$	KIE (K_H/K_D)
		30 s	60 s	90 s	30 s	60 s	90 s		
1	1:1 H/D-**3.1a**	167110	276341	367201	0.114	0.188	0.250	0.00295	3.14
		56674	87321	116399	0.039	0.059	0.079	0.00094	
2	1:1	182657	290499	382915	0.124	0.198	0.260	0.00310	3.26

	H/D-**3.1a**	42133	91205	120526	0.028	0.062	0.082	0.00095	

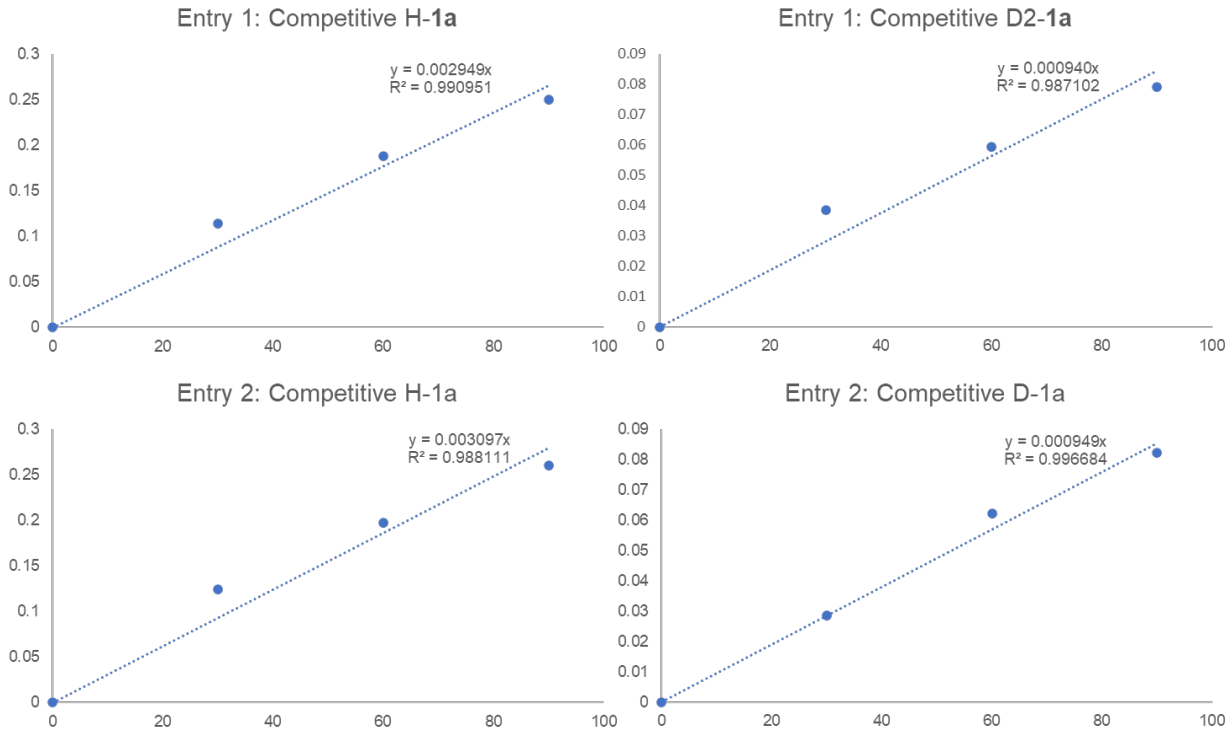

Figure C.S7. Duplicate of competitive kinetic isotope effect (KIE) experiments.

• KIE Experiments Summary

Entry		KIE	Avg. KIE	SD KIE	KIE
Non-competitive KIE	1	1.43	1.44	0.01	1.44 ± 0.01
	2	1.45			
Competitive KIE	1	3.14	3.20	0.08	3.20 ± 0.08
	2	3.26			

IV. Preparation and Characterization of the Azide Substrates

General procedure A:[4]

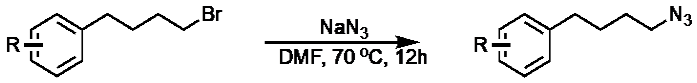

To a 100-mL flask were added alkyl bromide (5.0 mmol, 1.0 equiv.), sodium azide (487.6 mg, 7.5 mmol, 1.5 equiv.), and anhydrous DMF (50 mL). The mixture was stirred at 70 ºC for 12 h, then cooled to room temperature, and diluted with diethyl ether/water (50 mL, 1:1). The product was extracted by diethyl ether (30 mL × 3), and the combined organic layer was washed with brine (50 mL). The organic phase was further dried over Na_2SO_4 and concentrated to afford a yellow residue. Flash column chromatography was performed to afford pure product in 60% to 80% yield.

General procedure B:

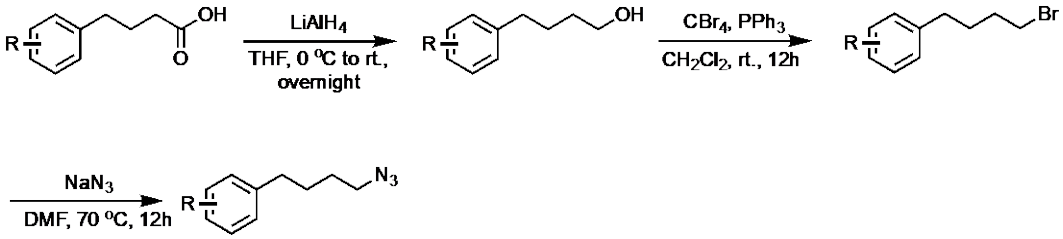

LAH reduction:[5] To a round-bottom flask containing carboxylic acids (1.0 equiv.) and anhydrous THF (0.1 M) at 0 ºC was slowly added $LiAlH_4$ (5.0 equiv.). The mixture was gradually warmed to room temperature and stirred for 18 h. Fieser method was conducted to workup the LAH reduction. After filtration, the organic phase was dried over Na_2SO_4 and further concentrated to afford a yellow residue. Flash column chromatography was performed to afford pure product in quantitative yield.

Bromination:[6] To a round-bottom flask containing alcohols (1.0 equiv.) and anhydrous dichloromethane (DCM, 0.3 M) was added CBr_4 (1.2 equiv.) and PPh_3 (1.2 equiv.) sequentially. The mixture was stirred at room temperature for 4 h before quenching with saturated aqueous $NaHCO_3$ and extracted with DCM (× 3). The combined organic layer was washed with brine,

further dried with Na_2SO_4, and concentrated to afford a colored residue. Flash column chromatography was performed to afford pure product in 70% to 80% yield.

Azidation: To a round-bottom flask were added alkyl bromide (1.0 equiv.), sodium azide (1.5 equiv.), and anhydrous DMF (0.1 M). The mixture was stirred at 70 °C for 12 h, then cooled to room temperature, and diluted with diethyl ether/water (1:1). The product was extracted by diethyl ether (× 3), and the combined organic layer was washed with brine (50 mL). The organic phase was further dried over Na_2SO_4 and concentrated to afford a yellow residue. Flash column chromatography was performed to afford pure product in 60% to 80% yield.

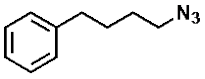

3.1a **(4-azidobutyl)benzene (3.1a):** The synthesis was conducted through general procedure A. **^{1}H NMR** (400 MHz, $CDCl_3$) δ 7.33 – 7.24 (m, 2H), 7.23 – 7.13 (m, 3H), 3.29 (t, *J* = 6.6 Hz, 2H), 2.65 (t, *J* = 7.4 Hz, 2H), 1.78 – 1.58 (m, 4H). **^{13}C NMR** (101 MHz, $CDCl_3$) δ 142.0, 128.5, 128.5, 126.0, 51.5, 35.5, 28.6.

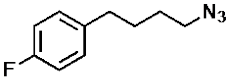

3.1b **1-(4-azidobutyl)-4-fluorobenzene (3.1b):** The synthesis was conducted through general procedure B. **^{1}H NMR** (400 MHz, $CDCl_3$) δ 7.15 – 7.03 (m, 4H), 3.28 (t, *J* = 6.7 Hz, 2H), 2.61 (t, *J* = 7.3 Hz, 2H), 2.32 (s, 3H), 1.78 – 1.57 (m, 4H). **^{13}C NMR** (101 MHz, $CDCl_3$) δ 161.4 (d, *J* = 243.5 Hz), 137.5 (d, *J* = 3.2 Hz), 129.8 (d, *J* = 7.7 Hz), 115.3 (d, *J* = 21.2 Hz), 51.4, 34.7, 28.7, 28.5. **^{19}F NMR** (376 MHz, $CDCl_3$) δ -117.6.

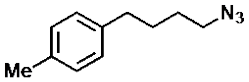

3.1c **1-(4-azidobutyl)-4-methylbenzene (3.1c):** The synthesis was conducted through general procedure B. **^{1}H NMR** (400 MHz, $CDCl_3$) δ 7.14 – 7.02 (m, 4H), 3.28 (t, J = 6.5

Hz, 2H), 2.61 (t, J = 7.2 Hz, 2H), 2.32 (s, 3H), 1.76 – 1.57 (m, 4H). **^{13}C NMR** (101 MHz, CDCl3) δ 138.9, 135.5, 129.2, 128.4, 51.5, 35.0, 28.7, 28.6, 21.1.

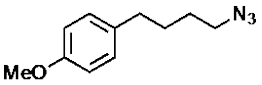

3.1d **1-(4-azidobutyl)-4-methoxybenzene (3.1d):** The synthesis was conducted through general procedure A. **^{1}H NMR** (400 MHz, $CDCl_3$) δ 7.13 – 7.06 (m, 2H), 6.87 – 6.79 (m, 2H), 3.79 (s, 3H), 3.28 (t, J = 6.5 Hz, 2H), 2.59 (t, J = 7.2 Hz, 2H), 1.74 – 1.56 (m, 4H). **^{13}C NMR** (101 MHz, $CDCl_3$) δ 158.0, 134.0, 129.4, 113.9, 55.4, 51.5, 34.6, 28.8, 28.5.

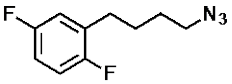

3.1e **2-(4-azidobutyl)-1,4-difluorobenzene (3.1e):** The synthesis was conducted through general procedure B. **^{1}H NMR** (400 MHz, $CDCl_3$) δ 6.96 (td, *J* = 8.8, 4.4 Hz, 1H), 6.92 – 6.80 (m, 2H), 3.30 (t, *J* = 6.5 Hz, 2H), 2.65 (t, *J* = 6.7 Hz, 2H), 1.74 – 1.60 (m, 4H). **^{13}C NMR** (101 MHz, $CDCl_3$) δ 158.7 (d, *J* = 239.4 Hz), 157.2 (d, *J* = 240.6 Hz), 130.5 (dd, *J* = 18.7, 7.7 Hz), 116.9 (dd, *J* = 23.6, 5.3 Hz), 116.3 (dd, *J* = 25.4, 8.8 Hz), 114.0 (dd, *J* = 24.0, 8.6 Hz), 51.3, 28.6, 28.5, 27.1. **^{19}F NMR** (376 MHz, $CDCl_3$) δ -119.6 (d, *J* = 18.0 Hz), -125.0 (d, *J* = 18.0 Hz).

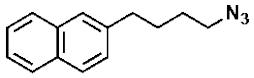

3.1f **2-(4-azidobutyl)naphthalene (3.1f):** The synthesis was conducted through general procedure B. **^{1}H NMR** (400 MHz, $CDCl_3$) δ 7.79 (ddd, *J* = 10.9, 7.7, 1.1 Hz, 3H), 7.61 (dd, *J* = 1.8, 0.9 Hz, 1H), 7.55 – 7.38 (m, 2H), 7.33 (dd, *J* = 8.5, 1.7 Hz, 1H), 3.31 (t, *J* = 6.8 Hz, 2H), 2.82 (t, *J* = 7.7 Hz, 2H), 1.87 – 1.74 (m, 2H), 1.74 – 1.59 (m, 2H). **^{13}C NMR** (101 MHz, $CDCl_3$) δ 139.4, 133.7, 132.2, 128.1, 127.8, 127.6, 127.3, 126.6, 126.1, 125.3, 51.5, 35.6, 28.6, 28.4.

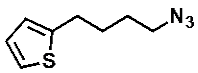

3.1g **2-(4-azidobutyl)thiophene (3.1g):** The synthesis was conducted through general procedure B. **^{1}H NMR** (400 MHz, $CDCl_3$) δ 7.13 (dd, *J* = 5.1, 1.2 Hz, 1H), 6.92 (dd, *J* = 5.1, 3.4 Hz, 1H), 6.79 (dq, *J* = 3.2, 1.0 Hz, 1H), 3.30 (t, *J* = 6.7 Hz, 2H), 2.87 (td, *J* = 7.3, 1.0 Hz, 2H), 1.83 – 1.72 (m, 2H), 1.72 – 1.61 (m, 2H). **^{13}C NMR** (101 MHz, $CDCl_3$) δ 144.7, 126.9, 124.4, 123.3, 51.4, 29.5, 28.9, 28.4.

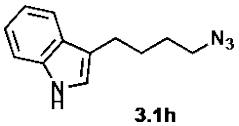

3.1h **3-(4-azidobutyl)-1H-indole (3.1h):** The synthesis was conducted through general procedure B. **^{1}H NMR** (400 MHz, $CDCl_3$) δ 7.92 (s, 1H), 7.61 (dq, *J* = 7.8, 0.9 Hz, 1H), 7.37 (dt, *J* = 8.1, 0.9 Hz, 1H), 7.21 (ddd, *J* = 8.1, 7.0, 1.2 Hz, 1H), 7.13 (ddd, *J* = 8.0, 7.0, 1.1 Hz, 1H), 6.99 (dt, *J* = 2.0, 0.9 Hz, 1H), 3.31 (t, *J* = 6.8 Hz, 2H), 2.81 (td, *J* = 7.4, 0.9 Hz, 2H), 1.86 – 1.76 (m, 2H), 1.76 – 1.66 (m, 2H). **^{13}C NMR** (101 MHz, $CDCl_3$) δ 136.5, 127.6, 122.1, 121.3, 119.3, 119.0, 116.3, 111.2, 51.6, 28.8, 27.3, 24.8.

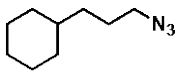

3.1i **(3-azidopropyl)cyclohexane (3.1i):** The synthesis was conducted through general procedure A. **^{1}H NMR** (400 MHz, $CDCl_3$) δ 3.24 (t, *J* = 7.0 Hz, 2H), 1.75 – 1.51 (m, 7H), 1.27 – 1.08 (m, 6H), 0.89 (tt, *J* = 11.6, 6.4 Hz, 2H). **^{13}C NMR** (101 MHz, $CDCl_3$) δ 52.0, 37.5, 34.6, 33.4, 26.7, 26.5, 26.4.

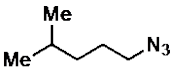

3.1j **1-azido-4-methylpentane (3.1j):** The synthesis was conducted through general procedure A. **^{1}H NMR** (400 MHz, $CDCl_3$) δ 3.25 (t, *J* = 7.0 Hz, 2H), 1.68 – 1.51 (m, 3H), 1.30 – 1.20 (m, 2H), 0.90 (d, *J* = 6.6 Hz, 6H). **^{13}C NMR** (101 MHz, $CDCl_3$) δ 51.9, 36.0, 27.9, 26.9, 22.6.

General procedure C:[7]

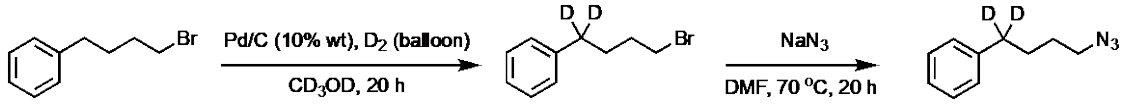

A mixture of (4-bromobutyl)benzene (0.53 g, 2.5 mmol, 1.0 equiv.) and Pd/C (10 wt%, 0.33 g, 60 mol%) in CD_3OD (5 mL) was placed under nitrogen and equipped with a deuterium balloon. After 20 h of reaction the mixture was filtered over celite, and the product diluted with diethyl ether (20 mL). The solution was washed with water (20 mL) and a saturated aqueous solution of sodium bicarbonate (× 2). The organic fraction was dried over $MgSO_4$ filtered and solvent removed to yield 4-bromo-1,1-bisdeutero-1-phenylbutane as a colorless oil which was used in the next step without additional purification.

The obtained 4-bromo-1,1-bisdeutero-1-phenylbutane was dissolved in DMF (10 mL) and sodium azide was added to the stirred solution. After heating at 70 °C for 20 hours the mixture was cooled to room temperature and water (20 mL) was added. The product was extracted with diethyl ether (20 mL), and the organic fraction was washed with water (5 × 30 mL), dried over $MgSO_4$, filtered and concentrated to afford a yellow residue. Flash column chromatography was performed to afford pure product as a colorless oil (0.25 g, 1.4 mmol, 90% deuteration rate, 56% overall yield).

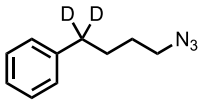

3.1aa **(4-azidobutyl-1,1-d2)benzene** (**3.1aa**): The synthesis was conducted through general procedure C (90% deuteration rate). ^{1}H NMR (400 MHz, $CDCl_3$) δ 7.29 (tt, J = 6.9, 0.9 Hz, 2H), 7.23 – 7.16 (m, 3H), 3.29 (t, J = 6.6 Hz, 2H), 1.75 – 1.59 (m, 3H). ^{13}C NMR (101 MHz, $CDCl_3$) δ 141.8, 128.4, 128.4, 125.9, 51.4, 35.2 – 34.4, 28.4, 28.3.

General procedure D:[8]

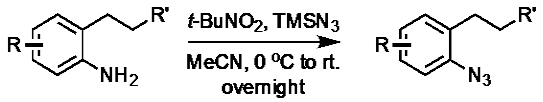

To a 100-mL flask at 0 ºC were added aniline (1.0 equiv.), MeCN (0.4 M), *t*-$BuNO_2$ (4.0 equiv.), and $TMSN_3$ (3.0 equiv.) dropwise, then the flask was warmed to room temperature and stirred overnight. De-ionized water was added after completion, the reaction mixture was extracted by diethyl ether (× 3), and the combined organic layer was washed with brine. The organic phase was further dried over Na_2SO_4 and concentrated to afford a yellow residue. Flash column chromatography was performed to afford pure product in 50% to 70% yield.

General procedure E:[9]

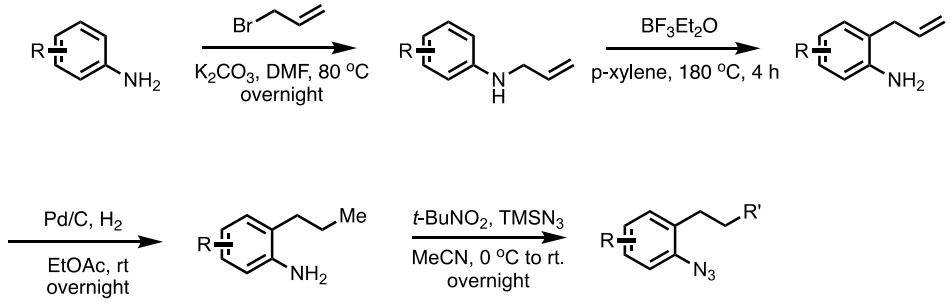

Allylation: To a 100-mL round-bottom flask were added aniline (1.0 equiv.), K_2CO_3 (2.4 equiv.), DMF (0.4 M) and allyl bromide (1.0 equiv.) dropwise. The solution was sealed and heated to 80 ºC overnight. The reaction mixture was filtered, washed with H_2O, and extracted with ethyl acetate twice. The combined organic layer was washed with brine, then dried over Na_2SO_4 and concentrated to afford a yellow residue. The crude product was purified by flash column chromatography (eluent: 10% Hex in EtOAc) to afford corresponding allyl aniline as a yellow oil with 40% to 50% yield.

Aza-Claisen rearrangement: To a 50-mL Schlenk tube were added allyl aniline (1.0 equiv.), *p*-xylene (2.0 M) and then added $BF_3 \cdot Et_2O$ (1.0 equiv.) dropwise. The Schlenk tube was sealed and heated to 180 °C for 4 h (sometimes longer based on how fast the rearrangement is).

Hydrogenation: To a 25-mL round-bottom flask were added corresponding aniline (1.0 equiv.) ethyl acetate (0.2 M) and Pd/C (100 mg/g of aniline) and then the mixture was degassed and recharged with a balloon of hydrogen. The reaction was vigorously stirred at room temperature overnight. After the reaction was completed, the mixture was filtered through a pad of celite before being concentrated to afford a yellow residue. The residue was directly used for the next step without any further purification.

Azidation: Same as General Procedure C described above.

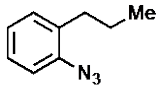

3.3a **1-azido-2-propylbenzene (3.3a):** The synthesis was conducted through general procedure C. **^{1}H NMR** (400 MHz, $CDCl_3$) δ 7.28 – 7.19 (m, 1H), 7.14 (ddd, *J* = 12.2, 7.7, 1.4 Hz, 2H), 7.06 (td, *J* = 7.4, 1.3 Hz, 1H), 2.58 – 2.50 (m, 2H), 1.66 – 1.52 (m, 2H), 0.94 (t, *J* = 7.3 Hz, 3H). **^{13}C NMR** (101 MHz, $CDCl_3$) δ 138.1, 134.3, 130.6, 127.3, 124.7, 118.2, 33.4, 23.6, 14.1.

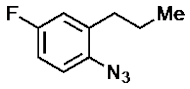

3.3b **1-azido-2-butylbenzene (3.3b):** The synthesis was conducted through general procedure C. **^{1}H NMR** (400 MHz, $CDCl_3$) δ 7.23 (td, *J* = 7.6, 1.7 Hz, 1H), 7.14 (ddd, *J* = 13.8, 7.7, 1.4 Hz, 2H), 7.06 (td, *J* = 7.4, 1.2 Hz, 1H), 2.56 (t, *J* = 7.6 Hz, 2H), 1.60 – 1.48 (m, 2H), 1.35 (dq, *J* = 14.6, 7.3 Hz, 2H), 0.93 (t, *J* = 7.3 Hz, 3H). **^{13}C NMR** (101 MHz, $CDCl_3$) δ 138.0, 134.5, 130.5, 127.2, 124.8, 118.2, 32.6, 31.1, 22.7, 14.1.

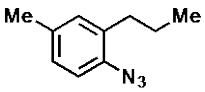

3.3c **1-azido-4-fluoro-2-propylbenzene (3.3c):** The synthesis was conducted through general procedure D. **^{1}H NMR** (400 MHz, $CDCl_3$) δ 7.06 (dd, *J* = 8.7, 4.8 Hz, 1H), 6.98 – 6.84 (m, 2H), 2.55 – 2.49 (m, 2H), 1.64 – 1.53 (m, 2H), 0.94 (t, *J* = 7.4 Hz, 3H). **^{13}C NMR** (101 MHz, $CDCl_3$) δ 159.9 (d, *J* = 243.7 Hz), 136.4 (d, *J* = 7.4 Hz), 133.8 (d, *J* = 2.8 Hz), 119.3 (d, *J* = 8.7 Hz), 117.2 (d, *J* = 22.4 Hz), 113.9 (d, *J* = 23.2 Hz), 33.3 (d, *J* = 1.4 Hz), 23.3, 14.0. **^{19}F NMR** (376 MHz, $CDCl_3$) δ -118.5.

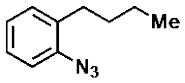

3.3d **1-azido-4-methyl-2-propylbenzene (3.3d):** The synthesis was conducted through general procedure D. **^{1}H NMR** (400 MHz, $CDCl_3$) δ 7.05 – 6.99 (m, 2H), 6.96 (s, 1H), 2.54 – 2.43 (m, 2H), 2.30 (s, 3H), 1.64 – 1.51 (m, 2H), 0.94 (t, *J* = 7.4 Hz, 3H). **^{13}C NMR** (101 MHz, $CDCl_3$) δ 135.2, 134.4, 134.0, 131.3, 127.8, 118.1, 33.4, 23.7, 21.0, 14.1.

3.3e **1-azido-2-isobutylbenzene (3.3e):** The synthesis was conducted through general procedure C. **^{1}H NMR** (400 MHz, $CDCl_3$) δ 7.26 – 7.20 (m, 1H), 7.12 (ddd, *J* = 7.6, 3.6, 1.5 Hz, 2H), 7.05 (td, *J* = 7.4, 1.2 Hz, 1H), 2.44 (d, *J* = 7.2 Hz, 2H), 1.95 – 1.82 (m, 1H), 0.89 (d, *J* = 6.6 Hz, 6H). **^{13}C NMR** (101 MHz, $CDCl_3$) δ 138.3, 133.4, 131.5, 127.3, 124.5, 118.2, 40.5, 29.3, 22.5.

V. Preparation and Characterization of the Racemic Standards of Products

***Notes*:** All the pyrrolidine derivative standard products were commercially available and purchased from vendors mentioned in **Section 3.4**. Unless otherwise noted, indoline derivative standard products were commercially available and purchased from vendors.

General procedure F:[10]

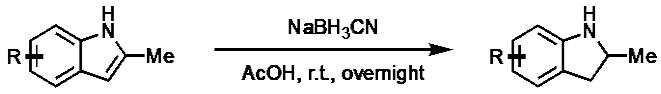

To a round-bottom flask at 0 ºC were added indole (1.0 equiv.), AcOH (0.2 M), and $NaBH_3CN$ (6.0 equiv.). The mixture was gradually warmed to room temperature and stirred overnight. After completion detected by TLC analysis, water and additional NaOH pellets were added until pH >12 before extracting with diethyl ether (three times). After extraction, the organic phase was combined, further dried over Na_2SO_4, and concentrated to afford a yellow residue. Flash column chromatography was performed to afford pure product in 50% to 60% yield.

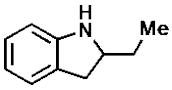

3.4b **2-ethylindoline (3.4b): ^{1}H NMR** (400 MHz, $CDCl_3$) δ 7.11 – 7.04 (m, 1H), 7.01 (dddd, *J* = 7.7, 6.8, 1.3, 0.7 Hz, 1H), 6.70 (td, *J* = 7.4, 1.0 Hz, 1H), 6.63 (d, *J* = 7.7 Hz, 1H), 3.79 (tt, *J* = 8.5, 6.6 Hz, 1H), 3.13 (dd, *J* = 15.5, 8.6 Hz, 1H), 2.69 (dd, *J* = 15.5, 8.4 Hz, 1H), 1.65 (dtd, *J* = 13.8, 7.3, 3.0 Hz, 2H), 0.98 (t, *J* = 7.4 Hz, 3H). **^{13}C NMR** (101 MHz, $CDCl_3$) δ 150.7, 129.2, 127.4, 124.8, 118.9, 109.5, 61.7, 35.9, 29.6, 10.9. **HRMS** (FD) Calcd for $C_{10}H_{13}N$ [M] 147.1048, found 147.1038.

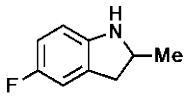

3.4c **5-fluoro-2-methylindoline (3.4c): ^{1}H NMR** (400 MHz, $CDCl_3$) δ 6.80 (ddt, *J* = 8.5, 2.5, 1.2 Hz, 1H), 6.70 (dddt, *J* = 9.3, 8.4, 2.7, 0.8 Hz, 1H), 6.53 (ddd, *J* = 8.4, 4.4, 1.1 Hz, 1H), 4.08 – 3.94 (m, 1H), 3.13 (dd, *J* = 16.3, 8.9 Hz, 1H), 2.63 (dd, *J* = 15.4, 7.6 Hz, 1H), 1.30 (d, *J* = 6.3 Hz, 3H). **^{13}C NMR** (101 MHz, $CDCl_3$) δ 157.3 (d, *J* = 235.2 Hz), 146.6 (d, *J* = 1.5 Hz), 131.0 (d, *J* = 8.2 Hz), 113.3 (d, *J* = 23.1 Hz), 112.3 (d, *J* = 23.7 Hz), 109.8 (d, *J* = 8.4 Hz), 56.1, 38.1 (d, *J* = 1.8 Hz), 22.2. **^{19}F NMR** (376 MHz, $CDCl_3$) δ -126.3. **HRMS** (FD) Calcd for $C_9H_{10}NF$ [M] 151.0797, found 151.0798.

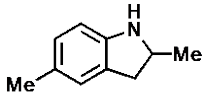

3.4d **2,5-dimethylindoline (3.4d): ^{1}H NMR** (400 MHz, $CDCl_3$) δ 6.92 (s, 1H), 6.83 (d, *J* = 7.8 Hz, 1H), 6.54 (d, *J* = 7.8 Hz, 1H), 3.98 (ddq, *J* = 8.4, 7.8, 6.2 Hz, 1H), 3.11 (dd, *J* = 15.4, 8.4 Hz, 1H), 2.61 (dd, *J* = 15.4, 7.8 Hz, 1H), 2.25 (s, 3H), 1.29 (d, *J* = 6.3 Hz, 3H). **^{13}C NMR** (101 MHz, $CDCl_3$) δ 148.0, 129.7, 128.6, 127.7, 125.7, 109.8, 55.6, 37.9, 22.2, 21.0. **HRMS** (FD) Calcd for $C_{10}H_{13}N$ [M] 147.1048, found 147.1046.

General procedure G:[11]

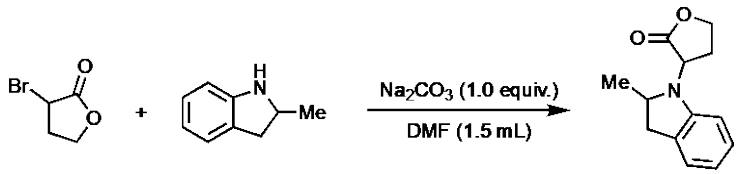

To a 40-mL dram vial were added a solution of alkylamine (2.2 mmol) in DMF (1.5 mL) and α-bromo-γ-butyrolactone (330 mg, 0.185 mL, 2 mmol). The resulting mixture was stirred at room temperature for 24 h. After reaction completion, the mixture was extracted with ethyl acetate (7

mL × 3), and the combined organic layer was washed with saturated $NaHCO_3$ solution (15 mL) and brine (15 mL). The organic phase was further dried over Na_2SO_4 and concentrated to afford a brown residue. The final product was purified through silica gel column chromatography.

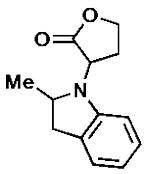

3.5 **3-(2-methylindolin-1-yl)dihydrofuran-2(3H)-one (3.5): ^{1}H NMR** (400 MHz, $CDCl_3$) δ 7.09 – 6.98 (m, 2H), 6.70 (dtd, *J* = 12.4, 7.4, 0.9 Hz, 1H), 6.30 (dd, *J* = 11.4, 7.9 Hz, 1H), 4.55 (tdd, *J* = 9.2, 6.7, 1.7 Hz, 1H), 4.39 – 4.22 (m, 2H), 4.07 – 3.70 (m, 1H), 3.28 – 3.13 (m, 1H), 2.77 – 2.45 (m, 2H), 2.43 – 2.29 (m, 1H), 1.34 (dd, *J* = 41.8, 6.2 Hz, 3H).**^{13}C NMR** (101 MHz, $CDCl_3$) δ 175.2, 174.8, 148.7, 148.2, 129.7, 129.1, 127.4, 127.3, 125.0, 124.9, 119.1, 118.6, 108.8, 107.0, 65.7, 65.5, 60.0, 59.5, 55.0, 54.4, 37.3, 37.2, 24.7, 22.7, 20.3, 20.2. **HRMS** (FD) Calcd for $C_{13}H_{15}NO_2$ [M] 217.1103, found 217.1108.

VI. Analytic Scale Enzymatic Reactions and Calibration Curves for Products

All enzymatic reactions for intramolecular alkyl/aryl nitrene C–H insertion on analytical scale were conducted following the general procedure described in **Section I (D)**. Reactions for every substrate were set up in triplicate. Product formation was quantified by LC-MS based on the calibration curve of the corresponding racemic standard compound (**Section IV**). All TTNs for different products were calculated as the concentration of products divided by the concentration of hemoproteins measured by the CO binding assay (**Section I (C)**).

LC-MS calibration curve:

Calibration curves of synthesized reference compounds were created for the determination of yield and TTN. For each substrate, five different concentrations of product (1.00, 2.00, 3.00, 4.00, and 5.00 mM) in 400-μL *E. coli* cell solutions were quenched, each with 400 μL of 5.00 mM internal standard (ethyl benzoate or 1,2,3-trimethoxylbenzene) acetonitrile solution. The mixtures were vortexed and then analyzed by LC-MS based on UV absorbance at 254 or 210 nm. All data points represent the average of duplicate runs. The calibration curves depict the ratio of product area to internal standard area (y-axis) against product concentration in mM (x-axis).

Notes: Pdt = product area, IS = internal standard area, [Pdt] = product concentration in reaction, [PC] = protein concentration in reaction, Avg. TTN = average total turnover number, SD TTN = standard deviation of TTN, Avg. Yield = average yield, SD Yield = standard deviation of yield.

2-Phenylpyrrolidine (3.2a)

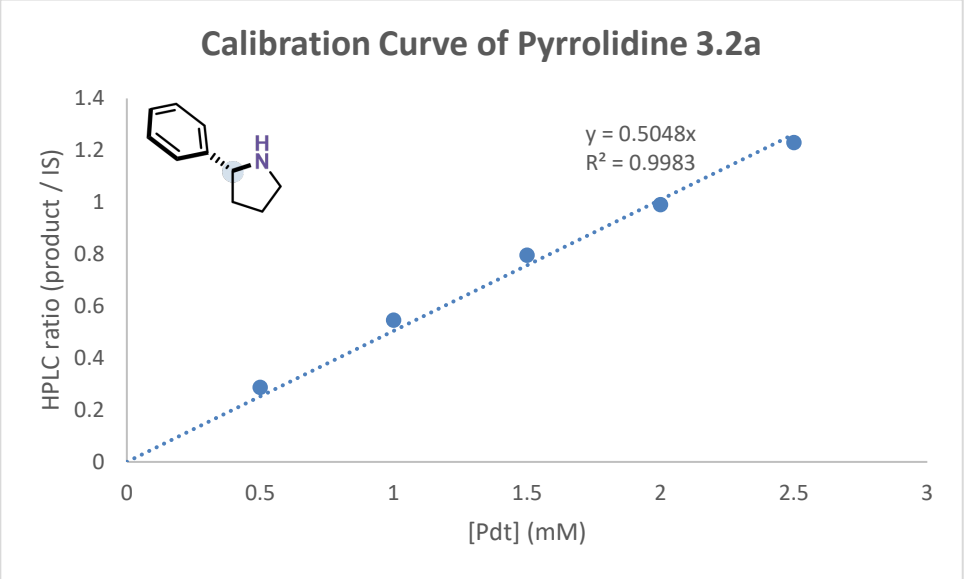

Data analysis for **P411-PYS-5141** catalyzed intramolecular C–H insertion with **3.1a** (2.5 mM, OD_{600} = 30):

Entry	Pdt	IS	Pdt/IS	[Pdt]/mM	[PC]/μM	Avg. TTN	SD TTN	Avg. Yield [%]	SD Yield [%]
1	50.6	967.3	0.0523	0.10	1.95	54	10	4	0.8
2	40.9	945.9	0.0432	0.086	1.95				
3	60.3	952.1	0.0633	0.13	1.95				

Data analysis for **P411-PYS-5142** catalyzed intramolecular C–H insertion with **3.1a** (2.5 mM, OD_{600} = 30):

Entry	Pdt	IS	Pdt/IS	[Pdt]/mM	[PC]/μM	Avg. TTN	SD TTN	Avg. Yield [%]	SD Yield [%]
1	159.7	964.7	0.166	0.33	1.58	210	3	13	0.2
2	161.9	952	0.170	0.34	1.58				
3	160.3	956.1	0.168	0.33	1.58				

Data analysis for **P411-PYS-5143** catalyzed intramolecular C–H insertion with **3.1a** (2.5 mM, OD_{600} = 30):

Entry	Pdt	IS	Pdt/IS	[Pdt]/mM	[PC]/μM	Avg. TTN	SD TTN	Avg. Yield [%]	SD Yield [%]
1	159.6	972.7	0.164	0.32	2.38	142	10	14	1.0
2	155.2	956	0.162	0.32	2.38				
3	179.5	970.8	0.185	0.37	2.38				

Data analysis for **P411-PYS-5144** catalyzed intramolecular C–H insertion with **3.1a** (2.5 mM, OD_{600} = 30):

Entry	Pdt	IS	Pdt/IS	[Pdt]/mM	[PC]/μM	Avg. TTN	SD TTN	Avg. Yield [%]	SD Yield [%]
1	241.6	932.6	0.259	0.51	2.21	224	10	20	0.9
2	240.9	951.2	0.253	0.50	2.21				
3	225.4	946.2	0.238	0.47	2.21				

Data analysis for **P411-PYS-5145** catalyzed intramolecular C–H insertion with **3.1a** (2.5 mM, OD_{600} = 30):

Entry	Pdt	IS	Pdt/IS	[Pdt]/mM	[PC]/μM	Avg. TTN	SD TTN	Avg. Yield [%]	SD Yield [%]
1	344.2	907.4	0.379	0.75	1.73	420	24	29	1.6
2	361.8	957.5	0.378	0.75	1.73				
3	329.4	960.3	0.343	0.68	1.73				

Data analysis for **P411-PYS-5146** catalyzed intramolecular C–H insertion with **3.1a** (2.5 mM, OD_{600} = 30):

Entry	Pdt	IS	Pdt/IS	[Pdt]/mM	[PC]/μM	Avg. TTN	SD TTN	Avg. Yield [%]	SD Yield [%]

1	369.4	916.5	0.403	0.80	1.68	463	15	31	1.0
2	368.8	931.8	0.396	0.78	1.68				
3	353	933.8	0.378	0.75	1.68				

Data analysis for **P411-PYS-5147** catalyzed intramolecular C–H insertion with **3.1a** (2.5 mM, OD_{600} = 30):

Entry	Pdt	IS	Pdt/IS	[Pdt]/mM	[PC]/μM	Avg. TTN	SD TTN	Avg. Yield [%]	SD Yield [%]
1	608.4	927.9	0.656	1.30	3.76	350	4	53	0.6
2	637.8	952.7	0.669	1.33	3.76				
3	628.5	938.6	0.670	1.33	3.76				

Data analysis for **P411-PYS-5148** catalyzed intramolecular C–H insertion with **3.1a** (2.5 mM, OD_{600} = 30):

Entry	Pdt	IS	Pdt/IS	[Pdt]/mM	[PC]/μM	Avg. TTN	SD TTN	Avg. Yield [%]	SD Yield [%]
1	635.7	958.9	0.663	1.31	3.76	361	11	54	1.6
2	645.5	938.4	0.688	1.36	3.76				
3	676.4	961.4	0.704	1.39	3.76				

Data analysis for **P411-PYS-5149** catalyzed intramolecular C–H insertion with **3.1a** (2.5 mM, OD_{600} = 30):

Entry	Pdt	IS	Pdt/IS	[Pdt]/mM	[PC]/μM	Avg. TTN	SD TTN	Avg. Yield [%]	SD Yield [%]
1	725.9	927.9	0.782	1.55	3.44	479	25	66	3.5
2	797.5	940.6	0.848	1.68	3.44				
3	812.8	938.3	0.866	1.72	3.44				

Data analysis for **P411-PYS-5149** (M9-N, pH = **8.4**) catalyzed intramolecular C–H insertion with **3.1a** (2.5 mM, OD_{600} = 30):

Entry	Pdt	IS	Pdt/IS	[Pdt]/mM	[PC]/μM	Avg. TTN	SD TTN	Avg. Yield [%]	SD Yield [%]
1	874.9	930.6	0.940	1.86	3.74	494	4	74	0.7
2	877.2	949.8	0.924	1.83	3.74				
3	877.7	940.7	0.933	1.85	3.74				

2-(4-Fluorophenyl)pyrrolidine (3.2b)

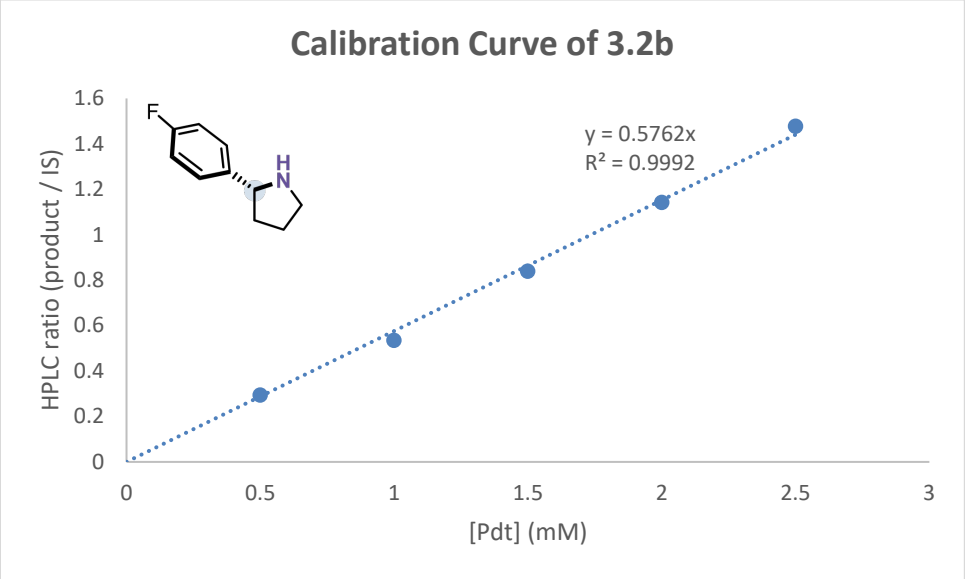

Data analysis for **P411-PYS-5149** (M9-N, pH = **8.4**) catalyzed intramolecular C–H insertion with **3.1b** (2.5 mM, OD_{600} = 30):

Entry	Pdt	IS	Pdt/IS	[Pdt]/mM	[PC]/μM	Avg. TTN	SD TTN	Avg. Yield [%]	SD Yield [%]
1	307	965.9	0.249	0.43	2.21	290	37	26	3.2
2	395.6	966.9	0.320	0.56	2.21				
3	371.1	974	0.301	0.52	2.21				

2-(*p*-Tolyl)pyrrolidine (3.2c)

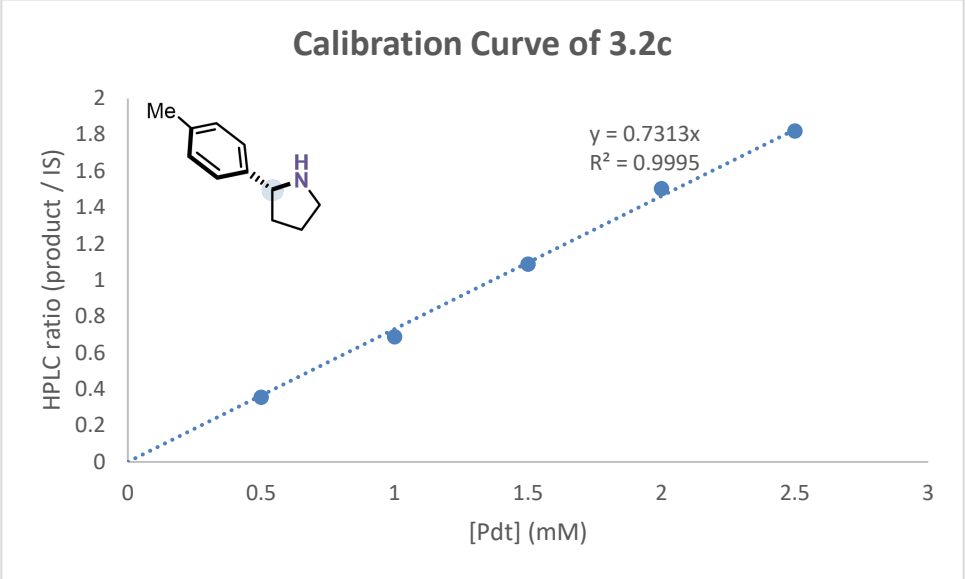

Data analysis for **P411-PYS-5149** (M9-N, pH = **8.4**) catalyzed intramolecular C–H insertion with **3.1c** (2.5 mM, OD_{600} = 30):

Entry	Pdt	IS	Pdt/IS	[Pdt]/mM	[PC]/μM	Avg. TTN	SD TTN	Avg. Yield [%]	SD Yield [%]
1	560.1	902.7	0.620	0.85	2.21	414	43	37	3.8
2	681.4	911	0.748	1.02	2.21				
3	576.7	902	0.639	0.87	2.21				

2-(4-Methoxyphenyl)pyrrolidine (3.2d)

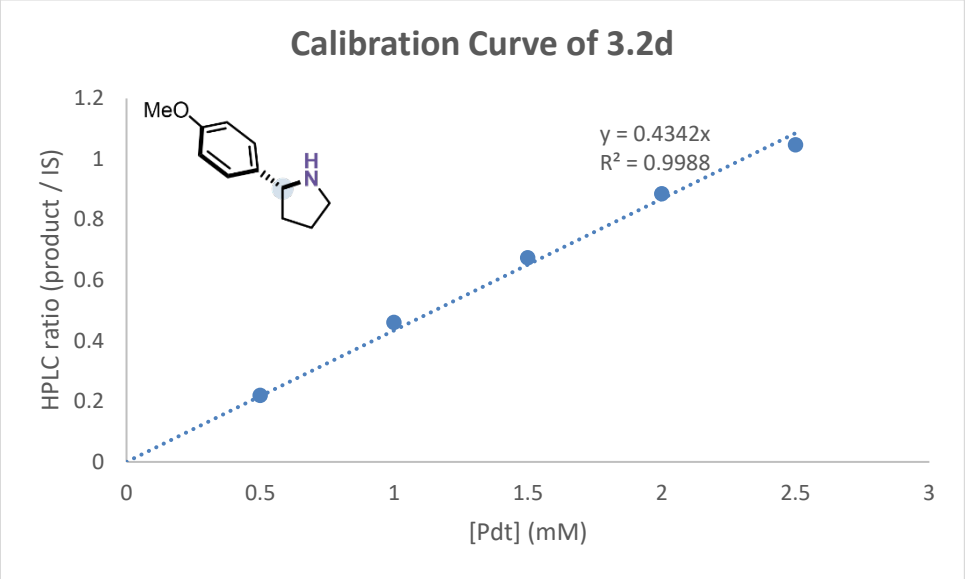

Data analysis for **P411-PYS-5149** (M9-N, pH = **8.4**) catalyzed intramolecular C–H insertion with **3.1d** (2.5 mM, OD_{600} = 30):

Entry	Pdt	IS	Pdt/IS	[Pdt]/mM	[PC]/μM	Avg. TTN	SD TTN	Avg. Yield [%]	SD Yield [%]
1	659.8	928.2	0.711	1.64	2.21	761	30	67	2.7
2	697.7	913.9	0.763	1.76	2.21				
3	656.5	916.3	0.716	1.65	2.21				

2-(2,5-Difluorophenyl)pyrrolidine (3.2e)

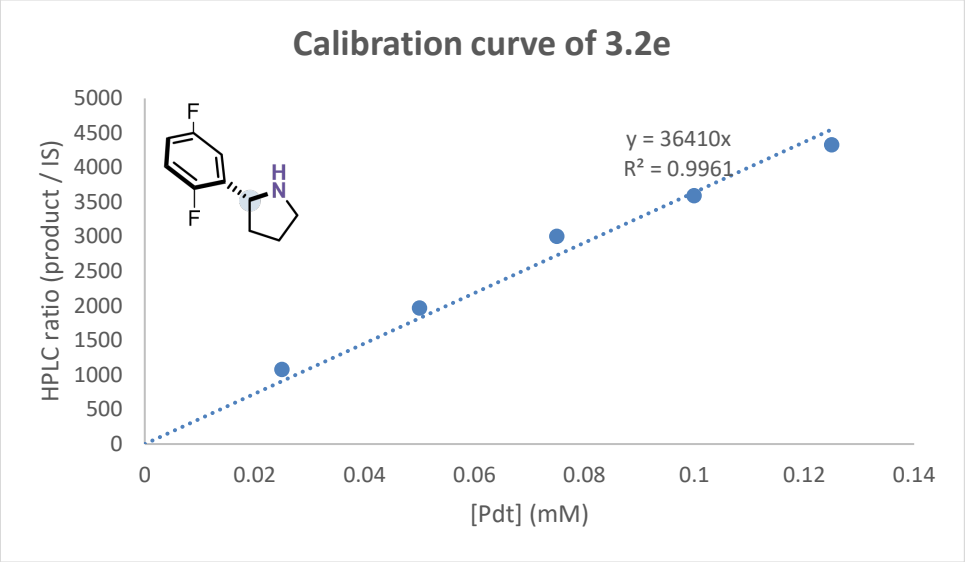

Data analysis for **P411-PYS-5149** (M9-N, pH = **8.4**) catalyzed intramolecular C–H insertion with **3.1e** (2.5 mM, OD_{600} = 30):

Entry	Pdt (Ion Count)	IS	Pdt/IS	[Pdt]/mM	[PC]/μM	Avg. TTN	SD TTN	Avg. Yield [%]	SD Yield [%]
1	2730675.0	919.7	2969.1	0.082	1.44	58	1	3.3	0.06
2	2790964.8	915.6	3048.2	0.084	1.44				
3	2751191.0	895.4	3072.6	0.084	1.44				

2-(Naphthalen-2-yl)pyrrolidine (3.2f)

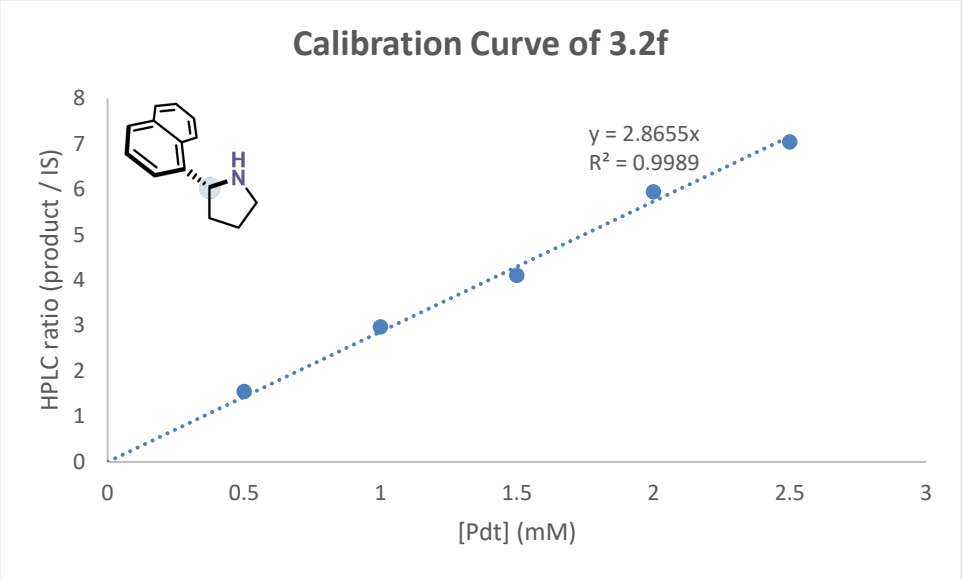

Data analysis for **P411-PYS-5149** (M9-N, pH = **8.4**) catalyzed intramolecular C–H insertion with **3.1f** (2.5 mM, OD_{600} = 30):

Entry	Pdt	IS	Pdt/IS	[Pdt]/mM	[PC]/μM	Avg. TTN	SD TTN	Avg. Yield [%]	SD Yield [%]
1	166.8	212.1	0.786	0.27	1.44	211	19	12	1.1
2	162.5	183.0	0.888	0.31	1.44				
3	155.6	165.8	0.938	0.33	1.44				

2-(Thiophen-2-yl)pyrrolidine (3.2g)

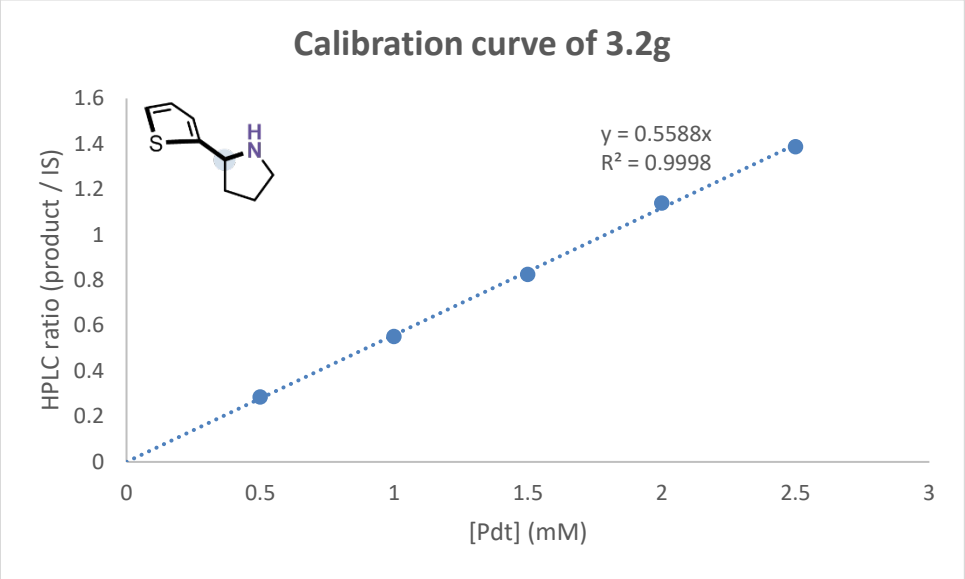

Data analysis for **P411-PYS-5149** (M9-N, pH = **8.4**) catalyzed intramolecular C–H insertion with **3.1g** (2.5 mM, OD_{600} = 30):

Entry	Pdt	IS	Pdt/IS	[Pdt]/mM	[PC]/μM	Avg. TTN	SD TTN	Avg. Yield [%]	SD Yield [%]
1	76.5	184.5	0.415	0.74	2.21	360	23	32	2.0
2	84.3	178.9	0.471	0.84	2.21				
3	80.4	179.9	0.447	0.80	2.21				

3-(Pyrrolidin-2-yl)-1H-indole (3.2h)

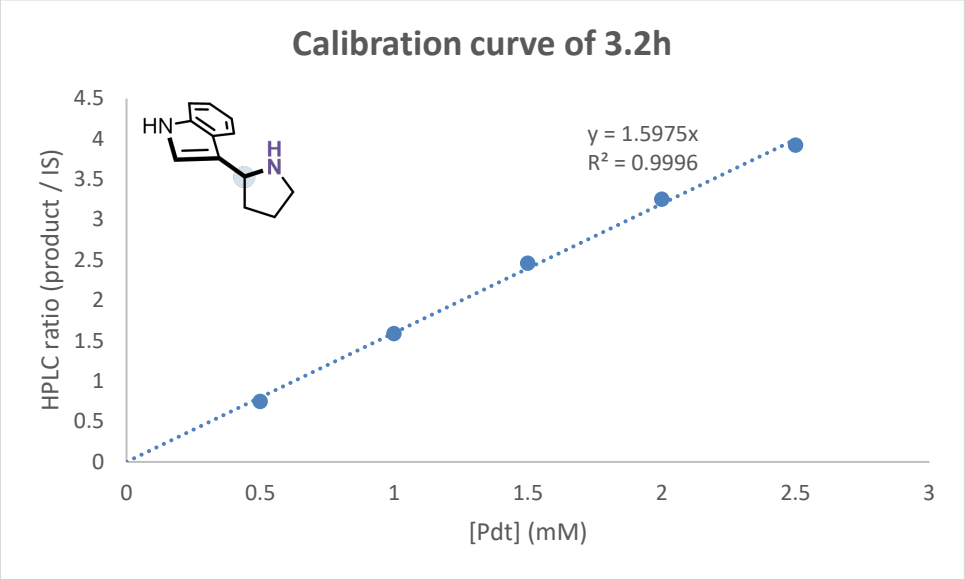

Data analysis for **P411-PYS-5149** (M9-N, pH = **8.4**) catalyzed intramolecular C–H insertion with **3.1h** (2.5 mM, OD_{600} = 30):

Entry	Pdt	IS	Pdt/IS	[Pdt]/mM	[PC]/μM	Avg. TTN	SD TTN	Avg. Yield [%]	SD Yield [%]
1	254.4	177.8	1.43	0.90	2.21	461	49	41	4.3
2	306.1	175.4	1.75	1.09	2.21				
3	290.4	170.1	1.71	1.07	2.21				

1-Azaspiro[4.5]decane (3.2i)

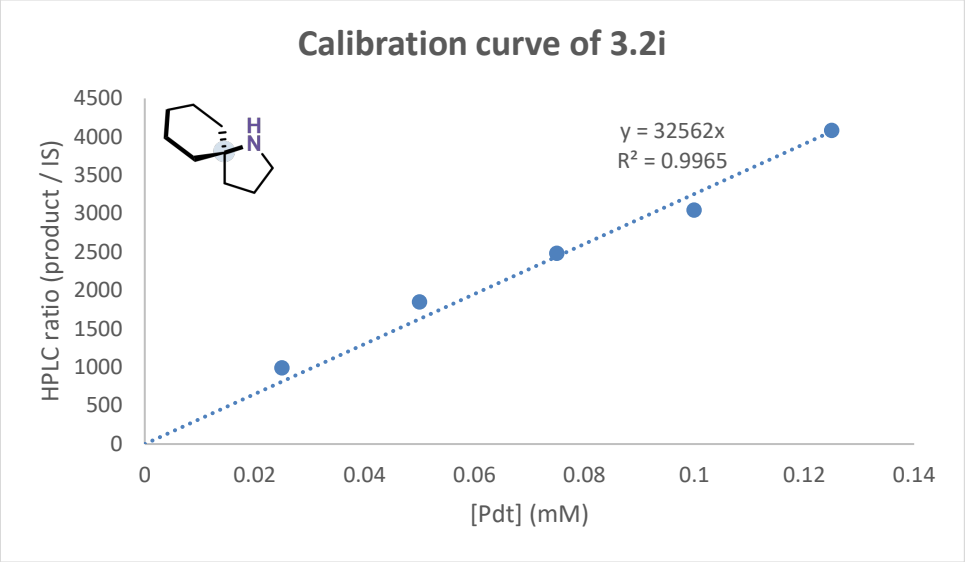

Data analysis for **P411-PYS-5149** (M9-N, pH = **8.4**) catalyzed intramolecular C–H insertion with **3.1i** (2.5 mM, OD_{600} = 30):

Entry	Pdt (Ion Count)	IS	Pdt/IS	[Pdt]/mM	[PC]/μM	Avg. TTN	SD TTN	Avg. Yield [%]	SD Yield [%]
1	2544228.3	931.9	2730.1516	0.084	1.44	57	2	3.3	0.1
2	2383615.3	931.8	2558.0761	0.079	1.44				
3	2489055.3	931.6	2671.8069	0.082	1.44				

2,2-Dimethylpyrrolidine (3.2j)

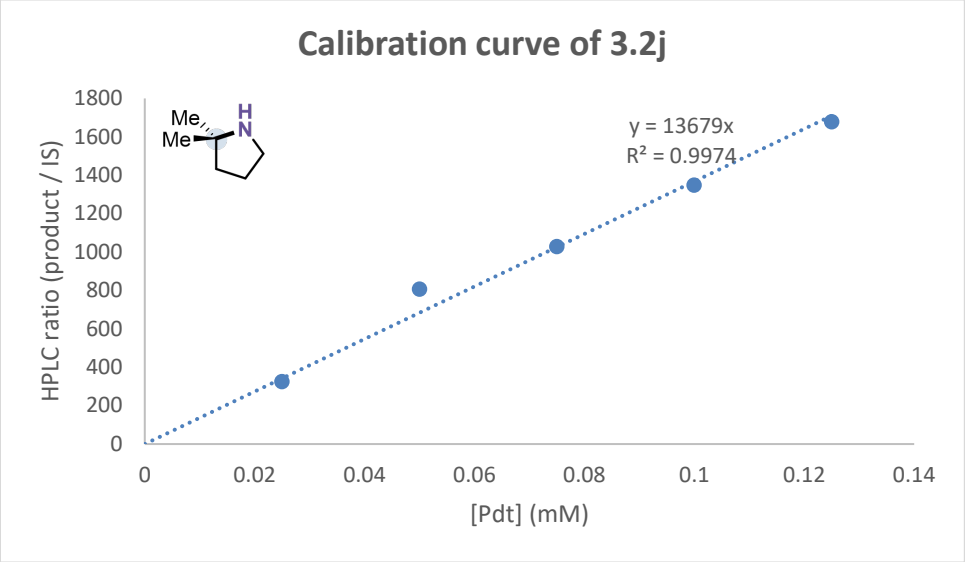

Data analysis for **P411-PYS-5149** (M9-N, pH = **8.4**) catalyzed intramolecular C–H insertion with **3.1j** (2.5 mM, OD_{600} = 30):

Entry	Pdt (Ion Count)	IS	Pdt/IS	[Pdt]/mM	[PC]/μM	Avg. TTN	SD TTN	Avg. Yield [%]	SD Yield [%]
1	657275.0	896.6	733.1	0.054	1.44	36	1	2.0	0.08
2	631301.0	915.8	689.3	0.050	1.44				
3	622256.9	916	679.3	0.050	1.44				

2-Methylindoline (3.4a)

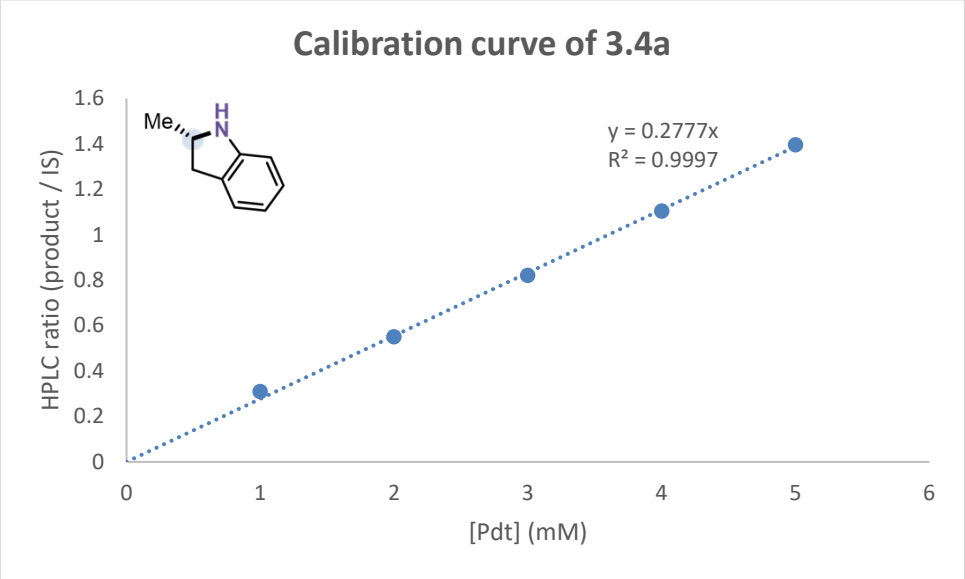

Data analysis for **P411-PYS-5148** (M9-N, pH = **7.4**) catalyzed intramolecular C–H insertion with **3.3a** (5.0 mM, OD_{600} = 40):

Entry	Pdt	IS	Pdt/IS	[Pdt]/mM	[PC]/μM	Avg. TTN	SD TTN	Avg. Yield [%]	SD Yield [%]
1	59.3	97.6	0.61	2.18	4.71	488	34	46	3.2
2	68.8	99.7	0.69	2.48	4.71				
3	58.2	94.2	0.62	2.22	4.71				

Data analysis for **P411-INS-5150** (M9-N, pH = **7.4**) catalyzed intramolecular C–H insertion with **3.3a** (5.0 mM, OD_{600} = 40):

Entry	Pdt	IS	Pdt/IS	[Pdt]/mM	[PC]/μM	Avg. TTN	SD TTN	Avg. Yield [%]	SD Yield [%]
1	66.3	95.2	0.70	2.51	3.29	742	25	49	1.7
2	63.7	97.7	0.65	2.35	3.29				
3	63.8	93.2	0.68	2.47	3.29				

Data analysis for **P411-INS-5151** (M9-N, pH = **7.4**) catalyzed intramolecular C–H insertion with **3.3a** (5.0 mM, OD_{600} = 40):

Entry	Pdt	IS	Pdt/IS	[Pdt]/mM	[PC]/μM	Avg. TTN	SD TTN	Avg. Yield [%]	SD Yield [%]
1	72.8	100.1	0.73	2.62	0.97	2690	49	52	1.0
2	67.8	92.3	0.73	2.65	0.97				
3	67.7	95.5	0.71	2.55	0.97				

Data analysis for **P411-INS-5151** (M9-N, pH = **8.4**) catalyzed intramolecular C–H insertion with **3.3a** (5.0 mM, OD_{600} = 40):

Entry	Pdt	IS	Pdt/IS	[Pdt]/mM	[PC]/μM	Avg. TTN	SD TTN	Avg. Yield [%]	SD Yield [%]
1	82.4	91.8	0.90	3.23	1.04	3100	48	64	1.0
2	88.5	97.5	0.91	3.27	1.04				
3	83.7	95.1	0.88	3.17	1.04				

Ethylindoline (3.4b)

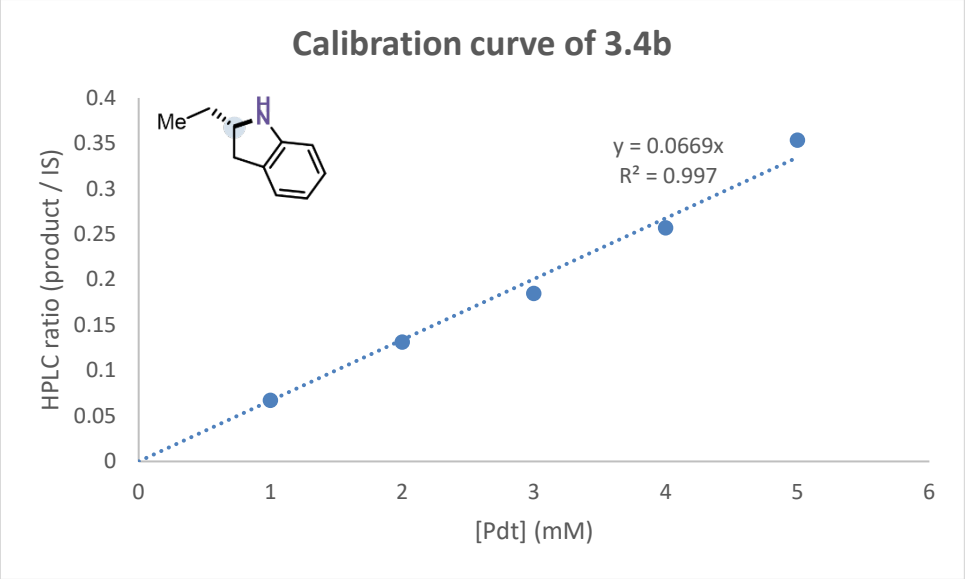

Data analysis for **P411-INS-5151** (M9-N, pH = **8.4**) catalyzed intramolecular C–H insertion with **3.3c** (5.0 mM, OD_{600} = 40):

Entry	Pdt	IS	Pdt/IS	[Pdt]/mM	[PC]/μM	Avg. TTN	SD TTN	Avg. Yield [%]	SD Yield [%]
1	258.0	5814.1	0.044	0.66	0.49	1310	57	13	0.6
2	261.0	5945.0	0.044	0.66	0.49				
3	232.6	5684.5	0.041	0.61	0.49				

5-Fluoro2-methylindoline (3.4c)

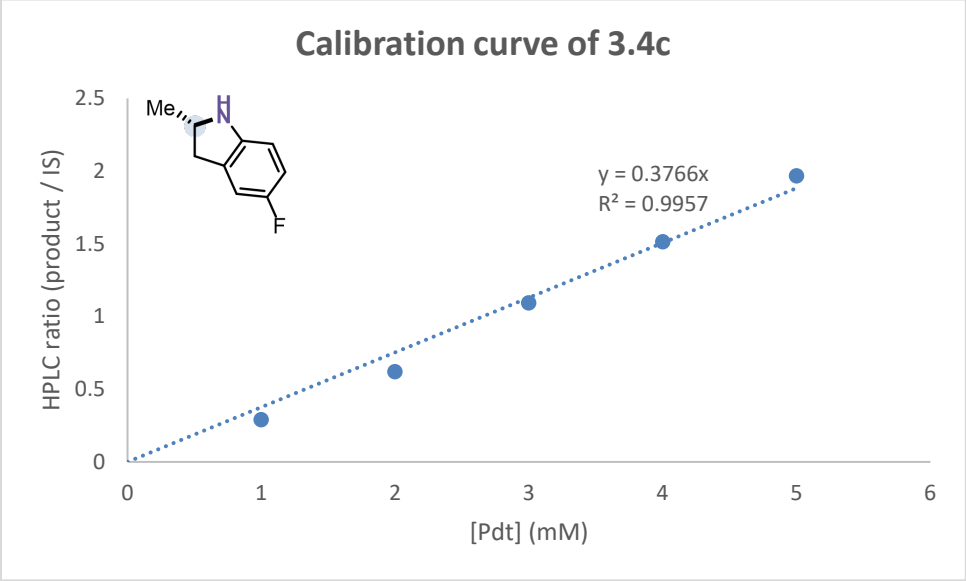

Data analysis for **P411-INS-5151** (M9-N, pH = **8.4**) catalyzed intramolecular C–H insertion with **3.3b** (5.0 mM, OD_{600} = 40):

Entry	Pdt	IS	Pdt/IS	[Pdt]/mM	[PC]/μM	Avg. TTN	SD TTN	Avg. Yield [%]	SD Yield [%]
1	17.9	95.3	0.19	0.51	0.49	1050	43	10	0.4
2	17.4	93.9	0.19	0.50	0.49				
3	19.1	95.5	0.20	0.54	0.49				

2,5-Dimethylindoline (3.4d)

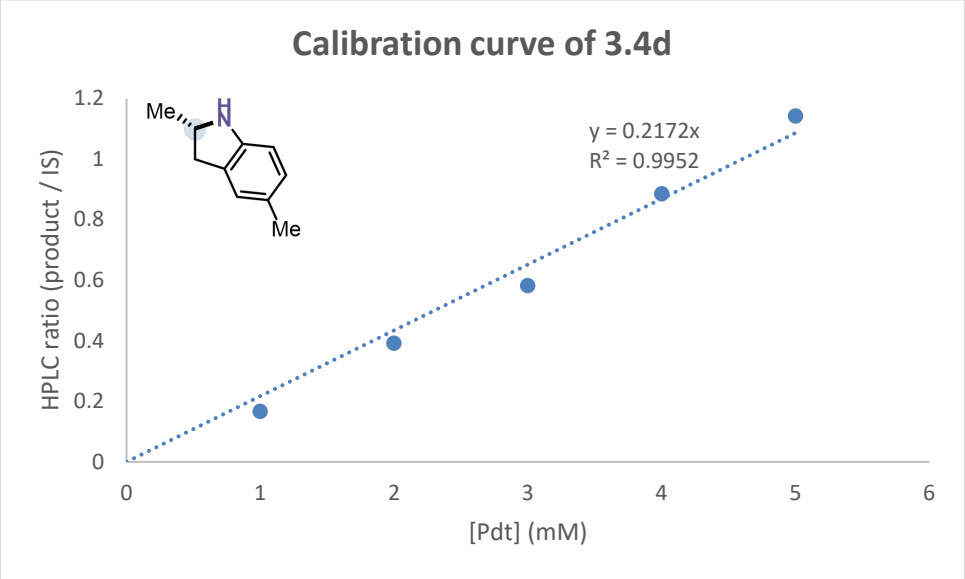

Data analysis for **P411-INS-5151** (M9-N, pH = **8.4**) catalyzed intramolecular C–H insertion with **3.3c** (5.0 mM, OD_{600} = 40):

Entry	Pdt	IS	Pdt/IS	[Pdt]/mM	[PC]/μM	Avg. TTN	SD TTN	Avg. Yield [%]	SD Yield [%]
1	48.2	6019.7	0.0080	0.11	0.49	211	18	2	0.2
2	40.1	5831.5	0.0069	0.10	0.49				
3	41.4	5869.6	0.0071	0.10	0.49				

3-(2-Methylindolin-1-yl)dihydrofuran-2(3H)-one (3.5)

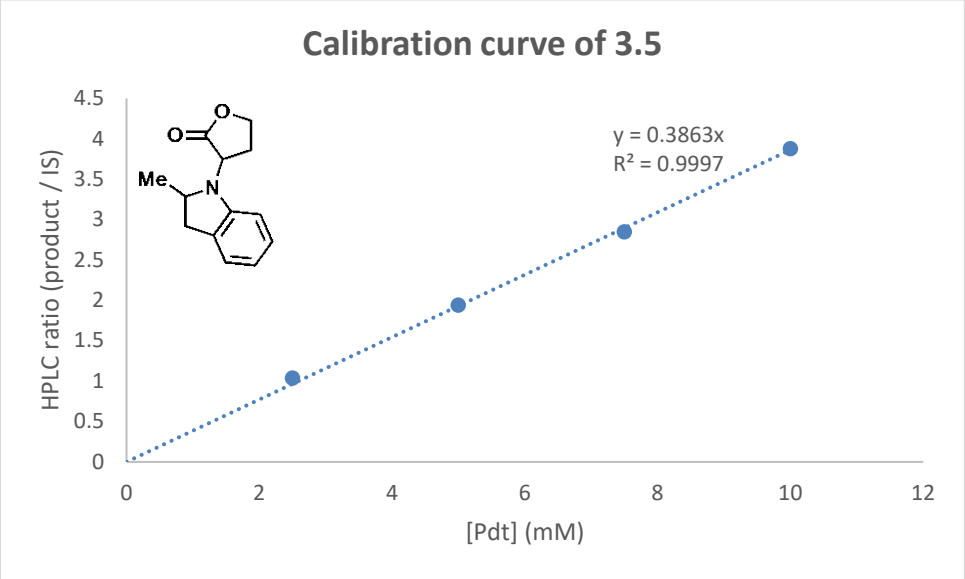

Data analysis for **L7_FL** (M9-N, pH = **7.4**) catalyzed intermolecular N–H insertion with **3.4a** (10.0 mM, OD_{600} = 30):

Entry	Pdt	IS	Pdt/IS	[Pdt]/mM	[PC]/μM	Avg. TTN	SD TTN	Avg. Yield [%]	SD Yield [%]
1	697.6	359.4	1.94	0.90	2.38	1985	115	47	2.7
2	621.8	357.6	1.74	1.09	2.38				
3	640.6	358.8	1.79	1.07	2.38				

VII. Preparative-Scale Enzymatic Synthesis

General procedure for 1-mmol scale enzymatic intramolecular C–H aminations with 3.3a:

In a 500-mL flask, a suspension of 150 mL *E. coli* expressing variant **P411-INS-5151** (OD_{600} = 40) in M9-N (pH = 8.4), 45 mL D-glucose (500 mM in M9-N, pH = 8.4), and 5 mL 1-azido-2-propylbenzene **3.3a** (161.2 mg, 200 mM in EtOH) were added sequentially under anaerobic conditions. The flask was capped and sealed with parafilm inside the anaerobic chamber. The mixture was shaken at 250 rpm in a shaker outside of an anaerobic chamber overnight.

After the reaction was completed, the reaction mixture was transferred to two 500-mL centrifuge bottles. The aqueous phase was extracted with organic solvent (hexane/EtOAc = 1:2, 120 mL × 4). The organic layers were combined in an Erlenmeyer flask, dried over Na_2SO_4, and concentrated under reduced pressure. Purification by preparative TLC with dichloromethane (with 0.5% NEt_3) as eluents afforded the cyclized product as a dark oil. TTNs were calculated based on measured protein concentration using CO binding and isolated product yield.

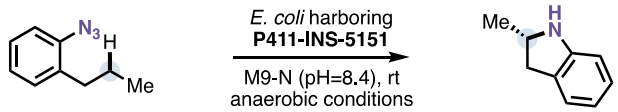

3.3a **3.4a**

(*S*)-2-Methylindoline

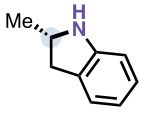

3.4a
largescale

(*S*)-**3.4a**: 79.8 mg, 60% yield, 2900 TTN, 92:8 *er* **^{1}H NMR** (400 MHz, $CDCl_3$) δ 7.08 (d, *J* = 7.3 Hz, 1H), 7.02 (dddd, *J* = 9.1, 7.6, 1.4, 0.8 Hz, 1H), 6.71 (td, *J* = 7.4, 1.0 Hz, 1H), 6.64 (d, *J* = 7.8 Hz, 1H), 4.01 (ddq, *J* = 8.5, 7.7, 6.2 Hz, 1H), 3.15 (dd, *J* = 15.3, 8.4 Hz, 1H), 2.65 (dd, *J* = 15.4, 7.7 Hz, 1H), 1.31 (d, *J* = 6.2 Hz, 3H). **^{13}C NMR** (101 MHz, $CDCl_3$) δ 150.6, 129.2, 127.4, 124.9, 119.0, 109.7, 55.4, 37.9, 22.3.

General procedure for 1-mmol scale enzymatic intramolecular C–H aminations with 3.3e:

In a 500-mL flask, a suspension of 150 mL *E. coli* expressing variant **P411-INS-5151** (OD_{600} = 40) in M9-N (pH = 8.4), 45 mL D-glucose (500 mM in M9-N, pH = 8.4), and 5 mL 1-azido-2-propylbenzene **3.3a** (175.2 mg, 200 mM in EtOH) were added sequentially under anaerobic conditions. The flask was capped and sealed with parafilm inside the anaerobic chamber. The mixture was shaken at 250 rpm in a shaker outside of an anaerobic chamber overnight.

After the reaction was completed, the reaction mixture was transferred to two 500-mL centrifuge bottles. The aqueous phase was extracted with organic solvent (hexane/EtOAc = 1:2, 120 mL × 4). The organic layers were combined in an Erlenmeyer flask, dried over Na_2SO_4, and concentrated under reduced pressure. Purification by preparative TLC with EtOAc/hexanes (10% hexanes in EtOAc) as eluents afforded the cyclized product as a dark oil. TTNs were calculated based on measured protein concentration using CO binding and isolated product yield.

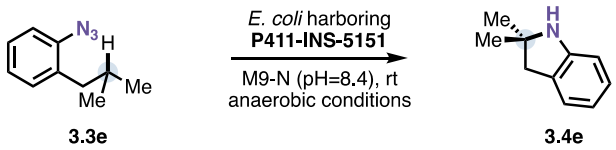

2,2-Dimethylindoline

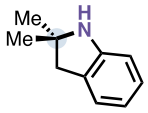

3.4e
largescale

3.4e: 58.6 mg, 40% yield, 1470 TTN **^{1}H NMR** (400 MHz, $CDCl_3$) δ 7.06 (d, *J* = 7.3 Hz, 1H), 7.01 (t, *J* = 7.6 Hz, 1H), 6.69 (t, *J* = 7.4 Hz, 1H), 6.58 (d, *J* = 7.7 Hz, 1H), 2.85 (s, 2H), 1.33 (s, 6H). **^{13}C NMR** (101 MHz, $CDCl_3$) δ 129.7, 127.6, 125.3, 120.2, 117.5, 111.2, 62.3, 44.1, 28.9. **HRMS** (FD) Calcd for $C_{10}H_{13}N$ [M] 147.1048, found 147.1046.

General procedure for 0.5-mmol scale enzymatic N–H insertion reactions:

In a 250-mL flask, a suspension of 45 mL *E. coli* expressing variant **L7_FL** (OD_{600} = 40) in M9-N (pH = 7.4), 2.5 mL D-glucose (500 mM in M9-N, pH = 7.4), 1.25 mL (*S*)-2-methylindoline **3.4a** (66.6 mg, 1.0 equiv. 400 mM in EtOH), and 1.25 mL lactone diazo (LAD, 67.2 mg, 1.2 equiv. 480 mM in EtOH) were added sequentially under anaerobic conditions. The flask was capped and sealed with parafilm inside the anaerobic chamber. The mixture was shaken at 250 rpm in a shaker outside of an anaerobic chamber overnight.

After the reaction was completed, the reaction mixture was transferred to four 50-mL Eppendorf tubes. The aqueous phase was extracted with organic solvent (hexane/EtOAc = 1:2, 120 mL × 4). The organic layers were combined in an Erlenmeyer flask, dried over Na_2SO_4, and concentrated under reduced pressure. Purification by silica column chromatography with EtOAc/hexanes as eluents afforded the desired product. TTNs were calculated based on measured protein concentration using CO binding and isolated product yield.

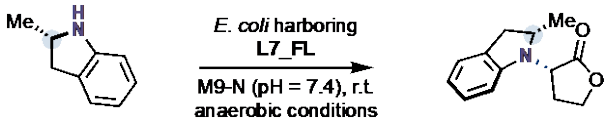

3.4a **3.5**

(S)-3-((S)-2-Methylindolin-1-yl)dihydrofuran-2(3H)-one (3.5)

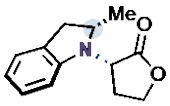

3.5 **3.5**: 46.6 mg, 43% yield, 2770 TTN, 98:2 *er*, >96:4 *dr* **^{1}H NMR** (400 MHz, $CDCl_3$) δ 7.11 – 6.97 (m, 2H), 6.72 (t, *J* = 7.4 Hz, 1H), 6.30 (d, *J* = 7.9 Hz, 1H), 4.54 (td, *J* = 9.2, 1.6 Hz, 1H), 4.36 – 4.20 (m, 2H), 3.76 (ddq, *J* = 9.5, 8.7, 6.1 Hz, 1H), 3.18 (dd, *J* = 15.5, 8.6 Hz, 1H), 2.71 (dd, *J* = 15.4, 9.4 Hz, 1H), 2.60 – 2.43 (m, 1H), 2.42 – 2.29 (m, 1H), 1.40 (d, *J* = 6.1 Hz, 3H). **^{13}C NMR** (101 MHz, $CDCl_3$) δ 174.8, 148.1, 129.8, 127.4, 124.9, 119.2, 108.8, 65.7, 60.0, 55.1, 37.3, 22.7, 20.2. **HRMS** (FD) Calcd for $C_{13}H_{15}NO_2$ [M] 217.1103, found 217.1104.

General procedure for 0.5-mmol scale enzymatic noncanonical amino acid synthesis:

In a 100-mL flask, a suspension of 25 mL kPi (pH = 8.0), L-serine (52.5 mg as a solid), (*S*)-2-methylindoline **3.4a** (66.6 mg, 1.0 equiv. 400 mM in EtOH), and 300 μL purified *Tm*TrpB synthase **TmE3** (238 μM in KPi buffer, 2.856 μM final concentration) were added sequentially under aerobic conditions. The flask was capped and sealed with parafilm. The mixture was shaken at 250 rpm in a shaker overnight.

After the reaction was completed, the reaction mixture was transferred to a 100-mL round-bottom flask. The aqueous phase was concentrated under reduced pressure. Purification by reverse column chromatography with EtOAc/hexanes as eluents afforded the desired product. TTNs were calculated based on measured protein concentration using CO binding and isolated product yield.

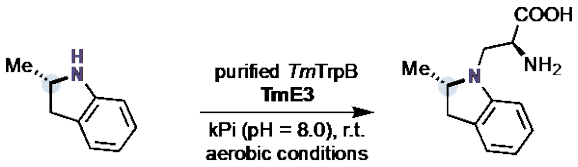

3.4a **3.6**

(2S)-2-Amino-3-(2-methylindolin-1-yl)propanoic acid (3.6)

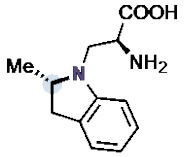

3.6 **3.6**: 32.5 mg, 30% yield, 2100 TTN, >94:6 *dr* **^{1}H NMR** (400 MHz, D_2O) δ 7.14 (tdd, *J* = 7.7, 4.2, 1.3 Hz, 2H), 6.73 (t, *J* = 7.4 Hz, 1H), 6.62 (d, *J* = 7.8 Hz, 1H), 3.82 – 3.72 (m, 1H), 3.69 (dd, *J* = 7.4, 5.5 Hz, 1H), 3.43 (qd, *J* = 14.8, 6.4 Hz, 2H), 3.15 (dd, *J* = 15.7, 8.4 Hz, 1H), 2.61 (dd, *J* = 15.7, 7.5 Hz, 1H), 1.23 (d, *J* = 6.2 Hz, 3H). **^{13}C NMR** (101 MHz, D_2O) δ 178.3, 151.8, 129.6, 127.5, 124.7, 118.0, 106.8, 61.3, 55.3, 50.0, 36.4, 17.8. **HRMS** (FD) Calcd for $C_{12}H_{16}N_2O_2$ [M] 220.1211, found 220.1214.

VIII. Chiral-Phase HPLC Traces

The absolute stereochemistry for enzymatic products **3.2a** and **3.4a** were assigned to be *R* and *S,* respectively, by comparing with their optical pure standard product. All other products **3.2b–3.2g**, **3.2j**, **3.4b–3.4d** were assigned by analogy. Before analysis of *ee*, all pyrrolidine products were protected by the benzoyl group, while indoline products were not.

Determination of absolute stereochemistry for **3.2a**:

Chiral-phase HPLC conditions: Chiralpak IC, 25% *i*-PrOH in hexane, 1.5 mL/min, 25 ºC, 210 nm

Racemic 2-Phenylpyrrolidine:

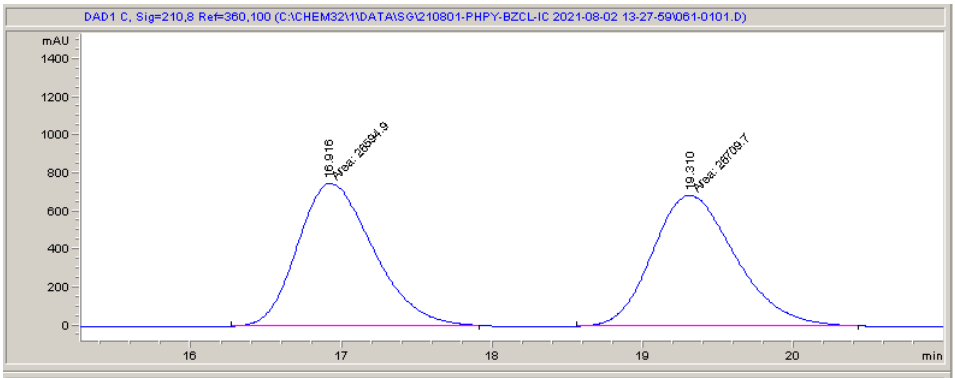

#	Time	Area	Height	Width	Area%	Symmetry
1	16.916	26594.9	753.9	0.5879	49.892	0.707
2	19.31	26709.7	691.5	0.6438	50.108	0.799

(*S*)-Phenylpyrrolidine: commercially available enantiopure compound

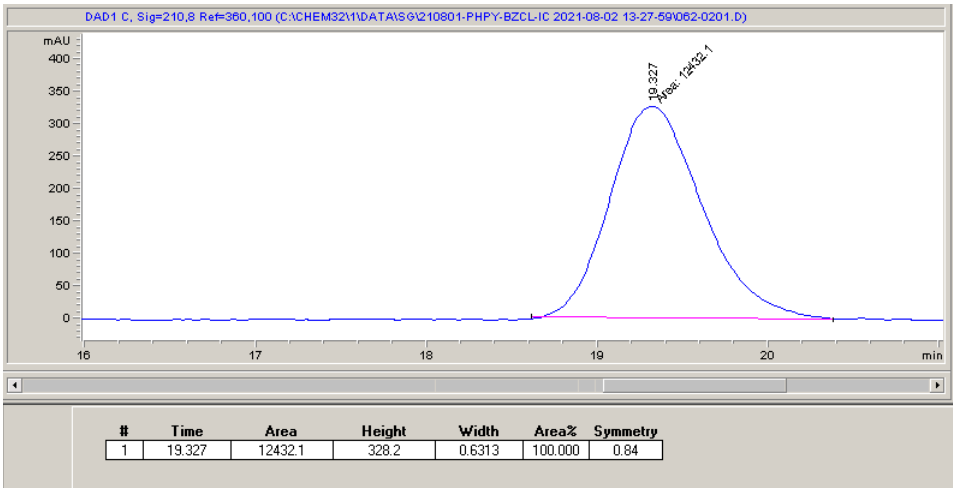

#	Time	Area	Height	Width	Area%	Symmetry
1	19.327	12432.1	328.2	0.6313	100.000	0.84

Determination of absolute stereochemistry for **3.4a**:

Chiral-phase HPLC conditions: Chiralpak IB, 2% *i*-PrOH in hexane, 1.0 mL/min, 25 ºC, 254 nm

Racemic 2-Methylindoline:

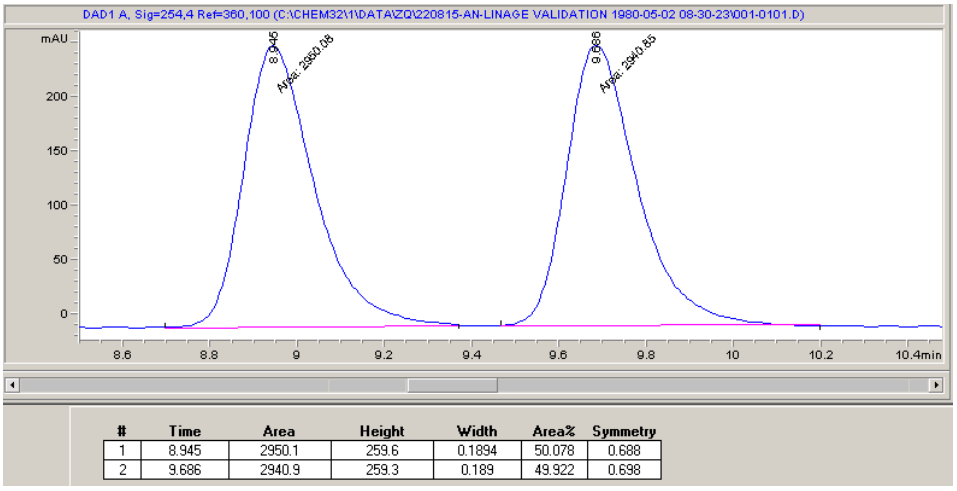

#	Time	Area	Height	Width	Area%	Symmetry
1	8.945	2950.1	259.6	0.1894	50.078	0.688
2	9.686	2940.9	259.3	0.189	49.922	0.698

(*R*)- 2-Methylindoline: commercially available enantiopure compound

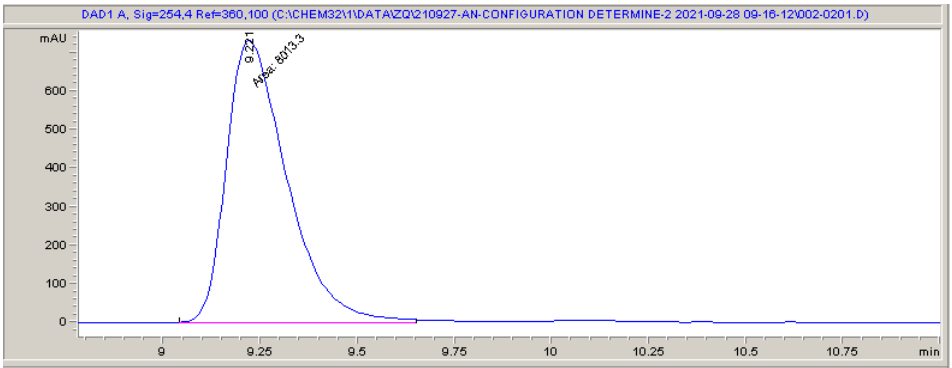

#	Time	Area	Height	Width	Area%	Symmetry
1	9.221	8013.3	735.8	0.1815	100.000	0.573

Determination of stereochemistry for all products:

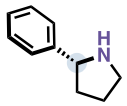

(*R*)-2-Phenylpyrrolidine (3.2a)

Chiral-phase HPLC conditions: Chiralpak IC, 25% *i*-PrOH in hexane, 1.5 mL/min, 25 ºC, 210 nm

Racemic 3.2a:

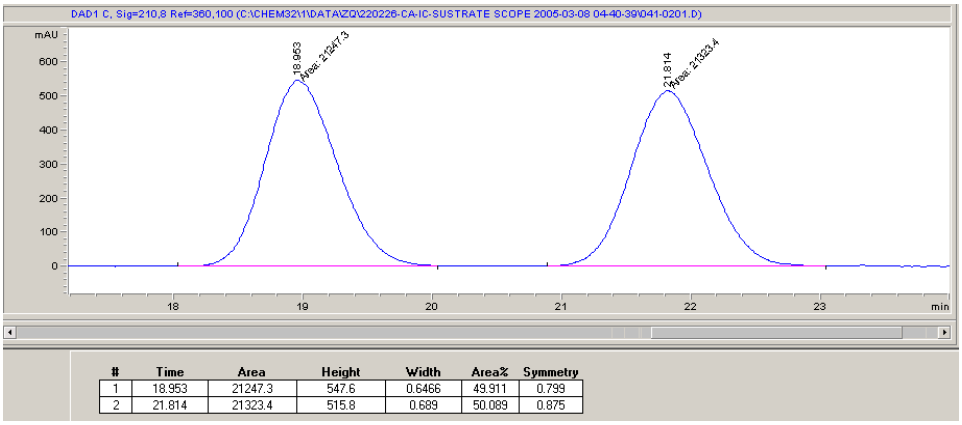

#	Time	Area	Height	Width	Area%	Symmetry
1	18.953	21247.3	547.6	0.6466	49.911	0.799
2	21.814	21323.4	515.8	0.689	50.089	0.875

Enzymatic preparation of 3.2a with P411-PYS-5149: 91:9 *er*

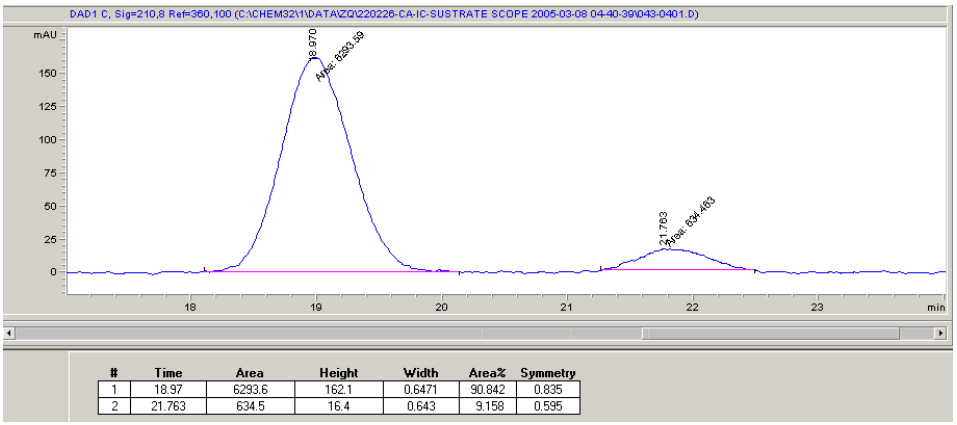

#	Time	Area	Height	Width	Area%	Symmetry
1	18.97	6293.6	162.1	0.6471	90.842	0.835
2	21.763	634.5	16.4	0.643	9.158	0.595

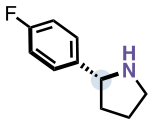

2-(4-Fluorophenyl)pyrrolidine (3.2b)

Chiral-phase HPLC conditions: Chiralpak IA, 10% *i*-PrOH in hexane, 1.5 mL/min, 25 ºC, 210 nm

Racemic 3.2b:

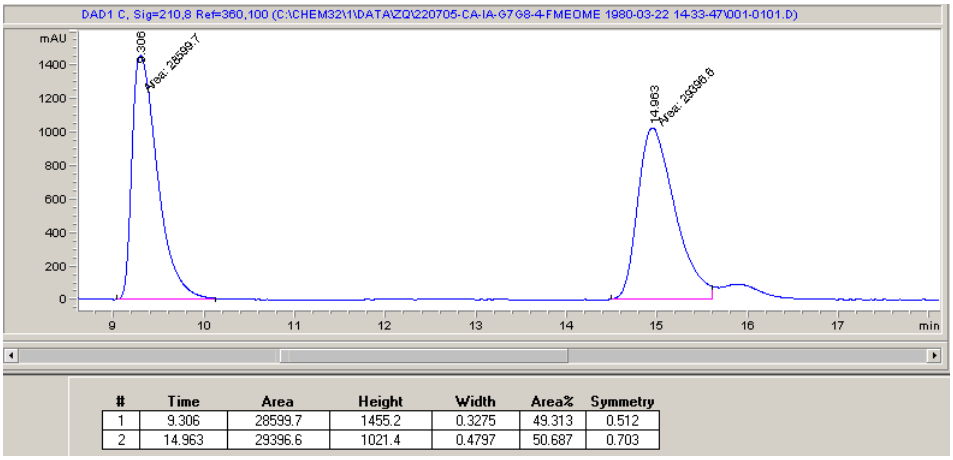

#	Time	Area	Height	Width	Area%	Symmetry
1	9.306	28599.7	1455.2	0.3275	49.313	0.512
2	14.963	29396.6	1021.4	0.4797	50.687	0.703

Enzymatic preparation of 3.2b with P411-PYS-5149: 92:8 *er*

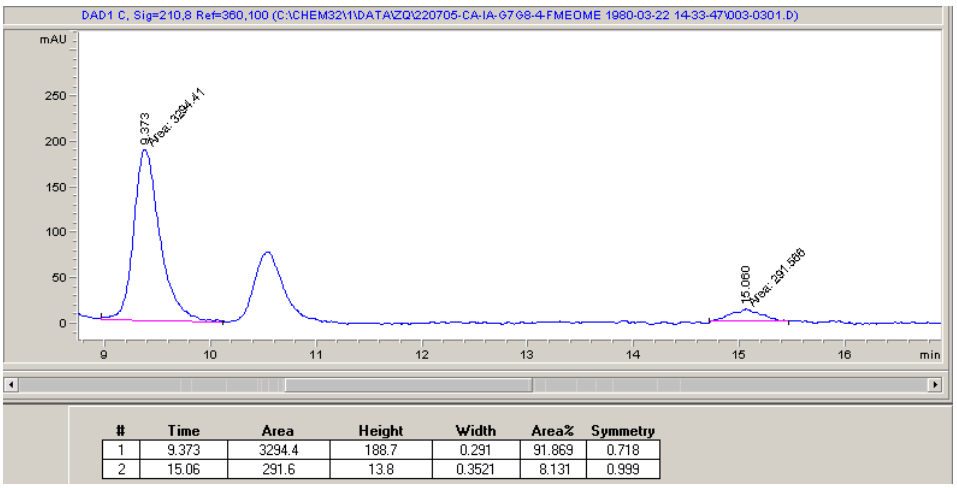

#	Time	Area	Height	Width	Area%	Symmetry
1	9.373	3294.4	188.7	0.291	91.869	0.718
2	15.06	291.6	13.8	0.3521	8.131	0.999

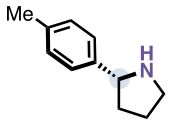

2-(*p*-Tolyl)pyrrolidine (3.2c)

Chiral-phase HPLC conditions: Chiralpak IA, 10% *i*-PrOH in hexane, 1.5 mL/min, 25 ºC, 210 nm

Racemic 3.2c:

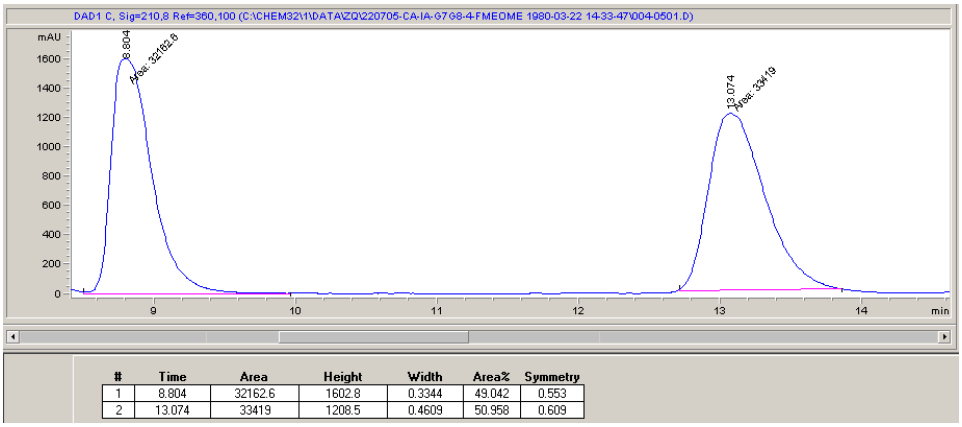

#	Time	Area	Height	Width	Area%	Symmetry
1	8.804	32162.6	1602.8	0.3344	49.042	0.553
2	13.074	33419	1208.5	0.4609	50.958	0.609

Enzymatic preparation of 3.2c with P411-PYS-5149: 92:8 *er*

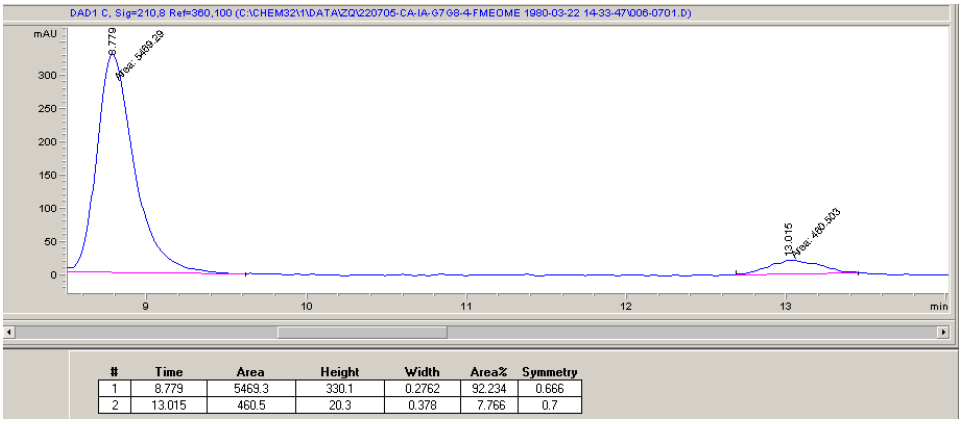

#	Time	Area	Height	Width	Area%	Symmetry
1	8.779	5469.3	330.1	0.2762	92.234	0.666
2	13.015	460.5	20.3	0.378	7.766	0.7

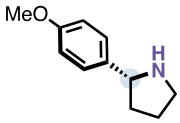

(*R*)-2-(4-Methoxyphenyl)pyrrolidine (3.2d)

Chiral-phase HPLC conditions: Chiralpak IA, 15% *i*-PrOH in hexane, 1.5 mL/min, 25 ºC, 210 nm

Racemic 3.2d:

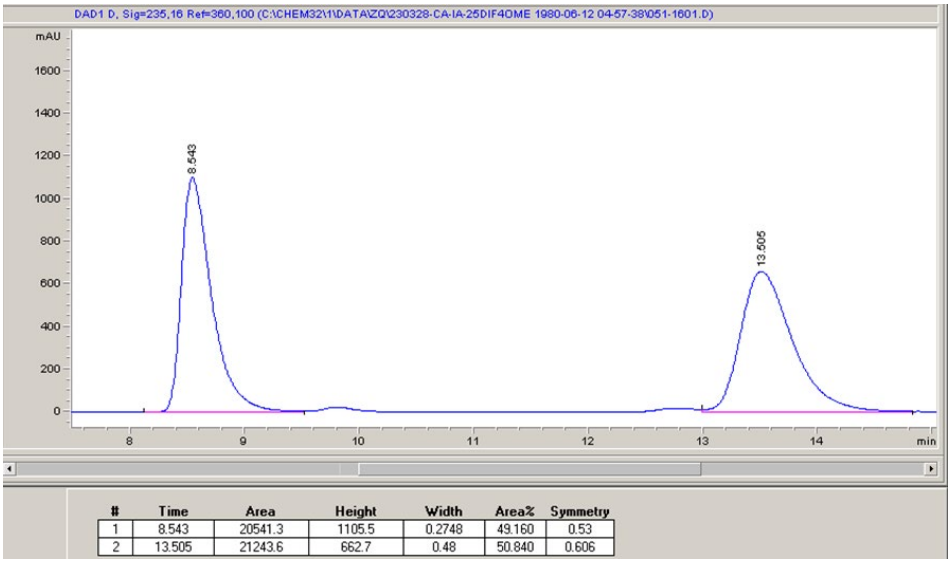

#	Time	Area	Height	Width	Area%	Symmetry
1	8.543	20541.3	1105.5	0.2748	49.160	0.53
2	13.505	21243.6	662.7	0.48	50.840	0.606

Enzymatic preparation of 3.2d with P411-PYS-5149: 99:1 *er*

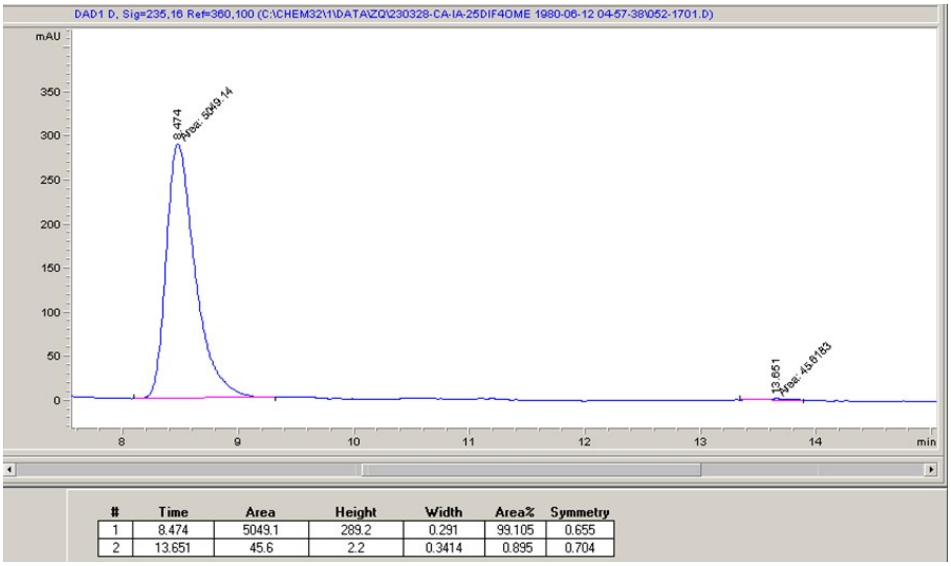

#	Time	Area	Height	Width	Area%	Symmetry
1	8.474	5049.1	289.2	0.291	99.105	0.655
2	13.651	45.6	2.2	0.3414	0.895	0.704

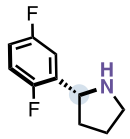

(*R*)-2-(2,5-Difluorophenyl)pyrrolidine (3.2e)

Chiral-phase HPLC conditions: Chiralpak IA, 7% *i*-PrOH in hexane, 1.5 mL/min, 25 ºC, 210 nm

Racemic 3.2e:

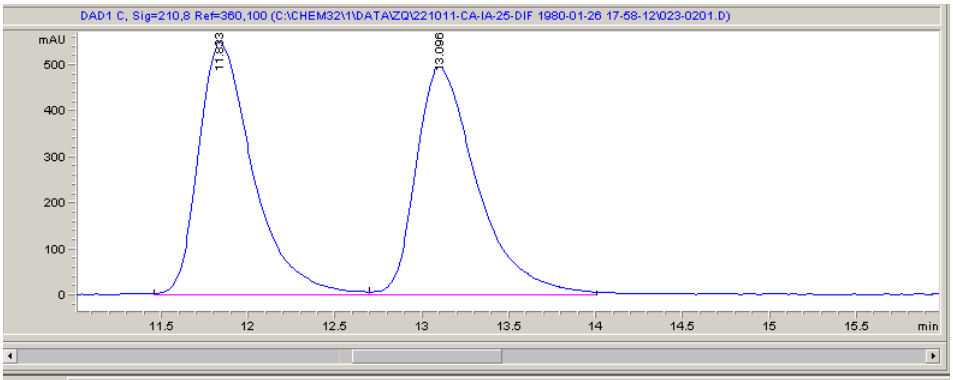

#	Time	Area	Height	Width	Area%	Symmetry
1	11.833	12083.3	551.4	0.3217	49.739	0.604
2	13.096	12210	497.2	0.3625	50.261	0.574

Enzymatic preparation of 3.2e with P411-PYS-5149: 85:15 *er*

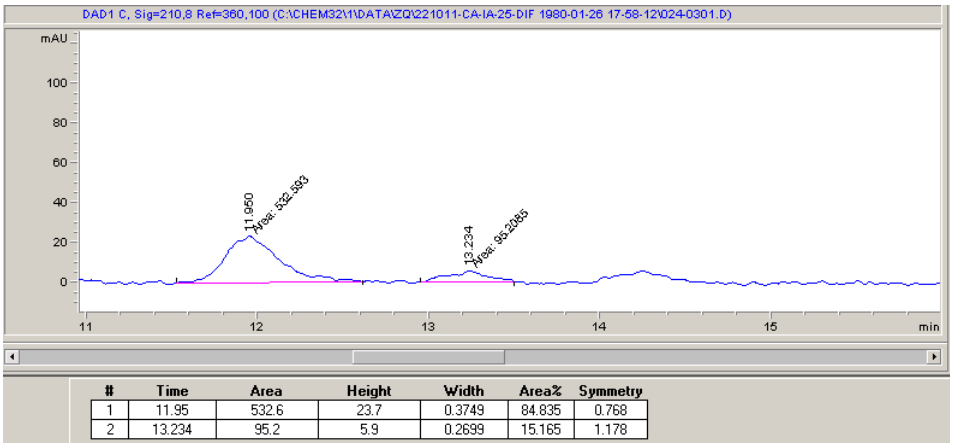

#	Time	Area	Height	Width	Area%	Symmetry
1	11.95	532.6	23.7	0.3749	84.835	0.768
2	13.234	95.2	5.9	0.2699	15.165	1.178

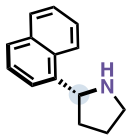

(*R*)-2-(Naphthalen-2-yl)pyrrolidine (3.2f)

Chiral-phase HPLC conditions: Chiralpak IA, 10% *i*-PrOH in hexane, 1.5 mL/min, 25 ºC, 210 nm

Racemic 3.2f:

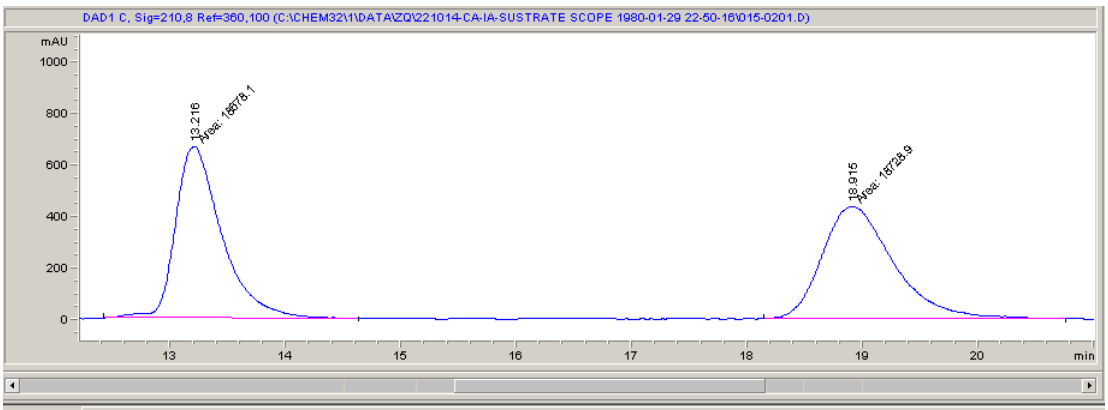

#	Time	Area	Height	Width	Area%	Symmetry
1	13.216	18678.1	667.2	0.4666	49.932	0.677
2	18.915	18728.9	437	0.7144	50.068	0.705

Enzymatic preparation of 3.2f with P411-PYS-5149: 60:40 *er*

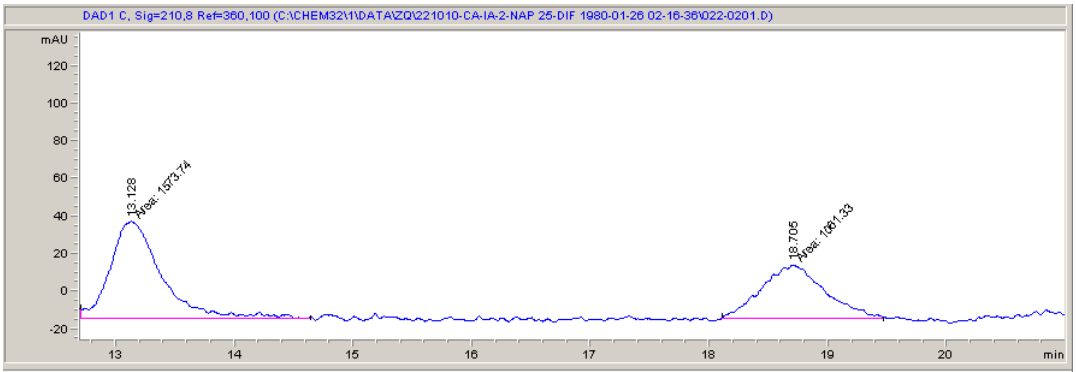

#	Time	Area	Height	Width	Area%	Symmetry
1	13.128	1573.7	52	0.5047	59.723	0.661
2	18.705	1061.3	28.5	0.6202	40.277	0.972

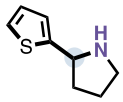

2-(Thiophen-2-yl)pyrrolidine (3.2g)

Chiral-phase HPLC conditions: Chiralpak IC, 25% *i*-PrOH in hexane, 1.5 mL/min, 25 ºC, 254 nm

Racemic 3.2g:

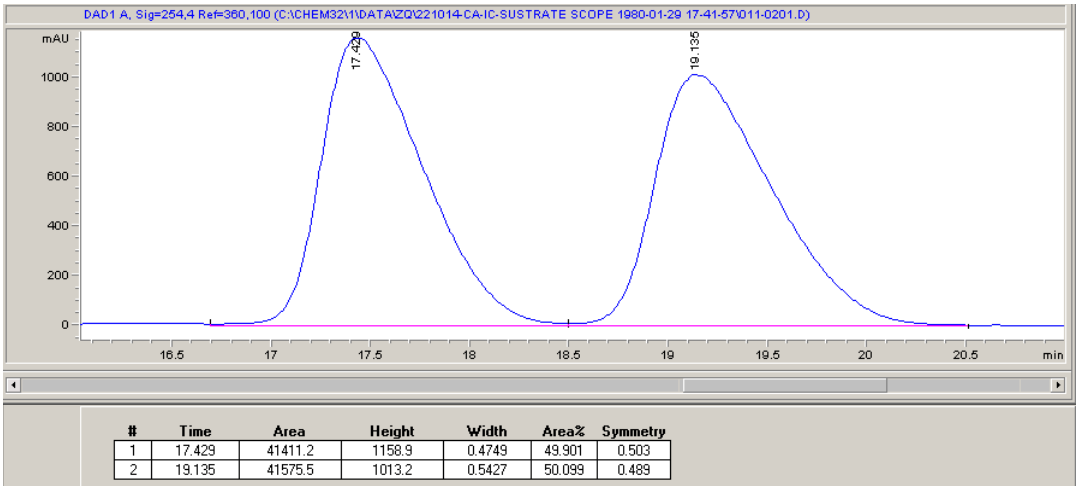

#	Time	Area	Height	Width	Area%	Symmetry
1	17.429	41411.2	1158.9	0.4749	49.901	0.503
2	19.135	41575.5	1013.2	0.5427	50.099	0.489

Enzymatic preparation of 3.2g with P411-PYS-5149: 23:77 *er*

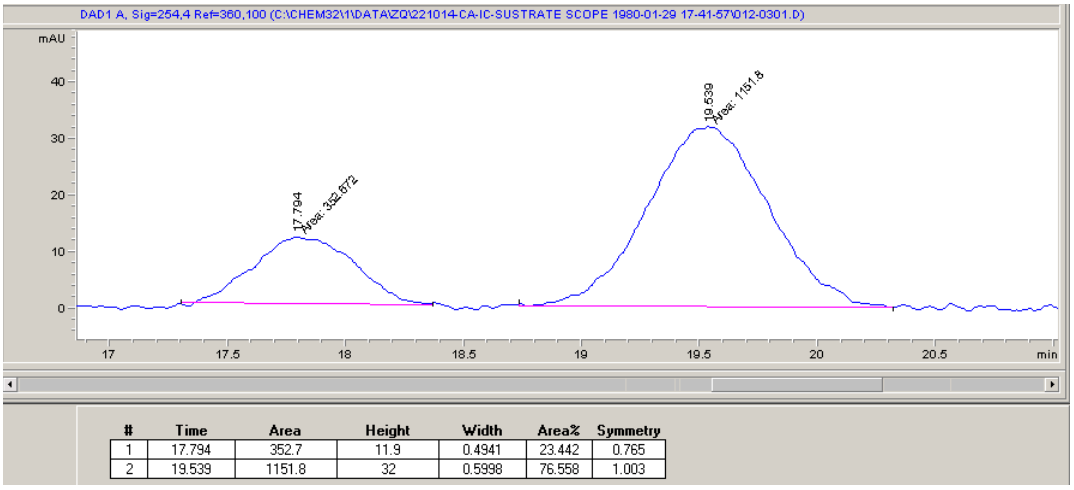

#	Time	Area	Height	Width	Area%	Symmetry
1	17.794	352.7	11.9	0.4941	23.442	0.765
2	19.539	1151.8	32	0.5998	76.558	1.003

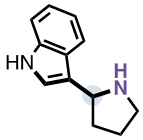

3-(Pyrrolidin-2-yl)-1H-indole (3.2h)

Chiral-phase HPLC conditions: Chiralpak IC, 20% *i*-PrOH in hexane, 1.5 mL/min, 25 ºC, 210 nm

Racemic 3.2h:

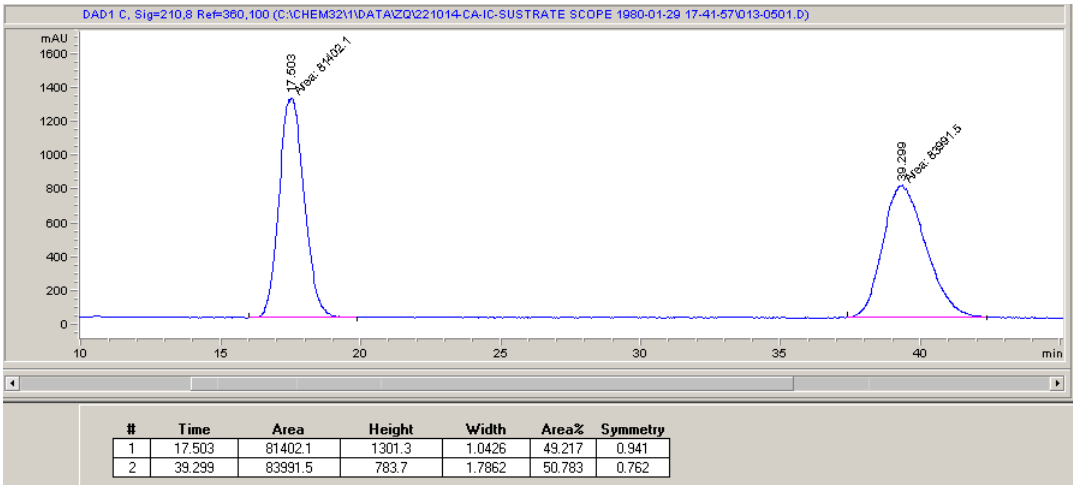

#	Time	Area	Height	Width	Area%	Symmetry
1	17.503	81402.1	1301.3	1.0426	49.217	0.941
2	39.299	83991.5	783.7	1.7862	50.783	0.762

Enzymatic preparation of 3.2h with P411-PYS-5149: 52:48 *er*

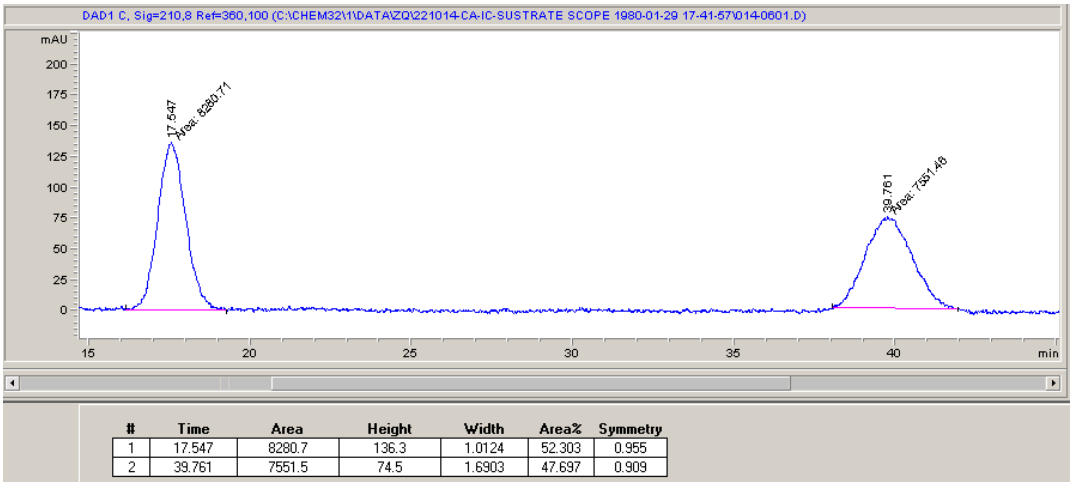

#	Time	Area	Height	Width	Area%	Symmetry
1	17.547	8280.7	136.3	1.0124	52.303	0.955
2	39.761	7551.5	74.5	1.6903	47.697	0.909

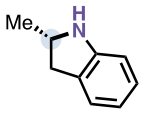

(*S*)-2-Methylindoline (3.4a)

Chiral-phase HPLC conditions: Chiralpak IB, 2% *i*-PrOH in hexane, 1.0 mL/min, 25 ºC, 254 nm

Racemic 3.4a:

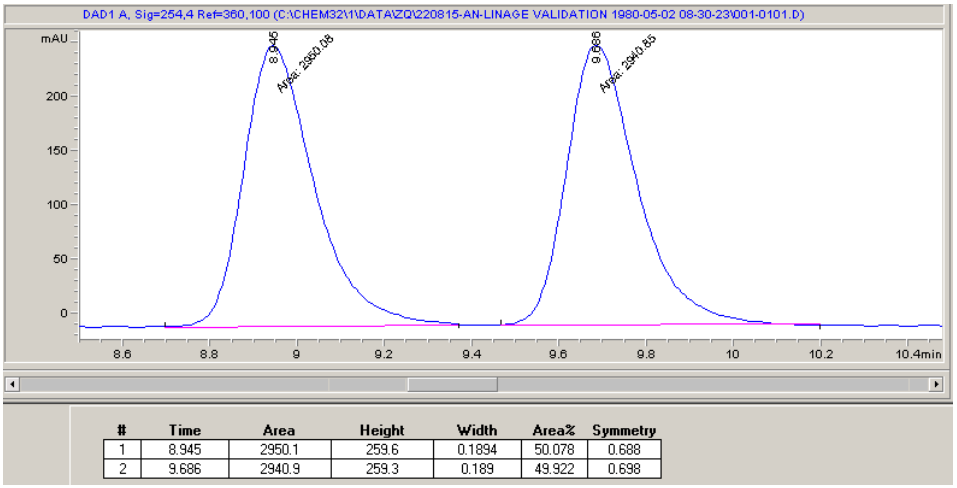

#	Time	Area	Height	Width	Area%	Symmetry
1	8.945	2950.1	259.6	0.1894	50.078	0.688
2	9.686	2940.9	259.3	0.189	49.922	0.698

Enzymatic preparation of 3.4a with P411-INS-5151: 8:92 *er*

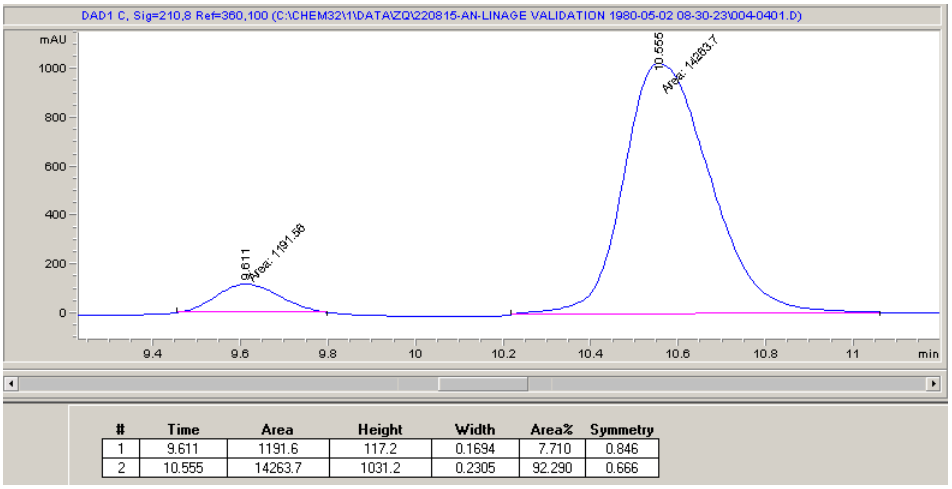

#	Time	Area	Height	Width	Area%	Symmetry
1	9.611	1191.6	117.2	0.1694	7.710	0.846
2	10.555	14263.7	1031.2	0.2305	92.290	0.666

Preparative scale enzymatic preparation of 3.4a with P411-INS-5151: 9:91 *er*

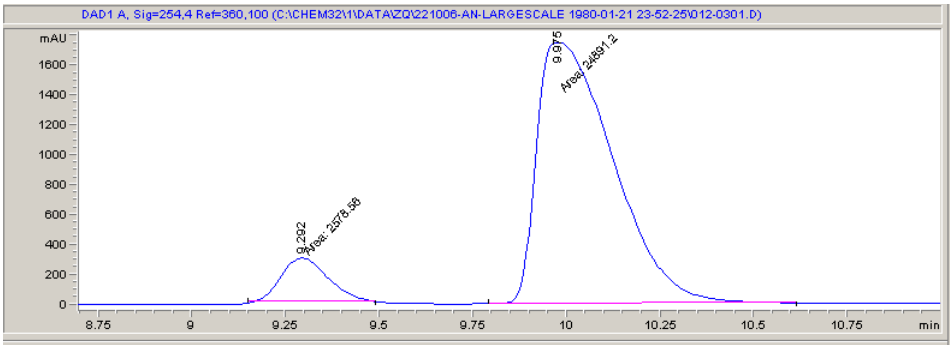

#	Time	Area	Height	Width	Area%	Symmetry
1	9.292	2578.6	293.8	0.1463	9.387	0.765
2	9.975	24891.2	1750.6	0.237	90.613	0.364

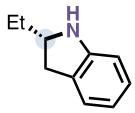

(*S*)-2-Ethylindoline (3.4b)

Chiral-phase HPLC conditions: Chiralpak IB, 2% *i*-PrOH in hexane, 1.0 mL/min, 25 ºC, 254 nm

Racemic 3.4b:

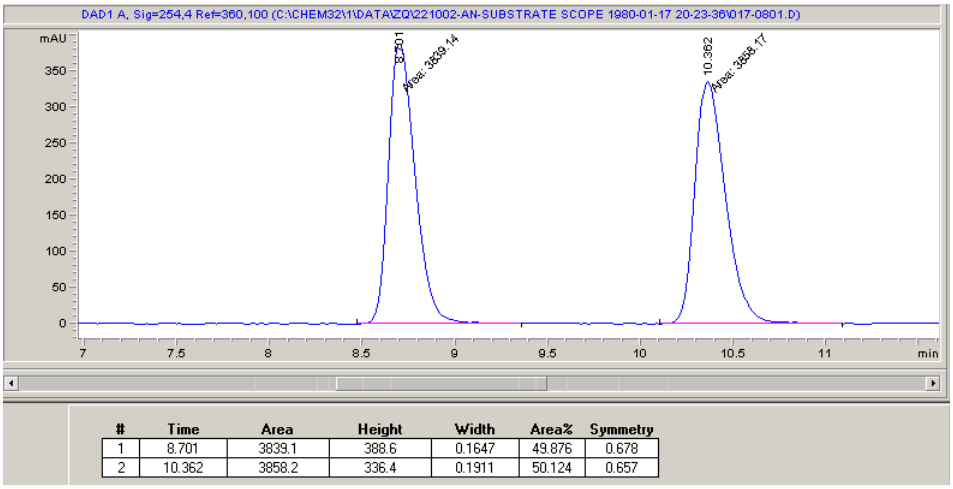

#	Time	Area	Height	Width	Area%	Symmetry
1	8.701	3839.1	388.6	0.1647	49.876	0.678
2	10.362	3858.2	336.4	0.1911	50.124	0.657

Enzymatic preparation of 3.4b with P411-INS-5151: 9:91 *er*

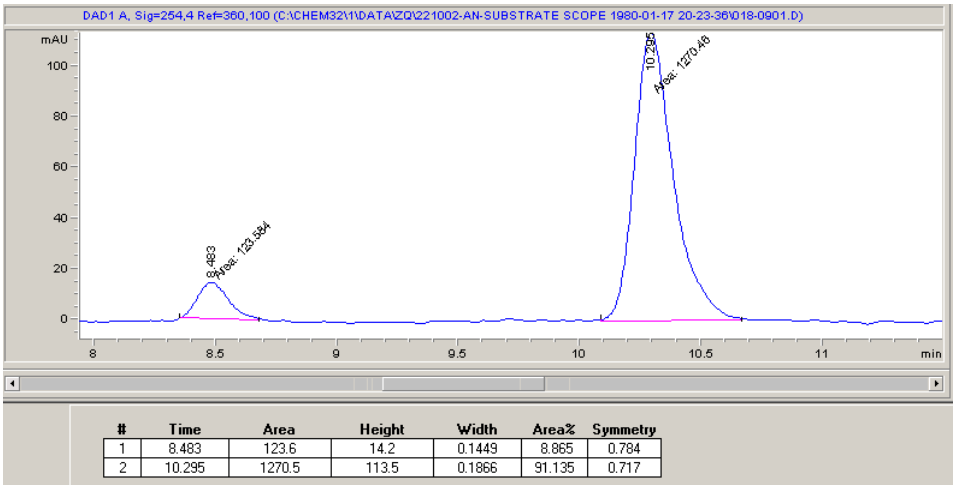

#	Time	Area	Height	Width	Area%	Symmetry
1	8.483	123.6	14.2	0.1449	8.865	0.784
2	10.295	1270.5	113.5	0.1866	91.135	0.717

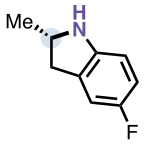

(*S*)-5-Fluoro-2-methylindoline (3.4c)

Chiral-phase HPLC conditions: Chiralpak IB, 2% *i*-PrOH in hexane, 1.0 mL/min, 25 ºC, 254 nm

Racemic 3.4c:

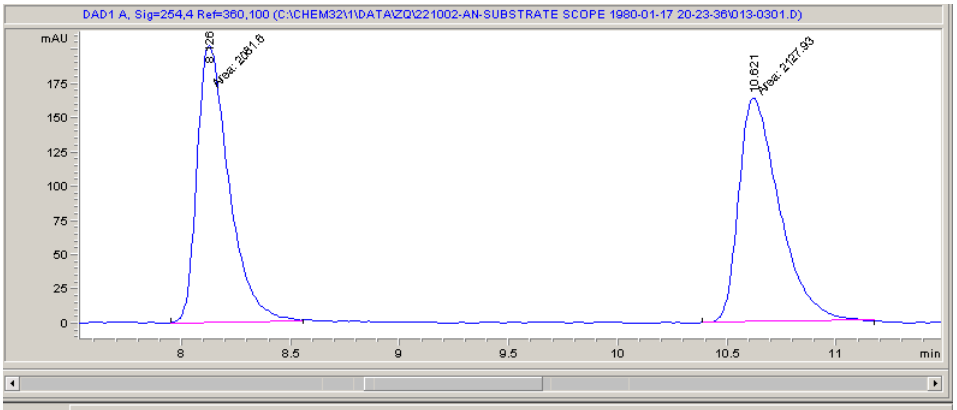

#	Time	Area	Height	Width	Area%	Symmetry
1	8.126	2081.6	203.3	0.1707	49.450	0.59
2	10.621	2127.9	163.7	0.2167	50.550	0.55

Enzymatic preparation of 3.4c with P411-INS-5151: 13:87 *er*

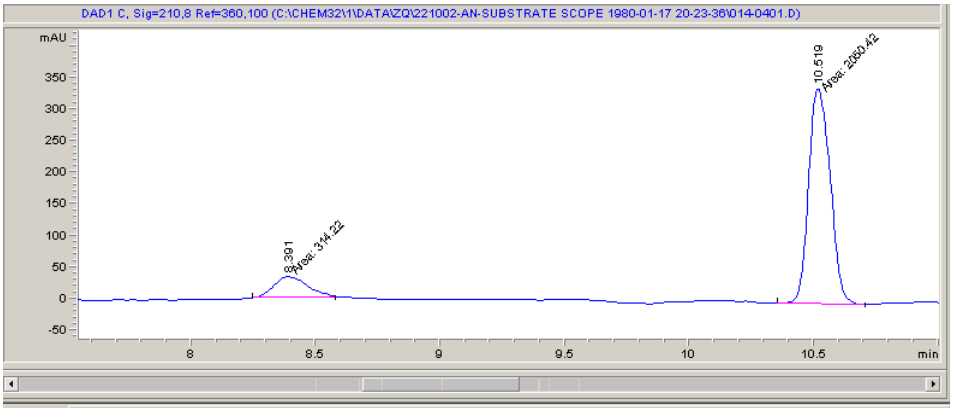

#	Time	Area	Height	Width	Area%	Symmetry
1	8.391	314.2	33.1	0.1583	13.288	0.74
2	10.519	2050.4	340.3	0.1004	86.712	0.751

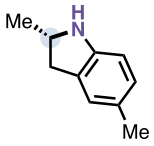

(*S*)-2,5-Dimethylindoline (3.4d)

Chiral-phase HPLC conditions: Chiralpak IB, 2% *i*-PrOH in hexane, 1.0 mL/min, 25 ºC, 254 nm

Racemic 3.4d:

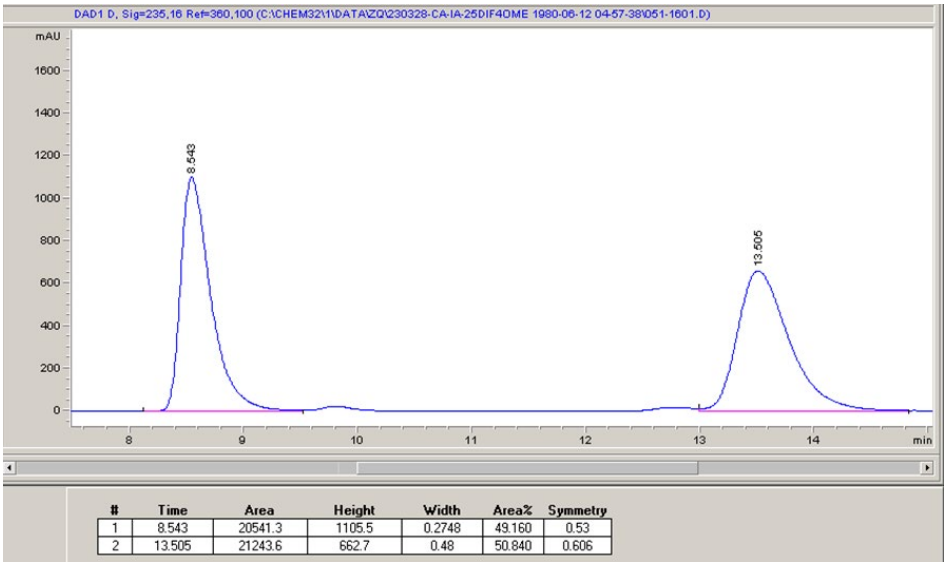

#	Time	Area	Height	Width	Area%	Symmetry
1	8.543	20541.3	1105.5	0.2748	49.160	0.53
2	13.505	21243.6	662.7	0.48	50.840	0.606

Enzymatic preparation of 3.4d with P411-INS-5151: 79:21 *er*

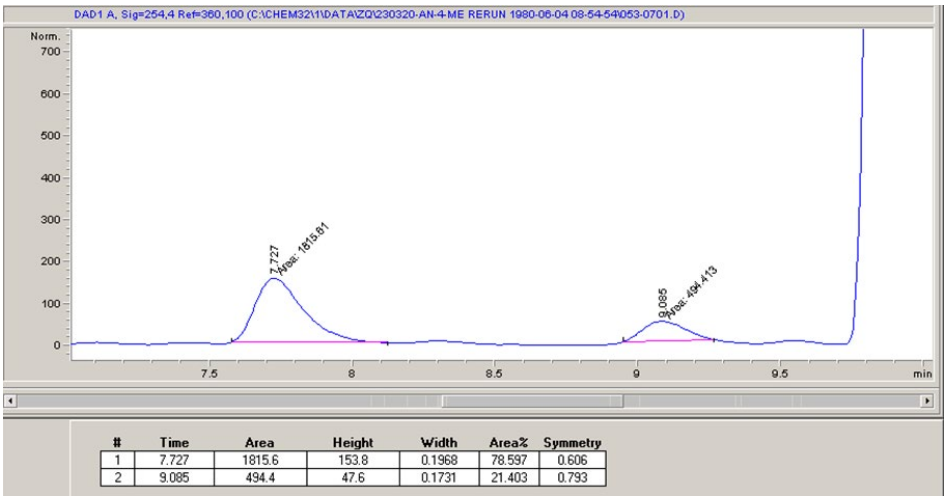

#	Time	Area	Height	Width	Area%	Symmetry
1	7.727	1815.6	153.8	0.1968	78.597	0.606
2	9.085	494.4	47.6	0.1731	21.403	0.793

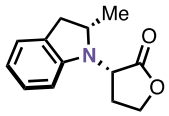

(S)-3-((S)-2-Methylindolin-1-yl)dihydrofuran-2(3H)-one (3.5):

Chiral-phase HPLC conditions: Chiralpak IC, 25% *i*-PrOH in hexane, 1.5 mL/min, 25 ºC, 254 nm

Racemic 3.5:

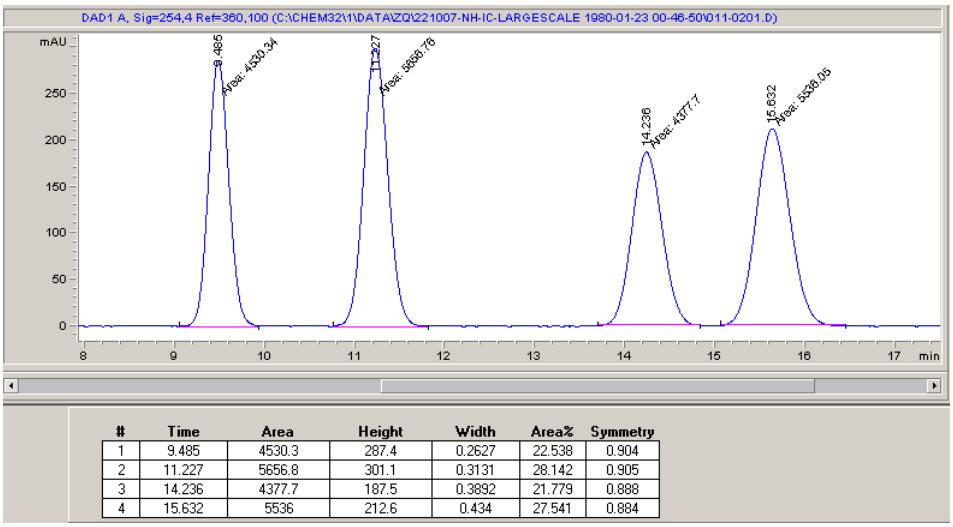

#	Time	Area	Height	Width	Area%	Symmetry
1	9.485	4530.3	287.4	0.2627	22.538	0.904
2	11.227	5656.8	301.1	0.3131	28.142	0.905
3	14.236	4377.7	187.5	0.3892	21.779	0.888
4	15.632	5536	212.6	0.434	27.541	0.884

Racemic 3-((S)-2-methylindolin-1-yl)dihydrofuran-2(3H)-one:

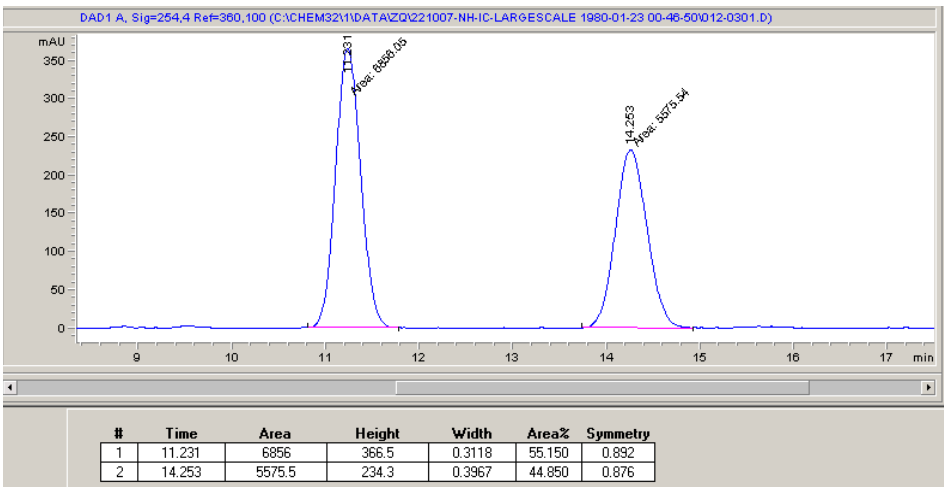

#	Time	Area	Height	Width	Area%	Symmetry
1	11.231	6856	366.5	0.3118	55.150	0.892
2	14.253	5575.5	234.3	0.3967	44.850	0.876

Preparative scale enzymatic preparation of 3.5 with L7_FL: 98:2 *er* and >24:1 dr

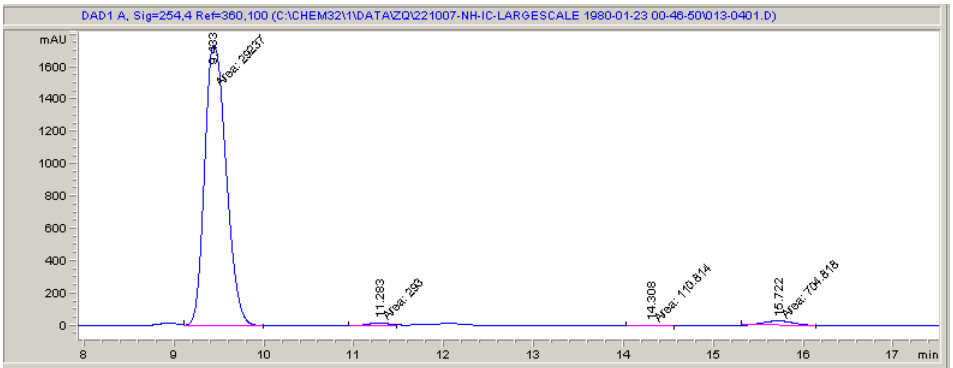

#	Time	Area	Height	Width	Area%	Symmetry
1	9.433	29237	1743.6	0.2795	96.347	0.684
2	11.283	293	16.8	0.2915	0.966	1.139
3	14.308	110.8	5.4	0.344	0.365	1.022
4	15.722	704.8	29.5	0.3986	2.323	1.055

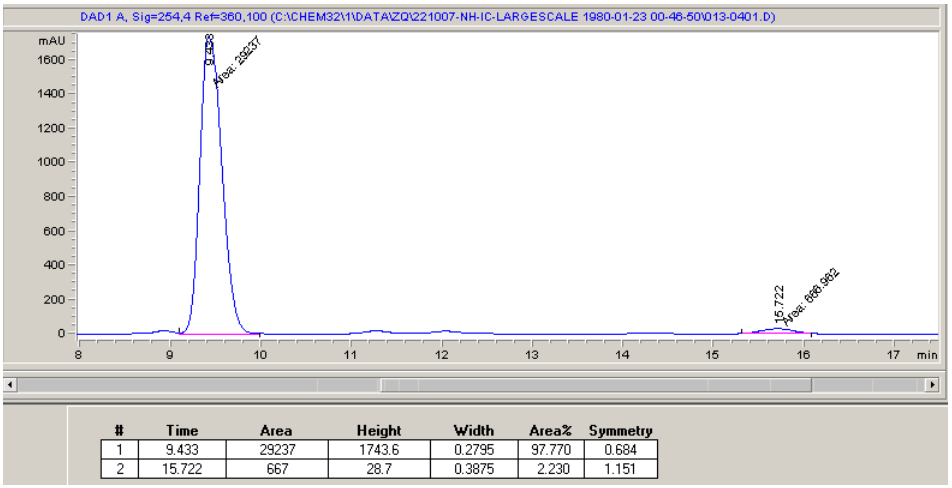

#	Time	Area	Height	Width	Area%	Symmetry
1	9.433	29237	1743.6	0.2795	97.770	0.684
2	15.722	667	28.7	0.3875	2.230	1.151

IX. Sequence Information

Mutations present in P411 variants described in this study:

P411 variant	Mutations relative to wild-type $P450_{BM3}$
P411-M177L (**P411-PYS-5141**)	A74G V78L A82L F87A P142S T175I M177L A184V S226R H236Q E252G I263Y H266V T268G A290V T327I A328V L353V I366V C400S T436L L437Q E442K
P411-PYS-5142	A74G **L75E** V78L A82L F87A P142S T175I M177L A184V S226R H236Q E252G I263Y H266V T268G A290V T327I A328V L353V I366V C400S T436L L437Q E442K
P411-PYS-5143	A74G **L75E** V78L A82L F87A P142S T175I M177L A184V S226R H236Q E252G I263Y H266V T268G A290V T327I A328V L353V I366V C400S T436L E442K
P411-PYS-5144	A74G **L75E** V78L A82L F87A P142S T175I M177L A184V S226R H236Q E252G I263Y H266V T268G A290V T327I A328V **A330Q** L353V I366V C400S T436L E442K
P411-PYS-5145	A74G **L75E** V78L A82L F87A **M118V** P142S T175I M177L A184V S226R H236Q E252G I263Y H266V T268G A290V T327I A328V **A330Q** L353V I366V C400S T436L E442K
P411-PYS-5146	A74G **L75E F77C** V78L A82L F87A **M118V** P142S T175I M177L A184V S226R H236Q E252G I263Y H266V T268G A290V T327I A328V **A330Q** L353V I366V C400S T436L E442K
P411-PYS-5147	**S72W** A74G **L75E F77C** V78L A82L F87A **M118V** P142S T175I M177L A184V S226R H236Q E252G I263Y H266V T268G A290V T327I A328V **A330Q** L353V I366V C400S T436L E442K
P411-PYS-5148	**S72W Q73A** A74G **L75E F77C** V78L A82L F87A **M118V** P142S T175I M177L A184V S226R H236Q E252G I263Y H266V T268G A290V T327I A328V **A330Q** L353V I366V C400S T436L E442K
P411-PYS-5149	**S72W Q73A** A74G **L75E F77C** V78L A82L F87A **M118V** P142S T175I M177L A184V S226R H236Q E252G I263Y H266V T268G A290V T327I A328V **A330Q** L353V I366V C400S **T436R** E442K
P411-INS-5150	**S72W Q73A** A74G **L75E F77C** V78L A82L F87A **M118V** P142S T175I M177L A184V S226R H236Q E252G I263Y H266V T268G A290V T327I A328V **A330Q** L353V I366V C400S T436L **L437P** E442K
P411-INS-5151	**S72W Q73A** A74G **L75E F77C** V78L A82L F87A **M118V** P142S T175I M177L **L181N** A184V S226R H236Q E252G I263Y H266V T268G A290V T327I A328V **A330Q** L353V I366V C400S T436L **L437P** E442K

Nucleotide and amino acid sequences of P411-M177L (P411-PYS-5141):

```
ATGACAATTAAAGAAATGCCTCAGCCAAAAACGTTTGGAGAGCTTAAAAATTTACCGTTATTAAACACAG
ATAAACCGGTTCAAGCTTTGATGAAAATTGCGGATGAATTAGGAGAAATCTTTAAATTCGAGGCGCCTGG
```

TCGTGTAACGCGCTACTTATCAAGTCAGCGTCTAATTAAAGAAGCATGCGATGAATCACGCTTTGATAAA
AACTTAAGTCAAGGTCTGAAATTTCTGCGTGATTTTCTTGGAGACGGGTTAGCCACAAGCTGGACGCATG
AAAAAAATTGGAAAAAAGCGCATAATATCTTACTTCCAAGCTTTAGTCAGCAGGCAATGAAAGGCTATCA
TGCGATGATGGTCGATATCGCCGTGCAGCTTGTTCAAAAGTGGGAGCGTCTAAATGCAGATGAGCATATT
GAAGTATCGGAAGACATGACACGTTTAACGCTTGATACAATTGGTCTTTGCGGCTTTAACTATCGCTTTA
ACAGCTTTTACCGAGATCAGCCTCATCCATTTATTATAAGTCTGGTCCGTGCACTGGATGAAGTAATGAA
CAAGCTGCAGCGAGCAAATCCAGACGACCCAGCTTATGATGAAAACAAGCGCCAGTTTCAAGAAGATATC
AAGGTGATGAACGACCTAGTAGATAAAATTATTGCAGATCGCAAAGCAAGGGGTGAACAAAGCGATGATT
TATTAACGCAGATGCTAAACGGAAAAGATCCAGAAACGGGTGAGCCGCTTGATGACGGGAACATTCGCTA
TCAAATTATTACATTCTTATATGCGGGAGTTGAAGGTACAAGTGGTCTTTTATCATTTGCGCTGTATTTC
TTAGTGAAAAATCCACATGTATTACAAAAAGTAGCAGAAGAAGCAGCACGAGTTCTAGTAGATCCTGTTC
CAAGCTACAAACAAGTCAAACAGCTTAAATATGTCGGCATGGTCTTAAACGAAGCGCTGCGCTTATGGCC
AATTGTTCCTGCGTTTTCCCTATATGCAAAAGAAGATACGGTGCTTGGAGGAGAATATCCTTTAGAAAAA
GGCGACGAAGTAATGGTTCTGATTCCTCAGCTTCACCGTGATAAAACAGTTTGGGGAGACGATGTGGAGG
AGTTCCGTCCAGAGCGTTTTGAAAATCCAAGTGCGATTCCGCAGCATGCGTTTAAACCGTTTGGAAACGG
TCAGCGTGCGTCTATCGGTCAGCAGTTCGCTCTTCATGAAGCAACGCTGGTACTTGGTATGATGCTAAAA
CACTTTGACTTTGAAGATCATACAAACTACGAGCTCGATATTAAAGAACTGCAGACGTTAAAACCTAAAG
GCTTTGTGGTAAAAGCAAAATCGAAAAAAATTCCGCTTGGCGGTATTCCTTCACCTAGCACTGAACAGTC
TGCTAAAAAAGTACGCAAAAAGGCAGAAAACGCTCATAATACGCCGCTGCTTGTGCTATACGGTTCAAAT
ATGGGTACCGCTGAAGGAACGGCGCGTGATTTAGCAGATATTGCAATGAGCAAAGGATTTGCACCGCAGG
TCGCAACGCTTGATTCACACGCCGGAAATCTTCCGCGCGAAGGAGCTGTATTAATTGTAACGGCGTCTTA
TAACGGTCATCCGCCTGATAACGCAAAGCAATTTGTCGACTGGTTAGACCAAGCGTCTGCTGATGAAGTA
AAAGGCGTTCGCTACTCCGTATTTGGATGCGGCGATAAAAACTGGGCTACTACGTATCAAAAAGTGCCTG
CTTTTATCGATGAAACGCTTGCCGCTAAAGGGGCAGAAAACATCGCTGACCGCGGTGAAGCAGATGCAAG
CGACGACTTTGAAGGCACATATGAAGAATGGCGTGAACATATGTGGAGTGACGTAGCAGCCTACTTTAAC
CTCGACATTGAAAACAGTGAAGATAATAAATCTACTCTTTCACTTCAATTTGTCGACAGCGCCGCGGATA
TGCCGCTTGCGAAAATGCACGGTGCGTTTTCAACGAACGTCGTAGCAAGCAAAGAACTTCAACAGCCAGG
CAGTGCACGAAGCACGCGACATCTTGAAATTGAACTTCCAAAAGAAGCTTCTTATCAAGAAGGAGATCAT
TTAGGTGTTATTCCTCGCAACTATGAAGGAATAGTAAACCGTGTAACAGCAAGGTTCGGCCTAGATGCAT
CACAGCAAATCCGTCTGGAAGCAGAAGAAGAAAAATTAGCTCATTTGCCACTCGCTAAAACAGTATCCGT
AGAAGAGCTTCTGCAATACGTGGAGCTTCAAGATCCTGTTACGCGCACGCAGCTTCGCGCAATGGCTGCT
AAAACGGTCTGCCCGCCGCATAAAGTAGAGCTTGAAGCCTTGCTTGAAAAGCAAGCCTACAAAGAACAAG
TGCTGGCAAAACGTTTAACAATGCTTGAACTGCTTGAAAAATACCCGGCGTGTGAAATGAAATTCAGCGA
ATTTATCGCCCTTCTGCCAAGCATACGCCCGCGCTATTACTCGATTTCTTCATCACCTCGTGTCGATGAA
AAACAAGCAAGCATCACGGTCAGCGTTGTCTCAGGAGAAGCGTGGAGCGGATATGGAGAATATAAAGGAA
TTGCGTCGAACTATCTTGCCGAGCTGCAAGAAGGAGATACGATTACGTGCTTTATTTCCACACCGCAGTC
AGAATTTACGCTGCCAAAAGACCCTGAAACGCCGCTTATCATGGTCGGACCGGGAACAGGCGTCGCGCCG
TTTAGAGGCTTTGTGCAGGCGCGCAAACAGCTAAAAGAACAAGGACAGTCACTTGGAGAAGCACATTTAT
ACTTCGGCTGCCGTTCACCTCATGAAGACTATCTGTATCAAGAAGAGCTTGAAAACGCCCAAAGCGAAGG
CATCATTACGCTTCATACCGCTTTTTCTCGCATGCCAAATCAGCCGAAAACATACGTTCAGCACGTAATG
GAACAAGACGGCAAGAAATTGATTGAACTTCTTGATCAAGGAGCGCACTTCTATATTTGCGGAGACGGAA
GCCAAATGGCACCTGCCGTTGAAGCAACGCTTATGAAAAGCTATGCTGACGTTCACCAAGTGAGTGAAGC
AGACGCTCGCTTATGGCTGCAGCAGCTAGAAGAAAAAGGCCGATACGCAAAAGACGTGTGGGCTGGGCTC
GAGCACCACCACCACCACCACTGA

MTIKEMPQPKTFGELKNLPLLNTDKPVQALMKIADELGEIFKFEAPGRVTRYLSSQRLIKEACDESRFDK
NLSQGLKFLRDFLGDGLATSWTHEKNWKKAHNILLPSFSQQAMKGYHAMMVDIAVQLVQKWERLNADEHI
EVSEDMTRLTLDTIGLCGFNYRFNSFYRDQPHPFIISLVRALDEVMNKLQRANPDDPAYDENKRQFQEDI
KVMNDLVDKIIADRKARGEQSDDLLTQMLNGKDPETGEPLDDGNIRYQIITFLYAGVEGTSGLLSFALYF
LVKNPHVLQKVAEEAARVLVDPVPSYKQVKQLKYVGMVLNEALRLWPIVPAFSLYAKEDTVLGGEYPLEK
GDEVMVLIPQLHRDKTVWGDDVEEFRPERFENPSAIPQHAFKPFGNGQRASIGQQFALHEATLVLGMMLK
HFDFEDHTNYELDIKELQTLKPKGFVVKAKSKKIPLGGIPSPSTEQSAKKVRKKAENAHNTPLLVLYGSN

MGTAEGTARDLADIAMSKGFAPQVATLDSHAGNLPREGAVLIVTASYNGHPPDNAKQFVDWLDQASADEV
KGVRYSVFGCGDKNWATTYQKVPAFIDETLAAKGAENIADRGEADASDDFEGTYEEWREHMWSDVAAYFN
LDIENSEDNKSTLSLQFVDSAADMPLAKMHGAFSTNVVASKELQQPGSARSTRHLEIELPKEASYQEGDH
LGVIPRNYEGIVNRVTARFGLDASQQIRLEAEEEKLAHLPLAKTVSVEELLQYVELQDPVTRTQLRAMAA
KTVCPPHKVELEALLEKQAYKEQVLAKRLTMLELLEKYPACEMKFSEFIALLPSIRPRYYSISSSPRVDE
KQASITVSVVSGEAWSGYGEYKGIASNYLAELQEGDTITCFISTPQSEFTLPKDPETPLIMVGPGTGVAP
FRGFVQARKQLKEQGQSLGEAHLYFGCRSPHEDYLYQEELENAQSEGIITLHTAFSRMPNQPKTYVQHVM
EQDGKKLIELLDQGAHFYICGDGSQMAPAVEATLMKSYADVHQVSEADARLWLQQLEEKGRYAKDVWAGL
EHHHHHH

Nucleotide and amino acid sequences of P411-PYS-5142:

ATGACAATTAAAGAAATGCCTCAGCCAAAAACGTTTGGAGAGCTTAAAAATTTACCGTTATTAAACACAG
ATAAACCGGTTCAAGCTTTGATGAAAATTGCGGATGAATTAGGAGAAATCTTTAAATTCGAGGCGCCTGG
TCGTGTAACGCGCTACTTATCAAGTCAGCGTCTAATTAAAGAAGCATGCGATGAATCACGCTTTGATAAA
AACTTAAGTCAAGGTGAGAAATTTCTGCGTGATTTTCTTGGAGACGGGTTAGCCACAAGCTGGACGCATG
AAAAAAATTGGAAAAAAGCGCATAATATCTTACTTCCAAGCTTTAGTCAGCAGGCAATGAAAGGCTATCA
TGCGATGATGGTCGATATCGCCGTGCAGCTTGTTCAAAAGTGGGAGCGTCTAAATGCAGATGAGCATATT
GAAGTATCGGAAGACATGACACGTTTAACGCTTGATACAATTGGTCTTTGCGGCTTTAACTATCGCTTTA
ACAGCTTTTACCGAGATCAGCCTCATCCATTTATTATAAGTCTGGTCCGTGCACTGGATGAAGTAATGAA
CAAGCTGCAGCGAGCAAATCCAGACGACCCAGCTTATGATGAAAACAAGCGCCAGTTTCAAGAAGATATC
AAGGTGATGAACGACCTAGTAGATAAAATTATTGCAGATCGCAAAGCAAGGGGTGAACAAAGCGATGATT
TATTAACGCAGATGCTAAACGGAAAAGATCCAGAAACGGGTGAGCCGCTTGATGACGGGAACATTCGCTA
TCAAATTATTACATTCTTATATGCGGGAGTTGAAGGTACAAGTGGTCTTTTATCATTTGCGCTGTATTTC
TTAGTGAAAAATCCACATGTATTACAAAAAGTAGCAGAAGAAGCAGCACGAGTTCTAGTAGATCCTGTTC
CAAGCTACAAACAAGTCAAACAGCTTAAATATGTCGGCATGGTCTTAAACGAAGCGCTGCGCTTATGGCC
AATTGTTCCTGCGTTTTCCCTATATGCAAAAGAAGATACGGTGCTTGGAGGAGAATATCCTTTAGAAAAA
GGCGACGAAGTAATGGTTCTGATTCCTCAGCTTCACCGTGATAAAACAGTTTGGGGAGACGATGTGGAGG
AGTTCCGTCCAGAGCGTTTTGAAAATCCAAGTGCGATTCCGCAGCATGCGTTTAAACCGTTTGGAAACGG
TCAGCGTGCGTCTATCGGTCAGCAGTTCGCTCTTCATGAAGCAACGCTGGTACTTGGTATGATGCTAAAA
CACTTTGACTTTGAAGATCATACAAACTACGAGCTCGATATTAAAGAACTGCAGACGTTAAAACCTAAAG
GCTTTGTGGTAAAAGCAAAATCGAAAAAAATTCCGCTTGGCGGTATTCCTTCACCTAGCACTGAACAGTC
TGCTAAAAAAGTACGCAAAAAGGCAGAAAACGCTCATAATACGCCGCTGCTTGTGCTATACGGTTCAAAT
ATGGGTACCGCTGAAGGAACGGCGCGTGATTTAGCAGATATTGCAATGAGCAAAGGATTTGCACCGCAGG
TCGCAACGCTTGATTCACACGCCGGAAATCTTCCGCGCGAAGGAGCTGTATTAATTGTAACGGCGTCTTA
TAACGGTCATCCGCCTGATAACGCAAAGCAATTTGTCGACTGGTTAGACCAAGCGTCTGCTGATGAAGTA
AAAGGCGTTCGCTACTCCGTATTTGGATGCGGCGATAAAAACTGGGCTACTACGTATCAAAAAGTGCCTG
CTTTTATCGATGAAACGCTTGCCGCTAAAGGGGCAGAAAACATCGCTGACCGCGGTGAAGCAGATGCAAG
CGACGACTTTGAAGGCACATATGAAGAATGGCGTGAACATATGTGGAGTGACGTAGCAGCCTACTTTAAC
CTCGACATTGAAAACAGTGAAGATAATAAATCTACTCTTTCACTTCAATTTGTCGACAGCGCCGCGGATA
TGCCGCTTGCGAAAATGCACGGTGCGTTTTCAACGAACGTCGTAGCAAGCAAAGAACTTCAACAGCCAGG
CAGTGCACGAAGCACGCGACATCTTGAAATTGAACTTCCAAAAGAAGCTTCTTATCAAGAAGGAGATCAT
TTAGGTGTTATTCCTCGCAACTATGAAGGAATAGTAAACCGTGTAACAGCAAGGTTCGGCCTAGATGCAT
CACAGCAAATCCGTCTGGAAGCAGAAGAAGAAAAATTAGCTCATTTGCCACTCGCTAAAACAGTATCCGT
AGAAGAGCTTCTGCAATACGTGGAGCTTCAAGATCCTGTTACGCGCACGCAGCTTCGCGCAATGGCTGCT
AAAACGGTCTGCCCGCCGCATAAAGTAGAGCTTGAAGCCTTGCTTGAAAAGCAAGCCTACAAAGAACAAG
TGCTGGCAAAACGTTTAACAATGCTTGAACTGCTTGAAAAATACCCGGCGTGTGAAATGAAATTCAGCGA
ATTTATCGCCCTTCTGCCAAGCATACGCCCGCGCTATTACTCGATTTCTTCATCACCTCGTGTCGATGAA
AAACAAGCAAGCATCACGGTCAGCGTTGTCTCAGGAGAAGCGTGGAGCGGATATGGAGAATATAAAGGAA

TTGCGTCGAACTATCTTGCCGAGCTGCAAGAAGGAGATACGATTACGTGCTTTATTTCCACACCGCAGTC
AGAATTTACGCTGCCAAAAGACCCTGAAACGCCGCTTATCATGGTCGGACCGGGAACAGGCGTCGCGCCG
TTTAGAGGCTTTGTGCAGGCGCGCAAACAGCTAAAAGAACAAGGACAGTCACTTGGAGAAGCACATTTAT
ACTTCGGCTGCCGTTCACCTCATGAAGACTATCTGTATCAAGAAGAGCTTGAAAACGCCCAAAGCGAAGG
CATCATTACGCTTCATACCGCTTTTTCTCGCATGCCAAATCAGCCGAAAACATACGTTCAGCACGTAATG
GAACAAGACGGCAAGAAATTGATTGAACTTCTTGATCAAGGAGCGCACTTCTATATTTGCGGAGACGGAA
GCCAAATGGCACCTGCCGTTGAAGCAACGCTTATGAAAAGCTATGCTGACGTTCACCAAGTGAGTGAAGC
AGACGCTCGCTTATGGCTGCAGCAGCTAGAAGAAAAAGGCCGATACGCAAAAGACGTGTGGGCTGGGCTC
GAGCACCACCACCACCACCACTGA

MTIKEMPQPKTFGELKNLPLLNTDKPVQALMKIADELGEIFKFEAPGRVTRYLSSQRLIKEACDESRFDK
NLSQGEKFLRDFLGDGLATSWTHEKNWKKAHNILLPSFSQQAMKGYHAMMVDIAVQLVQKWERLNADEHI
EVSEDMTRLTLDTIGLCGFNYRFNSFYRDQPHPFIISLVRALDEVMNKLQRANPDDPAYDENKRQFQEDI
KVMNDLVDKIIADRKARGEQSDDLLTQMLNGKDPETGEPLDDGNIRYQIITFLYAGVEGTSGLLSFALYF
LVKNPHVLQKVAEEAARVLVDPVPSYKQVKQLKYVGMVLNEALRLWPIVPAFSLYAKEDTVLGGEYPLEK
GDEVMVLIPQLHRDKTVWGDDVEEFRPERFENPSAIPQHAFKPFGNGQRASIGQQFALHEATLVLGMMLK
HFDFEDHTNYELDIKELQTLKPKGFVVKAKSKKIPLGGIPSPSTEQSAKKVRKKAENAHNTPLLVLYGSN
MGTAEGTARDLADIAMSKGFAPQVATLDSHAGNLPREGAVLIVTASYNGHPPDNAKQFVDWLDQASADEV
KGVRYSVFGCGDKNWATTYQKVPAFIDETLAAKGAENIADRGEADASDDFEGTYEEWREHMWSDVAAYFN
LDIENSEDNKSTLSLQFVDSAADMPLAKMHGAFSTNVVASKELQQPGSARSTRHLEIELPKEASYQEGDH
LGVIPRNYEGIVNRVTARFGLDASQQIRLEAEEEKLAHLPLAKTVSVEELLQYVELQDPVTRTQLRAMAA
KTVCPPHKVELEALLEKQAYKEQVLAKRLTMLELLEKYPACEMKFSEFIALLPSIRPRYYSISSSPRVDE
KQASITVSVVSGEAWSGYGEYKGIASNYLAELQEGDTITCFISTPQSEFTLPKDPETPLIMVGPGTGVAP
FRGFVQARKQLKEQGQSLGEAHLYFGCRSPHEDYLYQEELENAQSEGIITLHTAFSRMPNQPKTYVQHVM
EQDGKKLIELLDQGAHFYICGDGSQMAPAVEATLMKSYADVHQVSEADARLWLQQLEEKGRYAKDVWAGL
EHHHHHH

Nucleotide and amino acid sequences of P411-PYS-5143:

ATGACAATTAAAGAAATGCCTCAGCCAAAAACGTTTGGAGAGCTTAAAAATTTACCGTTATTAAACACAG
ATAAACCGGTTCAAGCTTTGATGAAAATTGCGGATGAATTAGGAGAAATCTTTAAATTCGAGGCGCCTGG
TCGTGTAACGCGCTACTTATCAAGTCAGCGTCTAATTAAAGAAGCATGCGATGAATCACGCTTTGATAAA
AACTTAAGTCAAGGTGAGAAATTTCTGCGTGATTTTCTTGGAGACGGGTTAGCCACAAGCTGGACGCATG
AAAAAAATTGGAAAAAAGCGCATAATATCTTACTTCCAAGCTTTAGTCAGCAGGCAATGAAAGGCTATCA
TGCGATGATGGTCGATATCGCCGTGCAGCTTGTTCAAAAGTGGGAGCGTCTAAATGCAGATGAGCATATT
GAAGTATCGGAAGACATGACACGTTTAACGCTTGATACAATTGGTCTTTGCGGCTTTAACTATCGCTTTA
ACAGCTTTTACCGAGATCAGCCTCATCCATTTATTATAAGTCTGGTCCGTGCACTGGATGAAGTAATGAA
CAAGCTGCAGCGAGCAAATCCAGACGACCCAGCTTATGATGAAAACAAGCGCCAGTTTCAAGAAGATATC
AAGGTGATGAACGACCTAGTAGATAAAATTATTGCAGATCGCAAAGCAAGGGGTGAACAAAGCGATGATT
TATTAACGCAGATGCTAAACGGAAAAGATCCAGAAACGGGTGAGCCGCTTGATGACGGGAACATTCGCTA
TCAAATTATTACATTCTTATATGCGGGAGTTGAAGGTACAAGTGGTCTTTTATCATTTGCGCTGTATTTC
TTAGTGAAAAATCCACATGTATTACAAAAAGTAGCAGAAGAAGCAGCACGAGTTCTAGTAGATCCTGTTC
CAAGCTACAAACAAGTCAAACAGCTTAAATATGTCGGCATGGTCTTAAACGAAGCGCTGCGCTTATGGCC
AATTGTTCCTGCGTTTTCCCTATATGCAAAAGAAGATACGGTGCTTGGAGGAGAATATCCTTTAGAAAAA
GGCGACGAAGTAATGGTTCTGATTCCTCAGCTTCACCGTGATAAAACAGTTTGGGGAGACGATGTGGAGG
AGTTCCGTCCAGAGCGTTTTGAAAATCCAAGTGCGATTCCGCAGCATGCGTTTAAACCGTTTGGAAACGG
TCAGCGTGCGTCTATCGGTCAGCAGTTCGCTCTTCATGAAGCAACGCTGGTACTTGGTATGATGCTAAAA
CACTTTGACTTTGAAGATCATACAAACTACGAGCTCGATATTAAAGAACTGCTGACGTTAAAACCTAAAG
GCTTTGTGGTAAAAGCAAAATCGAAAAAAATTCCGCTTGGCGGTATTCCTTCACCTAGCACTGAACAGTC

TGCTAAAAAAGTACGCAAAAAGGCAGAAAACGCTCATAATACGCCGCTGCTTGTGCTATACGGTTCAAAT
ATGGGTACCGCTGAAGGAACGGCGCGTGATTTAGCAGATATTGCAATGAGCAAAGGATTTGCACCGCAGG
TCGCAACGCTTGATTCACACGCCGGAAATCTTCCGCGCGAAGGAGCTGTATTAATTGTAACGGCGTCTTA
TAACGGTCATCCGCCTGATAACGCAAAGCAATTTGTCGACTGGTTAGACCAAGCGTCTGCTGATGAAGTA
AAAGGCGTTCGCTACTCCGTATTTGGATGCGGCGATAAAAACTGGGCTACTACGTATCAAAAAGTGCCTG
CTTTTATCGATGAAACGCTTGCCGCTAAAGGGGCAGAAAACATCGCTGACCGCGGTGAAGCAGATGCAAG
CGACGACTTTGAAGGCACATATGAAGAATGGCGTGAACATATGTGGAGTGACGTAGCAGCCTACTTTAAC
CTCGACATTGAAAACAGTGAAGATAATAAATCTACTCTTTCACTTCAATTTGTCGACAGCGCCGCGGATA
TGCCGCTTGCGAAAATGCACGGTGCGTTTTCAACGAACGTCGTAGCAAGCAAAGAACTTCAACAGCCAGG
CAGTGCACGAAGCACGCGACATCTTGAAATTGAACTTCCAAAAGAAGCTTCTTATCAAGAAGGAGATCAT
TTAGGTGTTATTCCTCGCAACTATGAAGGAATAGTAAACCGTGTAACAGCAAGGTTCGGCCTAGATGCAT
CACAGCAAATCCGTCTGGAAGCAGAAGAAGAAAAATTAGCTCATTTGCCACTCGCTAAAACAGTATCCGT
AGAAGAGCTTCTGCAATACGTGGAGCTTCAAGATCCTGTTACGCGCACGCAGCTTCGCGCAATGGCTGCT
AAAACGGTCTGCCCGCCGCATAAAGTAGAGCTTGAAGCCTTGCTTGAAAAGCAAGCCTACAAAGAACAAG
TGCTGGCAAAACGTTTAACAATGCTTGAACTGCTTGAAAAATACCCGGCGTGTGAAATGAAATTCAGCGA
ATTTATCGCCCTTCTGCCAAGCATACGCCCGCGCTATTACTCGATTTCTTCATCACCTCGTGTCGATGAA
AAACAAGCAAGCATCACGGTCAGCGTTGTCTCAGGAGAAGCGTGGAGCGGATATGGAGAATATAAAGGAA
TTGCGTCGAACTATCTTGCCGAGCTGCAAGAAGGAGATACGATTACGTGCTTTATTTCCACACCGCAGTC
AGAATTTACGCTGCCAAAAGACCCTGAAACGCCGCTTATCATGGTCGGACCGGGAACAGGCGTCGCGCCG
TTTAGAGGCTTTGTGCAGGCGCGCAAACAGCTAAAAGAACAAGGACAGTCACTTGGAGAAGCACATTTAT
ACTTCGGCTGCCGTTCACCTCATGAAGACTATCTGTATCAAGAAGAGCTTGAAAACGCCCAAAGCGAAGG
CATCATTACGCTTCATACCGCTTTTTCTCGCATGCCAAATCAGCCGAAAACATACGTTCAGCACGTAATG
GAACAAGACGGCAAGAAATTGATTGAACTTCTTGATCAAGGAGCGCACTTCTATATTTGCGGAGACGGAA
GCCAAATGGCACCTGCCGTTGAAGCAACGCTTATGAAAAGCTATGCTGACGTTCACCAAGTGAGTGAAGC
AGACGCTCGCTTATGGCTGCAGCAGCTAGAAGAAAAAGGCCGATACGCAAAAGACGTGTGGGCTGGGCTC
GAGCACCACCACCACCACCACTGA

MTIKEMPQPKTFGELKNLPLLNTDKPVQALMKIADELGEIFKFEAPGRVTRYLSSQRLIKEACDESRFDK
NLSQGEKFLRDFLGDGLATSWTHEKNWKKAHNILLPSFSQQAMKGYHAMMVDIAVQLVQKWERLNADEHI
EVSEDMTRLTLDTIGLCGFNYRFNSFYRDQPHPFIISLVRALDEVMNKLQRANPDDPAYDENKRQFQEDI
KVMNDLVDKIIADRKARGEQSDDLLTQMLNGKDPETGEPLDDGNIRYQIITFLYAGVEGTSGLLSFALYF
LVKNPHVLQKVAEEAARVLVDPVPSYKQVKQLKYVGMVLNEALRLWPIVPAFSLYAKEDTVLGGEYPLEK
GDEVMVLIPQLHRDKTVWGDDVEEFRPERFENPSAIPQHAFKPFGNGQRASIGQQFALHEATLVLGMMLK
HFDFEDHTNYELDIKELLTLKPKGFVVKAKSKKIPLGGIPSPSTEQSAKKVRKKAENAHNTPLLVLYGSN
MGTAEGTARDLADIAMSKGFAPQVATLDSHAGNLPREGAVLIVTASYNGHPPDNAKQFVDWLDQASADEV
KGVRYSVFGCGDKNWATTYQKVPAFIDETLAAKGAENIADRGEADASDDFEGTYEEWREHMWSDVAAYFN
LDIENSEDNKSTLSLQFVDSAADMPLAKMHGAFSTNVVASKELQQPGSARSTRHLEIELPKEASYQEGDH
LGVIPRNYEGIVNRVTARFGLDASQQIRLEAEEEKLAHLPLAKTVSVEELLQYVELQDPVTRTQLRAMAA
KTVCPPHKVELEALLEKQAYKEQVLAKRLTMLELLEKYPACEMKFSEFIALLPSIRPRYYSISSSPRVDE
KQASITVSVVSGEAWSGYGEYKGIASNYLAELQEGDTITCFISTPQSEFTLPKDPETPLIMVGPGTGVAP
FRGFVQARKQLKEQGQSLGEAHLYFGCRSPHEDYLYQEELENAQSEGIITLHTAFSRMPNQPKTYVQHVM
EQDGKKLIELLDQGAHFYICGDGSQMAPAVEATLMKSYADVHQVSEADARLWLQQLEEKGRYAKDVWAGL
EHHHHHH

Nucleotide and amino acid sequences of P411-PYS-5144:

ATGACAATTAAAGAAATGCCTCAGCCAAAAACGTTTGGAGAGCTTAAAAATTTACCGTTATTAAACACAG
ATAAACCGGTTCAAGCTTTGATGAAAATTGCGGATGAATTAGGAGAAATCTTTAAATTCGAGGCGCCTGG
TCGTGTAACGCGCTACTTATCAAGTCAGCGTCTAATTAAAGAAGCATGCGATGAATCACGCTTTGATAAA

AACTTAAGTCAAGGTGAGAAATTTCTGCGTGATTTTCTTGGAGACGGGTTAGCCACAAGCTGGACGCATG
AAAAAAATTGGGAAAAAAGCGCATAATATCTTACTTCCAAGCTTTAGTCAGCAGGCAATGAAAGGCTATC
ATGCGATGATGGTCGATATCGCCGTGCAGCTTGTTCAAAAGTGGGAGCGTCTAAATGCAGATGAGCATAT
TGAAGTATCGGAAGACATGACACGTTTAACGCTTGATACAATTGGTCTTTGCGGCTTTAACTATCGCTTT
AACAGCTTTTACCGAGATCAGCCTCATCCATTTATTATAAGTCTGGTCCGTGCACTGGATGAAGTAATGA
ACAAGCTGCAGCGAGCAAATCCAGACGACCCAGCTTATGATGAAAACAAGCGCCAGTTTCAAGAAGATAT
CAAGGTGATGAACGACCTAGTAGATAAAATTATTGCAGATCGCAAAGCAAGGGGTGAACAAAGCGATGAT
TTATTAACGCAGATGCTAAACGGAAAAGATCCAGAAACGGGTGAGCCGCTTGATGACGGGAACATTCGCT
ATCAAATTATTACATTCTTATATGCGGGAGTTGAAGGTACAAGTGGTCTTTTATCATTTGCGCTGTATTT
CTTAGTGAAAAATCCACATGTATTACAAAAAGTAGCAGAAGAAGCAGCACGAGTTCTAGTAGATCCTGTT
CCAAGCTACAAACAAGTCAAACAGCTTAAATATGTCGGCATGGTCTTAAACGAAGCGCTGCGCTTATGGC
CAATTGTTCCTCAGTTTTCCCTATATGCAAAAGAAGATACGGTGCTTGGAGGAGAATATCCTTTAGAAAA
AGGCGACGAAGTAATGGTTCTGATTCCTCAGCTTCACCGTGATAAAACAGTTTGGGGAGACGATGTGGAG
GAGTTCCGTCCAGAGCGTTTTGAAAATCCAAGTGCGATTCCGCAGCATGCGTTTAAACCGTTTGGAAACG
GTCAGCGTGCGTCTATCGGTCAGCAGTTCGCTCTTCATGAAGCAACGCTGGTACTTGGTATGATGCTAAA
ACACTTTGACTTTGAAGATCATACAAACTACGAGCTCGATATTAAAGAACTGCTGACGTTAAAACCTAAA
GGCTTTGTGGTAAAAGCAAAATCGAAAAAAATTCCGCTTGGCGGTATTCCTTCACCTAGCACTGAACAGT
CTGCTAAAAAAGTACGCAAAAAGGCAGAAAACGCTCATAATACGCCGCTGCTTGTGCTATACGGTTCAAA
TATGGGTACCGCTGAAGGAACGGCGCGTGATTTAGCAGATATTGCAATGAGCAAAGGATTTGCACCGCAG
GTCGCAACGCTTGATTCACACGCCGGAAATCTTCCGCGCGAAGGAGCTGTATTAATTGTAACGGCGTCTT
ATAACGGTCATCCGCCTGATAACGCAAAGCAATTTGTCGACTGGTTAGACCAAGCGTCTGCTGATGAAGT
AAAAGGCGTTCGCTACTCCGTATTTGGATGCGGCGATAAAAACTGGGCTACTACGTATCAAAAAGTGCCT
GCTTTTATCGATGAAACGCTTGCCGCTAAAGGGGCAGAAAACATCGCTGACCGCGGTGAAGCAGATGCAA
GCGACGACTTTGAAGGCACATATGAAGAATGGCGTGAACATATGTGGAGTGACGTAGCAGCCTACTTTAA
CCTCGACATTGAAAACAGTGAAGATAATAAATCTACTCTTTCACTTCAATTTGTCGACAGCGCCGCGGAT
ATGCCGCTTGCGAAAATGCACGGTGCGTTTTCAACGAACGTCGTAGCAAGCAAAGAACTTCAACAGCCAG
GCAGTGCACGAAGCACGCGACATCTTGAAATTGAACTTCCAAAAGAAGCTTCTTATCAAGAAGGAGATCA
TTTAGGTGTTATTCCTCGCAACTATGAAGGAATAGTAAACCGTGTAACAGCAAGGTTCGGCCTAGATGCA
TCACAGCAAATCCGTCTGGAAGCAGAAGAAGAAAAATTAGCTCATTTGCCACTCGCTAAAACAGTATCCG
TAGAAGAGCTTCTGCAATACGTGGAGCTTCAAGATCCTGTTACGCGCACGCAGCTTCGCGCAATGGCTGC
TAAAACGGTCTGCCCGCCGCATAAAGTAGAGCTTGAAGCCTTGCTTGAAAAGCAAGCCTACAAAGAACAA
GTGCTGGCAAAACGTTTAACAATGCTTGAACTGCTTGAAAAATACCCGGCGTGTGAAATGAAATTCAGCG
AATTTATCGCCCTTCTGCCAAGCATACGCCCGCGCTATTACTCGATTTCTTCATCACCTCGTGTCGATGA
AAAACAAGCAAGCATCACGGTCAGCGTTGTCTCAGGAGAAGCGTGGAGCGGATATGGAGAATATAAAGGA
ATTGCGTCGAACTATCTTGCCGAGCTGCAAGAAGGAGATACGATTACGTGCTTTATTTCCACACCGCAGT
CAGAATTTACGCTGCCAAAAGACCCTGAAACGCCGCTTATCATGGTCGGACCGGGAACAGGCGTCGCGCC
GTTTAGAGGCTTTGTGCAGGCGCGCAAACAGCTAAAAGAACAAGGACAGTCACTTGGAGAAGCACATTTA
TACTTCGGCTGCCGTTCACCTCATGAAGACTATCTGTATCAAGAAGAGCTTGAAAACGCCCAAAGCGAAG
GCATCATTACGCTTCATACCGCTTTTTCTCGCATGCCAAATCAGCCGAAAACATACGTTCAGCACGTAAT
GGAACAAGACGGCAAGAAATTGATTGAACTTCTTGATCAAGGAGCGCACTTCTATATTTGCGGAGACGGA
AGCCAAATGGCACCTGCCGTTGAAGCAACGCTTATGAAAAGCTATGCTGACGTTCACCAAGTGAGTGAAG
CAGACGCTCGCTTATGGCTGCAGCAGCTAGAAGAAAAAGGCCGATACGCAAAAGACGTGTGGGCTGGGCT
CGAGCACCACCACCACCACCACTGA

MTIKEMPQPKTFGELKNLPLLNTDKPVQALMKIADELGEIFKFEAPGRVTRYLSSQRLIKEACDESRFDK
NLSQGEKFLRDFLGDGLATSWTHEKNWKKAHNILLPSFSQQAMKGYHAMMVDIAVQLVQKWERLNADEHI
EVSEDMTRLTLDTIGLCGFNYRFNSFYRDQPHPFIISLVRALDEVMNKLQRANPDDPAYDENKRQFQEDI
KVMNDLVDKIIADRKARGEQSDDLLTQMLNGKDPETGEPLDDGNIRYQIITFLYAGVEGTSGLLSFALYF
LVKNPHVLQKVAEEAARVLVDPVPSYKQVKQLKYVGMVLNEALRLWPIVPQFSLYAKEDTVLGGEYPLEK
GDEVMVLIPQLHRDKTVWGDDVEEFRPERFENPSAIPQHAFKPFGNGQRASIGQQFALHEATLVLGMMLK
HFDFEDHTNYELDIKELLTLKPKGFVVKAKSKKIPLGGIPSPSTEQSAKKVRKKAENAHNTPLLVLYGSN
MGTAEGTARDLADIAMSKGFAPQVATLDSHAGNLPREGAVLIVTASYNGHPPDNAKQFVDWLDQASADEV

KGVRYSVFGCGDKNWATTYQKVPAFIDETLAAKGAENIADRGEADASDDFEGTYEEWREHMWSDVAAYFN
LDIENSEDNKSTLSLQFVDSAADMPLAKMHGAFSTNVVASKELQQPGSARSTRHLEIELPKEASYQEGDH
LGVIPRNYEGIVNRVTARFGLDASQQIRLEAEEEKLAHLPLAKTVSVEELLQYVELQDPVTRTQLRAMAA
KTVCPPHKVELEALLEKQAYKEQVLAKRLTMLELLEKYPACEMKFSEFIALLPSIRPRYYSISSSPRVDE
KQASITVSVVSGEAWSGYGEYKGIASNYLAELQEGDTITCFISTPQSEFTLPKDPETPLIMVGPGTGVAP
FRGFVQARKQLKEQGQSLGEAHLYFGCRSPHEDYLYQEELENAQSEGIITLHTAFSRMPNQPKTYVQHVM
EQDGKKLIELLDQGAHFYICGDGSQMAPAVEATLMKSYADVHQVSEADARLWLQQLEEKGRYAKDVWAGL
EHHHHHH

Nucleotide and amino acid sequences of P411-PYS-5145:

ATGACAATTAAAGAAATGCCTCAGCCAAAAACGTTTGGAGAGCTTAAAAATTTACCGTTATTAAACACAG
ATAAACCGGTTCAAGCTTTGATGAAAATTGCGGATGAATTAGGAGAAATCTTTAAATTCGAGGCGCCTGG
TCGTGTAACGCGCTACTTATCAAGTCAGCGTCTAATTAAAGAAGCATGCGATGAATCACGCTTTGATAAA
AACTTAAGTCAAGGTGAGAAATTTCTGCGTGATTTTCTTGGAGACGGGTTAGCCACAAGCTGGACGCATG
AAAAAAATTGGGAAAAAAGCGCATAATATCTTACTTCCAAGCTTTAGTCAGCAGGCAATGAAAGGCTATC
ATGCGGTGATGGTCGATATCGCCGTGCAGCTTGTTCAAAAGTGGGAGCGTCTAAATGCAGATGAGCATAT
TGAAGTATCGGAAGACATGACACGTTTAACGCTTGATACAATTGGTCTTTGCGGCTTTAACTATCGCTTT
AACAGCTTTTACCGAGATCAGCCTCATCCATTTATTATAAGTCTGGTCCGTGCACTGGATGAAGTAATGA
ACAAGCTGCAGCGAGCAAATCCAGACGACCCAGCTTATGATGAAAACAAGCGCCAGTTTCAAGAAGATAT
CAAGGTGATGAACGACCTAGTAGATAAAATTATTGCAGATCGCAAAGCAAGGGGTGAACAAAGCGATGAT
TTATTAACGCAGATGCTAAACGGAAAAGATCCAGAAACGGGTGAGCCGCTTGATGACGGGAACATTCGCT
ATCAAATTATTACATTCTTATATGCGGGAGTTGAAGGTACAAGTGGTCTTTTATCATTTGCGCTGTATTT
CTTAGTGAAAAATCCACATGTATTACAAAAAGTAGCAGAAGAAGCAGCACGAGTTCTAGTAGATCCTGTT
CCAAGCTACAAACAAGTCAAACAGCTTAAATATGTCGGCATGGTCTTAAACGAAGCGCTGCGCTTATGGC
CAATTGTTCCTCAGTTTTCCCTATATGCAAAAGAAGATACGGTGCTTGGAGGAGAATATCCTTTAGAAAA
AGGCGACGAAGTAATGGTTCTGATTCCTCAGCTTCACCGTGATAAAACAGTTTGGGGAGACGATGTGGAG
GAGTTCCGTCCAGAGCGTTTTGAAAATCCAAGTGCGATTCCGCAGCATGCGTTTAAACCGTTTGGAAACG
GTCAGCGTGCGTCTATCGGTCAGCAGTTCGCTCTTCATGAAGCAACGCTGGTACTTGGTATGATGCTAAA
ACACTTTGACTTTGAAGATCATACAAACTACGAGCTCGATATTAAAGAACTGCTGACGTTAAAACCTAAA
GGCTTTGTGGTAAAAGCAAAATCGAAAAAAATTCCGCTTGGCGGTATTCCTTCACCTAGCACTGAACAGT
CTGCTAAAAAAGTACGCAAAAAGGCAGAAAACGCTCATAATACGCCGCTGCTTGTGCTATACGGTTCAAA
TATGGGTACCGCTGAAGGAACGGCGCGTGATTTAGCAGATATTGCAATGAGCAAAGGATTTGCACCGCAG
GTCGCAACGCTTGATTCACACGCCGGAAATCTTCCGCGCGAAGGAGCTGTATTAATTGTAACGGCGTCTT
ATAACGGTCATCCGCCTGATAACGCAAAGCAATTTGTCGACTGGTTAGACCAAGCGTCTGCTGATGAAGT
AAAAGGCGTTCGCTACTCCGTATTTGGATGCGGCGATAAAAACTGGGCTACTACGTATCAAAAAGTGCCT
GCTTTTATCGATGAAACGCTTGCCGCTAAAGGGGCAGAAAACATCGCTGACCGCGGTGAAGCAGATGCAA
GCGACGACTTTGAAGGCACATATGAAGAATGGCGTGAACATATGTGGAGTGACGTAGCAGCCTACTTTAA
CCTCGACATTGAAAACAGTGAAGATAATAAATCTACTCTTTCACTTCAATTTGTCGACAGCGCCGCGGAT
ATGCCGCTTGCGAAAATGCACGGTGCGTTTTCAACGAACGTCGTAGCAAGCAAAGAACTTCAACAGCCAG
GCAGTGCACGAAGCACGCGACATCTTGAAATTGAACTTCCAAAAGAAGCTTCTTATCAAGAAGGAGATCA
TTTAGGTGTTATTCCTCGCAACTATGAAGGAATAGTAAACCGTGTAACAGCAAGGTTCGGCCTAGATGCA
TCACAGCAAATCCGTCTGGAAGCAGAAGAAGAAAAATTAGCTCATTTGCCACTCGCTAAAACAGTATCCG
TAGAAGAGCTTCTGCAATACGTGGAGCTTCAAGATCCTGTTACGCGCACGCAGCTTCGCGCAATGGCTGC
TAAAACGGTCTGCCCGCCGCATAAAGTAGAGCTTGAAGCCTTGCTTGAAAAGCAAGCCTACAAAGAACAA
GTGCTGGCAAAACGTTTAACAATGCTTGAACTGCTTGAAAAATACCCGGCGTGTGAAATGAAATTCAGCG
AATTTATCGCCCTTCTGCCAAGCATACGCCCGCGCTATTACTCGATTTCTTCATCACCTCGTGTCGATGA
AAAACAAGCAAGCATCACGGTCAGCGTTGTCTCAGGAGAAGCGTGGAGCGGATATGGAGAATATAAAGGA
ATTGCGTCGAACTATCTTGCCGAGCTGCAAGAAGGAGATACGATTACGTGCTTTATTTCCACACCGCAGT

CAGAATTTACGCTGCCAAAAGACCCTGAAACGCCGCTTATCATGGTCGGACCGGGAACAGGCGTCGCGCC
GTTTAGAGGCTTTGTGCAGGCGCGCAAACAGCTAAAAGAACAAGGACAGTCACTTGGAGAAGCACATTTA
TACTTCGGCTGCCGTTCACCTCATGAAGACTATCTGTATCAAGAAGAGCTTGAAAACGCCCAAAGCGAAG
GCATCATTACGCTTCATACCGCTTTTTCTCGCATGCCAAATCAGCCGAAAACATACGTTCAGCACGTAAT
GGAACAAGACGGCAAGAAATTGATTGAACTTCTTGATCAAGGAGCGCACTTCTATATTTGCGGAGACGGA
AGCCAAATGGCACCTGCCGTTGAAGCAACGCTTATGAAAAGCTATGCTGACGTTCACCAAGTGAGTGAAG
CAGACGCTCGCTTATGGCTGCAGCAGCTAGAAGAAAAAGGCCGATACGCAAAAGACGTGTGGGCTGGGCT
CGAGCACCACCACCACCACCACTGA

MTIKEMPQPKTFGELKNLPLLNTDKPVQALMKIADELGEIFKFEAPGRVTRYLSSQRLIKEACDESRFDK
NLSQGEKFLRDFLGDGLATSWTHEKNWKKAHNILLPSFSQQAMKGYHAVMVDIAVQLVQKWERLNADEHI
EVSEDMTRLTLDTIGLCGFNYRFNSFYRDQPHPFIISLVRALDEVMNKLQRANPDDPAYDENKRQFQEDI
KVMNDLVDKIIADRKARGEQSDDLLTQMLNGKDPETGEPLDDGNIRYQIITFLYAGVEGTSGLLSFALYF
LVKNPHVLQKVAEEAARVLVDPVPSYKQVKQLKYVGMVLNEALRLWPIVPQFSLYAKEDTVLGGEYPLEK
GDEVMVLIPQLHRDKTVWGDDVEEFRPERFENPSAIPQHAFKPFGNGQRASIGQQFALHEATLVLGMMLK
HFDFEDHTNYELDIKELLTLKPKGFVVKAKSKKIPLGGIPSPSTEQSAKKVRKKAENAHNTPLLVLYGSN
MGTAEGTARDLADIAMSKGFAPQVATLDSHAGNLPREGAVLIVTASYNGHPPDNAKQFVDWLDQASADEV
KGVRYSVFGCGDKNWATTYQKVPAFIDETLAAKGAENIADRGEADASDDFEGTYEEWREHMWSDVAAYFN
LDIENSEDNKSTLSLQFVDSAADMPLAKMHGAFSTNVVASKELQQPGSARSTRHLEIELPKEASYQEGDH
LGVIPRNYEGIVNRVTARFGLDASQQIRLEAEEEKLAHLPLAKTVSVEELLQYVELQDPVTRTQLRAMAA
KTVCPPHKVELEALLEKQAYKEQVLAKRLTMLELLEKYPACEMKFSEFIALLPSIRPRYYSISSSPRVDE
KQASITVSVVSGEAWSGYGEYKGIASNYLAELQEGDTITCFISTPQSEFTLPKDPETPLIMVGPGTGVAP
FRGFVQARKQLKEQGQSLGEAHLYFGCRSPHEDYLYQEELENAQSEGIITLHTAFSRMPNQPKTYVQHVM
EQDGKKLIELLDQGAHFYICGDGSQMAPAVEATLMKSYADVHQVSEADARLWLQQLEEKGRYAKDVWAGL
EHHHHHH

Nucleotide and amino acid sequences of P411-PYS-5146:

ATGACAATTAAAGAAATGCCTCAGCCAAAAACGTTTGGAGAGCTTAAAAATTTACCGTTATTAAACACAG
ATAAACCGGTTCAAGCTTTGATGAAAATTGCGGATGAATTAGGAGAAATCTTTAAATTCGAGGCGCCTGG
TCGTGTAACGCGCTACTTATCAAGTCAGCGTCTAATTAAAGAAGCATGCGATGAATCACGCTTTGATAAA
AACTTAAGTCAAGGTGAGAAATGTCTGCGTGATTTTCTTGGAGACGGGTTAGCCACAAGCTGGACGCATG
AAAAAAATTGGGAAAAAAGCGCATAATATCTTACTTCCAAGCTTTAGTCAGCAGGCAATGAAAGGCTATC
ATGCGGTGATGGTCGATATCGCCGTGCAGCTTGTTCAAAAGTGGGAGCGTCTAAATGCAGATGAGCATAT
TGAAGTATCGGAAGACATGACACGTTTAACGCTTGATACAATTGGTCTTTGCGGCTTTAACTATCGCTTT
AACAGCTTTTACCGAGATCAGCCTCATCCATTTATTATAAGTCTGGTCCGTGCACTGGATGAAGTAATGA
ACAAGCTGCAGCGAGCAAATCCAGACGACCCAGCTTATGATGAAAACAAGCGCCAGTTTCAAGAAGATAT
CAAGGTGATGAACGACCTAGTAGATAAAATTATTGCAGATCGCAAAGCAAGGGGTGAACAAAGCGATGAT
TTATTAACGCAGATGCTAAACGGAAAAGATCCAGAAACGGGTGAGCCGCTTGATGACGGGAACATTCGCT
ATCAAATTATTACATTCTTATATGCGGGAGTTGAAGGTACAAGTGGTCTTTTATCATTTGCGCTGTATTT
CTTAGTGAAAAATCCACATGTATTACAAAAAGTAGCAGAAGAAGCAGCACGAGTTCTAGTAGATCCTGTT
CCAAGCTACAAACAAGTCAAACAGCTTAAATATGTCGGCATGGTCTTAAACGAAGCGCTGCGCTTATGGC
CAATTGTTCCTCAGTTTTCCCTATATGCAAAAGAAGATACGGTGCTTGGAGGAGAATATCCTTTAGAAAA
AGGCGACGAAGTAATGGTTCTGATTCCTCAGCTTCACCGTGATAAAACAGTTTGGGGAGACGATGTGGAG
GAGTTCCGTCCAGAGCGTTTTGAAAATCCAAGTGCGATTCCGCAGCATGCGTTTAAACCGTTTGGAAACG
GTCAGCGTGCGTCTATCGGTCAGCAGTTCGCTCTTCATGAAGCAACGCTGGTACTTGGTATGATGCTAAA
ACACTTTGACTTTGAAGATCATACAAACTACGAGCTCGATATTAAAGAACTGCTGACGTTAAAACCTAAA
GGCTTTGTGGTAAAAGCAAAATCGAAAAAAATTCCGCTTGGCGGTATTCCTTCACCTAGCACTGAACAGT
CTGCTAAAAAAGTACGCAAAAAGGCAGAAAACGCTCATAATACGCCGCTGCTTGTGCTATACGGTTCAAA

TATGGGTACCGCTGAAGGAACGGCGCGTGATTTAGCAGATATTGCAATGAGCAAAGGATTTGCACCGCAG
GTCGCAACGCTTGATTCACACGCCGGAAATCTTCCGCGCGAAGGAGCTGTATTAATTGTAACGGCGTCTT
ATAACGGTCATCCGCCTGATAACGCAAAGCAATTTGTCGACTGGTTAGACCAAGCGTCTGCTGATGAAGT
AAAAGGCGTTCGCTACTCCGTATTTGGATGCGGCGATAAAAACTGGGCTACTACGTATCAAAAAGTGCCT
GCTTTTATCGATGAAACGCTTGCCGCTAAAGGGGCAGAAAACATCGCTGACCGCGGTGAAGCAGATGCAA
GCGACGACTTTGAAGGCACATATGAAGAATGGCGTGAACATATGTGGAGTGACGTAGCAGCCTACTTTAA
CCTCGACATTGAAAACAGTGAAGATAATAAATCTACTCTTTCACTTCAATTTGTCGACAGCGCCGCGGAT
ATGCCGCTTGCGAAAATGCACGGTGCGTTTTCAACGAACGTCGTAGCAAGCAAAGAACTTCAACAGCCAG
GCAGTGCACGAAGCACGCGACATCTTGAAATTGAACTTCCAAAAGAAGCTTCTTATCAAGAAGGAGATCA
TTTAGGTGTTATTCCTCGCAACTATGAAGGAATAGTAAACCGTGTAACAGCAAGGTTCGGCCTAGATGCA
TCACAGCAAATCCGTCTGGAAGCAGAAGAAGAAAAATTAGCTCATTTGCCACTCGCTAAAACAGTATCCG
TAGAAGAGCTTCTGCAATACGTGGAGCTTCAAGATCCTGTTACGCGCACGCAGCTTCGCGCAATGGCTGC
TAAAACGGTCTGCCCGCCGCATAAAGTAGAGCTTGAAGCCTTGCTTGAAAAGCAAGCCTACAAAGAACAA
GTGCTGGCAAAACGTTTAACAATGCTTGAACTGCTTGAAAAATACCCGGCGTGTGAAATGAAATTCAGCG
AATTTATCGCCCTTCTGCCAAGCATACGCCCGCGCTATTACTCGATTTCTTCATCACCTCGTGTCGATGA
AAAACAAGCAAGCATCACGGTCAGCGTTGTCTCAGGAGAAGCGTGGAGCGGATATGGAGAATATAAAGGA
ATTGCGTCGAACTATCTTGCCGAGCTGCAAGAAGGAGATACGATTACGTGCTTTATTTCCACACCGCAGT
CAGAATTTACGCTGCCAAAAGACCCTGAAACGCCGCTTATCATGGTCGGACCGGGAACAGGCGTCGCGCC
GTTTAGAGGCTTTGTGCAGGCGCGCAAACAGCTAAAAGAACAAGGACAGTCACTTGGAGAAGCACATTTA
TACTTCGGCTGCCGTTCACCTCATGAAGACTATCTGTATCAAGAAGAGCTTGAAAACGCCCAAAGCGAAG
GCATCATTACGCTTCATACCGCTTTTTCTCGCATGCCAAATCAGCCGAAAACATACGTTCAGCACGTAAT
GGAACAAGACGGCAAGAAATTGATTGAACTTCTTGATCAAGGAGCGCACTTCTATATTTGCGGAGACGGA
AGCCAAATGGCACCTGCCGTTGAAGCAACGCTTATGAAAAGCTATGCTGACGTTCACCAAGTGAGTGAAG
CAGACGCTCGCTTATGGCTGCAGCAGCTAGAAGAAAAAGGCCGATACGCAAAAGACGTGTGGGCTGGGCT
CGAGCACCACCACCACCACCACTGA

MTIKEMPQPKTFGELKNLPLLNTDKPVQALMKIADELGEIFKFEAPGRVTRYLSSQRLIKEACDESRFDK
NLSQGEKCLRDFLGDGLATSWTHEKNWKKAHNILLPSFSQQAMKGYHAVMVDIAVQLVQKWERLNADEHI
EVSEDMTRLTLDTIGLCGFNYRFNSFYRDQPHPFIISLVRALDEVMNKLQRANPDDPAYDENKRQFQEDI
KVMNDLVDKIIADRKARGEQSDDLLTQMLNGKDPETGEPLDDGNIRYQIITFLYAGVEGTSGLLSFALYF
LVKNPHVLQKVAEEAARVLVDPVPSYKQVKQLKYVGMVLNEALRLWPIVPQFSLYAKEDTVLGGEYPLEK
GDEVMVLIPQLHRDKTVWGDDVEEFRPERFENPSAIPQHAFKPFGNGQRASIGQQFALHEATLVLGMMLK
HFDFEDHTNYELDIKELLTLKPKGFVVKAKSKKIPLGGIPSPSTEQSAKKVRKKAENAHNTPLLVLYGSN
MGTAEGTARDLADIAMSKGFAPQVATLDSHAGNLPREGAVLIVTASYNGHPPDNAKQFVDWLDQASADEV
KGVRYSVFGCGDKNWATTYQKVPAFIDETLAAKGAENIADRGEADASDDFEGTYEEWREHMWSDVAAYFN
LDIENSEDNKSTLSLQFVDSAADMPLAKMHGAFSTNVVASKELQQPGSARSTRHLEIELPKEASYQEGDH
LGVIPRNYEGIVNRVTARFGLDASQQIRLEAEEEKLAHLPLAKTVSVEELLQYVELQDPVTRTQLRAMAA
KTVCPPHKVELEALLEKQAYKEQVLAKRLTMLELLEKYPACEMKFSEFIALLPSIRPRYYSISSSPRVDE
KQASITVSVVSGEAWSGYGEYKGIASNYLAELQEGDTITCFISTPQSEFTLPKDPETPLIMVGPGTGVAP
FRGFVQARKQLKEQGQSLGEAHLYFGCRSPHEDYLYQEELENAQSEGIITLHTAFSRMPNQPKTYVQHVM
EQDGKKLIELLDQGAHFYICGDGSQMAPAVEATLMKSYADVHQVSEADARLWLQQLEEKGRYAKDVWAGL
EHHHHHH

Nucleotide and amino acid sequences of P411-PYS-5147:

ATGACAATTAAAGAAATGCCTCAGCCAAAAACGTTTGGAGAGCTTAAAAATTTACCGTTATTAAACACAG
ATAAACCGGTTCAAGCTTTGATGAAAATTGCGGATGAATTAGGAGAAATCTTTAAATTCGAGGCGCCTGG
TCGTGTAACGCGCTACTTATCAAGTCAGCGTCTAATTAAAGAAGCATGCGATGAATCACGCTTTGATAAA
AACTTATGGCAAGGTGAGAAATGTCTGCGTGATTTTCTTGGAGACGGGTTAGCCACAAGCTGGACGCATG

AAAAAAATTGGGAAAAAAGCGCATAATATCTTACTTCCAAGCTTTAGTCAGCAGGCAATGAAAGGCTATC
ATGCGGTGATGGTCGATATCGCCGTGCAGCTTGTTCAAAAGTGGGAGCGTCTAAATGCAGATGAGCATAT
TGAAGTATCGGAAGACATGACACGTTTAACGCTTGATACAATTGGTCTTTGCGGCTTTAACTATCGCTTT
AACAGCTTTTACCGAGATCAGCCTCATCCATTTATTATAAGTCTGGTCCGTGCACTGGATGAAGTAATGA
ACAAGCTGCAGCGAGCAAATCCAGACGACCCAGCTTATGATGAAAACAAGCGCCAGTTTCAAGAAGATAT
CAAGGTGATGAACGACCTAGTAGATAAAATTATTGCAGATCGCAAAGCAAGGGGTGAACAAAGCGATGAT
TTATTAACGCAGATGCTAAACGGAAAAGATCCAGAAACGGGTGAGCCGCTTGATGACGGGAACATTCGCT
ATCAAATTATTACATTCTTATATGCGGGAGTTGAAGGTACAAGTGGTCTTTTATCATTTGCGCTGTATTT
CTTAGTGAAAAATCCACATGTATTACAAAAAGTAGCAGAAGAAGCAGCACGAGTTCTAGTAGATCCTGTT
CCAAGCTACAAACAAGTCAAACAGCTTAAATATGTCGGCATGGTCTTAAACGAAGCGCTGCGCTTATGGC
CAATTGTTCCTCAGTTTTCCCTATATGCAAAAGAAGATACGGTGCTTGGAGGAGAATATCCTTTAGAAAA
AGGCGACGAAGTAATGGTTCTGATTCCTCAGCTTCACCGTGATAAAACAGTTTGGGGAGACGATGTGGAG
GAGTTCCGTCCAGAGCGTTTTGAAAATCCAAGTGCGATTCCGCAGCATGCGTTTAAACCGTTTGGAAACG
GTCAGCGTGCGTCTATCGGTCAGCAGTTCGCTCTTCATGAAGCAACGCTGGTACTTGGTATGATGCTAAA
ACACTTTGACTTTGAAGATCATACAAACTACGAGCTCGATATTAAAGAACTGCTGACGTTAAAACCTAAA
GGCTTTGTGGTAAAAGCAAAATCGAAAAAAATTCCGCTTGGCGGTATTCCTTCACCTAGCACTGAACAGT
CTGCTAAAAAAGTACGCAAAAAGGCAGAAAACGCTCATAATACGCCGCTGCTTGTGCTATACGGTTCAAA
TATGGGTACCGCTGAAGGAACGGCGCGTGATTTAGCAGATATTGCAATGAGCAAAGGATTTGCACCGCAG
GTCGCAACGCTTGATTCACACGCCGGAAATCTTCCGCGCGAAGGAGCTGTATTAATTGTAACGGCGTCTT
ATAACGGTCATCCGCCTGATAACGCAAAGCAATTTGTCGACTGGTTAGACCAAGCGTCTGCTGATGAAGT
AAAAGGCGTTCGCTACTCCGTATTTGGATGCGGCGATAAAAACTGGGCTACTACGTATCAAAAAGTGCCT
GCTTTTATCGATGAAACGCTTGCCGCTAAAGGGGCAGAAAACATCGCTGACCGCGGTGAAGCAGATGCAA
GCGACGACTTTGAAGGCACATATGAAGAATGGCGTGAACATATGTGGAGTGACGTAGCAGCCTACTTTAA
CCTCGACATTGAAAACAGTGAAGATAATAAATCTACTCTTTCACTTCAATTTGTCGACAGCGCCGCGGAT
ATGCCGCTTGCGAAAATGCACGGTGCGTTTTCAACGAACGTCGTAGCAAGCAAAGAACTTCAACAGCCAG
GCAGTGCACGAAGCACGCGACATCTTGAAATTGAACTTCCAAAAGAAGCTTCTTATCAAGAAGGAGATCA
TTTAGGTGTTATTCCTCGCAACTATGAAGGAATAGTAAACCGTGTAACAGCAAGGTTCGGCCTAGATGCA
TCACAGCAAATCCGTCTGGAAGCAGAAGAAGAAAAATTAGCTCATTTGCCACTCGCTAAAACAGTATCCG
TAGAAGAGCTTCTGCAATACGTGGAGCTTCAAGATCCTGTTACGCGCACGCAGCTTCGCGCAATGGCTGC
TAAAACGGTCTGCCCGCCGCATAAAGTAGAGCTTGAAGCCTTGCTTGAAAAGCAAGCCTACAAAGAACAA
GTGCTGGCAAAACGTTTAACAATGCTTGAACTGCTTGAAAAATACCCGGCGTGTGAAATGAAATTCAGCG
AATTTATCGCCCTTCTGCCAAGCATACGCCCGCGCTATTACTCGATTTCTTCATCACCTCGTGTCGATGA
AAAACAAGCAAGCATCACGGTCAGCGTTGTCTCAGGAGAAGCGTGGAGCGGATATGGAGAATATAAAGGA
ATTGCGTCGAACTATCTTGCCGAGCTGCAAGAAGGAGATACGATTACGTGCTTTATTTCCACACCGCAGT
CAGAATTTACGCTGCCAAAAGACCCTGAAACGCCGCTTATCATGGTCGGACCGGGAACAGGCGTCGCGCC
GTTTAGAGGCTTTGTGCAGGCGCGCAAACAGCTAAAAGAACAAGGACAGTCACTTGGAGAAGCACATTTA
TACTTCGGCTGCCGTTCACCTCATGAAGACTATCTGTATCAAGAAGAGCTTGAAAACGCCCAAAGCGAAG
GCATCATTACGCTTCATACCGCTTTTTCTCGCATGCCAAATCAGCCGAAAACATACGTTCAGCACGTAAT
GGAACAAGACGGCAAGAAATTGATTGAACTTCTTGATCAAGGAGCGCACTTCTATATTTGCGGAGACGGA
AGCCAAATGGCACCTGCCGTTGAAGCAACGCTTATGAAAAGCTATGCTGACGTTCACCAAGTGAGTGAAG
CAGACGCTCGCTTATGGCTGCAGCAGCTAGAAGAAAAAGGCCGATACGCAAAAGACGTGTGGGCTGGGCT
CGAGCACCACCACCACCACCACTGA

MTIKEMPQPKTFGELKNLPLLNTDKPVQALMKIADELGEIFKFEAPGRVTRYLSSQRLIKEACDESRFDK
NLWQGEKCLRDFLGDGLATSWTHEKNWKKAHNILLPSFSQQAMKGYHAVMVDIAVQLVQKWERLNADEHI
EVSEDMTRLTLDTIGLCGFNYRFNSFYRDQPHPFIISLVRALDEVMNKLQRANPDDPAYDENKRQFQEDI
KVMNDLVDKIIADRKARGEQSDDLLTQMLNGKDPETGEPLDDGNIRYQIITFLYAGVEGTSGLLSFALYF
LVKNPHVLQKVAEEAARVLVDPVPSYKQVKQLKYVGMVLNEALRLWPIVPQFSLYAKEDTVLGGEYPLEK
GDEVMVLIPQLHRDKTVWGDDVEEFRPERFENPSAIPQHAFKPFGNGQRASIGQQFALHEATLVLGMMLK
HFDFEDHTNYELDIKELLTLKPKGFVVKAKSKKIPLGGIPSPSTEQSAKKVRKKAENAHNTPLLVLYGSN
MGTAEGTARDLADIAMSKGFAPQVATLDSHAGNLPREGAVLIVTASYNGHPPDNAKQFVDWLDQASADEV
KGVRYSVFGCGDKNWATTYQKVPAFIDETLAAKGAENIADRGEADASDDFEGTYEEWREHMWSDVAAYFN

LDIENSEDNKSTLSLQFVDSAADMPLAKMHGAFSTNVVASKELQQPGSARSTRHLEIELPKEASYQEGDH
LGVIPRNYEGIVNRVTARFGLDASQQIRLEAEEEKLAHLPLAKTVSVEELLQYVELQDPVTRTQLRAMAA
KTVCPPHKVELEALLEKQAYKEQVLAKRLTMLELLEKYPACEMKFSEFIALLPSIRPRYYSISSSPRVDE
KQASITVSVVSGEAWSGYGEYKGIASNYLAELQEGDTITCFISTPQSEFTLPKDPETPLIMVGPGTGVAP
FRGFVQARKQLKEQGQSLGEAHLYFGCRSPHEDYLYQEELENAQSEGIITLHTAFSRMPNQPKTYVQHVM
EQDGKKLIELLDQGAHFYICGDGSQMAPAVEATLMKSYADVHQVSEADARLWLQQLEEKGRYAKDVWAGL
EHHHHHH

Nucleotide and amino acid sequences of P411-PYS-5148:

ATGACAATTAAAGAAATGCCTCAGCCAAAAACGTTTGGAGAGCTTAAAAATTTACCGTTATTAAACACAG
ATAAACCGGTTCAAGCTTTGATGAAAATTGCGGATGAATTAGGAGAAATCTTTAAATTCGAGGCGCCTGG
TCGTGTAACGCGCTACTTATCAAGTCAGCGTCTAATTAAAGAAGCATGCGATGAATCACGCTTTGATAAA
AACTTATGGGCGGGTGAGAAATGTCTGCGTGATTTTCTTGGAGACGGGTTAGCCACAAGCTGGACGCATG
AAAAAAATTGGAAAAAAGCGCATAATATCTTACTTCCAAGCTTTAGTCAGCAGGCAATGAAAGGCTATCA
TGCGGTGATGGTCGATATCGCCGTGCAGCTTGTTCAAAAGTGGGAGCGTCTAAATGCAGATGAGCATATT
GAAGTATCGGAAGACATGACACGTTTAACGCTTGATACAATTGGTCTTTGCGGCTTTAACTATCGCTTTA
ACAGCTTTTACCGAGATCAGCCTCATCCATTTATTATAAGTCTGGTCCGTGCACTGGATGAAGTAATGAA
CAAGCTGCAGCGAGCAAATCCAGACGACCCAGCTTATGATGAAAACAAGCGCCAGTTTCAAGAAGATATC
AAGGTGATGAACGACCTAGTAGATAAAATTATTGCAGATCGCAAAGCAAGGGGTGAACAAAGCGATGATT
TATTAACGCAGATGCTAAACGGAAAAGATCCAGAAACGGGTGAGCCGCTTGATGACGGGAACATTCGCTA
TCAAATTATTACATTCTTATATGCGGGAGTTGAAGGTACAAGTGGTCTTTTATCATTTGCGCTGTATTTC
TTAGTGAAAAATCCACATGTATTACAAAAAGTAGCAGAAGAAGCAGCACGAGTTCTAGTAGATCCTGTTC
CAAGCTACAAACAAGTCAAACAGCTTAAATATGTCGGCATGGTCTTAAACGAAGCGCTGCGCTTATGGCC
AATTGTTCCTCAGTTTTCCCTATATGCAAAAGAAGATACGGTGCTTGGAGGAGAATATCCTTTAGAAAAA
GGCGACGAAGTAATGGTTCTGATTCCTCAGCTTCACCGTGATAAAACAGTTTGGGGAGACGATGTGGAGG
AGTTCCGTCCAGAGCGTTTTGAAAATCCAAGTGCGATTCCGCAGCATGCGTTTAAACCGTTTGGAAACGG
TCAGCGTGCGTCTATCGGTCAGCAGTTCGCTCTTCATGAAGCAACGCTGGTACTTGGTATGATGCTAAAA
CACTTTGACTTTGAAGATCATACAAACTACGAGCTCGATATTAAAGAACTGCTGACGTTAAAACCTAAAG
GCTTTGTGGTAAAAGCAAAATCGAAAAAAATTCCGCTTGGCGGTATTCCTTCACCTAGCACTGAACAGTC
TGCTAAAAAAGTACGCAAAAAGGCAGAAAACGCTCATAATACGCCGCTGCTTGTGCTATACGGTTCAAAT
ATGGGTACCGCTGAAGGAACGGCGCGTGATTTAGCAGATATTGCAATGAGCAAAGGATTTGCACCGCAGG
TCGCAACGCTTGATTCACACGCCGGAAATCTTCCGCGCGAAGGAGCTGTATTAATTGTAACGGCGTCTTA
TAACGGTCATCCGCCTGATAACGCAAAGCAATTTGTCGACTGGTTAGACCAAGCGTCTGCTGATGAAGTA
AAAGGCGTTCGCTACTCCGTATTTGGATGCGGCGATAAAAACTGGGCTACTACGTATCAAAAAGTGCCTG
CTTTTATCGATGAAACGCTTGCCGCTAAAGGGGCAGAAAACATCGCTGACCGCGGTGAAGCAGATGCAAG
CGACGACTTTGAAGGCACATATGAAGAATGGCGTGAACATATGTGGAGTGACGTAGCAGCCTACTTTAAC
CTCGACATTGAAAACAGTGAAGATAATAAATCTACTCTTTCACTTCAATTTGTCGACAGCGCCGCGGATA
TGCCGCTTGCGAAAATGCACGGTGCGTTTTCAACGAACGTCGTAGCAAGCAAAGAACTTCAACAGCCAGG
CAGTGCACGAAGCACGCGACATCTTGAAATTGAACTTCCAAAAGAAGCTTCTTATCAAGAAGGAGATCAT
TTAGGTGTTATTCCTCGCAACTATGAAGGAATAGTAAACCGTGTAACAGCAAGGTTCGGCCTAGATGCAT
CACAGCAAATCCGTCTGGAAGCAGAAGAAGAAAAATTAGCTCATTTGCCACTCGCTAAAACAGTATCCGT
AGAAGAGCTTCTGCAATACGTGGAGCTTCAAGATCCTGTTACGCGCACGCAGCTTCGCGCAATGGCTGCT
AAAACGGTCTGCCCGCCGCATAAAGTAGAGCTTGAAGCCTTGCTTGAAAAGCAAGCCTACAAAGAACAAG
TGCTGGCAAAACGTTTAACAATGCTTGAACTGCTTGAAAAATACCCGGCGTGTGAAATGAAATTCAGCGA
ATTTATCGCCCTTCTGCCAAGCATACGCCCGCGCTATTACTCGATTTCTTCATCACCTCGTGTCGATGAA
AAACAAGCAAGCATCACGGTCAGCGTTGTCTCAGGAGAAGCGTGGAGCGGATATGGAGAATATAAAGGAA
TTGCGTCGAACTATCTTGCCGAGCTGCAAGAAGGAGATACGATTACGTGCTTTATTTCCACACCGCAGTC
AGAATTTACGCTGCCAAAAGACCCTGAAACGCCGCTTATCATGGTCGGACCGGGAACAGGCGTCGCGCCG

TTTAGAGGCTTTGTGCAGGCGCGCAAACAGCTAAAAGAACAAGGACAGTCACTTGGAGAAGCACATTTAT
ACTTCGGCTGCCGTTCACCTCATGAAGACTATCTGTATCAAGAAGAGCTCGAAAACGCCCAAAGCGAAGG
CATCATTACGCTTCATACCGCTTTTTCTCGCATGCCAAATCAGCCGAAAACATACGTTCAGCACGTAATG
GAACAAGACGGCAAGAAATTGATTGAACTTCTTGATCAAGGAGCGCACTTCTATATTTGCGGAGACGGAA
GCCAAATGGCACCTGCCGTTGAAGCAACGCTTATGAAAAGCTATGCTGACGTTCACCAAGTGAGTGAAGC
AGACGCTCGCTTATGGCTGCAGCAGCTAGAAGAAAAAGGCCGATACGCAAAAGACGTGTGGGCTGGGCTC
GAGCACCACCACCACCACCACTGA

MTIKEMPQPKTFGELKNLPLLNTDKPVQALMKIADELGEIFKFEAPGRVTRYLSSQRLIKEACDESRFDK
NLWAGEKCLRDFLGDGLATSWTHEKNWKKAHNILLPSFSQQAMKGYHAVMVDIAVQLVQKWERLNADEHI
EVSEDMTRLTLDTIGLCGFNYRFNSFYRDQPHPFIISLVRALDEVMNKLQRANPDDPAYDENKRQFQEDI
KVMNDLVDKIIADRKARGEQSDDLLTQMLNGKDPETGEPLDDGNIRYQIITFLYAGVEGTSGLLSFALYF
LVKNPHVLQKVAEEAARVLVDPVPSYKQVKQLKYVGMVLNEALRLWPIVPQFSLYAKEDTVLGGEYPLEK
GDEVMVLIPQLHRDKTVWGDDVEEFRPERFENPSAIPQHAFKPFGNGQRASIGQQFALHEATLVLGMMLK
HFDFEDHTNYELDIKELLTLKPKGFVVKAKSKKIPLGGIPSPSTEQSAKKVRKKAENAHNTPLLVLYGSN
MGTAEGTARDLADIAMSKGFAPQVATLDSHAGNLPREGAVLIVTASYNGHPPDNAKQFVDWLDQASADEV
KGVRYSVFGCGDKNWATTYQKVPAFIDETLAAKGAENIADRGEADASDDFEGTYEEWREHMWSDVAAYFN
LDIENSEDNKSTLSLQFVDSAADMPLAKMHGAFSTNVVASKELQQPGSARSTRHLEIELPKEASYQEGDH
LGVIPRNYEGIVNRVTARFGLDASQQIRLEAEEEKLAHLPLAKTVSVEELLQYVELQDPVTRTQLRAMAA
KTVCPPHKVELEALLEKQAYKEQVLAKRLTMLELLEKYPACEMKFSEFIALLPSIRPRYYSISSSPRVDE
KQASITVSVVSGEAWSGYGEYKGIASNYLAELQEGDTITCFISTPQSEFTLPKDPETPLIMVGPGTGVAP
FRGFVQARKQLKEQGQSLGEAHLYFGCRSPHEDYLYQEELENAQSEGIITLHTAFSRMPNQPKTYVQHVM
EQDGKKLIELLDQGAHFYICGDGSQMAPAVEATLMKSYADVHQVSEADARLWLQQLEEKGRYAKDVWAGL
EHHHHHH

Nucleotide and amino acid sequences of P411-PYS-5149:

ATGACAATTAAAGAAATGCCTCAGCCAAAAACGTTTGGAGAGCTTAAAAATTTACCGTTATTAAACACAG
ATAAACCGGTTCAAGCTTTGATGAAAATTGCGGATGAATTAGGAGAAATCTTTAAATTCGAGGCGCCTGG
TCGTGTAACGCGCTACTTATCAAGTCAGCGTCTAATTAAAGAAGCATGCGATGAATCACGCTTTGATAAA
AACTTATGGGCGGGTGAGAAATGTCTGCGTGATTTTCTTGGAGACGGGTTAGCCACAAGCTGGACGCATG
AAAAAAATTGGAAAAAAGCGCATAATATCTTACTTCCAAGCTTTAGTCAGCAGGCAATGAAAGGCTATCA
TGCGGTGATGGTCGATATCGCCGTGCAGCTTGTTCAAAAGTGGGAGCGTCTAAATGCAGATGAGCATATT
GAAGTATCGGAAGACATGACACGTTTAACGCTTGATACAATTGGTCTTTGCGGCTTTAACTATCGCTTTA
ACAGCTTTTACCGAGATCAGCCTCATCCATTTATTATAAGTCTGGTCCGTGCACTGGATGAAGTAATGAA
CAAGCTGCAGCGAGCAAATCCAGACGACCCAGCTTATGATGAAAACAAGCGCCAGTTTCAAGAAGATATC
AAGGTGATGAACGACCTAGTAGATAAAATTATTGCAGATCGCAAAGCAAGGGGTGAACAAAGCGATGATT
TATTAACGCAGATGCTAAACGGAAAAGATCCAGAAACGGGTGAGCCGCTTGATGACGGGAACATTCGCTA
TCAAATTATTACATTCTTATATGCGGGAGTTGAAGGTACAAGTGGTCTTTTATCATTTGCGCTGTATTTC
TTAGTGAAAAATCCACATGTATTACAAAAAGTAGCAGAAGAAGCAGCACGAGTTCTAGTAGATCCTGTTC
CAAGCTACAAACAAGTCAAACAGCTTAAATATGTCGGCATGGTCTTAAACGAAGCGCTGCGCTTATGGCC
AATTGTTCCTCAGTTTTCCCTATATGCAAAAGAAGATACGGTGCTTGGAGGAGAATATCCTTTAGAAAAA
GGCGACGAAGTAATGGTTCTGATTCCTCAGCTTCACCGTGATAAAACAGTTTGGGGAGACGATGTGGAGG
AGTTCCGTCCAGAGCGTTTTGAAAATCCAAGTGCGATTCCGCAGCATGCGTTTAAACCGTTTGGAAACGG
TCAGCGTGCGTCTATCGGTCAGCAGTTCGCTCTTCATGAAGCAACGCTGGTACTTGGTATGATGCTAAAA
CACTTTGACTTTGAAGATCATACAAACTACGAGCTCGATATTAAAGAACGTCTGACGTTAAAACCTAAAG
GCTTTGTGGTAAAAGCAAAATCGAAAAAAATTCCGCTTGGCGGTATTCCTTCACCTAGCACTGAACAGTC
TGCTAAAAAAGTACGCAAAAAGGCAGAAAACGCTCATAATACGCCGCTGCTTGTGCTATACGGTTCAAAT
ATGGGTACCGCTGAAGGAACGGCGCGTGATTTAGCAGATATTGCAATGAGCAAAGGATTTGCACCGCAGG

TCGCAACGCTTGATTCACACGCCGGAAATCTTCCGCGCGAAGGAGCTGTATTAATTGTAACGGCGTCTTA
TAACGGTCATCCGCCTGATAACGCAAAGCAATTTGTCGACTGGTTAGACCAAGCGTCTGCTGATGAAGTA
AAAGGCGTTCGCTACTCCGTATTTGGATGCGGCGATAAAAACTGGGCTACTACGTATCAAAAAGTGCCTG
CTTTTATCGATGAAACGCTTGCCGCTAAAGGGGCAGAAAACATCGCTGACCGCGGTGAAGCAGATGCAAG
CGACGACTTTGAAGGCACATATGAAGAATGGCGTGAACATATGTGGAGTGACGTAGCAGCCTACTTTAAC
CTCGACATTGAAAACAGTGAAGATAATAAATCTACTCTTTCACTTCAATTTGTCGACAGCGCCGCGGATA
TGCCGCTTGCGAAAATGCACGGTGCGTTTTCAACGAACGTCGTAGCAAGCAAAGAACTTCAACAGCCAGG
CAGTGCACGAAGCACGCGACATCTTGAAATTGAACTTCCAAAAGAAGCTTCTTATCAAGAAGGAGATCAT
TTAGGTGTTATTCCTCGCAACTATGAAGGAATAGTAAACCGTGTAACAGCAAGGTTCGGCCTAGATGCAT
CACAGCAAATCCGTCTGGAAGCAGAAGAAGAAAAATTAGCTCATTTGCCACTCGCTAAAACAGTATCCGT
AGAAGAGCTTCTGCAATACGTGGAGCTTCAAGATCCTGTTACGCGCACGCAGCTTCGCGCAATGGCTGCT
AAAACGGTCTGCCCGCCGCATAAAGTAGAGCTTGAAGCCTTGCTTGAAAAGCAAGCCTACAAAGAACAAG
TGCTGGCAAAACGTTTAACAATGCTTGAACTGCTTGAAAAATACCCGGCGTGTGAAATGAAATTCAGCGA
ATTTATCGCCCTTCTGCCAAGCATACGCCCGCGCTATTACTCGATTTCTTCATCACCTCGTGTCGATGAA
AAACAAGCAAGCATCACGGTCAGCGTTGTCTCAGGAGAAGCGTGGAGCGGATATGGAGAATATAAAGGAA
TTGCGTCGAACTATCTTGCCGAGCTGCAAGAAGGAGATACGATTACGTGCTTTATTTCCACACCGCAGTC
AGAATTTACGCTGCCAAAAGACCCTGAAACGCCGCTTATCATGGTCGGACCGGGAACAGGCGTCGCGCCG
TTTAGAGGCTTTGTGCAGGCGCGCAAACAGCTAAAAGAACAAGGACAGTCACTTGGAGAAGCACATTTAT
ACTTCGGCTGCCGTTCACCTCATGAAGACTATCTGTATCAAGAAGAGCTCGAAAACGCCCAAAGCGAAGG
CATCATTACGCTTCATACCGCTTTTTCTCGCATGCCAAATCAGCCGAAAACATACGTTCAGCACGTAATG
GAACAAGACGGCAAGAAATTGATTGAACTTCTTGATCAAGGAGCGCACTTCTATATTTGCGGAGACGGAA
GCCAAATGGCACCTGCCGTTGAAGCAACGCTTATGAAAAGCTATGCTGACGTTCACCAAGTGAGTGAAGC
AGACGCTCGCTTATGGCTGCAGCAGCTAGAAGAAAAAGGCCGATACGCAAAAGACGTGTGGGCTGGGCTC
GAGCACCACCACCACCACCACTGA

MTIKEMPQPKTFGELKNLPLLNTDKPVQALMKIADELGEIFKFEAPGRVTRYLSSQRLIKEACDESRFDK
NLWAGEKCLRDFLGDGLATSWTHEKNWKKAHNILLPSFSQQAMKGYHAVMVDIAVQLVQKWERLNADEHI
EVSEDMTRLTLDTIGLCGFNYRFNSFYRDQPHPFIISLVRALDEVMNKLQRANPDDPAYDENKRQFQEDI
KVMNDLVDKIIADRKARGEQSDDLLTQMLNGKDPETGEPLDDGNIRYQIITFLYAGVEGTSGLLSFALYF
LVKNPHVLQKVAEEAARVLVDPVPSYKQVKQLKYVGMVLNEALRLWPIVPQFSLYAKEDTVLGGEYPLEK
GDEVMVLIPQLHRDKTVWGDDVEEFRPERFENPSAIPQHAFKPFGNGQRASIGQQFALHEATLVLGMMLK
HFDFEDHTNYELDIKERLTLKPKGFVVKAKSKKIPLGGIPSPSTEQSAKKVRKKAENAHNTPLLVLYGSN
MGTAEGTARDLADIAMSKGFAPQVATLDSHAGNLPREGAVLIVTASYNGHPPDNAKQFVDWLDQASADEV
KGVRYSVFGCGDKNWATTYQKVPAFIDETLAAKGAENIADRGEADASDDFEGTYEEWREHMWSDVAAYFN
LDIENSEDNKSTLSLQFVDSAADMPLAKMHGAFSTNVVASKELQQPGSARSTRHLEIELPKEASYQEGDH
LGVIPRNYEGIVNRVTARFGLDASQQIRLEAEEEKLAHLPLAKTVSVEELLQYVELQDPVTRTQLRAMAA
KTVCPPHKVELEALLEKQAYKEQVLAKRLTMLELLEKYPACEMKFSEFIALLPSIRPRYYSISSSPRVDE
KQASITVSVVSGEAWSGYGEYKGIASNYLAELQEGDTITCFISTPQSEFTLPKDPETPLIMVGPGTGVAP
FRGFVQARKQLKEQGQSLGEAHLYFGCRSPHEDYLYQEELENAQSEGIITLHTAFSRMPNQPKTYVQHVM
EQDGKKLIELLDQGAHFYICGDGSQMAPAVEATLMKSYADVHQVSEADARLWLQQLEEKGRYAKDVWAGL
EHHHHHH

Nucleotide and amino acid sequences of P411-INS-5150:

ATGACAATTAAAGAAATGCCTCAGCCAAAAACGTTTGGAGAGCTTAAAAATTTACCGTTATTAAACACAG
ATAAACCGGTTCAAGCTTTGATGAAAATTGCGGATGAATTAGGAGAAATCTTTAAATTCGAGGCGCCTGG
TCGTGTAACGCGCTACTTATCAAGTCAGCGTCTAATTAAAGAAGCATGCGATGAATCACGCTTTGATAAA
AACTTATGGGCGGGTGAGAAATGTCTGCGTGATTTTCTTGGAGACGGGTTAGCCACAAGCTGGACGCATG
AAAAAAATTGGAAAAAAGCGCATAATATCTTACTTCCAAGCTTTAGTCAGCAGGCAATGAAAGGCTATCA

TGCGGTGATGGTCGATATCGCCGTGCAGCTTGTTCAAAAGTGGGAGCGTCTAAATGCAGATGAGCATATT
GAAGTATCGGAAGACATGACACGTTTAACGCTTGATACAATTGGTCTTTGCGGCTTTAACTATCGCTTTA
ACAGCTTTTACCGAGATCAGCCTCATCCATTTATTATAAGTCTGGTCCGTGCACTGGATGAAGTAATGAA
CAAGCTGCAGCGAGCAAATCCAGACGACCCAGCTTATGATGAAAACAAGCGCCAGTTTCAAGAAGATATC
AAGGTGATGAACGACCTAGTAGATAAAATTATTGCAGATCGCAAAGCAAGGGGTGAACAAAGCGATGATT
TATTAACGCAGATGCTAAACGGAAAAGATCCAGAAACGGGTGAGCCGCTTGATGACGGGAACATTCGCTA
TCAAATTATTACATTCTTATATGCGGGAGTTGAAGGTACAAGTGGTCTTTTATCATTTGCGCTGTATTTC
TTAGTGAAAAATCCACATGTATTACAAAAAGTAGCAGAAGAAGCAGCACGAGTTCTAGTAGATCCTGTTC
CAAGCTACAAACAAGTCAAACAGCTTAAATATGTCGGCATGGTCTTAAACGAAGCGCTGCGCTTATGGCC
AATTGTTCCTCAGTTTTCCCTATATGCAAAAGAAGATACGGTGCTTGGAGGAGAATATCCTTTAGAAAAA
GGCGACGAAGTAATGGTTCTGATTCCTCAGCTTCACCGTGATAAAACAGTTTGGGGAGACGATGTGGAGG
AGTTCCGTCCAGAGCGTTTTGAAAATCCAAGTGCGATTCCGCAGCATGCGTTTAAACCGTTTGGAAACGG
TCAGCGTGCGTCTATCGGTCAGCAGTTCGCTCTTCATGAAGCAACGCTGGTACTTGGTATGATGCTAAAA
CACTTTGACTTTGAAGATCATACAAACTACGAGCTCGATATTAAAGAACTGCCGACGTTAAAACCTAAAG
GCTTTGTGGTAAAAGCAAAATCGAAAAAAATTCCGCTTGGCGGTATTCCTTCACCTAGCACTGAACAGTC
TGCTAAAAAAGTACGCAAAAAGGCAGAAAACGCTCATAATACGCCGCTGCTTGTGCTATACGGTTCAAAT
ATGGGTACCGCTGAAGGAACGGCGCGTGATTTAGCAGATATTGCAATGAGCAAAGGATTTGCACCGCAGG
TCGCAACGCTTGATTCACACGCCGGAAATCTTCCGCGCGAAGGAGCTGTATTAATTGTAACGGCGTCTTA
TAACGGTCATCCGCCTGATAACGCAAAGCAATTTGTCGACTGGTTAGACCAAGCGTCTGCTGATGAAGTA
AAAGGCGTTCGCTACTCCGTATTTGGATGCGGCGATAAAAACTGGGCTACTACGTATCAAAAAGTGCCTG
CTTTTATCGATGAAACGCTTGCCGCTAAAGGGGCAGAAAACATCGCTGACCGCGGTGAAGCAGATGCAAG
CGACGACTTTGAAGGCACATATGAAGAATGGCGTGAACATATGTGGAGTGACGTAGCAGCCTACTTTAAC
CTCGACATTGAAAACAGTGAAGATAATAAATCTACTCTTTCACTTCAATTTGTCGACAGCGCCGCGGATA
TGCCGCTTGCGAAAATGCACGGTGCGTTTTCAACGAACGTCGTAGCAAGCAAAGAACTTCAACAGCCAGG
CAGTGCACGAAGCACGCGACATCTTGAAATTGAACTTCCAAAAGAAGCTTCTTATCAAGAAGGAGATCAT
TTAGGTGTTATTCCTCGCAACTATGAAGGAATAGTAAACCGTGTAACAGCAAGGTTCGGCCTAGATGCAT
CACAGCAAATCCGTCTGGAAGCAGAAGAAGAAAAATTAGCTCATTTGCCACTCGCTAAAACAGTATCCGT
AGAAGAGCTTCTGCAATACGTGGAGCTTCAAGATCCTGTTACGCGCACGCAGCTTCGCGCAATGGCTGCT
AAAACGGTCTGCCCGCCGCATAAAGTAGAGCTTGAAGCCTTGCTTGAAAAGCAAGCCTACAAAGAACAAG
TGCTGGCAAAACGTTTAACAATGCTTGAACTGCTTGAAAAATACCCGGCGTGTGAAATGAAATTCAGCGA
ATTTATCGCCCTTCTGCCAAGCATACGCCCGCGCTATTACTCGATTTCTTCATCACCTCGTGTCGATGAA
AAACAAGCAAGCATCACGGTCAGCGTTGTCTCAGGAGAAGCGTGGAGCGGATATGGAGAATATAAAGGAA
TTGCGTCGAACTATCTTGCCGAGCTGCAAGAAGGAGATACGATTACGTGCTTTATTTCCACACCGCAGTC
AGAATTTACGCTGCCAAAAGACCCTGAAACGCCGCTTATCATGGTCGGACCGGGAACAGGCGTCGCGCCG
TTTAGAGGCTTTGTGCAGGCGCGCAAACAGCTAAAAGAACAAGGACAGTCACTTGGAGAAGCACATTTAT
ACTTCGGCTGCCGTTCACCTCATGAAGACTATCTGTATCAAGAAGAGCTCGAAAACGCCCAAAGCGAAGG
CATCATTACGCTTCATACCGCTTTTTCTCGCATGCCAAATCAGCCGAAAACATACGTTCAGCACGTAATG
GAACAAGACGGCAAGAAATTGATTGAACTTCTTGATCAAGGAGCGCACTTCTATATTTGCGGAGACGGAA
GCCAAATGGCACCTGCCGTTGAAGCAACGCTTATGAAAAGCTATGCTGACGTTCACCAAGTGAGTGAAGC
AGACGCTCGCTTATGGCTGCAGCAGCTAGAAGAAAAAGGCCGATACGCAAAAGACGTGTGGGCTGGGCTC
GAGCACCACCACCACCACCACTGA

MTIKEMPQPKTFGELKNLPLLNTDKPVQALMKIADELGEIFKFEAPGRVTRYLSSQRLIKEACDESRFDK
NLWAGEKCLRDFLGDGLATSWTHEKNWKKAHNILLPSFSQQAMKGYHAVMVDIAVQLVQKWERLNADEHI
EVSEDMTRLTLDTIGLCGFNYRFNSFYRDQPHPFIISLVRALDEVMNKLQRANPDDPAYDENKRQFQEDI
KVMNDLVDKIIADRKARGEQSDDLLTQMLNGKDPETGEPLDDGNIRYQIITFLYAGVEGTSGLLSFALYF
LVKNPHVLQKVAEEAARVLVDPVPSYKQVKQLKYVGMVLNEALRLWPIVPQFSLYAKEDTVLGGEYPLEK
GDEVMVLIPQLHRDKTVWGDDVEEFRPERFENPSAIPQHAFKPFGNGQRASIGQQFALHEATLVLGMMLK
HFDFEDHTNYELDIKELPTLKPKGFVVKAKSKKIPLGGIPSPSTEQSAKKVRKKAENAHNTPLLVLYGSN
MGTAEGTARDLADIAMSKGFAPQVATLDSHAGNLPREGAVLIVTASYNGHPPDNAKQFVDWLDQASADEV
KGVRYSVFGCGDKNWATTYQKVPAFIDETLAAKGAENIADRGEADASDDFEGTYEEWREHMWSDVAAYFN
LDIENSEDNKSTLSLQFVDSAADMPLAKMHGAFSTNVVASKELQQPGSARSTRHLEIELPKEASYQEGDH

LGVIPRNYEGIVNRVTARFGLDASQQIRLEAEEEKLAHLPLAKTVSVEELLQYVELQDPVTRTQLRAMAA
KTVCPPHKVELEALLEKQAYKEQVLAKRLTMLELLEKYPACEMKFSEFIALLPSIRPRYYSISSSPRVDE
KQASITVSVVSGEAWSGYGEYKGIASNYLAELQEGDTITCFISTPQSEFTLPKDPETPLIMVGPGTGVAP
FRGFVQARKQLKEQGQSLGEAHLYFGCRSPHEDYLYQEELENAQSEGIITLHTAFSRMPNQPKTYVQHVM
EQDGKKLIELLDQGAHFYICGDGSQMAPAVEATLMKSYADVHQVSEADARLWLQQLEEKGRYAKDVWAGL
EHHHHHH

Nucleotide and amino acid sequences of P411-INS-5151:

ATGACAATTAAAGAAATGCCTCAGCCAAAAACGTTTGGAGAGCTTAAAAATTTACCGTTATTAAACACAG
ATAAACCGGTTCAAGCTTTGATGAAAATTGCGGATGAATTAGGAGAAATCTTTAAATTCGAGGCGCCTGG
TCGTGTAACGCGCTACTTATCAAGTCAGCGTCTAATTAAAGAAGCATGCGATGAATCACGCTTTGATAAA
AACTTATGGGCGGGTGAGAAATGTCTGCGTGATTTTCTTGGAGACGGGTTAGCCACAAGCTGGACGCATG
AAAAAAATTGGAAAAAAGCGCATAATATCTTACTTCCAAGCTTTAGTCAGCAGGCAATGAAAGGCTATCA
TGCGGTGATGGTCGATATCGCCGTGCAGCTTGTTCAAAAGTGGGAGCGTCTAAATGCAGATGAGCATATT
GAAGTATCGGAAGACATGACACGTTTAACGCTTGATACAATTGGTCTTTGCGGCTTTAACTATCGCTTTA
ACAGCTTTTACCGAGATCAGCCTCATCCATTTATTATAAGTCTGGTCCGTGCAAATGATGAAGTAATGAA
CAAGCTGCAGCGAGCAAATCCAGACGACCCAGCTTATGATGAAAACAAGCGCCAGTTTCAAGAAGATATC
AAGGTGATGAACGACCTAGTAGATAAAATTATTGCAGATCGCAAAGCAAGGGGTGAACAAAGCGATGATT
TATTAACGCAGATGCTAAACGGAAAAGATCCAGAAACGGGTGAGCCGCTTGATGACGGGAACATTCGCTA
TCAAATTATTACATTCTTATATGCGGGAGTTGAAGGTACAAGTGGTCTTTTATCATTTGCGCTGTATTTC
TTAGTGAAAAATCCACATGTATTACAAAAAGTAGCAGAAGAAGCAGCACGAGTTCTAGTAGATCCTGTTC
CAAGCTACAAACAAGTCAAACAGCTTAAATATGTCGGCATGGTCTTAAACGAAGCGCTGCGCTTATGGCC
AATTGTTCCTCAGTTTTCCCTATATGCAAAAGAAGATACGGTGCTTGGAGGAGAATATCCTTTAGAAAAA
GGCGACGAAGTAATGGTTCTGATTCCTCAGCTTCACCGTGATAAAACAGTTTGGGGAGACGATGTGGAGG
AGTTCCGTCCAGAGCGTTTTGAAAATCCAAGTGCGATTCCGCAGCATGCGTTTAAACCGTTTGGAAACGG
TCAGCGTGCGTCTATCGGTCAGCAGTTCGCTCTTCATGAAGCAACGCTGGTACTTGGTATGATGCTAAAA
CACTTTGACTTTGAAGATCATACAAACTACGAGCTCGATATTAAAGAACTGCCGACGTTAAAACCTAAAG
GCTTTGTGGTAAAAGCAAAATCGAAAAAAATTCCGCTTGGCGGTATTCCTTCACCTAGCACTGAACAGTC
TGCTAAAAAAGTACGCAAAAAGGCAGAAAACGCTCATAATACGCCGCTGCTTGTGCTATACGGTTCAAAT
ATGGGTACCGCTGAAGGAACGGCGCGTGATTTAGCAGATATTGCAATGAGCAAAGGATTTGCACCGCAGG
TCGCAACGCTTGATTCACACGCCGGAAATCTTCCGCGCGAAGGAGCTGTATTAATTGTAACGGCGTCTTA
TAACGGTCATCCGCCTGATAACGCAAAGCAATTTGTCGACTGGTTAGACCAAGCGTCTGCTGATGAAGTA
AAAGGCGTTCGCTACTCCGTATTTGGATGCGGCGATAAAAACTGGGCTACTACGTATCAAAAAGTGCCTG
CTTTTATCGATGAAACGCTTGCCGCTAAAGGGGCAGAAAACATCGCTGACCGCGGTGAAGCAGATGCAAG
CGACGACTTTGAAGGCACATATGAAGAATGGCGTGAACATATGTGGAGTGACGTAGCAGCCTACTTTAAC
CTCGACATTGAAAACAGTGAAGATAATAAATCTACTCTTTCACTTCAATTTGTCGACAGCGCCGCGGATA
TGCCGCTTGCGAAAATGCACGGTGCGTTTTCAACGAACGTCGTAGCAAGCAAAGAACTTCAACAGCCAGG
CAGTGCACGAAGCACGCGACATCTTGAAATTGAACTTCCAAAAGAAGCTTCTTATCAAGAAGGAGATCAT
TTAGGTGTTATTCCTCGCAACTATGAAGGAATAGTAAACCGTGTAACAGCAAGGTTCGGCCTAGATGCAT
CACAGCAAATCCGTCTGGAAGCAGAAGAAGAAAAATTAGCTCATTTGCCACTCGCTAAAACAGTATCCGT
AGAAGAGCTTCTGCAATACGTGGAGCTTCAAGATCCTGTTACGCGCACGCAGCTTCGCGCAATGGCTGCT
AAAACGGTCTGCCCGCCGCATAAAGTAGAGCTTGAAGCCTTGCTTGAAAAGCAAGCCTACAAAGAACAAG
TGCTGGCAAAACGTTTAACAATGCTTGAACTGCTTGAAAAATACCCGGCGTGTGAAATGAAATTCAGCGA
ATTTATCGCCCTTCTGCCAAGCATACGCCCGCGCTATTACTCGATTTCTTCATCACCTCGTGTCGATGAA
AAACAAGCAAGCATCACGGTCAGCGTTGTCTCAGGAGAAGCGTGGAGCGGATATGGAGAATATAAAGGAA
TTGCGTCGAACTATCTTGCCGAGCTGCAAGAAGGAGATACGATTACGTGCTTTATTTCCACACCGCAGTC
AGAATTTACGCTGCCAAAAGACCCTGAAACGCCGCTTATCATGGTCGGACCGGGAACAGGCGTCGCGCCG
TTTAGAGGCTTTGTGCAGGCGCGCAAACAGCTAAAAGAACAAGGACAGTCACTTGGAGAAGCACATTTAT
ACTTCGGCTGCCGTTCACCTCATGAAGACTATCTGTATCAAGAAGAGCTCGAAAACGCCCAAAGCGAAGG
CATCATTACGCTTCATACCGCTTTTTCTCGCATGCCAAATCAGCCGAAAACATACGTTCAGCACGTAATG
GAACAAGACGGCAAGAAATTGATTGAACTTCTTGATCAAGGAGCGCACTTCTATATTTGCGGAGACGGAA

GCCAAATGGCACCTGCCGTTGAAGCAACGCTTATGAAAAGCTATGCTGACGTTCACCAAGTGAGTGAAGC
AGACGCTCGCTTATGGCTGCAGCAGCTAGAAGAAAAAGGCCGATACGCAAAAGACGTGTGGGCTGGGCTC
GAGCACCACCACCACCACCACTGA

MTIKEMPQPKTFGELKNLPLLNTDKPVQALMKIADELGEIFKFEAPGRVTRYLSSQRLIKEACDESRFDK
NLWAGEKCLRDFLGDGLATSWTHEKNWKKAHNILLPSFSQQAMKGYHAVMVDIAVQLVQKWERLNADEHI
EVSEDMTRLTLDTIGLCGFNYRFNSFYRDQPHPFIISLVRANDEVMNKLQRANPDDPAYDENKRQFQEDI
KVMNDLVDKIIADRKARGEQSDDLLTQMLNGKDPETGEPLDDGNIRYQIITFLYAGVEGTSGLLSFALYF
LVKNPHVLQKVAEEAARVLVDPVPSYKQVKQLKYVGMVLNEALRLWPIVPQFSLYAKEDTVLGGEYPLEK
GDEVMVLIPQLHRDKTVWGDDVEEFRPERFENPSAIPQHAFKPFGNGQRASIGQQFALHEATLVLGMMLK
HFDFEDHTNYELDIKELPTLKPKGFVVKAKSKKIPLGGIPSPSTEQSAKKVRKKAENAHNTPLLVLYGSN
MGTAEGTARDLADIAMSKGFAPQVATLDSHAGNLPREGAVLIVTASYNGHPPDNAKQFVDWLDQASADEV
KGVRYSVFGCGDKNWATTYQKVPAFIDETLAAKGAENIADRGEADASDDFEGTYEEWREHMWSDVAAYFN
LDIENSEDNKSTLSLQFVDSAADMPLAKMHGAFSTNVVASKELQQPGSARSTRHLEIELPKEASYQEGDH
LGVIPRNYEGIVNRVTARFGLDASQQIRLEAEEEKLAHLPLAKTVSVEELLQYVELQDPVTRTQLRAMAA
KTVCPPHKVELEALLEKQAYKEQVLAKRLTMLELLEKYPACEMKFSEFIALLPSIRPRYYSISSSPRVDE
KQASITVSVVSGEAWSGYGEYKGIASNYLAELQEGDTITCFISTPQSEFTLPKDPETPLIMVGPGTGVAP
FRGFVQARKQLKEQGQSLGEAHLYFGCRSPHEDYLYQEELENAQSEGIITLHTAFSRMPNQPKTYVQHVM
EQDGKKLIELLDQGAHFYICGDGSQMAPAVEATLMKSYADVHQVSEADARLWLQQLEEKGRYAKDVWAGL
EHHHHHH

X. Computational Methods

DFT Calculations

A conformational search was conducted using CREST of the XTB program (with the searching parameters -rthr 0.5 -metac -T 8).[12] DFT calculation of each low-energy conformer was performed using Gaussian 09 program package.[13] The structure of each species was submitted for geometry optimization at the level of B3LYP/(SDD for Fe and 6-31G(d) for other atoms) for singlet state and uB3LYP/(SDD for Fe and 6-31G(d) for other atoms) for triplet state, with CPCM solvation model for diethyl ether with the integration grid set to ultrafine level, followed by frequency calculation at the same theoretical level. All reported Gibbs free energies are for 298K and are after quasi-harmonic correction using the GoodVibes program.[14] Single point energy calculations of the optimized geometries were performed at uB3LYP-D3/DEF2TZVP level with CPCM solvation model for diethyl ether and with the integration grid set to ultrafine level. We have calculated energies for singlet, triplet, and quintet. All reported energies are in the lowest energy states of the corresponding species.

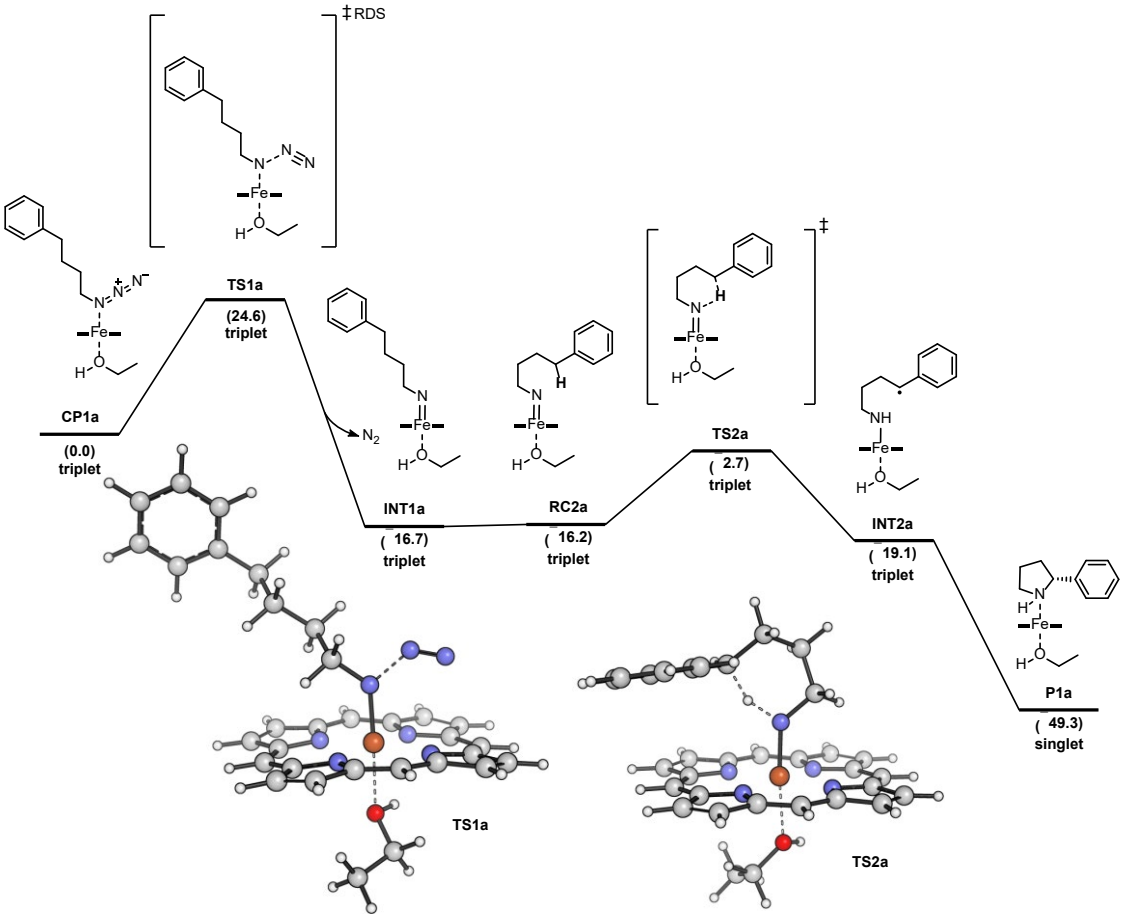

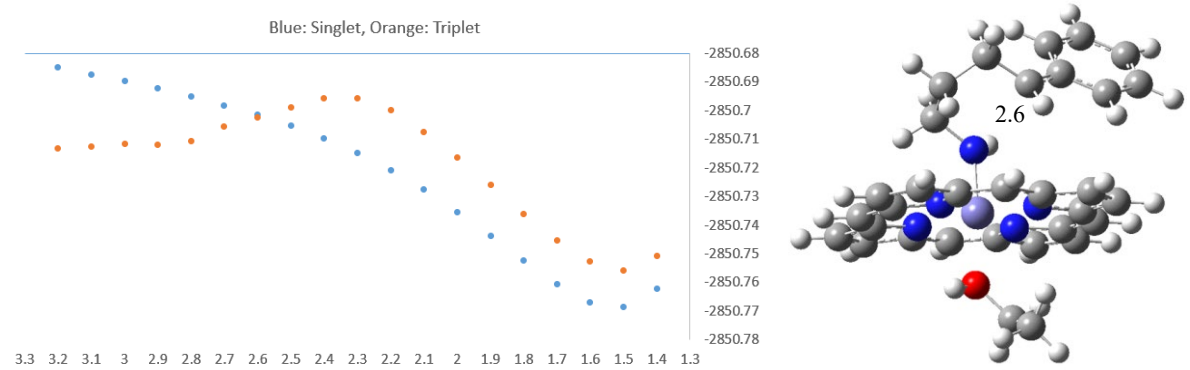

Figure C.S8. Calculated reaction pathway for the alkyl azide substrate **3.1a**. The MECP for triplet **INT2a** to singlet **P3.1a** occurs when the bond forming distance is 2.6 Angstrom.

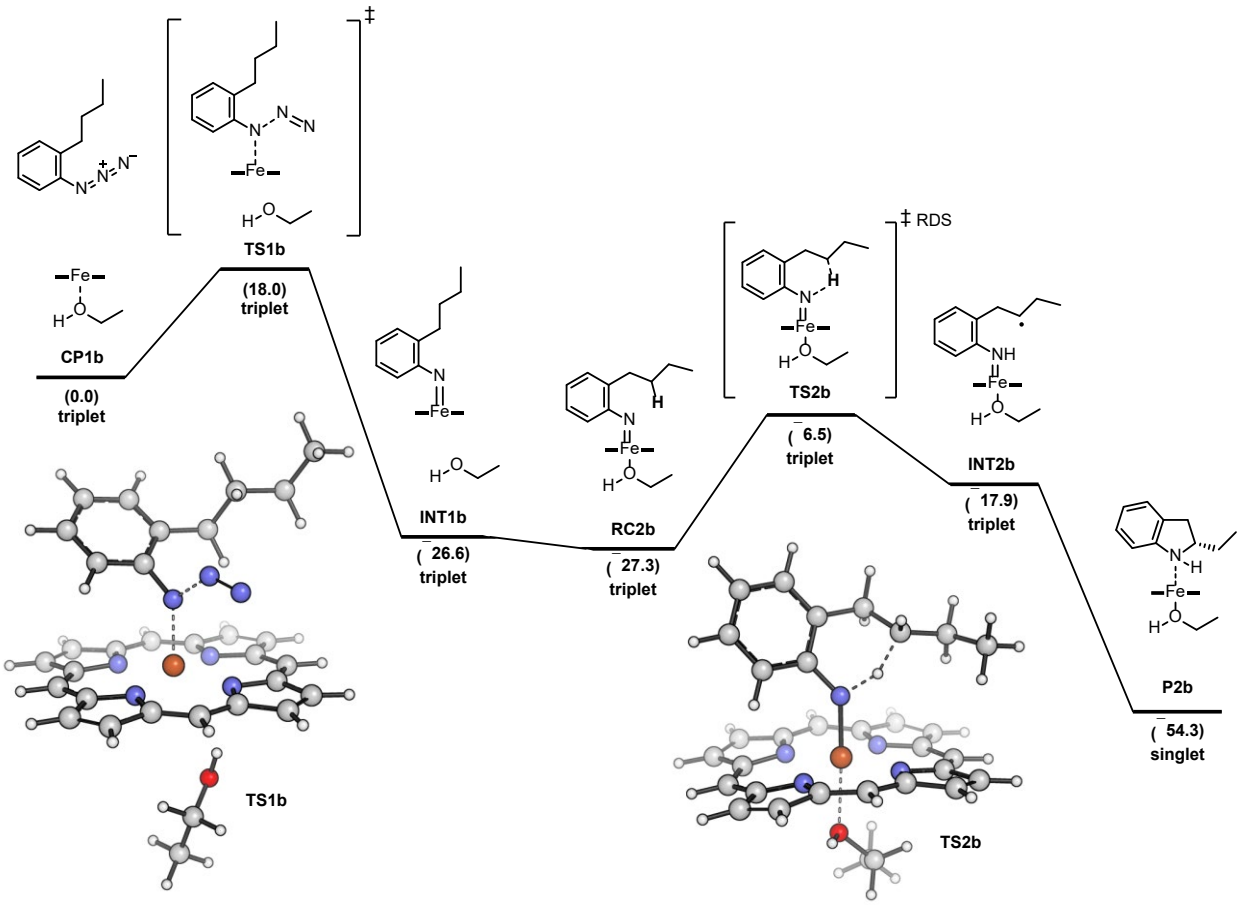

Figure C.S9. Calculated reaction pathway for the aryl azide substrate **3.3b**.

Molecular Dynamics Simulations

Molecular dynamics (MD) simulations were performed using the Amber 16 program and AmberTools 16 packages.[15] For the MD simulations of proteins with substrates, the structures resulting from the docking calculations were used for the simulations (where the intrinsically preferred antipode led to docked poses, whereas the opposite antipode does not provide any reasonable docking pose). The protonation state of each protein was first determined from the PDB2PQR Server using PROPKA[16] to assign protonation states at pH 7.3. MD simulations in explicit water were performed using the GPU-accelerated code (*pmemd*). For the protein scaffold, an evolved version of the Stony Brook modification of the Amber 99 force field (*ff14SB*)[17] parameters were applied. TIP3P[18] parameters were assigned to water molecules. MCPB.py[19] was applied to prepare for the force field of the ligand and Fe atom. The partial charges of the ligand were set to fit the electrostatic potential generated at the HF/6-31 G(d) level by the RESP (restrained electrostatic potential) model.[20] The charges were calculated according to the Merz-Singh-Kollman scheme using the Gaussian 09 program package. For the simulations involving a transition state bound, the two bond-forming distances of the ligand were restrained to the distances according to the QM optimized transition state structure, respectively, applying a harmonic constraint with a force constant with the number corresponding to the imaginary frequency obtained from DFT calculations. For the simulations not involving a transition state bound, no constraint was applied. Each protein complex was placed in a pre-equilibrated cubic box with a 12-Å buffer of TIP3P water molecules using the *leap* module. The systems were neutralized by the addition of explicit counter ions (Na^+). Long-range electrostatic effects were modeled using the particle mesh Ewald method with periodic boundary conditions.[21] An 8-Å cutoff was applied to Lennard-Jones and electrostatic interactions. Molecular dynamics simulations were performed according to the following steps:

(1) Each system was minimized with a maximum cycle of 50000 and with the steepest descent algorithm for the first 25000 cycles, with a periodic boundary for constant volume (NVT) and without the SHAKE algorithm activated. Positional restraint of 2 kcal mol^{-1} $Å^{-2}$ was applied on the protein backbone atoms (C and N) and heavy atoms of the ligand. (2) A 1 ns heating process was performed with a periodic boundary for constant volume (NVT) with the SHAKE algorithm turned on such that the angle between the hydrogen atoms was kept fixed. The temperature increased from 0 K to 300 K in a time period of 1 ns with Langevin dynamics with the collision

frequency of 5 ps^{-1}. Positional restraint of 2 kcal mol^{-1} $Å^{-2}$ was applied on the protein backbone atoms (C and N) and heavy atoms of the ligand. (3) a 2 ns equilibrium process was performed with a periodic boundary for constant pressure (NPT) and with a constant temperature of 300 K. Positional restraint of 2 kcal mol^{-1} $Å^{-2}$ was applied on the protein backbone atoms (C and N) and heavy atoms of the ligand. (4) a 2 ns equilibrium process was performed for constant pressure (NPT) and with a constant temperature of 300 K. Positional restraint of 0.5 kcal mol^{-1} $Å^{-2}$ was applied on the protein backbone atoms (C and N), and heavy atoms of the ligand. (5) A 1000 ns production was performed by applying the standard simulation condition for constant pressure (NPT) and with a constant temperature of 300K.

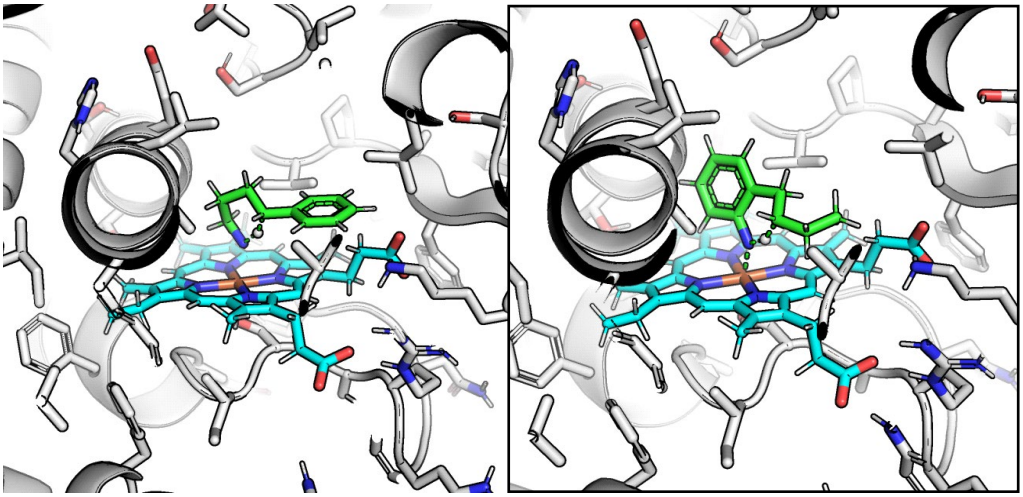

Figure C.S10. Reaction model of the hydrogen abstraction step derived from MD simulations.

XYZ coordinates and energies for the DFT calculations

CP3.1a

E[M06-2X/6-31G(d,p)/CPCM(ether)]= -1820.51428283
Zero-point correction= 0.575950
Thermal correction to Energy= 0.614033
Thermal correction to Enthalpy= 0.614978
Thermal correction to Gibbs Free Energy= 0.495862

Fe	0.398231	0.471892	0.434531
N	1.758604	1.927010	0.148921
N	1.239127	-0.591553	-1.057537
N	-0.410546	1.502004	1.966395
N	-0.913242	-1.031899	0.779858
C	1.853546	3.110522	0.842744
C	0.837109	-1.823878	-1.520222
C	2.778877	1.951030	-0.776262
C	2.328984	-0.240524	-1.823588
C	-0.020337	2.741315	2.416989
C	-1.039820	-2.196365	0.051618
C	-1.460871	1.122756	2.773501
C	-1.918756	-1.068271	1.725364
C	2.954467	3.899251	0.339520
C	1.689902	-2.254009	-2.604240
C	3.530270	3.178965	-0.663187
C	2.617145	-1.273308	-2.790305
C	-0.844872	3.152722	3.529687
C	-2.139706	-2.981863	0.556154
C	-1.737897	2.148346	3.751901
C	-2.683316	-2.283712	1.594612
H	3.238619	4.873012	0.718594
H	1.581566	-3.189010	-3.139751
H	4.382591	3.439426	-1.278010
H	3.424774	-1.236209	-3.510491
H	-0.738302	4.089527	4.062317
H	-2.444797	-3.941831	0.158451
H	-2.515469	2.090408	4.503166
H	-3.523619	-2.554460	2.221537
C	1.024802	3.495671	1.892230
C	-0.226597	-2.566599	-1.015593
C	-2.167558	-0.070916	2.663127
C	3.050459	0.941663	-1.693960
H	1.219631	4.460699	2.350604
H	-0.434888	-3.520991	-1.490173
H	-2.984198	-0.233895	3.360076
H	3.888789	1.091523	-2.367614
N	-0.812984	1.846132	-2.313686
N	-0.292833	2.077341	-3.303635
C	-5.859108	-0.368053	-1.961537
H	-5.706282	-0.337124	-3.048265
H	-5.487648	-1.342214	-1.617890
C	-5.014795	0.744592	-1.306740
H	-5.384744	1.722694	-1.643573
C	-2.693592	1.717165	-0.958267
H	-3.015349	2.710125	-1.297283
H	-5.162834	0.713689	-0.218623
H	-2.803275	1.677184	0.126868
C	-3.519796	0.614206	-1.626384
H	-3.147731	-0.360151	-1.286670
H	-3.370070	0.653926	-2.714315
N	-1.232379	1.563896	-1.186411
O	1.785157	-1.007076	2.278405
C	2.852538	-1.911255	1.961180
H	2.758595	-2.258960	0.923630
H	2.805050	-2.790912	2.619643
H	0.937854	-1.451560	2.102572
C	4.170793	-1.180918	2.153785
H	5.010736	-1.850521	1.937969
H	4.268641	-0.825164	3.185378
H	4.234424	-0.317794	1.482257
C	-7.336084	-0.245453	-1.650310
C	-7.887334	-0.866934	-0.520190
C	-8.181592	0.521760	-2.465185
C	-9.241868	-0.725304	-0.210418
H	-7.248500	-1.471676	0.120262
C	-9.536764	0.666982	-2.160282
H	-7.773765	1.006086	-3.350124
C	-10.071980	0.043567	-1.030134
H	-9.649439	-1.219068	0.668071
H	-10.175090	1.262810	-2.807711
H	-11.126918	0.152263	-0.792997

CP1b

E[M06-2X/6-31G(d,p)/CPCM(ether)]= -1820.51559468
Zero-point correction= 0.574840
Thermal correction to Energy= 0.613114

Thermal correction to Enthalpy= 0.614058
Thermal correction to Gibbs Free Energy= 0.495698

Fe	0.384426	0.145536	0.734914
N	1.255724	1.944407	0.510569
N	1.363161	-0.524411	-0.893477
N	-0.702617	0.853820	2.275452
N	-0.581265	-1.624159	0.886582
C	1.076436	3.054081	1.304906
C	1.286595	-1.783165	-1.445911
C	2.178371	2.313289	-0.445029
C	2.272491	0.167398	-1.664146
C	-0.618072	2.107506	2.836278
C	-0.406705	-2.733429	0.086503
C	-1.649242	0.177541	3.014278
C	-1.558215	-1.970509	1.798008
C	1.906354	4.141332	0.842224
C	2.168346	-1.884900	-2.584871
C	2.589052	3.682501	-0.244325
C	2.779374	-0.674615	-2.720896
C	-1.528303	2.221256	3.951610
C	-1.281834	-3.798969	0.511805
C	-2.169726	1.024649	4.060963
C	-1.996838	-3.325722	1.571608
H	1.947082	5.122427	1.298730
H	2.289079	-2.772671	-3.193145
H	3.305858	4.208304	-0.862470
H	3.504117	-0.364164	-3.463013
H	-1.651157	3.109694	4.558376
H	-1.335490	-4.774954	0.045674
H	-2.926806	0.727224	4.775548
H	-2.755925	-3.833348	2.153344
C	0.212290	3.131452	2.392674
C	0.471323	-2.814364	-0.989438
C	-2.051364	-1.135450	2.794513
C	2.655236	1.488259	-1.457754
H	0.174318	4.072865	2.932571
H	0.509953	-3.755368	-1.530139
H	-2.814857	-1.540084	3.452099
H	3.384432	1.909617	-2.143231
N	-2.955514	1.786966	-0.634009
N	-3.475239	2.259410	0.266669
N	-2.407241	1.107696	-1.506204
O	1.991669	-0.897686	2.298337
C	3.346859	-1.269750	1.984844
H	3.408121	-1.604077	0.941225
H	3.653172	-2.102844	2.631411
C	4.243350	-0.065582	2.213032
H	5.283941	-0.325041	1.988585
H	4.186785	0.266968	3.255295
H	3.946461	0.765580	1.565563
C	-2.055777	1.656252	-2.780078
C	-1.355332	2.427015	-5.371877
C	-1.541709	2.954525	-2.985048
C	-2.182067	0.754741	-3.846890
C	-1.837892	1.136768	-5.139977
C	-1.210048	3.308801	-4.302142
H	-2.562727	-0.240646	-3.640433
H	-1.947116	0.431356	-5.958606
H	-0.810406	4.304774	-4.479855
H	-1.080259	2.739981	-6.375015
C	-1.320339	3.960439	-1.873701
H	-0.398052	4.513214	-2.092435
H	-1.137649	3.451892	-0.920630
C	-2.469016	4.978801	-1.711014
H	-3.412208	4.450713	-1.517460
H	-2.608081	5.512373	-2.661597
C	-2.210353	5.989097	-0.586091
H	-1.263701	6.512743	-0.781142
H	-2.071144	5.446658	0.359607
H	1.434632	-1.693365	2.260417
C	-3.340031	7.012564	-0.429654
H	-4.292183	6.518631	-0.199882
H	-3.127424	7.720267	0.379910
H	-3.480357	7.591342	-1.351067

INT3.1a

E[M06-2X/6-31G(d,p)/CPCM(ether)]= -1710.99957173
Zero-point correction= 0.566329
Thermal correction to Energy= 0.601098
Thermal correction to Enthalpy= 0.602043
Thermal correction to Gibbs Free Energy= 0.494821

Fe	0.350852	0.151080	0.425007
N	1.061442	1.817449	-0.529137
N	1.471098	-1.004837	-0.818457
N	-0.497009	1.338082	1.805542

N	-0.072763	-1.467199	1.529698
C	0.731625	3.126617	-0.260773
C	1.579683	-2.372077	-0.794465
C	1.802132	1.845276	-1.688987
C	2.171526	-0.589764	-1.922811
C	-0.601395	2.710501	1.776452
C	0.245957	-2.774304	1.244155
C	-1.201303	0.927778	2.914345
C	-0.827397	-1.502221	2.677869
C	1.295182	4.000415	-1.262034
C	2.375679	-2.834131	-1.909762
C	1.959103	3.205494	-2.147717
C	2.743023	-1.726873	-2.610991
C	-1.382560	3.173635	2.898959
C	-0.316957	-3.653241	2.242660
C	-1.753440	2.069145	3.604652
C	-0.982298	-2.864726	3.131932
H	1.187888	5.077835	-1.271787
H	2.613142	-3.871260	-2.110749
H	2.508379	3.496869	-3.034229
H	3.345179	-1.664650	-3.508796
H	-1.604104	4.213002	3.106449
H	-0.202683	-4.729925	2.248956
H	-2.342630	2.013909	4.511446
H	-1.527732	-3.159558	4.019612
C	-0.037693	3.546733	0.818335
C	1.009865	-3.202215	0.164226
C	-1.358814	-0.391283	3.324420
C	2.324645	0.730391	-2.335119
H	-0.215533	4.612858	0.921663
H	1.177961	-4.270360	0.065357
H	-1.939082	-0.567852	4.224979
H	2.900633	0.904830	-3.239003
C	-5.781002	-0.616728	-2.241241
H	-5.640410	0.232635	-2.922563
H	-5.451819	-1.512998	-2.783214
C	-4.877441	-0.420641	-1.006412
H	-5.204980	0.475511	-0.461023
C	-2.498950	-0.097446	-0.128886
H	-2.827438	0.802234	0.420784
H	-5.018597	-1.267985	-0.320929
H	-2.640295	-0.948146	0.559939
C	-3.393122	-0.291384	-1.369494
H	-3.061361	-1.188279	-1.909430
H	-3.247211	0.558640	-2.049379
N	-1.122212	0.025542	-0.490115
O	2.368370	0.432244	1.585157
C	2.572706	0.573569	3.007924
H	1.665313	0.981738	3.467539
H	3.393025	1.281849	3.176407
H	2.474364	1.301998	1.162034
C	2.917261	-0.783595	3.596274
H	3.070464	-0.691820	4.677562
H	3.835926	-1.178136	3.148835
H	2.109174	-1.500051	3.421831
C	-7.246990	-0.746704	-1.884222
C	-8.068543	0.386478	-1.791037
C	-7.810910	-1.999770	-1.602079
C	-9.411712	0.273644	-1.425063
H	-7.651051	1.366676	-2.012248
C	-9.153399	-2.118834	-1.235623
H	-7.191402	-2.891334	-1.675039
C	-9.959348	-0.981017	-1.145277
H	-10.031219	1.164772	-1.363062
H	-9.570745	-3.100340	-1.025333
H	-11.005092	-1.071644	-0.863794

INT1b

E[M06-2X/6-31G(d,p)/CPCM(ether)]= -1711.01292976
Zero-point correction= 0.565376
Thermal correction to Energy= 0.600836
Thermal correction to Enthalpy= 0.601781
Thermal correction to Gibbs Free Energy= 0.492742

Fe	0.798039	1.359037	-0.028810
N	2.496994	2.360066	-0.355661
N	1.382009	-0.048803	-1.329699
N	0.504028	2.487562	1.639396
N	-0.616973	0.051963	0.665665
C	2.889336	3.547120	0.229815
C	0.690507	-1.187699	-1.691335
C	3.465602	2.075432	-1.295513
C	2.498039	-0.023941	-2.138993
C	1.148354	3.658120	1.963876
C	-1.076195	-1.076681	0.018404
C	-0.513013	2.360218	2.559142
C	-1.505038	0.269931	1.699663

C	4.112297	4.021948	-0.367996
C	1.379149	-1.877621	-2.754252
C	4.475564	3.103944	-1.305494
C	2.505542	-1.162663	-3.023716
C	0.536099	4.273119	3.117169
C	-2.253743	-1.589382	0.670970
C	-0.492696	3.463803	3.490405
C	-2.516290	-0.757144	1.718785
H	4.625085	4.929987	-0.077463
H	1.040253	-2.800749	-3.206895
H	5.345888	3.103410	-1.949284
H	3.282562	-1.372718	-3.747600
H	0.869473	5.196924	3.572675
H	-2.792571	-2.476253	0.362646
H	-1.183160	3.584985	4.315474
H	-3.316351	-0.819712	2.445455
C	2.250100	4.170286	1.291784
C	-0.470996	-1.652345	-1.090732
C	-1.448632	1.333909	2.590901
C	3.477818	0.959213	-2.120802
H	2.669702	5.104838	1.650746
H	-0.917677	-2.554943	-1.495819
H	-2.204806	1.372666	3.369023
H	4.308341	0.854145	-2.811675
N	-0.249871	2.266870	-1.072772
O	1.882506	-1.145173	2.165330
C	1.819875	-1.061666	3.590640
H	1.031634	-1.724592	3.979936
H	1.576756	-0.036562	3.907584
C	3.170227	-1.475175	4.153271
H	3.158227	-1.433643	5.248038
H	3.959502	-0.807823	3.789669
H	3.417307	-2.498090	3.848292
C	-0.384827	2.906300	-2.243737
C	-0.785738	4.274266	-4.687009
C	-1.581187	3.690405	-2.450799
C	0.578809	2.842603	-3.296183
C	0.375864	3.516278	-4.491169
C	-1.742620	4.349077	-3.666574
H	1.474383	2.256072	-3.140814
H	1.125073	3.453257	-5.276190
H	-2.640779	4.943774	-3.819920
H	-0.944746	4.804806	-5.621432
C	-2.644719	3.768867	-1.381135
H	-3.240010	4.678027	-1.536375
H	-2.171060	3.857173	-0.395952
C	-3.591375	2.549580	-1.366632
H	-2.996690	1.636713	-1.233189
H	-4.083215	2.464369	-2.346129
C	-4.653996	2.633405	-0.263603
H	-5.241134	3.553997	-0.392745
H	-4.153121	2.722247	0.710947
H	1.031186	-0.844820	1.801674
C	-5.594148	1.423180	-0.244488
H	-6.345932	1.513455	0.548447
H	-6.126219	1.319399	-1.198427
H	-5.035309	0.495123	-0.071864

INT2a

E[M06-2X/6-31G(d,p)/CPCM(ether)]= -1710.99829055
Zero-point correction= 0.565464
Thermal correction to Energy= 0.600051
Thermal correction to Enthalpy= 0.600995
Thermal correction to Gibbs Free Energy= 0.495476

N	-2.112991	23.301363	-28.790109
C	-3.118253	22.256637	-28.815395
C	-2.815304	21.136593	-29.830413
C	-1.609679	20.237523	-29.478909
C	-0.272067	20.892529	-29.644284
O	-2.576940	27.017087	-27.334655
H	-3.426271	27.342246	-27.677051
N	-0.766257	24.743747	-26.871507
N	-3.628050	24.458580	-26.729969
N	-0.995661	25.745808	-29.513620
C	1.107589	25.466882	-28.283790
C	-2.031759	23.872309	-24.953880
C	-5.741345	24.811318	-27.929977
C	-2.587873	26.248990	-31.318790
C	0.570603	24.960712	-27.103701
C	-3.315943	23.989170	-25.478387
C	-5.205337	25.286709	-29.123500
C	-1.305164	26.164579	-30.783893
C	1.347724	24.578724	-25.945861
C	-4.522643	23.648974	-24.757423
C	-5.979053	25.661862	-30.284535
C	-0.099690	26.527750	-31.497221

C	0.465135	24.123990	-25.014023
C	-5.566564	23.920959	-25.588441
C	-5.089054	26.056995	-31.237675
C	0.940072	26.318821	-30.642579
C	-0.852504	24.229292	-25.600901
C	-4.998358	24.424213	-26.818786
C	-3.770774	25.927544	-30.658856
C	0.370158	25.824626	-29.408881
N	-3.863430	25.459538	-29.369722
Fe	-2.306646	24.997162	-28.157029
H	-4.078790	22.709910	-29.079867
H	-3.256651	21.792374	-27.820370
H	-2.667007	21.580369	-30.824421
H	-3.706133	20.497377	-29.898055
H	-1.654371	19.351703	-30.137326
H	-1.738738	19.851971	-28.459466
H	-1.185919	22.921305	-28.599654
H	-0.155065	21.528910	-30.520788
H	2.186269	25.581018	-28.334001
H	-1.943899	23.482511	-23.943953
H	-6.821997	24.727292	-27.864036
H	-2.674057	26.605940	-32.341033
H	-6.626691	23.801519	-25.402589
H	-7.059570	25.622985	-30.345183
H	-5.289473	26.408962	-32.242052
H	-0.072598	26.894107	-32.515985
H	1.997520	26.477032	-30.814352
H	2.425458	24.655025	-25.874287
H	0.668257	23.750831	-24.017959
H	-4.547756	23.259927	-23.747119
C	-1.718201	29.095769	-28.360859
H	-0.998097	29.907301	-28.204648
H	-1.486977	28.601333	-29.308465
H	-2.715207	29.548617	-28.435413
C	-1.649528	28.114829	-27.200082
H	-1.856812	28.623755	-26.250052
H	-0.665653	27.648213	-27.130891
C	0.876137	20.710588	-28.832623
C	2.085342	21.399868	-29.157417
C	0.907640	19.860170	-27.686239
C	3.232888	21.250626	-28.393482
H	2.092394	22.055150	-30.025373
C	2.063455	19.717861	-26.929555
H	0.016669	19.309233	-27.402105
C	3.235448	20.407747	-27.271197
H	4.136020	21.789577	-28.668748
H	2.056870	19.060847	-26.063328
H	4.135385	20.290221	-26.674397

INT2b

E[M06-2X/6-31G(d,p)/CPCM(ether)]= -1710.99422569
Zero-point correction= 0.564434
Thermal correction to Energy= 0.599336
Thermal correction to Enthalpy= 0.600280
Thermal correction to Gibbs Free Energy= 0.496860

Fe	0.608653	0.502097	0.267943
N	2.257584	1.597183	-0.061896
N	1.223090	-0.805456	-1.141506
N	0.111133	1.672213	1.841079
N	-0.929898	-0.739622	0.757636
C	2.577565	2.782706	0.552635
C	0.535593	-1.912804	-1.578099
C	3.272018	1.345508	-0.954372
C	2.372263	-0.750304	-1.896323
C	0.720923	2.852463	2.187808
C	-1.336204	-1.843643	0.041748
C	-0.941094	1.516323	2.708769
C	-1.860494	-0.571075	1.757910
C	3.820872	3.298638	0.025146
C	1.265743	-2.565735	-2.640876
C	4.256166	2.401987	-0.902998
C	2.409546	-1.850862	-2.830949
C	0.035400	3.457394	3.308440
C	-2.544144	-2.389543	0.613897
C	-0.991613	2.625214	3.635946
C	-2.864934	-1.605691	1.682361
H	4.290525	4.220320	0.345095
H	0.936496	-3.460100	-3.154886
H	5.154889	2.436917	-1.505904
H	3.210670	-2.034323	-3.535921
H	0.321885	4.391738	3.774686
H	-3.063117	-3.263233	0.239981
H	-1.724591	2.735478	4.425291
H	-3.701101	-1.704174	2.363220
C	1.854862	3.381780	1.580254
C	-0.663624	-2.383467	-1.050030

C	-1.856752	0.467735	2.683942
C	3.342991	0.241674	-1.799026
H	2.231739	4.323698	1.967427
H	-1.092965	-3.269189	-1.508609
H	-2.648901	0.478535	3.426342
H	4.204680	0.166999	-2.455350
N	-0.520196	1.512391	-0.796246
O	1.671873	-0.716801	1.762683
C	2.968801	-1.358871	1.669530
H	3.209655	-1.522254	0.615066
H	2.903130	-2.333432	2.165423
C	4.011472	-0.486239	2.345925
H	4.996032	-0.961870	2.270289
H	3.774109	-0.348150	3.406165
H	4.066282	0.496599	1.869141
C	-0.405678	2.388908	-1.858259
C	-0.231358	4.133931	-4.088125
C	-1.268199	3.526315	-1.958246
C	0.531916	2.171895	-2.893799
C	0.618195	3.029528	-3.986241
C	-1.162376	4.363429	-3.070892
H	1.176146	1.305436	-2.834414
H	1.348076	2.826793	-4.766635
H	-1.822374	5.226605	-3.134688
H	-0.171320	4.806176	-4.939495
C	-2.273064	3.846140	-0.866971
H	-2.675171	4.858228	-1.058215
H	-1.762476	3.927564	0.107089
C	-3.411073	2.871726	-0.743629
H	-1.372325	1.688273	-0.268680
H	-3.738514	2.357709	-1.647180
C	-4.345296	2.919772	0.424413
H	-4.958046	3.841039	0.373607
H	-3.766602	3.016912	1.355979
H	0.976945	-1.395138	1.816792
C	-5.282318	1.707922	0.517566
H	-4.712512	0.780221	0.643355
H	-5.968204	1.803063	1.366964
H	-5.887287	1.609099	-0.391886

P3.1a

E[M06-2X/6-31G(d,p)/CPCM(ether)]= -1711.05336838
Zero-point correction= 0.572279
Thermal correction to Energy= 0.605238
Thermal correction to Enthalpy= 0.606182
Thermal correction to Gibbs Free Energy= 0.508138

N	-0.479298	23.466083	-29.370636
C	-1.116416	22.801133	-30.558550
C	-0.314385	21.501090	-30.826803
C	0.888969	21.590578	-29.867910
C	0.328480	22.408297	-28.674216
O	-2.143906	27.012356	-27.650766
N	0.547127	25.871634	-28.235337
N	-1.375273	24.562051	-26.562160
N	-1.385131	26.001687	-30.347243
C	0.913329	26.866100	-30.452579
C	0.919408	25.157747	-25.913756
C	-3.684805	23.735646	-26.445459
C	-3.682469	25.415950	-30.988395
C	1.326672	26.517147	-29.167184
C	-0.341319	24.621870	-25.656606
C	-4.075280	24.028774	-27.750961
C	-2.434853	25.986637	-31.233610
C	2.635816	26.797377	-28.617842
C	-0.755029	24.065345	-24.386510
C	-5.401468	23.788089	-28.283533
C	-2.055442	26.634038	-32.471404
C	2.636342	26.318170	-27.342050
C	-2.052038	23.674681	-24.533185
C	-5.399582	24.256374	-29.561983
C	-0.761274	27.034493	-32.324353
C	1.328562	25.742303	-27.111954
C	-2.430557	23.986677	-25.894138
C	-4.073341	24.786153	-29.808035
C	-0.351252	26.635633	-30.994511
N	-3.279018	24.617052	-28.701298
Fe	-1.360438	25.208944	-28.482379
H	-1.083259	23.498891	-31.396253
H	-2.166907	22.604484	-30.342600
H	-0.003982	21.415465	-31.872378
H	-0.922636	20.621414	-30.592278
H	1.637017	27.373990	-31.084249
H	1.642800	25.132162	-25.103298
H	-4.426077	23.274758	-25.798396
H	-4.420537	25.479826	-31.783398
H	-2.704202	23.216578	-23.799631

H	-6.215326	23.330834	-27.734013
H	-6.211649	24.264026	-30.278864
H	-2.705038	26.756980	-33.329493
H	-0.131754	27.554645	-33.036093
H	3.435201	27.299987	-29.148677
H	3.436542	26.347017	-26.612443
H	-0.125850	23.995786	-23.507493
C	-2.365015	29.395628	-27.143967
H	-1.922756	30.380440	-27.334356
H	-3.399508	29.405179	-27.503281
H	-2.377052	29.237922	-26.058521
C	-1.555902	28.316577	-27.848290
H	-0.515756	28.305885	-27.504859
H	-1.554953	28.462312	-28.929650
C	-0.395883	21.497929	-27.694938
C	0.383756	20.871014	-26.707970
C	-1.751191	21.154390	-27.778880
C	-0.165035	19.926096	-25.841364
H	1.438009	21.126249	-26.621910
C	-2.304923	20.206561	-26.912716
H	-2.393357	21.641097	-28.502870
C	-1.516368	19.584455	-25.944552
H	0.461523	19.458890	-25.085933
H	-3.360452	19.960631	-26.996338
H	-1.949211	18.847375	-25.273476
H	1.125776	22.923362	-28.132316
H	0.243010	24.065565	-29.768392
H	1.276320	20.612646	-29.568926
H	1.710903	22.150538	-30.332190
H	-2.071988	26.771726	-26.709862

P2b

E[M06-2X/6-31G(d,p)/CPCM(ether)]= -1711.05390925
Zero-point correction= 0.570621
Thermal correction to Energy= 0.603943
Thermal correction to Enthalpy= 0.604888
Thermal correction to Gibbs Free Energy= 0.507355

Fe	0.379977	0.444249	0.402194
N	1.685154	1.914431	-0.025457
N	1.099485	-0.650282	-1.141213
N	-0.214956	1.445068	2.046765
N	-0.873815	-1.079988	0.871035
C	1.801414	3.124436	0.612285
C	0.633240	-1.863154	-1.590122
C	2.645943	1.909863	-1.006721
C	2.169662	-0.334479	-1.943904
C	0.183156	2.697390	2.439268
C	-1.111389	-2.220612	0.135913
C	-1.039612	0.979692	3.040233
C	-1.664408	-1.179947	1.993428
C	2.843341	3.919913	-0.004191
C	1.426780	-2.321498	-2.710453
C	3.375601	3.160752	-1.001456
C	2.390227	-1.379647	-2.919040
C	-0.425873	3.045088	3.707148
C	-2.102334	-3.041696	0.795003
C	-1.173402	1.971938	4.087483
C	-2.434776	-2.402850	1.952906
H	3.128957	4.916147	0.310790
H	1.264747	-3.249568	-3.245013
H	4.184460	3.407556	-1.678247
H	3.174263	-1.373095	-3.666404
H	-0.274915	3.981447	4.230382
H	-2.467259	-3.990600	0.421336
H	-1.770101	1.849619	4.983200
H	-3.133150	-2.718971	2.718194
C	1.086460	3.502859	1.747584
C	-0.426643	-2.574332	-1.026276
C	-1.715271	-0.238920	3.020200
C	2.895122	0.853529	-1.879859
H	1.298967	4.483517	2.164374
H	-0.700588	-3.514151	-1.497441
H	-2.360939	-0.462218	3.865098
H	3.704301	0.979724	-2.593799
N	-1.264076	1.238403	-1.064572
O	1.730624	-0.588704	1.704762
C	3.169617	-0.700975	1.564856
H	3.435370	-0.604635	0.508491
H	3.465906	-1.698002	1.910202
C	3.840335	0.372358	2.403282
H	4.928622	0.297804	2.295751
H	3.588446	0.252840	3.462609
H	3.528666	1.369349	2.079463
C	-0.755986	1.842696	-2.275908
C	0.041532	3.413035	-4.428171
C	-1.000460	3.224113	-2.267161

C	-0.176663	1.224030	-3.378855
C	0.225904	2.028503	-4.453617
C	-0.589082	4.017551	-3.331618
H	-0.045569	0.149007	-3.419234
H	0.681463	1.560351	-5.322362
H	-0.782547	5.087592	-3.328729
H	0.358672	4.018777	-5.272701
C	-1.817444	3.553054	-1.040833
H	-2.585015	4.311436	-1.220939
H	-1.189646	3.892433	-0.204871
C	-2.419853	2.167787	-0.728826
H	-1.617911	0.298662	-1.239449
H	-3.186343	1.974712	-1.497682
C	-3.078395	1.991996	0.632252
H	-2.422932	2.374016	1.415685
H	-3.219926	0.923474	0.830093
H	1.329514	-1.463531	1.570928
C	-4.437092	2.704100	0.700596
H	-4.337308	3.785344	0.548573
H	-5.129651	2.323175	-0.060464
H	-4.901792	2.551017	1.680837

RC2a

E[M06-2X/6-31G(d,p)/CPCM(ether)]= -1710.99898058
Zero-point correction= 0.566426
Thermal correction to Energy= 0.600994
Thermal correction to Enthalpy= 0.601938
Thermal correction to Gibbs Free Energy= 0.495824

N	-2.221773	23.404981	-29.402152
C	-3.230321	22.393327	-29.399256
C	-2.730665	21.074100	-30.027097
C	-1.543698	20.417509	-29.305986
C	-1.856530	19.937657	-27.872357
O	-2.239508	27.177436	-28.059422
H	-1.982523	27.716344	-28.826163
N	-0.316512	24.849912	-27.949450
N	-2.987802	24.515711	-27.038393
N	-1.305792	25.854403	-30.454189
C	1.061211	25.601839	-29.840793
C	-0.962634	23.964355	-25.756853
C	-5.355326	24.801674	-27.633114
C	-3.325701	26.296703	-31.773075
C	0.890175	25.085541	-28.559653
C	-2.341875	24.056365	-25.914041
C	-5.182735	25.270554	-28.930919
C	-1.946122	26.259807	-31.600891
C	1.976905	24.723750	-27.676075
C	-3.304896	23.697971	-24.898759
C	-6.264187	25.625672	-29.821763
C	-0.981111	26.642592	-32.605580
C	1.410770	24.259723	-26.527559
C	-4.538307	23.945105	-25.421242
C	-5.693787	26.033753	-30.988797
C	0.251218	26.453062	-32.056887
C	-0.021410	24.340666	-26.710159
C	-4.331852	24.448861	-26.759300
C	-4.262762	25.934680	-30.810929
C	0.039718	25.951370	-30.717963
N	-3.973369	25.465911	-29.552023
Fe	-2.160528	25.037488	-28.791710
H	-4.111684	22.741943	-29.965126
H	-3.585363	22.211336	-28.371185
H	-2.447852	21.273288	-31.068835
H	-3.578487	20.374787	-30.058088
H	-0.703287	21.122442	-29.274040
H	-1.204901	19.555888	-29.896567
H	-2.722340	19.262499	-27.903104
H	-2.146428	20.796006	-27.253998
H	2.081025	25.732906	-30.190325
H	-0.592697	23.580696	-24.810812
H	-6.374388	24.697192	-27.273051
H	-3.702097	26.646282	-32.729704
H	-5.507423	23.805506	-24.958834
H	-7.315247	25.567081	-29.568076
H	-6.178718	26.382092	-31.892080
H	-1.231145	27.006109	-33.594451
H	1.222319	26.627065	-32.503344
H	3.027632	24.819906	-27.919680
H	1.899605	23.898088	-25.631589
H	-3.051226	23.315549	-23.918024
C	-0.349435	28.357728	-26.985710
H	-0.035619	28.809210	-26.037405
H	0.367634	27.577039	-27.254690
H	-0.316279	29.142591	-27.752239
C	-1.753842	27.788498	-26.847249
H	-2.460389	28.573734	-26.547979

H	-1.788024	26.996327	-26.096823
C	-0.683342	19.229763	-27.226953
C	-0.555641	17.834717	-27.294857
C	0.323930	19.957161	-26.574609
C	0.543780	17.183455	-26.730236
H	-1.328991	17.252813	-27.792216
C	1.425520	19.311306	-26.009312
H	0.240742	21.040118	-26.507142
C	1.539773	17.920488	-26.084983
H	0.619814	16.100685	-26.791105
H	2.192983	19.894039	-25.505898
H	2.394672	17.416114	-25.642374

RC2b

E[M06-2X/6-31G(d,p)/CPCM(ether)]= -1711.01513944
Zero-point correction= 0.565739
Thermal correction to Energy= 0.600543
Thermal correction to Enthalpy= 0.601487
Thermal correction to Gibbs Free Energy= 0.497100

Fe	0.786754	0.745042	0.382055
N	2.569022	1.604411	0.052759
N	1.143164	-0.588652	-1.087902
N	0.547975	1.898892	2.038420
N	-0.871468	-0.335526	0.911561
C	3.100057	2.685519	0.716185
C	0.310767	-1.596472	-1.517316
C	3.483276	1.264646	-0.915639
C	2.244476	-0.629712	-1.910564
C	1.340297	2.945272	2.431154
C	-1.449281	-1.362807	0.202774
C	-0.500079	1.861438	2.921852
C	-1.734295	-0.052511	1.944449
C	4.378771	3.040376	0.144290
C	0.898773	-2.280463	-2.646359
C	4.619776	2.155037	-0.862336
C	2.100504	-1.686435	-2.885391
C	0.781001	3.588000	3.600984
C	-2.696402	-1.753259	0.817155
C	-0.359965	2.912473	3.907989
C	-2.870809	-0.943583	1.900501
H	5.002437	3.855196	0.489997
H	0.442557	-3.113394	-3.166502
H	5.480233	2.094950	-1.516895
H	2.833812	-1.928103	-3.644552
H	1.221402	4.436710	4.109140
H	-3.339713	-2.547041	0.458586
H	-1.053534	3.092365	4.719910
H	-3.687897	-0.936326	2.610989
C	2.526058	3.324605	1.810272
C	-0.902189	-1.949780	-0.934159
C	-1.558244	0.957193	2.886294
C	3.342481	0.221238	-1.826105
H	3.061705	4.171203	2.229158
H	-1.455668	-2.764122	-1.391972
H	-2.320292	1.056154	3.653729
H	4.147750	0.069121	-2.538432
N	-0.109743	1.857245	-0.634967
O	1.744478	-0.715759	1.811570
C	2.947997	-1.499794	1.630327
H	3.136556	-1.626403	0.559346
H	2.784979	-2.489585	2.071808
C	4.109598	-0.799195	2.313161
H	5.027689	-1.380959	2.171944
H	3.924900	-0.699136	3.388113
H	4.265055	0.198066	1.891559
C	-0.226131	2.590591	-1.745789
C	-0.537901	4.173015	-4.073794
C	-1.342985	3.502296	-1.865073
C	0.706080	2.514361	-2.829557
C	0.545851	3.291069	-3.966457
C	-1.461204	4.264426	-3.023964
H	1.542991	1.834382	-2.740325
H	1.268553	3.214628	-4.774989
H	-2.298188	4.954676	-3.108981
H	-0.662209	4.785756	-4.962143
C	-2.377167	3.603039	-0.768993
H	-2.843968	4.596034	-0.809383
H	-1.890385	3.512927	0.209024
C	-3.482974	2.530889	-0.873512
H	-3.021370	1.535675	-0.834683
H	-3.971425	2.613018	-1.855047
C	-4.536418	2.651302	0.234916
H	-4.984603	3.654838	0.202443
H	-4.040250	2.567009	1.212019
H	0.971389	-1.305676	1.794715
C	-5.640102	1.593025	0.130415

H	-5.221766	0.581804	0.205000
H	-6.381577	1.708266	0.929875
H	-6.169160	1.665415	-0.828154

TS3.1a

E[M06-2X/6-31G(d,p)/CPCM(ether)]= -1820.47131100
Zero-point correction= 0.574028
Thermal correction to Energy= 0.610724
Thermal correction to Enthalpy= 0.611668
Thermal correction to Gibbs Free Energy= 0.501557

Fe	0.602248	0.899615	0.650682
N	2.276997	1.800920	1.362247
N	1.728081	-0.185175	-0.617423
N	-0.447485	1.786858	2.129557
N	-0.992118	-0.225822	0.181386
C	2.386741	2.658158	2.436419
C	1.320562	-1.229928	-1.410765
C	3.525227	1.761106	0.780542
C	3.052495	0.026592	-0.915654
C	0.017207	2.628486	3.113360
C	-1.047399	-1.266122	-0.715987
C	-1.808284	1.709647	2.309499
C	-2.279096	-0.033964	0.623988
C	3.734866	3.160196	2.536037
C	2.416366	-1.689272	-2.232448
C	4.436263	2.617432	1.500623
C	3.487796	-0.903297	-1.933072
C	-1.077989	3.091722	3.932598
C	-2.402431	-1.752161	-0.830586
C	-2.212500	2.535799	3.423647
C	-3.168012	-0.980480	-0.008884
H	4.081812	3.845945	3.298680
H	2.355432	-2.506727	-2.939824
H	5.478772	2.760261	1.245345
H	4.489979	-0.944670	-2.340799
H	-0.974904	3.762114	4.776543
H	-2.710754	-2.573064	-1.465696
H	-3.232541	2.647702	3.769146
H	-4.233533	-1.041245	0.173626
C	1.342588	3.013555	3.282465
C	0.031917	-1.752649	-1.446861
C	-2.669588	0.888725	1.588918
C	3.882824	0.954242	-0.294392
H	1.568094	3.689579	4.101408
H	-0.154459	-2.580357	-2.124250
H	-3.724436	0.927422	1.843302
H	4.910159	1.013017	-0.640818
N	0.190468	3.756522	-0.407423
N	0.478678	4.343733	0.535013
C	1.498448	2.457953	-5.534200
H	1.737188	3.522856	-5.413750
H	2.422761	1.902636	-5.327408
C	0.436336	2.064048	-4.486771
H	-0.491268	2.616735	-4.692374
C	-0.179681	1.946013	-2.012533
H	-1.102207	2.510166	-2.215657
H	0.193885	0.998691	-4.606898
H	-0.428176	0.887621	-2.119701
C	0.892060	2.330376	-3.046543
H	1.809053	1.766818	-2.834527
H	1.136939	3.394502	-2.927044
N	0.218222	2.143913	-0.624297
O	1.253086	-0.723308	2.193337
C	0.503872	-1.192974	3.338102
H	-0.199637	-0.414579	3.653618
H	1.205050	-1.378766	4.160301
H	1.975664	-0.152108	2.505798
C	-0.226669	-2.471401	2.966904
H	-0.795100	-2.836492	3.829868
H	0.482389	-3.249791	2.665079
H	-0.924532	-2.296992	2.142958
C	1.052792	2.193314	-6.957049
C	0.350468	3.165882	-7.684217
C	1.299200	0.956188	-7.570749
C	-0.094822	2.911446	-8.983312
H	0.154994	4.134128	-7.227844
C	0.856365	0.695899	-8.869594
H	1.848159	0.191156	-7.025366
C	0.156466	1.673743	-9.581126
H	-0.633687	3.681260	-9.529908
H	1.062036	-0.268499	-9.327241
H	-0.185911	1.474789	-10.593170

TS1b

E[M06-2X/6-31G(d,p)/CPCM(ether)]= -1820.47606862

Zero-point correction= 0.571115
Thermal correction to Energy= 0.609387
Thermal correction to Enthalpy= 0.610331
Thermal correction to Gibbs Free Energy= 0.494222

Fe	0.472053	0.724918	-0.091014
N	2.047016	1.906103	-0.507624
N	1.303865	-0.725289	-1.247118
N	0.018152	1.942403	1.465165
N	-0.731546	-0.681746	0.714060
C	2.304207	3.160232	0.007663
C	0.819123	-1.997389	-1.461629
C	3.013133	1.698020	-1.470461
C	2.356816	-0.578734	-2.123974
C	0.536509	3.193861	1.714129
C	-0.944124	-1.970505	0.250048
C	-1.004295	1.777649	2.374018
C	-1.659781	-0.501951	1.727312
C	3.441113	3.749091	-0.649606
C	1.578359	-2.657956	-2.492547
C	3.881319	2.841792	-1.565754
C	2.532723	-1.777228	-2.903873
C	-0.169741	3.823754	2.800300
C	-1.997835	-2.602815	0.993540
C	-1.126671	2.944789	3.209622
C	-2.442475	-1.692938	1.906413
H	3.844442	4.726800	-0.419214
H	1.396270	-3.667494	-2.838104
H	4.720969	2.919854	-2.244421
H	3.297577	-1.912795	-3.657764
H	0.054919	4.808208	3.190245
H	-2.342502	-3.615431	0.827889
H	-1.851217	3.056674	4.005963
H	-3.225389	-1.806371	2.645185
C	1.596927	3.772204	1.031733
C	-0.231574	-2.582856	-0.769798
C	-1.798141	0.645757	2.493295
C	3.155077	0.550260	-2.236572
H	1.909245	4.766287	1.334517
H	-0.506025	-3.598692	-1.034723
H	-2.568253	0.648985	3.257752
H	3.959851	0.527954	-2.964169
N	-2.278724	0.897173	-1.675805
N	-2.822355	-0.006486	-1.227480
N	-0.822599	1.474569	-1.412616
O	1.823966	-1.118795	2.600593
C	2.548151	-2.321369	2.330500
H	2.815206	-2.379990	1.264955
H	1.931786	-3.202439	2.567204
C	3.805768	-2.322555	3.184482
H	4.385053	-3.236344	3.011965
H	3.548987	-2.271212	4.248345
H	4.437013	-1.460687	2.941135
C	-0.652425	2.644011	-2.199688
C	-0.166653	4.914201	-3.789704
C	-1.299780	3.868025	-1.891420
C	0.209287	2.582836	-3.311452
C	0.464393	3.705357	-4.095334
C	-1.039076	4.981667	-2.703040
H	0.680594	1.632411	-3.541347
H	1.140917	3.635883	-4.943169
H	-1.527495	5.925396	-2.467811
H	0.017985	5.798748	-4.393778
C	-2.271654	4.000829	-0.739465
H	-2.079395	4.947704	-0.216181
H	-2.096675	3.195635	-0.020230
C	-3.750673	3.979749	-1.179891
H	-3.952586	3.049608	-1.727131
H	-3.928904	4.800045	-1.889895
C	-4.725196	4.102309	-0.001612
H	-4.513697	5.030344	0.548942
H	-4.541614	3.279704	0.704234
H	1.042405	-1.094578	2.022342
C	-6.195530	4.087338	-0.433589
H	-6.866968	4.175047	0.428600
H	-6.416441	4.918770	-1.114598
H	-6.444096	3.155801	-0.957084

TS2a

E[M06-2X/6-31G(d,p)/CPCM(ether)]= -1710.96742569
Zero-point correction= 0.561017
Thermal correction to Energy= 0.594784
Thermal correction to Enthalpy= 0.595729
Thermal correction to Gibbs Free Energy= 0.493900

N	-2.320466	23.136089	-28.743342
C	-3.365418	22.149725	-28.883638

C	-3.021034	21.117013	-29.976439
C	-1.661420	20.460265	-29.697354
C	-0.555557	21.508286	-29.634766
O	-2.555857	26.902471	-27.328292
H	-3.293448	27.276051	-27.839131
N	-0.839605	24.529244	-26.786562
N	-3.704328	24.352614	-26.697945
N	-0.977378	25.488019	-29.459843
C	1.084471	25.174758	-28.167384
C	-2.169842	23.718449	-24.886828
C	-5.775072	24.815059	-27.933249
C	-2.509436	26.067648	-31.292306
C	0.506954	24.704612	-26.992267
C	-3.437853	23.880593	-25.436974
C	-5.199092	25.264578	-29.118788
C	-1.241212	25.918766	-30.736444
C	1.248643	24.316015	-25.813081
C	-4.672750	23.605868	-24.735055
C	-5.938262	25.669288	-30.292229
C	-0.007529	26.237200	-31.421724
C	0.334249	23.895308	-24.896282
C	-5.686783	23.924847	-25.585850
C	-5.018688	26.012157	-31.237764
C	1.003086	25.999759	-30.539377
C	-0.967029	24.032066	-25.513121
C	-5.072124	24.390629	-26.809493
C	-3.715533	25.821462	-30.643354
C	0.386847	25.530322	-29.318251
N	-3.847204	25.373867	-29.348747
Fe	-2.340639	24.808187	-28.118376
H	-4.309436	22.650361	-29.136735
H	-3.534645	21.618042	-27.929141
H	-2.997963	21.619909	-30.952803
H	-3.812239	20.358524	-30.019258
H	-1.434135	19.718277	-30.477403
H	-1.722706	19.906650	-28.752134
H	-1.227271	22.501890	-29.053891
H	-0.368896	21.960770	-30.614550
H	2.166749	25.257507	-28.193243
H	-2.115447	23.335270	-23.871993
H	-6.859582	24.785933	-27.884964
H	-2.562509	26.422028	-32.317705
H	-6.754696	23.862750	-25.417057
H	-7.018603	25.683105	-30.366201
H	-5.189978	26.365115	-32.247166
H	0.057067	26.600919	-32.439775
H	2.068808	26.127113	-30.683819
H	2.326452	24.361804	-25.719852
H	0.505229	23.527780	-23.892081
H	-4.735050	23.228124	-23.722051
C	-1.349733	28.862569	-28.236102
H	-0.605038	29.621479	-27.969302
H	-0.991267	28.314440	-29.111728
H	-2.274578	29.388423	-28.506402
C	-1.578370	27.926919	-27.057711
H	-1.905403	28.492418	-26.175219
H	-0.665863	27.387273	-26.797379
C	0.699617	21.234566	-28.903881
C	1.922620	21.735721	-29.398516
C	0.735130	20.505810	-27.696040
C	3.124234	21.508159	-28.730239
H	1.921179	22.304373	-30.325503
C	1.936629	20.280555	-27.025557
H	-0.186169	20.114789	-27.273989
C	3.139278	20.776638	-27.538595
H	4.051685	21.898240	-29.142022
H	1.934392	19.713951	-26.097796
H	4.074836	20.595824	-27.016387

TS2b

E[M06-2X/6-31G(d,p)/CPCM(ether)]= -1710.97079311
Zero-point correction= 0.560320
Thermal correction to Energy= 0.594318
Thermal correction to Enthalpy= 0.595262
Thermal correction to Gibbs Free Energy= 0.494675

Fe	0.625537	0.956074	0.129973
N	2.143491	2.180649	-0.341501
N	1.298672	-0.378555	-1.237929
N	0.175881	2.107824	1.723854
N	-0.712041	-0.421593	0.782901
C	2.369420	3.429112	0.181384
C	0.674952	-1.546665	-1.618089
C	3.146972	1.960414	-1.252372
C	2.417501	-0.266216	-2.035293
C	0.660170	3.369598	1.966944
C	-1.063456	-1.584118	0.140003

C	-0.727350	1.844866	2.723511
C	-1.500971	-0.354688	1.905665
C	3.530955	4.027339	-0.439390
C	1.412148	-2.176535	-2.687533
C	4.022205	3.109736	-1.317068
C	2.500203	-1.392509	-2.934033
C	0.042134	3.920127	3.152695
C	-2.110811	-2.261972	0.870553
C	-0.806946	2.967794	3.631212
C	-2.369971	-1.508190	1.975411
H	3.918612	5.010439	-0.203353
H	1.132535	-3.108041	-3.163562
H	4.892457	3.186325	-1.956824
H	3.289155	-1.545342	-3.659790
H	0.255370	4.900021	3.561240
H	-2.562001	-3.200523	0.573727
H	-1.439570	3.007883	4.509190
H	-3.082797	-1.696782	2.768435
C	1.654810	4.004426	1.227955
C	-0.447987	-2.090911	-1.001941
C	-1.494583	0.688054	2.827639
C	3.299164	0.810385	-2.022434
H	1.946569	5.002690	1.540319
H	-0.831065	-3.025224	-1.401238
H	-2.172224	0.612164	3.672637
H	4.144418	0.772653	-2.702947
N	-0.588502	1.824327	-0.936974
O	2.207934	-0.141701	1.377177
C	2.126444	-0.587631	2.750802
H	2.648536	-1.547949	2.835575
H	1.076248	-0.740981	3.019898
C	2.776583	0.449271	3.650072
H	2.708069	0.129446	4.696124
H	2.276354	1.417055	3.551457
H	3.834321	0.575460	3.395057
C	-0.522769	2.615806	-2.068954
C	-0.461940	4.249249	-4.386854
C	-1.401009	3.737536	-2.197422
C	0.356456	2.337631	-3.142485
C	0.390355	3.147962	-4.274072
C	-1.356458	4.523059	-3.347377
H	1.001081	1.473209	-3.078007
H	1.080242	2.906539	-5.079237
H	-2.035347	5.369651	-3.428681
H	-0.441779	4.877686	-5.272818
C	-2.366260	4.020865	-1.071386
H	-3.166554	4.690185	-1.421113
H	-1.854527	4.549405	-0.251352
C	-2.943866	2.725620	-0.529105
H	-1.743611	2.055944	-0.456154
H	-3.449055	2.141245	-1.308045
C	-3.726935	2.806956	0.765003
H	-4.359292	3.711028	0.724027
H	-3.045098	2.967155	1.610360
H	2.189378	-0.915003	0.788635
C	-4.622510	1.591715	1.028285
H	-4.037322	0.667894	1.076263
H	-5.162695	1.697303	1.976356
H	-5.366996	1.476731	0.230776

XI. References

(1) Kille, S.; Acevedo-Rocha, C. G.; Parra, L. P.; Zhang, Z.-G.; Opperman, D. J.; Reetz, M. T.; Acevedo J. P. Reducing Codon Redundancy and Screening Effort of Combinatorial Protein Libraries Created by Saturation Mutagenesis. *ACS Synth. Biol.* **2013**, *2*, 83–92.

(2) Gibson, D. G.; Young, L.; Chuang, R.-Y.; Venter, J. C.; Hutchinson III, C. A.; Smith, H. O. Enzymatic Assembly of DNA Molecules up to Several Hundred Kilobases. *Nat. Methods* **2009**, *6*, 343–345.

(3) Vatsis, K. P.; Peng, H.-M.; Coon, M. J. Replacement of Active-Site Cysteine-436 by Serine Converts Cytochrome P450 2B4 into an NADPH Oxidase with Negligible Monooxygenase Activity. *J. Inorg. Biochem.* **2002**, *91*, 542–553.

(4) Seyfried, P.; Heinz, M.; Pintér, G.; Klötzner, D.-P.; Becker, Y.; Bolte, M.; Jonker, H. R. A.; Stelzl, L. S.; Hummer, G.; Schwalbe, H.; Heckel, A. Optimal Destabilization of DNA Double Strands by Single-Nucleobase Caging. *Chem. Eur. J.* **2018**, *24*, 17568–17576.

(5) Blair, L. M.; Sperry, J. Palladium-Catalyzed Heteroannulation Approach to 1,2-Bis(3-Indolyl)Ethanes. *Synlett* **2013**, *24*, 1931–1936.

(6) Hardouin, C.; Kelso, M. J.; Romero, F. A.; Rayl, T. J.; Leung, D.; Hwang, I.; Cravatt, B. F.; Boger, D. L. Structure−Activity Relationships of α-Ketooxazole Inhibitors of Fatty Acid Amide Hydrolase. *J. Med. Chem.* **2007**, *50*, 3359–3368.

(7) Kuijpers, P. F.; Tiekink, M. J.; Breukelaar, W. B.; Broere, D. L. J.; van Leest, N. P.; van der Vlugt, J. I.; Reek, J. N. H.; de Bruin, B. Cobalt-Porphyrin-Catalysed Intramolecular Ring-Closing C−H Amination of Aliphatic Azides: A Nitrene-Radical Approach to Saturated Heterocycles. *Chem. Eur. J.* **2017**, *23*, 7945–7952.

(8) Nguyen, Q.; Sun, K.; Driver, T. G. Rh_2(II)-Catalyzed Intramolecular Aliphatic C–H Bond Amination Reactions Using Aryl Azides as the N-Atom Source. *J. Am. Chem. Soc.* **2012**, *134*, 7262–7265.

(9) Zhang, H.-Y.; Mao, L.-L.; Yang, B.; Yang, S.-D. Copper-Catalyzed Radical Cascade Cyclization for the Synthesis of Phosphorated Indolines. *Chem. Commun.* **2015**, *51*, 4101–4104.

(10) Gotor-Fernández V.; Fernández-Torres, P.; Gotor, V. Chemoenzymatic Preparation of Optically Active Secondary Amines: A New Route to Enantiomerically Pure Indolines. *Tetrahedron Asymmetry* **2006**, *17*, 2558–2564.

(11) Liu, Z.; Calvó-Tusell, C.; Zhou, A. Z.; Chen, K.; Garcia-Borràs, M.; Arnold, F. H. Dual-Function Enzyme Catalysis for Enantioselective Carbon-Nitrogen Bond Formation. *Nat. Chem.* **2021**, *13*, 1166–1172.

(12) Grimme, S. Exploration of Chemical Compound, Conformer, and Reaction Space with Meta-Dynamics Simulations Based on Tight-Binding Quantum Chemical Calculations. *J. Chem. Theory Comput.* **2019**, *15*, 2847–2862.

(13) Frisch, M. J.; Trucks, G. W.; Schlegel, H. B.; Scuseria, G. E.; Robb, M. A.; Cheeseman, J. R.; Scalmani, G.; Barone, V.; Petersson, G. A.; Nakatsuji, H.; Li, X.; Caricato, M.; Marenich, A.; Bloino, J.; Janesko, B. G.; Gomperts, R.; Mennucci, B.; Hratchian, H. P.; Ortiz, J. V.; Izmaylov, A. F.; Sonnenberg, J. L.; Williams-Young, D.; Ding, F.; Lipparini, F.; Egidi, F.; Goings, J.; Peng, B.; Petrone, A.; Henderson, T.; Ranasinghe, D.; Zakrzewski, V. G.; Gao, J.; Rega, N.; Zheng, G.; Liang, W.; Hada, M.; Ehara, M.; Toyota, K.; Fukuda, R.; Hasegawa, J.; Ishida, M.; Nakajima, T.; Honda, Y.; Kitao, O.; Nakai, H.; Vreven, T.; Throssell, K.; Montgomery, J. A.; Peralta, Jr., J. E.; Ogliaro, F.; Bearpark, M.; Heyd, J. J.; Brothers, E.; Kudin, K. N.; Staroverov, V. N.; Keith, T.; Kobayashi, R.; Normand, J.; Raghavachari, K.; Rendell, A.; Burant, J. C.; Iyengar, S. S.; Tomasi, J.; Cossi, M.; Millam, J. M.; Klene, M.; Adamo, C.; Cammi, R.; Ochterski, J. W.; Martin, R. L.; Morokuma, K.; Farkas, O.; Foresman, J. B.; Fox, D. J. Gaussian 09, Revision A.02, Gaussian, Inc., Wallingford CT, 2016.

(14) Luchini, G.; Alegre-Requena, J. V.; Funes-Ardoiz, I.; Paton, R. S. GoodVibes: Automated Thermochemistry for Heterogeneous Computational Chemistry Data. *F1000Research* **2020**, *9*, 291–305.

(15) Case, D. A.; Betz, R. M.; Cerutti, D. S.; Cheatham, III, T. E.; Darden, T. A.; Duke, R. E.; Giese, T. J.; Gohlke, H.; Goetz, A. W.; Homeyer, N.; Izadi, S.; Janowski, P.; Kaus, J.; Kovalenko, A.; Lee, T. S.; LeGrand, S.; Li, P.; Lin, C.; Luchko, T.; Luo, R.; Madej, B.; Mermelstein, D.; Merz, K. M.; Monard, G.; Nguyen, H.; Nguyen, H. T.; Omelyan, I.; Onufriev, A.; Roe, D. R.; Roitberg, A.; Sagui, C.; Simmerling, C. L.; Botello-Smith, W. M.; Swails, J.; Walker, R. C.; Wang, J.; Wolf, R. M.;X. Wu, L. Xiao and P.A. Kollman (2016), AMBER 2016, University of California, San Francisco.)

(16) Søndergaard, C. R.; Olsson, M. H. M.; Rostkowski, M.; Jensen, J. H. Improved Treatment of Ligands and Coupling Effects in Empirical Calculation and Rationalization of pKa Values. *J. Chem. Theory Comput.* **2011**, *7*, 2284–2295.

(17) Maier, J. A.; Martinez, C.; Kasavajhala, K.; Wickstrom, L.; Hauser, K. E.; Simmerling, C. ff14SB: Improving the Accuracy of Protein Side Chain and Backbone Parameters from ff99SB. *J. Chem. Theory Comput.* **2015,** *11*, 3696–3713.

(18) Jorgensen, W. L., Chandrasekhar, J., Madura, J. D., Impey, R. W.; Klein, M. L. Comparison of Simple Potential Functions for Simulating Liquid Water. *J. Chem. Phys.* **1983**, *79***,** 926–935.

(19) Li, P.; Jr. Merz, K. M. MCPB.py: a Python Based Metal Center Parameter Builder. *J. Chem. Inf. Model.* **2016**, *56*, 599–604.

(20) (a) Bayly, C. I., Cieplak, P., Cornell, W. D.; Kollman, P. A. A Well-Behaved Electrostatic Potential Based Method Using Charge Restraints for Deriving Atomic Charges: the RESP Model. *J. Phys. Chem.* **1993**, *97*, 10269–10280. (b) Besler, B. H., Merz, K. M.; Kollman, P. A. Atomic Charges Derived from Semiempirical Methods. *J. Comput. Chem.* **1990**, *11*, 431–439. (c) Singh, U. C.; Kollman, P. A. An Approach to Computing Electrostatic Charges for Molecules. *J. Comput. Chem.* **1984**, *5*, 129–145.

(21) Darden, T., York, D.; Pedersen, L. Particle mesh Ewald: An N-log(N) Method for Ewald Sums in Large Systems. *J. Chem. Phys.* **1993**, *98*, 10089–10092.